SOVIET PHYSICS

JETP

A translation of the Zhurnal Éksperimental'noĭ i Teoreticheskoĭ Fiziki.

Vol. 12, No. 5, pp. 819-1033 (Russ. orig. Vol. 39, No. 5, pp. 1177-1487, Nov., 1960) May, 1961

MULTIPLE PARTICLE PRODUCTION IN THE INTERACTION BETWEEN $> 10^{11}$-ev *NUCLEONS AND EMULSION NUCLEI*

A. P. ZHDANOV, I. M. KUKS, N. V. SKIRDA, and R. M. YAKOVLEV

Radium Institute, Academy of Sciences, U.S.S.R.

Submitted to JETP editor April 6, 1960

J. Exptl. Theoret. Phys. (U.S.S.R.) 39, 1177-1185 (November, 1960)

We analyze 80 events of multiple meson production detected in an emulsion stack, using methods of mathematical statistics. The experimental material is compared with the hydrodynamical theory of particle production. Meson production due to central collisions between the nucleons and heavy nuclei is considered in particular detail.

1. EXPERIMENTAL DATA

A stack consisting of 180 layers of NIKFI-R emulsion, each 10 cm × 10 cm and 400 μ thick, was irradiated for 9 hours at 24 km altitude. A total of 120 interactions with more than five relativistic particles produced by singly-charged particles or neutral particles was found in the systematic scanning of the stack. In the scanning, the number of thin (N_s), grey (N_g), and black (N_h) tracks was counted for each of these stars, and the angle $\theta_{1/2}$ containing one half of the relativistic particles was approximately measured with a goniometer. 64 events were selected for subsequent measurements according to two criteria: the value of the half-angle $\theta_{1/2} < 10°$, or (independently of $\theta_{1/2}$) the multiplicity $N_s > 25$. These data were supplemented by 16 events from another stack of 0.25-liter volume irradiated for 15 hours at 20 km altitude.

The grain count and accurate angle measurements were made with MBI-8, MBI-8M, and Cooke 4005 microscopes. Tracks with a grain density 1.3 to 4 times greater than minimum were regarded as grey. The method of measuring the angles of the shower particles with respect to the direction of motion of the primary particle has been described earlier.[1] In order to ensure a constant relative error in the determination of both small and large angles, sections of the tracks were usually measured in two or three cross sections of the shower. The error in the determination of the smallest angle in each cross section was not greater than 20%. As a rule, the measurements were carried out in one emulsion layer. The shrinkage of the emulsion was determined immediately after the measurements, by determining the thickness of the emulsion layer at five points.

The main characteristics of the analyzed showers are presented in the table. (The notation used in the table is explained in the text.)

2. MULTIPLICITY OF PARTICLE PRODUCTION AND THE NUMBER OF NUCLEONS TAKING PART IN MESON PRODUCTION

To determine the number l of target-nucleus nucleons that take part in the meson production, the following relation was used:

$$N_s = (2l)^{1/4}(l+1)\gamma_c^{1/2}, \qquad \gamma_c = [1-(v_c/c)^2]^{-1/2}, \qquad (1)$$

which is correct within the framework of the hydrodynamical theory of Landau (v_s is the center-of-mass velocity of the system containing the primary nucleon and the l nucleons of the nucleus). The values of l calculated in this manner (see table) are often found to be greater than those expected from the model of a cylindrical tunnel. (Not more than 7 nucleons can be found in the emulsion nuclei along the line of motion of the primary particle.)

Moreover, the variation of $\log N_s$ with $\log \gamma_c$ yields a correlation coefficient $r = -0.33 \pm 0.18$, which indicates a monotonically decreasing function. Showers with $\gamma_c \geq 6$ were used in the calculation, since the selection of such showers was carried out independently of their multiplicity (according to the criterion $\theta_{1/2} \geq 10°$.).

The results obtained can be explained in the following manner: In the $10^{11} - 10^{12}$ ev energy range, the factor γ_c is small, and a considerable part of the primary-nucleon energy can be transferred to a part of the nucleus lying outside the

Serial No.	Z	N_s	N_g	N_h	$\gamma_c(\overline{x})$	$\gamma_c(\theta_{1/2})$	l	E_0^{****}, 10^{10} ev	s	σ	$\overline{\gamma}$	w_k	$P(w < w_k)$
1	2	3**	4	5	6***	7	8	9	10	11	12	13	14
1	1	18	2	9	2.5	2.9	6	7.2	0.29	0.62			
2	1	38(5)	12	22	2.6	2.6	11	13.2	0.54	0.50		0.063	0.60
3	1	13	6	6	2.8	2.8	4	5,6	0.45	0.68			
4	1	39(6)	7	18	2.9	2.4	10	16.0	0.69	0.58	2.3	0.123	0.92
5	1	20(2)	11	15	2.9	2.9	6	10.8	0.51	0.66	1.5		
6	1	18	4	18	3.0	3.2	5	8.5	0.53	0.67	2.5		
7	1	26	6	10	3.02	3.0	7	12.6	0,31	0.64			
8	1	19	8	15	3.1	4.1	6	10.8	0.54	0.67			
9	1	17	3	6	3.4	3.6	5	9.5	0.44	0.74			
10	1	9	3	21	3.6	4.0	3	6.9	0.56	0,74			
11	0	15	5	20	3.7	4.5	4	10.5	0.36	0,72			
12	1	30	9	19	3.7	3.7	8	11.2	0.41	0.60		0.027	0.13
13	1	14(1)	4	6	3.8	3.6	3	5.1	0.29	0.72			
14*	1	36	10	17	3.8	3.2	9	26.0	0.61	0.64		0.146	0.96
15	1	21(1)	3	2	4.2	4.5	5	16.0	0.40	0,72			
16	1	8	5	13	4.2	6.3	2	6.6	0.32	0.88			
17	1	44(1)	10	18	4.24	3.24	10	32.0	0.51	0.74		0.093	0.84
18	1	31(1)	2	11	4.3	5.3	8	28.0	0.53	0,67		0.032	0.14
19*	1	11	9	10	8.1	4.3	2	20.0	1.02	0.94			
20	0	17	4	13	4.6	5.7	4	14.0	0.26	0.75			
21	1	8	2	6	4.4	4.4	2	7.4	0.15	0.75			
22	1	16(3)	6	10	4.7	5.0	4	16.4	0.46	0,75			
23	0	23	0	13	4.8	4.0	5	21.5	0.44	0.74			
24	1	15	9	12	4,9	4.5	4	17.6	0,56	0.76			
25	1	25	7	12	4.9	4.4	6	26.4	0.50	0.72			
26	1	18	1	10	5.5	8.5	4	34.0	0.49	0.80	1.5		
27	1	41	17	21	5.1	5.3	9	47,7	0.43	0.69		0.046	0.40
28	0	15	1	7	5.3	5.1	4	21.0	0.39	0.78			
29*	1	38(1)	4	11	5.3	5,4	8	40.0	0.58	0.70		0.030	0.14
30	1	7	8	17	5.4	7.6	2	11,0	0.30	0.82			
31	1	14	0	6	6.2	6.3	3	16.6	0.45	0.79			
32	1	16	8	17	5.6	6.8	4	23.2	0.39	0.78			
33	1	17	4	11	5.6	6.0	4	23.2	0.71	0.78			
34	1	10	3	6	6.0	7.1	2	13,5	0.40	0.81			
35	0	14	2	5	6.2	7.3	2	14.0	0.35	0.84			
36*	1	22	2	15	6.3	7.6	5	37.5	0.30	0.78			
37	1	8	3	14	6.4	5.9	1	7.5	0.28	0.88			
38	1	14	7	11	6.5	8.2	3	23.4	0,23	0.82			
39	1	9	5	6	7.2	7.6	2	15.6	0,42	0.86			
40	1	23	4	8	6.5	7.8	5	39.0	0.53	0.775			
41*	1	28	5	9	6.6	6.8	6	48.5	0.51	0.71			
42	1	9	8	18	6.7	6.3	2	16.5	0.30	0.85			
43	0	19	1	4	7.2	8.2	4	33.0	0.54	0.81			
44*	1	13	3	9	6.7	7.1	3	25.0	0.61	0.88	1.5		
45	1	9	7	3	7.3	10.9	2	20.0	0.35	0.84			
46	1	21	4	4	7.9	7.8	4	44.0	0,52	0.83			
47	1	33	3	3	7.9	7.7	6	66.0	0.51	0.79		0.065	0.61
48	1	24	0	6	8.2	9.9	5	65.0	0,62	0.82			
49	1	8	1	8	8.4	11.8	1	13.0	0.36	0.90			
50	1	14	4	12	8.5	13.3	3	39.0	0.65	0.86	1.5		
51	1	11	3	12	8.7	11.0	2	28.0	0.53	0.88			
52	1	18	2	10	8.7	8.8	3	42,0	0,56	0.86			
53	1	8	6	4	8.9	8.9	1	15.0	0.50	0.91			
54	1	51	3	10	8.9	9,6	8	120.0	0.49	0.79		0.063	0.65
55*	1	25	6	2	8,9	8.3	5	75.0	0.43	0.83			
56	1	6	3	6	9.5	8.3	1	17.0	0.37	0.92			
57	1	6	3	9	9.5	9.6	1	17.0	0.51	0.92			
58	1	17	6	11	10.5	10.5	3	60.0	0.50	0.88			
59	1	12	2	13	10.6	12,4	2	42.0	0.34	0.91			
60	1	18	6	9	11.7	12.5	3	66.0	0.57	0.89			
61	0	8	2	7	10.9	14.0	1	22.0	0.31	0.93			
62	1	8	2	7	11.0	18.8	1	22,0	0.33	0.93	1.5		
63	1	12	2	7	11.8	14.0	2	52.0	0.38	0.90			
64	1	8	1	7	11.8	10.9	1	26.0	0.40	0,95			
65*	1	68(1)	13	17	12,6	11.2	9	261.0	0.54	0.81		0,103	0,89

1	2	3**	4	5	6***	7	8	9	10	11	12	13	14
66	1	18	3	7	13.3	28.3	3	105.0	0.65	0.91	2.3		
67	0	10	1	10	13.8	18.2	1	37.0	0.59	0.97			
68*	1	10	2	15	15	19.0	2	82.0	0.34	0.95			
69	0	8	3	9	16.3	14.0	1	50.0	0.25	0.98			
70*	0	69(2)	13	16	17.5	15.4	8	456.0	0.63	0.87		0.046	0.30
71	1	11	1	1	18,0	28.9	1	65,0	0,52	1.00			
72	1	17	1	5	28.1	28.2	2	240.0	0.72	1.01			
73*	0	27	4	5	37,6	29.6	3	780.0	0.51	1.03			
74*	1	7	3	10	43,0	32,0	1	340.0	0.86	1.09			
75	0	10	2	3	31,5	32.5	1	180,0	0.86	1.09			
76	1	5	0	5	24.5	32,0	1	270.0	0.63	1.08			
77	1	5	2	2	58.6	54.7	1	360.0	0.38	1.10			
78*	0	46	5	6	49.1	60.3	4	1800.0	0.46	1.04			
79*	1	14	1	8	72,4	85.4	1	960,0	0.48	1.13			
80*	1	14	2	2	56.9	107.4	1	700,0	0,62	1.11			

*Jets detected in the small chamber.

**The numbers in the parentheses denote the number of shower particles in the backward hemisphere.

***The value γ_c was estimated (assuming a symmetrical angular distribution of shower particles about the angle $\pi/2$ in the c.m.s.) in two ways: $\gamma_c(\bar{x}) = -(1/N_s)\times \Sigma \log \tan \theta_i$ and $\gamma_c = \cot \theta_{1/2}$ (column 7).

****Energy of the primary nucleon E_0 was calculated according to the formula $E_0 = Mc^2 2\gamma_c^2 l$ (where M is the nucleon mass).

cylindrical tunnel. Within the framework of the hydrodynamical model, we can approximately estimate the dilatation of the tunnel during the process of its "drilling" through the nucleus. We shall consider this process at any moment of time in the laboratory system (l.s.). A part of the matter in the future tunnel behind the front of the shock wave moves in the direction of the primary particle (along the x axis), and undergoes a Lorentz contraction in the ratio γ, which varies from $\gamma_0 = E_0/Mc^2$ to γ_c as the added mass of the matter joins the motion. In the coordinate system of the moving matter, the walls of the tunnel expand with the velocity of propagation of the shock wave $v'_\perp = c/3$. Using the Lorentz transformation formula, we obtain $v_\perp = c/3\gamma$ for the velocity of dilatation of the tunnel wall in the l.s. We find γ by using the momentum conservation law: $\gamma = (M_0/M_X)\gamma_0 \lesssim \gamma_0/X$, where M_X is the mass of the matter which is already moving along the path X measured in nucleon diameters. Finally, an account of the dilatation of the tunnel leads to the following increase of the number l of nucleons that can take part in the meson production, as compared to the number of nucleons in the cylindrical tunnel l_{geom}:

$$l/l_{geom} \gtrsim 1 + 0.68\, l_{geom}/\gamma_0^{1/2} + 0.175\, l_{geom}^3/\gamma_0. \qquad (2)$$

If, instead of the values of l calculated by means of Eq. (1), we now take those found from Eq. (2), then the contradiction with the geometrical dimensions of the emulsion nuclei disappears. In addition, it is also possible to explain the anomalous correlation between N_s and γ_c. In fact, with increasing energy of the primary nucleon, two competing effects in the meson production appear: the mean multiplicity per nucleon increases, and the number of excited nucleons of the target nucleus decreases. In the energy range up to 10^{12} ev, the second effect is more pronounced.*

The tunnel dilatation can also be useful in studying the excitation energy of the residual nucleus. Thus, according to our data, the mean number of grey and black tracks in stars at $E_0 < 5 \times 10^{11}$ ev equal to $\overline{N}_g + \overline{N}_h = 4.7 + 11.2$ is greater than at $E_0 \geq 5 \times 10^{11}$ ev, where $\overline{N}_g + \overline{N}_h = 3.7 + 7.2$.

3. ANISOTROPY OF THE ANGULAR DISTRIBUTION OF SHOWER PARTICLES

In the analysis of the angular distribution of shower particles, it is convenient to consider the quantity $x_i = \log \tan \theta_i$. In the variables x_i, the mean square deviation σ of the distribution serves as a measure of the shower anisotropy. The estimates of s found for each shower[*] are given in column 10 of the table. In column 11, the values of σ^2 calculated from the hydrodynamical model according to the following formula of Milekhin[2] are shown for comparison:

---

*Equation (2) gives the volume contained between the radial front of the shock wave and two planes with separation l_{geom}. The influence of the spherical form of the target nucleus for $\gamma_0 > 100$ and for heavy target nuclei is negligible, especially since the shock-wave model completely loses its meaning for meson-production events at $\gamma_0 < 100$. However, an effect analogous to the tunnel expansion can, at low energies, be represented by a branching off of the meson-producing cascade, independently of the hydrodynamical model.

$$L = \sigma^2 = 0.25 \log \gamma_0 + 0.7 \log \frac{2}{l+1} + 0.3. \qquad (3)$$

The values of σ obtained from Eq. (3) are greatly overestimated, as can be seen from the table. At the same time, Eq. (3) apparently reflects the increase of the anisotropy with increasing primary-particle energy correctly. Thus, for the variation of $\sigma^2(\log \gamma_0)$, the slope of the straight line as found by the least-squares method from the data for all 80 showers is $+0.32 \pm 0.07$ for a correlation coefficient $r = +0.61^{-0.06}_{+0.08}$.

For a constant primary-particle energy, one should observe a marked difference in the anisotropy for nucleon-nucleon showers and for those showers that result from central collisions between the primary nucleon and a heavy nucleus. According to Eqs. (2) and (3), we have calculated the mean value of s for two groups of showers with the same mean energy of about 10^{12} ev. The first group, which, for simplicity's sake, will henceforth be called the "high-multiplicity" group, includes twelve showers with maximum tunnel length $l \geq 7$. The second group (nucleon-nucleon collisions) contains data sent from the laboratories in Moscow, Alma-Ata, Warsaw, Prague, and Berlin, and selected according to the following criteria: $N_g + N_h \leq 3$; $20 \leq \gamma \leq 100$; $N_s \leq 18$ (in all, 32 jets with a total number of shower particles equal to 398). For nucleon-nucleon showers, we obtained the mean value s = 0.55 for showers of high-multiplicity 0.54.[†] If Eq. (2) were correct and our results due only to statistical fluctuations, the probability of such an event would be less than 0.01%.

In a narrow range of γ_c ($4 \leq \gamma \leq 8$), the disagreement between predictions of the hydrodynamical theory[‡] and our data is even more marked, since the dispersion σ^2 is found to be an increasing function of $\log l$: the slope of the straight line obtained by the least-squares method is 0.39 for a correlation coefficient $r = 0.43^{+0.11}_{-0.12}$. Analogous results have also been obtained by other authors.[3-5] Since the conclusion about decreasing anisotropy with an increasing length of the nuclear tunnel follows from the hydrodynamical approach (which is independent of additional postulates, say the equation of state), serious doubts arise as to the validity of applying such an approach to the description of multiple-meson production.

4. TEST OF THE UNIFORMITY OF THE ANGULAR DISTRIBUTION OF SHOWER PARTICLES

The fact that the anisotropy of the angular distribution does not decrease with increasing number of excited nucleons is understandable if we use those meson-production models in which there is no assumption about the existence of a common excited state of the system (the two-center model,[5] the "accompanying-showers" model of Chernavskiĭ,[7] the scheme of plural-multiple processes). In connection with the above, it would be very interesting to obtain some information on the general properties, not related to anisotropy, of the angular distribution.

In theories with one center of emission, the angular distributions of produced particles are given for the variables $x = \log \tan \theta$ by the probability of approximately Gaussian form $f(x; a, \sigma^2)$, where the mathematical expectation and the dispersion σ^2 of the variable x determine all the individual features of the showers. A two- or a multi-center theory leads to a superposition of functions of the same type $G(x) = \Sigma \alpha_i f(x; a_i, \sigma_i^2)$, and the mathematical expectation and the dispersion of the value x no longer determine the function G(x) fully. These distributions will be non-uniform in the Gaussian sense.

Thus, the choice of one or the other approach to the description of the multiple particle production depends on the uniformity of the experimentally obtained angular distributions. Since it is assumed that the hydrodynamical theory is most applicable to those interactions in which a large number of secondary particles are produced,[6] it becomes especially important to verify the uniformity in the group of high-multiplicity stars. In this section, we shall describe only the results of the investigation, the details being given in the Appendix.

The integral angular distributions of the shower particles of a group of nucleon-nucleon collisions and of a group of high-multiplicity stars

---

[*] Here and in the following discussion we differentiate between the mathematical expectation E(x), the mean-square deviation σ of the quantity x in the general set, and the estimates of these parameters from direct measurements, $\bar{x}$ and $\bar{s}$ respectively.

[†] It is interesting to note that the spreads of individual values in the group of nucleon-nucleon collisions (mean-square value 0.17) and in the high-multiplicity group (0.08) are strictly proportional to their statistical estimates based on the different mean multiplicity of the jets in these groups.

[‡] We can, in the present case, compare the experimental results with the hydrodynamical theory because of the high average multiplicity of the showers.

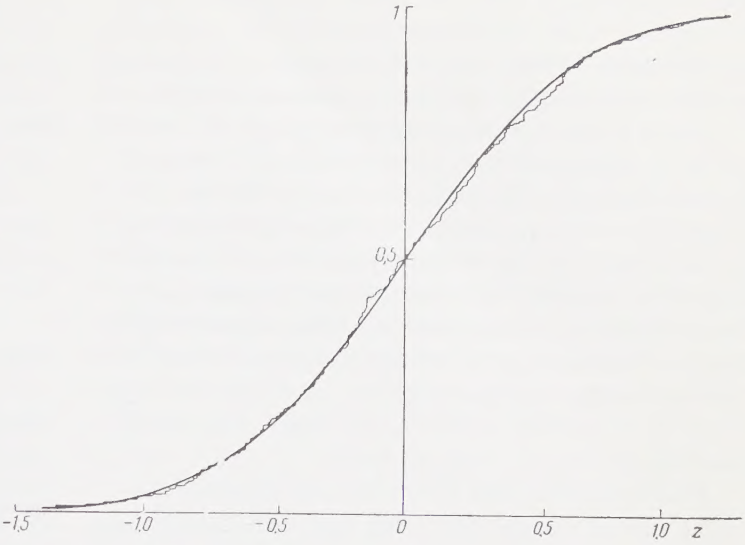

FIG. 1. Integral angular distribution for a group of nucleon-nucleon collisions in normalized variables $z = (x - \bar{x})/s$.

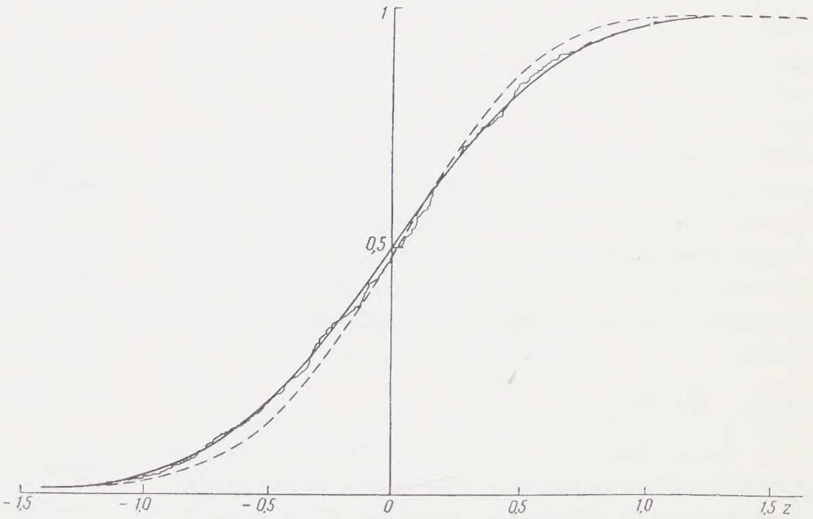

FIG. 2. Angular distribution of particles for a group of high-multiplicity interactions in normalized variables.

are shown in Figs. 1 and 2 in normalized variables $z = (x - \bar{x})/s$, where s^2 is the measure of dispersion obtained from experimental data. The solid curves represent the Gaussian function with the parameter equal to 0 and 1. It can be seen that, in both cases, the empirical distribution functions can be considered as normal ones. The w-test does not reveal marked deviations even at a significance level of 20%. The corresponding values of w_k for separate jets are shown in column 13 of the table. The arithmetical mean in the group of high-multiplicity jets $\bar{w} = 0.07$ is in good agreement with the assumption of the uniformity of the distribution. With a fit of 94%, the mean difference between the angular distribution of these jets and the normal distribution is less than 3×10^{-4}.

Chernavskiĭ[7] proposed a hypothesis suggesting the existence of a special type of non-uniformities in nucleon-nucleus collisions connected with the production of an accompanying shower by virtual π mesons, independent of the main shower. Stars of such a type should differ by possessing a large number of grey and black prongs, i.e., the same features as are characteristic of high-multiplicity stars. One can therefore separate showers of such type in the last group only by the form of the angular distribution of shower particles.

The dotted curve in Fig. 2 represents, in normalized variables, the calculated total angular distribution of the main shower and of the accompanying one. For constructing the curves, we used Eq. (2) with $E_0 = 10^{12}$ ev, $l = 5$, and under the following assumptions: the angular distribution for the accompanying shower is shifted from the main one by the quantity $\log\sqrt{M/\mu}$, the dispersion is decreased by $0.25 \log(M/\mu)$, and the number of particles in it amounts to 0.4 of the total. The quantity characterizing the difference between the solid and the dotted line $\Delta = 9 \times 10^{-4}$ (see Appendix). The probability of an agreement between the calculated distribution and the total distribution of all groups of high-multiplicity showers is less than 0.01%.

For all the 12 showers of this group, the comparison with the dotted curve produced a value of Δ less than with the solid curve only for No. 14 (see table). If we assume that the agreement is, in that case, not due to purely accidental factors, and if we take into account the fact that the detection probability of the accompanying showers in the high-multiplicity group should be greater than the corresponding total probability, we obtain the upper limit of probability of the appearance of an accompanying shower as equal to 0.04.*

It follows from the above that the angular distributions of shower particles are sufficiently uniform so that the fraction of showers of the two-center type cannot be great. In fact, in the variables $x = \log \tan \theta$, $y = \log [F/(1 - F)]$, only eight out of 80 showers are represented by curves with a well-marked split into two branches, characteristic of two-center stars. The value of $\bar{\gamma}$ (the Lorentz factor of the emission centers in the general center-of-mass system) for these showers is shown in column 12 of the table. Thus, the two-center mechanisms of particle production cannot be responsible for the anomalous behavior of the distribution anisotropy, as is maintained by Bartke et al.[5]

CONCLUSIONS

1. In the analysis of the interactions of high-energy nucleons (up to 10^{12} ev) with heavy nuclei, it is necessary to take the widening of the tunnel in the course of penetrating through the nucleus into account.
2. The anisotropy of the angular distribution of nucleon-nucleus showers does not decrease with an increase in the number of excited nucleons, at least not up to energies of 5×10^{12} ev.
3. Within the same energy range, the relative probability for the appearance of accompanying showers in the form predicted by Chernavskiĭ is smaller than 0.04. Apparently, an "accompanying" tunnel cannot be considered independently of the main one.
4. The angular distributions of relativistic particles in the showers are uniform and, expressed in terms of the variables $x = \log \tan \theta$, are well described by Gaussian functions.

The authors are greatly indebted to A. A. Blyudzin, who was very helpful in collecting the experimental material. The authors would like to thank D. M. Samoĭlovich for the processing of the emulsion stack, A. N. Charakhch'yan and V. P. Grigor'ev for help in organizing the flight, and E. L. Feĭnberg and G. A. Milekhin for their interest in the experiment and for their comments.

APPENDIX

In the article, we have made use of the w test to check the agreement between the experimental results and a hypothetic curve for a small amount of data. The test is based on the use of the quantity w_n which relates the integral empirical distribution function $\tilde{F}(x; \bar{x}, s)$, for a chosen volume n out of the total Gaussian set, to the Gaussian function

$$F(x; a, \sigma) = (2\pi\sigma^2)^{-1/2} \int_{-\infty}^{x} e^{-(x-a)^2/2\sigma^2} dx,$$

where

$$w_n = \int [\tilde{F}(x) - F(x \mid a = \bar{x},\ \sigma = s)]^2 \, dF(x \mid \bar{x}, s)$$

$$= 1/12n + \sum_{\nu=1}^{n} [F(x_\nu \mid \bar{x}, s) - (2\nu - 1)/2n]^2,$$

where $\bar{x}$, s are the estimates of the parameters a and σ corresponding to the given choice, and the quantities x_ν are ordered according to increasing value. It has been shown[8] that the distribution of w is independent of the values $\bar{x}$ and s and, for increasing n, soon becomes independent of the chosen volume. In the same reference, tables for the asymptotic form of the distribution w and the distribution w_n for n = 25 and n = 100 are given.

Let us consider r showers with multiplicity n_k each with a corresponding empirical distribution function $\tilde{G}_k(x)$. We wish to test whether the observed $\tilde{G}_k(x)$ is better described by a Gaussian function (assumption I) or by a superposition of such functions $G'_k(x) = \sum_i \alpha_{ik} F(x; a_{ik}, \sigma_{ik})$ (assumption II).

---

*Let us denote the number of the ordinary showers and of the Chernavskiĭ-type showers by N_0 and N_{ch} respectively. The high-multiplicity group consists of events with $l \geq 7$. The values of l calculated for the Chernavskiĭ-type showers using Eq. (1) take the nucleons both in the main and in the accompanying tunnel into account. The total value $l \geq 7$ is obtained if the main tunnel contains five nucleons. The relative probability in the high-multiplicity group is therefore

$$N_{ch}(l_{main} \geqslant 5) / [N_{ch}(l_{main} \geqslant 5) + N_0(l \geqslant 7)],$$

and the total probability from geometrical considerations is

$$N_{ch}(l_{main} \geqslant 5) / [N_0(l \geqslant 5) + N_{ch}(l_{main} \geqslant 5)] \approx N_{ch}(l_{main} \geqslant 5) / N(l \geqslant 5).$$

The number of showers with $N(l \geq 5)$ is taken from the table.

For each shower, we shall pass from the variable x to the normalized variable $z_{\nu k} = (x_{\nu k} - \bar{x}_k)/s_k$, where

$$\bar{x}_k = \frac{1}{n_k}\sum_{\nu}^{n_k} x_{\nu k}, \qquad s_k = \frac{1}{n_k - 1}\sum_{\nu}^{n_k}(x_{\nu k} - \bar{x}_k)^2,$$

and we shall construct the total empirical distribution function

$$\tilde{G}(z) = (1/r)\sum_{k}^{r} \tilde{G}_k(z).$$

If the assumption II is correct, then the following two cases can occur:

a) The parameters α_{ik}, a_{ik}, and σ_{ik} are such that all the distributions $G_k(z)$, or a considerable part of them, are identical. The function $\tilde{G}(z)$, for a sufficient amount of data, is then markedly different from the function $F(z;\, 0,\, 1)$, which can easily be established, e.g., by means of the w test.

b) Let us consider the case where α_{ik}, a_{ik}, and σ_{ik} are not connected by any relation in individual showers, and all $G_k(z)$ values are different. The function $\tilde{G}(z)$ can then coincide with $F(z)$, but $\tilde{G}_k(z)$ differs for different showers by more than can be ascribed to purely statistical fluctuations.

We define the variance of the functions $G_k(z)$ and $F(z)$ as

$$\Delta_k = \int [G_k(z) - F(z)]^2\, dF(z).$$

For each of the r showers, let us find the quantity

$$w'_k = n_k \int (F - \tilde{G}_k)^2\, dF(z).$$

If F and G_k are different, then

$$\begin{aligned} w'_k &= n_k \int [(F - G_k) + (G_k - \tilde{G}_k)]^2 dF(z) \\ &= n_k \int (F - G_k)^2\, dF(z) + n_k \int (G_k - \tilde{G}_k)^2\, dF(z). \end{aligned}$$

The first term of the sum equals $n_k\Delta_k$, and the second term is distributed approximately according to the w-distribution law. Averaging w'_k over all showers, we find

$$\frac{1}{r}\sum_{k}^{r} w'_k = \bar{w} + \overline{n_k\Delta_k} \approx \bar{w} + \bar{n}_k\bar{\Delta}_k.$$

For a large r, we can find such a value of w_P that, with probability $1 - P$, we have

$$\bar{w} \leqslant w_P = E(w) + \lambda_r(P), \qquad \lambda_r(P) \to 0 \text{ as } r \to \infty$$

where $E(w)$ denotes the mathematical expectation of w. In order to find $\lambda_r P$ for a finite r, we can use the limiting theorem of Lyapunov.

In principle, if we desire a given accuracy of $1 - P$, we can always select a sufficiently large r in order to determine the accuracy of the standard deviation $(\bar{\Delta}_k)$ for the angular distribution functions of single showers and of the total distribution.

Finally, if for the selected level of significance P, we simultaneously find that

$$\frac{1}{r}\sum w'_k < E(w) + \lambda_r(P),$$

$$\Big(\sum_{k}^{r} n_k\Big) \int [\tilde{G}(z) - F(z)]^2\, dF(z) < E(w) + \lambda_r(P),$$

then we can consider the assumption I as correct, and the functions $\tilde{G}_k(z)$ as homogeneous within the limits of the variance

$$\Big[E(w) - \lambda_r(P) - \frac{1}{r}\sum w'_k\Big](1/\bar{n}_k).$$

---

[1] Zhdanov, Berkovich, Lepekhin, Skirda, and Khokhlova, Приборы техника и эксперимента (Instruments and Exptl. Techniques) **4**, 32 (1957).

[2] G. A. Milekhin, JETP **35**, 1185 (1958), Soviet Phys. JETP **8**, 829 (1959).

[3] Gurevich, Mishakova, Nikol'skiĭ, and Surkova, JETP **34**, 265 (1958), Soviet Phys. JETP **7**, 185 (1958).

[4] G. Bozoki and E. Gombozi, Nucl. Phys. **9**, 400 (1958).

[5] Bartke, Ciok, Gierula, Holyński, Mięsowicz, and Saniewska, Proceedings of the Moscow International Conference on Cosmic Rays **1**, 1960.

[6] E. L. Feĭnberg, Usp. Fiz. Nauk **70**, 333 (1960), Soviet Phys.-Uspekhi **3**, 147 (1960).

[7] D. S. Černavskij, Suppl. Nuovo cimento **8**, 775 (1958).

[8] Kac, Kiefer, and Wolfowitz, Ann. Math. Stat. **26**, 189 (1955).

Translated by H. Kasha
223

DOUBLE CHARGE EXCHANGE OF ALKALI METAL IONS

Ya. M. FOGEL', V. F. KOZLOV, and G. N. POLYAKOVA

Kharkov State University; Crimean Astrophysical Observatory, Academy of Sciences, U.S.S.R.

Submitted to JETP editor May 10, 1960

J. Exptl. Theoret. Phys. (U.S.S.R.) **39**, 1186-1192 (November, 1960)

New experimental data on double charge exchange of Li^+, Na^+, and K^+ ions in a number of gases are presented which confirm the possibility of using Massey's adiabatic hypothesis to account for the shapes of the $\sigma_{1-1}(v)$ curves. Conclusions are stated regarding the behavior of some of these curves for $v < v_{max}$ near v_{max}.

INTRODUCTION

In earlier work[1,2] we have shown that double-exchange processes of the type

$$A^+ + B \rightarrow A^- + B^{++} \qquad \text{(I)}$$

obey Massey's adiabatic hypothesis, i.e., the maximum of the $\sigma_{1-1}(v)$ curve is reached at a velocity v_{max} determined from

$$a\,|\Delta E|/hv_{\max} \approx 1, \qquad (1)$$

where a is the range of interaction between the colliding particles,* ΔE is the so-called resonance defect (the change in internal energy of the particles that results from the given process), and h is Planck's constant. a was found to be only slightly dependent on the nature of the colliding particles, and to have the average value 1.5 A.

Similar relations hold true for

$$A + B \rightarrow A^- + B^+ \qquad \text{(II)}$$

(electron capture by fast neutral particles[4-6]), and for

$$A^+ + B \rightarrow A + B^+ \qquad \text{(III)}$$

(ordinary charge exchange[7,8]), with the sole difference that the average values of a for these processes are 3 and 8 A, respectively.

Another important consequence of the adiabatic hypothesis is the theorem that for large values of the adiabatic parameter $(a\,|\Delta E|\,hv \gg 1)$ the cross sections for inelastic processes are small but increase with velocity according to the formula

$$\sigma = \sigma_0 \exp\{-ka\,|\Delta E|/hv\}. \qquad (2)$$

Practically nothing is known regarding the shape of the $\sigma(v)$ curve in the adiabatic region $a\,|\Delta E|/hv \gg 1$. On the basis of data that he had obtained previously[7,8] Hafsted has concluded in reference 9 that $\sigma_{10}(v)$ for ordinary charge exchange obeys Eq. (2) at velocities that are not very far from the maximum.

The present work presents measured cross sections for double charge exchange of Li^+, Na^+, and K^+. These data further confirm (1) for double charge exchange, and also permit some conclusions regarding the shape of $\sigma_{1-1}(v)$ for primary-ion velocities $v < v_{max}$.

EXPERIMENTAL RESULTS

We measured the cross sections σ_{1-1} for $Li^+ \rightarrow Li^-$ in H_2, Ar, Kr, and Xe at 5 — 60 kev, for $Na^+ \rightarrow Na^-$ in H_2, Ar, Kr, and Xe at 10 — 55 kev, and for $K^+ \rightarrow K^-$ in H_2, Ne, Ar, Kr, and Xe at 10 — 80 kev. Beams of alkali metal ions were obtained from either a high-frequency ion source[10] or a thermionic source. The apparatus and technique have been described in references 11 — 14.

Curves of $\sigma_{1-1}(v)$ for $Li^+ \rightarrow Li^-$, $Na^+ \rightarrow Na^-$ and $K^+ \rightarrow K^-$ are shown in Figs. 1 — 3. For each energy the magnitude of σ_{1-1} was obtained by averaging two measurements. For those portions of the curves where low peaks appeared ($Na^+ \rightarrow Na^-$ and $K^+ \rightarrow K^-$ in H_2) and for low velocities, where σ_{1-1} is small, the cross sections were obtained by averaging five or six measurements. The most probable error is ±15%.

A comparison of the $\sigma_{1-1}(v)$ curves for $Li^+ \rightarrow Li^-$ and $Na^+ \rightarrow Na^-$, obtained with the aid of both thermionic and high-frequency sources, shows that the curve shape depends on the type of ion source producing the primary beam. Curves obtained with a high-frequency source exhibit maxima which do not appear on corresponding curves obtained with a thermionic source. As we have shown previously,[1,2] the complex structure of

---

*A different interpretation of a in (1) has been given by Drukarev.[3]

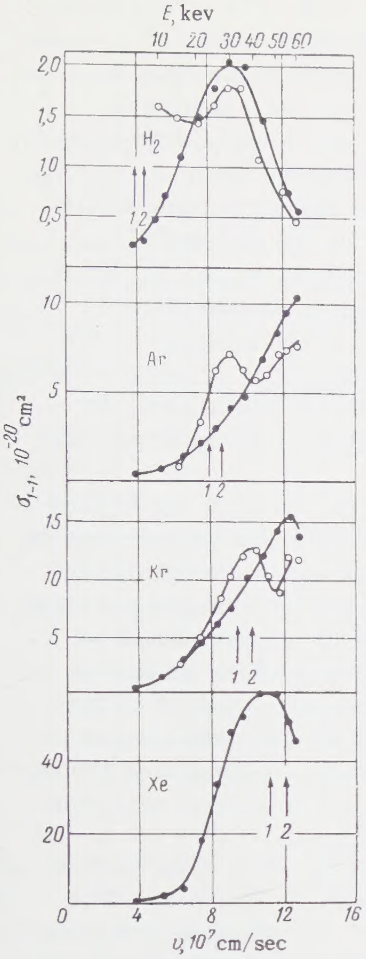

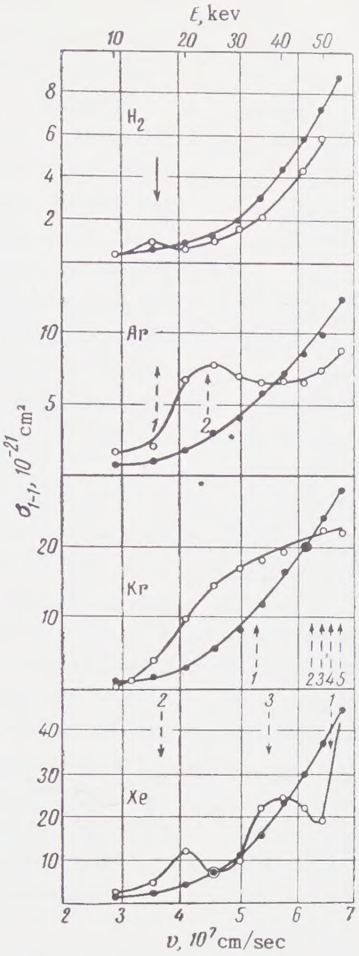

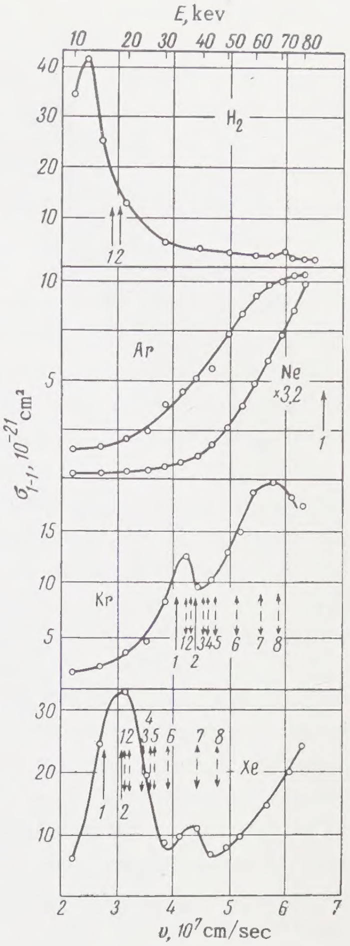

FIG. 1. $Li^+ \to Li^-$ process. ● – thermionic source, ○ – high-frequency source. Excited levels of fast ions: $1 - 2s^3S_1$; $2 - 2s\,^1S_0$.

FIG. 2. $Na^+ \to N^-$ process. ● – thermionic source, ○ – high-frequency source. Excited level of fast ions (process IV in H_2): $3s^5\,^3P^0_{2,0}$. Dashed arrows indicate the following combinations of excited levels of fast and slow ions:

Ar:
$1-Na^+(3s^5\,^3P^0_{2,0})-Ar^{++}(3p^4\,^1D_2)$,
$2-Na^+(3s^5\,^3P^0_{2,0})-Ar^{++}(3p^4\,^1S_0)$;

Kr:
$1-Na^+(3s^5\,^3P^0_{2,0})-Kr^{++}(4p^5\,^3P^0_{2,1,0})$,
$2-Na^+(3s^5\,^3P^0_{2,0})-Kr^{++}(4d\,^5D^0_{0,1,2,3,4})$,
$3-Na^+(3s^5\,^3P^0_{2,0})-Kr^{++}(4p^5\,^1P^0_1)$,
$4-Na^+(3s^5\,^3P^0_{2,0})-Kr^{++}(5s\,^5S^0_2)$,
$5-Na^+(3s^5\,^3P^0_{2,0})-Kr^{++}(4d\,^3D^0_{3,2,1})$.

Xe:
$1-Na^+(3s^5\,^3P^0_{2,0})-Xe^{++}(7s\,^5S_2^0)$,
$2-Na^+(3s^5\,^3P^0_{2,0})-Xe^{++}(5d\,^5D_0)$,
$3-Na^+(3s^5\,^3P^0_{2,0})-Xe^{++}(6p\,^5P_3)$;

FIG. 3. $K^+ \to K^-$ process. ● – thermionic source. Excited levels of fast ions: $1 - 3d\,^1F^0_3$; $2 - 4s\,^3P^0_2$. Dashed arrows indicate the following combinations of excited levels of fast and slow ions:

Kr:
$1, 2-K^+(3d\,^1F^0_8)-Kr^{++}(4p^4\,^3P_{1,0})$,
$3, 4-K^+(4s\,^3P^0_2)-Kr^{++}(4p^4\,^3P_{1,0})$,
$5-K^+(3d\,^1F^0_3)-Kr^{++}(4p^4\,^1D_2)$,
$6-K^+(4s\,^3P^0_2)-Kr^{++}(4p^4\,^1D_2)$,
$7-K^+(3d\,^1F^0_3)-Kr^{++}(4p^4\,^1S_0)$,
$8-K^+(4s\,^3P^0_2)-Kr^{++}(4p^4\,^1S_0)$;

Xe:
$1, 2-K^+(3d\,^1F^0_8)-Xe^{++}(5p^4\,^3P_{1,0})$,
$3, 4-K^+(4s\,^3P^0_2)-Xe^{++}(5p^4\,^3P_{1,1})$,
$5-K^+(3d\,^1F^0_3)-Xe^{++}(5p^4\,^1D_2)$,
$6-K^+(4s\,^3P^0_2)-Xe^{++}(5p^4\,^1D_2)$,
$7-K^+(3d\,^1F^0_3)-Xe^{++}(5p^4\,^1S_0)$,
$8-K^+(4s\,^3P^0_2)-Xe^{++}(5p^4\,^1S_0)$

$\sigma_{1-1}(v)$ curves obtained with high-frequency sources is accounted for by the fact that the primary beam in such cases contains some ions in metastable excited states. During beam passage through a gas, process I (double charge exchange in which only ground-state particles participate) will then be accompanied by other processes:

$$A^{+*} + B \to A^- + B^{++} \qquad \text{(IV)}$$

(double charge exchange of fast excited ions) and

$$A^{+*} + B \to A^- + B^{++*} \qquad \text{(V)}$$

(double charge exchange of fast excited ions with the formation of slow excited ions).

Unlike the cases of $Li^+ \rightarrow Li^-$ and $Na^+ \rightarrow Na^-$, identical $\sigma_{1-1}(v)$ curves for $K^+ \rightarrow K^-$ charge exchange are obtained with high-frequency and thermionic sources, i.e., peaks are observed at identical velocities in the two cases. The difference which is found in the respective heights of these peaks results from different numbers of excited ions in the beams. Since thermionic emission cannot be accompanied by the excitation of K^+ ions evaporating from the emitter (potassium aluminosilicate), excited ions must be produced through collisions of primary ions with residual gas molecules and with the metal surfaces of beam-defining slits and of the magnetic mass-monochromator cover. The apparatus was redesigned for the purpose of determining the part played by residual gas in the excitation of ions in a K^+ beam. The ion beam path from the source to the collision chamber was reduced. The residual gas pressure was considerably reduced by a modified pumping system and by the use of liquid-nitrogen traps. In this manner the number of residual gas molecules in the beam path from the source to the collision chamber was reduced by a factor of about 10, without affecting the $\sigma_{1-1}(v)$ curve for the $K^+ \rightarrow K^-$ process. We can thus conclude that excited ions in a K^+ beam from a thermionic source are produced by collisions with metal surfaces. The absence of excited ions in Li^+ and Na^+ beams from thermionic sources evidently results from the fact that the excitation energy of metastable Li^+ and Na^+ is considerably above that of K^+.

In our earlier work[1,2] we have shown that (1) is applicable to double charge exchange processes and that a is approximately identical, with an average value of 1.5 A, for double charge exchange of unexcited and excited ions. On this basis we have analyzed the $\sigma_{1-1}(v)$ curves for $Na^+ \rightarrow Na^-$ and $K^+ \rightarrow K^-$.

The simplest of the $Na^+ \rightarrow Na$ processes is that of Na^+ in H_2, when excited gas ions cannot result. The peak of the curve obtained with a high-frequency source is associated with an admixture of Na^+ ions in the metastable excited states $3s_5\,{}^3P_2$ and $3s_3\,{}^3P_0$ (with very close excitation energies). The shape of $\sigma_{1-1}(v)$ for $Na^+ \rightarrow Na^-$ in Ar, Kr and Xe, using a high-frequency source, can be attributed to double charge exchange of excited Na^+ ions in $3s_5\,{}^3P_{2,0}$ states, with the simultaneous formation of exeited doubly-charged gas ions. The arrows in Figs. 2 and 3 indicate the positions of the additional peaks associated with processes IV and V (solid arrows for IV and dashed arrows for V). The level of the fast excited ion participating in process IV is stated in the captions of Figs. 1 – 3. The levels of the fast ion and of the gas ion participating in process V are stated in the captions of Figs. 2 and 3.

When $K^+ \rightarrow K^-$ processes were analyzed similarly, the case of K^+ in H_2 was found to be especially interesting. Here the main and secondary peaks associated with charge exchange of K^+ in the metastable states $3d\,{}^1F_3^0$ and $4s\,{}^3P_2^0$ are within the investigated velocity range. In Fig. 3 the secondary peak is seen to be considerably higher than the main peak. The explanation for this lies in the rapid falling-off of $\sigma_{1-1\max}$ with increasing resonance defect,[15] while $|\Delta E|$ for $K^+(3p^6\,{}^1S_0$, the ground state$) \rightarrow K^-$ is larger than for $K^+(3d\,{}^1F_3^0) \rightarrow K^-$.

The shape of $\sigma_{1-1}(v)$ for $K^+ \rightarrow K^-$ in Kr and Xe can be attributed to double charge exchange of K^+ in $3d\,{}^1F_3^0$ and $4s\,{}^3P_2^0$ states, accompanied by the production of excited doubly-charged gas ions. For $K^+(3d\,{}^1F_3^0) \rightarrow K^-$ in Ar a peak should be found at 90 kev, with all other peaks located at higher energies. Fig. 3 shows a peak at 80 kev for K^+ in Ar. For K^+ in Ne the peak closest to the investigated energy range is located at 360 kev $[K^+(3d\,{}^1F_3^0) \rightarrow K^-]$; $\sigma_{1-1}(v)$ increases monotonically in the investigated range.

The shapes of $\sigma_{1-1}(v)$ for $Na^+ \rightarrow Na^-$ and $K^+ \rightarrow K^-$, as well as for $H^+ \rightarrow H^-$, $Li^+ \rightarrow Li^-$, $B^+ \rightarrow B^-$, $O^+ \rightarrow O^-$ and $F^+ \rightarrow F^-$, which we had investigated previously, are fully accounted for by the adiabatic criterion (1).

In order to account for the shape of σ_{1-1} at velocities $v < v_{\max}$ we may use $\sigma_{1-1}(v)$ for $Li^+ \rightarrow Li^-$ and $Na^+ \rightarrow Na^-$ in the case of a thermionic source, as well as for $K^+ \rightarrow K^-$ in Ne and Ar, since in these cases the velocity region of interest is not distorted by secondary peaks that represent double charge exchange involving excited particles.

It must be remembered that our velocity region $v < v_{\max}$ is not adiabatic for any of the aforementioned cases (with the possible exception of K^+ in Ne), since the condition $a|\Delta E|/hv \gg 1$ is not fulfilled. We could therefore not expect $\sigma_{1-1}(v)$ in this region to be described by (2). In actuality, a considerable portion of $\sigma_{1-1}(v)$ almost up to the peak obeys (2) for all of the cases mentioned ($Li^+ \rightarrow Li^-$ and $K^+ \rightarrow K^-$ in Ar). This can be seen from the plot (Fig. 4a) of $\ln \sigma_{1-1}$ as a function of $1/v$ for $Li^+ \rightarrow Li^-$ in H_2; here two points lie off the straight line near the peak of $\sigma_{1-1}(v)$ (which corresponds to the smallest value of $1/v$), and an additional point at the smallest velocity (3.7×10^7 cm/sec). The number of points not lying on the rectilinear segment of $\ln \sigma_{1-1} = f(1/v)$ increases at lower velocities. This is seen for Na^+

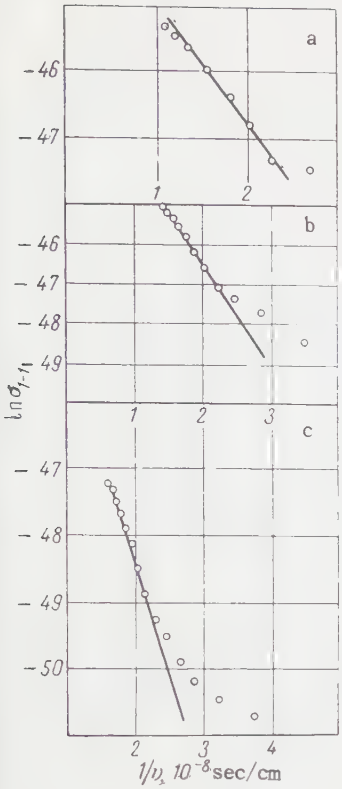

FIG. 4. $\ln \sigma_{1-1} = f(1/v)$ for (a) $Li^+ \rightarrow Li^-$ in H_2; (b) $Na^+ \rightarrow Na^-$ in H_2; (c) $K^+ \rightarrow K^-$ in Ne

$\rightarrow Na^-$ in H_2 (Fig. 4b), where three points lie off the straight line, and is even more prominent for $K^+ \rightarrow K^-$ in Ne (Fig. 4c), where five points lie off the straight line.

The $\sigma_{1-1}(v)$ curve thus obeys (2) wherever the condition $a|\Delta E|/hv \gg 1$ is not satisfied, and ceases to obey (2) wherever the condition is satisfied to any extent ($a|\Delta E|/hv \approx 7$ for the lowest velocity on $\sigma_{1-1}(v)$ in the case of $K^+ \rightarrow K^-$ in Ne). The situations for processes II[15] and III[9] are analogous.

In connection with the observed characteristics of $\sigma_{1-1}(v)$ in the region $v < v_{max}$ for electron capture by fast ions and atoms, during a discussion at the conference on electronic and atomic collisions held in Riga during June of 1959, V. M. Dukel’skiĭ suggested that (2) is not fully obeyed because the relative velocity of particles involved in the given process does not equal their relative velocity before collision. The manner in which points depart from the straight line in plots of $\ln \sigma_{1-1} = f(1/v)$ indicates that if this suggestion is correct, then $v_{true} > v$, where v_{true} is the true velocity at which the process occurs and v is the velocity before collision. The increment $\Delta v = v_{true} - v$ results from the interaction between the colliding particles. The relative velocity change resulting from the acceleration induced by the interaction forces is easily calculated from the departure of points lying off the rectilinear segment of $\ln \sigma_{1-1} = f(1/v)$. From the most extremely deviating point for K^+ in Ne we obtain $\Delta v/v \approx 60\%$, which is too large to result from the known attractive forces between atomic particles. Dukel’skiĭ’s suggestion can therefore not account for the way in which $\sigma_{1-1}(v)$ departs from (2).

In disagreement with Hafsted,[9] we maintain that the way in which σ_{1-1} falls off in the region $v < v_{max}$ near the peak according to (2) has no relation to the adiabatic hypothesis, since $a|\Delta E|/hv \gg 1$ is clearly unfulfilled in this velocity region. This condition is evidently not fulfilled even for K^+ in Ne, in which case we obtained the highest values of $a|\Delta E|/hv$. This is evident from the fact that the points of $\ln \sigma_{1-1} = f(1/v)$ that lie off the straight line do not determine a second straight line, which would have been evidence of a true adiabatic region. Moreover, even in a true adiabatic region $\sigma_{1-1}(v)$ might not obey (2) since a can be velocity dependent. The experimental information required for determining $\sigma_{1-1}(v)$ in the adiabatic region is still extremely meager. Therefore the further investigation of $\sigma(v)$ for different processes at low velocities remains a very important task in the physics of atomic collisions.

In conclusion the authors wish to thank Prof. A. K. Val’ter for his constant interest, and V. I. Muratov and O. I. Ekhichev for assistance with the measurements.

---

[1] Fogel’, Mitin, Kozlov, and Romashko, JETP **35**, 565 (1958), Soviet Phys. JETP **8**, 390 (1959).

[2] Fogel, Kozlov, Kalmykov, and Muratov, JETP **36**, 1312 (1959), Soviet Phys. JETP **9**, 929 (1959).

[3] G. F. Drukarev, JETP **37**, 847 (1959), Soviet Phys. JETP **10**, 603 (1960).

[4] Fogel’, Ankudinov, Pilipenko, and Topolya, JETP **34**, 579 (1958), Soviet Phys. JETP **7**, 400 (1958).

[5] Fogel, Ankudinov, and Pilipenko, JETP **35**, 868 (1958), Soviet Phys. JETP **8**, 601 (1959).

[6] Fogel, Ankudinov, and Pilipenko, JETP **38**, 26 (1960), Soviet Phys. JETP **11**, 18 (1960).

[7] J. B. H. Stedeford and J. B. Hasted, Proc. Roy. Soc. (London) **A227**, 466 (1955).

[8] H. B. Gilbody and J. B. Hasted, Proc. Roy. Soc. (London) **A238**, 334 (1957).

[9] J. B. Hasted, J. Appl. Phys. **30**, 25 (1959).

[10] Kozlov, Marchenko, and Fogel’, Приборы и техника эксперимента (Instruments and Exptl. Techniques) (in press).

[11] Ya. M. Fogel’ and L. I. Krupnik, JETP **29**, 209 (1955), Soviet Phys. JETP **2**, 252 (1956).

[12] Ya. M. Fogel’ and R. V. Mitin, JETP **30**, 450

(1956), Soviet Phys. JETP **3**, 334 (1956).

[13] Fogel', Mitin, and Koval', JETP **31**, 397 (1956), Soviet Phys. JETP **4**, 359 (1957).

[14] Ya. M. Fogel' and A. D. Timofeev, Тр. физ.-мат. фак-та ХГУ (Trans. Phys.-Math. Faculty, Kharkov State University) No. 7, 147 (1958).

[15] Ya. M. Fogel', Usp. Fiz. Nauk **71**, 243 (1960), Soviet Phys. Uspekhi **3**, 390 (1960).

Translated by I. Emin
224

SOVIET PHYSICS JETP VOLUME 12, NUMBER 5 MAY, 1961

MEASUREMENT OF THE ANISOTROPY OF THERMAL CONDUCTIVITY OF ZINC AND CADMIUM IN THE SUPERCONDUCTING STATE

N. V. ZAVARITSKIĬ

Institute for Physics Problems, Academy of Sciences, U.S.S.R.

Submitted to JETP editor June 17, 1960

J. Exptl. Theoret. Phys. (U.S.S.R.) 39, 1193-1197 (November, 1960)

The thermal conductivity of zinc and cadmium in the superconducting state has been measured along different crystallographic directions. The anisotropy in the temperature dependence of the electronic thermal conductivity is ascribed to an anisotropy in the width of the gap in the energy spectrum of the excitations in these metals.

RECENT investigations have shown the existence of an anisotropy in the energy spectrum of the excitations in the superconducting state for gallium[1] and tin.[2] In the present work these measurements are extended to zinc and cadmium. As before,[1] the form of the anisotropy of the spectrum was determined from the anisotropy of the electronic thermal conductivity in the superconducting state.

The conductivity of zinc and cadmium specimens, grown along the principal crystallographic directions by Kapitza's method,[3] was measured between 0.1 and 1° K. The method of measurement was similar to that used previously,[4] the change in the apparatus consisting only in a considerable improvement in the thermal contact between specimen and cooling salt. Figure 1 shows the results of the thermal conductivity measurements and Fig. 2 the relative change in conductivity of the specimens in the superconducting state. At $T = T_c$ the values of K (in w/cm-deg.) are as follows:

Zn-1	Zn-2	Zn-7	Zn-4	Zn-5	Cd-1	Cd-2	Cd-3
18	8.3	7.5	4.6	2.1	6.92	28.2	9.1

In order to determine the critical temperature T_c of the metals studied, the temperature dependence of the critical magnetic field H_c was measured, as previously.[1] The table gives the chief quantities characterizing the $H_c(T)$ dependence and the heat capacity of the metal in the normal state, based on these data. The critical temperature for zinc derived from these measurements agrees with Phillips' data,[5] but the critical temperature for cadmium comes out somewhat lower than that obtained earlier,[6] due evidently to the improvement in the magnetic temperature scale achieved by Cooke et al.[7]

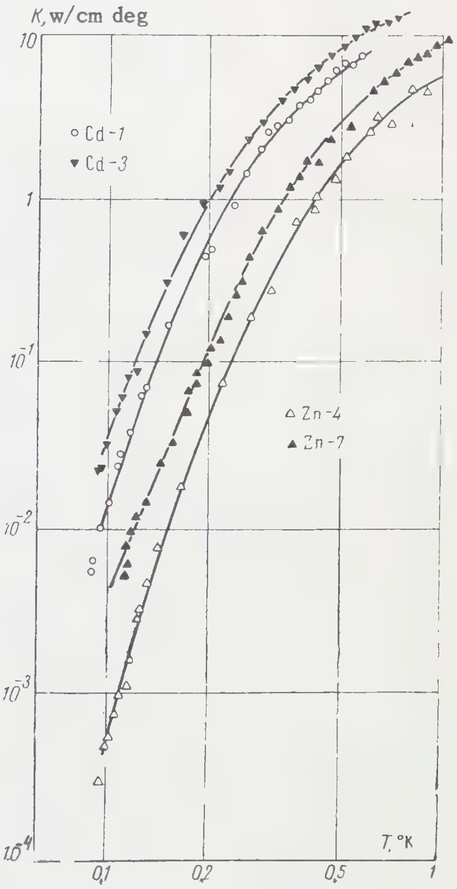

FIG. 1. The thermal conductivity of specimens of zinc and cadmium along the hexagonal axis (open points) and perpendicular to the hexagonal axis (full points).

DISCUSSION OF RESULTS

We shall first consider the results for zinc. It can be seen from Fig. 2 that the temperature dependence of the thermal conductivity is a function

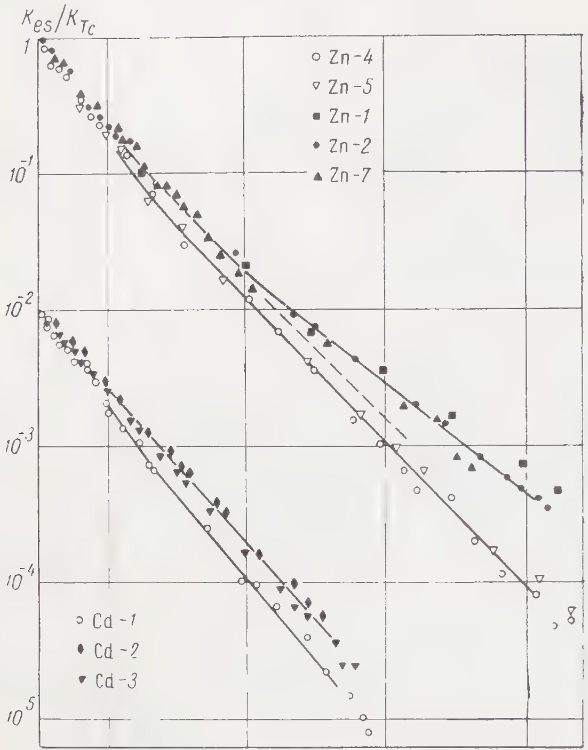

FIG. 2. The variation with temperature of the electronic thermal conductivity of zinc and cadmium in the superconducting state: open points – specimens along the hexagonal axis, full points – specimens perpendicular to the hexagonal axis.

of the crystallographic direction. The greatest difference is observed between the temperature dependence of the conductivity along the hexagonal axis and in a direction perpendicular to it. The results obtained previously[8] for zinc specimens of intermediate orientation lie between these two curves. The anisotropy in the temperature dependences of the thermal conductivity shows up most clearly in the variation of the ratio of conductivities along different crystallographic axes, as shown in Fig. 3. The mean values of K_{es}/K_{Tc} for all specimens of one orientation have been used for calculating these ratios, and we have taken the value $\rho_\perp/\rho_\parallel = 1.4$ for the residual resistance range, according to the measurements of V. B. Zernov (private communication), which corresponds to $K_{Tc\parallel}/K_{Tc\perp} = 1.40$. Since the lattice conductivity — the upper limit of which can be estimated from Casimir's formula (see, for example, reference 1) — is small compared with the electronic conductivity for the specimens studied, the results evidently reflect a temperature variation in the electronic thermal conductivity of zinc.

Quantity	Zn	Cd
T_c	0.82_5	0,53
$(dH_c/dT)_{T\rightarrow T_c}$	100	95
$(H_c)_{T\rightarrow 0^\circ K}$	52(±0.5)	28.5(±0.5)
$(d^2H_c/dT^2)_{T\rightarrow 0}$	90	107
$10^3\,\gamma$, Joule/g-mole-deg	0,68(±0,03)	0.63(±0.06)

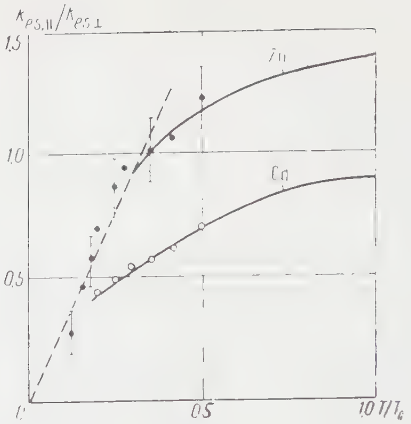

FIG. 3. The temperature dependence of the relative anisotropy of electronic thermal conductivity of zinc and cadmium ($K_\parallel$ and $K_\perp$ are the thermal conductivities of specimens along and perpendicular to the hexagonal axis). The dashed curve is the variation of the ratio $K_{\perp,\Delta_{min}}/K_{\parallel,\Delta_{min}}$ according to theory.

The anisotropy of the temperature variation of electronic thermal conductivity of a superconductor in the temperature region $T \ll T_c$ can be ascribed to an anisotropy in the width of the gap Δ which separates the excited state from the "superconductive" ground state of the electrons.[1,9] The more rapid change in conductivity along the hexagonal axis therefore indicates a more rapid reduction in excitation density with decreasing temperature, corresponding to a maximum of Δ in this direction.

We can compare the results obtained with the theoretical analysis of the change in conductivity of an anisotropic superconductor, made by Khalatnikov.[9] If the directions for which the values of Δ are the minimum lie in a plane perpendicular to the principal direction, then for isotropic scattering of the excitations

$$K_{\perp,\Delta_{min}}/K_{\parallel,\Delta_{min}} = 4.1\ T/\Delta'', \tag{1}$$

where $K_\parallel, \Delta_{min}$ and $K_\perp, \Delta_{min}$ are the conductivities in the direction of Δ_{min} and perpendicular to it and Δ'' is the derivative of Δ in the direction of Δ_{min} with respect to angle,* or if we approximate Δ by an ellipsoid of revolution,

$$K_{\perp,\Delta_{min}}/K_{\parallel,\Delta_{min}} = 4.1\ \Delta_{min}T/(\Delta^2_{max} - \Delta^2_{min}). \tag{1a}$$

---

*The calculation of the thermal conductivity for the case of anisotropy was carried out by A. F. Rusinov (private communication).

It can be seen from Fig. 3 that this dependence is close to that obtained experimentally in the temperature region $T/T_c < 0.3$, so that we can use the results of the calculation to determine $\Delta_{\min}$ and the anisotropy* of Δ. The direct proportionality of $K_{\perp, \Delta_{\min}}$ to $\exp(-\Delta_{\min}/T)$ for temperatures where $(\Delta_{\max} - \Delta_{\min})/T > 1$ was used to determine $\Delta_{\min}$, and Eq. (1a) was used to determine $\Delta_{\max} - \Delta_{\min}$. Comparison of the results of this calculation with the data of Figs. 2 and 3 shows that for zinc $\Delta_{\min} \approx 1.2\ T_c$, i.e. $\sim 1.0°$ K and $\Delta_{\max} - \Delta_{\min} \sim 0.55\ T_c$.

Let us now consider the results for the thermal conductivity of cadmium. Here the temperature dependence in the superconducting state is also a function of the crystallographic direction. The form of the anisotropy of K_{es} is similar to that found for zinc (Figs. 2 and 3). The nature of the anisotropy of Δ in these two metals is evidently similar. A quantitative comparison with theory can not be made in this case. An estimate of the value of $\Delta_{\min}$ leads to the value $\Delta_{\min} \sim 1.35\ T_c$, i.e. $\sim 0.67°$ K for cadmium.

Measurements made up to the present thus indicate the existence of an anisotropy in the energy spectrum of the excitations in a whole range of superconductors: gallium, tin, zinc and cadmium — all the metals which have so far been studied. The form of the anisotropy in the energy gap can, apparently, differ. For example, while in the case of gallium the value of Δ can be represented to a first approximation by an ellipsoid compressed along the axis of rotation, in the case of zinc and cadmium this ellipsoid is stretched out along the axis of rotation. The considerable magnitude of the anisotropy in Δ and its differing character show that one must be very wary of the comparison of the properties of different metals according to the mean value of the gap width[8,10] and of the results of comparing the properties of real superconductors with the results of a theory based on an isotropic model. There is as yet insufficient data to relate unambiguously the anisotropy of Δ with the anisotropy of the properties of a metal in the normal state, but the agreement between the form of the anisotropy of Δ for gallium and the details of the Fermi surface, which can be derived from the galvanomagnetic properties by using the theory of Lifshitz et al.,[12] can hardly be considered fortuitous. There is obviously a similar correlation for zinc and cadmium.

In conclusion, I take the opportunity of expressing my sincere thanks to P. L. Kapitza and A. I. Shal'nikov for their constant interest in this work.

---

*In the earlier[1] analysis of the anisotropy of Δ for gallium it was impossible to compare the experimental results with the theory since, owing to the large anisotropy of thermal conductivity in the normal state over the whole temperature range studied, the added condition $K_{\perp, \Delta_{\min}}/K_{\parallel, \Delta_{\min}} < 1$ which follows from (1) and the conditions for the calculation, $(\Delta_{\max} - \Delta_{\min})/T > 1$ was not fulfilled.

---

[1] N. V. Zavaritskiĭ, JETP **37**, 1506 (1959), Soviet Phys. JETP **10**, 1069 (1960).

[2] Bezuglyĭ, Galkin, and Korolyuk, JETP **36**, 1951 (1959), Soviet Phys. JETP **9**, 1388 (1959). Morse, Olsen, and Gavenda, Phys. Rev. Letters **3**, 15 (1959).

[3] P. L. Kapitza, Proc. Roy. Soc. **A119**, 358 (1928).

[4] N. V. Zavaritskiĭ, JETP **33**, 1085 (1957), Soviet Phys. JETP **6**, 837 (1958).

[5] N. E. Phillips, Phys. Rev. Letters **1**, 363 (1958).

[6] B. B. Goodman and E. Mendoza, Phil. Mag. **42**, 594 (1951). B. N. Samoĭlov, Dokl. Akad. Nauk SSSR **81**, 791 (1951).

[7] Cooke, Meyer, and Wolf, Proc. Roy. Soc. **A233**, 536 (1956).

[8] N. V. Zavaritskiĭ, JETP **34**, 1116 (1958), Soviet Phys. JETP **7**, 773 (1958).

[9] I. M. Khalatnikov, JETP **36**, 1818 (1959), Soviet Phys. JETP **9**, 1296 (1959).

[10] B. B. Goodman, Compt. rend. **246**, 3031 (1958), P. L. Richards and M. Tinkham, Phys. Rev. Letters **1**, 318 (1958).

[11] J. Yahia and J. A. Marcus, Phys. Rev. **113**, 137 (1959).

[12] I. M. Lifshitz and V. G. Peschanskiĭ, JETP **35**, 1251 (1958), Soviet Phys. JETP **8**, 875 (1959).

Translated by R. Berman
225

SOVIET PHYSICS JETP VOLUME 12, NUMBER 5 MAY, 1961

THE STUDY OF THE ASYMMETRY IN THE DECAY OF NEGATIVE MUONS IN A NUCLEAR EMULSION

A. O. VAĬSENBERG, É. D. KOLGANOVA, and V. A. SMIRNIT-SKIĬ

Submitted to JETP editor May 28, 1960

J. Exptl. Theoret. Phys. (U.S.S.R.) **39**, 1198-1200 (November, 1960)

The spatial asymmetry of electrons from the $\mu^- \rightarrow e^-$ decay in NIKFI-R emulsions was studied in an 11-koe and in zero field. It is shown that no asymmetry can be observed in either of the cases in a total of approximately 10^4 decay events.

In the first experiment by Lederman et al.,[1] which was performed by electronic methods and which demonstrated the parity nonconservation in $\pi \rightarrow \mu \rightarrow e$ decay, it was shown that the coefficient of asymmetry for negatively-charged muons stopped in graphite is approximately six or seven times less than for positive muons, and its value is $a \approx -0.05$. The mechanism by which the negative muons can be so greatly depolarized was considered by Shmushkevich[2] and Dzhrbashyan,[3] who showed that in cascade transitions in mesic atoms the negative muons lose the greater part of their polarization, and retain only 15–17% of the initial polarization on the K shell of the mesic atom, where they decay. This result is in agreement with the experimental data obtained by Ignatenko et al.[4] If the nucleus of the mesic atom has a magnetic moment, then the interaction between the magnetic moments of the nucleus and the negative muon will cause even this residual part of the polarization to be lost, and it can no longer be restored in ordinary magnetic fields obtainable under laboratory conditions. However, if the nucleus has no spin (such nuclei are the C^{12} and O^{16}, which make up the main part of the gelatine in emulsions), then the additional depolarization on the K shell will be due only to the interaction of the magnetic moment of the negative muon with the magnetic field of the electron shell, and such a depolarization can be destroyed by ordinary magnetic fields, similar to what takes place in muonium. Actually, the energy of interaction between the magnetic moments of the negative muon and of the peripheral electron can be only less than the energy of interaction of the hyperfine structure in muonium, since the electron has an effective quantum number greater than unity. Consequently, a field of approximately 10^4 oe, which is sufficient for the annihilation of the depolarization of positive muons, should be sufficient also for the annihilation of this depolarization mechanism.

With these considerations in mind, along with the thought that the presence of a measurable polarization of the negative muons stopped in nuclear emulsion would permit investigation of asymmetry in many secondary processes connected with the capture of negative muons by the light nuclei of the emulsion, we undertook a measurement of the asymmetry coefficient in $\mu^- \rightarrow e^-$ decay in a nuclear emulsion without a magnetic field ($H < 0.1$ oe), and in a strong magnetic field ($H = 11$ koe) directed along the axis of a negative-meson beam.*

The NIKFI-R emulsions were exposed in the synchrocyclotron of the Joint Institute for Nuclear Research to a negative-muon beam first slowed down by copper filters in such a way that the negative muons were stopped in the first 3 or 4 cm of emulsion.

The initial polarization of the negative-muon beam was not measured, and apparently cannot differ greatly from the initial polarization of the positive muon beam, which amounts to 0.81 ± 0.11 according to Mukhin, Ozerov, and Pontecorvo.[5]

In measurements of the asymmetry coefficient, the initial direction was taken to be the direction of the negative-muon beam, about which the decay electrons have a distribution of the form $1 + a \cos \vartheta$. To measure the value of a, the observers noted the emission of the decay electrons in the angular intervals $\vartheta = (0 \pm 45)^\circ$ (forward) and $(180 \pm 45)^\circ$ (backward).† A total of 9279 decays were observed without the magnetic field and 3403 decays were observed in the 11-koe field. The conditions and results of the measurement are as follows:

---

*This field was produced by an iron-free solenoid, graciously furnished by A. E. Ignatenko.

†All the μ–e decays more than 50μ away from the glass or the surface of the emulsion were registered.

Magnetic field H	$\leqslant 10^{-1}$ oe	11 koe
Number of decays forward	4580	1707
Number of decays backward	4699	1696
Asymmetry coefficient	+0.02 ± 0.017	0.00 ± 0.025
Number of observers	6	14
Agreement (by the χ^2 test)	$\chi^2 \sim 8$	$\chi^2 \sim 25$

It follows from these data that within the indicated statistical errors we observed neither noticeable asymmetry nor an effect of the magnetic field on this asymmetry. The positive sign of the asymmetry for H = 0 may be the result of a small systematic measurement error. It should be noted that in the case of μ^- decays the danger of systematic errors is considerably higher than for μ^+ decays. Actually, in the latter case practically each stoppage of the positive muon is accompanied by the appearance of a decay electron (thus, in 99442 decays of positive muons no decay electron was observed in only 20 cases). The stoppings of the negative muons are approximately equally distributed among the light (C, N, O) and heavy (Ag, Br) components of the emulsion, and consequently approximately half of all the stoppings in the emulsion occur without the appearance of a decay electron. This contributes to the occurrence of systematic scanning errors, connected, for example, with the different efficiency of observing decay electrons in different parts of the field of view of the microscope.

In connection with the possibility of subjective systematic errors of the observers, we have analyzed the agreement between the date of 14 individual observers, using the usual χ^2 criterion. The data above indicate that the results obtained by individual observers, particularly in the case H = 0, are in sufficiently good agreement with each other.

Further measurements consisted of attempting to detect a spatial asymmetry at the end of the decay-electron spectrum, where the asymmetry coefficient is approximately three times greater than the asymmetry coefficient averaged over the entire spectrum.[6] For this purpose we selected 612 flat electron tracks (306 decays each for H = 0 and H = 11 koe), in which the energy could be measured by the multiple-scattering method, and measured the energy distributions of these electrons by means of a semi-automatic scattering measuring apparatus, as well as the angles ϑ between the directions of these tracks and the direction of the negative-muon beam.

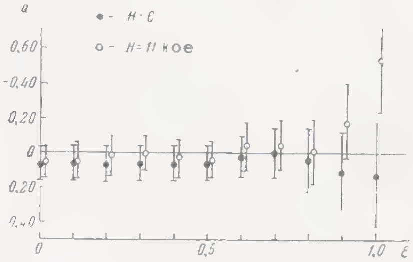

Coefficient of asymmetry a for electrons with energy greater than a given value (ε).

The procedure of these measurements and the criterion for selecting the tracks were in complete agreement with those indicated in earlier works.[6,7] The results are shown in the figure. The values of the asymmetry coefficient shown in the graph have been calculated from the average value of $\overline{\cos\vartheta}$ using the formula

$$a = 2\,\overline{\cos\vartheta} \pm 1{,}57/\sqrt{N},$$

for N is the number of electrons with energy greater than a given energy ϵ. The energy dependence thus obtained for the asymmetry coefficient points, in agreement with the data given above, to the absence of noticeable asymmetry. A striking fact is that at H = 11 koe a certain increase in the average value of a is observed at the end of the spectrum. The statistical significance of this increase, which does not exceed one and a half times the standard error, is however very small.

The measurements performed make it therefore possible to state that our experiments show practically no asymmetry effect in the decay of negative muons in the NIKFI-R nuclear emulsion, independently of the presence of an external magnetic field. This makes it almost impossible to observe by the emulsion method such secondary effects connected with the polarization of negative muons as the asymmetry of emission of protons from stars produced upon absorption of negative muons by a nucleus, or the asymmetry of emission of the electrons from β-active recoil nuclei formed in such an absorption.

The authors are grateful to N. V. Rabin and E. A. Pesotskaya for participating in the measurements of the decay-electron spectrum.

---

[1] Garwin, Lederman, Weinrich, Phys. Rev. **105**, 1415 (1957).

[2] P. M. Shmushkevich, JETP **36**, 645 (1959), Soviet Phys. JETP **9**, 449 (1959).

[3] V. A. Dzhrbashyan, JETP **36**, 277 (1959), Soviet Phys. JETP **9**, 188 (1959).

[4] Ignatenko, Egorov, Khalupa, and Chultém, JETP **35**, 1131 (1958), Soviet Phys. JETP **8**, 792 (1959).

[5] Mukhin, Ozerov, and Pontecorvo, JETP **35**, 340 (1958), Soviet Phys. JETP **8**, 237 (1959).

[6] A. O. Weissenberg and V. A. Smirnitsky, Nucl. Phys. **5**, 33 (1958).

[7] Vaĭsenberg, Kolganova, and Rabin, JETP **37**, 326 (1959), Soviet Phys. JETP **10**, 231 (1960).

Translated by J. G. Adashko
226

SOVIET PHYSICS JETP VOLUME 12, NUMBER 5 MAY, 1961

THE FERMI SURFACE OF TIN

N. E. ALEKSEEVSKIĬ, Yu. P. GAĬDUKOV, I. M. LIFSHITZ, and V. G. PESCHANSKIĬ

Institute of Physics Problems, Academy of Sciences, U.S.S.R.

Submitted to JETP editor June 17, 1960

J. Exptl. Theoret. Phys. (U.S.S.R.) 39, 1201-1214 (November, 1960)

Possible topological shapes of the Fermi surface of tin are discussed. The most probable shape of the Fermi surface of tin is chosen by comparison with the experimental results of galvanomagnetic measurements.

It has been concluded from an experimental investigation of the galvanomagnetic properties of tin that this metal has a Fermi surface of the open type.[1,2] The Fermi surface of a metal with tetragonal crystal lattice can in principle be of the "corrugated cylinder," "corrugated plane," or "three-dimensional grid" type, unlike metals with cubic structure for which the first two types are excluded.[3-5]

The experimental data obtained for tin[1,2] pertain mainly to samples with axes located in the principal crystallographic planes. It was possible to conclude from these data that the [100], [010], and [110] directions are open for the Fermi surface of tin. However, to explain all the topological features of the Fermi surface of tin, it was necessary to carry out a more detailed investigation of the anisotropy of the resistance of tin single crystals in large magnetic fields. It was also desirable to consider in greater detail the possible types of Fermi surfaces of metals with tetragonal lattices.

1. ANALYSIS OF GEOMETRY OF FERMI SURFACES FOR CRYSTALS WITH TETRAGONAL STRUCTURE

To investigate the topological features of the constant energy surfaces of metals with tetragonal crystal lattices, we use the following expression for the dispersion of $\epsilon(\mathbf{p})$:

$$\varepsilon(\mathbf{p}) = A_0 - A_1 \cos\frac{cp_z}{\hbar} - A_2 \cos\frac{cp_z}{2\hbar}\left(\cos\frac{ap_x}{2\hbar} + \cos\frac{ap_y}{2\hbar}\right) - A_3 \cos\frac{ap_x}{2\hbar}\cos\frac{ap_y}{2\hbar} - A_4\left(\cos\frac{ap_x}{\hbar} + \cos\frac{ap_y}{\hbar}\right). \quad (1)$$

Here c is the period of the lattice in the direction of the [001] tetragonal axis, and a is the period in the direction of the [100] and [010] binary axes. This expression represents the first harmonics of the Fourier series of the periodic function $\epsilon(\mathbf{p})$ for the tetragonal lattice of the metal.* We do not discuss here the question of the genesis of the spectrum, and in this connection we consider a priori the constants $A_0, \ldots, A_4$ to be arbitrary.

For values of ϵ close to minimum, the constant-energy surfaces are ellipsoids. The position of the centers of these ellipsoids depends on the relation between the coefficients A_i. For example, if all $A_i > 0$, then the centers of the closed constant-energy surfaces $\epsilon(\mathbf{p}) = \epsilon_{\min} + \delta\epsilon$ ($\delta\epsilon$ is small) coincide with the origin. As ϵ increases, the volumes of the constant-energy surfaces increase, and at a certain value $\epsilon = \epsilon_1$ (where $\epsilon_1 = A_0 - A_1 - 2A_4 + A_3$) the surface becomes tangent to the faces of the first Brillouin zone.

If the coefficient A_1 is the largest of the A_i, then the surface (1) will in the first place be tangent to the (100) and (010) planes. When $\epsilon > \epsilon_1$ surface (1) is an open surface comprising a plane grid of "corrugated cylinders" parallel to the [100] and [010] axes. For sufficiently large values of ϵ surface (1) will also become tangent to the (111) planes of the Brillouin zone.

If the relations between the coefficients A_i are different (if A_2 and A_3 are greater than the coefficients A_1 and A_4), the surface (1) will with increasing ϵ become tangent to the (111) planes of the Brillouin zone earlier than to the (100) and (010) planes. If the Fermi surface of indium were open it would intersect the (111) planes of the Brillouin zone, somewhat similar to the Fermi surface of gold or copper. (The lattice constant a and the nearest neighboring atoms are $\frac{1}{2}(a_2 + c_2)^{1/2}$ apart. Therefore $A_2 > A_1$ and $A_3 > A_4$.)

---

*If the coefficients of the Fourier series decrease with increasing number of the harmonic (which is true in the approximation of the strongly-bound electrons), it is sufficient for the analysis of the topology of the constant-energy surfaces $\varepsilon(\mathbf{p}) = \varepsilon$ to retain several of the first harmonics in $\varepsilon(\mathbf{p})$.

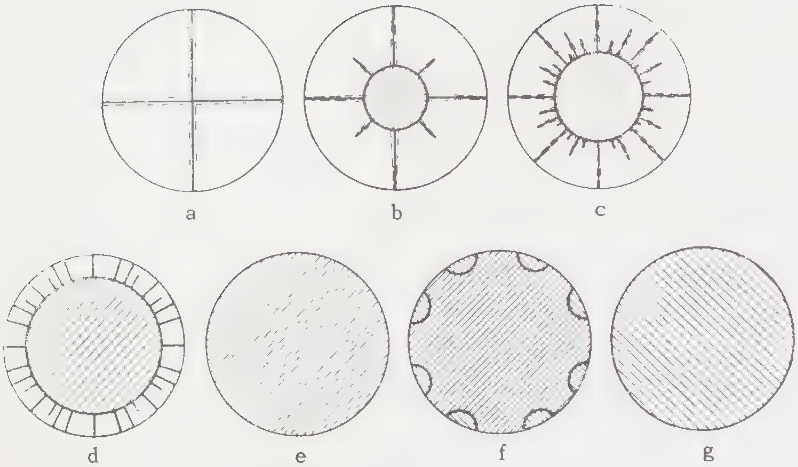

FIG. 1. Transformation of stereographic projections of the special directions of the magnetic field with increasing ε for Fermi surfaces of metals with tetragonal structure of crystal lattice.

If A_4 is the largest among the coefficients A_i, then constant-energy surfaces (1) of the "corrugated cylinder" type are possible. This case takes place when c is much greater than a. However, no metals exist in nature with such a tetragonal structure.

The edge of the elementary crystal cell of the tin lattice in the direction of the [001] axis is much smaller than the edge of the cell in the [100] direction ($a/c \approx 1.8$). We therefore assumed that the coefficients A_i satisfy the inequalities

$$A_1 > A_2 > A_3 > A_4. \tag{2}$$

For the sake of simplicity, we shall assume that all $A_i > 0$, and investigate in detail the constant-energy surfaces described by equation (1)* with relation (2) for the coefficients A_i.

If $(\epsilon - \epsilon_{min}) < 2(A_2 + A_3)$, the surfaces (1) are closed. If $(\epsilon - \epsilon_{min}) > 2(A_2 + A_3)$, the surface (1) will be an open surface comprising a plane grid of "corrugated cylinders."

At not too large values of ϵ, the average direction of the open trajectories $\epsilon = \text{const}$, $p_z = \text{const}$ is located in the (001) plane. With increasing ϵ, the diameters of the "corrugated cylinders" increase, and the surface (1) recalls a pair of "corrugated planes" connected by tubes in the [001] direction. With increasing ϵ these tubes become narrower and narrower, and can in general vanish before the surface (1) touches the (111) faces of the Brillouin zone (if A_1 is much greater than the individual coefficients A_2, A_3, or A_4). If A_1 differs little from A_2, A_3 or A_4, then the tangency of the surface (1) with the (111) faces of the Brillouin zone will take place earlier than the vanishing of the openings in the "corrugated planes." In this case, along with open trajectories in (001), there will exist open trajectories parallel to the [001] axis. (It must be noted that for certain directions of the magnetic field, open trajectories will exist simultaneously with different average directions.)

When ϵ is close to ϵ_{max} the surfaces (1) are closed surfaces located around the points of intersection of the three planes (100), (110), and (111) (and their like).

Figure 1 shows the transformation of the stereographic projections of the directions of the magnetic field which lead with increasing ϵ to open plane sections $p_z = \text{const}$ of the constant-energy surface (1).

If A_1 differs greatly from A_2, A_3 or A_4 (for $A_1 > 2A_2$), then the case f on Fig. 1 will not take place. The surface (1) will be a "corrugated plane" with openings at $2(A_2 + A_3) < (\epsilon - \epsilon_{min}) < 4A_2$. When $(\epsilon - \epsilon_{min}) > 4A_2$, the surface (1) degenerates into two solid "corrugated sheets." When $(\epsilon - \epsilon_{min}) \geq 2A_1$, these sheets form new pairs (i.e., "corrugated planes" joined by tubes), and as ϵ increases the transformation of the stereographic projections proceeds in reverse order from g to d, c, b, and a.

If these "corrugated planes" are pairwise interconnected by straight circular cylinders, then the boundary of the two-dimensional shaded region on the stereographic projections b, c, and d can be accurately calculated. Let d and h be the diameter and the height of the cylinder, b the re-

---

*In the approximation of strongly-bound electrons, the dependence of the energy on the momentum for tin has a somewhat different closed form

$$\varepsilon(\mathbf{p}) = A_0 + A\cos\frac{cp_z}{\hbar} \pm B\left[\cos^2\frac{ap_x}{4\hbar}\cos^2\frac{ap_y}{4\hbar}\cos^2\frac{ap_z}{4\hbar} + \sin^2\frac{ap_x}{4\hbar}\sin^2\frac{ap_y}{4\hbar}\sin^2\frac{cp_z}{4\hbar}\right]^{1/2}. \tag{1a}$$

Naturally, each of the two branches of the function (1a) can be expanded in a Fourier series similar to (1), and the surfaces (1) and (1a) are equivalent in their topological properties. (The coefficients A_i in (1) are different for the different branches.)

ciprocal lattice constant in the [100] direction; then, when $\theta < \theta_0$, the open trajectories exist for any value of the angle φ (θ and φ are the angular coordinates of the vector **H**, with θ reckoned from [001]. θ_0 is determined from the condition

$$\tan\theta_0 = h/d. \tag{3}$$

We note that when $\theta < \theta_0$ there exist, along with the open trajectories, closed trajectories with different directions about the electrons, and when $\theta > \theta_0$ only closed trajectories with like directions exist.

When $\theta > \theta_0$ the open trajectories exist only for rational directions of the projections **H** on the (001) plane, i.e., when $\tan\varphi = n/m$ (n and m are integers). The maximum value of the angle $\theta_{n,m}$, at which open trajectories still exist, is obtained from the following condition (n/m is an irreducible fraction)

$$\tan\theta_{n,m} = \frac{\tan\theta_0}{1 - b/d\sqrt{n^2 + m^2}}. \tag{4}$$

2. DETERMINATION OF THE DIRECTIONS OF PLANE SECTIONS OF THE OPEN FERMI SURFACE

To estimate the agreement between the surfaces considered above and the experimental data, it is necessary to analyze not only the stereographic projections of the special directions of the magnetic field, but also the open directions, which can be obtained by investigating the dependence of the resistance on the angle between the current and the crystallographic axes at a fixed direction of the magnetic field.

Several types of such current diagrams $\rho_{\mathbf{H}=\text{const}}(\alpha)$ are possible, where α is the angle between the current and the open section, or a certain crystallographic direction ($\mathbf{J} \perp \mathbf{H}$):

1. If for a specified direction of the magnetic field there exists a layer of open trajectories with a single average direction, then the dependence $\rho_{\mathbf{H}=\text{const}}(\alpha)$ will have the following form

$$\rho_{\mathbf{H}=\text{const}}(\alpha) = AH^2\cos^2\alpha + B. \tag{5}$$

When $\alpha = \pm\pi/2$, the current diagram has a minimum, in the direction of which the resistance reaches saturation. For all the remaining angles the resistance will increase without limit in the magnetic field: $\rho \sim H^2$.

2. If for a given direction of the magnetic field there are no open trajectories at all, or there are isolated open trajectories, and $V_1 = V_2$, then the resistance for any value of α increases quadratically with the field. By V_1 and V_2 we mean the following expressions [see Eq. (25) in reference 3]:

$$V_1 = \int S_1(\varepsilon_1, p_z)\,dp_z, \qquad S_1 = \oint p_x \frac{\partial p_y}{\partial\tau}\,d\tau > 0; \tag{6}$$

$$V_2 = -\int S_2(\varepsilon_1, p_z)\,dp_z, \qquad S_2 = \oint p_x \frac{\partial p_y}{\partial\tau}\,d\tau < 0. \tag{7}$$

Here it must be noted that for closed Fermi surfaces the volume compensation is not an accident of low probability, but a regular phenomenon. For metals with even valence a small overlap of the bands should always cause the appearance of compensation of the volumes V_1 and V_2. However, attention must be called to the fact that even for open Fermi surfaces we can speak of relative volumes (in p space within the limits of one cell of the reciprocal lattice) with energy $\epsilon > \epsilon_0$ and $\epsilon < \epsilon_0$, i.e., of "electrons" and "holes" respectively. Therefore, in the absence of open trajectories, the compensation of the volumes V_1 and V_2 is just as regular as in the case of closed surfaces. But in the presence of open trajectories the corresponding expressions in the kinetic coefficients do not reduce to those volumes, and consequently the effects connected with volume compensation do not take place.

3. If, for a given direction of the magnetic field, there exists a layer of open trajectories with different average directions, or there are no open trajectories at all, and $V_1 \neq V_2$, then the resistance reaches saturation in the magnetic field for any value of the angle α.

Thus, the polar current diagrams make it possible to explain the cause of the quadratic increase in resistance for a given direction of the magnetic field, to show whether it is due to compensation of volumes ($V_1 = V_2$) or to the presence of open trajectories, and to determine the directions of the latter.

When speaking of volume compensation, we have in mind the integrals (6) and (7), taken over entire sheets of the Fermi surface. This means that the compensation can take place either spontaneously in the case of an open surface, or as a result of addition with volumes of supplementary surfaces, if such exist.

It is of interest to clarify the character of the variation of resistance on approaching special directions of the magnetic field (at which open trajectories appear or disappear, see Fig. 3 in reference 4). We speak here of the specific case when the compensation of volumes V_1 and V_2 takes place for field directions at which only closed trajectories exist, and consequently there is a quadratic increase in the resistance for all angles α.

The formulas of reference 4 cannot be used in this case directly in the vicinity of singular points, but their analysis makes it possible to obtain the following expression for ρ:

$$\rho=\rho_0\frac{D\cos^2\alpha+\lambda_1\gamma_0^2}{[(\Delta V/V+cD)^2+c'D]\,\gamma_0^2+\lambda\gamma_0^4}, \tag{8}$$

where $\Delta V = V_1 - V_2$, and $V = (V_1 + V_2)/2$, c, c', λ, λ_1 are quantities of the same order of magnitude; D is of the same order of magnitude as the thickness of the layer of open trajectories $-\Delta p_z/b\hbar$. When the thickness of the layer of open trajectories vanishes ($D = 0$), we get $\Delta V = 0$.

Let us consider two cases

1) An entire layer of open trajectories ($D \neq 0$) occurs in a special direction of the magnetic field, and there are near this direction strongly elongated closed trajectories. (This case recalls somewhat the case of a "corrugated cylinder" type of surface.)

When $D \neq 0$ the values V_1 and V_2 "become uncompensated," and the resistance can be represented as follows (for $\mathbf{H} \perp \mathbf{J}$)

$$\rho\approx AH^2\cos^2\alpha+B.$$

If the direction of the magnetic field deviates noticeably from the special direction $\theta_1 \gg \gamma_0$ (θ_1 is the angle between $\mathbf{H}$ and the special direction), then $\rho = \lambda_1 H^2/\lambda$.

Near the special direction ($\theta_1 \lesssim \gamma_0$) there are no open trajectories of the type indicated above, but the presence of strongly stretched out closed trajectories, passing through many cells (on the order of $1/\gamma_0$) of the reciprocal lattice, does not make it possible to attain compensation of V_1 and V_2, owing to the fact that ρ cannot be expanded in powers of γ_0 in this region (see references 3–5).

As a result of the fact that over a very small angle interval ($\theta_1 \sim \gamma_0$) a change takes place in the analytic expression for the resistance as a function of the angle $\rho(\vartheta)$ (ϑ is the angle of rotation of the magnetic field in a plane perpendicular to the current), a very narrow resistance extremum should be observed. The relative magnitude of this extremum is independent of the magnitude of the magnetic field, and the half-width diminishes with increasing magnetic field as $1/H$.

2) Let us consider another case of a special direction of the magnetic field, in which the thickness of the layer of open trajectories vanishes. These special directions correspond to the boundary between the two-dimensional regions of the direction of the magnetic field, in which there are open trajectories, and the region of directions of the magnetic field in which there are no open trajectories and $V_1 = V_2$. In the region of magnetic-field directions for which only closed trajectories exist

$$\rho=\rho_0\lambda_1H^2/\lambda H_0^2+C, \tag{9}$$

and in the region of field directions for which there are open trajectories, the resistance in the two extreme cases is of the following form:

$$\rho=AH^2\cos^2\alpha+B,\quad \theta_1\gg\gamma_0^2;$$

$$\rho=\rho_0\lambda_1H^2/\lambda H_0^2+C,\quad \theta_1\ll\gamma_0^2. \tag{10}$$

When open trajectories exist, the volumes V_1 and V_2 do not compensate each other, but $\Delta V/V \approx \theta_1$. Therefore, for magnetic field directions with which open trajectories exist in a very narrow region ($\Delta\theta_1 \sim \gamma_0^2$) near $\theta_1 = 0$ we can assume, as before, that $\Delta V = 0$ in the expression for ρ. In this case, a very sharp kink should be observed in the angular dependence $\rho(\vartheta)$.

$$d\rho/d\vartheta=\Lambda H^4\cos^2\alpha+\Lambda_1H^2. \tag{11}$$

3) Finally, it should be noted that in a two-dimensional region of directions of the magnetic field $\Delta V/V$ is a monotonic function of the angle θ_1, whereas the thickness of the layer of open trajectories Δp_z vanishes at the center and at the boundary of the two-dimensional region. We can therefore expect ρ to have an additional maximum, which is not sharp, and which is located somewhere inside the two-dimensional region.

3. EXPERIMENTAL RESULTS AND DISCUSSION

The samples were made from a batch of tin obtained by zone melting in the Technology Division of the Institute of Physics Problems, U.S.S.R. Academy of Sciences.* Single crystals were made by several methods: by the Czochralski method, by the Bridgeman method, and also by electric erosion from a bulk single-crystal block. The diameters of the samples ranged from 1 to 2 mm. For measuring the Hall emf, cylindrical samples as well as single-crystal plates measuring 12 × 4 × 0.3 mm were used.

The orientations of the samples were determined optically with an accuracy of ±1°. The samples were mounted in accordance with the remarks made in reference 6. The anisotropy of the resistance of single crystals of tin was investigated in a magnetic field up to 34 koe at 4.2°K.

---

*The authors take this opportunity to thank N. N. Mikhaĭlov and L. N. Vasil'ev for the preparation of very pure metal.

TABLE I

Sample	Orientation* φ; ϑ'	$\rho_{300°K}/\rho_{4,2°K}$	Sample	Orientation φ; ϑ'	$\rho_{300°K}/\rho_{4.2°K}$
Sn-1	0°; 0 ° [001]	11 200	Sn-20	24°; 68°	62 500
Sn-2	0°; 26°	14 500	Sn-21	12°; 64°	57 000
Sn-3	0°; 36°	11 100	Sn-22	32°; 62°	49 600
Sn-4	0°; 51°	13 600	Sn-23	23°; 52°	64 000
Sn-5	0°; 62° [011]	11 000	Sn-24	22°; 50°	42 000
Sn-6	0°; 71°	10 800	Sn-25	33°; 48°	46 500
Sn-7	0°; 83°	10 800	Sn-26	37°; 44°	55 000
Sn-8	0°; 90° [010]	48 300	Sn-27	22°; 43°	~60 000
Sn-9	7°; 90°	48 500	Sn-28	4°; 41°	~60 000
Sn-10	15°; 90°	54 000	Sn-29	30°; 39°	~60 000
Sn-11	24°; 90°	45 000	Sn-30	17°; 37°	~60 000
Sn-12	32°; 90°	38 600	Sn-31	12°; 35°	64 500
Sn-13	38°; 90°	47 400	Sn-32	26°; 35°	50 600
Sn-14	45°; 90° [110]	24 200	Sn-33	38°; 35°	~50 000
Sn-15	45°; 71°	55 000	Sn-34	12°; 32°	~50 000
Sn-16	45°; 53°	45 800	Sn-35	20°; 29°	~50 000
Su-17	45°; 41°	44 000	Sn-36	24°; 28°	~50 000
Sn-18	45°; 36°	40 600	Sn-37	38°; 28°	~50 000
Sn-19	45°; 23°	66 700	Sn-38	22°; 26°	~60 000

---

*φ and ϑ' are the polar coordinates of the axes of the samples: φ is measured from the (010) or (100) plane, and ϑ' is the angle between the [001] axis and the axis of the sample. The directions of the axes of the samples are noted on the stereographic projection in Fig. 4a.

All the measurements were made for the case **H** ⊥ **J** (**J** is the measuring current).

The data on the samples are listed in Table I. For all the tin samples, polar resistance diagrams $\rho_{H = \text{const}}(\vartheta)$ were obtained in a constant magnetic field H = 23.5 koe.

The diagram of the sample Sn-1 is an eight-folium rosette, on which the resistance minima are observed along the directions [010] and [110] (see Fig. 1 in reference 1). For the same directions a clearly pronounced saturation of resistance is observed in the magnetic field.

For the tin specimens whose axes make a small angle with the [001] axis ($0° < \vartheta' \lesssim 30°$), the resistance diagrams retain in general the shape of eight-folium rosettes, although the relative depths of the minima decrease, and some maxima become smoother. All the minima observed on the resistance diagrams for these samples lie on the line in which the plane of rotation of the magnetic field intersects the (010) and (110) planes. An investigation of the dependence of $\rho(H)$ in the direction of the minima has shown that the saturation of resistance is observed only in samples whose axes lie in the (010) or (110) planes (corresponding to $\varphi = 0°$ and $\varphi = 45°$), and only for those minima, whose directions coincide with the direction of the line of intersection of the final rotation of the magnetic field with the plane passing through the axis of the sample and the [001] axis.

As the angle between the axis of the samples and the crystallographic [001] axis is increased (the angle ϑ' changes approximately from 30° to

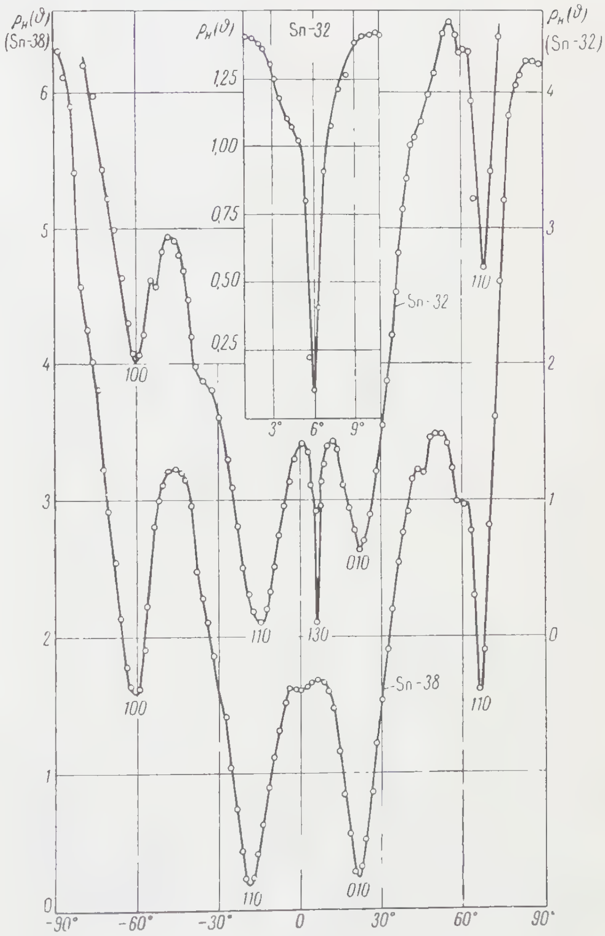

FIG. 2. Polar resistance diagrams in a constant magnetic field H = 23.5 koe for the single crystals Sn-32 and Sn-38 and T = 4.2°K. The values $\rho_{H=\text{const}}(\vartheta)$ are plotted in arbitrary units. The upper curve is the narrow minimum ($\vartheta_{\min} = 6°$) for Sn-32, plotted on a larger scale.

50°), there appears on the diagrams $\rho_H = \text{const}(\vartheta)$ a series of new very narrow and deep minima. The directions of these minima coincide with the directions of the lines of intersection of the plane of the magnetic field with the planes of type (120), (130), (150), and (230). As ϑ' is increased, the first to appear is a minimum in the direction of the (130) plane ($\vartheta'_{(130)} \approx 29°$) (see Fig. 2), after which appear minima in the planes (120) ($\vartheta'_{(120)} \approx 38°$) and (150) ($\vartheta'_{(150)} \approx 37°$), and, finally, in the (230) plane ($\vartheta'_{(230)} \approx 43$?).

In spite of the considerable depth of these minima, no resistance saturation in the magnetic field could be observed for them. This may be explained by the fact that the minima are very narrow, and it is quite probable that an averaging of the resistance over the angle ϑ takes place here. [It should be noted that the widths of all the observed minima decrease (from ~20° to ~1°) with increasing sum of the indices of the corresponding planes.]

The polar resistance diagrams of the samples of tin, for which the angles $\vartheta' \gtrsim 50°$, are in the form of bifoliate rosettes. The changeover from the resistance maximum to the minimum is smooth. The direction corresponding to the minimum on the resistance diagrams coincides in this series of samples with the direction of the line of intersection of the plane of rotation of the magnetic field with the plane passing though the axis of the sample and the [001] crystallographic axis. In the direction of such a minimum, $\rho(H)$ has the form of a saturation curve. For most samples, we investigated also the dependence of the resistance on the magnetic field in directions not coinciding with the directions of the minima. For these directions the resistance increases without limit in a magnetic field, following a nearly-quadratic law.

Figure 3 shows the variation of the form of the polar diagrams of resistance (in the most interesting region of the angles ϑ) with deviation of the sample axis from the [001] axis. Two circumstances must be noted: a) the change from the diagram of the Sn-27 type to the diagram of the Sn-25 type occurs for different angles φ at different angles ϑ'. Thus, it was qualitatively established that the values of ϑ' are approximately 45, 50, and 55° for $\varphi = 0$, 22, and 45° respectively; b) in the polar resistance diagrams of tin samples with the angle ϑ' close to 90°, two additional weekly pronounced minima are observed (at $\vartheta \approx \pm 40°$ and at $\vartheta \approx \pm 17°$).

Table II lists certain characteristic details of polar diagrams of resistance of all the investigated single crystals of tin. All the observed minima are plotted on the stereographic projection shown in Fig. 4 b and c.

The large number of samples of different orientation has made it possible to plot current diagrams of resistance and to draw conclusions concerning the causes of the square-law increase in the resistance or its saturation for different directions of the magnetic field. In the construction of the current diagrams of resistance $\rho_H = \text{const}(\alpha)$, the diagrams $\rho_H = \text{const}(\vartheta)$ have been reduced to a single scale. Examples of typical current diagrams are shown in Fig. 5.

The current diagram I (lower curve) is encountered only once for a field direction **H** ∥ [001]. In this case for any orientation of the current (**H** ⊥ **J**) the resistance in large fields is almost independent of the magnitude of the magnetic field. It follows, therefore, that there are no open sections of the Fermi surface for this direction of the field (however, one cannot exclude here the existence of isolated open sections), and the volumes V_1 and V_2 do not compensate each other.

The current diagram II (central curve) is characteristic of the directions of the magnetic field located in the planes (010) and (110) (for all angles θ) and in the planes (150), (130), (120), and (230); here the angle θ for the orientations of **H** is limited in the following manner: $\theta_{(130)} \lesssim 61°$; $\theta_{(150)} \lesssim 53°$, $\theta_{(120)} \lesssim 52°$, and $\theta_{(230)} \approx 47°$. [It must be noted that the angle $\theta_{(230)}$ is obviously not a maximum, since it was impossible to establish convincingly the vanishing of the minimum in these directions on the $\rho_H = \text{const}(\vartheta)$ diagrams.] In addition, a current diagram of type II is observed for magnetic field orientations occupying an entire region (over the angles φ and θ) centered about the [001] axis. The boundary of this region was determined only approximately, and only three points are known for it (with not very great accuracy): 1) $\varphi = 0°$, $\theta \approx 45°$; 2) $\varphi = 22°$, $\theta \approx 40°$, 3) $\varphi = 45°$, $\theta \approx 35°$. Similar current diagrams should exist for those magnetic-field directions, for which open sections of the Fermi surface exist. Knowing the direction of the maximum (or minimum) on the current diagram, we can determine the average direction of these sections. An analysis of the experimental data has shown that all the open sections of the Fermi surface of tin are located in the basal (001) plane.

For all the remaining directions of the magnetic field, current diagrams of the third type (upper curve) are observed. These diagrams are characterized by a quadratic increase of the resistance in the magnetic field for any current

TABLE II

Sample	Positions of the minima and maxima (in degrees) on the diagrams $\rho_{H=\mathrm{const}}(\vartheta)$*; the parentheses contain the ratio of the resistance for the given value of the angle and the resistance at the lowest minimum	$\Delta\rho_H/\rho_0$ in the direction of the lowest minimum
Sn-1	0 [010] (1); ±33(127); ±45[110] (3)	5.5
Sn-2	0 (1); ±22(45); ±26(44); ±30(45); ±43(19); ±65(93); ±90(37)	10
Sn-3	0 (1); ±12(44); ±15(41); ±25(67); ±40(40); ±52(150); ±70(142); ±75(143); ±90(86)	6
Sn-4	0(1); ±8 и ±18 **(small minima)** ; ±26(31); ±30(30); ±78(92); ±90(87)	7.5
Sn-5	0(1); ±25(12); ±29(10); ±78(34); ±88(33); ±90(37)	8
Sn-6	0(1); ± 19(66); ± 24(57); ± 82(203); ± 90(197)	8
Sn-7	0(1); ± 17(28); ± 22(25); ± 82(102); ± 90(100)	20
Sn-8	0(1); ± 18(150); ± 25(90); ± 90(420)	
Sn-9	0(1); ± 15(200); ± 25(125); ± 90(450)	
Sn-10	0(1); ± 15(65); ± 24(40); ± 90(165)	
Sn-11	0(1); ± 17(10); ± 23(9); ± 90(35)	
Sn-12	0(1); ± 17(42); ± 23(26); ± 90(110)	
Sn-13	0(1); ± 16(250); ± 22(132); ± 32(320); ± 35(185); ± 90(550)	40
Sn-14	0(1); ± 16(210); ± 22(143); ± 35(365); ± 43(320); ± 90(490)	27
Sn-15	0(1); ± 70(355); ± 75(335); ± 80(385); ± 90(360)	6
Sn-16	0(1); ± 82(1500); ± 90(1440)	10
Sn-17	0(1); ± 14(420); ± 17(300); ± 30(600); ± 35(500); ± 80(1860); ± 90(1230)	9
Sn-18	0(1); ±19(140); ±21(120); ±24(195); ±26(60); ±29(200); ±78(550); ±90(300)	20
Sn-19	0(1); ± 17(158); ± 42(24); ± 78(280); ± 90(100)	58
Sn-20	0(1); ± 39(56); ± 40(65); ± 42(56); ± 90(110)	
Sn-21	0(1); ± 90(550)	50
Sn-22**	0(1); + 20(430); + 25(400); — 87(2600)	24
Sn-23**	0(1); + 53(112); + 54(100); + 60(112); ± 90(185)	160
Sn-24**	0(1); + 16. + 23 **and** + 26 **(minute minima)** ; + 85(262)	72
Sn-25	— 48(415); — 46(523); — 35(239); — 34(264); — 29.5(170); — 29(165); —19.5 (121); — 19(105); — 9.5(32); — 9(27); 0(1); + 2(7.5) + 2.5(1.5); +7.5(24); + 8(18); + 15.5(73); +16(68); +21(157); +22(118); +30(209); + 30.5(197); + 35(285); + 37(274); + 68(652); + 70(630); + 90(1000)	
Sn-26**	— 44 (32); — 38(34); — 31(14); — 26 (25); — 6(1); + 5(8.5); + 8(3); +10 (7.5); + 15(3); + 22(12.5); + 28(9)	
Sn-27**	—18(35); —7(77); —3(8); 0(45); +4(1); +9(36); +10(6); +12(50); +18(25)	
Sn-28	— 83(156); — 71(168); — 35(49); — 33(54); — 11(5); — 7(18); —6(5.5); — 5,5(18); + 3(1); + 13(27); + 13.5(23); + 14(28); + 18(16.5); + 31(77); +40(68); + 74(185)	
Sn-29**	—88(78); — 70(40); — 58(45); — 39(24); — 38(28.5); — 20(8.2); — 16(10); —13(7); — 12(8.7); — 8(1,5); — 3,5(7); — 3(2.6); + 1(10); + 12(1); +30(20,5); + 35 (14)	
Sn-30	— 70 (133); — 57(155); — 22(27); — 10(53); — 2(1); + 2(33); + 13(7.8); +26(100); + 28(70); + 30(100); + 46(117); + 55(102); + 79(246)	
Sn-31	— 87(900); — 60(1340); — 30(275); — 13(556); — 5(55); 0°(380); + 10(1); + 25(486); + 25.5(147); + 26(490); + 38(685); +53(466); + 75(1690)	10
Sn-32	— 60(19); — 48(26); — 15(1); 0(13); + 6(1); + 10(13); + 22(5.7); + 55(39); + 69(26); + 86(62)	
Sn-33	— 82(39); **from** — 75 **to** —69(66); —32(12,5); —22(20); —16(13); —12 (17); +6(1); + 35(28); + 45(22); + 85(84)	
Sn-34	— 76(200); — 60(310); — 30(63); — 13(131); — 8(100); — 6(14.5); — 3(97); + 10(1); +25(140); +26(57); +26,5(145); +37(186); + 53(115); +78(428)	
Sn-35**	— 22(1); — 3(11); 0(4,5); + 2(11); + 17(1,5);	
Sn-36	— 64(2,7); —48(6.5); — 20(1); + 4(4); + 21(1.1); + 48(9.8); + 66(4.5) ; + 88(7.5)	
Sn-37**	— 47(133); — 36(274); —8(1); + 18(226); + 32(116); + 67(583)	
Sn-38	— 62(8); — 46(16); — 19(1); + 4(8); + 6(8,5); + 21(1.3); + 54(17.5); +66(8); + 86(31)	

---

*For $\vartheta = 0$ we chose the direction of the line of intersection of the plane of rotation of the magnetic field with the plane passing through the axis of the sample and the [001] axis.

**Samples for which the diagrams $\rho_{H=\mathrm{const}}(\vartheta)$ have not been fully investigated.

orientation. Thus, for these directions of the magnetic field there are no open sections of the Fermi surface, and the resistance increases as H^2 because $V_1 = V_2$.

The appearance of additional maxima on the polar diagrams of the samples, the angle ϑ' of which is close to 90°, is probably due to the circumstances mentioned in Article 3 of Sec. 2.

On the basis of an analysis of the diagrams $\rho_{H = \mathrm{const}}(\vartheta)$ and $\rho_{H = \mathrm{const}}(\alpha)$, a stereographic projection was plotted for the special directions of the magnetic field for the Fermi surface of tin (Fig. 4d). This projection is significantly supplemented by a stereographic projection of the

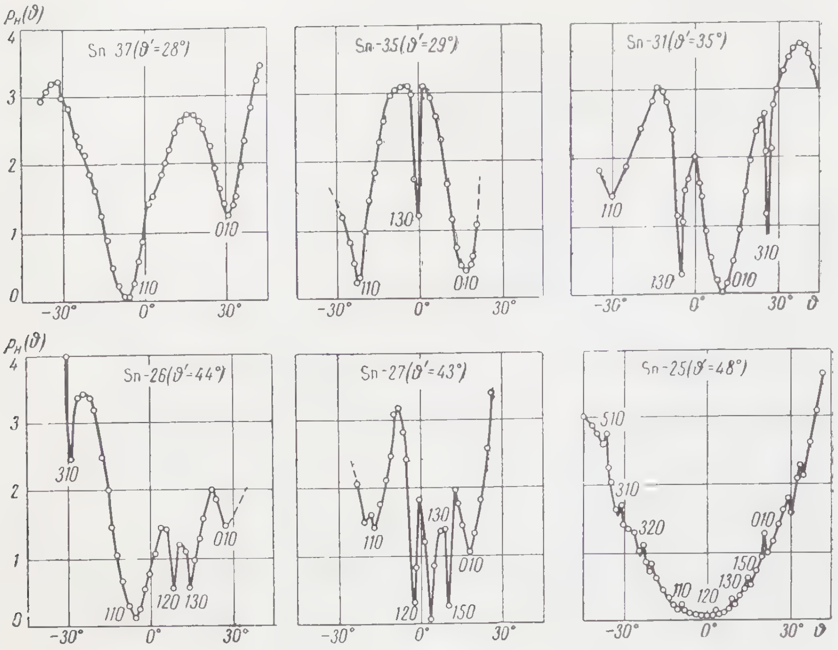

FIG. 3. Variation of the form of the polar diagrams of resistance in a constant magnetic field H = 23.5 koe for a single crystals of tin with increasing ϑ. The values $\rho_{H=\text{const}}(\vartheta)$ are in arbitrary units.

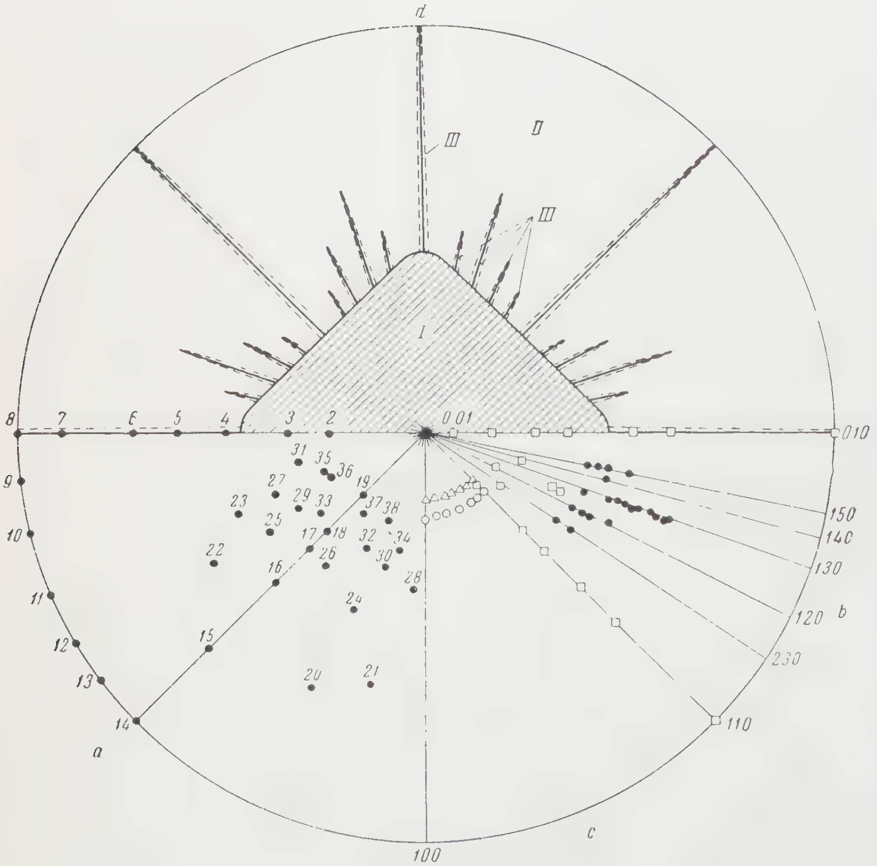

FIG. 4. Stereographic projections. a – directions of the axes of the investigated tin samples (the numbers label the points); b – directions of the minima on the polar resistance diagram; □ – minima for which ϑ = 0; ● – narrow minima; c (○ and △) – directions of weakly-pronounced additional broad minima and maxima; d – special directions of the magnetic field for the Fermi surface of tin: region I – two-dimensional region of magnetic field directions for which open trajectories exist (the thickness of the layer of open trajectories vanishes on the boundary of region I and in the [001]); there are no open trajectories in region II, and the "electron" and "hole" volumes compensate each other, $V_1 = V_2$; regions III are those regions of magnetic-field directions, for which strongly elongated trajectories exist and the compensation of the volumes is violated, $V_1 \neq V_2$. Open trajectories occur only for those directions of the magnetic field which lie on the axial lines.

average directions of the open sections of the Fermi surface of tin, which is a circle with a center corresponding to the [001] direction.

According to the previously employed terminology,[4] region I on Fig. 4d is the two-dimensional region of the directions of the magnetic field, for which open sections of the Fermi surface exist. The special directions are here the center of the region (direction [001]) and the boundary of the region. For these special directions of **H**, the thickness of the layer of the open trajectories vanishes.

In regions II there are no open sections of the Fermi surface and $V_1 = V_2$. For regions III there

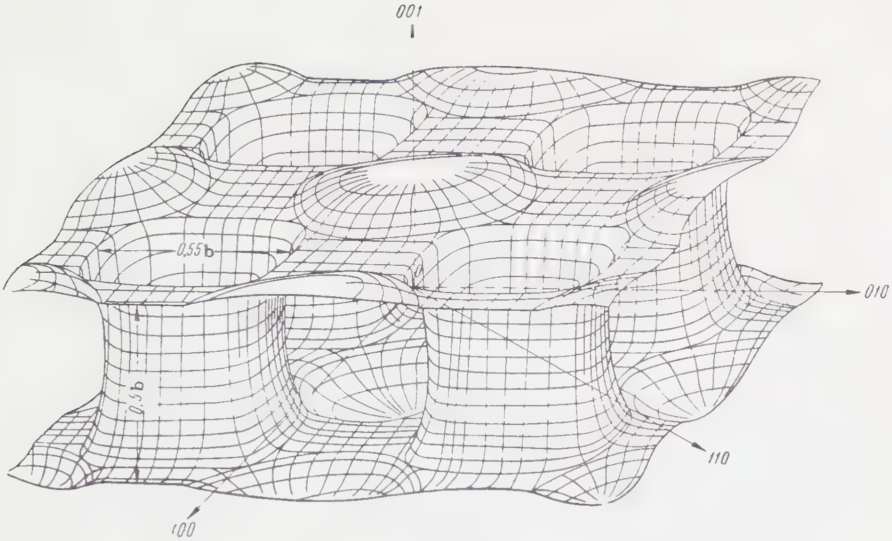

FIG. 6. Open Fermi surface of tin.

exist strongly elongated closed sections [the open sections appear only when the direction **H** is located along the central line — planes with rational indices (100), (110), (120), (130), (150), and (230)].

4. THE FERMI SURFACE OF TIN

The stereographic projection shown in Fig. 4d can be set in correspondence with the Fermi surface comprising a network of "corrugated cylinders" the axes of which coincide with the directions [010], [100], and [110]. Such a surface is topologically equivalent to two corrugated planes, parallel to the (001) plane and joined by tubes, the axes of which have the same direction as the [001] of the reciprocal lattice of tin (Fig. 6).

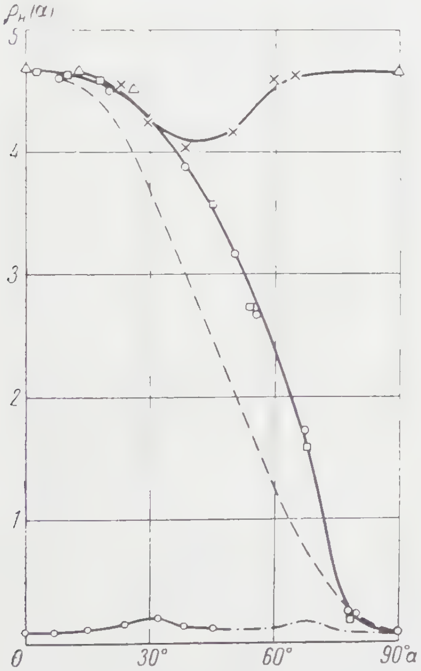

FIG. 5. Typical current diagrams for single-crystal tin; H = 23.5 koe, T = 4.2°K (α is the angle of rotation of the measuring current **J** in the plane perpendicular to the fixed direction of the magnetic field). The experimental curves were obtained for different orientations of the magnetic field: ○ – **H** ∥ [010]; □ – **H** ∥ [110]; × – field in direction determined by the angles $\varphi = 22°$, $\theta = 90°$; △ – field in direction $\varphi = 32°$, $\theta = 90°$ (with this, $\alpha = 90°$ when **J** ∥ [001]); lower curve – **H** ∥ [001] (with this $\alpha = 0°$ when **J** ∥ [010]). The dashed line is the curve of $\cos^2 \alpha$.

However, such a surface alone cannot explain the current diagrams of type III (Fig. 5). As was already noted, such a current diagram is obtained in the case of volume compensation ($V_1 = V_2$). In this connection it is necessary to assume that tin has still other constant-energy surfaces, the presence of which makes it possible to obtain such a volume compensation. We assume that at least two branches of the energy spectrum $\epsilon(\mathbf{p})$ are very important for the Fermi surface of tin.

The second isoenergetic surface can be either closed or open. Both versions of the Fermi surface of tin can be reconciled with the stereographic projection of the special directions of the magnetic field (Fig. 4d). If it is assumed that the Fermi surface of tin consists of two surfaces of equal volume, one of which is open and the other closed, then the measurements of the Hall emf* in the [001] direction make it possible to conclude that the open surface is a "hole" surface and the closed one is an "electron" surface.

The experimental results allow us also to estimate some of the parameters of the open Fermi surface of tin. The form of the two-dimensional region I, and the relation between the angles $\theta_{n,m}$ on the stereographic projection (Fig. 4d) indicate that the form of the tubes (bridges between the planes) of the Fermi surface of tin do

---

*A more detailed description of the results of the measurements of the Hall emf for single crystals of tin will be published soon in JETP.

TABLE III

φ	$\theta_0(\varphi,)$ deg	$\theta_{n,m}(\varphi)$, deg.	$d(\varphi)$	$h(\varphi)$
[150]	41	53	0.57	0.5
[130]	38	61	0.57	0.46
[120]	37	52	0.62	0.46
[230]	36	47?	0.93?	
[010]	45		0.52	
[110]	46		0.64	

not differ greatly from straight cylinders. Therefore, to estimate the distance between the planes and the "diameter" of the tube we can use relations (3) and (4). The results of the calculations are given in Table III. The quantities $d(\varphi)$ and $h(\varphi)$ are given in units of the reciprocal lattice constant of tin, b (in the direction [010]). The boundary value θ_{230} could not be established for the [230] direction. In the calculations for the [010] and [110] directions we put respectively $h \approx 0.5$ and $h \approx 0.45$. The data of Table III were used to plot the open Fermi surface of tin (Fig. 6). The presence of two Fermi surfaces in tin ("electron" and "hole") sharply distinguishes the character of the anisotropy of the resistance of tin in a magnetic field from the anisotropy of the resistance of copper, silver, and gold, which also has open Fermi surfaces, made of "corrugated cylinders." A quadratic increase of the resistance in the magnetic field predominates in tin, whereas saturation predominates in copper, silver, and gold. This excludes the possibility of obtaining a linear increase of resistance in polycrystalline tin when averageing in a magnetic field (Kapitza's law).

It should also be noted that the assumption that the Fermi surface is multifoliate can explain the specific features of the galvanomagnetic properties of lead, cadmium, zinc, and other metals, which have open Fermi surfaces.[2]

In conclusion, we consider it our pleasant duty to thank Academician P. L. Kapitza for continuous attention and interest in this investigation.

---

[1] N. E. Alekseevskiĭ and Yu. P. Gaĭdukov, JETP **36**, 447 (1959), Soviet Phys. JETP **9**, 311 (1959).

[2] N. E. Alekseevskiĭ and Yu. P. Gaĭdukov, JETP **37**, 672 (1959), Soviet Phys. JETP **10**, 481 (1960).

[3] Lifshitz, Azbel', and Kaganov, JETP **31**, 63 (1956), Soviet Phys. JETP **4**, 41 (1957).

[4] I. M. Lifshitz and V. G. Peschanskiĭ, JETP **35**, 1251 (1958), Soviet Phys. JETP **8**, 875 (1959).

[5] I. M. Lifshitz and V. G. Peschanskiĭ, JETP **38**, 180 (1960), Soviet Phys. JETP **11**, 131 (1960).

[6] Alekseevskiĭ, Brandt, and Kostina, JETP **34**, 139 (1958), Soviet Phys. JETP **7**, 96 (1958).

Translated by J. G. Adashko
227

SOVIET PHYSICS JETP VOLUME 12, NUMBER 5 MAY, 1961

ELECTRON PARAMAGNETIC RESONANCE AND PARAMAGNETIC RELAXATION IN LIQUID AND SUPERCOOLED SOLUTIONS OF Ti^{+++} SALTS

V. I. AVVAKUMOV, N. S. GARIF'YANOV, and E. I. SEMENOVA

Kazan' Branch, Academy of Sciences, U.S.S.R.

Submitted to JETP editor June 17, 1960

J. Exptl. Theoret. Phys. (U.S.S.R.) 39, 1215-1220 (November, 1960)

Electron paramagnetic resonance measurements in alcohol and glycerine solutions of the salts $TiCl_3 \cdot 6H_2O$ and $Ti_2(SO_4)_3 \cdot 4H_2O$ were carried out at frequencies 300 — 9460 Mc/sec and at temperatures of 300°, 200° and 77°K. Symmetric lines with ΔH dependent on the solvent and on the concentration of the solution were observed in supercooled solutions at a frequency $\nu = 300$ Mc/sec. Broad asymmetric lines due to the asymmetry of the g-factor were observed at a frequency of 9460 Mc/sec. The values of $g_{||}$ and $g_{\perp}$ have been determined for supercooled glycerine and alcohol solutions. Narrow symmetric lines have been observed in dilute liquid solutions. Relaxation measurements in parallel fields were also carried out at frequencies of 300, 17, and 6 Mc/sec. The order of magnitude of the spin-lattice relaxation time, ρ_l, has been estimated, and it has been found that ρ_l depends both on the solvent and on the concentration of the solution.

1. INTRODUCTION

TRIVALENT titanium salts are among the paramagnetic compounds of elements of the iron group which have received very little study. This is related to the fact that the spin-lattice relaxation time has turned out to be very short in the majority of the Ti^{+++} salts that have been investigated. Therefore in the work of Bleaney et al.[1] electron paramagnetic resonance (e.p.r.) could be successfully observed in a single crystal of titanium cesium alum only at $T = 4.2 - 2.5°K$ with $g_{||} = 1.25$ and $g_{\perp} = 1.14 \pm 0.02$.

Bijl[2] has also investigated e.p.r. in powdered samples of the same alum at helium temperatures. The effective g-factor for the powders has turned out to depend on the temperature: $g_{\text{eff}} = 1.35$ at $T = 6.33°K$ and $g_{\text{eff}} = 1.53$ at $T = 7.88°K$.

Wong[3] has made measurements of e.p.r. in a single crystal of $(TiAl)Cl_3 \cdot 6H_2O$ at liquid hydrogen and helium temperatures as a function of the concentration of Ti^{+++}. He has observed a symmetric line of width ~ 100 oe with an isotropic g-factor equal to 1.93 ± 0.02. It turned out that the line width does not depend strongly on the temperature and was ascribed by the author to the accidental inhomogeneities of the crystalline field. In the paper by Bowers and Owen[4] an investigation was made of e.p.r. in $KTi(C_2O_4)_2 \cdot 2H_2O$ at $T = 90 - 20°K$. Measurements have shown that $g_{||} = 1.86$ and $g_{\perp} = 1.96$.

Finally, Jarrett[5] has, for the first time, found in $Ti[(CH_3CO)_2CH_3]_2$ at room temperature, paramagnetic resonance absorption which is due to the presence in this compound of a strong axial crystalline field. The values of $g_{||} = 2$ and $g_{\perp} = 1.93$ were obtained.

It should also be pointed out that titanium cesium alum was the object of theoretical investigations[6,7] in which the mechanism of spin-lattice relaxation in magnetically diluted paramagnetic crystals was elucidated for the first time.

We have observed e.p.r. both in liquid glycerine and alcohol solutions of $TiCl_3 \cdot 6H_2O$, and also in the supercooled state at temperatures of 77 and 200°K. Investigation of e.p.r. in these solutions was carried out at 300 and 9460 Mc/sec.

In addition we have also carried out relaxation measurements (by the parallel field method) in supercooled solutions at 77°K. The method of carrying out these measurements has been described in an article by one of the present authors.[8] Finally, we have made an attempt to study by the e.p.r. method the pyridine complexes of Ti^{+++}, and also samples of silicate and borate glasses containing titanium compounds.

2. RESULTS OF MEASUREMENTS

1. $\nu = 300$ Mc/sec. As is well known, the majority of the investigated compounds of Ti^{+++} possess a strongly anisotropic g-factor. This

Table I

Concentration of solution, mole/liter	ΔH, oe			Concentration of solution, mole/liter	ΔH, oe		
	77 °K	200 °K	295 °K		77° K	200° K	295° K
Glycerine solution of $TiCl_3 \cdot 6H_2O$				Alcohol solution of $TiCl_3 \cdot 6H_2O$			
2	54	60	—	1	63	—	—
1	32	35	—	0,5	35	—	20
0.5	17	18	—	0,25	27	—	10
0,25	14	17	10	0,1	17	—	10
0,1	13	16	10	0,05	16	—	10
0,01	13	16	10	0,01	16	—	10

leads to the result that when e.p.r. is measured in polycrystalline samples in the microwave frequency range the form of the resonance line is primarily determined by the anisotropy of the g-factor. Therefore, we have carried out investigations of the concentration and the temperature dependence of the line at $\nu = 300$ Mc/sec.

Table I shows the dependence of the line width ΔH on the concentration of Ti^{+++} in different solvents at three different temperatures (the line width ΔH has been measured between the points on the absorption curve corresponding to half of the maximum intensity). The value of the g-factor is everywhere equal to 1.9 ± 0.1.

As can be seen from the table, ΔH in supercooled solutions falls off rapidly as the concentration is diminished and tends to a constant value independent of the concentration. It should be noted that in 2 mole/liter glycerine and in 1 mole/liter alcohol supercooled solutions there exists at 77°K zero-field absorption $\chi''(H = 0)$. The intensity of this zero-field absorption falls off rapidly both as the frequency ν is increased and as the concentration is diminished.

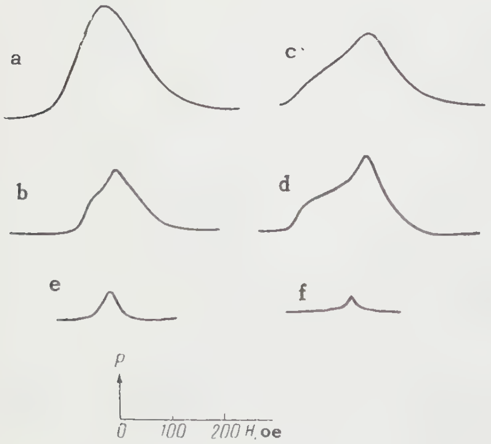

E.p.r. lines for solutions of $TiCl_3 \cdot 6H_2O$ at a frequency of 9460 Mc/sec. The supercooled state (77°K) of the solution in glycerine of concentration: a) 2 mole/liter, b) 0.05 mole/liter; in alcohol: c) 1 mole/liter, d) 0.05 mole/liter. The liquid state of the solution (295°K) in glycerine: e) 0.25 mole/liter; in alcohol: f) 0.25 mole/liter

The line width is greater in supercooled alcohol solutions than in glycerine solutions. In going over from the supercooled state to the liquid state the intensity of the e.p.r. line diminishes strongly. At the same time for low concentrations the line width becomes somewhat narrower.

2. $\nu = 9460$ Mc/sec. In supercooled alcohol and glycerine solutions of $TiCl_3 \cdot 6H_2O$ there is observed at 77°K a wide asymmetric e.p.r. line with an unresolved second absorption maximum (cf. diagram, a, b, c, d). As the concentration of the magnetic ion is decreased the asymmetry of the line increases, although the line width diminishes slightly at the same time. The values of $g_{\parallel}$ and $g_{\perp}$ determined from the experimental e.p.r. curves (at $\nu = 9460$ Mc/sec) are shown in Table II.

Table II

$g_{\parallel}$	$g_{\perp}$	g_{eff}
77 °K		290 °K
Glycerine solution of $TiCl_3 \cdot 6H_2O$		
1.99	1,93	1,95
Alcohol solution of $TiCl_3 \cdot 6H_2O$		
2.00	1,90	1,94

As can be seen from this table, the anisotropy of the g-factor in supercooled alcohol solutions is greater than in glycerine solutions. As the temperature is increased the line widths and the asymmetry of the curves in supercooled solutions diminish, and when the liquid state is reached symmetric and fairly narrow lines are observed (cf. diagrams e and f).

At the same time it should be noted that in liquid alcohol solutions a line with $\Delta H = 10$ oe is observed for 0.25 mole/liter at $T = 295°K$ both at 9460 Mc/sec, and at 300 Mc/sec, while in a glycerine solution at the same temperature and concentration the line width depends on the frequency: $\Delta H = 50$ oe at $\nu = 9460$ Mc/sec and $\Delta H = 10$ oe at $\nu = 300$ Mc/sec. As the temperature is increased above room temperature (~400°K) the frequency dependence disappears, and the line width decreases and becomes equal to $\Delta H = 10$ oe. Finally, in pyridine complexes fairly broad lines are observed, whose asymmetry is considerably greater than in alcohol supercooled solutions. We have not succeeded in observing e.p.r. in silicate and borate glasses containing titanium compounds.

Also we have not succeeded in observing resonance absorption in aqueous solutions of $TiCl_3 \cdot 6H_2O$ and $Ti_2(SO_4)_3 \cdot 4H_2O$.

3. Relaxation measurements in parallel fields. At a frequency of 300 Mc/sec one can observe the absorption $\chi''_s(H)$ due to spin-spin relaxation in a 2-molar glycerine solution of $TiCl_3 \cdot 6H_2O$ at 77°K. As the concentration of the solution is decreased by only a factor of two the intensity of this absorption practically falls to zero. Such a rapid decrease in the intensity of $\chi''_s(H)$ can be explained by the disappearance of the "zero-field absorption" $\chi''(H = 0)$. At a frequency of 17 Mc/sec at 77°K the form of the relaxation depends on the concentration of the solution: from 2 to 1.5 mole/liter inclusive the absorption $\chi''_l(H)$ due to spin-lattice relaxation is observed, while from 1.5 to 0.1 mole/liter the absorption $\chi''_s(H)$ due to spin-spin relaxation is observed.

At a frequency of 6 Mc/sec in these supercooled solutions, the absorption $\chi''_l(H)$ is observed over the greater range from 2 to 0.05 mole/liter, while $\chi''_s(H)$ occurs in solutions of concentrations from 0.5 to 0.1 mole/liter. Thus, the domain of spin-spin relaxation depends on the concentration of the magnetic ions: the lower the concentration the lower the frequencies at which the absorption $\chi''_s(H)$ is observed.

Moreover, the shape of the curves $\chi''_l(H)$ and $\chi''_s(H)$ also depends on the concentration: the lower the concentration of the magnetic ions, the lower the values of H at which $\chi''_s(H)$ and $\chi''_l(H)$ cease to depend on the intensity of the constant magnetic field. For those concentrations of the supercooled solutions of $TiCl_3 \cdot 6H_2O$ which we have investigated, the curves of $\chi''_s(H)$ are described by Shaposhnikov's theory, while the curves of $\chi''_l(H)$ are described by the theory of Casimir and Du Pre.[10]

Finally, it should be noted that the curves of $\chi''_s(H)$ for alcohol solutions at 77°K are observed at higher frequencies than in glycerine solutions of corresponding concentrations at the same temperature.

3. DISCUSSION OF RESULTS

At a frequency of 300 Mc/sec the e.p.r. line in concentrated glycerine and alcohol solutions has at 77°K a Gaussian shape and, as has already been noted, its width ΔH depends on the concentration. Therefore the ΔH of the e.p.r. curves in these solutions is due to dipole-dipole magnetic interactions. This assumption is also supported by the very weak dependence of ΔH on T in the temperature range 200 – 77°K.

In dilute solutions the width ΔH which does not depend on the concentration is due to the anisotropy of the g-factor and to the contribution of the magnetic moments of the protons from molecules of the immediate surroundings. Moreover, the insignificant increase in ΔH of dilute supercooled solutions as the temperature is raised from 77 to 200°K indicates that spin-lattice relaxation makes a contribution to ΔH in accordance with the relation

$$\Delta H \sim 1/\rho_s + 1/\rho_l.$$

A decrease in the line width in the transition from a supercooled solution to the liquid state is due to the influence of motion. In liquid alcohol and glycerine solutions the intensity of the e.p.r. line is very low in spite of the narrowness of the absorption curves. This can be explained by the presence in liquid solutions of two types of Ti^{+++} ions: Ti^{+++} ions whose crystalline electric field has a high symmetry, and ions in which the crystalline field has a sufficiently strong component of low symmetry that is not averaged out by motion. Therefore e.p.r. in liquid solutions is due only to Ti^{+++} ions of the latter type. In aqueous solutions of Ti^{+++} salts only electric fields of the first type are present.

At a frequency of 9460 Mc/sec the shape of the e.p.r. curves in the supercooled state is typical of ions with a strongly anisotropic g-factor.[11]

As can be seen from the figure, in concentrated glycerine solutions in the supercooled state the line is more symmetric than in alcohol and in dilute glycerine solutions. This is explained by the fact that in a 2-molar glycerine solution the width due to the magnetic dipole-dipole interactions dominates over the width associated with the anisotropy of the g-factor.

The frequency dependence of ΔH in liquid glycerine solutions at room temperature referred to previously is explained by the fact that, owing to the high value of the viscosity, the frequency of rotation of the "magnetic complex" formed with the immediate surroundings is lower than the Larmor precession frequency. Therefore, at this frequency the line width is due to the anisotropy of the g-factor.

As the temperature is raised the average frequency of rotation of the "magnetic complex" increases, and the g-factor takes on the averaged effective value $g_{\text{eff}} = \frac{1}{3}(g_{\parallel} + 2g_{\perp})$. In this case the e.p.r. line is described by the following spin-Hamiltonian:

$$\mathcal{H} = \sum_{i=1}^{N} g\beta H S_{zi} + \Delta g\beta H \left(\cos^2\theta_i - \tfrac{1}{3}\right) S_{zi} + \tfrac{1}{2}\Delta g\beta H \sin\theta_i \cos\theta_i \cdot [S_{+i} + S_{-i}],$$

where $g = \frac{1}{3}(g_{\parallel} + 2g_{\perp})$ and $\Delta g = g_{\parallel} - g_{\perp}$.

One of the present authors[12] has shown earlier that the constant b of the magnetic specific heat of the spin-system is related to the half width $\Delta H_{\parallel}$ of the $\chi''_S(H)$ curves by the expression

$$b = C(1 + \sqrt{2})\,\Delta H_{\parallel}, \tag{1}$$

where C is the Curie constant. It follows from the results of our relaxation measurements that as the supercooled solutions of Ti^{+++} are made more dilute the half width $\Delta H_{\parallel}$ of the $\chi''_S(H)$ curves decreases to a very small value. Therefore, according to relation (1) the constant b will also diminish. Such a decrease in the constant b is explained by the fact that for compounds of Ti^{+++} with $S = \frac{1}{2}$ the specific heat of the spin-system will be determined only by the value of the dipole-dipole magnetic interactions.[8]

The displacement of spin-spin relaxation into the low frequency region as the concentration is diminished indicates an increase in the spin-lattice relaxation time which could be explained by means of the heat reservoirs proposed by Bloembergen and Wang[13-15] if exchange interaction existed at the high concentrations utilized by us. However, this assumption is untenable since in concentrated solutions in parallel fields narrow relaxation curves $\chi''_S(H)$ are observed.[16]

The absence of exchange is also confirmed by the fact that as the solution is made more dilute the e.p.r. lines become narrower, while they should have a tendency to become more broad. It is therefore possible that the variation of ρ_l with concentration is related to the existence of cross-relaxation effects[17] in the concentrated supercooled solutions.

Relaxation measurements (at 77°K) have also enabled us to estimate the order of magnitude of ρ_l and the dependence of ρ_l on concentration and on solvent. It has turned out that for a 2 mole/liter glycerine solution the value is $\rho_l \sim 5 \times 10^{-8}$ sec and for 0.1 mole/liter the value is $\rho_l \sim 5 \times 10^{-7}$ sec. In alcohol solutions the value of ρ_l is smaller by approximately an order of magnitude than in glycerine solutions. This result is in good agreement with the estimated value of the splitting of the lowest orbital triplet Δ due to the axially symmetric field; an estimate of Δ for the supercooled glycerine and alcohol solutions may be obtained from a comparison of the theoretical and the experimental values of the g-factor.

Indeed, for a field possessing trigonal symmetry $g_{\parallel} = 2.0$, $g_{\perp} = 2(1 - 3\lambda/\Delta)$, where $\lambda = 154\ \text{cm}^{-1}$ is the spin-orbit coupling constant. From this by utilizing the data of Table II we obtain $\Delta \sim 15000\ \text{cm}^{-1}$ for glycerine solutions and $\Delta \sim 9000\ \text{cm}^{-1}$ for alcohol solutions. On the other hand, in accordance with reference 7 we have $\rho_l \sim \Delta^4$. Therefore, assuming that the other parameters determining ρ_l do not vary significantly when the solvent is replaced, we obtain

$$\rho_{l\,\text{glycerine}} / \rho_{l\,\text{alcohol}} \approx (\Delta_{\text{glycerine}} / \Delta_{\text{alcohol}})^4 \approx 7.8,$$

as is observed experimentally. The absence of e.p.r. in silicate and borate glasses indicates that in the glasses titanium has a valence of four, since the symmetry of the electric field in the glasses does not differ significantly from the electric field in the supercooled solutions.

In conclusion the authors express their gratitude to B. M. Kozyrev for discussion of results, and to Yu. M. Ryzhmanov for aid with the experiment.

---

[1] Bleaney, Bogle, Cooke, Duffus, O'Brien and Stevens, Proc. Phys. Soc. (London) **A68**, 57 (1955).

[2] D. Bijl, Proc. Phys. Soc. (London) **A63**, 405 (1950).

[3] E. J. Wong, J. Chem. Phys. **32**, 598 (1960).

[4] K. D. Bowers and J. Owen, Rep. Prog. Phys. **18**, 304 (1955).

[5] H. S. Jarrett, J. Chem. Phys. **27**, 1298 (1957).

[6] R. Kronig, Physica **6**, 33 (1939).

[7] J. H. Van Vleck, Phys. Rev. **57**, 426 (1940).

[8] N. S. Garif'yanov, JETP **37**, 1551 (1959), Soviet Phys. JETP **10**, 1101 (1960).

[9] I. G Shaposhnikov, JETP **18**, 533 (1948).

[10] H. B. Casimir and F. K. Du Pre, Physica **5**, 507 (1938).

[11] R. H. Sands, Phys. Rev. **99**, 1222 (1955).

[12] N. S. Garif'yanov, JETP **25**, 359 (1953).

[13] N. Bloembergen and S. Wang, Phys. Rev. **93**, 72 (1954).

[14] N. S. Garif'yanov and M. M. Aksel'rod, Химия и технология топлива и масел (Chemistry and Technology of Fuel and Oils) **3**, 65 (1959).

[15] Goldsbrough, Mandel, and Pake, Phys. Rev. Letters **1**, 13 (1960).

[16] B. M. Kozyrev, Doctoral Thesis, Moscow, Physics Institute, Academy of Sciences, U.S.S.R. 1957.

[17] Bloembergen, Shapiro, Pershan, and Artman, Phys. Rev. **114**, 445 (1959).

Translated by G. Volkoff
228

SOVIET PHYSICS JETP VOLUME 12, NUMBER 5 MAY, 1961

THE β^+ SPECTRUM OF Si^{27}

S. S. VASIL'EV and L. Ya. SHAVTVALOV

Institute of Nuclear Physics, Moscow State University

Submitted to JETP editor June 23, 1960

J. Exptl. Theoret. Phys. (U.S.S.R.) 39, 1221-1223 (November, 1960)

The β^+ spectrum of Si^{27} was investigated with a magnetic-lens β spectrometer. End points were observed at 3.65 and 1.45 Mev with intensities 90% and 10%, respectively.

THE β^+ end-point energy of Si^{27} has been given as 3.48 ± 0.1 Mev by Boley and Zaffarano,[1] whose work was done with a scintillation spectrometer. On the basis of several investigations,[1-3] the most reliable value of the corresponding half-life appears to be 4.14 ± 0.03 sec.

We have used a magnetic-lens β spectrometer to investigate the β^+ spectrum of Si^{27} produced in the reaction $Al^{27}(p, n)Si^{27}$, with 6.7-Mev protons from the 120-cm cyclotron of the Institute of Nuclear Physics, Moscow State University. Figure 1 is a schematic diagram of the experimental apparatus. The extracted proton beam was focused by quadrupole lenses on a rotating target positioned 9 m from the cyclotron behind a concrete shield; this differs from the setup used in our earlier work.[4] Before reaching the target the protons passed through a grid coupled to an integrator, which registered the relative beam intensity. The target, which was subjected to continuous proton bombardment, consisted of a rotating aluminum ring 2.7 mg/cm^2 thick. Each bombarded area of the target reached the focus of the β spectrometer in a period of time which was variable, from a few hundredths of a second to one second, by changing the speed of rotation in accordance with the radioactive half-life under investigation; reduced target activity was compensated by intensifying the proton beam. The troublesome background was reduced by an additional shield. In addition, the materials used for parts of the apparatus subject to proton bombardment were selected with a view to reducing the gamma-ray and neutron backgrounds.

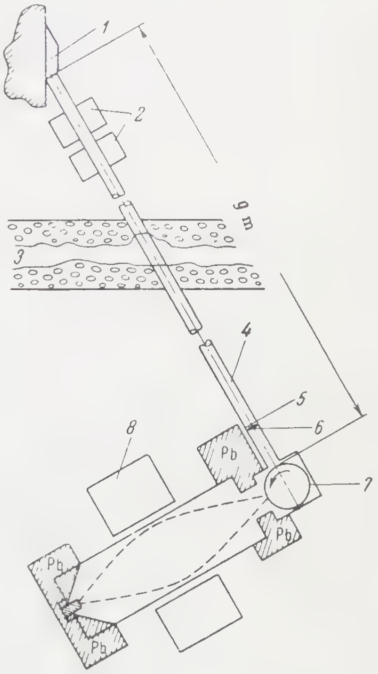

FIG. 1. Schematic diagram of experiment: 1 – exit window of cyclotron, 2 – quadrupole lenses, 3 – concrete wall, 4 – proton beam, 5 – to integrator, 6 – grid, 7 – rotating target, 8 – β spectrometer.

Figure 2 shows the Fermi plot for the complex β^+ spectrum of Si^{27}, consisting of two partial spectra. The principal end point, corresponding to ~ 90% of the intensity, is located at 3.65 ± 0.05 Mev, while not more than 10% of the intensity is represented by the partial β^+ spectrum having its end point at 1.45 ± 0.1 Mev. The decay scheme of Si^{27} given in the book by Dzhelepov and Peker[5] must therefore be amended by introducing the latter partial spectrum and end point, representing the transition to the 2270-kev level of Al^{27} (Fig. 3), which is observed in connection with inelastic scattering.[5,6]

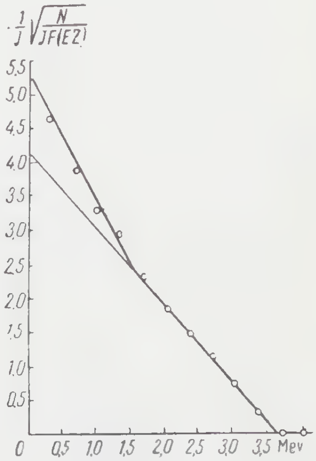

FIG. 2

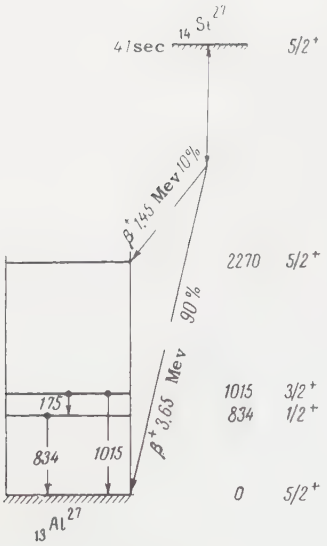

FIG. 3

According to reference 5, the given level has positive parity and spin $^5/_2$, like the ground state of Si^{27}. Therefore there is greater probability of a β transition to this level than to other Al^{27} levels having different spins.

The observed half-life of Si^{27} was 4.1 ± 0.4 sec, agreeing with the previously known value within experimental error. The given value was determined as follows. The current in the magnetic lenses of the β spectrometer was adjusted to focus 1650-kev electrons. The proton beam was then switched off, and pulses in the counter of the spectrometer were recorded magnetically. By means of a timing device, the magnetic record was read out so that pulses recorded within 2-second intervals were registered successively by a 100-channel pulse-height analyzer.

We wish to express our thanks to V. S. Zazulin, who was responsible for the indicated method of determining the half-life, to the cyclotron crew, especially Yu. A. Vorob'ev, and to Z. I. Tikhomirova, B. M. Makuni and N. S. Kirpichev for assistance.

---

[1] F. I. Boley and D. J. Zaffarano, Phys. Rev. **84**, 1059 (1951).

[2] Summers-Gill, Haslam, and Katz, Can. J. Phys. **31**, 70 (1953).

[3] Kuscer, Mihailovic, and Park, Phil. Mag. **2**, 998 (1957).

[4] S. S. Vasil'ev and L. Ya. Shavtvalov, Izv. Akad. Nauk SSSR, Ser. Fiz. **22**, 788 (1958), Columbia Tech. Transl. p. 782; JETP **36**, 317 (1959), Soviet Phys. JETP **9**, 218 (1959).

[5] B. S. Dzhelepov and L. K. Peker, Схемы распада радиоактивных ядер (Decay Schemes of Radioactive Nuclei), Acad. Sci. Press, 1958.

[6] P. M. Endt and G. M. Braams, Revs. Modern Phys. **29**, 683 (1957).

Translated by I. Emin
229

SOVIET PHYSICS JETP VOLUME 12, NUMBER 5 MAY, 1961

INELASTIC SCATTERING OF PHOTONS ON Rh¹⁰³ *NUCLEI*

O. V. BOGDANKEVICH, L. E. LAZAREVA, and A. M. MOISEEV

P. N. Lebedev Physics Institute, Academy of Sciences, U.S.S.R.

Submitted to JETP editor June 23, 1960

J. Exptl. Theoret. Phys. (U.S.S.R.) 39, 1224-1228 (November, 1960)

The yields of the reaction $Rh^{103}(\gamma, \gamma')Rh^{103m}$ were measured by the induced-radioactivity method for various maximum bremsstrahlung energies between 5.9 and 25.5 Mev from a 30-Mev synchrotron. In this energy range the cross section for the reaction $Rh^{103}(\gamma, \gamma')Rh^{103m}$ was calculated from the yield curve by the Penfold and Leiss method. The cross section has two peaks, one at 9.3 Mev near the threshold of the (γ, n) reaction, and the second at ~20 Mev. The peak cross section values are respectively 4.8 and ~ 2.5 mb. The ratio of the radiative and neutron widths is estimated.

THE cross section of inelastic nuclear scattering of γ quanta by rhodium was measured by del Rio y Sierra and Telegdi,[1] who used the method of registering the β activity of Rh^{103m}. The curve for the cross section of the reaction $Rh^{103}(\gamma, \gamma')Rh^{103m}$, obtained by these authors in the energy interval from 8 to 18 Mev, has a sharp peak at 12.8 Mev; the half-width of the peak is 2.9 Mev, and the cross section at the maximum is 12.5 mb. Both the position of the peak and its magnitude contradict other data on inelastic scattering of photons by Y^{87}, Ag^{107}, In^{115}, and Au^{197}, available in the literature.[2-7] For all these nuclei the cross section of the (γ, γ') reaction has a sharp peak near the threshold of the (γ, n) reaction, usually attributed to the competition between the radiative and neutron widths. The height of the peak amounts to ~ 2 — 4 mb. In this connection, we deemed it advisable to make new measurements on rhodium.

Measurements were carried out with the 30-Mev synchrotron of the Physics Institute of the Academy of Sciences. The yields of the $Rh^{103}(\gamma, \gamma')Rh^{103m}$ reaction were measured at different bremsstrahlung energies E_{max} from 5.9 to 25.5 Mev in intervals of ~ 1 Mev. The number of isomer nuclei Rh^{103m} ($T = 56 \pm 1$ min, $E_\gamma = 40 \pm 0.5$ kev) was determined from the induced-radioactivity decay curves.

MEASUREMENT OF THE YIELD CURVE

Samples of high-purity (99.99%) metallic rhodium were in the form of discs 40 mm in diameter. The measurements were carried out with two sample thicknesses: 20 and 50μ (24.8 and 62 mg/cm²). The samples were irradiated at a distance of 60 cm from the synchrotron target; at the lowest energies the distance was reduced to 40 cm.

The γ-quantum flux incident on the sample during the irradiation time was measured by a thin-wall integrating ionization chamber located in the beam at a distance 50 cm behind the sample. The sensitivity of this chamber was calibrated before and after each irradiation against an "absolute" ionization chamber with thick walls (7.5 cm) of aluminum[8] which replaced the sample in the beam. To obviate a correction for the distribution of the γ-radiation intensity in the beam, the section of the air gap of the "absolute" chamber had the same shape and dimensions as the sample. The gap thickness was 7 mm.

The samples were irradiated from 20 minutes to 2 hours. To introduce corrections for the fluctuation in the intensity of the x rays during the time of irradiation, the voltage of the output of the current integrator of the thin-wall chamber, located in the beam behind the sample, was recorded on the chart of an electronic ÉPP-0.9 potentiometer.

The decay of the Rh^{103m} isomer nuclei is characterized by the following quantities:[9,10]

Transition energy, kev	40
Coefficient of conversion from the K shell, α_K	40
Ratio of conversion coefficients	
on K and L shells	0.09 ± 0.01
on L and M shells	7 ± 1

The yield of the $Rh^{103}(\gamma, \gamma')Rh^{103m}$ reaction was measured with a scintillation counter recording the characteristic x-rays accompanying the conversion from the K shell ($h\nu = 22.7$ and 20.3

kev). Registration of the gamma radiation made it possible to increase the efficiency by increasing the thickness of the samples, and simplified the corrections for absorption and scattering in the samples. The irradiated sample of rhodium was placed between two NaI(Tl) crystals 40 mm in diameter and 2 mm thick, and consequently the radiation was registered in a solid angle close to 4π. The crystals were hermetically sealed in flat cylindrical boxes. The ends of the boxes, facing the sample, were made of 100-μ aluminum foil. The opposite ends, in contact with the photomultipliers were made of optical glass 1 mm thick. FÉU-29 photomultipliers, connected in parallel had a noise level corresponding to 3—5 kev.

Table I

Reaction	Reaction threshold, Mev	Residual nucleus	Half-life
(γ, γ')	—	Rh^{103m}	56 min
(γ, n)	9.3	Rh^{102}	213 days
$(\gamma, 2n)$	~ 17.1	Rh^{101m}	4.5 days
$(\gamma, 2n)$	16.8	Rh^{101}	~ 5 years
$(\gamma, 2p)$	16.5	Tc^{101}	14 min
$(\gamma, 2pn)$	24.8	Tc^{100}	15. sec

In the irradiation of the rhodium by x rays with a maximum energy up to 25.5 Mev, the radioactive isotopes were formed as result of the reactions listed in Table I. The main reactions, the yield of which at these energies amounts to ~90% of the total of all the disintegrations of the rhodium nuclei, are the (γ, n) and (γ, 2n) reactions. The yield of the reaction (γ, 2p) cannot exceed a fraction of a percent, since the total of the protons from the rhodium due to the reactions (γ, p), (γ, np) and others amounts to not more than 6% of the neutron yield at a maximum energy of 25 Mev.[11] In order to separate most completely the Rh^{103m} decay in the registration of the induced radioactivity of the samples, the amplified pulses from the photomultipliers were fed through a single-channel pulse-height analyzer. This made it possible to reduce considerably the background of the apparatus and the background due to the reactions (γ, n) and (γ, 2n). No decay of Tc^{101} was observed under these conditions.

The measurement of the induced activity began 10 or 20 minutes after the end of the irradiation, so as to eliminate the influence of the short-lived isotopes Rh^{104} (T = 44 sec) and Rh^{104m} (T = 4.5 min), which are produced through capture of slow background neutrons [(n, γ) reaction].

A special circuit with electronic "memory," developed by Shtranikh,[12] was used to record the number of pulses every 4 minutes on a telegraph tape. Each decay curve was measured during 2.5 hours. The sensitivity of the apparatus was monitored against a standard source.

In the reduction of the results, corrections were introduced for absorption in the samples (for which purpose the yields from samples of different thickness, simultaneously irradiated, were measured), for the width of the "window" of the pulse-height analyzer, for the solid angle of the apparatus, and for the absorption in the aluminum foil covering the NaI(Tl) crystals.

The irradiation of the rhodium samples in the synchrotron beam could produce, in addition to the (γ, γ′) reaction, also metastable Rh^{103m} states due to inelastic scattering of photoneutrons produced in the sample itself and background neutrons around the accelerator. Two control experiments were carried out to estimate these effects:

1) With x rays of maximum energy E_{max} = 25.5 Mev incident on the samples, when the effect due to the background neutrons should be a maximum, one rhodium sample was placed in the beam and the other at the same distance from the synchrotron outside the γ-ray beam. The activity of the latter sample, due to the neutrons and scattered gamma radiation, did not exceed 1% of the activity of the samples placed in the beam.

2) During irradiation at E_{max} = 23 Mev, several rhodium samples were placed between discs of the same diameter, made of cadmium 0.5 mm thick. The yield of the (n, n′) reaction due to the neutrons formed in the cadmium should have increased by approximately 20 times. Measurements have shown that the number of Rh^{103m} isomer nu-

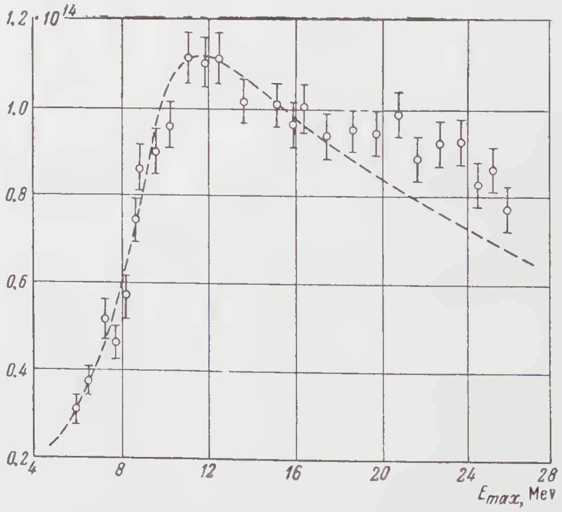

FIG. 1. Yield of the reaction $Rh^{103}(\gamma, \gamma')Rh^{103m}$ at various maximum x-ray energies E_{max}. Ordinates – saturated activity per second per mole per ampere of ionization current of the absolute chamber. The dashed curve is the yield curve calculated under the assumption that the reaction cross section is zero at energies above 12.5 Mev.

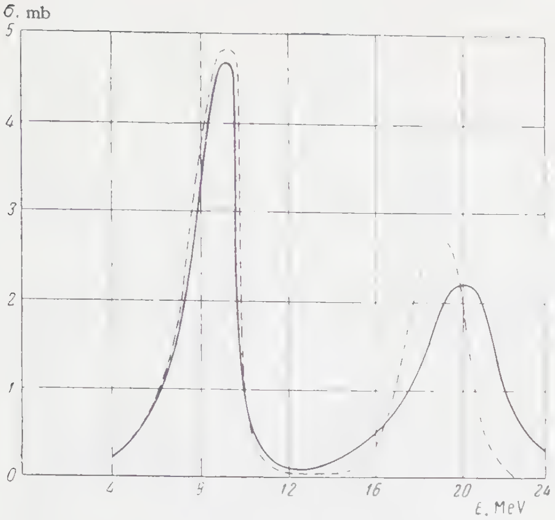

FIG. 2. Cross section of the reaction $Rh^{103}(\gamma,\gamma')\,Rh^{103m}$. Two versions of the calculation are given; other versions yield intermediate values.

clei produced in irradiation with and without cadmium were the same within 5%, i.e., the effect is negligibly small for the sample thicknesses used.

Figure 1 shows the yields of the reaction $Rh^{103}(\gamma, \gamma')Rh^{103m}$ obtained at different maximum bremsstrahlung energies. Each experimental point is the average of 6 — 10 individual measurements (mean-square errors).

INELASTIC SCATTERING CROSS SECTION

The cross section of the reaction $Rh^{103}(\gamma, \gamma')$ Rh^{103m} in the energy interval 5 — 25 Mev was calculated by the method of Penfold and Leiss[13] from the yields obtained. Figure 2 shows the curves corresponding to the two versions of the calculation.

The cross section has 2 maxima. The position of the first maximum coincides, within the accuracy of the experiment, with the threshold of the (γ, n) reaction. The second maximum is located at ~ 20 Mev, i.e., 3 or 4 Mev above the energy corresponding to the maximum cross section of nuclear photon absorption (16 Mev).[14] The calculated cross section in the vicinity of the first maximum is much less accurate. As a check, Fig. 1 shows dotted the yield curve calculated under the assumption that the cross section of the reaction is zero at energies below 12.5 Mev. A comparison of the dotted curve with the experimental points shows that there is no doubt that the cross section increases in the vicinity of 20 Mev.

The cross section obtained for the $Rh^{103}(\gamma, \gamma')$ Rh^{103m} reaction gives the lower limit for the cross section of inelastic nuclear scattering on rhodium. To obtain from this the total cross section of the (γ, γ') reaction, it is necessary to know the relative probability of production of the isomer state κ in inelastic photon scattering. It is impossible to calculate this quantity with any degree of accuracy, since the branching ratio of the transitions to the ground and metastable states is determined for each excitation energy by all the lower levels of the given nucleus. A rough statistical analysis of the process,[15,16] which agrees qualitatively with the experimental data, yields in the case of rhodium $\kappa = 0.2 - 0.25$.

Knowing the cross section of the (γ, γ') reaction, we can estimate the radiative width Γ_γ for different excitation energies. Table II lists the inelastic scattering cross section $\sigma(\gamma, \gamma') \approx 4.5\sigma[Rh^{103}(\gamma, \gamma')Rh^{103m}]$, and the photoneutron cross section $\sigma_n = \sigma(\gamma, n) + \sigma(\gamma, 2n)$, measured by Parsons.[14] Starting with the threshold of the (γ, n) reaction, the neutron width Γ_n increases rapidly, and the cross section of the reaction (γ, γ') accordingly diminishes rapidly. In the energy interval 9.35 — 11 Mev the ratio of the cross sections $\sigma(\gamma, \gamma')/\sigma_n$, the value of which is 2 at 9.35 Mev, decreases to 0.09 at 10 Mev, and to 0.03 at 11 Mev. Up to 16 Mev, the ratio of the cross sections $\sigma(\gamma, \gamma')/\sigma_n$ remains approximately constant at ~ 0.01. Starting at 16 or 17 Mev, the relative probability of inelastic scattering increases and amounts to ~10% at 20 Mev.

Table II

E, Mev	$\sigma(\gamma, \gamma')$, mb	σ_n, mb	$\sigma(\gamma, \gamma')/\sigma_n$	E, Mev	$\sigma(\gamma, \gamma')$, mb	σ_n, mb	$\sigma(\gamma, \gamma')/\sigma_n$
5	1.8	—	—	12	0.6	62.1	0.01
7	8.5	—	—	14	1.2	155.2	~0.01
9.3	21.2	—	—	16	2.7	193.1	~0.01
9.35	21.1	10.3	2.04	18	6.1	169.0	0.04
9.5	14.8	17.2	0.86	19	9.2	136.2	0.07
9.75	4.4	25.2	0.18	20	10.3	111.0	0.09
10	2.6	27.6	0.09	21	8.7	87.9	0.10
11	1.0	37.2	0.03	22	4.4	71.7	0.06

If the nuclear excitation energy is several Mev higher than the threshold energy of the (γ, n) reaction, the emission of a photon can with a large probability be accompanied by an emission of a neutron [reaction $(\gamma, \gamma n)$]. In this case the ratio $\sigma(\gamma, \gamma')/\sigma_n < \Gamma_\gamma/\Gamma_n$. According to an estimate made by Goldemberg and Katz,[4] $\Gamma_\gamma/\Gamma_n \approx 3\sigma(\gamma, \gamma')/\sigma_n$ near 20 Mev. This means that in the case of rhodium the radiative width at 20 — 22 Mev amounts to 25 — 30% of the neutron width. The strong increase in the radiative width in the 20-Mev region, obtained for rhodium, confirms the results obtained earlier[3,6] for Ag^{107} and In^{115}.

---

[1] C. S. del Rio y Sierra and V. L. Telegdi, Phys. Rev. **90**, 439 (1953).

[2] E. Silva and J. Goldemberg, Phys. Rev. **110**, 1102 (1958).

[3] Bogdankevitch, Dolbikin, Lazareva, and Nikolaiev, Comptes Rendus du Congres International de Physique Nucleaire, Paris, (1958) Dunod, Paris (1959), p. 697.

[4] J. Goldemberg and L. Katz, Phys. Rev. **90**, 308 (1953).

[5] Burkhardt, Winhold, and Dupree, Phys. Rev. **100**, 199 (1955).

[6] Bogdankevich, Lazareva, and Nikolaev, JETP **31**, 405 (1956), Soviet Phys. JETP **4**, 320 (1957).

[7] L. Meyer-Schutzmeister and V. L. Telegdi, Phys. Rev. **104**, 185 (1956).

[8] Flowers, Lawson, and Fossey, Proc. Phys. Soc. **B65**, 286 (1952).

[9] Avignon, Michalowicz, and Bouchez, J. Phys. et Radium, **16**, 404 (1955).

[10] Drabkin, Orlov, and Rusinov, Izv. Akad. Nauk SSSR, Ser. Fiz. **19**, 324 (1955), Columbia Tech. Transl. p. 294.

[11] A. Mann and J. Halpern, Phys. Rev. **82**, 733 (1951).

[12] I. V. Shtranikh, Автоматизация измерений на призме (The Automatization of Prism Measurements), paper at the Physics Institute, Academy of Sci., 1951.

[13] A. S. Penfold and J. E. Leiss, Phys. Rev. **114**, 1332 (1959).

[14] R. W. Parsons, Canad. J. Phys. **37**, 1344 (1959).

[15] Martin, Diven, and Taschek, Phys. Rev. **93**, 199 (1954).

[16] S. A. Moszkowski, Phys. Rev. **89**, 474 (1953).

Translated by J. G. Adashko
230

SOVIET PHYSICS JETP VOLUME 12, NUMBER 5 MAY, 1961

ASYMMETRY IN THE DECAY OF Λ^0 HYPERONS GENERATED BY 2.8 Bev/c NEGATIVE PIONS, DETERMINED BY OBSERVATIONS IN A FREON BUBBLE CHAMBER

V. V. BARMIN, Yu. S. KRESTNIKOV, I. I. PERSHIN, V. P. RUMYANTSEVA, Ya. Ya. SHALAMOV, and V. A. SHEBANOV

Submitted to JETP editor July 2, 1960

J. Exptl. Theoret. Phys. (U.S.S.R.) **39**, 1229-1231 (November, 1960)

The asymmetry in the decay of Λ^0 hyperons relative to the plane of creation was investigated in a freon bubble chamber for Λ^0 particles created on carbon, chlorine, and fluorine nuclei by 2.8-Bev/c negative pions. The measured value of the asymmetry coefficient is $\alpha\overline{P} = -0.30 \pm 0.15$.

WE know[1,2] that the decay products of Λ^0 hyperons generated in the reaction

$$\pi^- + p \rightarrow \Lambda^0 + K^0, \tag{1}$$

are emitted asymmetrically with respect to the plane of creation of the Λ^0, owing to the transverse polarization of the Λ^0 hyperons due to parity nonconservation in the process of decay of the Λ^0 particles. The distribution of the decay products of the Λ^0 particles relative to the plane of their creation is described by the relation

$$W(\xi)\,d\xi \sim (1 + \alpha\overline{P}\xi)\,d\xi, \tag{2}$$

where α is the asymmetry coefficient characterizing the degree of parity nonconservation in the Λ^0 decay, $\overline{P}$ is the hyperon polarization averaged over all the values of the angles of emission of the Λ^0 during creation, and $\boldsymbol{\xi} = [\mathbf{p}_{\pi\ \mathrm{pri}} \times \mathbf{p}_\Lambda] \times \mathbf{p}_{\pi\ \mathrm{decay}}$, where $\mathbf{p}_\Lambda$, $\mathbf{p}_{\pi\ \mathrm{pri}}$ and $\mathbf{p}_{\pi\ \mathrm{decay}}$ are the momentum vectors of the Λ^0 particle, primary pion, and "decay" pion respectively. Usually the value of $\alpha\overline{P}$ is calculated from the formula

$$\alpha\overline{P} = 2(N_\uparrow - N_\downarrow)/(N_\uparrow + N_\downarrow), \tag{3}$$

where $N_\uparrow$ and $N_\downarrow$ are the numbers of pions emitted upward and downward relative to the plane of creation.

This asymmetry was investigated in several researches (see, for example, references 3 – 6) at a generating pion energy near 1 Bev. According to the latest data, the value of $\alpha\overline{P}$ measured in a hydrogen chamber[6] is 0.73 ± 0.14. In a xenon bubble chamber $\alpha\overline{P} = 0.45 \pm 0.15$.[6]

Of considerable interest are the values of $\alpha\overline{P}$ at energies above 1 Bev, since they can give an idea of the polarization of the Λ^0 hyperons created at this energy.

We have set up experiments on the asymmetry of the decay of Λ^0 hyperons generated by negative pions with momenta (2.8 ± 0.3) Bev/c on light nuclei, in a 17-liter freon bubble chamber[7] without a magnetic field. The measurements were made with the negative-pion beam from the proton synchrotron of the Joint Institute for Nuclear Research.

The Λ^0 particles are generated by 2.8-Bev/c negative pions essentially via the reaction

$$\pi^- + N \rightarrow \Lambda^0 + K + n\pi \tag{4}$$

(with a tentative estimate $\bar{n} \approx 1.5$).

In addition, the considered Λ^0 decays contain several Λ^0 hyperons due to the decay of the Σ^0 hyperons generated in a reaction analogous to (4). Because of the Λ^0-particle contamination due to the decay $\Sigma^0 \rightarrow \Lambda^0 + \gamma$, our calculated value of $\alpha\overline{P}$ may be somewhat too low.

A total of about 60 thousand stereophotographs were obtained, in which the first scanning disclosed approximately 1200 "forks" connected with termination of a pion track. The Λ^0 particles in these events were identified by estimating ionization, multiple scattering, and in many cases also the ranges of the protons or pions, and also by kinematic analysis, with the aid of the tables of reference 8, of the angles between the direction of motion of the Λ^0 particle and its decay products.

By the same token, the result included only the Λ^0-hyperon decays for which a noticeable difference in ionization was observed for at least one of the decay products, relative to the minimum ionization corresponding to the beam particles.

A total of 183 Λ^0-decay cases were selected, of which 165 were due to the production of Λ^0 particles by the freon, i.e., by the C, F, or Cl nuclei, and 18 cases were due to production by the propane-

Material in the chamber	Total no. of Λ^0 decay events	No. of negative pions from the Λ^0-hyperon decay emitted			$\alpha\overline{P}$
		upward	downward	in the creation plane	
Freon	165	67	95	3	-0.34 ± 0.16
Xenon-propane	18	9	8	1	$+0.12 \pm 0.47$
Total number of events	183	76	103	4	-0.30 ± 0.15

xenon mixture, i.e., the H, C, or Xe nuclei. The average momentum of the Λ^0 particles used in the measurements was 650 Mev/c in the laboratory system. Owing to the stringent selection criteria, the K^0-decay contamination of the Λ^0 decays did not exceed 5%.

The measured values of $\alpha\overline{P}$ are listed in the table (the errors indicated are statistical). The systematic errors connected with the measurement procedure do not change our result by more than 20%. It follows from the data obtained, with considerable probability, that a negative value of $\alpha\overline{P}$ is observed in the decay of hyperons generated by negative ~3-Bev pions on light nuclei. This may be connected with the fact that on going from 1 Bev to higher negative-pion energies a change takes place in sign of the polarization of the Λ^0 hyperons. However, the statistical accuracy of our experiment is insufficient for an unequivoval conclusion that $\alpha\overline{P}$ is negative.

In connection with the foregoing result, it should be noted that the authors of reference 4 conclude that $\alpha\overline{P}$ decreases somewhat on going from a generating-meson energy of 0.9 — 1.0 Bev to 1.2 — 1.3 Bev. In another investigation,[5] carried out with 1.3 — 1.9 Bev generating mesons for targets made of iron, no asymmetry was observed. However, the statistical accuracy of both results is low.

The authors express deep gratitude to A. I. Alikhanov, A. G. Meshkovskiĭ, and I. Yu. Kobzarev for a discussion of the results obtained, to V. I. Veksler for an opportunity to perform the experiment with the negative-pion beam of the Dubna proton synchrotron, and also to the proton-synchrotron crew and to the laboratory staff who participated in the reduction of the photographs of the Λ^0-hyperon decay.

---

[1] T. D. Lee and C. N. Yang, Phys. Rev. **104**, 254 (1956).

[2] Lee, Steinberger, Feinberg, Kabir, and Yang, Phys. Rev. **106**, 1367 (1957).

[3] Crawford, Cresti, Good, Gottstein, Lyman, Solmitz, Stevenson, and Ticho, Phys. Rev. **108**, 1102 (1957).

[4] Eisler, Plano, Prodell, Samions, Schwartz, Steinberger, Bassi, Borelli, Puppi, Tanaka, Woloschek, Zoboti, Conversi, Franzini, Mannelli, Santangelo, Silvestrini, Glaser, Graves, and Perl, Phys. Rev. **108**, 1353 (1957).

[5] Boldt, Bridge, Caldwell, and Pall, Phys. Rev. Lett. **1**, 256 (1958).

[6] D. A. Glaser, Тр. Конференции по физике частиц высоких энергий (Trans. Conference on the Physics of High-Energy Particles), Kiev, 1959 (in press).

[7] Blinov, Lomanov, Meshkovskiĭ, Shalamov, and Shebanov, Приборы и техника эксперимента (Instr. and Exptl. Techniques) **1**, 35 (1958).

[8] L. B. Leipuner, Some Relativistic Two-Body Kinematics Tables, preprint, Brookhaven National Laboratory, 1958.

Translated by J. G. Adashko
231

SOVIET PHYSICS JETP VOLUME 12, NUMBER 5 MAY, 1961

PRODUCTION OF π^0 MESONS IN COLLISIONS BETWEEN 2.8-Bev/c π^- MESONS AND PROTONS

Ya. Ya. SHALAMOV and V. A. SHEBANOV

Submitted to JETP editor July 2, 1960

J. Exptl. Theoret. Phys. (U.S.S.R.) **39**, 1232-1236 (November, 1960)

The production of π^0 mesons in the $\pi^- + p \rightarrow m\pi^0 + n$ ($m = 1, 2, 3$) reactions was investigated at $p_{\pi^-} = 2.8$ Bev/c in a 17-liter bubble chamber filled either with a propane-xenon or a freon 12- freon 13 mixture. The cross section for hydrogen was determined by the difference method as (2.2 ± 0.3) mb. The mean number of γ rays per interaction is 4.0 ± 0.4. The angular distribution of the γ rays in the c.m.s. is anisotropic and possesses a sharp peak in the forward direction. The small cross section for exchange scattering, $\sigma(\pi^- + p \rightarrow \pi^0 + n) = (0.20 \pm 0.25)$ mb, indicates that, for the given π^--meson energy, the partial interaction cross sections with isotopic spins $3/2$ and $1/2$ are equal. The cross sections for processes involving the production of two or three π^0 mesons are estimated by analyzing the distribution of the events with respect to the number of γ quanta.

INTRODUCTION

THE multiple production of mesons in π^-p collisions at π-meson energy > 1 Bev has been studied by a number of investigators. In experiments with diffusion chambers in a magnetic field and filled with hydrogen, the meson production in π^-p collisions was studied at a π^--meson energy of 5 and 1.85 Bev.[1,2] Walker[3] carried out similar experiments using nuclear emulsions for 4.5-Bev π mesons. As a result of these investigations, the angular and momentum distributions of π mesons, as well as the distributions of mesons with respect to various charged states, have been obtained. The most complete data relate to the production of charged mesons. The reactions accompanied by a simultaneous production of charged and neutral mesons have only been partially investigated. Reactions of the type

$$\pi^- + p \rightarrow m\pi^0 + n \qquad (1)$$

where only neutral particles are emitted have not been investigated. A logical interpretation of the data on the multiple production of π mesons becomes possible if one makes an assumption about the ratio of the production cross sections for different isotopic spins of the system. In particular, the number of events of type (1) was determined in references 1 and 2 by using such a method.

It would be of interest to obtain direct data on the production of π^0 mesons in these reactions, and on the magnitude of the exchange scattering of π^- mesons with energies > 1 Bev.

The cross sections for processes of the type (1) were measured by us for 2.8-Bev/c π^- mesons by means of a bubble chamber[4] filled with a heavy hydrogen-containing liquid.[5] The measurements were carried out with the extracted π^--meson beam of the proton synchrotron of the Joint Institute for Nuclear Research.

1. EXPERIMENTAL METHOD

About 3000 stereoscopic photographs were taken in experiments with the π^--meson beam, using a bubble chamber filled with a propane-xenon mixture. The cross section for hydrogen was determined by the difference method. In order to determine the background due to the quasi-free collisions of π^- mesons with protons in the nuclei, 2800 additional stereoscopic photographs taken in analogous experiments with the π^- beam and the same bubble chamber, but using a mixture of freon 12 (CCl_2F_2) and freon 13 ($CClF_3$), were analyzed.

All photographs were scanned by three independent observers. In the scanning, prongless stars were noticed, i.e., events where, in the observation region, a π^- meson track stopped abruptly without any visible nuclear-interaction products. Usually, it was possible to correlate such a point of track disappearance with one or more electron-positron conversion pairs appearing as a result of the process (1) with consecutive decays $\pi^0 \rightarrow 2\gamma$.

In order to find the absolute cross section for the process, the total number of π mesons passing through the working volume of the chamber was counted. Particles were counted in 10 out of every 50 squares. The total number of π mesons was found to equal 42,300 and 38,300 for the propane-xenon and freon fillings, respectively. A 5-cm x 15-cm lead collimator was placed at the entrance to the chamber. The strict delimitation of the beam region considerably increased the conversion efficiency, but also the relative fraction of μ mesons in the beam. The admixture of μ mesons in the beam was not measured and, therefore, to compute the cross section, the ratio of the total number of interactions to the given number of π-meson passages was determined.

Estimates of possible background events were made. Possible imitating processes are events of the types

$$\pi^- + p \to \Lambda^0 + K^0 + m\pi^0, \tag{2}$$

$$\pi^- + p \to K^0 + \tilde{K}^0 + n\pi^0 \tag{3}$$

on a free proton or on a weakly-bound proton of a nucleus. About 120 events of the V-decay type were detected in 3000 pictures. It was found that the number of events in which K^0 mesons or Λ^0 hyperons are produced, and which can be regarded as reactions (2) or (3), is less than 5%. Such a correction amounts to not more than 2 to 3% of the events studied, and was not taken into account in the final results.

The number of chance electron-positron pairs directed towards the point of disappearance of π^- mesons was estimated. The estimate was obtained by noting that, among the 120 V-decay events detected in the photographs, not a single electron-positron pair was directed towards the vertex of the V event. This makes the probability of a chance superposition less than 1% of the total number of detected electron-positron pairs directed towards prongless stars.

2. EXPERIMENTAL RESULTS

As a result of the multiple scanning of the photographs, 125 prongless stars were found in the propane-xenon mixture, and 102 in the freon filling. The distribution with respect to the number of electron-positron pairs directed towards the point of disappearance of the π^- mesons is given below:

Number of pairs $e^+ + e^-$	0	1	2	3	4	5	6
Number of events in the propane-xenon mixture	13	30	41	26	9	5	1
Number of events in the freon mixture	13	52	22	11	3	1	—

The angle θ_γ with the direction of the incident π mesons was determined for each pair. In order to obtain data on the angular γ-ray distribution, the detection efficiency was calculated by two methods. In the first method, the maximum possible γ-ray path length in the working volume of the chamber was measured and the probability of observing a given pair was determined from the known conversion length (equal to 19 and 30 cm for the two working liquids, respectively). In the second method, the mean detection efficiency of the γ rays in the chamber was calculated for different angles of emission θ_γ with an electronic computer.

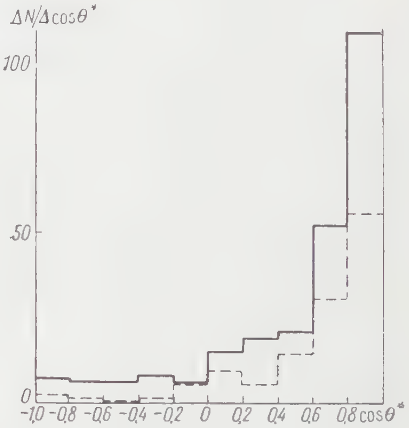

FIG. 1. Angular distribution of γ rays in the c.m.s. without taking the detection efficiency into account: solid curve – propane and xenon, dashed curve – freon.

The angular γ-ray distributions in the pion-nucleon c.m.s., obtained without taking the detection efficiency into account, are shown in Fig. 1. The angular distributions obtained with account of the efficiency are shown in Figs. 2 and 3. Both methods of calculating the efficiency gave similar results.

From the observed number of events we calculated the probabilities for the production of prongless stars on the nuclei of C, F, Cl (freon) and H, C, Xe (propane-xenon mixture). These were found to equal respectively (0.93 ± 0.1)% and (1.6 ± 0.15)% of the total cross section for the inelastic interaction of π^- mesons with nuclei. The cross section per free proton calculated from these data is (2.2 ± 0.3) mb. In calculating the results for freon, it was assumed that the charac-

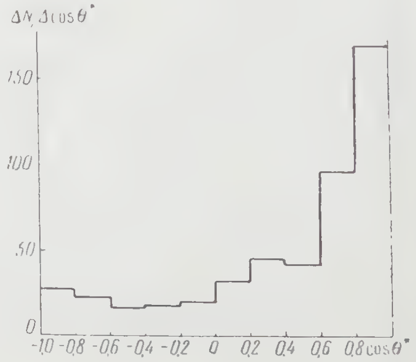

FIG. 2. Angular distribution of γ rays from reaction (1) in the c.m.s. (propane-xenon).

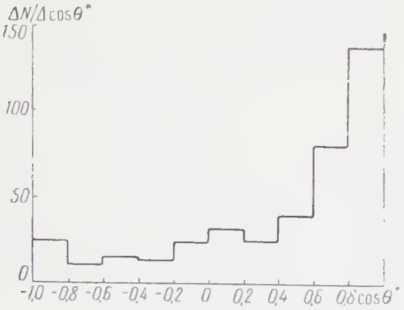

FIG. 3. Angular distribution of γ rays from the reaction $\pi^- + C \to m\pi^0 + C'$ in the c.m.s. (freon).

ter of the nuclear interactions differs little for a lighter nucleus (C) and for a heavier nucleus (Cl). For the xenon nuclei, it was assumed that the production cross section for prongless stars on xenon is proportional to the number of protons in the nucleus.* It is important to note that, out of 125 events detected in the xenon-propane mixture, two thirds occurred on free protons and only one third on the bound protons of the nuclei. Thus, the results depend little on the assumptions made in the calculation.

From a comparison of the angular γ-ray distributions obtained for the two different mixtures (see Fig. 1), it can be seen that the distributions are identical within the limits of experimental error. One can therefore assume that Fig. 2 represents the distribution of γ rays originating in the decay of π^0 mesons produced on free protons.

The mean number of γ rays per interaction of the above type equals 4.0 ± 0.4, i.e., two π^0 mesons are on the average produced per collision.

From six events in which five or six conversion pairs were observed (5γ, 6γ), it was found that the number of events of the type $\pi^- + p \to 3\pi^0 + n$ lies between 30 and 60. Moreover, from the number of events in which only one pair was observed (1γ), it was found that the number of exchange scattering events $\pi^- + p \to \pi^0 + n$ is not greater than 25. Such an estimate made it possible to determine the cross section for the process (1) for m = 1, 2, and 3:

$$\sigma_{\pi^0 n} = (0.2 \pm 0.25)\ \text{mb}, \quad \sigma_{2\pi^0 n} = (1.3 \pm 0.4)\ \text{mb},$$

$$\sigma_{3\pi^0} = (0.7 \pm 0.4)\ \text{mb}.$$

The mean number of γ rays calculated from these cross-section values is 5.6 ± 0.6, which disagrees with the value 4.0 ± 0.4 given above. It is natural to ascribe this discrepancy to the low detection efficiency of the reaction $\pi^- + p \to 3\pi^0 + n$, and to the resulting large statistical errors in the cross sections.

3. DISCUSSION OF RESULTS

As can be seen from Figs. 2 and 3, the angular γ-ray distribution in the c.m.s. is strongly anisotropic. We can observe one section in the distribution that is strongly peaked in the forward direction ($\cos\theta^* \gg 0.6$, where θ^* is the angle in the c.m.s.), while another section is isotropic. It should be mentioned that the angular π^0-meson distribution will practically coincide with the γ-ray angular distribution provided the energy spectrum of the π^0 mesons is sufficiently hard, which is evidently true for the energy of π^- mesons used. The conclusions reached concerning the angular γ-ray distribution will then apply to the same extent to the angular distribution of π^0 mesons produced in reaction (1). Similar regularities detected by us on π^0 mesons were also observed for charged mesons.[1,2]

Reaction products	Probability of a given reaction in percent of the total cross section for inelastic interaction	
	According to statistical theory	Experimental values
n 0	2.4	1 ± 1.2
n 00	5.3	5.9 ± 1.8
n 000	2.6	3.2 ± 1.8
n 0000	0.4	–
Total	10.7	10.1 ± 1.4

It is known that calculations based on the statistical theory of multiple π-meson production do not explain the anisotropy of the angular distribution, although they are in good agreement with the data on the multiplicity of the production processes.[6] The same is true for our results. Maksimenko,[7] using statistical theory, calculated that for 2.8-Bev π^- mesons the processes of the type (1) should amount to 10.7% of the cross section for inelastic interactions of π^- mesons with protons. This is in good agreement with our experimental result of (10.1 ± 1.4)%. A satisfactory agreement with the statistical theory can also be obtained by comparing the calculations on the multiplicity of process (1) with the experimental data obtained (see table), although large statistical errors in the cross section make such a comparison not very effective. Moreover, the observed anisotropy in the angular distribution of π^0 mesons cannot be explained by a statistical theory. An interesting possibility for explaining the peculiarity in the angular π-meson distribution was considered by Barashenkov.[8] It was demonstrated by him that the resulting asymmetry in the angular distribution of the mesons produced can be explained by assuming that the peripheral collisions amount to $\gtrsim 20\%$ of the total cross section for π^-p collisions.

---

*We have also made use of preliminary results, obtained in a xenon bubble chamber, for which we thank E. V. Kuznetsov. According to these data, the ratio of prongless stars to the total number of interactions is equal to (0.5 ± 0.2)% per xenon nucleus.

The cross section for exchange scattering can be written in terms of the amplitudes f and g corresponding to isotopic states with $T = 3/2$ and $T = 1/2$ respectively:

$$\sigma(\pi^- + p \rightarrow \pi^0 + n) = \tfrac{2}{9}[f - g]^2.$$

Okun' and Pomeranchuk[9] have drawn attention to the fact that, at high energies, the exchange-scattering cross section should amount to only a small fraction of the total cross section for inelastic scattering, and that, consequently, $f \approx g$. From the data of the present experiment, we can conclude that, even for ~3-Bev π mesons, the reaction probabilities for channels with different isotopic spins are practically equal. Using the dispersion relations, we can also show that the differential charge-exchange cross section at 0° decreases sharply with increasing π-meson energy from 0.8 to 2 Bev.[10] Similarly, the total cross section for exchange scattering should also decrease, a fact which is also confirmed by the results obtained.

In conclusion, the authors would like to thank Academician A. I. Alikhanov for help and support in the experiment, and Academician V. I. Veksler for enabling us to carry out the present experiment. We would like to thank the synchrotron operation team, who made it possible to execute the work, and also Yu. S. Krestnikov, Yu. I. Makarov, and N. S. Khropov for help in carrying out the measurements. We are indebted to N. G. Birger for helpful comments, to V. M. Maksimenko for calculating the results of the statistical theory, to I. S. Bruk for providing the facilities of the M-2 electronic computer of the Institute for Electronic and Control Machinery, U.S.S.R. Academy of Sciences, and to G. M. Adel'son for carrying out the computations.

---

[1] Maenchen, Fowler, Powell, and Wright, Phys. Rev. **108**, 850 (1957).

[2] R. C. Whitten and M. M. Block, Phys. Rev. **111**, 1676 (1958).

[3] W. D. Walker, Phys. Rev. **108**, 872 (1957).

[4] Blinov, Lomanov, Meshkovskiĭ, Shalamov, and Shebanov, Приборы и техника эксперимента (Instruments and Exptl. Techniques) **1**, 35 (1958).

[5] Ya. Ya. Shalamov and V. A. Shebanov, ibid. **3**, 141 (1960).

[6] Belen'kiĭ, Maksimenko, Nikishov, and Rozental', Usp. Fiz. Nauk **62**, 1 (1957).

[7] V. M. Maksimenko, Dissertation, Physics Institute of the Academy of Sciences, U.S.S.R, 1960.

[8] V. S. Barashenkov, Nucl. Phys. **15**, 486 (1960).

[9] L. B. Okun' and I. Ya. Pomeranchuk, JETP **30**, 424 (1956), Soviet Phys. JETP **3**, 307 (1956).

[10] Cool, Piccioni, and Clark, Phys. Rev. **103**, 1082 (1956).

Translated by H. Kasha
232

SOVIET PHYSICS JETP VOLUME 12, NUMBER 5 MAY, 1961

PRODUCTION OF CHARGED HYPERONS BY 9-Bev PROTONS INTERACTING WITH PHOTOGRAPHIC EMULSION NUCLEI

L. P. DZHANELIDZE, D. K. KOPYLOVA, Yu. B. KOROLEVICH, N. I. KOSTANASHVILI,
K. V. MANDRITSKAYA, N. I. PETUKHOVA,* M. I. PODGORETSKIĬ, D. TUVDENDORZH,
O. A. SHAKHULASHVILI, and CHENG P'U-YING

Joint Institute for Nuclear Research; Institute of Physics, Academy of Sciences, Georgian S.S.R.; Tbilisi State University

Submitted to JETP editor July 9, 1960

J. Exptl. Theoret. Phys. (U.S.S.R.) **39**, 1237-1241 (November, 1960)

The angular distribution of $\pi^\pm$ mesons from decaying $\Sigma^\pm$ hyperons, produced by interaction of 9-Bev protons with emulsion nuclei, was investigated. An estimate is obtained of the charge composition of the hyperons. The value of the cross section for the production of charged hyperons on emulsion nuclei is estimated.

CONDITIONS OF THE EXPERIMENT

Two pellicle stacks measuring $10 \times 10 \times 6$ and $10 \times 15 \times 4$ cm (stacks 1 and 2 respectively), and made up of NIKFI type BR-400 emulsions were used. The stacks were exposed to the 9-Bev proton beam from the proton synchrotron of the High-Energy Laboratory. The purpose was to investigate, in particular, the angular distributions of the charged-hyperon decay products; principal attention was therefore paid to finding the hyperons by a method as free as possible from experimental sampling, and also to a careful identification of the observed decay events. In this connection, the search for hyperons was conducted by continuing the tracks in stars produced by primary protons. The particle-decay events in flight produced by one relativistic particle were registered. The cases thus obtained could be due to decay in flight of either $\Sigma^\pm$ hyperons or $K^\pm$ mesons, with the admixture of the latter being exceedingly insignificant, owing to the large difference between the lifetimes of these particles.

The final identification of the decaying particle was by measuring the multiple scattering and the ionization. The prongs, produced by the primary protons, which were to be continued satisfied certain energy and geometry conditions. These conditions, as well as the details of searching and identifying the hyperons decaying in flight by the scheme $\Sigma^\pm \rightarrow \pi^\pm + n$, are given in reference 1.

The entire procedure of finding and processing was the same for both stacks, except that in stack 1 primary stars with $N_h \geq 10$ were selected, while the selection in stack 2 was independent of the number of prongs in the stars. A total of 76 $\Sigma^\pm \rightarrow \pi^\pm + n$ decays in flight were found, of which 33 were in stack 1 and 43 in stack 2.*

RESULTS

1. Angular distribution of the $\Sigma^\pm$-hyperon decay products. Solov'ev[2] emphasized the importance of investigating the longitudinal asymmetry in the angular distribution of the pions produced in the decay of hyperons. As was already reported in reference 1, we undertook to refine the data on the angular distribution of the $\pi^\pm$ mesons from the decay of $\Sigma^\pm$ hyperons. The resultant angular distribution in the hyperon rest system relative to its direction of motion is shown in Fig. 1.

If we approximate the distribution by the expression $1 + a\cos\theta^*$, then the coefficient of asymmetry is found to be

$$a \equiv \alpha \overline{P}_\Sigma = \frac{3}{N}\sum_{i=1}^{N}\cos\theta_i^* \pm \left(\frac{3-a^2}{N}\right)^{1/2} = 0.03 \pm 0.2,$$

where α is the coefficient of asymmetry for complete polarization of the hyperons, $\overline{P}_\Sigma$ is the component of the vector of the average polarization of the Σ hyperon along the direction of its motion, θ_i^* is the angle between the direction of hyperon flight and the pion flight in the rest system of the hyperon, and N is the number of observed hyperons.

We also investigated the angular distribution of

---

*Deceased.

*Stack 1 was scanned in the High-Energy Laboratory of the Joint Institute for Nuclear Research, while stack 2 was scanned in the Physics Institute of the Georgian Academy of Sciences, and at the Tbilisi State University.

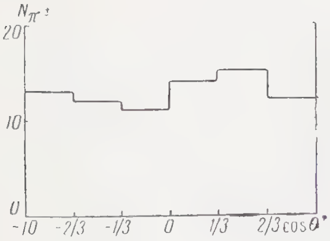

FIG. 1. Angular distribution of $\pi^\pm$ mesons in the rest system of the hyperon, relative to the direction of its motion.

the pions relative to the plane of creation of the Σ hyperons. The normal to the plane of creation was determined by the vector product $[\mathbf{p}\times\mathbf{\Sigma}]$ where **p** and **Σ** are unit vectors in the direction of motion of the proton beam and the hyperon respectively, and the "upward" and "downward" directions relative to this plane were determined from the sign of the mixed product $[\mathbf{p}\times\mathbf{\Sigma}]\cdot\pi$. The coefficient of asymmetry of this distribution is

$$b = 2\,(N_{\text{up}} - N_{\text{down}})\,/\,(N_{\text{up}} + N_{\text{down}}) = 0.36 \pm 0.22.$$

2. Angular and energy distributions of the $\Sigma^\pm$ hyperons. Two corrections were introduced in the angular and energy distributions of the $\Sigma^\pm$ hyperons. The first took into account the hyperons that decayed beyond the potential range. This correction amounts to approximately 16% of the observed number of hyperons. The second correction is purely geometric, and is connected with the circumstance that not all the hyperons traveling in the forward hemisphere relative to the motion of the beam proton have been registered, but only those for which the dip angle did not exceed 7.5° (reference 1).

Figure 2 shows the resultant angular distribution of $\Sigma^\pm$ hyperons with allowance for the corrections. As can be seen from the distribution, it can apparently be assumed that practically all the hyperons produced by interactions of 9-Bev protons with the emulsion nuclei are emitted in the forward hemisphere. Then, taking the foregoing corrections into account, the total number of hyperons is 488.

Figure 3 shows the total energy spectrum of charged hyperons. We see that the spectrum has a maximum and a sufficiently sharp fall-off towards higher energies. In addition, there are no hyperons with energies greater than 290 Mev, although hyperons with energies 410 — 420 Mev could have been registered according to the search rules applied in the present investigation. It is not excluded that these peculiarities of the spectrum are due to the fact that the produced hyperons interact effectively with the nucleons contained in the parent nucleus.

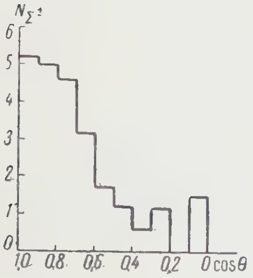

FIG. 2. Angular distribution of $\Sigma^\pm$ hyperons. The number of hyperons is given in arbitrary units.

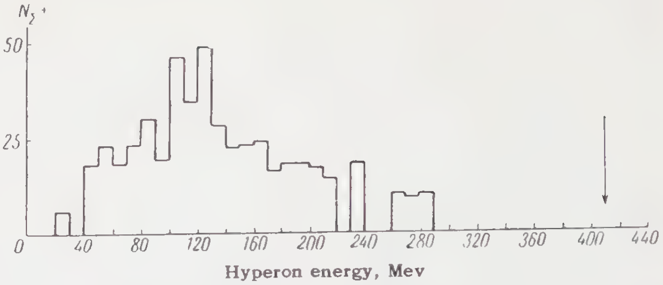

FIG. 3. Experimental energy spectrum of charged hyperons. The arrow indicates the upper limit of the hyperon energy which could still be registered.

Figure 4 shows the limiting curves for angles and the kinetic energy of the Σ hyperons produced in the reactions

$$p + N \rightarrow \Sigma + K + N, \qquad (1)$$
$$\pi + N \rightarrow \Sigma + K, \qquad (2)$$

calculated with allowance for the intranuclear motion of the nucleons. The possible generation of a certain number of additional pions in reactions (1) and (2) can cause only a narrowing of the limiting curves, which in this case will be completely located inside the corresponding curves of Fig. 4. The limiting curve of reaction (2) was calculated for an 8-Bev pion, corresponding to the maximum energy possible for pions generated by 9-Bev pro-

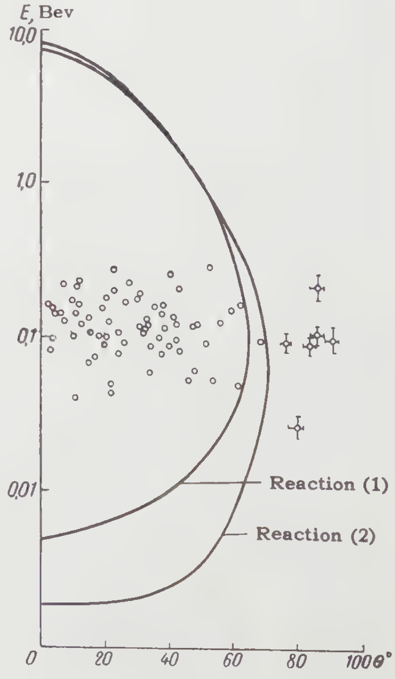

FIG. 4. Limiting curves for the angles of emission of hyperons in a laboratory system of coordinates, θ, and of the kinetic energy E of the Σ hyperons, produced in reactions (1) and (2).

tons, and emitted in the direction of the beam.*

Among the 76 hyperons shown in Fig. 4, six cases have been noticed which did not fall within the 3-fold error limits into the region bounded by the limit curves. It is natural to assume that these hyperons were initially produced in reactions (1) and (2), but upon further passage through the parent nucleus they experienced a nuclear interaction. Nor is it excluded that they were formed in an interaction between a primary proton and a nuclear tunnel.

3. Signs of Σ hyperons and the cross section for the creation of charged hyperons. The statistical estimate of the ratio of the number of positive to negative hyperons was obtained from a comparison of the times of flight of all the observed hyperons, from the point of their production to the point of decay, with the average time of flight expected at the given differential range under the assumption that all the observed hyperons are Σ^+ or Σ^- hyperons.

In the calculation of the average value of the time of flight of each hyperon, in the two variants indicated above, the average lifetimes with Σ^+ and Σ^- hyperons were taken to be respectively 0.75×10^{-10} sec, and 1.59×10^{-10} sec.[3] The fraction of Σ^+ hyperons was found to be 0.62 ± 0.07. If one considers that the ratio of the decay frequencies of Σ^+ hyperons along the two possible channels is unity, we obtain for the ratio of the positive to negative hyperons

$$N_{\Sigma^+}/N_{\Sigma^-} = 3.2 \pm 1.0.$$

An estimate of the cross section for the generation of the hyperons was made separately for stacks 1 and 2. Necessary information concerning the mean free path for the interaction of the 9-Bev protons with the emulsion nuclei, on the percentage of interactions of the 9-Bev protons with the light and heavy nuclei of the emulsion, and on the elementary composition of the emulsion used to calculate the cross section were taken from references 4—6. The following values for the cross section σ_g for the generation of charged hyperons in interactions between the primary protons and emulsion nuclei (stack 2), and heavy emulsion nuclei (stack 1) respectively were obtained:

$$\sigma_g^{\text{e.nuc.}}(\Sigma^\pm) = 4.2 \pm 0.9 \text{ mb}, \quad \sigma_g^{\text{h.nuc.}}(\Sigma^\pm) = 3.7 \pm 0.9 \text{ mb},$$

It is easy to show from general considerations of isotopic invariance that in the interaction of primary protons with nuclei having zero isotopic spin, the number of produced charged Σ is twice the number of neutral Σ hyperons. The emulsion nuclei satisfy in practice these conditions. Therefore

$$\sigma_g^{\text{e.nuc.}}(\Sigma^{\pm,0}) = 6.3 \pm 1.4 \text{ mb}, \quad \sigma_g^{\text{h.nuc.}}(\Sigma^{\pm,0}) = 5.6 \pm 1.4 \text{ mb}.$$

4. Additional remarks. In this investigation we traced all the black and grey prongs in 76 stars, in which Σ hyperons decaying by the scheme $\Sigma^\pm \rightarrow \pi^\pm + n$ were observed. As a result we found four cases of paired production of a Σ^+ and K^+ meson, two cases of paired production of K^+ and K^- mesons, and a case of production of two hyperons in a single star. A star of the type (17 + 7p) contained two "grey" particles decaying in flight per relativistic particle. The values of the masses of these particles, obtained from the results of measurement of multiple scattering and ionization, were found to be

$$m_1 = (1.78 \pm 0.45)\, m_p, \quad m_2 > (1.91 \pm 0.44)\, m_p.$$

Assuming that both particles are hyperons, it must be admitted that this star contained also neutral or charged K mesons, which were not observed.

In addition, in the continuation of the selected prongs we observed one case of annihilation of an antiproton in flight. The range of the antiproton from the parent star to the point of annihilation was 17.4 mm. The kinetic energy of the antiproton at the point of annihilation was $A_{\text{kin}}(\bar{p}) = 92 \pm 15$ Mev. The annihilation star contains 9 "black" and "grey" particles, and one relativistic particle.

The authors are grateful to É. L. Andronikashvili and V. I. Veksler for interest in the work, and also to the accelerator crew and the laboratory staff who participated in the scanning of the emulsions.

---

[1] Dzhanelidze, Kopylova, Korolevich, Kostanashvili, Mandritskaya, Petukhova, Tuvdendorzh, Shakhulashvili, and Cheng P'u-Ying, JETP **38**, 1004 (1960), Soviet Phys. JETP **11**, 722 (1960).

[2] V. G. Solov'ev, preprint R-147, Joint Institute for Nuclear Research, 1958.

[3] L. V. Alvarez, Paper at the International Conference on the Physics of High-Energy Particles, Kiev, 1959.

[4] V. I. Veksler, ibid.

[5] Barashenkov, Belyakov, Wang Shu-Fen, Glagolev, Dolkhozhav, Kirillova, Lebedev, Mal'tsev, Markov, Tolstov, Tsyganov, Shafranova, and Yao Ch'ing-Hsieh, preprint R-331, Joint Institute for Nuclear Research, 1959.

[6] M. F. Rodicheva, Scientific-Technical Report, Res. Inst. of Motion Picture Industry, No. 39/3, 1959.

Translated by J. G. Adashko
233

---

*It should be noted that as the energy of the incoming pion is decreased, the region covered by the limiting curve becomes narrower.

SOVIET PHYSICS JETP VOLUME 12, NUMBER 5 MAY, 1961

DEPENDENCE OF THE DEPTH OF PENETRATION OF THE MAGNETIC FIELD IN A SUPERCONDUCTOR ON THE MAGNETIC FIELD STRENGTH

Yu. V. SHARVIN and V. F. GANTMAKHER

Institute of Physics Problems, Academy of Sciences, U.S.S.R.

Submitted to JETP editor July 15, 1960

J. Exptl. Theoret. Phys. (U.S.S.R.) **39**, 1242-1250 (November, 1960)

The dependence of the depth of penetration δ of the magnetic field in a superconductor on the field was measured in 10 samples placed in the coil of the resonant circuit of an oscillator operating at 2 Mc/sec. The change in frequency accompanying the application of the field was measured accurate to 0.005 cps, corresponding to a change in δ of about 10^{-9} cm.

THE depth of penetration of a magnetic field in an isotropic superconductor is defined as the ratio of the magnetic flux in a surface layer of the superconductor to the value of the magnetic field on this surface, i.e.,

$$\delta = \int\limits_0^\infty H(z)\,dz/H(0)$$

(it is assumed that the permeability $\mu = 1$). This quantity can be considered independent of the magnetic field only in first approximation, at small values of H/H_c, when the equations of superconductor electrodynamics are assumed linear. In general, we can put

$$\delta(H) = \delta(0)[1 + \alpha(H/H_c)^2 + \beta(H/H_c)^4 + \ldots], \qquad (1)$$

since δ is obviously an even function of H.

The question of the magnitude and the character of the nonlinear effects in real superconductors has not yet been sufficiently clarified both in its experimental and theoretical aspects. At temperatures sufficiently close to T_c, the phenomenological theory of Ginzburg and Landau[1] leads to the relation

$$\alpha = \frac{\varkappa(\varkappa + 2\sqrt{2})}{8(\varkappa + \sqrt{2})^2}, \qquad \varkappa = \frac{\sqrt{2}\,|e_{\text{eff}}|}{\hbar c} H_c \delta^2(0). \qquad (2)$$

Using the method indicated in reference 1, expressions can also be derived for the succeeding expansion coefficients in (1). The exact expression for β is quite cumbersome. Approximately, when $\kappa \ll 1$,

$$\beta = 4.7 \cdot 10^{-2} \varkappa^2 (1 - 5.1\varkappa + 7\varkappa^2) \text{ and } \beta \ll \alpha. \qquad (3)$$

Gor'kov[2] has shown, starting with the modern microscopic theory of superconductivity,[3,4], that e_{eff} in (2) should be taken equal to twice the electron charge, and the validity of relations (2) and (3) should be restricted both by the condition $(T_c - T)/T_c \ll 1$ and by the condition $\delta \gg \xi_0$, where ξ_0 is the nonlocality parameter.[3] For tin this condition corresponds approximately to $T_c - T < 0.1°$ (see reference 5).

There exists apparently no theoretical analysis of the nonlinear effects in the region where the local relations of the Ginzburg and Landau theory are not applicable.

The first attempts at an experimental investigation of the dependences for tin and mercury were made quite long ago, simultaneously with the first measurements of δ in weak fields. For mercury, Laurman and Shoenberg[6] found the changes in δ to be beyond the limits of the sensitivity of their method, corresponding to $\alpha < 0.05$.

The function $\delta(H)$ for tin was investigated[7,8] by low-frequency ($\nu = 4$ cps) modulation of the sample temperature. It was noted that polycrystalline mechanically worked and annealed samples exhibit strong and complicated dependences of δ on the applied field. In single-crystal tin samples[8] the increments of δ were several times smaller, and the $\delta(H)$ plot became approximately parabolic. Still the value $\alpha = 0.06$ for $2.4° \le T \le 3.67°$, determined from these experiments, exceeded appreciably the theoretical value $\alpha = 0.025$, obtained by substituting in (2) the expression

$$\delta(0) = 2.5 \cdot 10^{-6} (1 - T/T_c)^{-1/2}\ \text{cm}, \qquad (4)$$

which is valid near T_c.[6,8-10]

To ascertain the reasons for this discrepancy, we have decided to carry on further investigations on a large number of samples, using a more accurate and more sensitive radio-frequency procedure for the measurements.

Pippard[9,11] has demonstrated that the use of high frequencies for the investigation of the depth of penetration has considerable methodological advantages over low-frequency statistical measurement methods. In this case the errors due to the presence of an included normal phase in the sample are considerably reduced (if the depth of penetration of the field in the normal phase is less than the dimensions of these inclusions). The sensitivity of the apparatus to changes in the depth of penetration can also be appreciably increased by raising the frequency of the measuring field, since the reactive component X of the surface impedance of the sample is connected with the depth of penetration, at not too high frequencies, by the formula

$$X = 4\pi c^{-2}\delta\omega \qquad (5)$$

and increases consequently as the frequency. The closer the temperature of the sample is to T_c, the more stringent is the limitation that should be imposed on the frequency in order to satisfy the equality (5).

Theoretical estimates for the frequency interval in which relation (5) can be used for the determination of the statistical value of δ have been made by Abrikosov, Gor'kov, and Khalatnikov.[12] However, our own choice of the operating frequency is based only on the experimental data, which call for more stringent limitations.

From this point of view, the 9400 Mcs/sec frequency used by Pippard[13] in the investigation of the dependence of the impedance of tin on the field is too high. In this case the linear dependence of X on δ is noticeably violated even at temperatures above 3°K.[11] When $T_c - T = 0.1°$, the difference between the static value[6] of $\delta(0)$ and the value $\delta_\omega(0)$ as given by formula (5) amounts to approximately 40% of $\delta(0)$. A reliable determination of the static value of α near T_c is impossible in this case.

In Pippard's measurements[9] at 1200 Mc/sec with no constant field, a value of approximately 10% was obtained for $[\delta(0) - \delta_\omega(0)]/\delta(0)$ at $T_c - T = 0.1°$. A still lower frequency should make the difference $\delta(0) - \delta_\omega(0)$ increase even more rapidly, since it follows from general considerations that at low frequencies ω we have $\delta - \delta_\omega \sim \omega^2$ (see reference 14).

We note that an analogous frequency dependence, proportional to ω^2 was actually found by Sturge[15] for the active component of the surface impedance of tin at frequencies from 10^3 to 10^2 Mc/sec.

In the development of the measurement procedure, we decided on a frequency near 2 Mc/sec, which is certainly sufficiently low in the investigated temperature region, where $T_c - T > 0.01°$. On the other hand, it was possible to attain at this frequency an accuracy and sensitivity which were fully adequate for our purposes.

THE METHOD

Construction of the instrument. The heart of the measuring apparatus were two identical oscillator circuits using 06-P2B low-power pentodes placed in a Dewar vessel with liquid helium (the parts kept at low temperature are separated in Fig. 1 by a dashed line). The two oscillators together dissipated in the helium approximately 0.05 w. The investigated sample, in the form of a cylinder with pointed ends (diameter 8 — 9 mm, length of cylindrical part 40 mm, overall length 60 mm), was placed in the coil (approximately 20 mm long) of the tank circuit of one of the oscillators (Fig. 2). The coil was placed in the homogeneous magnetic field of solenoid A (Fig. 3). The earth's field was compensated for during the experiment with an accuracy of ~0.01 oe. The change in the surface impedance of the sample due to the application of the external magnetic field changed the frequency f_1 of the first oscillator. The second oscillator served as a frequency standard. Both oscillators were connected to a common power pack through dependable decoupling filters. In these Hartley oscillators the B voltage was applied to the screen grids of the pentodes, and the signal was picked off the plates, to reduce the coupling between the output and the tank circuits. Small resistances (R in Fig. 1) were inserted in the cathode circuits to reduce the frequency shift due to variation of the filament current. The second oscillator and the tube of the first oscillator were shielded against external magnetic fields by lead superconducting shields. The frequency f_0 of the second generator could be varied over a small range during the time of the experiment by

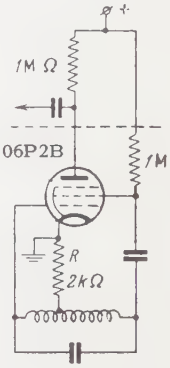

FIG. 1. Diagram of the measuring and standard oscillators.

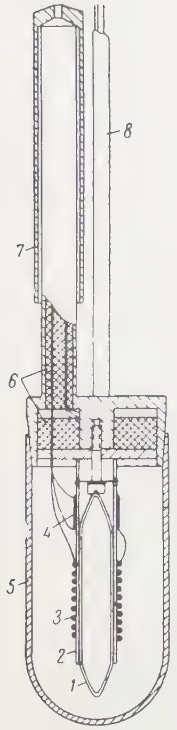

FIG. 2. Section through the measuring oscillator. 1 – sample in ampule, 2 – quartz form of the tank circuit, 3 – coil winding – 100 turns of copper wire (0.15 mm dia.), 4 – mica capacitors of the tank circuit, 5 – copper vacuum-tight screen with lapped seal, 6 – foamed styrol heat insulation between the tube and the sample, 7 – lead shield, 8 – tube for vacuum and wire leads.

means of a lead plunger traveling in the coil of its own tank circuit.

The signals from both oscillators were fed to a mixer M (Fig. 3), which separated the difference frequency $f_1 - f_0$. The value of the difference frequency was set equal to approximately 100 cps. The value of $f_1 - f_0$ was adjusted and roughly measured by means of an ICh-6 frequency meter feeding an ÉPP-09 automatic recorder, and by means of an oscillograph with a sweep signal from a ZG-12 audio oscillator. For exact measurement of the frequency, the sinusoidal signal was converted in the shaping network S into a sequence of pulses, the interval between which was increased by a factor k_1 in a PS-64 scaler (in most experiments, $k_1 = 64$). The interval between pulses was measured with a chronograph comprising a crystal oscillator G, an electronic switch SW which passed a signal of frequency $\varphi = 10^5$ cps from the crystal oscillator in the interval between two pulses, and PS-10000 counters, which counted the number of cycles in the interval between the pulses. The measurements were made with the magnetic field of solenoid A alternately switched on and off several times (usually 16 times); the number of cycles counted with the field off, N_1, was summed by one PS-10000 counter, while the number of cycles with the field on, N_2, was counted by the second counter. Relay Rel was used to actuate the devices and to apply the magnetic field, and the number of switchings k_2 was set by means of a supplementary PS-64 scaler.

Calibration of the instrument. The frequency shift Δf_1 due to application of the magnetic field could be determined from the relation $\Delta f_1 = k_1 k_2 \varphi (N_1 - N_2)/N_1 N_2$. The accuracy of the measurement of Δf_1 was determined by the stability of the oscillators and by the duration of the measurements, and amounted to approximately 0.005 cps. To calibrate the instrument, the frequency f_1 was determined for lead samples of different radii r. The same measurements were repeated with aluminum samples in normal state, and the results were in agreement. These data were used to calculate, accurate to 4 or 5%, the value of dr/df_1 as a function of the radius of the sample. For the investigated tin samples, $dr/df_1 = (3 - 4) \times 10^{-7}$ cm/cps. Thus, depth-of-penetration changes on the order of 10^{-9} cm could be detected.

Control experiments. The influence of the field on the oscillation frequency in the absence of a sample were checked between individual measurements. To reduce this influence, we had to make the tank-circuit coil of specially prepared copper wire, the surface of which was free of iron. All the joints in and near the tank circuit were made with a solder which was not superconducting in the operating frequency range (60% Bi, 40% Cd). With these precautions, the absolute frequency shift due to application of a field ranging from 0 to 100 oe could not exceed 0.02 – 0.03 cps. This effect could appreciably reduce the measurement accuracy only at temperatures below 3° K. It can be assumed that the frequency shift was due essentially to mechanical displacement of the parts of the instru-

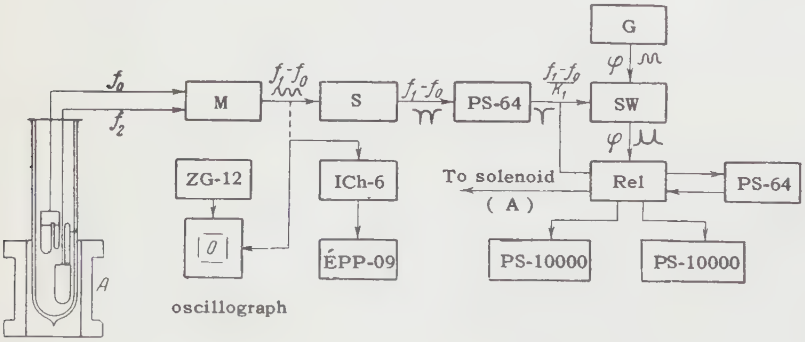

FIG. 3. Block diagram of the measuring apparatus.

ment due to switching on the magnetic field, since the magnitude of the observed displacement was not consistently reproducible.

Data reduction. In determining $\delta(H)$ from our data it is necessary to take it into account that if δ depends on the magnetic field Eq. (5) is not applicable directly, for it is necessary then to allow for the periodic variation of δ induced by the measuring field. Assuming the oscillation frequency to be sufficiently low, we can write down, accurate to the fifth power of the field, the instantaneous value of the magnetic flux through the surface layer of the sample per unit length of its circumference as

$$\Phi = H\delta(0)(1 + \alpha H^2/H_c^2 + \beta H^4/H_c^4), \qquad (6)$$

where H is the sum of the constant and measuring fields, i.e., $H = H_0 + H_1 \sin \omega t$. Substituting this expression in (6), we should single out the terms that oscillate at a frequency ω and depend on H_0, for only these terms can change the oscillation frequency. In most of our experiments, $H_0 \parallel H_1$. Then, putting $H_0/H_c = h$ and $H_1/H_c = h_1$, we obtain

$$\Phi_\omega = \delta(0)\left[\left(3\alpha + \tfrac{15}{2}\beta h_1^2\right)h^2 + 5\beta h^4\right] H_1 \sin \omega t. \qquad (7)$$

The measuring field H_1 was measured in separate experiments under different conditions, and was set at 0.1 — 0.2 oe during the measurements. The quantity $15\beta h_1^2/2$ amounted to a fraction of one percent of the total coefficient of h^2, and could therefore be neglected. The effective increase in δ, determined experimentally as $\Delta_{\mathrm{eff}}\delta = (dr/df_1) \times \Delta f_1$, was expressed thus in terms of α and β as

$$\Delta_{\mathrm{eff}}\delta = \delta(0)(3\alpha h^2 + 5\beta h^4). \qquad (8)$$

The value of α could therefore be determined from the initial slope of the Δ_{eff} vs. h^2 curve. $\delta(0)$ was calculated here from (4).

Samples. The characteristics of the investigated samples are listed in the table. At the preliminary stage of the investigation we used samples grown in glass ampules, which were removed from the samples prior to the investigation. One such sample is numbered 1 in the table. The remaining samples were placed in the coil in quartz ampules, the internal surface of which was coated with a thin layer of lampblack to provent the tin from sticking during casting. The ampules removed from the samples were placed in the coil during the control experiments. The crystal orientation of the samples was determined from the etch figures. Samples 3 and 4 consisted of several crystals, turned 1 — 2° relative to each other. These crystals apparently came from a single seeding under conditions where the tin was considerably supercooled.

Sample number	$\frac{\rho\,(4{,}2°\mathrm{K})}{\rho\,(20°\mathrm{C})} \cdot 10^5$	Impurities,* 10^{-4} %	φ**, deg	ψ***, deg
1	4	8	65	30
2	1	1	90	0
3	1	1	40	30
4	1	1	75	0

*Impurity content estimated according to reference 16.

**φ – angle between the axis of the sample and the [001] axis.

***ψ – angle between the projection of the sample axis on the (001) plane and the [100] axis.

RESULTS

The general form of the function $\Delta f_1(H)$ is shown for one of these samples in Fig. 4. The curve was obtained with the ICh-6 frequency meter and an automatic recorder. The instant when superconductivity is destroyed is noted from the sharp kink on the curve. Superconductivity was sometimes destroyed at fields somewhat higher than H_c, and consequently the values of the critical field were determined by observation of the reverse transition from the intermediate to the superconducting state.

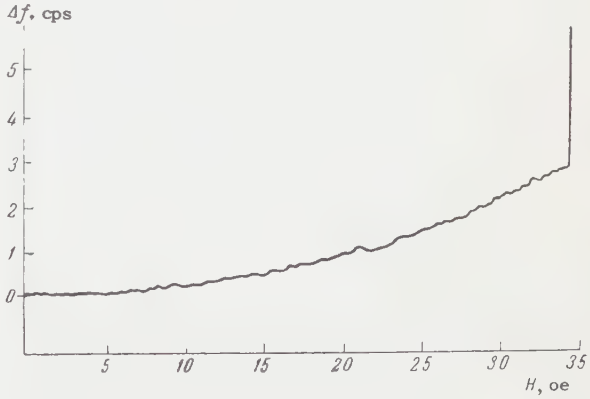

FIG. 4

Figure 5 shows the results of the measurements of $\Delta_{\mathrm{eff}}\delta$ for sample 3, made with the aid of a chronograph. The dependence of $\Delta_{\mathrm{eff}}\delta$ on h was close to parabolic, although noticeable deviations from a parabola were observed at large values of H, particularly at low temperatures. The initial slopes of the curves were determined by using two points carefully measured at small values of h^2. The dispersion in repeated measurements usually did not exceed 2 or 3%. The values of

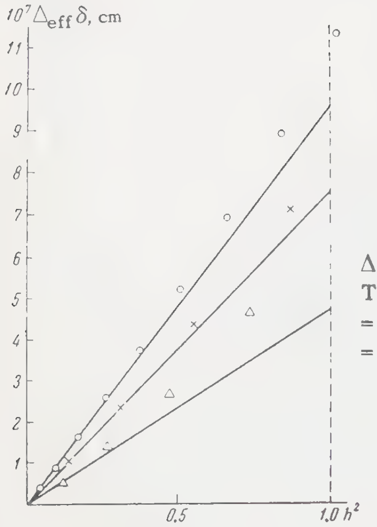

FIG. 5. The function $\Delta_{\text{eff}}\delta(h^2)$ for sample 3. o) $T_c - T = 0.059°K$. ×) $T_c - T = 0.107°K$, △) $T_c - T = 0.773°K$.

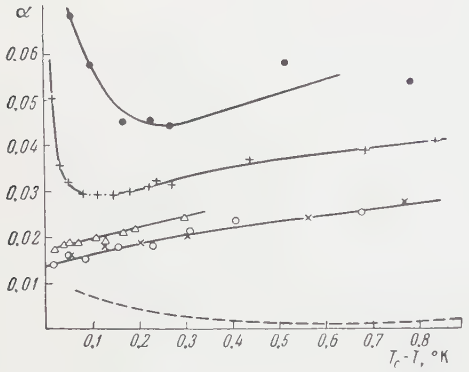

FIG. 6. The function α(T). +) sample 1; △) sample 2; ×) sample 3; o) sample 4; ●) sample 4 after removal of the ampule.

α (T), calculated for all samples listed in the table, are shown in Fig. 6. Measurements on sample 1 led to values of α which increased rapidly as $T \rightarrow T_c$. Further experiments showed, however, that this temperature variation of α was due to secondary causes. Although the tin surface was carefully protected against scratches, the sample might have been slightly bent during the installation and cooling. Samples 2 — 4, protected by ampules against possible damage, yielded considerably smaller, nearly equal values of α, which tended to a finite limit as $T \rightarrow T_c$. After the ampule was taken off sample 4, the values of α for this sample increased sharply and the α (T) curve assumed the same form as for sample 1. It must be noted that the anomalous behavior of the deformed specimens was not due to the incompleteness of the Meissner effect, for the results with all specimens were practically independent of the magnitude and direction of the field in which the specimen was cooled.

At this stage of the investigation, we undertook to study the crystalline anisotropy of δ (H). It would have been necessary in this case to change over to flat samples, so that the field and current would have the same direction relative to the crystal axis over the entire surface of the sample. In our case the current in the sample was made to flow in circles, and we dealt always only with suitably averaged values $\Delta_{\text{eff}}\delta$. We therefore did not introduce in the foregoing formulas the complicating modifications necessary to allow for the anisotropy. The fact that samples 2 — 4, with different crystal orientations, yielded values of α that were close to each other justifies this data reduction method.

We attempted also to investigate the variation of δ (H) in a transverse field. In this case the constant and alternating fields were perpendicular to each other on the main part of the sample surface, so that the numerical coefficients in front of α and β in (8) are changed. In the case of homogeneous crossed fields these coefficients would be unity. In our case it is necessary to allow for the fact that the constant field is different at different sections of the sample surface. Considering the sample to be a long cylinder and averaging over its perimeter, we obtain for the transverse field

$$\Delta_{\text{eff}}\,\delta = \delta(0)\left(\tfrac{1}{2}\,\alpha h_\perp^2 + \tfrac{3}{8}\,\beta h_\perp^4\right), \qquad (9)$$

where $h_\perp$ is the ratio of the external field to the value of the field at which superconductivity begins to disappear.

The conditions for measuring α were much more favorable for our samples in a transverse field than in a longitudinal field. From (8) and (9) it follows that the effect quadratic in h should be six times smaller for an isotropic sample in a transverse field than in a longitudinal one. In addition, the ends of the sample make a larger contribution to $\Delta_{\text{eff}}\delta$ in a transverse field than in a longitudinal field, while the surface finish of the samples is undoubtedly poorer near the ends than on the cylindrical part.

The $\Delta_{\text{eff}}(h^2_\perp)$ curves obtained with sample 3 disclose noticeable deviations from linearity at small values, $h_\perp^2 < 0.2$, and the slope of the curve increases with increasing field. These deviations were apparently due to loss of superconductivity of some parts of the sample surface near the ends. With increasing temperature, the deviations become less noticeable, so that a limiting value $\alpha_\perp = 2 \times 10^{-2}$ could be estimated for $T \rightarrow T_c$. The maximum difference between the values of $\alpha_\perp$, measured at different directions of the transverse field in the horizontal plane, was 10 to 15% (the dependence of $\alpha_\perp$ on the angle was sinusoidal, as expected in a cylindrical sample, independently of the character of the true anisotropy α).

It can be concluded from all these experiments that the average value of α for tin lies between 1.4×10^{-2} and 2×10^{-2} at temperatures close to T_c.

Our data give for temperatures close to T_c estimated values $\beta = 1 \times 10^{-3}$ to 2×10^{-3}, which, however, must be considered only as upper limits, since the values of $\Delta_{\text{eff}}\delta$ used for this calculation were those for large values of the external field, when loss of superconductivity on the damaged portions of the sample surface was possible.

DISCUSSION OF RESULTS

The experimental values of α obtained for $T \rightarrow T_c$ were somewhat lower than the values calculated by the Ginzburg and Landau (GL) theory from data on the depth of penetration. According to (2) and (4), $\alpha = 2.5 \times 10^{-2}$, whereas the experimental values are $\alpha = (1.4 \text{ to } 2) \times 10^{-2}$, and the lower limit is the more reliable one, for defects in the samples cause, as has been shows, an increase in the experimental values of α.

The theoretical value of β, calculated from (3) and (4), is 4.5×10^{-4}, and agrees in order of magnitude with the given experimental estimates.

It is interesting to note, that if $\delta(0)$ is calculated from our values of $\Delta_{\text{eff}}\delta$ and the formulas of the GL theory, the resultant value is only 10 or 15% lower than that usually assumed. A similar result can be obtained by calculating $\delta(0)$ with the formulas of the GL theory using data on surface tension at the boundary between the superconducting and normal phases.[17,18] From this point of view, the discrepancies which arise in the present paper and in references 17 and 18 are of the same sign and magnitude.

In any case, the discrepancies obtained are not very large, particularly considering the inaccuracy due to neglecting the anisotropy of the effect. On the whole, our results for temperatures close to T_c should be viewed as confirming the GL theory for tin when $T_c - T$ is on the order of $0.1 - 0.01°$.

The results obtained should also be compared with the data on the dependence of the impedance of tin on the field, as obtained by Pippard[13] at 9400 Mc/sec and by Spiewak[19] at 1000 Mc/sec. From theoretical considerations[12] one could assume that all three investigations should yield like results at temperatures not too close to T_c, since the temperature used by Pippard is already quite low compared with the width Δ_0 of the energy gap for superconducting tin ($\hbar\omega/\Delta_0 = 7 \times 10^{-2}$). In fact, however, the relationships obtained from the data of these investigations differ so much in character, that a quantitative comparison becomes impossible. According to Pippard, the curve $\alpha(T)$ has a minimum at 3°K, where α practically vanishes (dotted curve in Fig. 6). On going to frequencies one order of magnitude lower, Spivak observed even sharper anomalies. Thus, for example, at temperatures higher than 2.5° the variation of the reactance with the field was non-monotonic in character, and the sign of the coefficient of h^2 in the expansion in terms of the field was reversed, corresponding to a decrease in the depth of penetration after application of the field. A comparison of Pippard's and Spiewak's data with respect to the value of α is possible only at temperatures lower than 2.4°K, where the values obtained by Spiewak are approximately twice those obtained by Pippard (according to Pippard, α ranges from 0.8×10^{-2} to 0.5×10^{-2} as the temperature is increased from 1.5 to 2.4°K). Our own measurements did not extend to this temperature region. An extrapolation of our data, which depend little on the temperature, leads to values of α some two or three times greater than those obtained by Spiewak.

These discrepancies show that a further investigation of the dependence of the surface impedance of superconductors on the field at relatively low frequencies, on the order of $10^6 - 10^9$ cps, is of undoubted interest. The results of measurements of the reactive component of the impedance at frequencies on the order of 10^6 cps can apparently be considered here as characterizing the static properties of superconductors.

We express our sincere gratitude to Academician P. L. Kapitza and to A. K. Shal'nikov for interest in the work and for discussion of the results.

---

[1] V. L. Ginzburg and L. D. Landau, JETP **20**, 1064 (1950).

[2] L. P. Gor'kov, JETP **36**, 1918 (1959), Soviet Phys. JETP **9**, 1364 (1959).

[3] Bardeen, Cooper, and Schrieffer, Phys. Rev. **108**, 1175 (1958).

[4] N. N. Bogolyubov, JETP **34**, 58 (1958), Soviet Phys. JETP **7**, 41 (1958).

[5] V. L. Ginzburg, JETP **36**, (1930), (1959), Soviet Phys. JETP **9**, 1372 (1959).

[6] E. Laurman and D. Shoenberg, Proc. Roy. Soc. **A198**, 560 (1949).

[7] A. I. Shal'nikov and Yu. V. Sharvin, Izv. Akad. Nauk SSSR, Ser. Fiz. **12**, 195 (1948).

[8] Yu. V. Sharvin, JETP **22**, 367 (1952).

[9] A. B. Pippard, Proc. Roy. Soc. **A191**, 399 (1947).

[10] A. L. Schawlow and G. E. Devlin, Phys. Rev. **113**, 120 (1959).

[11] A. B. Pippard, Proc. Roy. Soc. **A203**, 98 (1950).

[12] Abrikosov, Gor'kov, and Khalatnikov, JETP **37**, 187 (1959), Soviet Phys. JETP **10**, 132 (1960).

[13] A. B. Pippard, Proc. Roy. Soc. **A203**, 210 (1950).

[14] L. D. Landau and E. M. Lifshitz, Электродинамика сплошных сред (Electrodynamics of Continuous Media), Gostekhizdat, 1957.

[15] M. D. Sturge, Proc. Roy. Soc. **A246**, 570 (1958).

[16] V. B. Zernov and Yu. V. Sharvin, JETP **36**, 1038 (1959), Soviet Phys. JETP **9**, 737 (1959).

[17] Yu. V. Sharvin, JETP **33**, 1341 (1957), Soviet Phys. JETP **6**, 1031 (1958).

[18] Yu. V. Sharvin, JETP **38**, 298 (1960), Soviet Phys. JETP **11**, 216 (1960).

[19] M. Spiewak, Phys. Rev. **113**, 1479 (1959).

Translated by J. G. Adashko
234

SOVIET PHYSICS JETP VOLUME 12, NUMBER 5 MAY, 1961

HYDRODYNAMIC STABILITY OF A LIQUID LAYER ON A VERTICAL WALL

V. K. BUSHMANOV

Ivanovo State Pedagogical Institute

Submitted to JETP editor February 5, 1960

J. Exptl. Theoret. Phys. (U.S.S.R.) **39**, 1251-1257 (November, 1960)

We consider the flow of a liquid layer on a vertical wall under the influence of gravitation. The stability of the plane flow preceding wave flow is investigated in the first approximation.

REYNOLDS' number, given by the equation

$$\mathrm{Re} = 4Q/\gamma, \tag{1}$$

determines the way in which a thin layer of liquid will flow down a vertical wall under the influence of gravity. In Eq. (1), Q is the volume of liquid crossing unit width perpendicular to the flow per second and γ is the kinematic viscosity. The flow is two dimensional. Up to Reynolds numbers of about 1500, the flow is laminar and such that the relation

$$Q = ga^3/3\gamma \tag{2}$$

holds, where a is the thickness of the layer and g is the acceleration due to gravity. Equation (2) is derived for flow parallel to the wall and has been verified experimentally, provided that a is taken to be the mean thickness of the layer. However, the instantaneous thickness can be greater. Several investigators[1] have confirmed the hypothesis that there are waves on the surface of such a layer. Waves can exist for Reynolds numbers ranging from 25 to 1500.

P. L. Kapitza has done both theoretical[1] and experimental[2] work on the wave flow. He used an original method to find the least value of Re for which the wave flow was stable. His result agrees well with experimental data.

The purpose of the present paper is to investigate the stability of the parallel flow preceding the wave flow. This problem is different from that of P. L. Kapitza: the wave flow can appear at a Reynolds number different from that at which it disappears.

THE METHOD OF SMALL PERTURBATIONS

We proceed in the usual way by introducing small disturbances in the flow. Let x, y be coordinates parallel to the wall (and along the flow) and perpendicular to the wall (away from it) respectively; let u and v be the corresponding velocities. In the undisturbed flow the speed is given by

$$U = \frac{g}{\gamma}\left(ay - \frac{y^2}{2}\right). \tag{3}$$

Now let this flow be perturbed:

$$u = U + w, \qquad v = 0 + v, \qquad p = P + \pi. \tag{4}$$

The perturbed flow is described by the equation of continuity and the linearized Navier-Stokes equations. These are as follows, differentiation with respect to y being denoted by a prime:

$$\frac{\partial w}{\partial t} + U\frac{\partial w}{\partial x} + vU' = -\frac{1}{\rho}\frac{\partial \pi}{\partial x} + \gamma\left(\frac{\partial^2 w}{\partial x^2} + w''\right),$$
$$\frac{\partial v}{\partial t} + U\frac{\partial v}{\partial x} = -\frac{1}{\rho}\pi' + \gamma\left(\frac{\partial^2 v}{\partial x^2} + v''\right), \qquad \frac{\partial w}{\partial x} + v' = 0. \tag{5}$$

For periodic perturbations,

$$w, v \sim \exp\left[in(x - kt)\right] \tag{6}$$

the system of equations (5) becomes the Orr-Sommerfeld equation.[3]

Let us formulate the boundary conditions. At the wall,

$$y = 0, \qquad v = 0, \qquad v' = 0. \tag{7}$$

Let us assume that at the surface there is no interaction with the gas and the tangential stress is zero:

$$w' + \partial v/\partial x = 0. \tag{8}$$

The equation of continuity, together with (8), gives the first condition on the surface:

$$y = a, \qquad v'' + n^2 v = 0. \tag{9}$$

The stress normal to the surface is balanced by the capillary pressure. This leads to a second condition:

$$y = a, \qquad \pi - 2\eta v' = -\sigma\,\partial^2 a/\partial x^2, \tag{10}$$

where η is the viscosity and σ is the surface tension (the surface is assumed to be only slightly curved). Upon substitution of π from (10) into the first equation of (5) followed by differentiation with respect to time, this last condition becomes

$$y = a, \qquad v''' + \left(\frac{ink}{\gamma} - \frac{inga^2}{2\gamma^2} - 3n^2\right) v' - \frac{i\delta n^3}{k\gamma} v = 0. \quad (11)$$

In Eq. (11), δ is the kinematic surface tension.

Without defining any new symbols, we introduce the dimensionless quantities

$$1 - y/a \to y, \qquad na \to n, \qquad ka/\gamma \to k. \quad (12)$$

If, furthermore, we have

$$R = ga^3/2\gamma^2, \qquad S = \delta a/\gamma^2, \quad (13)$$

$$A = n(k - R), \qquad B = nR, \qquad C = n^3 S/k, \quad (14)$$

then the Orr-Sommerfeld equation, together with its boundary conditions, becomes

$$v'''' + [(iA - 2n^2) + iBy^2]\, v'' - \{[i(n^2 A + 2B) - n^4] + in^2 By^2\}\, v = 0,$$

$$y = 1, \qquad v = 0, \qquad v' = 0,$$

$$y = 0, \qquad v'' + n^2 v = 0, \qquad v''' + (iA - 3n^2)\, v' + iCv = 0. \quad (15)$$

We seek a solution of (15) in the form

$$v = \alpha_0 + \alpha_1 y + \alpha_2 y^2 + \alpha_3 y^3 + \alpha_4 y^4 + \alpha_5 y^5 + \ldots. \quad (16)$$

The series (16) can be cut off at the fifth power and the resulting fifth-order polynomial substituted into (15) and into the boundary conditions. The determinant of the resulting system of equations is then calculated and its real and imaginary parts set equal to zero, with the following result:

$$n^2 A^3 + A^2 B + (720 + 480\, n^2 + 18 n^4 - 11\, n^6)\, A + 2\,(120 + 48 n^2 - n^4)\, B - 4\,(120 + 24 n^2 + n^4)\, C = 0,$$

$$(120 + 4n^2 - 11 n^4)\, A^2 + 4\,(10 - n^2)\, AB - 8\,(12 + n^2)\, AC + 4B^2 - 16\, BC - 15\,(192 + 384\, n^2 + 64\, n^4 - n^8) = 0. \quad (17)$$

The next step should be to substitute for A, B, and C, to express S in terms of R, and to eliminate k. Then the curve R(n) would be the curve of equilibrium. However, this procedure is algebraically difficult, so that it becomes necessary to find the equilibrium curve numerically. Our calculations were carried out for water.

From (13) and the experimental data quoted in reference,[2] we have

$$S = \frac{\delta}{\gamma}\left(\frac{2}{g\gamma}\right)^{1/3} R^{1/3} = 3657\, R^{1/3}. \quad (18)$$

Considering (14) as a system of equations for n, k, and R, that is,

$$3657\, n^{11/3} = C\,(A + B)\, B^{-1/3}, \qquad nk = A + B, \quad nR = B, \quad (19)$$

we assign arbitrary values to n. We choose a value of A to satisfy the first equation in (19) if B and C are obtained from (17). The other two equations determine k and R. From (1), (2), and (13) we find

$$\mathrm{Re} = \tfrac{8}{3} R. \quad (20)$$

The results are shown in the figure. Curve 1 corresponds to positive phase velocities, while curve 2 corresponds to negative ones. The phase velocities and wave lengths can be calculated from (12), (13), and (20).

Data applicable to the threshold of instability are shown in the table. It appears that the most "dangerous" perturbations are those traveling upward at 15.1 cm/sec. They break up the flow at a Reynolds number Re ~ 72, when wave conditions are produced.

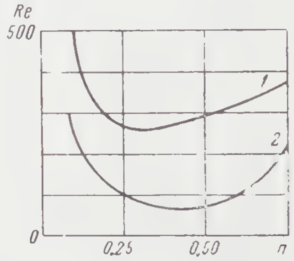

	$k > 0$	$k < 0$	[1.2]
Re	260	72	22
$n = 2\pi a/\lambda$	0.3	0.4	0.1
λ, cm	0.62	0.30	0.89
k, cm/sec	27.7	—15.1	12.4

At first glance it would appear that these conclusions contradict the data shown in the last column of the table, which are the results of P. L. Kapitza and have been verified experimentally.[1,2] However, the comparison must be made carefully. According to the experiments, the lower bound for the stability of wave flow is Re = 22. To establish this, artificial regular perturbations were introduced (photographs II, 6 — 12 in reference 2). Without these, wave flow occurs at a higher Reynolds number. The Reynolds numbers are easy to find from the data of photographs I, 1 — 2, and are 46, 55, and 54 respectively. The photographs do not show the volume rates of flow; however, these were presumably close to critical since the photographs must have been made as soon as wave flow was observed.

Wave flow appears and disappears at different

Reynolds numbers. Conditions for the existence of plane and wave flows are not mutually exclusive, but overlap partially. The process by which wave flow is established may be visualized as follows for the case when there are no artificial perturbations. As the rate of flow increases no waves appear as Re = 22 is reached. At Re = 72, waves will run upward at 15.1 cm/sec. As will appear shortly, these waves are not stable and will exist for only a short time. The plane flow will be disturbed, so that waves running downward can appear and establish stable wave flow. Wave flow will persist as the flow rate is decreased to Re = 22, when plane flow is again established.

The above considerations make it clear that there is no contradiction with the experimental data shown in the table. It would be desirable to measure the upper bound for stability of plane flow.

It is usually believed that P. L. Kapitza has theoretically established the transition between plane and wave flow and found it to occur in water at a Reynolds number of 21.6. In what follows we compare Kapitza's method with the method of small perturbations.

THE METHOD OF P. L. KAPITZA

1. Before proceeding with the comparison, we present a brief exposition of Kapitza's work,[1] using our notation.

Assume that the distribution of longitudinal velocity is the same in wave flow as it is in plane flow. The average (over y) velocity, together with its square, is substituted into the Navier-Stokes equation, without the third term on the left hand side:

$$\frac{\partial u}{\partial t} + \frac{1}{2}\frac{\partial u^2}{\partial x} = -\frac{1}{\rho}\frac{\partial p}{\partial x} + g + \gamma\nabla^2 u. \tag{21}$$

The pressure is assumed to be constant over the cross section of the flow, and equal to the capillary pressure at the surface.

Taking the phase velocity in the profile of the liquid surface to be k, a constant, and writing the variable thickness of the layer in the form

$$a = a_0(1+\varphi), \tag{22}$$

P. L. Kapitza obtained the following equation in the second approximation:

$$\delta a_0 \dddot{\varphi}(1+3\varphi) + \bar{u}_0^2(z-1)(z-1.2)\left(1-\frac{z}{5z-6}\varphi\right)\dot{\varphi} + 3g\varphi^2$$
$$+3\left(g - z\frac{\gamma\bar{u}_0}{a_0^2}\right)\varphi + \left(g - 3\frac{\gamma\bar{u}_0}{a_0^2}\right) = 0. \tag{23}$$

In this equation, a subscript zero denotes the middle cross section, a short horizontal bar over a symbol means an average over y, and the ratio of the phase velocity to the mean velocity has been written as z, the ratio being taken at the middle cross section.

The solution of (23) is

$$\varphi = \alpha\sin nx + 0.28\alpha^2\cos 2nx - \frac{g\alpha^2}{4n^3\delta a_0}\sin 2nx + \ldots \tag{24}$$

subject to the following supplementary conditions:

$$g = z\gamma\bar{u}_0/a_0^2, \qquad g(1+3\alpha^2/2) = 3\gamma\bar{u}_0/a_0^2, \tag{25}$$

$$n^2 = (z-1)(z-1.2)\,\bar{u}_0^2/\delta a_0. \tag{26}$$

The amplitude α and the number z are determined from the equilibrium and energy-balance conditions. The fact that the average dissipated energy equals the work of the force of gravity leads to the relation

$$a_0^3 = 3\gamma QF/g,$$

$$F = \frac{1}{\lambda}\int_0^\lambda \frac{(1+z\varphi)^2}{(1+\varphi)^3}dx = \frac{1}{2}\{2+\alpha^2[1-6z$$
$$+z^2(1+2\alpha^2)]\}(1-\alpha^2)^{-5/2}. \tag{27}$$

As a function of the two variables z and α, the quantity F has a minimum at

$$\alpha = 0.46, \qquad z = 2.4 \tag{28}$$

The mean potential energy associated with the surface tension is

$$\bar{E}_\sigma = \tfrac{1}{4}\sigma a_0^2\alpha^2 n^2[1 + 4(g\alpha/4a_0\delta)^2 n^{-6} + \ldots] \tag{29}$$

and from this expression the critical value for Re can be found as follows:

Imagine wave flow to be established. As long as the quantity in the brackets is small, the surface energy will decrease with increasing λ and decreasing n. However, for some critical value of λ the part in brackets will become large and the energy will begin to grow. Such waves are presumably unstable and so the wave flow will disappear. Hence the condition

$$\partial\bar{E}_\sigma/\partial n = 0 \tag{30}$$

defines the limiting wave length beyond which wave flow is unstable. From (26), (27), (29), and (30) it follows that

$$\lambda/a_0 = 13.5Q/\gamma, \qquad \mathrm{Re} = 2.43(\delta^3/g\gamma^4)^{1/11} = 0.3\,\lambda/a_0, \tag{31}$$

For water this yields Re = 21.6.

The above method, due to P. L. Kapitza, gives the lower boundary for stability of wave flow, while the method of small perturbations gives the upper boundary for stability of plane flow. The results obtained by use of these two methods are not contradictory.

2. Kapitza's results have been experimentally verified. However, the following comments can be made about the theory, as summarized above.

First, the longitudinal velocity cannot be distributed parabolically in wave flow, for if it were, then the equation of continuity would imply a cubically-distributed transverse velocity. The Orr-Sommerfeld equation (15) would then be satisfied by a cubic polynomial (16), which in fact is not the case. Unfortunately, it is difficult to see what this fundamental assumption could be replaced by. Furthermore, in the Navier-Stokes equation the quantities u and u^2 should be the true velocities, not mean values. It is the whole equation that should be averaged over y. The third term on the left hand side of the Navier-Stokes equation is of the same order of magnitude as the second term and so cannot be discarded (this follows from the equation of continuity). On the other hand, derivatives with respect to x can be neglected in comparison with derivatives taken with respect to y. Hence the equations to be considered are

$$\frac{\partial u}{\partial t}+u\frac{\partial u}{\partial x}+v\frac{\partial u}{\partial y}=-\frac{1}{\rho}\frac{\partial p}{\partial x}+g+\gamma\frac{\partial^2 u}{\partial y^2}, \quad \frac{\partial u}{\partial x}+\frac{\partial v}{\partial y}=0. \tag{32}$$

To avoid a complicated analysis of both equations, we must take the pressure to be constant over the cross section. This is only an approximation, since without a transverse pressure gradient there can be no transverse velocity and hence no wave flow.

It is difficult to find the minimum of the function F. It is easier to consider F as a function of one variable. From (25) we obtain

$$\alpha^2 = 2(3-z)/z. \tag{33}$$

From this it follows that waves with $z < 0$, i.e., those traveling upward, are impossible.

3. If the above comments are accepted, then Kapitza's method can be developed more rigorously. From (32) we obtain in lieu of (23)

$$3\delta a_0\varphi\dddot{\varphi}+\delta a_0\dddot{\varphi}-\tfrac{2}{5}z^2\overline{u_0^2}\varphi\dot{\varphi}+\tfrac{1}{5}(5z^2-12z+6)\overline{u_0^2}\dot{\varphi}$$
$$-3g\varphi^2+3(g-z\gamma\bar{u}_0/a_0^2)\varphi+(g-3\gamma\bar{u}_0/a_0^2)=0. \tag{34}$$

Conditions (25) and (33) still hold. The solution

$$\varphi=\alpha\sin nx-\frac{g\alpha^2}{4n^3\delta a_0}\sin 2nx$$
$$-\frac{17z^2-36z+18}{12(5z^2-12z+6)}\alpha^2\cos 2nx+\cdots \tag{35}$$

leads to the following improved approximation to the wave number

$$n^2=\tfrac{1}{5}(5z^2-12z+6)(\overline{u_0^2}/\delta a_0). \tag{36}$$

Considering the integrand in (27) to be a function of φ, we expand it in a power series and keep no terms higher than quadratic. Using (35) and (33) we find

$$F=1+(3-z)(z^2-6z+6)/3z, \tag{37}$$

and hence upon comparing (27) with the first equation of (25) we obtain

$$F=z/3. \tag{38}$$

From (37) and (38) we obtain

$$(3-z)(z^2-5z+6)=0. \tag{39}$$

One root of this equation corresponds to wave flow and leads, instead of (28), to

$$z=2, \quad \alpha=0.58. \tag{40}$$

The remaining two equal roots give plane flow ($z = 3$, $\alpha = 0$).

It was not necessary to find the minimum of F because the stable solution had already been found in (35). However, the same result could be obtained by finding the minimum of the function (37).

For comparison with experiment, it is not difficult to find, from (25), (36) and (40), parameters such as wave length, phase velocity, maximal longitudinal velocity (the rate at which a dye would spread), mean thickness of the layer, amplitude, and the thickness of the plane flow which would give the same volume rate of flow. All these quantities, as functions of the volume rate of flow, differ but little from those obtained by Kapitza, so that they can be thought of as verified by experiment.[2] The biggest discrepancy with experiment occurs for the amplitude; however, the authors themselves do not consider the experimental values for the amplitude to be a good test of the theory.

The situation is quite different for the critical value of Re. Let us compute it using Kapitza's method. Substituting (40) into (35) we find

$$\varphi=0.58\Big(\sin nx-0.145\frac{g}{n^3\delta a_0}\sin 2nx$$
$$+0.338\cos 2nx+\cdots\Big). \tag{41}$$

From (41), the mean surface energy can be calculated, as follows:

$$\overline{E}_\sigma=\sigma\,\overline{[1+(a_0\dot{\varphi})^2]^{1/2}} \tag{42}$$

so that, computing the derivative (30), we obtain

$$g/n^3\delta a_0\leqslant 2.94. \tag{43}$$

From (36), (27) and (38) it follows that

$$n^2=0.2gQ/\gamma\delta, \quad \lambda=14.1(\gamma\delta/gQ)^{1/2}, \quad a_0=1.26(\gamma Q/g)^{1/3}. \tag{44}$$

Substituting these into (43), instead of (31), it turns out that

$$\mathrm{Re} = 1.08\,\lambda / a_0 = 7.32\,(\delta^3 / g\gamma^4)^{1/11}. \tag{45}$$

For water, the data of reference 2 give

$$\mathrm{Re} = 64. \tag{46}$$

It thus appears that Kapitza's value of the lower limit of stable wave flow disagrees with experiment. This is not surprising in view of the comments made above.

CONCLUSION

The methods described above, together with the results obtained by their use, are first attempts to understand a new, important, problem in hydrodynamic stability. Both methods could be developed further, though this would be accompanied by great computational difficulties. The method of small perturbations could be improved by taking more terms in the series (16), or by solving the Orr-Sommerfeld equation differently. It would be interesting to apply Kapitza's method to the complete system of hydrodynamic equations for this problem.

The author would like to thank V. S. Sorokin for suggesting this problem and S. P. Kapitza for useful discussions.

---

[1] P. L. Kapitza, JETP **18**, 3, 19 (1948).

[2] P. L. Kapitza and S. P. Kapitza, JETP **19**, 105 (1949).

[3] C. C. Lin, The Theory of Hydrodynamic Stability, Cambridge, 1955.

Translated by R. Krotkov
235

SOVIET PHYSICS JETP VOLUME 12, NUMBER 5 MAY, 1961

THE USE OF LAPLACE TRANSFORMS FOR EVALUATING THE PARTITION FUNCTION

A. A. ZAĬTSEV

Ivanovo Institute for Chemical Technology

Submitted to JETP editor March 21, 1960; resubmitted June 13, 1960

J. Exptl. Theoret. Phys. (U.S.S.R.) **39**, 1258-1262 (November, 1960)

The problem of the evaluation of the partition function can be reduced to the problem of finding the trace of the operator $(\hat{H} + p)^{-1}$ where $\hat{H}$ is the energy operator and p a complex parameter, if one uses Laplace transforms. One can use this fact to find the partition function for a fairly wide class of energy operators $\hat{H}$ in the form of a power series in 1/kT.

INTRODUCTION

If one wishes to evaluate the partition function

$$Q = \sum_n \exp(-E_n/kT)$$

of a physical system, there are some useful methods which enable one to evaluate Q without knowing the eigenvalues E_n of the energy operator $\hat{H}$ of that system; these are based upon the possibility to write the partition function as the trace of the operator $\exp(-\hat{H}/kT)$. We may mention here the method of expanding Q in a power series in ħ (see, for instance references 1 and 2) or in a power series in some other small parameter on which $\hat{H}$ may depend.

One is, however, not able to use such methods to expand Q in powers of T or 1/T, so as to be able to evaluate the thermodynamic functions in the corresponding temperature ranges. A formal expansion of Q in powers of 1/T by using the definition of the operator

$$\exp(-\hat{H}/kT) = 1 - \frac{1}{kT}\hat{H} + \frac{1}{(kT)^2}\frac{\hat{H}^2}{2!} - \frac{1}{(kT)^3}\frac{\hat{H}^3}{3!} + \cdots,$$

yields nothing, for although one can easily evaluate the matrix elements of the operator $\hat{H}^n/(kT)^n n!$ for not too large values of n in any suitable representation, the trace of such an operator turns out to diverge.

We shall give in the present paper a method for expanding the partition function in powers 1/kT, based upon the application of the Laplace transformation to the function $Q(1/kT)$.

THE USE OF THE LAPLACE TRANSFORMATION FOR THE EVALUATION OF THE TRACE OF THE OPERATOR EXP $(-\tau\hat{H})$

When we use the Laplace transformation (see reference 3) we change from the function $Q(\tau)$, which is defined by the equation

$$Q(\tau) = \sum_n \exp(-\tau E_n)$$

(E_n are the eigenvalues of the Hamiltonian $\hat{H}$ of the system, and $\tau = 1/kT$) to its transform $\overline{Q}(p)$. One sees that the function $Q(\tau)$ satisfies all requirements necessary for it to have a Laplace transform.

The transform of the function $\exp(-\tau E_n)$ is the function $(E_n + p)^{-1}$,

$$\exp(-\tau E_n) \risingdotseq (E_n + p)^{-1}.$$

Using the fact that the Laplace transformation is a linear operator we find

$$\overline{Q}(p) = \sum_n \frac{1}{E_n + p} = \operatorname{Sp}\frac{1}{\hat{H} + p}. \qquad (1)$$

When we have evaluated the trace of the operator $(\hat{H} + p)^{-1}$ we find the partition function by taking the inverse Laplace transform. The advantage of this method is that it is in most cases simpler to evaluate the trace of the operator $(\hat{H} + p)^{-1}$ than to evaluate the trace of the operator $\exp(-\tau\hat{H})$. This is connected, first, with the fact that one can use the Green function of the operator $\hat{H} + p$ to evaluate the trace of the operator $(\hat{H} + p)^{-1}$, and, second, with the possibility of using the results of a number of mathematical investigations which have been published recently. In these papers methods are developed for the evaluation of the trace of similar operators,[4,5] and we can use the results of these papers together with the method presented here to evaluate the partition function.*

If the Green function $G(\mathbf{r}, \mathbf{r}', p)$ of the operator $\hat{H} + p$ is known (see, for instance, reference 6) one can find $\overline{Q}(p)$ by means of the equation

---

*See references 7 and 8 for some applications of Eq. (1) in quantum statistics.

$$\overline{Q}(p) = \sum_n \frac{1}{E_n + p} = \int G(\mathbf{r}, \mathbf{r}, p)\, dv,$$

where dv is a volume element and where the integration is over the region where the operator $\hat{H}$ is defined.

An explicit expression for the Green function is known only for some simple operators, for instance for the operator $d^2/dx^2 + p$ and its determination is connected with appreciable difficulties. It is therefore natural to use other methods which are based upon an application of Eq. (1) to evaluate $\overline{Q}(p)$.

EXPRESSIONS FOR $Q(\tau)$ FOR DIFFERENT CASES

The final result of a calculation of the partition function is independent of the set of basis functions in which the trace of the operator $(\hat{H} + p)^{-1}$ is evaluated. For some particular cases one can use directly the results of a paper by Dikiĭ[4] to evaluate the trace of the operator $(H + p)^{-1}$; in that paper he found an expression for the trace of the operator $[-d^2/dx^2 + V(x) + p]^{-1}$.

In Dikiĭ's paper the operator $\hat{H}$ had to satisfy the condition that all odd derivatives of the potential energy $V(x)$ vanish at the end points of the interval $0 - \pi$, and the eigenfunctions ψ_n of this operator had to satisfy the boundary conditions $\psi(0) = \psi(\pi) = 0$. The trace was evaluated in the basis of the functions $\sqrt{2/\pi}\sin nx$.

Let our energy operator be of the form

$$\hat{H} = -\frac{\hbar^2}{2m}\frac{d^2}{dx^2} + V(x)$$

and let it satisfy all conditions mentioned a moment ago. We find then from theorem (5.1) of Dikiĭ's paper[4]

$$\mathrm{Sp}\left(-\frac{\hbar^2}{2m}\frac{d^2}{dx^2} + V(x) + p\right)^{-1}$$
$$= \frac{m}{\hbar^2}\sum_{k=0}^{\infty}\frac{(-1)^k}{p^{k+1/2}}\left(\frac{\hbar^2}{2m}\right)^{k+1/2}\int_0^{\pi} A_{2k}\left(k - \frac{1}{2}, x\right)dx$$
$$+ \sum_{k=0}^{\infty}\frac{(-1)^k}{p^{k+1}}\left(\frac{\hbar^2}{2m}\right)^k \sum_{l=0}^{2k}(2i)^{l-2k-2}\,[A_l^{(2k-l)}(k, 0)$$
$$+ A_l^{(2k-l)}(k, \pi)].$$

Here k, l, m, and s are integers;

$$A_l(s, x) = \sum_{m=0}^{l} C^s_{(l+m)/2}\, B_{l,m}(x),$$

where $C^s_{(l+m)/2}$ is a binomial coefficient, and the functions $B_{1,m}$ are determined by the recurrence relations: $B_{0,0}(x) = 1$, and $B_{1,m}(x) = 0$ if either l or $m < 0$,

$$B_{l,m}(x) = -B''_{l-2,m}(x) + V(x)\,2m\hbar^{-2}B_{l-2,m}(x)$$
$$+ 2iB'_{l-1,m-1}(x).$$

Using operational techniques to change over from $\overline{Q}(p)$ to its inverse Laplace transform we find, according to what we said earlier, the initial expression for the partition function $Q(\tau)$

$$Q(\tau) = \frac{1}{2}\sum_{k=0}^{\infty}(-1)^k\frac{\tau^{k-1/2}}{\Gamma(k+1/2)}\left(\frac{\hbar^2}{2m}\right)^{k-1/2}\int_0^{\pi} A_{2k}(k - 1/2, x)\,dx$$
$$+ \sum_{k=0}^{\infty}\frac{\tau^k}{k!}\left(-\frac{\hbar^2}{2m}\right)^k\sum_{l=0}^{2k}(2i)^{l-2k-2}\,[A_l^{(2k-l)}(k, 0)$$
$$+ A_l^{(2k-l)}(k, \pi)], \tag{2}$$

where Γ is the gamma function.

If the form of the operator $\hat{H}$, the region in which it is defined, or the boundary conditions imposed on its eigenfunctions are different, the equation for $Q(\tau)$ will have a different form.

Let the operator $\hat{H}$ depend on three coordinates and let it be of the usual form of a single particle Hamiltonian

$$\hat{H} = -\frac{\hbar^2}{2m}\nabla^2 + V(\mathbf{r}).$$

Generalizing the results of Dikiĭ's paper[4] to the three-dimensional case we write the operator $(\hat{H} + p)^{-1}$ in the form

$$\frac{1}{\hat{H}+p} = \sum_{l=0}^{\infty}\sum_{m,k,j=0}^{l} B_{l,m,k,j}(\mathbf{r})\left(\frac{\partial}{\partial x}\right)^m\left(\frac{\partial}{\partial y}\right)^k\left(\frac{\partial}{\partial z}\right)^j$$
$$\times\left(-\frac{\hbar^2}{2m}\nabla^2 + p\right)^{-1-(l+m+k+j)/2}. \tag{3}$$

Our problem is thus to determine the coefficients $B_{l,m,k,j}$ in such a way that the equation indeed holds, i.e., that if we multiply both sides of Eq. (3) by $\hat{H} + p$ they turn out to be equal. Let us multiply both sides of the equation from the left by $\hat{H} + p$ and let us interchange the positions of the ∇^2 and the operator multiplying the function $B_{l,m,k,j}$ by using the commutation relations

$$\nabla^2(B_{l,m,k,j}f) = (\nabla^2 B_{l,m,k,j})f + B_{l,m,k,j}(\nabla^2 f)$$
$$+ 2\frac{\partial B_{l,m,k,j}}{\partial x}\frac{\partial f}{\partial x} + 2\frac{\partial B_{l,m,k,j}}{\partial y}\frac{\partial f}{\partial y} + 2\frac{\partial B_{l,m,k,j}}{\partial z}\frac{\partial f}{\partial z}.$$

Equating the coefficients of the same powers of

$$\left(\frac{\partial}{\partial x}\right)^m\left(\frac{\partial}{\partial y}\right)^k\left(\frac{\partial}{\partial y}\right)^j\left(-\frac{\hbar^2}{2m}\nabla^2 + p\right)^n,$$

we find recurrence relations for the functions $B_{l,m,k,j}$: $B_{l,m,k,j} = 0$, if either l, m, k, or j are less than zero; $B_{0,0,0,0} = 1$

$$B_{l,m,k,j} = \frac{\hbar^2}{2m}\left(\nabla^2 B_{l-2,m,k,j} + \frac{2m}{\hbar^2}V(\mathbf{r})\,B_{l-2,m,k,j}\right.$$
$$\left. + 2\frac{\partial B_{l-1,m-1,k,j}}{\partial x} + 2\frac{\partial B_{l-1,m,k-1,j}}{\partial y} + 2\frac{\partial B_{l-1,m,k,j-1}}{\partial z}\right). \tag{4}$$

We note also that $B_{l,m,k,j} = 0$, if $m + k + j > 1$, or if $l + m + k + j$ is an odd number, as is proved at once by induction with respect to l.

Let our operator $\hat{H}$ be defined in a finite, but sufficiently large region of the volume b. We can then use Eq. (3) for the operator $\overline{Q}(p)$ and evaluate the trace in the base of the orthonormal functions $u = v^{-1/2} \exp[i(k_l x + k_m y + k_n z)]$ (replacing the summation over the possible values of $\mathbf{k}$ by an integration over $dk_1 dk_2 dk_3$) and so get the following expression for $\overline{Q}(p)$

$$\overline{Q}(p) = \frac{1}{(2\pi)^3} \int_v dv \int d\mathbf{k} \sum_{l=0}^{\infty} \sum_{m=0}^{l} \sum_{k=0}^{l-m} \sum_{j=0}^{l-m-k} B_{l,m,k,j} \times (ik_1)^m (ik_2)^k (ik_3)^l \left[\frac{\hbar^2}{2m}(k_1^2 + k_2^2 + k_3^2) + p\right]^{-1-(l+m+k+j)/2} \tag{5}$$

(the limits of the summation are changed here in correspondence to the fact that $B_{l,m,k,j} = 0$, if $m + k + j > 1$).

To change over from $\overline{Q}(p)$ to $Q(\tau)$ we must find the inverse transform corresponding to the transform

$$\left[\frac{\hbar^2}{2m}(k_1^2 + k_2^2 + k_3^2) + p\right]^{-1-(l+m+k+j)/2}$$

We use the following property of the transforms: $\overline{f}^{(n)}(p) \doteqdot (-1)^n \tau^n f(\tau)$. We have therefore

$$\left[\frac{\hbar^2}{2m}(k_1^2 + k_2^2 + k_3^2) + p\right]^{-1-(l+m+k+j)/2} = (-1)^{(l+m+k+j)/2} \left[\left(\frac{l+m+k+j}{2}\right)!\right]^{-1} \frac{\partial^{(l+m+k+j)/2}}{\partial p^{(l+m+k+j)/2}} \left[\frac{\hbar^2}{2m}(k_1^2 + k_2^2 + k_3^2) + p\right]^{-1} \doteqdot \tau^{(l+m+k+j)/2} \left[\left(\frac{l+m+k+j}{2}\right)!\right]^{-1} \times \exp\left\{-\tau \frac{\hbar^2}{2m}(k_1^2 + k_2^2 + k_3^2)\right\}.$$

Substituting this expression into (5) we get

$$Q(\tau) = \frac{1}{(2\pi)^3} \int dk \int_v dv \sum_{l=0}^{\infty} \sum_{m=0}^{l} \sum_{k=0}^{l-m} \sum_{j=0}^{l-m-k} \tau^{(l+m+k+j)/2} \times \left[\left(\frac{l+m+k+j}{2}\right)!\right]^{-1} B_{l,m,k,j} (ik_1)^m (ik_2)^k (ik_3) \times \exp\left\{-\tau \frac{\hbar^2}{2m}(k_1^2 + k_2^2 + k_3^2)\right\}. \tag{6}$$

We integrate now over k_1, k_2, and k_3. It is clear that if m, k, or j is odd, the integral

$$I = \int dk\, (ik_1)^m (ik_2)^k (ik_3)^j \exp\left\{-\tau \frac{\hbar^2}{2m}(k_1^2 + k_2^2 + k_3^2)\right\}$$

vanishes, while for even m, k, and j it is equal to

$$I = (-1)^{(m+k+j)/2} \frac{m!\,k!\,j!}{2^{m+k+j}} \left[\left(\frac{m}{2}\right)! \left(\frac{k}{2}\right)! \left(\frac{j}{2}\right)!\right]^{-1} \times \pi^{3/2} \left(\frac{\hbar^2}{2m}\tau\right)^{-[(m+k+j)/2]-3/2}$$

Substituting this expression into (6) we find the final expression for $Q(\tau)$

$$Q(\tau) = \frac{1}{8}\left(\pi \frac{\hbar^2}{2m}\tau\right)^{-3/2} \sum_{l=0}^{\infty} \sum_{m=0}^{l} \sum_{k=0}^{l-m} \sum_{j=0}^{l-m-k} \left(-\frac{\hbar^2}{2m}\right)^{-(m+k+j)/2} \tau^{l/2} \times \frac{m!\,k!\,j!}{2^{m+k+j}} \left[\left(\frac{m}{2}\right)! \left(\frac{k}{2}\right)! \left(\frac{j}{2}\right)! \times \left(\frac{l+m+k+j}{2}\right)!\right]^{-1} \int_v B_{l,m,k,j}\, dv. \tag{7}$$

The summation is over even values of l, m, k, and j.

One can use this expression to evaluate the partition function for an arbitrary form of the potential energy $V(\mathbf{r}) = V(x, y, z)$, and the functions $B_{l,m,k,j}$ are determined from $V(\mathbf{r})$ using the recurrence relations (4). The method could immediately be generalized to the case where the energy operator depends on a larger number of coordinates.

I express my gratitude to Professor I. N. Godnev for a useful discussion of the problems considered here.

---

[1] L. D. Landau and E. M. Lifshitz, Статистическая физика (Statistical Physics), Gostekhizdat, 1951 [Pergamon, 1958].

[2] I. M. Khalatnikov, Doklady Akad. Nauk SSSR **87**, 539 (1952).

[3] M. A. Lavrent'ev and B. V. Shabat, Методы теории функций комплексного переменного (Methods of the theory of functions of a complex variable), Gostekhizdat, 1951.

[4] L. A. Dikiĭ, Usp. Mat. Nauk **13**, 111 (1958).

[5] I. M. Gel'fand, Usp. Mat. Nauk **2**, 191 (1956).

[6] R. Courant and D. Hilbert, Methoden der mathematischen Physik, Vol. 1, Springer, 1931.

[7] J. E. Kimball, J. Chem. Phys. **18**, 626 (1950).

[8] K. M. Watson, Phys. Rev. **103**, 489 (1956).

Translated by D. ter Haar
236

SOVIET PHYSICS JETP VOLUME 12, NUMBER 5 MAY, 1961

BEHAVIOR OF DOMAIN STRUCTURE UNDER THE INFLUENCE OF ELASTIC STRESSES

L. V. KIRENSKIĬ, V. A. IGNATCHENKO, and A. M. RODICHEV

Institute of Physics, Siberian Division, Academy of Sciences, U.S.S.R.

Submitted to JETP editor March 24, 1960

J. Exptl. Theoret. Phys. (U.S.S.R.) **39**, 1263-1268 (November, 1960)

The problem of the behavior of the simplest domain structure under the influence of homogenous elastic stresses is solved by the thermodynamic method developed for ferromagnetic materials by Landau and Lifshitz. A crystallite of the iron type, a surface of which coincides with a (001) plane, is considered. The good agreement of the calculation with experimental data permits use of the formulas derived for estimation of the density of magnetic poles on the boundaries between crystallites.

As is shown by experiment, in a plane crystallite of iron, whose surface coincides with the crystallographic plane (001), there occurs a plane-parallel domain structure, with domains oriented along one of the easy axes. At the edges of the crystallite, at the place of emergence of the vector $\mathbf{I}_s$, there may be a formation of closure domains; sometimes this is not advantageous. In general we may assume the presence of partial-closure domains (Fig. 1), whose width d may take a value from zero to D, the width of the basic domains. We shall calculate the free energy of such a structure. We take the coordinate axes along the tetragonal axes of the crystallite; we denote by x_0, y_0, z_0 the dimensions of the crystallite along the respective coordinate axes.

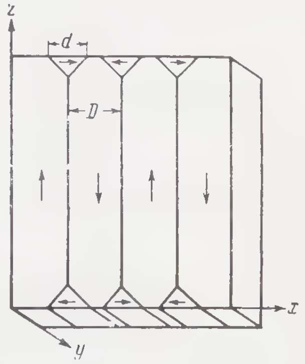

FIG. 1

1. THE FREE ENERGY

Kittel[2] gave a general method of calculating the energy of magnetic poles. He showed that for a structure periodic along one axis, the surface density of pole energy is given by the expression

$$\gamma_M = \pi \sum_{-\infty}^{+\infty} C_m C_{-m} P_m^{-1}, \qquad P_m = |m|\pi/D,$$

where the C_m's are the Fourier coefficients of the pole density. On applying this method to our case, we get

$$\gamma_M = \frac{4\omega^2 D}{\pi^2}\left[1.05 + \sum_{m=1}^{\infty} \frac{\cos(2m-1)\pi k}{(2m-1)^3}\right], \qquad (1.1)$$

where ω is the surface density of magnetic poles, and where $k = d/D$.

For poles on an iron-air boundary, in the absence of wedge-shaped domains, ω is equal to the saturation magnetization I_s. On the boundary between two crystallites, for a number of reasons, ω may be appreciably less than I_s. For example, if the domains in the adjacent crystallite are prolongations of the domains under consideration (Fig. 2), then $\omega = I_s(1 - \cos\varphi)$; a finer domain structure in the adjacent crystallite also leads to a diminution of ω; there may occur a formation of a sort of interdomain partition on small sections of the boundary between crystallites; the effective value of ω is sharply decreased by wedge-shaped domains, which may remain unnoticed if they are located in the body of the material and do not extend to the surface of observation. Therefore ω for the crystallite must be considered an unknown quantity, lying in the interval 0 to I_s. For each specific case, the value of ω can be calculated

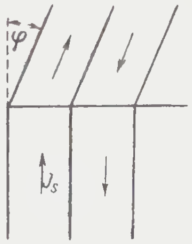

FIG. 2

from observation of the domain structure, as will be shown below. Assuming that the effective densities ω are the same on both faces of the crystallite, we write the magnetic pole energy, referred to unit volume, in the form

$$F_{\text{M}} = \frac{8\omega^2}{\pi^2 z_0} Df(k). \tag{1.2}$$

Here and below, all energies are referred to unit volume of the crystallite. By f(k) we denote the expression enclosed in square brackets in formula (1.1). Its value can be calculated with tables compiled by Kitover.[11] For rough estimates we approximated f(k) with the cubic polynomials

$$f(k) = \begin{cases} 5.28\,k^3 - 6.84\,k^2 + 2.1, & k \leqslant 0.5 \\ 5.28\,k^3 - 9\,k^2 + 2.16\,k - 1.56, & k \geqslant 0.5 \end{cases}.$$

If a surface of the crystallite does not coincide exactly with the direction [001], then the energy of the magnetic poles on this surface is

$$F^{*}_{\text{M}} = 1.7 I_s^2 \sin^2\theta \cdot 2D/(1+\mu^*)\,y_0 = aD/y_0,$$
$$\mu^* = 1 + 2\pi I_s/K, \tag{1.3}$$

where θ is the angle between the crystallite surface and the direction [001], and where K is the magnetic anisotropy constant.

The problem of calculating the magnetostrictive energy connected with the formation of closure domains (a problem in the theory of elasticity) has not been solved in its general form. Use is usually made of crude approximations, which give (for complete-closure domains) satisfactory agreement with experiment.[2,3] To calculate the dependence of the energy on k = d/D, we shall also make use of simplifying assumptions.

Because of the inequality of the magnetostrictive deformations along and across the magnetization, the closure domains are, in effect, squeezed between the basic ones. The latter prevent them from deforming in accordance with the requirements of magnetostriction, and this produces internal stress both in the closure domains and in the basic domains. The diagram (Fig. 3) may clarify this statement. We suppose at first that magnetostrictive deformation is absent; then a closure domain occupies the region aOb. Now we take account of magnetostriction, taking the point O fixed. The basic domain elongates along the z axis, with relative elongation λ_{100}, and contracts along the x axis, with relative contraction $\lambda_{100}/2$. As a result it tries to take the position a′Ob′; for the same reasons, the closure domain tries to take the position a″Ob″. In actuality, one may reason, the points a′ and a″, and likewise the points b′ and b″, will coincide, and there will occur some equilibrium state with a complicated distribution of the stress tensor, both in the basic and in the closure domains.

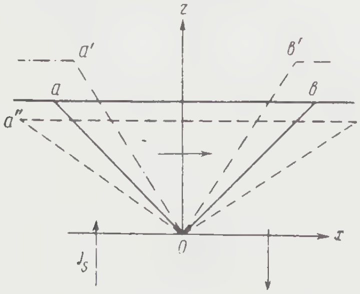

FIG. 3

We suppose for simplicity that deformation occurs only along the x axis, and we calculate the density of energy in the closure domains. Each half of such a domain (Fig. 4) undergoes at its top part an absolute deformation $\lambda_{100}d/2$. Consequently the relative deformation of the segment aa′ will be $\bar{u}_{11} = -\lambda_{100}d/D$. By assuming that the deformation decreases linearly with z and taking $u_{11} = 0$ at z = 0, we get for the mean deformation $u_{11} = -\lambda_{100}k/2$. We take all the other components of the strain tensor equal to zero. Since the energy density of magnetostriction is connected with the components of the strain tensor by the relation[3]

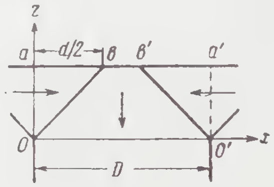

FIG. 4

$$f_{\text{ms}} = -3c_2\lambda_{100}\left(\sum_i \alpha_i^2 u_{ii} - \tfrac{1}{3} u_{ii}\right) - 3c_3\lambda_{111}\sum_{i \neq k}\alpha_i\alpha_k u_{ik}, \tag{1.4}$$

we get for the magnetostriction energy the expression

$$F_{\text{ms}} = c_2\lambda_{100}^2 Dk^3/2z_0. \tag{1.5}$$

The wall energy is determined with sufficient accuracy by the formula

$$F_{\text{w}} = \gamma/D, \tag{1.6}$$

where γ is the surface density of wall energy.

The energy density of elastic stresses, in the case in which the magnetization is parallel to an easy axis,[4] is

$$f_\sigma = -\tfrac{3}{2}\lambda_{100}\sigma\left(\cos^2\alpha - \tfrac{1}{3}\right), \tag{1.7}$$

where α is the angle between the direction of the applied stress and the vector $\mathbf{I_s}$. Calculation of the energy leads, both for the basic and for the closure domains, to the expression

$$F_\sigma = -\tfrac{3}{2}\lambda_{100}\sigma\left(\cos^2\varphi - \tfrac{1}{3}\right) + \tfrac{3}{4}\lambda_{100}\sigma\cos 2\varphi\,\frac{Dk^2}{z_0}, \quad (1.8)$$

where φ is the angle between the stress direction and the z axis (the direction [001]).

The complete free energy of the structure,

$$F = F_M + F_M^* + F_{ms} + F_w + F_\sigma \quad (1.9)$$

is in our case a function of the two parameters D and k.

2. BEHAVIOR OF THE STRUCTURE UNDER THE INFLUENCE OF STRESS

For an arbitrary value of σ, the equilibrium state of the structure is determined by the conditions

$$\partial F(D,\ k)/\partial D = 0, \qquad \partial F(D,\ k)/\partial k = 0, \quad (2.1)$$

which lead to the equations

$$D = \left[\frac{\gamma z_0}{az_0/y_0 + 8\omega^2\pi^{-2}f(k) + c_2\lambda_{100}^2k^3/2 + {}^3/_4\lambda_{100}\sigma k^2\cos 2\varphi}\right]^{1/2}, \quad (2.2)$$

$$(16\omega^2/3\pi^2)f'(k) + \lambda_{100}^2c_2k^2 + \lambda_{100}k\sigma\cos 2\varphi = 0. \quad (2.3)$$

The type of behavior of the structure depends on the value of the angle φ at which the stress acts. For $\varphi = \pi/4$, the stress has no effect on the structure. For $\varphi < \pi/4$, the value of k decreases with increase of σ and becomes zero when

$$\sigma\cos 2\varphi \approx 7.4\omega^2/\lambda_{100}. \quad (2.4)$$

Things are more complicated as regards the parameter of the basic structure, D. On increase of σ, one term in the denominator of (2.2) increases, the others decrease. According to the value of ω, either decrease or increase of D upon increase of σ may occur in the same material. When k becomes zero, D ceases to depend directly on the stress:

$$D = \left[\frac{\gamma z_0}{az_0/y_0 + 8\omega^2\pi^{-2}\cdot 2.1}\right]^{1/2}.$$

However, even for k = 0 a change of structure is possible, because of a change of the value of ω; for it is determined by conditions at the boundary of the crystallites, i.e., depends on the structure in adjoining crystallites.

For $\varphi > \pi/4$, the value of k increases with the value of σ, though complete closure does not occur. The direction of change of D now depends on ω. For k = 1

$$D = \left[\frac{\gamma z_0}{az_0/y_0 + \lambda_{100}c_2/2 + {}^3/_4\lambda_{100}\sigma\cos 2\varphi}\right]^{1/2}, \quad (2.5)$$

i.e., from the moment of complete closure, D increases with increase of σ. However, this formula does not completely describe the behavior of the structure for k = 1. Physically, the tendency toward increase of D is a consequence of the tendency toward increase of the volume of the closure domains, in which the vector I_S is more favorably oriented with respect to the applied stress. Increase of the volume of the closure domains can occur not only by increase of D, but also by growth of some of the closure domains and shrinking of their neighbors, without violation of the closure condition (Fig. 5). Consequently, the structure has an additional degree of freedom which must be taken into account. The energy of elastic stresses for such a structure is

$$F_\sigma = -\frac{3}{2}\lambda_{100}\sigma\left(\cos^2\varphi - \frac{1}{3}\right) + \frac{3}{4}\lambda_{100}\sigma\cos 2\varphi\cdot\frac{D}{z_0}(\eta^2 - 2\eta + 2), \quad (2.6)$$

where $\eta = d_1/D$, $d_1 + d_2 = 2D$, and d_1 is the width of the larger of the adjoining closure domains.

The magnetostriction energy we compute by the same approximation as before. The mean deformation along the x axis (Fig. 6) is, for the volumes Oaa′O′ and abb′a′ respectively,

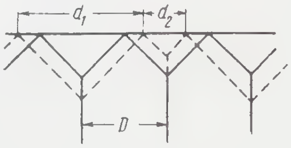

FIG. 5

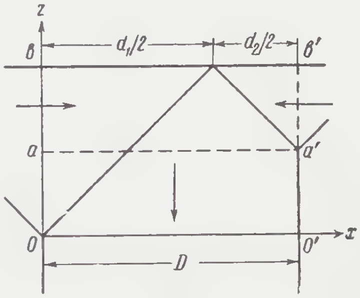

FIG. 6

$$\overline{u}_{11}^{(1)} = -\lambda_{100}d_1/4D \quad \text{and} \quad \overline{u}_{11}^{(2)} = -\lambda_{100}(d_1 + d_2)/4D.$$

Hence

$$F_{ms} = \tfrac{1}{2}\lambda_{100}^2c_2Dz_0^{-1}(\eta^3 - 3\eta^2 + 3\eta). \quad (2.7)$$

A systematic consideration of the case $\varphi > \pi/4$ requires introduction of the variable η from the beginning, and solution of the problem of a minimum of a free energy dependent on three parameters: D, k, and η. For simplicity we have assumed that the influence of η begins to be felt only after closure has occurred. The free energy F_η

of such a structure is the sum of the energies determined by formulas (1.3), (1.6), (2.6), and (2.7). The equilibrium conditions

$$\partial F_\eta(D, \eta)/\partial D = 0, \qquad \partial F_\eta(D, \eta)/\partial \eta = 0 \tag{2.8}$$

lead to the equations

$$D = \left[\frac{\gamma z_0}{a z_0/y_0 + \lambda_{100}^2 c_2(\eta^3 - 3\eta^2 + 3\eta)/2 + {}^3/_4 \lambda_{100}\sigma \cos 2\varphi\,(\eta^2 - 2\eta + 2)}\right]^{1/2}, \tag{2.9}$$

$$\eta = 1 - \sigma \cos 2\varphi/\lambda_{100}c_2. \tag{2.10}$$

With increase of σ, η increases; as $\sigma \cos 2\varphi \to -\lambda_{100}c_2$, η approaches the value 2, corresponding to the usual structure with uniform complete closure domains (Fig. 7, c). Under these conditions, D also increases. Upon increase of σ, sooner or later there comes a moment when F_X becomes less than F_Z (here F_Z is the free energy of a structure in which the basic domains are parallel to the z axis, and F_X is the energy of a structure whose basic domains are parallel to the x axis). Then there occurs a complete reorganization, and a new structure is formed, with domains parallel to the x axis.

We summarize the results obtained. In the absence of stress in the crystallite (Fig. 7) one of the three structures a, b, c is established, according to the value of ω. Suppose structure a has been established. Upon application of a homogeneous tensile stress at an angle greater than $\pi/4$ to the z axis, closure appears at some value of σ (b); it increases, until complete closure occurs (c); meanwhile D may either increase or decrease. There further occurs a growth of some closure domains and a shrinking of other (adjoining) ones, until structure e is formed; in this stage, D increases. When F_X becomes smaller than F_Z, there occurs a changeover to basic domains along the x axis; in the new direction one of the three structures f, g, h may form, according to the value of ω on the new boundary and to the value of σ at which the changeover occurred. On increase of σ, the closure will diminish (g), until state h occurs. Further increase of σ will have no effect on the nature of the domain structure (unless it produces a change of ω).

3. COMPARISON WITH EXPERIMENT

Various aspects of the process pictured in Fig. 7 have been observed by many authors. Structure b has been produced[5,6] with $k \sim 0.5$ at $\sigma = 0$; calculation by formula (2.3) gives for this case $\omega \approx 5$ gauss. A process similar to the transition from c to d has been described;[5] the stress was applied at an angle slightly exceeding $\pi/4$ (in the paper it was erroneously implied that $\varphi = \pi/2$). The transition occurred by a jump; this is presumably attributable to the usual departure of the system from a state of macroscopic equilibrium, because the crystallite is not "ideal." In these same researches, transitions from state b to c and from state f to h were observed. In the latter case the value of ω was about 70 gauss. A transition from f to g was observed by Shur and Zaĭkova.[7] In other work of the same authors[8] a transition from b to g was observed; in this case the intermediate stages turned into a complication of the structure inside the crystallite, a fact explained by peculiar circumstances (in the crystal, of inaccurate shape, there were always two domains in the initial state).

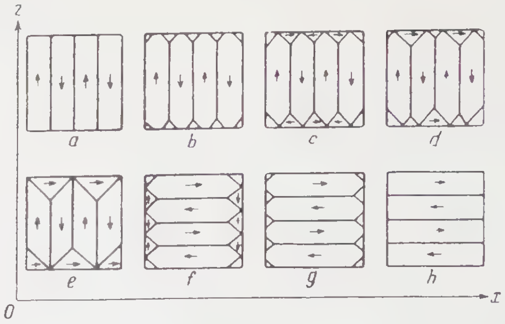

FIG. 7. Successive stages of change of the domain structure with extension [(100) plane; extension in a direction at angle greater than $\pi/4$ to the z axis].

Thus the calculation carried out agrees well with known experiments and forecasts the possibility of producing structure e, which has not yet been observed under the influence of elastic stresses. The formulas obtained make it possible to estimate, from observation of the partly closed structure of type b, the effective density ω of magnetic poles on the boundaries of the crystallites; this is of interest in relation to several questions in the theory of the technical magnetization curve. Such an estimate, carried out by us in two cases, gave values of ω appreciably less than the value I_S. It is possible that this sheds light on the disagreements with experiment of the theoretical predictions of the magnetic influence of the crystallites in the law of approach to saturation.[9,10]

---

[1] L. Landau and E. Lifshitz, Physik. Z. Sowjetunion **8**, 153 (1935).

[2] C. Kittel, Revs. Modern Phys. **21**, 541 (1949).

[3] S. V. Vonsovskiĭ and Ya. S. Shur, Ферромагнетизм (Ferromagnetism), Gostekhizdat, 1948.

[4] V. A. Ignatchenko and S. V. Vonsovskiĭ, Физика металлов и металловедение (Phys. of Metals and Metallurgy) **9**, 456 (1960).

[5] Kirenskiĭ, Savchenko, and Rodichev, Izv, Akad. Nauk SSSR, Ser. Fiz., **22**, 1181 (1958), Columbia Tech. Transl. p. 1171.

[6] L. V. Kirenskiĭ and M. K. Savchenko, Изв. высш. уч. зав., Физика (News of the Universities-Physics) **1**, 35 (1958).

[7] Ya. S. Shur and V. A. Zaĭkova, op. cit. ref. 4 **6**, 545 (1958).

[8] V. A. Zaĭkova and Ya. S. Shur, Izv. Akad. Nauk SSSR, Ser. Fiz., **22**, 1185 (1958), Columbia Tech. Transl. p. 1177.

[9] T. Holstein and H. Primakoff, Phys. Rev. **59**, 388 (1941).

[10] L. Néel, J. phys. radium **9**, 193 (1948).

[11] K. A. Kitover, Прикл. матем. и мех. (Appl. Math. and Mech.) **12**, 233 (1948).

Translated by W. F. Brown, Jr.
237

SOVIET PHYSICS JETP VOLUME 12, NUMBER 5 MAY, 1961

ON THE EFFECT OF INTERELECTRON INTERACTION IN METALS ON THE FINE STRUCTURE OF X-RAY SPECTRA

V. V. SHMIDT

Institute of Metallurgy, Academy of Sciences, U.S.S.R.

Submitted to JETP editor April 28, 1960

J. Exptl. Theoret. Phys. (U.S.S.R.) **39**, 1269-1275 (November, 1960)

Absorption of an x-ray quantum in a metal, with simultaneous excitation of a plasma, is considered for wavelengths close to the absorption edge. The calculations performed are valid for transition metals in the Fe group. It is demonstrated that the effect under consideration is very probable, the probability decreasing from Ti to Fe. A new interpretation of some short-wave satellites of the extreme short-wave emission line of the series is proposed.

1. INTRODUCTION

THE correspondence between the fine structure of x-ray absorption spectra and the characteristic energy levels of the electrons in metals has been noted by many researchers[1-4] who treated the characteristic electron energy losses from the point of view of the single-electron mechanism of transitions between bands. The fine structure of the x-ray spectra was considered from this same point of view. Establishment of a correspondence between the two phenomena has confirmed, in the opinion of many authors, the single-electron interpretation of the characteristic losses.

Ferrell[5] advanced the hypothesis that the excitation of plasma oscillation of the electron gas in a metal upon absorption of an x-ray quantum can complicate the fine structure of the x-ray absorption spectrum. Sobel'man and Feĭnberg[6] considered theoretically the effects of the excitation of plasma oscillations of the electron gas in a metal on the fine structure of the x-ray absorption spectrum for the region far from the absorption edge, that is, for the case when $E_f - E_F \gg \hbar\omega$, where E_f is the energy of the final state of an electron that has absorbed an x-ray quantum, E_F is the electron energy on the Fermi surface, and $\hbar\omega$ is the plasmon energy.

The results of the experimental investigations have pointed, however, to the necessity of investigating the question of the absorption of an x-ray quantum with simultaneous excitation of a plasmon (or with simultaneous single-electron transition between bands) for the region close to the absorption edge, that is, where the inequality given above is not satisfied and where, consequently, the deductions of Sobel'man and Feĭnberg cannot be directly applied. As will be made clear in the sequel, the process of absorption of an x-ray quantum with simultaneous excitation of the plasmon is of particular significance for transition metals.

2. FORMULATION OF THE PROBLEM

Our problem will consist of calculating the ratio of the coefficient of x-ray absorption, τ, with allowance for a simultaneous production of a plasmon, and the coefficient of absorption τ_0, given by the single-electron theory of x-ray spectra. In other words, the problem consists of finding the absorption coefficient with allowance for the interaction between an electron that has absorbed an x-ray quantum with all the free electrons of the metal (which interact with each other).

Let us consider a system consisting of the following: 1) An electron located in the periodic field of the ions (with a radius vector $\mathbf{R}$); in the initial state the electron is in the K shell (the generalization to other cases is easy), and goes over during the process of absorbing the x-ray quantum to the free states of the metal above the Fermi surface. 2) A gas of N free electrons of the metal, the common negative charge of which is offset by the positive background of the metal ions. 3) The field of the x-ray photons.

The Schrödinger equation of such a system will be written in the form

$$i\hbar\partial\varphi/\partial t = \mathscr{H}\varphi, \tag{1}$$

$$\mathscr{H} = H_1(\mathbf{R}) + H_e(\mathbf{r}_1, \ldots, \mathbf{r}_N) + H_{ph} + H_2,$$

$$H_1 = -\frac{\hbar^2}{2m}\nabla_{\mathbf{R}}^2 + U(\mathbf{R}), \qquad H_2 = \sum_j \frac{e^2}{|\mathbf{r}_j - \mathbf{R}|} + \hat{V},$$

$$H_e = -\sum_j \frac{\hbar^2}{2m}\nabla_j^2 + \frac{1}{2}\sum_{j_1 \neq j_2} \frac{e^2}{|\mathbf{r}_{j_1} - \mathbf{r}_{j_2}|} + H_{ei}.$$

Here H_{ph} is the self energy of the x-ray photons, $U(\mathbf{R})$ is the periodic lattice potential, H_{ei} is the energy operator of the interaction between the electrons and the positive background,* and $\hat{V}$ is the energy operator of the interaction between the electron $(\mathbf{R})$ and the x-ray photon.

Following Zubarev,[9] we introduce the particle-density operator $\rho(\mathbf{r}) = \Sigma_j \delta(\mathbf{r} - \mathbf{r}_j)$. Its Fourier amplitudes are

$$\rho_{\mathbf{k}} = N^{-1/2} \sum_j \exp\{-i\mathbf{k}\mathbf{r}_j\}, \qquad k < k_c,$$

where k_c is the maximum wave number of the plasma wave. The operators

$$b_{\mathbf{k}} = \tfrac{1}{2}(\partial/\partial q_{-\mathbf{k}} + q_{\mathbf{k}}), \qquad b_{\mathbf{k}}^{+} = \tfrac{1}{2}(-\partial/\partial q_{\mathbf{k}} + q_{-\mathbf{k}}) \tag{2}$$

satisfy the commutation relations of the Bose creation and annihilation operators. Here

$$q_{\mathbf{k}} = \rho_{\mathbf{k}}/\sqrt{2}\,\lambda_k, \qquad \lambda_k = \sqrt{(\hbar^2 k^2/2m)/\hbar\omega_p},$$

$$\omega_p = \sqrt{4\pi N e^2/Vm}.$$

The operators a and a^{+} are the Fourier amplitudes of the Fermi-field operators

$$\hat{\psi}(\mathbf{r}, s_z) = \frac{1}{\sqrt{V}} \sum_{\sigma\mathbf{p}} a_{\mathbf{p}\sigma} e^{i\mathbf{p}\mathbf{r}} S_\sigma(s_z),$$

$$\hat{\psi}^{+}(\mathbf{r}, s_z) = \frac{1}{\sqrt{V}} \sum_{\sigma\mathbf{p}} \overset{+}{a}_{\mathbf{p}\sigma} e^{-i\mathbf{p}\mathbf{r}} S_\sigma(s_z). \tag{2'}$$

We now change over to a mixed second-quantization representation, using expression (2) and (2′). Then H_2 is transformed, after expansion of the first term in a Fourier series in plane waves, into the form

$$H_2 = \frac{\sqrt{N}}{V} \sum_{k<k_c} \frac{4\pi e^2}{k^2} \lambda_k (b_{\mathbf{k}} + b_{-\mathbf{k}}^{+}) e^{i\mathbf{k}\mathbf{R}} + \frac{1}{V} \sum_{\substack{k>k_c,\\ \mathbf{p}}} \frac{4\pi e^2}{k^2} e^{i\mathbf{k}\mathbf{R}} \overset{+}{a}_{\mathbf{p}-\mathbf{k}} a_{\mathbf{p}} + \hat{V}, \tag{3}$$

and the initial equation (1), after canonical transformations similar to those introduced by Zubarev,[9] becomes

$$i\hbar\, \partial\Psi/\partial t = \mathcal{H}_1 \Psi,$$

where

$$\mathcal{H}_1 = H_0 + H, \qquad H_0 = H_1 + H_B + H_F + H_{ph},$$

$$H = H_2 + H_{BB} + H_{BF} + H_{FF},$$

$$H_B = \sum_{k<k_c,\ k\neq 0} \hbar\omega(k)\, b_{\mathbf{k}}^{+} b_{\mathbf{k}}, \quad H_F = \sum_{\mathbf{p}\sigma} \frac{\hbar^2 p^2}{2m} \overset{+}{a}_{\mathbf{p}\sigma} a_{\mathbf{p}\sigma}. \tag{4}$$

Here H_B is the self energy of the Bose excitations of the electron gas (plasmons); H_F is the self energy of the electron gas; H_{BB}, H_{BF}, and H_{FF} describe the interaction between the plasmons themselves, the plasmons and the electrons, and the electrons themselves.

The problem of finding the probability of the absorption of an x-ray quantum with simultaneous excitation of a plasmon (or the creation of an electron-hole pair) reduces the problem to finding the probability of transition between the eigenstates of the Hamiltonian H_0 under the influence of the perturbation H. The problem is solved by the methods of the non-stationary perturbation theory with allowance for damping.[10]

3. CALCULATION OF THE MATRIX ELEMENTS

We consider transitions between the following eigenstates Ψ_μ of the operator H_0:

1. The ground state $\Psi_0 = \psi_0 \Phi_{B_0} \Phi_{F_0} \Phi_{ph}$. The function $\psi_0(\mathbf{R})$ describes the state of an absorbing electron in the K shell of the atom, Φ_{B_0} corresponds to the absence of plasmons, Φ_{F_0} corresponds to the ground state of the Fermi-particle state, and Φ_{ph} corresponds to a certain photon distribution.

2. Intermediate state, $\Psi_\nu = \psi_n \Phi_{B_0} \Phi_{F_0} \alpha_\lambda \Phi_{ph}$. It corresponds to a transition of an absorbing electron into the intermediate state ψ_n with absorption of an x-ray quantum, characterized by the index λ. This index takes into account the wavelength of the absorbed photon, the direction of propagation, and the state of polarization; α_λ is the annihilation operator of such a photon.

3. Final state

$$\Psi_{\varphi_1} = \psi_f b_{\varkappa}^{+} \Phi_{B0} \Phi_{F0} \alpha_\lambda \Phi_{ph} \quad \text{or} \quad \Psi_{\varphi_2} = \psi_f \Phi_{B0} \overset{+}{a}_{\mathbf{p}_1} a_{\mathbf{p}_2} \Phi_{F0} \alpha_\lambda \Phi_{ph}.$$

We are interested in the transition from the ground state to the final state. The investigated process should be considered in the second order of perturbation theory, and its probability per unit time is

$$w_{\varphi 0} = 2\pi\hbar^{-1} |\widetilde{\mathcal{H}_{\varphi 0}}|^2 \delta(E_\varphi - E_0),$$

$$|\widetilde{\mathcal{H}}_{\varphi 0}| = \sum_{\nu} \langle\varphi|H|\nu\rangle \langle\nu|H|0\rangle \left(E_\varphi - E_\nu + \tfrac{1}{2} i\hbar\gamma_\nu\right)^{-1}. \tag{5}$$

Here γ_ν is a total width of the level ν or a quantity reciprocal to the lifetime of the system in the state Ψ_ν; E_φ and E_ν are eigenvalues of the operator H_0 respectively for the functions Ψ_φ and Ψ_ν.

Using relations (3) and (4), we obtain

$$\langle\varphi_1|H|\nu\rangle = \frac{\sqrt{N}}{V} \frac{4\pi e^2}{\varkappa^2} \lambda_\varkappa \langle\psi_f|e^{i\varkappa\mathbf{R}}|\psi_n\rangle, \qquad \varkappa < k_c, \tag{6}$$

---

*The energy of interaction between the electrons and the homogeneous positive background is equal and opposite to the zeroth term (k = 0) of the Fourier expansion for the energy

$$\tfrac{1}{2} \sum_{j_1 \neq j_2} e^2/|\mathbf{r}_{j_1} - \mathbf{r}_{j_2}|.$$

$$\langle\varphi_2|H|\nu\rangle = \frac{1}{V}\frac{4\pi e^2}{|\mathbf{p}_2-\mathbf{p}_1|^2}\langle\psi_f|\exp\{i(\mathbf{p}_2-\mathbf{p}_1)\mathbf{R}\}|\psi_n\rangle,$$

$$|\mathbf{p}_2-\mathbf{p}_1| > k_c, \tag{7}$$

$$\langle\nu|H|0\rangle = \left\langle\psi_n\left|-\frac{ie\hbar}{mc}\mathbf{A}_0\nabla\right|\psi_0\right\rangle, \tag{8}$$

where $\mathbf{A}_0$ is the amplitude of the vector potential of the electromagnetic wave.

Inasmuch as we are directly interested in the fine structure of the main absorption edge, the eigenvalue of the energy of the absorbing electron in the final state is $E_f \sim E_F$. In addition, it follows from (5) that the greatest contribution to the effect under consideration would be given by those intermediate states ψ_n, for which the relation $E_n - E_f \sim \hbar\omega$ is satisfied, that is, $E_n - E_F \sim 10$ ev, since $\hbar\omega \sim 10$ ev.

The curve of the energy distribution of the free-electron states N(E) is shown in the figure for transition metals of the Fe group.[11] The Fermi level passes through the region of high state density, corresponding to the 3d band of the metal, whose wave functions correspond, as is well known, to the strong-coupling approximation.

The intermediate states ψ_n, for which $E_n - E_F \sim 10$ ev, correspond to the region of considerably smaller values of N(E) (the 4p band), and here N(E) is a slowly-varying function of E. The latter indicates that ψ_n should be considered in the weak-coupling approximation, the limiting case of which is a plane wave. Therefore, for a concrete calculation of (6), (7) and (8), we specify the wave functions:

$$\psi_0 = -(Z_0/a^3\pi)^{1/2}\exp\{-Z_0R/a\}, \tag{9}$$

i.e., the 1s state of the electron in an atom with atomic number Z_0; furthermore

$$\psi_n = V^{-1/2}\exp\{i\mathbf{k}_2\mathbf{R}\},$$

$$\psi_f = G^{-1/2}\sum_j \varphi_{3d}(\mathbf{R}-\mathbf{R}_j)\exp\{i\mathbf{k}_1\mathbf{R}_j\}, \tag{10}$$

i.e., the final state of the absorbing electron, ψ_f, is represented in the strong-coupling approximation, φ_{3d} is the atomic function describing the 3d state, $\mathbf{R}_j$ is the radius vector of the j-th atom, and G is the number of atoms in the lattice.

We shall make the calculations for the final state Ψ_{φ_1}, and drop the subscript 1 from now on. Substitution of (9) and (10) in (6) and (8) yields

$$\langle\varphi|H|\nu\rangle = 1.1\pi^{3/2}\frac{\sqrt{NG}}{V^{3/2}}\frac{e^2\hbar}{\varkappa\sqrt{2m\varepsilon_p}}\left(\frac{Z}{a}\right)^{9/2}(\mathbf{k}_2+\varkappa)^{-6}$$
$$\times\left[1+\frac{Z^2}{9a^2(\mathbf{k}_2+\varkappa)^2}\right]^{-4}\delta_{\mathbf{k}_2+\varkappa-\mathbf{k}_1}, \tag{11}$$

$$\langle\nu|H|0\rangle = 8\sqrt{\frac{\pi}{V}}\frac{\hbar e}{mck_2^3}A_0\left(\frac{Z_0}{a}\right)^{5/2}(1+Z_0^2/k_2^2a^2)^{-2}. \tag{12}$$

Considering that $Z_0^2/k_2^2a^2 \gg 1$, expression (12) can be written in the form

$$\langle\nu|H|0\rangle = 8\sqrt{\frac{\pi}{V}}\frac{\hbar ek_2}{mc}A_0\left(\frac{Z_0}{a}\right)^{-3/2} \tag{13}$$

Here a is the Bohr radius, Z the effective charge of the nucleus for 3d electrons, and $\epsilon_p = \hbar\omega_p$.

4. CALCULATION OF THE PROBABILITY OF ABSORPTION OF AN X-RAY QUANTUM

The coefficient of absorption of x-rays is determined by the value W_q of the total probability of absorption of an x-ray quantum by an atom of matter per unit time. In our case, W_q is given by

$$W_q = \int\frac{2V}{(2\pi)^3}d^3k_1\cdot\frac{V}{(2\pi)^3}d^3\varkappa\cdot w_{\varphi 0}, \tag{14}$$

where $w_{\varphi 0}$ is determined from (5).

We introduce the notation

$$M^2 = \frac{V}{(2\pi)^3}\int d^3\varkappa\,|\tilde{\mathscr{H}}_{\varphi 0}|^2. \tag{15}$$

Then

$$W_q = \frac{2\pi}{\hbar}\overline{M^2}N_{3d}(E), \qquad N_{3d}(E) = \frac{2V}{(2\pi)^3}\int_S dS/|\nabla_{\mathbf{k}_1}E_{3d}|, \tag{16}$$

where $N_{3d}(E)$ is the state density in the 3d band, $\overline{M^2}$ denotes averaging of M^2 over the surface S, defined by the equation $E_{3d}(\mathbf{k}_1) = \text{const}$, and satisfying the law of conservation of energy.

Substituting the expressions (11) and (13) into (15), we obtain after several simplifications the following estimate of the order of magnitude of W_q:

$$W_q \sim \frac{10^{10}\pi^7NG}{V^3}\frac{e^6A_0^2a^{10}k_c}{\hbar m^2c^2\varepsilon_pZ_0^3Z^7\gamma^2d^4}(E_{3d}+\varepsilon_p)N_{3d}, \tag{17}$$

where $\epsilon_p \equiv \hbar\omega_p$, and d is the parameter of the crystal lattice.

In the derivation of (17) the following simplifying assumptions were made: 1) the width of the intermediate state γ_ν is constant and is independent of ν, that is, $\gamma_\nu \equiv \gamma$; 2) $\hbar\omega(\kappa) = \hbar\omega_p = \epsilon_p$; 3) $k_1 \sim \pi/d$ on the surface S (over which M^2 is averaged).

Let us compare now the expression (17) with the total probability W_q^0 of absorption of an x-ray quantum by an atom of matter per unit time as a result of the direct transition $\psi_0 \rightarrow \psi_n$:

$$W_q^0 = \frac{2\pi}{\hbar}\overline{|H_{\nu 0}|^2}N_{4p} = 64\frac{\pi^3}{V}\frac{\hbar^2e^2A_0^2}{m^2c^2d^2}\left(\frac{a}{Z_0}\right)^3N_{4p}. \tag{18}$$

Here N_{4p} is the density of states in the 4p band of the metal.

The ratio $\chi = \tau/\tau_0 = W_q/W_q^0$ of the coefficient of absorption τ with simultaneous plasmon creation taken into account and of the coefficient of absorption τ_0 given by the single-electron theory is obtained from (17) and (18):

$$\chi \sim \frac{3\cdot 10^7 \pi^3 N G}{V^2} \frac{e^4 a^7 k_c}{\gamma^2 d^2 \hbar^2} \frac{E_{3d} + \varepsilon_p}{\varepsilon_p} \frac{N_{3d}}{N_{4p}} \frac{1}{Z^7}. \tag{19}$$

We assume the following estimates: the volume of the system $V = 1\ cm^3$, $N = G = 10^{23}$, $k_c = 1\ A^{-1}$, $d = 3\ A$, $(E_{3d} + \epsilon_p)/\epsilon_p \sim 1$, $N_{3d}/N_{4p} = 5$ (see figure). To estimate the width of the excited state γ, we can use the results from reference 12, from which it follows that for electrons whose energy exceeds the Fermi energy by ~ 10 ev, the width of the state will be on the order of several electron volts. We therefore assume $\gamma = 3 \times 10^{15}\ sec^{-1}$, corresponding to width of ~ 2 ev of the state. Then an estimate of the order of magnitude of (19) yields

$$\chi \sim 10^5/Z^7. \tag{20}$$

The value of Z — the effective charge of the nucleus for the 3d electrons of the atom — can be estimated following Slater;[13] we then obtain the following values of χ for Ti, Cr and Fe:

	Z (after Slater)	χ
Ti	4	5
Cr	5	1
Fe	7	0.1

5. DISCUSSION OF THE RESULTS

The results obtained show that the probability of absorption of x-ray quanta with simultaneous excitation of plasmons is of the same order of magnitude as the probability of direct transition without plasmon excitation; this transition pertains to the region of the main edge of the absorption spectrum. This effect becomes particularly significant for transition metals, since the factor N_{3d}/N_{4p}, which enters into the expression (19) for χ, may reach large values for these metals (see diagram).

The very strong dependence of χ on Z, given by (20) is connected with the choice of ψ_n in the form of a plane wave. Another form of intermediate-state function was considered

$$\psi_n = \frac{1}{\sqrt{G}} \sum_{j} \varphi_{4p}(\mathbf{R} - \mathbf{R}_j) \exp\{i\mathbf{k}_2\mathbf{R}_j\},$$

since the other extreme case, that of a strong coupling with the lattice, was assumed. In this case $\chi \sim 100/Z^2$ where Z is the effective averaged charge of the nucleus for the 3d and 4p electrons. Obviously, χ remains of the same order of magnitude, but its dependence on Z becomes weaker.

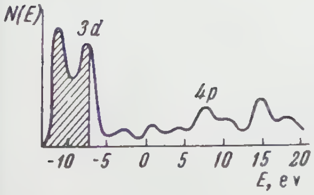

Energy distribution of the density of states of the free electrons for the transition elements of the iron group. The shaded area denotes the occupied states for the case of iron.[11]

Thus, we can conclude with regard to the absorption spectrum that the experimentally observed absorption spectrum should be a superposition of the true absorption spectrum (which would be produced only by direct transitions $\psi_0 \rightarrow \psi_n$), and of the same spectrum, but shifted by ϵ_p towards shorter wavelengths.

An experimental confirmation of this deduction is seen in the results of Borovskiĭ and Batyrev,[7] who investigated the fine structure of the x-ray absorption spectra of the elements of the iron group: Ti, V, Cr, Fe, Co, Ni, Cu. The details of the fine structure (which are considered by the authors as a plasma repetition) manifest themselves most clearly in titanium and chromium; in iron and chromium they are much less clearly pronounced, and dissappear completely in the case of nickel. This corresponds to our conclusion that χ decreases gradually on going from titanium through chromium to iron. Another experimental confirmation of our conclusion with regard to the absorption spectra has been obtained by Borovskiĭ and the author[8] in an investigation of the temperature dependence of the fine structure of the absorption spectrum of iron, and its connection with the characteristic losses of electron energy.

We note still another possible application of the results obtained here to the theory of emission spectra. All the calculations remain in force if we consider the reverse transition $\Psi_\varphi \rightarrow \Psi_\nu \rightarrow \Psi_0$, that is, if the initial state is considered to be a hole in the K shell, and if we consider the plasma excitation of the electron gas (appearing simultaneously with the production of the hole). Since the lifetime of the hole in the K shell and the lifetime of the plasmon are of the same order of magnitude (~ 10^{-16} sec), the existence of such a state is quite feasible. The transition to the intermediate state ψ_n is executed by the electron of the conduction band with absorption of a plasmon, after which it fills the hole in the K shell with emission of a short-wave satellite of the last (short-wave) emission line of the series. In this case the energy distance between the short-wave satellite and the generating line coincide with the magnitude of the characteristic energy loss of the electrons in the given substance. The following table, based on literature data, does not pretend to be systematic

Element	Distance from line to satellite, ev (reference 14)	Characteristic energy losses, ev (reference 15)	Element	Distance from line to satellite, ev (reference 14)	Characteristic energy losses, ev (reference 15)
Mg	$K_{\beta_1}-K_{\beta}^{V}$ 9.1	10.2	Fe	$K_{\beta_5}\ K-{}_{\beta}^{III}$ 7.9	7.5
Al	$K_{\beta_1}-K_{\beta}^{IV}$ 14.8	14.6	Mo	$L_{\beta_2}-L_{\beta_2}^{I}$ 24.8	24.7
K	$K_{\beta_5}-K_{\beta}^{III}$ 31.3	32.0	Sb	$L_{\beta_7}-L_{\beta_2}^{II}$ 18.0	18—20
Ca	$K_{\beta_5}-K_{\beta}^{III}$ 27.0	29.0	Te	$L_{\beta_7}-L_{\beta_2}^{II}$ 18.5	17.9

or complete, and is given merely to illustrate this conclusion. In this table the energy distance of the considered satellite from the last short-wave line of the series is compared with the characteristic loss for the given material. All the satellites have an energy greater than the energy of the corresponding edge of the absorption band.

I am deeply grateful to I. B. Borovskiĭ, V. L. Ginzburg, and K. P. Gurov for discussions and valuable remarks.

---

[1] Leder, Mandlowitz, Marton, Phys. Rev. **101**, 1460 (1956).

[2] H. Watanabe, J. Phys. Soc. Japan **9**, 920, 1035 (1954).

[3] H. Watanabe, Phys. Rev. **95**, 1684 (1954).

[4] Y. Cauchois, Acta Cryst. **5**, 351 (1952).

[5] R. Ferrell, Revs. Modern Phys. **28**, 308 (1956).

[6] I. I. Sobel'man and E. L. Feĭnberg, JETP **34**, 494 (1958), Soviet Phys. JETP **7**, 339 (1959).

[7] I. B. Borovskiĭ and V. A. Batyrev, Тр. Института металлургии АН СССР (Trans. Inst. of Metallurgy, USSR Acad. of Sci.) **6**, Acad. of Sci. Press, 1960, p. 60.

[8] I. B. Borovskiĭ and V. V. Shmidt, Doklady Akad. Nauk SSSR **127**, 997 (1959), Soviet Phys. Doklady **4**, 855 (1959).

[9] D. N. Zubarev, JETP **25**, 548 (1953).

[10] W. Heitler, The Quantum Theory of Radiation, Oxford, Clarendon Press, 1954.

[11] W. W. Beeman and H. Friedman, Phys. Rev. **56**, 392 (1939).

[12] Quinn and R. Ferrell, Phys. Rev. **112**, 812 (1959).

[13] J. S. Slater, Phys. Rev. **36**, 57 (1930).

[14] Справочные таблицы по рентгеновской спектроскопии (Reference Tables for X-Ray Spectroscopy), Acad. of Sci. Press, 1953.

[15] Сб. Характеристические потери энергии электронов в твердых телах (Coll. Characteristic Energy Losses of Electrons in Solids) Russian Translation, IIL, 1959.

Translated by J. G. Adashko
238

SOVIET PHYSICS JETP VOLUME 12, NUMBER 5 MAY, 1961

QUASICLASSICAL QUANTIZATION IN THE NEIGHBORHOOD OF SINGULAR CLASSICAL TRAJECTORIES

M. Ya. AZBEL'

Physico-Technical Institute, Academy of Sciences, Ukrainian S.S.R.

Submitted to JETP editor May 6, 1960; resubmitted July 11, 1960

J. Exptl. Theoret. Phys. (U.S.S.R.) **39**, 1276-1285 (November, 1960)

It is shown that in general the only singular trajectories in phase space which are important in thermodynamics are trajectories which are self-intersecting. Such trajectories necessarily exist if the potential well has several minima. In the case of a metal in a magnetic field this corresponds to a non-convex bounding Fermi-surface. The system of equations for these cases is found and it is shown that near the point of self-intersection the separation between levels contains a part which oscillates with the magnetic field.

1. INTRODUCTION

1. It is known[1] that to determine the energy levels in the quasi-classical case it is sufficient to express the energy ϵ as a function of the action variables I_i and to replace I_i in zeroth approximation by $2\pi n_i \hbar$ (n_i is an integer, $\hbar$ is Planck's constant) and in first approximation by $2\pi(n_i + \gamma_i)\hbar$, $0 < \gamma_i < 1$.

For a one-dimensional motion (two-dimensional in phase space)

$$\varepsilon = \varepsilon(I), \qquad I = \oint p\,dq = \Sigma(\varepsilon),$$

where $\Sigma(\epsilon)$ is the area bounding the classical orbit in phase space, and p and q are the generalized momentum and coordinate.

For the actual determination of the value of γ it is necessary to solve the Schroedinger equation; however, to find the separation $\Delta\epsilon$ between levels in the zeroth approximation it is not necessary to know γ, since in any case it is a slowly varying function of n (compared with n). Thus $\gamma \approx$ const, and

$$\Sigma(\varepsilon) = 2\pi(n+\gamma)\hbar, \tag{1.1}$$

$$\Delta\varepsilon = \hbar\omega, \qquad \omega = 2\pi(\partial\Sigma/\partial\varepsilon)^{-1}. \tag{1.2}$$

I. M. Lifshitz and Kosevich[2] pointed out that the quantization rules (1.1) and (1.2) can be used directly to obtain the system of levels for an electron with an arbitrary dispersion law $\epsilon = \epsilon(\mathbf{p})$ ($\mathbf{p}$ is the quasimomentum) in a constant magnetic field $\mathbf{H}(0, 0, H)$. In momentum space the motion occurs in the plane (p_x, p_y), and p_y and $q_y = cp_x/eH$, for which $[\hat{p}_y, \hat{q}_y] = \hbar/i$, can be regarded as the generalized coordinate and momentum. We therefore obtain immediately from (1.1) and (1.2) for this case (cf. reference 2)

$$S(\varepsilon, p_z) = \oint p_y\,dp_x = (n+\gamma)\,2\pi\alpha, \tag{1.3}$$

$$\alpha = \frac{|e|H\hbar}{c}, \qquad \Delta\varepsilon = \hbar\omega, \quad \omega = \frac{\alpha}{m^*\hbar}, \qquad m^* = \frac{1}{2\pi}\frac{\partial S}{\partial\varepsilon}. \tag{1.4}$$

Here m^* is the effective mass. Obviously (1.3) and (1.4) coincide with (1.1) and (1.2), if we replace S by Σ and α by $\hbar$.

If the velocity $\dot{\mathbf{p}}$ in momentum space [case (1.3) and (1.4)] or the velocity $(\dot{p}, \dot{q})$ in phase space [the case of (1.1) and (1.2)] does not vanish, then it is known[1] that $\gamma = 1/2$. This fact was first established for an arbitrary dispersion law by Zil'berman.[3]

However, in both cases the presence of one free parameter (the energy ϵ for the potential well and the momentum p_z for the case of fixed energy equal to the chemical potential ζ, which alone is important for the electrons in a metal) has the result that in general there exists a quasi-classical trajectory on which, for the electrons in the metal, there is a point with $\dot{\mathbf{p}} = 0$:

$$\varepsilon(\mathbf{p}) = \zeta, \qquad v_x = v_y = 0. \tag{1.5}$$

Here we have used the relations

$$\dot{\mathbf{p}} = \frac{e}{c}[\mathbf{v}\times\mathbf{H}], \qquad \mathbf{v} = \frac{\partial\varepsilon}{\partial\mathbf{p}}, \qquad \dot{p}_z = 0,$$

so that p_z is conserved.

For a one-dimensional potential well we have in this case $\dot{p} = 0$, $\dot{q} = 0$, so that

$$u'(q) = 0, \qquad \varepsilon = u(q), \tag{1.6}$$

where $u(q)$ is the potential energy. In deriving (1.6) we have used the relation

$$\dot{p} = -\partial u/\partial q, \qquad \dot{q} = p/m = \sqrt{2[\varepsilon - u(q)]/m}.$$

It is easy to see that the equations (1.5) and (1.6) determine a trajectory which is self-intersecting (in momentum and phase space respectively). Such a trajectory is always present if the bounding Fermi surface is nonconvex or if the potential well has more than one minimum. In the neighborhood of this trajectory, naturally, $\gamma \neq \frac{1}{2}$.

2. We shall, to be specific, consider throughout the following the more general case of an electron with an arbitrary dispersion law in a magnetic field; all the results are easily taken over to the case of a potential well with one or more "bumps."

It might seem that since the value of γ does not affect the distance between levels in zeroth approximation (as is to be expected since this separation is immediately obtained from the correspondence principle), the actual calculation of γ would be of no interest. However, this is not so. It turns out (cf. below) that the dependence of γ on n (and consequently on H) in the neighborhood of the point of self-interaction appears, not in the next approximation in $1/n$ as for the usual trajectories, but in the next approximation in $1/\ln n$:

$$\gamma = \gamma\,[(n - n_0)/\ln n] \tag{1.7}$$

($n_0 \gg 1$ is the number labelling the level which is closest to the point of self-intersection), and if we carry out a computation correct to terms of order $1/n$ the dependence of $\gamma(n)$ must be taken into account.

This dependence is extremely important in computing the partition function, since the function (1.7) has, as a function of n in the complex plane, singularities at distances from n_0 of the order of $|n - n_0| \sim \ln n_0$, which gives a quantum correction to the partition function of the order of some power of $1/n_0$ (whereas the complex neighborhood of an ordinary point gives an exponentially small contribution, in accordance with the fact that the singularities are located at distances $\sim n_0$ or $\sim \sqrt{n_0}$ (cf. below).

This contribution can turn out to be especially large because of the fact that for real magnetic fields $\ln n_0 \sim \ln(S/\alpha)$ is very small (for $H \sim 10^4$ oe, for the anomalously small zones which mainly determine quantum effects, $\ln n_0 \sim 1 - 4$; for the fundamental zones, $\ln n_0 \sim 10$) and it can turn out, especially in sufficiently strong magnetic fields or in the case of strong anisotropy, that this contribution is comparable to, or even smaller than, the dimensionless characteristics of the orbit (which have a magnitude of the order of unity; how these enter we shall see later on). In this case, naturally, even the distance between levels is not given correctly by formulas (1.2) and (1.4), since these refer to the case $n_0 \to \infty$, $\ln n_0 \to \infty$.

In this sense it is important that the quantity $\ln n_0$ be bounded for the section we are considering both from below and from above, since the magnetic field must be sufficiently large so that the magnitude of the quantum corrections to the thermodynamic quantities shall not be exponentially small:

$$\mu H \gtrsim 2\pi^2 kT, \qquad H \gtrsim 2\pi^2 kT/\mu \tag{1.7'}$$

(μ is the Bohr magneton for a conduction electron), and sufficiently small so that even one period of oscillation in the reversed magnetic fields is significant. These oscillations essentially alone permit us to distinguish the classical part of the given quantity from the quantum part:

$$H < 1/\Delta(H^{-1}) \sim cS/e\hbar. \tag{1.8}$$

Thus $\ln n_0$ varies within a very limited range under ordinary experimental conditions.

In addition, as it turns out, γH depends periodically on the magnetic field, which results in a new phenomenon: on top of the monotonic dependence of the distance between levels on magnetic fields there is superposed a periodic dependence which already makes itself manifest in the next approximation in $1/\ln(S/\alpha)$.

Thus the determination of the function $\gamma(n, H)$ is very important for two reasons: first, only a knowledge of this function allows us correctly to compute the quantum part of the partition function (as well as, it is understood, the quantum part of the kinetic coefficients); and, secondly, finding γ enables us to clarify the interesting feature of the levels in the neighborhood of the trajectory which intersects itself: the presence of a part of the level separation which oscillates with the magnetic field.

3. We must explain why it is that in the present case the dependence of γ on n and H appears even in the next approximation in $1/\ln n$, and not in the approximation in some power of $1/n$. From what we have said above it is clear that the latter case is not of interest, and neither is the consideration of open trajectories, which give a much smaller contribution (except possibly for specially selected directions of the magnetic field) than the closed trajectories which are always present.

In order to answer this question, we note that the special feature of our case could make itself felt also in a somewhat different way. It is clear that formula (1.3) with $\gamma = \frac{1}{2}$ is always correct if in (1.4) the quantity $m^* = (2\pi)^{-1}\partial S/\partial\epsilon$ is finite and not equal to zero, so that $\Delta\epsilon \neq 0$ and $\Delta\epsilon \neq \infty$. A priori this formula could break down for $m^* = \infty$ or $m^* = 0$. The latter case is not at all possible: $S(\epsilon)$ is always a monotonic function, since the intersection of orbits corresponding to different values of ϵ for a given p_Z and the same zone is impossible for a Hermitian energy operator. (This was pointed out by I. M. Lifshitz.) As for the case $m^* = \infty$, this just corresponds, as one easily sees from the definition of S, to the case we are considering of a trajectory which is self-intersecting.

It might seem that those cases should also be "suspect" where there are several areas corresponding to different zones. However, this is not so, since the probability of transitions between corresponding orbits is exponentially small if the orbits do not intersect, and in general is proportional to $\hbar^{3/2}$, if the orbits intersect (Zil'berman[3]), so that $\gamma = \gamma(\sqrt{n})$.

Contact of orbits with $\epsilon = \zeta$ is an exceptional case, since it requires simultaneously satisfying the two relations

$$\varepsilon_1(\mathbf{p}) = \zeta, \quad \varepsilon_2(\mathbf{p}) = \zeta; \quad v_{1x} = v_{2x}, \quad v_{1y} = v_{2y},$$

$$(\mathbf{v}_1 = \partial\varepsilon_1/\partial\mathbf{p}, \quad \mathbf{v}_2 = \partial\varepsilon_2/\partial\mathbf{p}). \tag{1.9}$$

4. The only singular case of interest is thus the case of self-intersecting orbits. The form of the orbit near the point of self intersection is determined, for a given p_Z, by the equations

$$v_x = v_y = 0, \tag{1.10}$$

$$\varepsilon = \varepsilon_0(p_z) \tag{1.11}$$

and can be found easily. Choosing the origin of coordinates at the point of self intersection and directing the coordinate axis so that at this point

$$\partial^2\varepsilon/\partial p_x\partial p_y = 0, \quad \partial^2\varepsilon/\partial p_x^2 = 1/m_1 > 0,$$

$$\partial^2\varepsilon/\partial p_y^2 = -1/m_2 < 0, \tag{1.12}$$

we have

$$\varepsilon(\mathbf{p}) = \varepsilon_0(p_z) + p_x^2/2m_1 - p_y^2/2m_2. \tag{1.13}$$

The closing of the curves in regions far from the origin can occur in two ways, as shown in Figs. 1 and 2 (we recall that, in accordance with the definition (1.12), all three axes have been chosen uniquely). The first case (Fig. 1) is realized for a Fermi surface with a "neck," (Fig. 3), and the second (Fig. 2) for a surface with an indentation (Fig. 4). In the following we shall, for brevity, call the case corresponding to Fig. 1 the case of a "neck" and that of Fig. 2 the case of an "indentation."

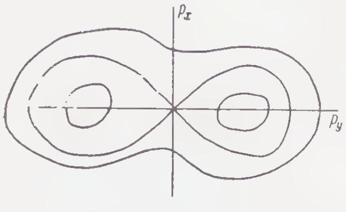

FIG. 1

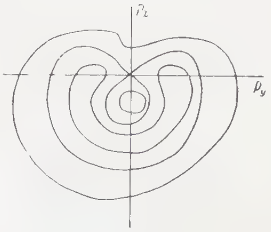

FIG. 2

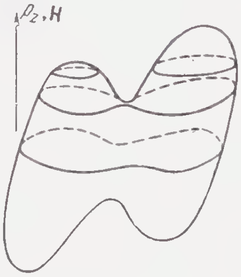

FIG. 3

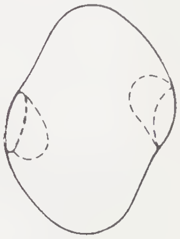

FIG. 4

As we approach the trajectory which is self intersecting, the velocity of the electron in the neighborhood of the point of self intersection tends to zero, while the time for passage of the segment in the neighborhood of the point of self intersection goes to infinity logarithmically[4] with $\epsilon_0(p_Z)(\epsilon - \epsilon_0(p_Z))^{-1}$. Almost the entire self-intersecting trajectory is travsersed by the electron in a finite time, but then the electron takes an infinite time to approach the point of self-intersection; passage through this point does not occur classically.

In coordinate space in the (x, y) plane the motion differs from the motion in momentum space, aside from a proportionality factor, by a rotation through $-\pi/2$[5]

$$x = \int v_x dt = -cp_y/eH, \quad y = \int v_y dt = cp_x/eH. \tag{1.14}$$

Let us now proceed immediately to the determination of the function γ. For the singular case of orbits which are symmetric with respect to the two axes for arbitrary p_Z (which, it is understood, is possible only for selected directions of the magnetic field), this was done by Zil'berman.[6] However, it is precisely in this (and only in this) case that there is no correction to the level separation which is an oscillating function of H. The thermodynamic quantities themselves have not even been found for this special case.

2. FORMULATION OF THE PROBLEM

Suppose that in the absence of a magnetic field the dispersion law has the form

$$\varepsilon = \varepsilon(p_x, p_y, p_z). \tag{2.1}$$

Then[1,3] the Hamiltonian operator in the magnetic field should be obtained by replacing P_X by P_X

$-(\hbar eH/ic)\,\partial/\partial p_y$:

$$\hat{\varepsilon} = \varepsilon\left(P_x + \Delta\frac{\partial}{\partial p_y},\ p_y,\ p_z\right),\quad \Delta = -i\Delta_0,\quad \Delta_0 = -\frac{eH\hbar}{c}. \tag{2.2}$$

It is understood that formula (2.2) still does not determine the energy operator so long as we are not given the rule for symmetrization of the non-commuting operators $\Delta\partial/\partial p_y$ and p_p. The correct rules for symmetrization can be stated starting from very general considerations (cf. Zil'berman[3] and I. M. Lifshitz and Kaganov[4]).

However, the precise symmetrization is not necessary for the solution of the questions we are interested in (finding the levels in the neighborhood of points whose contributions to the thermodynamic quantities are not exponentially small), since it is sufficient to know the operator $\hat{\epsilon}$ written to terms including Δ_0^2. To this accuracy, ϵ is already determined by the requirement of Hermiticity[7].

As a matter of fact,[7] any two Hermitian operators which are obtained from (2.2) by different symmetrizations can obviously differ from one another only by an even number of commutations (Δ is pure imaginary!), that is, by terms of no lower order than Δ^2. Consequently, to find the energy levels, i.e., the eigenvalues, of the equation

$$\hat{\varepsilon}\psi = \varepsilon(P_x + \Delta\partial/\partial p_y,\ p_y,\ p_z)\,\psi(P_x, p_y, p_z) = \varepsilon\psi(P_x,\ p_y,\ p_z), \tag{2.3}$$

the operator $\hat{\epsilon}$ can, in accordance with what we have said above, be given for example as follows. If

$$\varepsilon(P_x + \xi,\ p_y,\ p_z) = \sum \tfrac{1}{2}\alpha_{jk}(P_x,\ p_z)\,\xi^j p_y^k, \tag{2.4}$$

we may define $\hat{\epsilon}$ as

$$\hat{\varepsilon} = \sum \frac{1}{4}\alpha_{jk}(P_x,\ p_z)\left\{\left(\Delta\frac{\partial}{\partial p_y}\right)^j p_y^k + p_y^k\left(\Delta\frac{\partial}{\partial p_y}\right)^j\right\}. \tag{2.5}$$

Equations (2.3) – (2.5) are already sufficient for solving the problem. Now we shall show that there is an infinite degeneracy with respect to P_x (in the quasiclassical approximation), so that even for the determination of $\gamma(H)$ in our case we can set $P_x = 0$ in (2.3) – (2.5).

We shall show for the general case how, to an accuracy of terms of order Δ, this follows directly from (2.3). (Zil'berman[3] first proved by direct calculations that there was an infinite degeneracy with respect to P_x.) Setting

$$\psi = \exp\{\widetilde{S}/\Delta - P_x p_y/\Delta\}, \tag{2.6}$$

and introducing the notation

$$\pi_x = \frac{\partial\widetilde{S}}{\partial p_y},\qquad \widetilde{S} = \int \pi_x(p_y)\,dp_y,\qquad v_x(p_y) = \frac{\partial\varepsilon}{\partial\pi_x}, \tag{2.7}$$

we find the equation for $\pi_x(p_y, p_z)$ where p_z is a parameter:

$$\varepsilon(\pi_x,\ p_y,\ p_z) + \tfrac{1}{2}\Delta\partial v_x/dp_y = \varepsilon, \tag{2.8}$$

and this equation is just as general as (2.3) and (2.5).

Since (2.8) does not contain P_x, it is already evident that with the same accuracy as before (up to terms Δ^2, inclusive) there is an infinite degeneracy with respect to P_x. Equation (2.8) also shows that, to this same accuracy, for the determination of the energy levels in equation (2.3) we can formally set $P_x = 0$, writing the equation in the form

$$\varepsilon(\Delta\partial/\partial p_y,\ p_y,\ p_z)\,\psi_1 = \varepsilon\psi_1,\qquad \psi_1 = \psi\exp(P_x p_y/\Delta). \tag{2.9}$$

To find the levels when there is a self intersection, it is sufficient to solve (2.9) in the neighborhood of the point of self intersection and to join on to the wave function in other regions where one can use the usual solution*.

Before we go on to determine the energy levels, let us make one further comment. The classical orbits $\epsilon(p_x, p_y, p_z) = \epsilon$, $p_z = \text{const}$, in general are asymmetric with respect to the p_x axis (Figs. 1 and 2) [except for the region near the point of self intersection, where the symmetry follows from equations (1.5) and (1.6)], and the turning points do not lie on the p_x axis. However, since the quantization is determined only by the corresponding areas, it is natural to expect that a deformation of the curves far from the singular point, i.e., the point of self-intersection, will have no effect on the quantization if this deformation does not change the areas of the orbits $S(\epsilon)$ and $\partial S/\partial\epsilon$. This theorem can be proven rigorously. Using it, we can simplify the problem by assuming that the turning points lie on the p_x axis.

If in addition we have the case shown in Fig. 1, a still further simplification is possible – replacement of all the curves by curves which are symmetric with respect to the p_x axis and have the same area as before and the same value of $\partial S/\partial\epsilon$. We note that, as is clear from (1.13), symmetrization of the operator (2.9) in the neighborhood of singular points is not necessary in general.

3. DETERMINATION OF ENERGY LEVELS

As was shown in the preceding sections, the determination of the quasi-classical energy levels in the general case reduces to determining the largest eigenvalues of Eq. (2.9), when the turning points of the corresponding orbits (2.9) lie on the p_x axis. To do this in the quasiclassical case, we must join the solution far from the point of self-intersection with the solution near this point. The joining is accomplished as usual in the region where the solution far from the point of self intersection is still valid, and where one can still use asymptotic formulas for the solution near the point of self intersection. (Such a region is known always to exist in the quasiclassical case.) In doing this it is sufficient to restrict oneself to considering orbits close to the point of self intersection, since the arguments given below are suitable for "distances" $\Delta\epsilon$ in energy from the point of selfintersection such that $\Delta\epsilon \ll \epsilon$, while corrections to levels because of the presence of two orbits with possible transitions becomes exponentially small already for $\Delta\epsilon \gg \mu H$ ($\epsilon \gg \mu H$!).

---

*It is therefore more convenient in solving to use (2.9) instead of (2.8).

Comparing the coefficients for the linearly independent functions, we obtain a system of homogeneous equations whose determinant must be equal to zero. This gives the energy levels of the system.

4. INVESTIGATION OF THE LEVEL STRUCTURE

The level system when there is a self intersection has the form (n an integer)

$$\cos(S_1 \pm S_2 + \varphi(k)) = -\frac{e^{\mp k\pi}}{\sqrt{2\cosh 2k\pi}} \cos(S_1 \mp S_2), \quad (4.1)$$

$$f_{\pm}^{(1)}(k) \equiv S_1 \pm S_2 + \varphi(k) + \cos^{-1}\left\{\frac{e^{\mp k\pi}}{\sqrt{2\cosh 2k\pi}} \cos(S_1 \mp S_2)\right\} = (2n+1)\pi, \quad (4.2)$$

$$f_{\pm}^{(2)}(k) \equiv S_1 \pm S_2 + \varphi(k) - \cos^{-1}\left\{\frac{e^{\mp k\pi}\cos(S_1 \mp S_2)}{\sqrt{2\cosh 2k\pi}}\right\} = (2n+1)\pi, \quad (4.3)$$

$$\varphi(k) = 2\left\{k \ln\frac{|k|}{e} - \frac{1}{2i}\ln\frac{\Gamma(1/4 + ik)}{\Gamma(1/4 - ik)}\right\} - \tan^{-1}\tanh k\pi,$$

$$S_{1,2} = \frac{S_{1,2}(p_z)}{2\Delta_0}, \qquad k = \frac{\varepsilon - \varepsilon_0(p_z)}{2\hbar e H} c\sqrt{m_1 m_2}. \quad (4.4)$$

Here the upper sign refers to the case of "necking-in" (Figs. 1 and 3) and the lower sign to the "indentation" (Figs. 2, 4); the meaning of $S_1(p_z)$ and $S_2(p_z)$ is clear from Figs. 5 and 6.* (It is understood that after determining the function $\epsilon^{(1,2)}(n, p_z)$ from Eqs. (4.2) – (4.4) we should still take account of the presence of spin by adding both to $\epsilon^{(1)}(n, p_z)$ and $\epsilon^{(2)}(n, p_z)$ the term $\pm e\hbar/2m_0c$, where m_0 is the mass of the free electron; for brevity we shall not write down this term which is of no interest to us.)

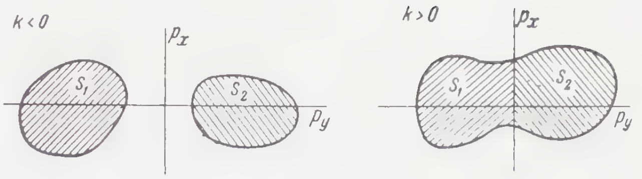

FIG. 5

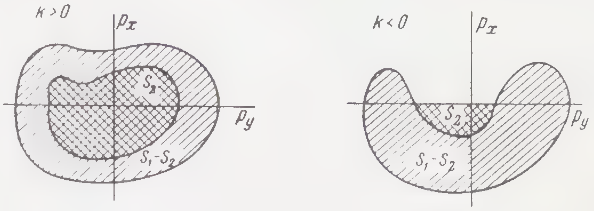

FIG. 6

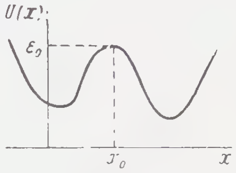

FIG. 7

First let us consider the limiting cases when the orbits are still far from the point of self-intersection, i.e., $|k| \gg 1$ and $\varphi(k) \to 0$. If $k \to +\infty$ in the case of the "neck", or $k \to -\infty$ for the "indentation",

$$S_1 \pm S_2 = (n + \tfrac{1}{2})\pi, \quad (4.4a)$$

which corresponds to the usual quasiclassical quantization rules for a single orbit with area $S_1 + S_2$ in the case of the "neck" (Fig. 5, k > 0) and with an area $S_1 - S_2$ in the case of an "indentation" (Fig. 6, k < 0).

If $k \to -\infty$ for the "neck" or $k \to +\infty$ for the "indentation,"

$$S_{1,2} = \left(n_{1,2} + \tfrac{1}{2}\right)\pi, \quad (4.4b)$$

which corresponds to the usual quantization rules for individual orbits (Figs. 5 and 6).

It may at first sight seem strange that formulas (4.4a) and (4.4b) for $|k| \gg 1$ hold not with an accuracy which is exponential in $|k|$, but only with an accuracy $1/|k|$, whereas it is physically clear that the probability of transition between different orbits associated with the tunneling effect is exponentially small.

For $\Delta p_z \sim p_0$ this is related to the fact that from the very beginning the accuracy of writing the equations and their solutions was not exponential, but of order $1/n$ in formulas of the type (4.4a),

---

*In the case of a potential well with a "hump" (Fig. 7)

$$S(k) = S/2\hbar, \qquad k = (\varepsilon - \varepsilon_0)\sqrt{m}\,[2\hbar\sqrt{|U''(x_0)|}]^{-1/2},$$

where S is the area of the orbit in phase space.

(4.4b), while in the formula for the energy the error was of the order of $1/n^2$. For $\Delta p_z \ll p_0$, the non-exponentially small terms give a correction to the usual quantization formulas for a single section, in the case of the geometry we are studying for the Fermi surface (the presence of a nearby saddle point).

Let us follow this transition directly from the two-level systems (4.2), (4.3). As an example we shall consider the case of a "neck." For $k \to \infty$ it follows from (4.2) and (4.3) that

$$S_1 + S_2 = (2n + \tfrac{1}{2})\pi, \ (2n + 1 + \tfrac{1}{2})\pi,$$

i.e., these level systems have the same separation between levels and are shifted with respect to one another by half the level separation, so that altogether they lead to the usual equations:

$$S_1 + S_2 = (n + \tfrac{1}{2})\pi.$$

Now let $k \to -\infty$. Let us consider two cases:

$$1)\ \left[\frac{S_1 - S_2}{\pi}\right] = 2m, \ S_1 = (n + m + \tfrac{1}{2})\pi,$$

$$S_2 = (n - m + \tfrac{1}{2})\pi:$$

$$2)\ \left[\frac{S_1 - S_2}{\pi}\right] = 2m - 1, \ S_1 = (n - m + \tfrac{1}{2})\pi,$$

$$S_2 = (n + m + \tfrac{1}{2})\pi$$

(m is an integer, $[x]$ is the largest integer contained in x).

Thus for $k < 0$, each of the branches "builds up" a level system corresponding in turn to one and then to the other of the individual areas, where each time we "build up" levels corresponding to the two areas.

Let us follow this process in more detail. Suppose that, in a certain energy interval $[(S_1 - S_2)/\pi]$ is even. Then the first branch in this energy interval begins to form a level system corresponding to S_1 and the second a branch corresponding to S_2. Later on, as the energy changes, $[(S_1 - S_2)/\pi]$ becomes odd and the first branch begins to extend the "work" of the second branch, the construction of levels corresponding to S_2, while the second branch starts the building up of those corresponding to S_1. Later on the roles of the branches are alternated once again, etc. This process for larger and larger values of $|k|$ is shown in Fig. 8 (where, since k is in the argument of the arc cos in the exponent, it is practically sufficient already to have $|k| > 1$).

Obviously, in the case of an "indentation" one can repeat these same arguments with a replacement of k by $-k$.

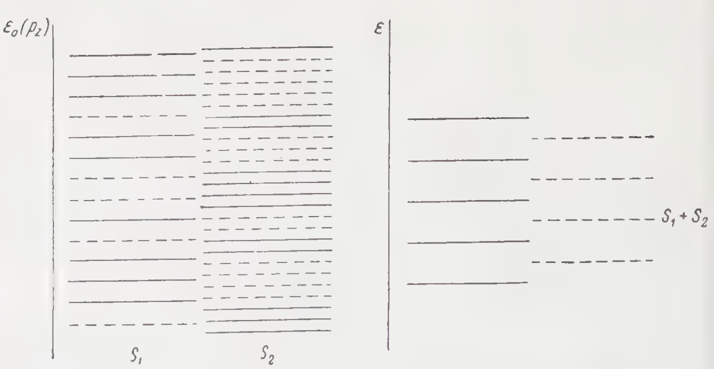

FIG. 8. Picture of levels for a self-intersecting trajectory. The solid lines show the first branch, the dotted lines the second; on the left $\varepsilon < \varepsilon_0(p_z)$, on the right $\varepsilon > \varepsilon_0(p_z)$.

2. Now let us explain how the distance between levels changes [we are especially interested in this for levels near $\epsilon_0(p_z)$]. By using formula (1.13) for $|k| \ll k_0$, it is easy to show that the functions $f_{\pm}^{(1,2)}(k)$ in (4.2) and (4.3) are always monotonic differentiable functions, so that the distance between levels in each of the branches corresponds to $\Delta k \sim (\partial S/\partial k)^{-1}$ and never becomes zero or infinity. (For levels near the point of self intersection this was not obvious beforehand.) As for the dependence of the distance Δk between levels on magnetic field, as one easily shows, it has an oscillatory correction.

From formulas (4.1) — (4.3) and our remarks above, it is clear that the only case considered by Zil'berman,[6] the case of a "neck" for $S_1 = S_2 = S$ is a case of degeneracy where

$$2S + \varphi(k) \pm \cos^{-1}\left(e^{-k\pi}/\sqrt{2\cosh 2k\pi}\right) = (2n + 1)\pi,$$

and where both for $k \gg 1$, as well as for $-k \gg 1$, there is a single equation system

$$2S = (n + \tfrac{1}{2})\pi \quad (k \gg 1), \qquad S = (n + \tfrac{1}{2})\pi \quad (-k \gg 1),$$

there is no "alternation" of levels as in Fig. 8, and there is no oscillation of levels with magnetic field in the neighborhood of $\epsilon_0(p_z)$.

If we go over from closed sections of the Fermi surface to open sections, we should see a picture analogous to that described by us, but possibly complicated still more by broadenings of the levels (Zil'berman[4] considered only the special case of sections which are periodic throughout the lattice).

---

[1] L. D. Landau and E. M. Lifshitz, Quantum Mechanics, Pergamon (1958).

[2] I. M. Lifshitz and A. M. Kosevich, JETP **29**, 730 (1955), Soviet Phys. JETP **2**, 636 (1956).

[3] G. E. Zil'berman, JETP **32**, 296 (1957) and **33**, 387 (1957), Soviet Phys. JETP **5**, 208 (1957) and **6**, 299 (1958).

[4] I. M. Lifshitz and M. I. Kaganov, Usp. Fiz. Nauk **69**, 419 (1959), Soviet Phys. Uspekhi **2**, 831 (1960).

[5] M. Ya. Azbel' and É. A. Kaner, JETP **32**, 896 (1957), Soviet Phys. JETP **5**, 730 (1957).

[6] G. E. Zil'berman, JETP **34**, 748 (1958), Soviet Phys. JETP **7**, 513 (1958).

[7] M. Ya. Azbel', JETP **34**, 969 (1958), Soviet Phys. JETP **7**, 669 (1958).

Translated by M. Hamermesh
239

SOVIET PHYSICS JETP VOLUME 12, NUMBER 5 MAY, 1961

THE ELASTIC SCATTERING OF γ RAYS BY DEUTERONS BELOW THE PION-PRODUCTION THRESHOLD

L. I. LAPIDUS and CHOU KUANG-CHAO

Joint Institute for Nuclear Research

Submitted to JETP editor May 12, 1960

J. Exptl. Theoret. Phys. (U.S.S.R.) **39**, 1286-1295 (November, 1960)

Dispersion relations and the conditions for unitarity of the S matrix are used for the analysis of the elastic scattering of γ rays by deuterons below the threshold for pion production. The low-energy limit is examined for the scattering of γ rays by nuclei of arbitrary spin. The energy dependence of elastic γd scattering is deduced on the basis of the experimental data on the photodisintegration of the deuteron. The result differs decidely from that of the impulse approximation over a wide range of energies. It is found that it is not important to include the influence of photoproduction of pions from deuterons in the range of energy considered.

1. INTRODUCTION

THE scattering of γ rays by deuterons is an example of a process whose amplitude is decidedly affected by inelastic processes, such as the photodisintegration of the deuteron and the photoproduction of mesons. Inclusion of the influence of pion photoproduction, which is important at γ-ray energies near and above the photoproduction threshold, requires a rather detailed analysis of the processes

$$\gamma + d \rightarrow NN\pi, \qquad \gamma + d \rightarrow d + \pi^0$$

and is not dealt with here.

The influence of the photodisintegration of the deuteron on the elastic γd scattering near the threshold for photodisintegration, and the departures from monotonic variation with the energy, which lead to a sharp decrease of the cross section, have been considered previously.[1] The purpose of the present paper is to make an analysis of γd scattering on the basis of dispersion relations over a wider energy range, in which meson production still does not have much effect.

The experimental data[2] on the scattering of γ rays by deuterons in the energy range 50 — 100 Mev do not fit into the framework of the impulse approximation,[3] and this forces us to carry through an analysis that does not involve this approximation. On the other hand, the contribution to the scattering amplitude from meson-production processes falls off rapidly below the threshold for photoproduction of mesons.

We shall confine ourselves to the forward scattering. In the calculation of the dispersion integrals we take into account the cross sections for the electric-dipole and magnetic-dipole photodisintegrations. We begin with the phase-shift analysis, so as to express the imaginary parts of the scattering amplitudes in terms of the quantities that characterize the photodisintegration of the deuteron. We then consider the dispersion relations for forward scattering and the low-energy theorem. The dispersion integrals are evaluated in the range of γ-ray energies below ~ 100 Mev. The real and imaginary parts of the amplitudes are obtained, and the polarizabilities of the deuteron and of nucleons are discussed.

2. THE PHENOMENOLOGICAL ANALYSIS

As is well known, the formulas for the electric and magnetic multipole waves $\mathbf{Y}^{(\lambda)}_{lm}(\mathbf{k})$ of a photon are ($\lambda = 0, 1$)

$$\mathbf{Y}^{(0)}_{lm} = \sum_{\mu} C^{lm}_{l\, m-\mu\, 1\mu} Y_{l\, m-\mu}(\mathbf{k})\, \zeta_{\mu}, \tag{1a}$$

$$\mathbf{Y}^{(1)}_{lm} = -i\,[\mathbf{k} \times \mathbf{Y}^{(0)}_{lm}], \tag{1b}$$

where **k** is the unit vector along the momentum of the photon in the center-of-mass system, $Y_{lm}(\mathbf{k})$ are normalized spherical functions, and

$$\zeta_{+} = -(\mathbf{i} + i\mathbf{j})/\sqrt{2},$$

$$\zeta_0 = \mathbf{k}, \qquad \zeta_{-} = (\mathbf{i} - i\mathbf{j})/\sqrt{2} \tag{2}$$

— the eigenfunctions of the photon spin — satisfy the transversality condition

$$\mathbf{k}\mathbf{Y}^{(\lambda)}_{lm}(\mathbf{k}) = 0.$$

If we write

$$\eta_+ = -\frac{1}{\sqrt{2}}\begin{pmatrix}1\\ i\\ 0\end{pmatrix}, \qquad \eta_0 = \begin{pmatrix}0\\ 0\\ 1\end{pmatrix}, \qquad \eta_- = \frac{1}{\sqrt{2}}\begin{pmatrix}1\\ -i\\ 0\end{pmatrix} \tag{3}$$

for the spin functions of the deuteron, then for the γd system we can construct eigenfunctions of the total angular momentum J^2, the component J_z, and the parity from Eqs. (1) and (3):

$$\mathbf{Y}^{(\lambda)}_{jlM}(\mathbf{k}) = \sum_r C^{jM}_{lM-r1r}\mathbf{Y}^{(\lambda)}_{l\,M-r}(\mathbf{k})\,\eta_r. \tag{4}$$

In the center-of-mass system (c.m.s.) all quantities in the final state are denoted by symbols with primes; for example, $\mathbf{k}'$ denotes the direction of the photon momentum in the final state.

By means of Eq. (4) we can write the scattering matrix T in the form

$$(\mathbf{e}'\mathbf{T}\mathbf{e}) = \sum_{\substack{jMll'\\ \lambda\lambda'}} Y^{(\lambda')}_{jl'M}(\mathbf{k}')\,Y^{(\lambda)}_{jlM}(\mathbf{k})\,a^{\lambda\lambda'}_{jll'}, \tag{5}$$

where $\mathbf{e}$ and $\mathbf{e}'$ are the respective polarization vectors of the photon in the initial and final states.

Parity conservation requires that

$$a^{\lambda\lambda'}_{jll'} = 0 \text{ for } (-1)^{l+\lambda} \neq (-1)^{l'+\lambda'}. \tag{6}$$

Time-reversal invariance leads to the symmetry condition

$$a^{\lambda\lambda'}_{jll'} = a^{\lambda'\lambda}_{jl'l}. \tag{7}$$

The usual arguments show that for forward scattering the spin dependence of the matrix T is of the form

$$(\mathbf{e}'\mathbf{T}\mathbf{e}) = A(\mathbf{e}'\mathbf{e}) + iB(\mathbf{S}[\mathbf{e}'\times\mathbf{e}]) + \tfrac{1}{2}C[(\mathbf{S}\mathbf{e})(\mathbf{S}\mathbf{e}') + (\mathbf{S}\mathbf{e}')(\mathbf{S}\mathbf{e})] + \tfrac{1}{2}D[(\mathbf{S}[\mathbf{k}\times\mathbf{e}])(\mathbf{S}[\mathbf{k}'\times\mathbf{e}']) + (\mathbf{S}[\mathbf{k}'\times\mathbf{e}'])(\mathbf{S}[\mathbf{k}\times\mathbf{e}])]. \tag{8}$$

Here $\mathbf{S}$ is the operator of the spin vector of the deuteron; its components S_i satisfy the Duffin-Kemmer commutation relations:

$$[S_i, S_j] = i\varepsilon_{ijk}S_k, \qquad S_iS_jS_k + S_kS_jS_i = \delta_{ij}S_k + \delta_{jk}S_i. \tag{9}$$

Using the Stokes parameters to describe the polarization of the photon, as was done in our paper on γN scattering,[4] we get without difficulty from Eqs. (2) and (8):

$$(\zeta^*_\pm \mathbf{T}\zeta_\pm) = A \mp B(\mathbf{S}\mathbf{k}) + \tfrac{1}{2}(D+C)[2-(\mathbf{S}\mathbf{k})^2],$$

$$(\zeta^*_\pm \mathbf{T}\zeta_\mp) = \tfrac{1}{2}(D-C)\{(\mathbf{S}\mathbf{i})^2 - (\mathbf{S}\mathbf{j})^2 \mp i[(\mathbf{S}\mathbf{i})(\mathbf{S}\mathbf{j}) + (\mathbf{S}\mathbf{j})(\mathbf{S}\mathbf{i})]\}. \tag{10}$$

By means of Eq. (10) and the method developed previously[4] we can construct the density matrix of the final state and calculate all observable quantities. The unpolarized forward scattering cross section is given by

$$\sigma_0(0^\circ) = |A + \tfrac{2}{3}(C+D)|^2 + \tfrac{1}{18}|C + D|^2 + \tfrac{2}{3}|B|^2 + \tfrac{1}{3}|D-C|^2, \tag{11}$$

and we have

$$4\pi\,\mathrm{Im}\,(A + \tfrac{2}{3}C + \tfrac{2}{3}D) = q\sigma_t, \tag{11'}$$

where σ_t is the total interaction cross section, including both elastic and inelastic interactions; $\mathbf{q} = |q|\mathbf{k}$.

Let us turn to the phase-shift analysis. We include the amplitudes for electric-dipole and magnetic-dipole transitions. The magnetic-dipole transition is characterized by the matrix

$$F^0_j = \sum Y^{(0)}_{j\,1M}(\mathbf{k})\,Y^{(0)}_{j\,1M}(\mathbf{k}) = \frac{3}{4\pi}\sum C^{jM}_{1M-r\,1r}C^{jM}_{1M-r'1r'}C^{1M-r}_{10\,1M-r}C^{1M-r'}_{10\,1M-r'}\eta_r\eta^*_{r'}\zeta_{M-r}\zeta^*_{M-r'}, \tag{12}$$

where we have used the fact that for forward scattering

$$Y_{lm} = \delta_{lm}\sqrt{(2l+1)/4\pi}.$$

From Eqs. (12) we easily obtain

$$(\zeta^*_+F\zeta_+) + (\zeta^*_-F\zeta_-) = \frac{3}{8\pi}\left[\alpha_j + \beta_jS^2_z\right],$$

$$(\zeta^*_+F\zeta_+) - (\zeta^*_-F\zeta_-) = \frac{3}{8\pi}\gamma_jS_z,$$

$$(\zeta^*_+F\zeta_-) = -\frac{3}{8\pi}\beta_jT_{2,-2} = -\frac{3}{8\pi}\beta_j\frac{1}{2}(S_x - iS_y)^2,$$

$$(\zeta^*_-F\zeta_+) = -\frac{3}{8\pi}\beta_jT_{2,2} = -\frac{3}{8\pi}\beta_j\frac{1}{2}(S_x + iS_y)^2. \tag{13}$$

For $j = 0, 1, 2$ the quantities α_j, β_j, γ_j are

$$\begin{array}{llll} j = & 2 & 1 & 0\\ \alpha_j = & 1 & 1 & 0\\ \beta_j = & 1/6 & -1/2 & 1/3\\ \gamma_j = & 5/6 & -1/2 & -1/3 \end{array} \tag{14}$$

In obtaining the relations (13) we have used the relations

$$\eta_+\eta^*_+ = \tfrac{1}{2}(S^2_z + S_z), \quad \eta_-\eta^*_- = \tfrac{1}{2}(S^2_z - S_z), \quad \eta_0\eta^*_0 = 1 - S^2_z,$$

$$\eta_+\eta^*_- = T_{2,2} = \tfrac{1}{2}[S^2_x - S^2_y + i(S_xS_y + S_yS_x)],$$

$$\eta_-\eta^*_+ = T_{2,-2} = \tfrac{1}{2}[S^2_x - S^2_y - i(S_xS_y + S_yS_x)]. \tag{15}$$

The case of the electric-dipole transition is obtained from the relations (13) by replacing $\boldsymbol{\zeta}_+$ by $i[\boldsymbol{\zeta}_+ \times \mathbf{k}] = -\boldsymbol{\zeta}_+$ and $\boldsymbol{\zeta}_-$ by $i[\boldsymbol{\zeta}_- \times \mathbf{k}] = \boldsymbol{\zeta}_-$. Comparing Eqs. (13) and (14) with Eq. (10), we get

$$2A = \frac{3}{8\pi}\sum_j(\alpha_j + 2\beta_j)(a^{(m)}_j + a^{(e)}_j),$$

$$2B = -\frac{3}{8\pi}\sum_j\gamma_j(a^{(m)}_j + a^{(e)}_j),$$

$$C = -\frac{3}{8\pi}\sum_j\beta_ja^{(e)}_j, \qquad D = -\frac{3}{8\pi}\sum_j\beta_ja^{(m)}_j. \tag{16}$$

The condition for unitarity of the S matrix reduces to the relation

$$2\pi i\,[T^{*}(-\mathbf{k}', -\mathbf{k}, -\mathbf{e}', -\mathbf{e}, -\mathbf{S})_{\gamma d\to\gamma d} - T(\mathbf{k}', \mathbf{k}, \mathbf{e}', \mathbf{e}, \mathbf{S})_{\gamma d\to\gamma d}] = q\int d\Omega_{n+p}\, T^{+}_{\gamma d\to np} T_{\gamma d\to np}, \tag{17}$$

where q is the relative momentum of the γd system. Let us represent $T_{\gamma d\to np}$ in the form

$$T_{\gamma d\to np} = \sum Y^{s}_{je'M}(\mathbf{n})\, Y^{(\lambda)*}_{jlM}(\mathbf{k})\, d^{s\lambda}_{jl'l}, \tag{18}$$

where j is the total angular momentum, l' is the orbital angular momentum in the final state, and s is the total spin of the np system.

Parity conservation requires that

$$(-1)^{l+\lambda+1} = (-1)^{l'}.$$

The quantities $d^{s\lambda}_{jl'l}$ are connected with the partial cross sections for photodisintegration:

$$24\pi\sigma^{s(m)}_{jl'} = (2j+1)\,|d^{s0}_{jl'1}|^2, \qquad 24\pi\sigma^{s(e)}_{jl'} = (2j+1)\,|d^{s1}_{jl'1}|^2. \tag{19}$$

The total cross section for photodisintegration is given by

$$24\pi\sigma_{\gamma d\to np} = \sum_{jl's} (2j+1)\,[\,|d^{s0}_{jl'1}|^2 + |d^{s1}_{jl'1}|^2]. \tag{20}$$

Substitution of Eqs. (18) and (5) in Eq. (17) gives

$$4\pi \operatorname{Im} a^{\lambda\lambda'}_{jll'}(q) = q\sum_{l''s} (d^{s\lambda}_{jl''l})^{*} d^{s\lambda'}_{jl''l'}, \tag{21}$$

and using Eqs. (16) and (14) we get the results

$$\operatorname{Im}\left[A + \tfrac{2}{3}(C+D)\right] = \frac{3}{16\pi}\sum_{j}\left(\alpha_j + \tfrac{2}{3}\beta_j\right)\left(\operatorname{Im} a^{(m)}_j + \operatorname{Im} a^{(e)}_j\right) = \frac{q}{4\pi}\sigma_{\gamma d\to np};$$

$$\operatorname{Im} A = (3\sigma_0 + \tfrac{6}{5}\sigma_2)\, q/4\pi,$$

$$\operatorname{Im} B = (\tfrac{3}{2}\sigma_0 + \tfrac{3}{4}\sigma_1 - \tfrac{3}{4}\sigma_2)\, q/4\pi,$$

$$\operatorname{Im} C = (-3\sigma^{(e)}_0 + \tfrac{3}{2}\sigma^{(e)}_1 - \tfrac{3}{10}\sigma^{(e)}_2)\, q/4\pi,$$

$$\operatorname{Im} D = (-3\sigma^{(m)}_0 - \tfrac{3}{10}\sigma^{(m)}_2)\, q/4\pi, \tag{22}$$

where σ_j denotes the partial cross section for photodisintegration in the state j, including the factor $(2j+1)$.

3. CROSSING SYMMETRY AND THE DISPERSION RELATIONS

The retarded amplitude for γd forward scattering can be written in the form

$$\langle\mu'|\mathbf{e}'\mathbf{N}^{ret}\mathbf{e}|\mu\rangle = -2\pi^2 i\int d^4z e^{-iqz}\langle \mathbf{p}', \mu'|\Theta(z_0)[\mathbf{e}'\mathbf{j}(z/2), \mathbf{e}\mathbf{j}(-z/2)]|\mathbf{p}, \mu\rangle, \tag{23}$$

where μ and μ' are the spin indices of the deuteron.

For the advanced amplitude we have the analogous expression

$$\langle\mu'|\mathbf{e}'\mathbf{N}^{adv}\mathbf{e}|\mu\rangle = 2\pi^2 i\int d^4z e^{-iqz}\langle \mathbf{p}', \mu'|\Theta(-z_0)[\mathbf{e}'\mathbf{j}(z/2), \mathbf{e}\mathbf{j}(-z/2)]|\mathbf{p}, \mu\rangle. \tag{24}$$

For the case of forward scattering the deuteron momentum p can be set equal to zero.

Considering the relations complex conjugate to Eqs. (23) and (24), we get

$$\langle\mu'|\mathbf{e}'\mathbf{N}^{ret(adv)}(q)\mathbf{e}|\mu\rangle^{*} = \langle\mu|\mathbf{e}'\mathbf{N}^{ret(adv)}(-q)\mathbf{e}|\mu'\rangle. \tag{25}$$

Interchanging the order of $(\mathbf{e}'\mathbf{j}(z/2))$ and $(\mathbf{e}\mathbf{j}(-z/2))$ in Eqs. (23) and (24) and changing the sign of the variable z, we arrive at the relation

$$\langle\mu'|\mathbf{e}'\mathbf{N}^{ret(adv)}(q)\mathbf{e}|\mu\rangle = \langle\mu'|\mathbf{e}\mathbf{N}^{adv(ret)}(-q)\mathbf{e}'|\mu\rangle. \tag{26}$$

Let us represent $N^{ret(adv)}$ in the form (8). The conditions (25) and (26) reduce to the following symmetry properties of the scalar functions A, B, C, D:

$$A^{ret(adv)}(\nu)^{*} = A^{ret(adv)}(-\nu), \quad B^{ret(adv)}(\nu)^{*} = -B^{ret(adv)}(-\nu),$$

$$C^{ret(adv)}(\nu)^{*} = C^{ret(adv)}(-\nu), \quad D^{ret(adv)}(\nu)^{*} = D^{ret(adv)}(-\nu); \tag{27}$$

$$A^{adv}(\nu) = A^{ret}(-\nu), \qquad B^{adv}(\nu) = -B^{ret}(-\nu),$$

$$C^{adv}(\nu) = C^{ret}(-\nu), \qquad D^{adv}(\nu) = D^{ret}(-\nu). \tag{28}$$

Denoting hereafter the quantities $A(\nu)$, $C(\nu)$, and $D(\nu)$ by $L_1(\nu)$, $L_2(\nu)$, and $L_3(\nu)$, respectively, and $B(\nu)$ by $L_4(\nu)$, we write the dispersion relations for the scalar functions in the form

$$\operatorname{Re} L_{1,2,3}(\nu_0) - \operatorname{Re} L_{1,2,3}(0) = \frac{2\nu_0^2}{\pi} P\int_{\nu_d}^{\infty} \frac{d\nu \operatorname{Im} L_{1,2,3}(\nu)}{\nu(\nu^2-\nu_0^2)}, \tag{29}$$

$$\operatorname{Re} L_4(\nu_0) - \nu_0 \operatorname{Re} L_4'(0) = \frac{2\nu_0^3}{\pi} P\int_{\nu_d}^{\infty} \frac{d\nu \operatorname{Im} L_4(\nu)}{\nu^2(\nu^2-\nu_0^2)}, \tag{30}$$

where ν_d is the threshold for photodisintegration of the deuteron, approximately equal to the binding energy of the deuteron.

In order for it to be possible to use the relations (29) and (30) for an actual analysis, it is necessary to know $L_{1,2,3}(0)$ and $L_4'(0)$, i. e., to calculate the γd scattering amplitude in the energy region close to zero. The result of the calculations carried out in the following section is that

$$\operatorname{Re} L_1(0) = -e^2/M, \qquad \operatorname{Re} L_{2,3}(0) = 0,$$

$$\operatorname{Re} L_4'(0) = (\mu_0 - e/M_d)^2, \tag{31}$$

where μ_0 is the magnetic moment and M_d the mass of the deuteron.

4. THE LOW-ENERGY LIMIT FOR γd SCATTERING

Thirring, Low, Gell-Mann, and Goldberger[5] have shown that the limiting values at $\nu_0 = 0$ of the scattering amplitude and of its derivative with respect to the photon frequency are determined by the statistical properties of the system, for systems with spin ½. Following a method developed by Low, we shall show that analogous results are also valid for systems with arbitrary spin.

The S matrix for the scattering of photons from the state (q, e) into the state (q′, e′) is given by the expression

$$S' = -e'_i q_{ij} e_j (4q_0 q'_0)^{-1/2}, \tag{32}$$

$$q_{ij} = \int \mathrm{P}\,[j_i(x),\ j_j(y)]\, e^{iqx - iq'x}\, dx dy. \tag{33}$$

Using the technique of Low, it is not hard to get the results*

$$g_{ij} = g_{ij}^{(0)} + A\delta_{ij} + B\varepsilon_{ijk} S_k + D(S_i S_j + S_j S_i), \tag{34}$$

$$A(\mathbf{q}'\mathbf{q}) + B(\mathbf{S}\,[\mathbf{q}'\times\mathbf{q}]) + D\,[(\mathbf{S}\mathbf{q}')(\mathbf{S}\mathbf{q}) + (\mathbf{S}\mathbf{q})(\mathbf{S}\mathbf{q}')] = q_0 q'_0 C, \tag{35}$$

$$C = \frac{(2\pi)^4}{i}\,\delta^{(4)}(p' + q' - p - q) \sum \Big[\frac{\langle \mathbf{q} - \mathbf{q}' \,|\, j_0 \,|\, \mathbf{q}\rangle \langle \mathbf{q} \,|\, j_0 \,|\, 0\rangle}{E(q) - E(0) - q_0} - \frac{\langle \mathbf{q} - \mathbf{q}' \,|\, j_0 \,|\, -\mathbf{q}'\rangle \langle -\mathbf{q}' \,|\, j_0 \,|\, 0\rangle}{E(q') - E(0) + q'_0} \Big], \tag{36}$$

$$g_{ij}^{(0)} = \frac{(2\pi)^4}{i}\,\delta^{(4)}(p' + q' - p - q) \sum \Big[\frac{\langle \mathbf{q} - \mathbf{q}' \,|\, j_i \,|\, \mathbf{q}\rangle \langle \mathbf{q} \,|\, j_j \,|\, 0\rangle}{E(q) - E(0) - q_0} + \frac{\langle \mathbf{q} - \mathbf{q}' \,|\, j_j \,|\, -\mathbf{q}'\rangle \langle -\mathbf{q}' \,|\, j_i \,|\, 0\rangle}{E(q') - E(0) + q'_0} \Big]. \tag{37}$$

The summation in Eqs. (36) and (37) is taken over the spins of the particles involved in the reaction.

Let us consider the case in which the states $|\mathbf{q}\rangle$ and so on are eigenstates of a system with spin S. For the calculation of Eqs. (36) and (37) we need the expression for the current matrix $\langle \mathbf{p}_2 | \mathbf{j} | \mathbf{p}_1 \rangle$ in the low-energy region to accuracy v/c, and for $\langle \mathbf{q}' | j_0 | \mathbf{q} \rangle$ to accuracy v^2/c^2. It turns out that these matrix elements can be determined with the required accuracy on the basis of general principles.

Since $\mathbf{j}$ and j_0 are Hermitian operators and the interaction is invariant under three-dimensional rotations and time reversal, the most general form of the matrix element of the current is, in the approximation in question,

$$\langle p_2 | \mathbf{j} | p_1 \rangle = (e/2M)(\mathbf{p}_1 + \mathbf{p}_2) + i\mu\mathbf{S}\times[\mathbf{p}_2 - \mathbf{p}_1] + c\{\mathbf{S}(\mathbf{S}, \mathbf{p}_1 + \mathbf{p}_2) + (\mathbf{S}, \mathbf{p}_1 + \mathbf{p}_2)\mathbf{S}\}, \tag{38}$$

$$\langle \mathbf{p}_2 | j_0 | \mathbf{p}_1 \rangle = a + b(p_1^2 + p_2^2) + d(\mathbf{p}_1\mathbf{p}_2) + if(\mathbf{S}\,[\mathbf{p}_2\times\mathbf{p}_1]) + h\,[(\mathbf{S}\mathbf{p}_1)(\mathbf{S}\mathbf{p}_1) + (\mathbf{S}\mathbf{p}_2)(\mathbf{S}\mathbf{p}_2) + g\,[(\mathbf{S}\mathbf{p}_1)(\mathbf{S}\mathbf{p}_2) + (\mathbf{S}\mathbf{p}_2)(\mathbf{S}\mathbf{p}_1)], \tag{39}$$

where e is the total charge, $\mu s = \mu_0$ is the total magnetic moment, and the quantities a, b, c, d, f, h, g are invariant constants.

Under Lorentz transformations j_1 behaves like a component of a four-vector. Being an irreducible representation of the inhomogeneous Lorentz group, the wave function $|\mathbf{p}, \mu\rangle$ transforms in the following way:

$$|\mathbf{p}, \mu\rangle \xrightarrow{L} |\mathbf{p}, \mu\rangle' = R_{\mu\mu'}(L, \mathbf{p})\,|L^{-1}\mathbf{p}, \mu'\rangle, \tag{40}$$

where $R_{\mu\mu'}(L, \mathbf{p})$ is the rotation of the spin in the Lorentz transformation, which has been treated by a number of authors.[6,7]

Let us consider two coordinate systems. In one

$$\mathbf{p}_1 = 0, \qquad \mathbf{p}_2 = \mathbf{p},$$

and in the other

$$\mathbf{p}_1 = \mathbf{q}, \qquad p_{10} = E_q = \sqrt{q^2 + M^2},$$

$$\mathbf{p}_2 = \mathbf{p} + \frac{\mathbf{q}}{E_q}\left[\frac{(\mathbf{p}\mathbf{q})}{q^2}\,E_q\left(1 - \frac{E_q}{M}\right) + \frac{E_q}{M}E_p\right],$$

$$p_{20} = \frac{E_q}{M}\left[E_p + \frac{(\mathbf{p}\mathbf{q})}{E_q}\right]. \tag{41}$$

The second system moves with the velocity $-\mathbf{q}/E_q$ relative to the first. For the Lorentz transformation from the first system to the second we have to accuracy v^2/c^2

$$R(L, \mathbf{p}) = 1 + i(\mathbf{S}\,[\mathbf{p}\times\mathbf{q}])/2M^2. \tag{42}$$

We also have to accuracy v/c

$$\begin{aligned} \langle \mathbf{p} + \mathbf{q} | \mathbf{j} | \mathbf{q}\rangle' &= e(\mathbf{p} + 2\mathbf{q})/2M + i\mu\,[\mathbf{S}\times\mathbf{p}] + c\{\mathbf{S}(\mathbf{S},\ \mathbf{p} + 2\mathbf{q}) + (\mathbf{S}, \mathbf{p} + 2\mathbf{q})\mathbf{S}\} \\ &= \langle \mathbf{p} | \mathbf{j} | 0\rangle + (\mathbf{q}/M)\langle \mathbf{p} | \mathbf{j} | 0\rangle \\ &= e\mathbf{p}/2M + i\mu\,[\mathbf{S}\times\mathbf{p}] + c\,[\mathbf{S}(\mathbf{S}\mathbf{p}) + (\mathbf{S}\mathbf{p})\mathbf{S}] + a\mathbf{q}/M \end{aligned} \tag{43}$$

and to accuracy v^2/c^2

$$\begin{aligned} \langle \mathbf{p} + \mathbf{q} | j_0 | \mathbf{q}\rangle' &= a + b(p^2 + 2\mathbf{p}\mathbf{q} + 2q^2) + d(\mathbf{p}\mathbf{q} + q^2) \\ &+ if(\mathbf{S}\,[\mathbf{p}\times\mathbf{q}]) + h\{\mathbf{S}, \mathbf{p} + \mathbf{q})(\mathbf{S}, \mathbf{p} + \mathbf{q}) + (\mathbf{S}\mathbf{q})(\mathbf{S}\mathbf{q})\} \\ &+ g\{(\mathbf{S}, \mathbf{p} + \mathbf{q})(\mathbf{S}\mathbf{q}) + (\mathbf{S}\mathbf{q})(\mathbf{S}, \mathbf{p} + \mathbf{q})\} \\ &= [1 - i(\mathbf{S}\,[\mathbf{p}\times\mathbf{q}])/2M^2]\,E_q M^{-1}\,[\langle \mathbf{p} | j_0 | 0\rangle \\ &+ (qM^{-1}, \langle \mathbf{p} | \mathbf{j} | 0\rangle)] = a - ia(\mathbf{S}[\mathbf{p}\times\mathbf{q}])/2M^2 + aq^2/2M^2 \\ &+ bp^2 + h(\mathbf{S}\mathbf{p})(\mathbf{S}\mathbf{p}) + e(\mathbf{p}\mathbf{q})/2M^2 + i\mu(\mathbf{S}\,[\mathbf{p}\times\mathbf{q}])/M. \end{aligned} \tag{44}$$

From Eq. (43) it follows that

$$a = e, \qquad c = 0,$$

and from Eq. (44) that

$$d + 2b = e/2M^2, \qquad f = \mu/M - e/2M^2, \qquad g = h = 0.$$

---

*This is the most general expression for an arbitrary S, if we are not concerned with terms with energy dependence higher than linear.

Finally we have the covariant expressions

$$\langle \mathbf{p}_2 | \mathbf{j} | \mathbf{p}_1 \rangle = e(\mathbf{p}_1 + \mathbf{p}_2)/2M + i\mu \mathbf{S} \times [\mathbf{p}_2 - \mathbf{p}_1],$$

$$\langle \mathbf{p}_2 | j_0 | \mathbf{p}_1 \rangle = e + i(\mu/M - e/2M^2)(\mathbf{S}[\mathbf{p}_{-}\ \mathbf{p}_1]) + e(\mathbf{p}_1\mathbf{p}_2)/2M^2 + 2b(\mathbf{p}_1 - \mathbf{p}_2)^2, \tag{45}$$

and, as must be so, the first of these is the same as the matrix element of the current of a nonrelativistic particle interacting with a magnetic field (cf., e. g., the book of Landau and Lifshitz[8]). It turns out that the term contained in the expression (45) makes no contribution to the final result.

By means of Eq. (45) one easily gets

$$S = i(2\pi)^4\delta^{(4)}(p' + q' - p - q)(4q_0q_0')^{-1/2}\{e^2(\mathbf{e}'\mathbf{e})/M - 2ie(\mathbf{S}[\mathbf{e}'\times\mathbf{e}])M(\mu - e/2M) - (i\mu^2/q_0)(\mathbf{S}[[\mathbf{e}\times\mathbf{q}]\times[\mathbf{e}'\times\mathbf{q}']]) - (ie\mu/Mq_0)[(\mathbf{e}\mathbf{q}')(\mathbf{S}[\mathbf{q}'\times\mathbf{e}']) - (\mathbf{e}'\mathbf{q})(\mathbf{S}[\mathbf{q}\times\mathbf{e}])]\} \tag{46}$$

or for the matrix T

$$-T = e^2(\mathbf{e}'\mathbf{e})/M - 2i(e/M)\nu(\mu - e/2M)(\mathbf{S}[\mathbf{e}'\times\mathbf{e}] - i(\mu^2/\nu)(\mathbf{S}[[\mathbf{e}\times\mathbf{q}]\times[\mathbf{e}'\times\mathbf{q}']]) - (ie\mu/M\nu)[(\mathbf{e}\mathbf{q}')(\mathbf{S}[\mathbf{q}'\times\mathbf{e}']) - (\mathbf{e}'\mathbf{q})(\mathbf{S}[\mathbf{q}\times\mathbf{e}])]\}. \tag{47}$$

For forward scattering, in particular, we have

$$-T = e^2(\mathbf{e}'\mathbf{e})/M - i\nu(\mathbf{S}[\mathbf{e}'\times\mathbf{e}])[\mu_0/S - e/M]^2, \tag{48}$$

from which the result (31) indeed follows for $S = 1$.

In the energy range below the threshold for photoproduction of mesons from deuterons the terms that depend on the spin make an insignificant contribution to the cross section, since the mass of the nucleus is doubled in comparison with that of a nucleon, and the magnetic moment is much smaller.

5. RESULTS OF THE ANALYSIS. DISCUSSION

Experimental data on the photodisintegration of the deuteron are available right up to ~ 500 Mev.[9] The results of the calculation of Re $[L_1 + (2/3)(L_2 + L_3)]$, for which it is sufficient to know the total cross sections, are shown in Fig. 1, where the values of the real part of the amplitude are represented as fractions of e^2/M_pc^2. The photon energy is measured as a multiple of the threshold for photodisintegration of the deuteron: $\nu_0/\nu_d = \gamma_0$. The diagram also shows the energy dependence of the imaginary part of the quantity $L_1 + (2/3)(L_2 + L_3)$.

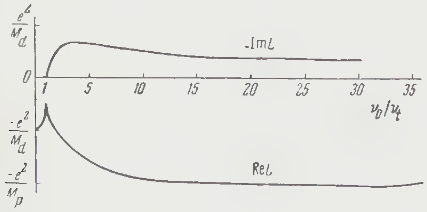

FIG. 1

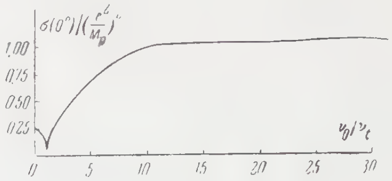

FIG. 2

In the energy range considered, $\nu_0 \lesssim 100$ Mev, the dominant contribution is that of photodisintegration with $\nu \lesssim 75$ Mev. For the other amplitudes a more detailed analysis of the photodisintegration is required. If we assume that the contribution from photodisintegration with $\nu_0 \lesssim 80$ Mev is also decisive for the other amplitudes and use the analysis of de Swart and Marshak,[10] it is possible to estimate the dispersion parts of all the scalar amplitudes. But for γd scattering the spin-dependent amplitudes play a much smaller part as compared with the case of γN scattering. Figure 2 shows the energy dependence of the γd forward scattering. With increase of the γ-ray energy the γd scattering cross section at first shows a marked decrease as compared with the Thomson limit, and then ($\nu \gtrsim 4$ Mev) rapidly rises, and in the range $20 < \nu < 80$ Mev reaches values larger than $(e^2/M_dc^2)^2$ by a factor four.

Inclusion of the magnetic-dipole absorption, especially near the threshold, leads to an additional sharp "dip" of the cross section,[1] with a total half-width ~ 200 — 300 kev. The width of the total decrease of the cross section is considerably larger.

The large influence of inelastic processes that involve the deuteron as a whole, in addition to the processes involving the individual nucleons of the deuteron, makes it impossible to apply the impulse approximation to elastic γd scattering over a wide range of energies.* The presence of the inelastic process of photodisintegration of the deuteron has an especially strong effect on the polarizability of the deuteron. If, as A. M. Baldin has shown, the polarizability of nucleons is entirely due to the process of meson production, on the other hand the main contribution to the polarizability of the deuteron, and of nuclei in general, comes from photonuclear processes at much smaller energies.

---

*In a preprint received very recently, Schult and Capps have made a new examination of the corrections to the impulse approximation for γd scattering and have come to a similar conclusion.

It follows from Eq. (29) that the polarizability of the deuteron is given by

$$\alpha_d = \frac{d}{d\nu^2}[\mathrm{Re}\,(L_1 + {}^2/_3\,L_2 + {}^2/_3\,L_3)]_{\nu=0} = \frac{\hbar c}{2\pi^2}\,\mathrm{P}\int\limits_{\nu_d}^{\infty}\frac{\sigma_t\,(\nu)\,d\nu}{\nu^2}. \tag{49}$$

An analogous formula is also valid for other nuclei. Dipole absorption plays the fundamental role in the total interaction cross section $\sigma_t(\nu)$. When this is taken into account Eq. (49) goes over into the well known formula of Migdal[11] (cf. also reference 12).

Substitution into Eq. (49) of the expressions (41) and (46) of reference 1 gives for the sum of the electric and magnetic polarizabilities of the deuteron

$$\alpha_e + \alpha_m = \alpha_d = \frac{e^2}{M_p c^2}\left(\frac{\hbar c}{\varepsilon}\right)^2\left\{\frac{3}{64} + \frac{1}{12}\left(1 + \sqrt{\frac{\varepsilon'}{\varepsilon}}\right)^2\frac{\varepsilon}{M_p c^2}\right.$$
$$\left.\times(\mu_p - \mu_n)^2\right\} = 0.64\cdot 10^{-39}\,\mathrm{cm}^3, \tag{50}$$

which agrees with the result of Levinger and Rustgi (cf. reference 12).

The presence of sizable contributions from photodisintegration in the γd elastic scattering amplitude and in the polarizability of the deuteron prevents our obtaining reliable conclusions about the polarizability of neutrons from the experimental data on the scattering of low-energy γ rays by deuterons.

To get information on the magnetic polarizability of the deuteron one must evidently have a much more detailed analysis of the photodisintegration of the deuteron and of processes of photoproduction of mesons from deuterons.*

Strictly speaking, the treatment carried out in the present paper is valid only for forward scattering. In the dipole approximation, however, the main results remain valid for other scattering angles also. But we have not made a direct comparison with the experimental data, since in the experiments[2] inelastic scattering of γ rays by deuterons,

$$\gamma + d \to n + p + \gamma,$$

was observed along with the elastic scattering. Recently A. M. Baldin (private communication) has examined the corrections to the impulse approximation in the inelastic scattering of γ rays and has arrived at the conclusion that for this process also there are appreciable corrections associated with the photodisintegration.

Thus we can evidently conclude that the results of an analysis that takes into account the photodisintegration of the deuteron (and the production of mesons), and the experimental data on the scattering of γ rays by deuterons in the energy range ~50 — 100 Mev are in agreement with each other. For a more reliable comparison of calculated results with experiment one first needs an analysis of the inelastic processes over a wider range of energies.

The writers are grateful to A. M. Baldin, V. I. Gol'danskii, and Ya. A. Smorodinskiĭ for numerous discussions.

---

*All conclusions concerning the magnetic polarizability of the proton are very sensitive to the assumptions that have to be made in the analysis of the photoproduction of pions. When one uses the analysis of Watson it follows from the results[4] that the magnetic polarizability of the proton is small. (In the case of the analysis of Watson it goes to zero.) This conclusion evidently is not in contradiction with the experimental data.[13]

[1] L. I. Lapidus and Chou Kuang-Chao, JETP **39**, 112 (1960), Soviet Phys. JETP **12**, 82 (1961).

[2] Hyman, Ely, Frisch, and Wahlig, Phys. Rev. Letters **3**, 93 (1959).

[3] R. H. Capps, Phys. Rev. **106**, 1031 (1957); **108**, 1032 (1957).

[4] L. I. Lapidus and Chou Kuang-Chao, JETP **37**, 1714 (1959), Soviet Phys. JETP **10**, 1213 (1960); JETP **38**, 201 (1960), Soviet Phys. JETP **11**, 147 (1960).

[5] F. E. Low, Phys. Rev. **96**, 1428 (1954). M. Gell-Mann and M. L. Goldberger, Phys. Rev. **96**, 1453 (1954).

[6] Chou Kuang-Chao and M. I. Shirokov, JETP **34**, 1230 (1958), Soviet Phys. JETP **7**, 851 (1958).

[7] L. Zastavenko and Chou Kuang-Chao, JETP **35**, 1417 (1958), Soviet Phys. JETP **8**, 990 (1959).

[8] L. Landau and E. Lifshitz, Quantum Mechanics, Pergamon, 1958.

[9] Barnes, Carver, Stafford, and Wilkinson, Phys. Rev. **86**, 359 (1952). J. Halpern and E. V. Weinstock, Phys. Rev. **91**, 934 (1953). Lew Allen, Jr., Phys. Rev. **98**, 705 (1955). J. C. Keck and A. V. Tollestrup, Phys. Rev. **101**, 360 (1956). Whalin, Schriever, and Hanson, Phys. Rev. **101**, 377 (1956). D. R. Dixon and K. C. Bandtel, Phys. Rev. **104**, 1730 (1956). Aleksandrov, Delone, Slovokhotov, Sokol, and Shtarkov, JETP **33**, 614 (1957), Soviet Phys. JETP **6**, 472 (1958). Tatro, Palfrey, Whaley, and Haxby, Phys. Rev. **112**, 932 (1958).

[10] J. J. de Swart, Physica **25**, 233 (1959). J. J. de Swart and R. E. Marshak, Physica **25**, 1001 (1959).

[11] A. B. Migdal, JETP **15**, 81 (1948).

[12] J. S. Levinger, Phys. Rev. **107**, 554 (1957).

[13] G. Bernardini, Report at the International Conference on the Physics of High-Energy Particles, Kiev, 1959.

Translated by W. H. Furry
240

SOVIET PHYSICS JETP VOLUME 12, NUMBER 5 MAY, 1961

ON THE THEORY OF RUNAWAY ELECTRONS

A. V. GUREVICH

P. N. Lebedev Physics Institute, Academy of Sciences, U.S.S.R.

Submitted to JETP editor May 23, 1960

J. Exptl. Theoret. Phys. (U.S.S.R.) **39**, 1296-1308 (November, 1960)

The influence of a relatively weak electric field on the velocity distribution of plasma electrons in the range of high velocities is considered. An expression for the stationary electron distribution function is obtained and analyzed. The magnitude of the flux of runaway electrons in a completely ionized plasma is determined. The effect on this flux of neutral plasma particles is taken into account. It is shown that under certain conditions instabilities in the plasma may occur during the development of the discharge which are due to the runaway electron flux. The results obtained are in qualitative agreement with experiment.

1. INTRODUCTION

As is well known, the frequency of collisions of an electron with ions, and also with other electrons in the plasma, falls off sharply as its velocity increases. Therefore, friction is always negligibly small for electrons possessing a sufficiently high energy. If a constant electric field is present in the plasma the velocity of such electrons increases continuously with time; they are usually called "runaway" electrons.

Clearly, in a very strong electric field (or in a plasma of sufficiently low density) all the electrons are accelerated by the field, i.e., become "runaway" electrons. In a weak field only very fast electrons will run away, i.e., those whose velocity v exceeds a certain critical value v_c. The velocity v_c depends in an essential manner on the magnitude of the field; in a weak field it is, naturally, much larger than the average thermal velocity of the electrons in the plasma and, therefore, the number of runaway electrons is not very great in this case. In order to determine it we must know the way in which the density of electrons having a velocity $v \sim v_c$ varies, i.e., we must know the velocity distribution for the electrons for $v \sim v_c$. The corresponding problem must, naturally, be solved taking collisions into account (since they determine the critical velocity v_c, and, consequently also the number of runaway electrons), and is therefore very complicated in general. In previous papers[1] only some numerical calculations for completely ionized plasma have been carried out (Dreicer, Bernstein and Rabinowitz), and also a solution has been obtained for a very strong electrical field when collisions may be neglected in the first approximation (Kovrizhnykh).

The investigation of the phenomenon of runaway electrons in the case of a weak electrical field in a completely ionized plasma is the aim of Sec. 2 of the present paper. The effect on the runaway electrons of neutral particles in the plasma is taken into account in Sec. 3.

2. THE DISTRIBUTION FUNCTION AND THE FLUX OF RUNAWAY ELECTRONS IN A COMPLETELY IONIZED PLASMA

The equation for the electron distribution function $f(v, \theta, t)$ in the domain of high velocities ($v \gg \sqrt{kT_e/m}$) in a completely singly ionized plasma situated in a constant uniform electric field **E** has the following form*

$$\frac{\partial f}{\partial t} + \frac{eE}{m}\left(\cos\theta\frac{\partial f}{\partial v} - \frac{\sin\theta}{v}\frac{\partial f}{\partial\theta}\right) - \frac{1}{v^2}\frac{\partial}{\partial v}\left\{v^2\nu_e(v)\left[\frac{kT_e}{m}\frac{\partial f}{\partial v} + vf\right]\right\}$$

$$- \frac{\nu(v)}{2\sin\theta}\frac{\partial}{\partial\theta}\left\{\sin\theta\frac{\partial f}{\partial\theta}\right\} = 0. \qquad (1)$$

Here, as usual, e, m and T_e are the charge, mass and temperature of the electrons; k is the Boltzmann constant; θ is the angle between **E** and **v**; $\nu_e(v)$ is the collision frequency of an electron of velocity v with other electrons in the plasma:

---

*In the velocity range $v \lesssim \sqrt{kT_e/m}$ the terms in Eq. (1) which describe collisions between electrons should be written in a more complicated form (cf., for example, references 2 and 3). However, this circumstance is not essential in our case in view of the fact that in a weak field ($E \ll E_{ci}$), which is the only one considered in the present article, any significant deviations of the distribution function from the equilibrium one appear only at high velocities, $v \gg \sqrt{kT_e/m}$ (cf. below).

$$\nu_e(v) = (4\pi e^4 N_e/m^2 v^3)\ln(mv^2 D/e^2), \qquad (2)$$

where N_e is the electron density, $D = \sqrt{kT_e/4\pi e^2 N_e}$ is the Debye radius. We have further

$$\nu(v) = \nu_i(v) + \nu_e(v)(1 - kT_e/2mv^2)$$

giving the frequency of collisions of an electron with ions and with electrons [$\nu_i(v)$ is also given by formula (2), but with N_e replaced by N_i]. We shall in future, as usual, neglect the variation of the logarithmic term in (2) and set $mv^2 = mv_c^2$ in the argument of the logarithm, where v_c is the characteristic velocity of the electrons under consideration: $mv_c^2 \approx kT_e E_{ci}/E$ (cf. below).

For subsequent developments it is convenient to go over to the dimensionless variables

$$\mu = \cos\theta, \qquad u = v/\sqrt{kT_e/m},$$
$$\tau = \nu_e(\sqrt{kT_e/m})\,t = 4\pi e^4 N_e m^{-1/2}(kT_e)^{-3/2}\ln(mv_c^2 D/e^2)\,t.$$

In terms of these variables, Eq. (1) assumes the following form

$$\frac{\partial f}{\partial\tau} + \frac{E}{E_{ci}}\left(\mu\frac{\partial f}{\partial u} + \frac{1-\mu^2}{u}\frac{\partial f}{\partial\mu}\right) - \frac{1}{u^2}\frac{\partial}{\partial u}\left\{\frac{1}{u}\frac{\partial f}{\partial u} + f\right\}$$
$$- \frac{1-1/4u^2}{u^3}\frac{\partial}{\partial\mu}\left\{(1-\mu^2)\frac{\partial f}{\partial\mu}\right\} = 0, \qquad (1a)$$

where E_{ci} is the characteristic (critical) field in a completely ionized plasma:

$$E_{ci} = \frac{4\pi e^3 N_e}{kT_e}\ln\left(\frac{mv_c^2 D}{e^2}\right)$$
$$\approx 2.6\cdot 10^{-13}\frac{N_e}{kT_e}\ln\left\{4\cdot 10^9\frac{(kT_e)^{1/2} mv_c^2}{N_e^{1/2}}\right\} \qquad (3)$$

(here in the last equation E_{ci} is in v/cm; kT_e and mv_c^2 are in ev). In what follows we shall consider only the case of a weak electric field $E \ll E_{ci}$. We note that the field E_c utilized in Dreicer's papers[1,4] is related to E_{ci} by the expression $E_c = \frac{1}{2}E_{ci}T_e/T_0$.

A. STATIONARY SOLUTION

Under stationary conditions ($\partial f/\partial\tau = 0$) it is natural to seek the solution of equation (1a) in the form

$$f = C\exp\{\varphi(u,\mu)\}, \qquad (4)$$

where C is a certain constant determined by the normalization conditions. The function $\varphi(u,\mu)$ must then satisfy the following nonlinear equation:

$$u^2\frac{E}{E_{ci}}\left[\mu u\frac{\partial\varphi}{\partial u} + (1-\mu^2)\frac{\partial\varphi}{\partial\mu}\right] - \left(\frac{\partial\varphi}{\partial u}\right)^2 - \frac{\partial^2\varphi}{\partial u^2}$$
$$- u\left(1-\frac{1}{u^2}\right)\frac{\partial\varphi}{\partial u} + 2\left(1-\frac{1}{4u^2}\right)\mu\frac{\partial\varphi}{\partial\mu} - \left(1-\frac{1}{4u^2}\right)$$
$$\times(1-\mu^2)\frac{\partial^2\varphi}{\partial\mu^2} - \left(1-\frac{1}{4u^2}\right)(1-\mu^2)\left(\frac{\partial\varphi}{\partial\mu}\right)^2 = 0. \qquad (5)$$

Before undertaking the solution of this equation we shall point out one essential characteristic feature of the electron velocity distribution in the domain of high velocities in the presence of a constant electric field. Under the action of the electric field the electrons acquire an additional velocity (with respect to the thermal velocity) directed parallel to the field. It is redistributed among other directions as a result of collisions of electrons with each other and with ions. The change in the distribution function due to the collisions is described by the last two terms in (1). The first of them describes the change in the absolute value of the velocity or of the energy of a fast electron colliding with another electron (as is well known, the change in electron energy in a collision with an ion is very small). The second term describes the change of only the direction of the momentum as a result of the collision. Collisions with electrons as well as collisions with ions contribute equally to such changes.

In a weak field ($E \ll E_{ci}$) in the domain of thermal velocities ($u \sim 1$) the distribution function is, naturally, close to Maxwellian. Under these conditions collisions between electrons are of little significance; in particular, the Maxwellian distribution function results in the vanishing of that term in (1) which describes the change in the absolute value of the electron velocity as a result of a collision. Under these conditions the principal role is played by collisions accompanied by a change of only the direction of the velocity, as a result of which, at thermal velocities, the additional velocity communicated to the electrons as a result of the action of the field turns out to be uniformly distributed among all the directions. Under these conditions the distribution function depends primarily only on the absolute value of the velocity, as is well known (cf., for example, reference 3).

At high velocities, when the collisions are infrequent and when as a result of this the electric field can produce considerable deviations of the distribution function from Maxwellian, the situation is significantly different. Under these conditions [for $u > (E_{ci}/E)^{1/4} \gg 1$] the most important collisions turn out to be those between electrons accompanied by a change in the absolute value of the velocity. The reason for this is that the gradient of a function of the Maxwellian type increases rapidly (in absolute value) as the velocity increases: $|df/du| \sim uf$; therefore for large u the change in the distribution function resulting from a change in the absolute value of u is very large [this can be clearly seen from Eq. (1)]. The last term in (1), describing the change in the direction of the velocity, is comparatively small; consequently, the redistribution of the electron energy over the different directions of the velocity is hindered. Therefore, for large values of u, when the collisions are infrequent and the electric field can produce a large increase in the component of the velocity u_z over a mean free path (the z axis is parallel to the field), this direction of the velocity must be strongly favored. The velocity distribution of the electrons for high velocities must acquire a directional character.

Taking into account the above peculiarity of the distribution function in the domain of high velocities it is natural to seek the solution of Eq. (5) in the form of a series in powers of μ in the neighborhood of $\mu = 1$ (i.e., near the z axis, since $\mu = \cos\theta$):

$$\varphi(u, \mu) = \varphi(u, 1) + (\mu - 1)\left(\frac{\partial\varphi}{\partial\mu}\right)_{\mu=1} + \frac{(\mu-1)^2}{2!}\left(\frac{\partial^2\varphi}{\partial\mu^2}\right)_{\mu=1} + \cdots$$
$$= \varphi_0(u) + (\mu - 1)\varphi_1(u) + (\mu - 1)^2\varphi_2(u) + \ldots.$$

On substituting this expansion into (5), and on equating terms containing various powers of $\mu - 1$, we obtain the following chain of equations for the functions $\varphi_0, \varphi_1, \varphi_2, \ldots$:

$$u^3\frac{E}{E_{ci}}\frac{d\varphi_0}{du} - \left(\frac{d\varphi_0}{du}\right)^2 - \frac{d^2\varphi_0}{du^2} - u\left(1 - \frac{1}{u^2}\right)\frac{d\varphi_0}{du} + 2\left(1 - \frac{1}{4u^2}\right)\varphi_1 = 0, \tag{5a}$$

$$u^3\frac{E}{E_{ci}}\left(\frac{d\varphi_0}{du} + \frac{d\varphi_1}{du}\right) - 2u^2\varphi_1\frac{E}{E_{ci}} - 2\frac{d\varphi_0}{du}\frac{d\varphi_1}{du} - \frac{d^2\varphi_1}{du^2} - u\left(1 - \frac{1}{u^2}\right)\frac{d\varphi_1}{du} + 2\left(1 - \frac{1}{4u^2}\right)(\varphi_1 + \varphi_1^2) + 8\left(1 - \frac{1}{4u^2}\right)\varphi_2 = 0, \tag{5b}$$

$$u^3\frac{E}{E_{ci}}\left(\frac{d\varphi_1}{du} + \frac{d\varphi_2}{du}\right) - u^2\frac{E}{E_{ci}}(\varphi_1 + 4\varphi_2) - 2\frac{d\varphi_0}{du}\frac{d\varphi_2}{du} - \left(\frac{d\varphi_1}{du}\right)^2 - \frac{d^2\varphi_1}{du^2} - u\left(1 - \frac{1}{u^2}\right)\frac{d\varphi_2}{du} + \left(1 - \frac{1}{4u^2}\right)(6\varphi_2 + 8\varphi_2\varphi_1 + \varphi_1^2) + 18\left(1 - \frac{1}{4u^2}\right)\varphi_3 = 0, \ldots. \tag{5c}$$

Equations (5) can be easily solved by successively terminating the chain of equations. By setting as a first approximation $\varphi_1 = 0$ and by omitting for simplicity small terms (of order $1/u^2$) we obtain

$$\varphi_0^{(1)} = -\int_0^u u\left(1 - u^2\frac{E}{E_{ci}}\right)du = -\frac{u^2}{2} + \frac{u^4}{4}\frac{E}{E_{ci}}. \tag{6}$$

In the next approximation, on setting $\varphi_2 = 0$ we obtain $\varphi_0 = \varphi_0^{(1)} + \varphi_0^{(2)}$, $\varphi_1 = \varphi_1^{(1)}$, where

$$\varphi_0^{(2)} = -\left(\frac{2E_{ci}}{E}\right)^{1/2}\left[1 - \left(1 - \frac{E}{2E_{ci}}u^2\right)^{1/2}\right],$$
$$\varphi_1^{(1)} = u^2\left[\frac{E}{2E_{ci}}\left(1 - \frac{E}{E_{ci}}u^2\right)\right]^{1/2} \tag{7}$$

etc.* Naturally, the stationary solution under discussion has sense only up to the runaway-electron limit, i.e., for $1 - u^2E/E_{ci} > 0$.

In order to determine the convergence of the sequence of successive approximations we rewrite expressions (6) and (7) for φ_0 and φ_1, by introducing the new variable $z = u^2E/E_{ci}$:

$$\varphi_0^{(1)} = -(E_{ci}/E)\left(\tfrac{1}{2}z - \tfrac{1}{4}z^2\right),$$
$$\varphi_0^{(2)} = -2^{1/2}(E_{ci}/E)^{1/2}[1 - (1 - z)^{1/2}],$$
$$\varphi_0^{(3)} = \tfrac{1}{4}(1 - z)^{-1} + \tfrac{1}{4}\ln[z^{3/2}(1 - z)^{-1}], \ldots;$$
$$\varphi_1^{(1)} = 2^{-1/2}(E_{ci}/E)^{1/2}z(1 - z)^{1/2},$$
$$\varphi_1^{(2)} = (-3 + 10z - 5z^2)/4(1 - z), \ldots.$$

From this it is clear that the expansion is in fact made in powers of the parameter $(E/E_{ci})^{1/2}$, which in the case of a weak field $E \ll E_{ci}$ is always small.

Thus, in the case $E \ll E_{ci}$ the stationary electron distribution function has the following form at high velocities ($u^2 = mv^2/kT_e \gtrsim \sqrt{E_{ci}/E}$)

$$f(v, \theta) = C\exp\left\{-\frac{mv^2}{2kT_e} + \frac{E}{4E_{ci}}\left(\frac{mv^2}{kT_e}\right)^2 - \left(\frac{2E_{ci}}{E}\right)^{1/2}\left[1 - \left(1 - \frac{E}{E_{ci}}\frac{mv^2}{kT_e}\right)^{1/2}\right] - \left(\frac{E}{2E_{ci}}\right)^{1/2}\frac{mv^2}{kT_e}\left(1 - \frac{E}{E_{ci}}\frac{mv^2}{kT_e}\right)^{1/2}(1 - \cos\theta)\right\}, \tag{8}$$

---

*We can also indicate a somewhat different, but a more consistent, method of solving the system of equations (5). In particular, with the aid of Eq. (5a) we can easily express the function φ_1 in terms of φ_0; with the aid of Eq. (5b) we can express φ_2 in terms of φ_1 and φ_0, etc., i.e., in the final result we can easily obtain a solution of the system of equations (5) in which all the functions $\varphi_1, \varphi_2, \varphi_3 \ldots$ will be expressed in terms of φ_0. In order to determine the function φ_0 it is necessary to use an additional condition. Indeed, a stationary electron distribution is established both when there exist no sources of particles, and also when there are δ-like sources of particles; naturally, the distribution in the two cases will be different, although Eq. (5) is valid in all cases. The condition imposed on the sources (or on the flux) of electrons is the required additional condition for the determination of φ_0 (cf., for example, reference 3). In particular, in the case under consideration at present there are no sources of particles; consequently, the total flux of particles over any closed surface must be equal to zero. This condition leads to a certain complicated integral equation for the function φ_0. A solution of this equation obtained by the method of successive approximations leads to expressions agreeing with (6) and (7).

where the normalization constant is $C = (m/2\pi kT_e)^{3/2}N_e$ (N_e is the electron density). For not very high velocities $v^2 \sim kT_e/m$ (or more accurately, for $v^2 \ll (kT_e/m)\sqrt{E_{ci}/E}$) the distribution function (8) is close to Maxwellian.* For large velocities $v^2 \gg (kT_e/m)\sqrt{E_{ci}/E}$ the distribution function (8) differs from it considerably: as the velocity increases it falls off significantly slower than the Maxwellian one does. Moreover, in the high velocity domain the distribution function (8) acquires a directional character, which is in complete agreement with the qualitative analysis of the solution of Eq. (1) carried out earlier. The directional nature of the distribution (8) is most clearly manifested for $v^2 = 2kT_eE_{ci}/3mE$. The average angular spread

$$\overline{\theta} = \int \theta f(v,\theta)\,d\Omega / \int f(v,\theta)\,d\Omega$$

has in this case a minimum value:

$$\overline{\theta} = \overline{\theta}_{min} = (27\pi^2/8)^{1/4}(E/E_{ci})^{1/4}.$$

It is of interest that not only at speeds $v^2 < 2kT_eE_{ci}/3mE$, but also at high speeds $v^2 > 2kT_eE_{ci}/3mE$ (i.e., near the runaway-electron limit), does the distribution function become less directional.†

B. THE FLUX OF RUNAWAY ELECTRONS

The average velocity of an electron parallel to the direction of the field $v_z = u_z(kT_e/m)^{1/2}$ is much greater in the high velocity domain than is its velocity in the direction orthogonal to the field $v_r = u_r(kT_e/m)^{1/2}$. Because of this, it is the distribution with respect to the velocity u_z which is particularly significant for runaway electrons:

$$F(u_z,\tau) = 2\pi \int_0 f(u,\theta,\tau)\,u_r\,du_r.$$

On multiplying Eq. (1) by $2\pi u_r$ and on integrating it over du_r (neglecting small terms of order u_r^2/u_z^2) we obtain the following equation for $F(u_z,\tau)$:

$$\frac{\partial F}{\partial \tau} - \frac{\partial}{\partial u_z}\left\{\frac{1}{u_z^2}\left(3 - \frac{E}{E_{ci}}u_z^2\right)F + \frac{1+\overline{u_r^2}}{u_z^3}\frac{\partial F}{\partial u_z}\right\} = 0. \quad (9)$$

Here

$$\overline{u_z^2} = \overline{u_r^2}(u_z) = \int_0^\infty u_r^3 f\,du_r \Big/ \int_0^\infty u_r f\,du_r$$

is the mean square velocity of the electron in the direction orthogonal to the field (for a given u_z). For the determination of $\overline{u_r^2}$ we can utilize the stationary distribution function (8) obtained earlier. We then find that (for $u_z^2 < E_{ci}/E$)

$$\overline{u_r^2} = 2\left[1 - \frac{E}{E_{ci}}u_z^2 + \frac{(E/E_{ci})^{1/2}(3 - u_z^2E/E_{ci})}{2^{1/2}(1 - u_z^2E/E_{ci})^{1/2}}\right]^{-1}. \quad (10)$$

The problem of finding the flux of runaway electrons has thus been reduced to finding the nonstationary solution of Eq. (9); we have obtained it earlier.[5] By utilizing this solution we obtain for the flux of the runaway electrons S the following expression:

$$S = \frac{N_e\nu_{e0}}{\sqrt{2\pi}}\left[\int_0^\infty \frac{u_z^3\,du_z}{1+\overline{u_r^2}}\exp\left\{\int_0^{u_z} u_z\,du_z\,\frac{3 - u_z^2E/E_{ci}}{1+\overline{u_r^2}}\right\}\right]^{-1}. \quad (11)$$

where $N_e = N_e(t)$ is the number of electrons in the principal stationary domain of velocities, $\nu_{e0} = \nu_e(\sqrt{kT_e/m})$ is the mean collision frequency for an electron. On taking it into account that $E_{ci}/E \gg 1$, we can carry out the integration in the last expression. We then obtain

$$S = \frac{2}{\sqrt{\pi}}N_e\nu_{e0}\left(\frac{E}{E_{ci}}\right)^{1/2}\exp\left\{-\frac{E_{ci}}{4E} - \sqrt{2}\left(\frac{E_{ci}}{E}\right)^{1/2}\right\}. \quad (12)$$

It is shown in reference 5 that the flux of runaway particles determined by formulas (11) and (12) is established within a time $\Delta t_y \gtrsim (E_{ci}/E)^{3/2}\nu_{e0}^{-1}$. Therefore, the weakly nonstationary solution, (11) and (12), is applicable only if the parameters N_e, T_e, E do not change appreciably during this time. In particular, since the density of electrons in the principal velocity domain N_e is decreased as a result of the running away process $dN_e/dt = -S$, then in order to be able to utilize expression (12) it is necessary to have $S\Delta t_y \ll N_e$, i.e., it is necessary that the following inequality hold

$$\frac{E_{ci}}{E}\exp\left\{-\frac{E_{ci}}{4E} - \left(\frac{2E_{ci}}{E}\right)^{1/2}\right\} \ll 1,$$

---

*It has been pointed out earlier that both the initial equation (1) and the method of solving it utilized in this paper are valid only at high velocities. However, only at such velocities can the electron distribution function differ appreciably from Maxwellian. For low (thermal) velocities the electron distribution is Maxwellian, and the solution of (8) which we have obtained coincides with it. Consequently, the distribution function (8) represents well the nature of electron distribution over the whole stationary domain of velocities: $E_{ci}kT_e/Em \geqslant v^2 \geqslant 0$.

†An analogous problem was recently investigated by Dreicer.[4] However, he assumed that the distribution function could be represented in the form $f(v) = f_0(v) + f_1(v)\cos\theta$, where $|f_1| \ll f_0$. He obtained the result that the distribution function is Maxwellian right up to the runaway-electron limit. As is clear from (8), the above assumption, and, consequently, the result obtained, are erroneous in the domain of high velocities $v^2 \gg (kT_e/m)\sqrt{E_{ci}/E}$, and even more so at the runaway-electron limit $v_c^2 = kT_eE_{ci}/mE$.

which, naturally, is always satisfied in the case of a sufficiently weak field $E \lesssim 0.1\, E_{ci}$.

If we estimate the flux of runaway electrons in the simplest possible manner, assuming that the distribution function is Maxwellian right up to the runaway-electron limit (cf., for example, Harrison's paper[1]), we obtain* $S \sim \nu_e N_e \exp\{-E_{ci}/2E\}$. This expression for the number of runaway electrons qualitatively agrees well with the exact formula (12), although the quantitative discrepancy between them is quite large for large values of E_{ci}/E. It should be emphasized that the agreement which we have mentioned is to a certain extent accidental. Indeed, as is clear from the exact calculation, the friction that determines the flux of runaway electrons is primarily determined by collisions between electrons which are accompanied by an appreciable change in electron energy. This constitutes only a part of the total friction experienced by electrons in a plasma, but this part differs from the total friction only by a numerical factor. As a result qualitative agreement is obtained between an elementary estimate of the flux taking the total friction into account and the result of an exact calculation.†

It should be emphasized that the assumptions made above in the calculation of the flux (neglect of terms of order $\overline{u_r^2}/\overline{u_z^2}$, the utilization for the determination of $\overline{u_r^2}$ of the stationary distribution function, in the evaluation of which, moreover, only the first terms of the expansion in powers of the parameter E/E_{ci} have been taken into account) have enabled us to pick out only the principal terms in the exponential factor in formula (12). If the next approximations are taken into account this should lead to corrections of order unity in the exponential term.

3. INCLUSION OF THE EFFECT OF NEUTRAL PARTICLES

a) Weakly ionized plasma. The possibility of electrons being accelerated in a completely ionized plasma is a consequence of the fact that the frequency of collisions of an electron with ions and with other electrons falls off rapidly as its velocity increases. As a result friction is always negligibly small for electrons possessing a sufficiently high energy, and they are accelerated by even a very weak electric field. If the plasma contains a considerable number of neutral particles the situation is, in general, completely analogous, since the frequency of collisions of an electron with the neutral particles (atoms, molecules) also decreases with increasing velocity in the case of electrons possessing a sufficiently high energy $\epsilon \gtrsim (3-5)\epsilon_i$, where ϵ_i is the ionization energy. However, for $\epsilon \lesssim \epsilon_i$ the frequency of collisions usually increases with increasing ϵ. Therefore, in weakly ionized plasma, when the principal role is played by the collisions of an electron with neutral particles, only the fast electrons may run away in a relatively weak electric field; their energy must, in any case, exceed $(3 \text{ to } 5)\epsilon_i$.

Because of this, it is possible to simplify considerably the kinetic equation for the electron distribution function in a weakly ionized plasma $f(v, \theta, t)$ by utilizing the differential representation for the integral due to the inelastic collisions of an electron with neutral particles (cf. reference 3). In this case the kinetic equation assumes the following form:

$$\frac{\partial f}{\partial t} + \frac{eE}{m}\left(\cos\theta\ \frac{\partial f}{\partial v} - \frac{\sin\theta}{v}\frac{\partial f}{\partial\theta}\right) - \frac{1}{v^2}\frac{\partial}{\partial v}\left\{v^2\left[D(v)\frac{\partial f}{\partial v} + \frac{F(v)}{m}f\right]\right\}$$
$$-\frac{\nu_n(v)}{2\sin\theta}\frac{\partial}{\partial\theta}\left(\sin\theta\ \frac{\partial f}{\partial\theta}\right) = 0. \qquad (13)$$

Here

$$F(v) = N_n\left\{(\varepsilon_i + \Delta\varepsilon)\, Q_i(v) + \sum_k \hbar\omega_k Q_k(v)\right\}$$

is the effective retarding force on an electron moving with a velocity v in a gas of density N_n. Here $\Delta\epsilon$ is the energy transferred to the knock-on electron, $Q_i(v)$ is the total ionization cross section, $Q_k(v)$ is the total cross section for the excitation of the level $\hbar\omega_k$. As is well known, the retarding force F may be approximately written in the form

$$F(v) = (4\pi e^4 N_n Z / mv^2)\ln(mv^2/\varepsilon), \qquad (14)$$

where $\overline{\epsilon}$ is some average excitation energy (the calculation in reference 6 yields $\overline{\epsilon} \approx Z \times 13.5$ ev, in particular $\overline{\epsilon} = 15$ ev in hydrogen, $\overline{\epsilon} = 30$ ev in helium). For not very high electron energies the force F increases with increasing v, while at high energies it diminishes. It reaches the maximum value of $F_{max} = 4\pi e^4 N_n Z/2.72\overline{\epsilon}$ for $\epsilon_{max} = 1.36$.*

---

*A similar expression for the main exponential term was also obtained in Dreicer's paper.[4]

†Naturally, other cases are also possible when there is no such agreement. For example, in the case of statistical acceleration mechanisms estimates of the magnitude of the flux of runaway particles made with the aid of simple formulas of the type given above turned out to be completely useless.[5]

*It should be noted that if we use the calculation of F_{max} experimental values of the cross sections which, as is well known, are considerably lower in the neighborhood of the maximum than the theoretical ones,[7] then the value of the force

Further,

$$D(v) = \frac{N_n}{2m^2 v}\left\{\varepsilon_i(\varepsilon_i + \Delta\varepsilon)\,Q_i(v) + \sum_k (\hbar\omega_k)^2 Q_k(v)\right\}, \qquad (15)$$

is the coefficient characterizing the velocity diffusion of an electron. For subsequent discussion it is convenient to write this expression in the form

$$D(v) = \varepsilon_i F(v)\,d(v)\,/\,2m^2 v. \qquad (15a)$$

Here $d(v)$ turns out to be a very slowly varying dimensionless function of v; its values are close to unity. In the case of hydrogen, for example, $d(v) \approx \bar{d} = 0.94$, in the case of helium $\bar{d} = 0.99$.

Finally, $\nu_n(v)$ is the frequency of collisions of electrons with neutral particles:

$$\nu_n(v) = N_n \int Q(v, \theta)(1 - \cos\theta)\,d\Omega,$$

where $Q(v, \theta)$ is the differential cross section for the scattering of an electron by a molecule, including elastic scattering, excitation of all levels, and ionization.

The stationary electron distribution function in a weakly ionized plasma determined by Eq. (13) turns out qualitatively to be completely analogous to the distribution function in a strongly ionized plasma: with increasing velocity it falls off more and more slowly; at sufficiently high velocities it acquires a directed character. In the first approximation, just as in the case of the strongly ionized plasma, the distribution function is symmetric; it has the following form

$$f = f(v) = f(v_0)\exp\left\{-\frac{2m}{\varepsilon_i}\int_{v_0}^{v}\frac{v\,dv}{d(v)}\left[1 - \frac{eE}{F(v)}\right]\right\}, \qquad (16)$$

where v_0 is the lower limit starting at which Eq. (13) becomes valid: $v_0 \sim (5\epsilon_i/m)^{1/2}$; $f(v_0)$ is the distribution function at the boundary v_0. If, for example, the distribution for $v \leq v_0$ is Maxwellian in the temperature T_e, then we have*

$$f(v_0) = (m/2\pi kT_e)^{3/2} N_e \exp\{-mv_0^2/2kT_e\}.$$

For sufficiently high velocities $v > v_0$, the account of $f(v_0)$ naturally introduces only a small correction in expression (16) for the function $f(v)$.

As is clear from (16), the limit for the stationary solution $v = v_c$ is determined by the condition

$$F(v_c) = eE. \qquad (17)$$

From this it may be seen that the stationary solution exists only under the condition

$$E < E_{cn} = F_{max}/e = 4\pi e^3 N_n Z/2.72\,\bar{\varepsilon} \approx 7\cdot 10^{-15} N_n\ \mathrm{v/cm} \qquad (18)$$

Consequently the field E_{cn} is the critical field in a weakly ionized plasma.

When condition (18) is fulfilled only electrons of velocity greater than v_c are accelerated. Naturally, the flux of runaway electrons is in this case determined by the expression

$$S = -\frac{dN_e}{dt} = \frac{eE}{mv_c} v_T^3 f(v_0)\exp\left\{-\frac{2m}{\varepsilon}\int_{v_0}^{v}\frac{v\,dv}{d(v)}\left[1 - \frac{eE}{F(v)}\right]\right\}$$

$$\approx \frac{eE}{mv_c} v_T^3 f(v_0)\exp\left\{\frac{mv_0^2}{\bar{d}\varepsilon_i}\left(1 - \frac{E}{E_{cn}}\right)\right\}$$

$$\times\exp\left\{-\frac{2\pi e^3 N_n Z\ln(\overline{mv^2}/\bar{\varepsilon})}{E\varepsilon_i\bar{d}}\right\}, \qquad (19)$$

where $\overline{mv^2} \approx (0.3\text{ to }0.4)\,mv_c^2$, $v_T^2 = 2kT_e/m$. In the last expression we have taken into account the fact that the function d is practically independent of v and may be replaced by its average value $\bar{d}$. We note that the last exponential factor in (19) may also be represented in the form

$$\exp\left\{-\frac{E_{cn}}{4E}A\right\},$$

$$A = 8\pi e^4 N_n Z\ \ln\frac{\overline{mv^2}}{\bar{\varepsilon}}\Big/\varepsilon_i\bar{d}F_{max} \approx 5{,}4\,\bar{\varepsilon}\ln\frac{\overline{mv^2}}{\bar{\varepsilon}}\Big/\varepsilon_i\bar{d}.$$

Here the constant A turns out to be a very large quantity, $A \gtrsim 10$. This means that the flux of runaway particles for $E < E_{cn}$ is not large; it falls off very sharply with increasing ratio E_{cn}/E, considerably faster than in the case of a fully ionized plasma [cf. (12)]. Qualitatively the nature of the dependence of the flux of runaway electrons on the intensity of the field E in a weakly ionized plasma is almost the same as in a strongly ionized plasma, which is as it should be.

F_{max} is considerably diminished, while ε_{max} increases (for example, in helium such a calculation yields $\varepsilon_{max} = 120$ ev and $F_{max} = 6\times 10^{-26} N_n$ dynes, while formula (14) gives $F_{max} = 10\times 10^{-26} N_n$ dynes and $\varepsilon_{max} = 35$ ev). Moreover, the differential representation of the integral due to the inelastic collisions of an electron with atoms utilized in Eq. (13) is valid only at sufficiently high electron energies $\varepsilon \gg \varepsilon_i$. This condition is not sufficiently well satisfied even in the region of maximum retardation force, and more so when $\varepsilon < \varepsilon_{max}$. As a result of this the values of the force F_{max}, and, consequently, also of the field E_{cn} (cf. below) are determined here only very approximately. We also note that the expressions given here for the retarding force F and for the diffusion coefficient D are valid only at not too high plasma temperatures, when $\exp\{-\hbar\omega_k/kT\} \ll 1$; for $kT \gtrsim \hbar\omega_k \approx \varepsilon_i$ it is necessary to take into account that some of the molecules are in an excited state (cf. reference 3).

*For $v < v_0$ the distribution function $f(v)$ can, of course, differ considerably from Maxwellian. For example, in inert gases the Druyvesteyn distribution holds up to $\varepsilon \sim \varepsilon_i$, while above ε_i there applies a function $f(v)$ which falls off even more sharply with increasing velocity (cf., for example, reference 3).

b) Arbitrary degree of ionization. The equation for the electron distribution function in the domain of high velocities for an arbitrary degree of plasma ionization is completely analogous to Eqs. (1) and (13) discussed previously; only we must now take into account in this equation collisions both with neutral particles and with free electrons and ions. The stationary solution of this equation has at high velocities the same character as before; in the first approximation the following expression holds for f(v)

$$f(v) = f(v_0) \exp \left\{ - \int_{v_0}^{v} mv\, dv \frac{F(v) + mv\nu_e(v) - eE}{\varepsilon_i F(v)\, d(v)/2 + kT_e mv\nu_e(v)} \right\}, \tag{20}$$

where all the quantities have the same meaning as before.*

The boundary v_c of the domain in which the stationary solution is valid is determined by the condition

$$F(v_c) + mv_c\nu_e(v_c) - eE = 0, \tag{21}$$

and, correspondingly, in the first approximation the flux of runaway electrons is given by

$$S = R(v_c)\, v_T^3 f(v_0) \exp \left\{ - \int_{v_0}^{v_c} mv\, dv \frac{F(v) + mv\nu_e(v) - eE}{\varepsilon_i F(v)\, d(v)/2 + kT_e mv\nu_e(v)} \right\}, \tag{22}$$

where $R(v_c)$ is some effective frequency which varies from eE/mv_c to $\nu_{e0}(E/E_c)^{1/2}$ depending on the degree of plasma ionization. For sufficiently high degrees of plasma ionization [when the electron distribution in the principal domain of velocities is Maxwellian (cf. reference 3)] the exponential term in formula (22) can be written in the form $\exp\{-E_c/4E\}$; if the next approximation is also taken into account (cf. Sec. 2) the expression for the flux assumes the form

$$S = N_e \nu_{e0} (E/E_c)^{1/2} \exp\{-E_c/4E - \sqrt{2}(E_c/E)^{1/2}\}, \tag{23}$$

where E_c is the critical field:

$$E_c = 4\pi e^3 \Big(N_e \ln \frac{mv_c^2 D}{e^2} \\ + N_n Z \ln \frac{\overline{mv^2}}{\bar{\varepsilon}} \Big)^2 \Big/ \Big(kT_e N_e \ln \frac{mv_c^2 D}{e^2} + \frac{\varepsilon_i \bar{d}}{2} N_n Z \ln \frac{\overline{mv^2}}{\bar{\varepsilon}} \Big). \tag{24}$$

At high degrees of plasma ionization formula (23) agrees with (12), while at low degrees of ionization (in the first approximation) it agrees with (19), as it should.* At low temperatures $kT_e < \epsilon_i$ the field E_c increases monotonically with increasing degree of plasma ionization.

c) Instability of a spatially homogeneous plasma. It was shown above that the flux of runaway electrons in a plasma in the case of a relatively weak electric field increases sharply with increasing electron temperature and usually falls off with increasing degree of plasma ionization. Both these quantities vary appreciably in the course of the development of a discharge in a gas in a constant field. The flux of runaway electrons varies correspondingly.

It is obvious that the magnitude of the flux S is uniquely related to the value of the electron distribution function with respect to the velocity v_z (the z axis is parallel to the field **E**) in the domain of very high velocities, beyond the limit for runaway electrons $v_z^2 \gg v_c^2 = E_c kT_e/Em$:

$$F(v_z) = F\left(\frac{eE}{m}(t - t_0)\right) = \frac{m}{eE} S(t_0).$$

From this it follows that if the flux $S(t_0)$ decreases with time then the distribution function $F(v_z)$ acquires a region in which $\partial F/\partial v_z > 0$, since

$$\frac{\partial F}{\partial v_z} = -\frac{m}{eE}\frac{\partial F}{\partial t_0} = -\frac{m^2}{e^2E^2}\frac{dS}{dt_0}.$$

However, it is well known that a spatially homogeneous plasma may become unstable with respect to longitudinal excitations[8] (plasma waves) if the distribution function has a domain in which $\partial F/\partial v_z > 0$. The criterion for instability

$$\pi (\partial F/\partial v_z) v_z^2 \omega_0 / 2N_e\nu \gtrsim 1$$

can in our case be rewritten in the following form

$$(-dS/dt_0)(\Delta t)^2 \omega_0 / N_e\nu \gtrsim 1. \tag{25}$$

Here $\Delta t = t - t_0$ is the time which will have elapsed from the instant t_0 when the flux begins to decrease to the instant t when an instability will arise in the plasma; $\omega_0 = (4\pi e^2 N/m)^{1/2}$ is the plasma frequency. The characteristic size of the excited inhomogeneities is $\lambdabar \sim eE\Delta t/m\omega_0$ [the time Δt is determined by relation (25)]; their characteristic frequency is $\omega \approx \omega_0$.

An experimental investigation of runaway electrons in a helium plasma placed in a constant electric field was carried out in a stellarator.[9] In this case the electron temperature at first increased sharply, but later if the field was lower than $E_p \approx 1.5 \times 10^2 p_0$ v/cm it stayed for a certain length of time at an almost stationary level $kT_e \sim (0.5 \text{ to } 0.9)\epsilon_i$ (cf. references 10 and 11). During this period (the period of the temperature or the current "plateau") the degree of plasma ionization q_i continued to increase slowly. Therefore, the flux of runaway electrons diminished, since at a constant temperature the flux decreases with increasing degree of plasma ionization. Consequently it was maximum at a time close to the instant of formation of the plateau; in this case the field is given by $E_c = E_{c\,\min} \approx (50 \text{ to } 35)E$. Consequently, the total number of runaway (accelerated) electrons is given by*

---

*If the electrons in the principal stationary domain of velocities do not have a Maxwellian distribution, then in formula (20) we have to replace kT_e by $mv_T^2/3$, where $mv_T^2/2$ is the average electron energy.

*For low degrees of plasma ionization formulas (23) and (24) given here, which take the second approximation [i.e., terms of order $(E_c/E)^{1/2}$] into account, are valid only for hydrogen (Z = 1). For other gases the coefficient $\sqrt{2}$ in front of this term must be replaced by $\sqrt{Z+1}$; the index of the power of the ratio E/E_c in the factor preceding the exponential is also changed.

$$\Delta N_e = \int S dt \approx S\left(\frac{E_{c\,min}}{E}\right) \Big/ \frac{dq_i}{dt} \sim (10^{-7} - 10^{-5})\, N_e.$$

Further, in virtue of the fact that during the current "plateau" the flux of runaway electrons decreases with time, an instability of a spatially homogeneous plasma should arise. The criterion (25) for instability to occur will be satisfied after a time

$$\Delta t \sim \left(\frac{1}{\omega_0 dq_i/dt} \frac{N_e}{\Delta N_e}\right)^{1/2} \sim 10^{-4} - 10^{-5} \text{ sec}$$

elapsed since the beginning of a decrease in the flux. Consequently, such an instability must arise during the current "plateau". Experimentally,[9] bursts of hard x rays were observed just at this time, due to the impact of a large number of accelerated electrons against the walls of the vessel; they are generally accompanied by powerful microwave radiation from the discharge at frequencies $\omega \sim (1 \text{ to } 3) \times 10^{11}$ (under these conditions the plasma frequency is of the same order of magnitude). Apparently, it can be concluded that these bursts of radiation during the current "plateau" (according to the terminology of reference 9 — bursts of "type A") are a result of the mechanism for the instability of a homogeneous plasma indicated above.

We should also point out another type of instability produced by runaway electrons in an equilibrium plasma pinch confined by a strong longitudinal magnetic field.* This instability is associated with the inhomogeneity of the electron density in the pinch, and arises only in the case of a high degree of plasma ionization. Indeed, the electron density in an equilibrium pinch falls off as it approaches the boundary: $N_e \to 0$ as $r \to a$. Correspondingly the field $E_c(r)$ also decreases: $E_c(r) \to E_{cn}$ as $r \to a$, with E_{cn} being very small at sufficiently high degrees of plasma ionization. Therefore, even if in the principal region of the pinch the electric field E is weak ($E \ll E_c$), yet in a layer of thickness

$$\Delta r = EkT_e / 4\pi e^3 \left(\frac{\partial N_e}{\partial r}\right)_{r=a} \ln \frac{kT_e D}{e^2}$$

near the boundary of the pinch it is always strong ($E \gtrsim E_c$). In this layer, therefore, all the electrons run away at once. Therefore, in this region the plasma consists of a stream of electrons moving among the ions. As is well known,[8] such a system is unstable with respect to excitation of plasma waves as soon as the velocity of the electron stream v_0 exceeds their mean thermal velocity. If an instability arises the amplitude of those waves builds up most rapidly whose wavelength is given by $\lambda = v_0/\omega_0 = Dv_0/(kT_e/m)^{1/2}$. Their frequency ω is determined in this case by the following expression:

$$\omega \approx \left(EkT_e / 2^{7/3} e m^{1/3} M^{2/3} \ln \frac{kT_e D}{e^2}\right)^{1/2}$$
$$\approx 1.2 \cdot 10^9 \left(\frac{M_p}{M}\right)^{1/3} (kT_e)^{1/2} E^{1/2}. \qquad (26)$$

Here M is the ion mass, M_p is the proton mass; numerically kT_e is expressed in ev and E in v/cm. The velocity of the stream required for the excitation of the above instability, $v_0 \approx (2 \text{ to } 3)(kT_e/m)^{1/2}$, is attained after a time $\Delta t = mv_0/eE$ has elapsed since the electric field has been switched on. The excitation of such an instability must be accompanied by a burst of radiation at a frequency of order ω determined by formula (26), and also by a sharp decrease in the current associated with the runaway electrons, i.e., by a decrease of the total current I_0 by a quantity of order $I_0 \Delta r/a$. At the same time x rays may be completely absent since the instability is excited by electrons of low energy $\epsilon = mv_0^2/2 \sim (2 \text{ to } 5)kT_e$.

---

*The first of the numbers quoted here corresponds to the case $E = 0.6\, E_p$, the second corresponds to $E = 0.9\, E_p$ [in making these estimates the values of $T_e(q_i, E/E_p)$ calculated in reference 11 were utilized]. It should also be emphasized that the total number of runaway electrons is very sensitive to the parameters. For example, if the temperature or electron density is changed by 10% then ΔN_e changes by almost an order of magnitude. In virtue of this, an investigation of the flux of runaway particles (with respect to number and to the energy distribution of the fast electrons) could serve as a good method for the measurement of electron temperature.

*The whole investigation is carried out here without taking into account the magnetic field H_I due to the current itself. This is only valid in the presence of a strong external longitudinal magnetic field $H_0 \gg H_I$.

The author is grateful to V. L. Ginzburg and V. P. Silin for useful discussions.

---

[1] H. Dreicer, Phys. Rev. **115**, 238 (1959); Proc. II Int. Conf. Geneva, 1958. I. Bernstein and I. Rabinowitz, Proc. Conf. on Phys. of Plasma, Uppsala, 1959. L. M. Kovrizhnykh, JETP **37**, 1394 (1959), Soviet Phys. JETP **10**, 989 (1960). E. Harrison, Phil. Mag. **3**, 1318 (1958).

[2] L. D. Landau, JETP **7**, 203 (1937).

[3] V. L. Ginzburg and A. V. Gurevich, Usp. Fiz. Nauk 70, 201 (1960), Soviet Phys. Uspekhi **3**, 115 (1960). A. V. Gurevich, Изв. Высш. уч. зав. (News of the University—Radiophysics) **2**, 355 (1959).

[4] H. Dreicer, Phys. Rev. **117**, 329 (1960).

[5] A. V. Gurevich, JETP **38**, 1597 (1960), Soviet Phys. JETP **11**, 1150 (1960).

[6] L. D. Landau and E. M. Lifshitz, Электродинамика сплошных сред (Electrodynamics of Continuous Media), Gostekhizdat, 1957, § 84. L. D. Landau and E. M. Lifshitz, Quantum Mechanics, Pergamon, 1958, § 121. H. Bethe, Ann. Physik **5**, 325 (1930). F. Bloch, Z. Physik **81**, 363 (1933).

[7] H. S. W. Massey and E. Burhop, Electron and Ion Collisions (Russ. Transl.) IIL, 1958.

[8] A. I. Akhiezer and Ya. B. Faĭnberg, JETP **21**, 1262 (1951). G. V. Gordeev, JETP **27**, 19, 24 (1954).

[9] Bernstein, Chen, Heald, and Kranz, Phys. Fluids **1**, 430 (1958).

[10] Coor, Cunningham, Ellis, Heald, and Kranz, Phys. Fluids **1**, 411 (1958).

[11] A. V. Gurevich, JETP **38**, 165 (1960), Soviet Phys. JETP **11**, 120 (1960).

Translated by G. Volkoff
241

SOVIET PHYSICS JETP VOLUME 12, NUMBER 5 MAY, 1961

ON THE THEORY OF THE MAGNETIC PROPERTIES OF A NONIDEAL FERMI GAS AT LOW TEMPERATURES

I. A. AKHIEZER and S. V. PELETMINSKIĬ

Physico-Technical Institute, Academy of Sciences, Ukrainian S.S.R.

Submitted to JETP editor May 25, 1960

J. Exptl. Theoret. Phys. (U.S.S.R.) **39**, 1308-1316 (November, 1960)

The methods of quantum field theory are used to study the effect of the interaction between particles on the oscillations of the magnetic moment of a Fermi gas. The forces between the particles are assumed to be of the short-range type, and the calculations are made in the gas approximation. Values are found for the changes of period and amplitude of the oscillations of the magnetic moment that are caused by the interaction between particles. At not too low temperatures the amplitude of the oscillations contains a factor that decreases exponentially with decrease of the magnetic field.

1. In the study of the magnetic properties of a degenerate Fermi gas the interaction between particles is usually taken into account only by the introduction of a generalized dispersion law to replace the free-particle relation between energy and momentum (L. D. Landau,[1] I. M. Lifshitz and A. M. Kosevich[2]). A paper by Dingle[3] has been devoted to effects of the finite widths of the energy levels of the particles, which are also due to the interaction, but in this paper the width is introduced in a purely formal way and is assumed to be the same for all levels.

Therefore it is interesting to study the effects of the interaction between particles on the magnetic properties of a Fermi gas in the framework of the microscopic theory.

In the present paper we examine this problem for the simplest model, assuming that the interaction between the particles is of the short-range type. Our final results apply to the domain of not too low temperatures [cf. the condition (13)], at which the influence of the magnetic field on the collisions of the particles can be neglected. This condition, however, is used only at the last stage of the calculation as we have arranged it, so that it is possible to study the character of the approximation and find the region of applicability of the results.

2. The thermodynamic quantities that characterize a system of interacting particles can be obtained by means of the one-particle thermodynamic Green's function

$$G(\mathbf{r}_1, \mathbf{r}_2; t_1 - t_2) = \langle T\{\psi(\mathbf{r}_1, t_1)\psi^+(\mathbf{r}_2, t_2)S(\beta)\}\rangle\langle S(\beta)\rangle^{-1}, \qquad (1)$$

where ψ^+, ψ are the operators for creation and annihilation of Fermi particles in the "thermodynamic interaction representation," $S(\beta)$ is the thermodynamic scattering matrix (β is the reciprocal of the temperature), and the averaging is carried out with the density matrix of noninteracting particles.

The quantity most simply expressed in terms of the Green's function is the density of the gas,

$$\mathfrak{N} = -\frac{\partial}{\partial\mu}\Omega = -\operatorname{Sp} G(\mathbf{r}, \mathbf{r}; -0), \qquad (2)$$

where $\mu = p_0^2/2m$ is the chemical potential and Ω is the thermodynamic potential per unit volume of the gas. Knowing the Green's function G, we can use this formula to find Ω and then calculate the magnetic moment per unit volume, which is given by

$$M = -\frac{\partial}{\partial\mathcal{H}}\Omega = -\frac{e}{mc}\frac{\partial}{\partial\omega}\Omega, \qquad (3)$$

where $\omega = e\mathcal{H}/mc$ is the Larmor frequency of a particle in the magnetic field $\mathcal{H}$.

Following the work of Abrikosov, Gor'kov, and Dzyaloshinskiĭ[4] and of Fradkin,[5] we expand the function $G(\mathbf{r}_1, \mathbf{r}_2; t)$ in Fourier series with respect to the variable t:

$$G(\mathbf{r}_1, \mathbf{r}_2; t) = \frac{1}{\beta}\sum_{p_4} G(\mathbf{r}_1, \mathbf{r}_2; p_4)e^{-ip_4 t}$$

$$\left(p_4 = \frac{2k+1}{\beta}\pi, \quad k = 0, \pm 1, \ldots\right).$$

Using the fact that the Green's function $G(\mathbf{r}_1, \mathbf{r}_2; t)$ has a discontinuity at the point $t = 0$,

$$G(\mathbf{r}_1, \mathbf{r}_2; +0) - G(\mathbf{r}_1, \mathbf{r}_2; -0) = \delta(\mathbf{r}_1 - \mathbf{r}_2),$$

we get:

$$\frac{1}{\beta}\sum_{p_4} G(\mathbf{r}_1, \mathbf{r}_2; p_4) = \tfrac{1}{2}\{G(\mathbf{r}_1, \mathbf{r}_2; +0) + G(\mathbf{r}_1, \mathbf{r}_2; -0)\}$$
$$= G(\mathbf{r}_1, \mathbf{r}_2; -0) + \tfrac{1}{2}\delta(\mathbf{r}_1 - \mathbf{r}_2).$$

Therefore the formula (2) can be rewritten in the form

$$\mathfrak{N} = -\lim_{\mathbf{r}_2\to\mathbf{r}_1} \mathrm{Sp}\left\{\frac{1}{\beta}\sum_{p_4} G(\mathbf{r}_1, \mathbf{r}_2; p_4) - \tfrac{1}{2}\delta(\mathbf{r}_1 - \mathbf{r}_2)\right\}. \quad (4)$$

To calculate the Green's function G we shall use the Feynman-diagram method, using a solid line for the Green's function of noninteracting particles in the magnetic field, $G_0(\mathbf{r}_1, \mathbf{r}_2; t_1 - t_2)$, and a dashed line for the interaction potential $V(\mathbf{r}_1 - \mathbf{r}_2)\,\delta(t_1 - t_2)$. The function $G_0(\mathbf{r}_1, \mathbf{r}_2; p_4)$ is of the following form:

$$G_0(\mathbf{r}_1, \mathbf{r}_2; p_4) = \sum_\alpha \frac{\psi_\alpha(\mathbf{r}_1)\,\psi_\alpha^*(\mathbf{r}_2)}{\varepsilon_\alpha - \mu + ip_4} \equiv \sum_\alpha \psi_\alpha(\mathbf{r}_1)\,G_0(\alpha; p_4)\,\psi_\alpha^*(\mathbf{r}_2), \quad (5)$$

where $\alpha \equiv (n, p_z, q)$ is a set of quantum numbers for the particle in the magnetic field*

$$\varepsilon_\alpha = \omega\left(n + \tfrac{1}{2}\right) + p_z^2/2m,$$
$$\psi_\alpha(\mathbf{r}) = (2\pi)^{-1}\exp\{i(p_z z + qy)\}\,\Phi_n(x - q/m\omega),$$

and $\Phi_n(x)$ are the wave functions of an oscillator with the frequency ω.

Noting that

$$\int_{-\infty}^{\infty} d\xi e^{i\xi m\omega y}\Phi_n\left(\xi + \frac{x}{2}\right)\Phi_n\left(\xi - \frac{x}{2}\right)$$
$$= \exp\left\{-\frac{m\omega}{4}(x^2 + y^2)\right\} L_n\left\{\frac{m\omega}{2}(x^2 + y^2)\right\}$$

[$L_n(x)$ are the Laguerre polynomials], we bring Eq. (5) into the form

$$G_0(\mathbf{r}_1, \mathbf{r}_2; p_4) = \exp\left\{i\frac{x_1 + x_2}{2}(y_1 - y_2)\,m\omega\right\}\frac{m\omega}{(2\pi)^2}$$
$$\times \sum_{n=0}^{\infty}\exp\left\{-\frac{m\omega}{4}[(x_1 - x_2)^2 + (y_1 - y_2)^2]\right\} L_n\left\{\frac{m\omega}{2}[(x_1 - x_2)^2 + (y_1 - y_2)^2]\right\}\int_{-\infty}^{\infty} dp_z \frac{\exp\{ip_z(z_1 - z_2)\}}{\omega(n + {}^1\!/_2) + p_z^2/2m - \mu + ip_4}.$$

By considering an arbitrary diagram for the one-particle Green's function, one can verify without difficulty that $G(\mathbf{r}_1, \mathbf{r}_2; p_4)$ is of the form

$$G(\mathbf{r}_1, \mathbf{r}_2; p_4) = \exp\left\{\tfrac{1}{2}i(x_1 + x_2)(y_1 - y_2)\,m\omega\right\} G(\mathbf{r}_1 - \mathbf{r}_2; p_4), \quad (6)$$

where $G(\mathbf{r}_1 - \mathbf{r}_2; p_4)$ is a function that involves only the difference of the coordinates, $\mathbf{r}_1 - \mathbf{r}_2$.

Let us expand the Green's function $G(\mathbf{r}_1, \mathbf{r}_2; p_4)$ in terms of the functions $\psi_\alpha(\mathbf{r})$. We get:

$$G(\mathbf{r}_1, \mathbf{r}_2; p_4) = \sum_{\alpha_1, \alpha_2} \psi_{\alpha_1}(\mathbf{r}_1)\,\psi_{\alpha_2}^*(\mathbf{r}_2)\,G(\alpha_1, \alpha_2; p_4).$$

It follows from Eq. (6) that the Green's function in the α representation is diagonal in the variables p_z, q:

$$G(\alpha_1, \alpha_2; p_4) = \delta(p_{z1} - p_{z2})\,\delta(q_1 - q_2)\,G(n_1, n_2; p_{z1}; p_4),$$

where the function $G(n_1, n_2; p_z; p_4)$ does not depend on the variable q.

The density of the gas, defined by the formula (4), is expressed in terms of the function $G(n_1, n_2; p_z; p_4)$ in the following way:

$$\mathfrak{N} = -\frac{m\omega}{(2\pi)^2}\,\mathrm{Sp}\sum_{n=0}^{\infty}\int_{-\infty}^{\infty} dp_z\left\{\frac{1}{2}\sum_{p_4} G(n, n; p_z; p_4) - \frac{1}{2}\right\}. \quad (7)$$

3. The Green's function $G(\mathbf{r}_1, \mathbf{r}_2; p_4)$ satisfies the well known equation

$$(H_0 - \mu + ip_4)\,G(\mathbf{r}_1, \mathbf{r}_2; p_4)$$
$$+ \int d\mathbf{r}'\,\Sigma(\mathbf{r}_1, \mathbf{r}'; p_4)\,G(\mathbf{r}', \mathbf{r}_2; p_4) = \delta(\mathbf{r}_1 - \mathbf{r}_2),$$

where H_0 is the Hamiltonian of a free particle in the magnetic field and Σ is the mass operator which takes account of the interaction between the particles. In the α representation this equation takes the form

$$(\varepsilon_{\alpha_1} - \mu + ip_4)\,G(\alpha_1, \alpha_2; p_4)$$
$$+ \sum_{\alpha'} \Sigma(\alpha_1, \alpha'; p_4)\,G(\alpha', \alpha_2; p_4) = \delta_{\alpha_1\alpha_2}. \quad (8)$$

We shall calculate the mass operator Σ in the gas approximation (cf. the paper by Galitskiĭ[6]). Then, as can be seen from the diagrams shown in Fig. 1 (which have weight factors − 2 and 1, respectively), the quantity Σ can be connected with the four-fermion vertex function Γ:

$$\Sigma(\alpha_1, \alpha_2; p_4) = \frac{1}{\beta}\sum_{p_4'; \alpha_3} G_0(\alpha_3; p_4')$$
$$\times \{\Gamma(\alpha_1, \alpha_3; \alpha_3, \alpha_2; p_4 + p_4')$$
$$- 2\Gamma(\alpha_1, \alpha_3; \alpha_2, \alpha_3; p_4 + p_4')\}. \quad (9)$$

(The function Γ corresponds to the shaded squares in the diagrams.)

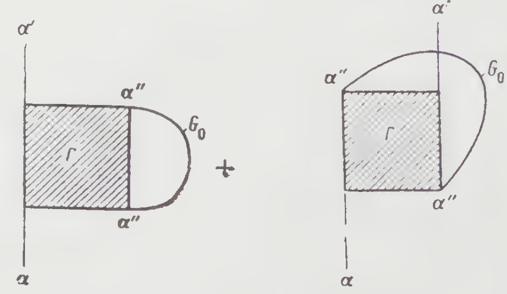

FIG. 1

---

*Here and hereafter ħ = 1.

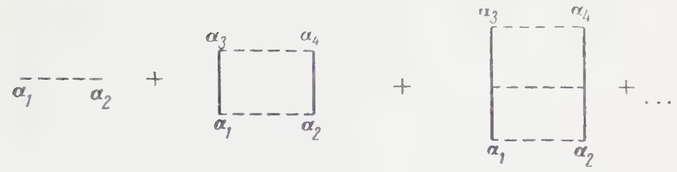

FIG. 2

In the gas approximation the quantity Γ corresponds to the set of diagrams shown in Fig. 2. As was stated above, the solid lines in the diagrams correspond to the function $G_0(\mathbf{r}_1, \mathbf{r}_2; p_4)$ and the dashed lines to the function $V(\mathbf{r}_1 - \mathbf{r}_2)$. Applying the method developed by Galitskiĭ,[6] we can get the equation satisfied by the operator $\Gamma(p_4)$:

$$\Gamma(p_4) = \Gamma_0(p_4) + \Gamma_0(p_4)\frac{\mathfrak{N}_1 + \mathfrak{N}_2}{H_1^0 + H_2^0 - 2\mu - ip_4}\Gamma(p_4),$$

$$\Gamma_0(p_4) = V - V[H - 2\mu - ip_4]^{-1}V. \qquad (10)$$

Here H_1^0 and H_2^0 are the Hamiltonians of the first and second particles in the magnetic field in the absence of interaction; $H = H_1^0 + H_2^0 + V$; and

$$\mathfrak{N}_{1,2} = [1 + \exp\{\beta(H_{1,2}^0 - \mu)\}]^{-1}.$$

The quantity $\Gamma(\alpha_1, \alpha_2; \alpha_3, \alpha_4; p_4)$ is the matrix element of the operator $\Gamma(p_4)$ in the α representation:

$$\Gamma(\alpha_1, \alpha_2; \alpha_3, \alpha_4; p_4) = \langle\alpha_1, \alpha_2|\Gamma(p_4)|\alpha_3, \alpha_4\rangle.$$

We now note that in the Schrödinger equation for two interacting particles in a constant magnetic field one can separate the variables belonging to the center of mass and to the relative motion of the particles. Therefore it is convenient to go over to a representation in which both the Hamiltonian that describes the motion of the center of mass, and the Hamiltonian that describes the relative motion of two noninteracting particles, are diagonal. In this representation the matrix element of the operator $\Gamma_0(p_4)$ has the form

$$\langle\alpha A|\Gamma_0(p_4)|\alpha' A'\rangle = \delta_{AA'}\Gamma_0(\alpha, \alpha'; p_4),$$

where $\alpha \equiv (n, p_z, q)$ is a set of quantum numbers for a particle with the mass $m/2$ and the charge $e/2$, and $A \equiv (N, P_z, Q)$ is a set of quantum numbers for a particle with the mass $2m$ and the charge $2e$, in the magnetic field $\mathcal{H}$.

The quantity $\Gamma_0(\alpha, \alpha'; p_4)$ can be connected with the amplitude $T_{\alpha\alpha'}$ for the scattering of particles with the mass $m/2$ and the charge $e/2$ by the short-range potential $V(\mathbf{r})$ in the magnetic field $\mathcal{H}$:

$$\Gamma_0(\alpha, \alpha'; p_4) = T^*_{\alpha'\alpha} + \sum_{\alpha''} T_{\alpha\alpha''}T^*_{\alpha'\alpha''}\left\{\frac{1}{\varepsilon_{\alpha''} - \varepsilon_\alpha + i0} - \frac{1}{\varepsilon_{\alpha''} + \varepsilon_A - 2\mu - ip_4}\right\},$$

$$\varepsilon_\alpha = \omega\left(n + \tfrac{1}{2}\right) + p_z^2/m, \qquad \varepsilon_A = \omega\left(N + \tfrac{1}{2}\right) + P_z^2/4m. \qquad (11)$$

4. The scattering amplitude $T_{\alpha\alpha'}$, which has been calculated in a paper by Skobov,[7] is of the form

$$T_{\alpha\alpha'} = \frac{f_0}{\pi m}\varphi_n\left(-\frac{2q}{m\omega}\right)\varphi_{n'}\left(-\frac{2q'}{m\omega}\right)\frac{1}{1 + if_0K(\varepsilon_\alpha)}, \qquad (12)$$

where $\varphi_n(x)$ is a wave function of an oscillator with the mass $m/2$ and the frequency ω, f_0 is the scattering amplitude of particles of zero energy in the absence of the magnetic field, and

$$K(\varepsilon) = \frac{m\omega}{2}\sum_{n=0}^{n_0}[m\omega(n_0 - n - \xi)]^{-1/2}$$

(the quantities n_0 and ξ are connected with the energy ϵ by the relation $\epsilon = \omega(n_0 + 1/2 - \xi)$, $0 < \xi \leq 1$).

Thus to determine the Green's function in the gas approximation it is necessary to calculate the quantity $\Gamma_0(\alpha, \alpha', p_4)$, using the expression (12) for $T_{\alpha\alpha'}$, and then, in accordance with Eqs. (9) and (10), to find the mass operator Σ that appears in (8). It follows from the expression for $K(\epsilon)$ that the quantity $f = f_0(1 + if_0K)^{-1}$ differs from f_0 only in the regions $0 < \xi < \xi_0$ and $1 - \xi_0 < \xi < 1$, where $\xi_0 = 1/4 m\omega f_0^2$. In the formula (9) for the mass operator Σ the main contribution for $\beta^{-1} \ll \mu$ obviously comes from the energy range $\mu - 1/2\beta^{-1} \lesssim \epsilon_\alpha \lesssim \mu + 1/2\beta^{-1}$; therefore if the conditions $\xi_0 \ll 1$ and $\beta^{-1} \gg \omega\xi_0$ are satisfied we can neglect the difference between f and f_0. In what follows we shall assume that these conditions are satisfied.

For $\beta^{-1} \lesssim \omega\xi_0$ the difference between the quantities f and f_0 can be important, since the region in which the step of the Fermi function is smeared out can enter one of the intervals $(0, \xi_0)$ or $(1 - \xi_0, 1)$. In the present paper, however, we shall not consider this low a range of temperatures.

As is customary in the study of the magnetic properties of a Fermi gas, we shall assume the magnetic field weak enough so that $\omega \ll \mu$. Thus we are assuming that the following conditions are satisfied:

$$p_0 f_0 \ll 1, \qquad \omega/\mu \ll 1, \qquad (\omega/\mu)^2(p_0 f_0)^2 \ll (\beta\mu)^{-1} \ll 1. \qquad (13)$$

The scattering amplitude then takes the form

$$T_{\alpha\alpha'} = \frac{f_0}{\pi m}\varphi_n\left(-\frac{2q}{m\omega}\right)\varphi_{n'}\left(-\frac{2q'}{m\omega}\right).$$

Since $\omega \ll \mu$, large quantum numbers n are important; therefore in Eq. (11) we replace the summation over n″ by an integration over k_t, where $k_t^2/m = \omega(n'' + 1/2)$, $\mathbf{k} \equiv (\mathbf{k}_t, k_z)$:

$$\Gamma_0(\alpha, \alpha'; p_4) = \frac{1}{(2\pi)^2}\varphi_n\left(-\frac{2q}{m\omega}\right)\varphi_{n'}\left(-\frac{2q'}{m\omega}\right)$$

$$\times\left\{\frac{f_0}{m} + \frac{f_0^2}{m^2}\int\frac{d\mathbf{k}}{(2\pi)^3}\left[\frac{1}{\frac{1}{m}k^2 - \varepsilon_\alpha + i0}\right.\right.$$

$$\left.\left.-\frac{1}{\frac{1}{m}k^2 + \varepsilon_A - 2\mu - ip_4}\right]\right\}.$$

The fractional error so introduced is of the order of $(\omega/\mu)^{1/2}$, and by the conditions (13) it is small. In fact, let us use the Poisson summation formula

$$\sum_{n=0}^{\infty} F(n + 1/2) = \int_0^\infty F(x)\,dx + 2\sum_{r=1}^{\infty}(-1)^r\int_0^\infty F(x)\cos 2\pi r x\,dx. \tag{14}$$

In the case in question, by Eqs. (11) and (12), the function F(x) is

$$F(x) = f_0^2\int_{-\infty}^{\infty}dk_z\left\{\frac{1}{k_z^2/m + \omega x - \varepsilon_\alpha + i0}\right.$$

$$\left.-\frac{1}{k_z^2/m + \omega x + \varepsilon_A - 2\mu - ip_4}\right\}\int_{-\infty}^{\infty}dq''\,\frac{[\varphi_n(-2q''/m\omega)]^2}{(2\pi)^2}$$

$$= \frac{m\omega}{2(2\pi)^2}f_0^2\int_{-\infty}^{\infty}\left\{\frac{1}{k_z^2/m + \omega x - \varepsilon_\alpha + i0}\right.$$

$$\left.-\frac{1}{k_z^2/m + \omega x + \varepsilon_A - 2\mu - ip_4}\right\}dk_z.$$

Making the change of variable $\omega x = k_t^2/m$ and integrating over the angles of the vector $\mathbf{k} = (\mathbf{k}_t, k_z)$, one easily verifies that the ratio of the sum of the oscillating terms in Eq. (14) to the first term, which we are keeping, is of the order of $(\omega/\mu)^{1/2}$.

Writing the operator equation (10) in the α representation and replacing the summation over the indices n, n′, N, n_3 in this equation and in the relation (9) by integration over the variables p_t, p_t', P_t, p_{t3}, with

$$p_t^2/m = \omega(n + 1/2), \quad p_t'^2/m = \omega(n' + 1/2),$$

$$P_t^2/4m = \omega(N + 1/2), \quad p_{t3}^2/2m = \omega(n_3 + 1/2)),$$

we get

$$\Sigma(\alpha_1, \alpha_2; p_4) = \delta(p_{z1} - p_{z2})\,\delta(q_1 - q_2)\,\delta_{n_1 n_2}\Sigma(\mathbf{p}_1, p_4),$$

$$\Sigma(\mathbf{p}, p_4) = -\frac{f_0^2}{m^2}\int\frac{d\mathbf{p}'d\mathbf{k}}{(2\pi)^6}\left\{1 - \mathfrak{N}\left(\frac{\mathbf{p}+\mathbf{p}'}{2} + \mathbf{k}\right)\right.$$

$$\left.-\mathfrak{N}\left(\frac{\mathbf{p}+\mathbf{p}'}{2} - \mathbf{k}\right)\right\}\left\{\mathfrak{N}(\mathbf{p}') + \left[\exp\beta\left(\frac{k^2}{m} + \frac{[\mathbf{p}+\mathbf{p}']^2}{4m} - 2\mu\right)\right.\right.$$

$$\left.\left.-1\right]^{-1}\right\}\frac{1}{k^2/m - (\mathbf{p}-\mathbf{p}')^2/4m - \mu + p^2/2m + ip_4} + \frac{f_0}{m}\int\frac{d\mathbf{p}'}{(2\pi)^3}$$

$$\times\mathfrak{N}(\mathbf{p}') + \frac{f_0^2}{m^2}\,\mathrm{P}\int\frac{d\mathbf{p}'d\mathbf{k}}{(2\pi)^6}\,\mathfrak{N}(\mathbf{p}')\,\frac{1}{k^2/m - (\mathbf{p}-\mathbf{p}')^2/4m}, \tag{15}$$

where

$$\mathfrak{N}(\mathbf{p}) = [1 + \exp\{\beta(p^2/2m - \mu)\}]^{-1}$$

and the quantum number n_1 is connected with the variable p_1 by the relation $p_{t1}^2/2m = \omega(n_1 + 1/2)$.

By making estimates as we did for the calculation of $\Gamma_0(\alpha, \alpha'; p_4)$, we can verify that the terms omitted in the function $\Sigma(\alpha_1, \alpha_2; p_4)$ do not exceed $(\omega/\mu)^{1/2}(p_0 f_0)^2\mu$. Also it follows from Eq. (15) that

$$\mathrm{Re}\,\Sigma(\mathbf{p}, p_4) = \mathrm{Re}\,\Sigma(\mathbf{p}, -p_4);$$

$$\mathrm{Im}\,\Sigma(\mathbf{p}; p_4) = -\mathrm{Im}\,\Sigma(\mathbf{p}; -p_4). \tag{16}$$

We note that the quantity $\Sigma(\mathbf{p}, p_4)$ does not depend on the angles of the vector **p** and has different analytical forms in different ranges of variation of the variables p and p_4. It is important that in the first approximation in the gas parameter $p_0 f_0$ this quantity is real and positive; the difference between the analytical expressions for Σ in the different ranges of p, p_4 arises only in the second gas approximation.

In what follows we shall need the value of the mass operator[*] $\Sigma(\mathbf{p}, p_4)$ for $ip_4 = \mu - p^2/2m$ in the region of negative and nearly zero values of the quantity $p - p_0$ ($|p - p_0| \ll p_0$):

$$\Sigma\left(p,\ i\frac{p^2}{2m} - i\mu\right) = -\Delta\mu + \frac{m^* - m}{m}\left(\frac{p^2}{2m} - \mu\right)$$

$$-\frac{i}{\tau}\left[1 + \frac{2}{\pi^2}\beta^2\left(\frac{p^2}{2m} - \mu\right)^2\right]; \tag{17}$$

$$-\frac{\Delta\mu}{\mu} = \frac{4}{3\pi}(p_0 f_0)\left[1 + \frac{11 - 2\ln 2}{5\pi}(p_0 f_0)\right],$$

$$\frac{m^*}{m} = 1 + \frac{8}{15\pi^2}(p_0 f_0)^2(7\ln 2 - 1), \quad \tau^{-1} = \frac{\pi}{4}\,\frac{1}{\mu\beta^2}(p_0 f_0)^2. \tag{18}$$

Substituting the expression (15) for Σ in Eq. (8), we find the Green's function

$$G(\alpha_1, \alpha_2; p_4) = \frac{\delta_{\alpha_1\alpha_2}}{\varepsilon_{\alpha_1} - \mu + ip_4 + \Sigma(\mathbf{p}, p_4)};$$

$$\frac{p_t}{2m} = \omega\left(n_1 + \frac{1}{2}\right). \tag{19}$$

5. Applying the Poisson summation formula (14), we rewrite the relation (7) in the form

$$\mathfrak{N} = \mathfrak{N}_0 + 2\sum_{r=1}^{\infty}(-1)^r\mathfrak{N}_r,$$

where

$$\mathfrak{N}_r = -\frac{2m\omega}{(2\pi)^2}\int_{-\infty}^{\infty}dp_z\int_0^\infty dx\left\{\frac{1}{\beta}\sum_{p_4}G\left(x - \frac{1}{2},\ x - \frac{1}{2};\ p_z;\ p_4\right)\right.$$

$$\left.-\frac{1}{2}\right\}\cos 2\pi r x.$$

---

[*] The expression for the mass operator at temperature equal to zero has been obtained in a paper by V. Galitskiĭ.[6]

Making the change of variable $\omega x = p_t^2/2m$ and using the formula (19) for G, we get

$$\mathfrak{N}_r = -\frac{2}{(2\pi)^8}\int d\mathbf{p}\left\{\frac{1}{\beta}\sum_{p_4}\frac{1}{p^2/2m-\mu+ip_4+\Sigma(p,\ p_4)}\right.$$
$$\left.-\frac{1}{2}\right\}\cos\frac{\pi r p_t^2}{m\omega}. \qquad (20)$$

The quantity $\mathfrak{N}_r$ is real in virtue of the relations (16).

We note that by neglecting the oscillating terms in Σ we incur a fractional error of the order $(p_0f_0)^2$ in $\mathfrak{N}_r$.

Integrating over the angles of the vector $\mathbf{p}$ in the formula (20) and dropping the nonoscillating terms, we rewrite $\mathfrak{N}_r$ in the form

$$\mathfrak{N}_r^{osc} = -\frac{m}{2\pi^2}\left(\frac{m\omega}{r}\right)^{1/2}\operatorname{Re}\exp\left(\frac{2\pi ir\mu}{\omega}\right.$$
$$\left.-\frac{\pi i}{4}\right)\frac{1}{\beta}\sum_{p_4}\int_{-\infty}^{\infty}\frac{e^{2\pi irz/\omega}}{z+ip_4+\Sigma(z,\ p_4)}\,dz, \qquad (21)$$

where $z = p^2/2m - \mu$.

To calculate the integral that appears in Eq. (21), we introduce an analytic function $\tilde{\Sigma}(z,\ p_4)$ that coincides with the function $\Sigma(z,\ p_4)$ in the region of negative values of z close to zero. Using the fact that for $\beta\mu \gg 1$ the main contribution to the integral in question comes from the region of small negative values of z, to accuracy $(p_0f_0)^2$ we can replace the integration of the function $e^{2\pi irz/\omega}[z + ip_4 + \Sigma(z,\ p_4)]^{-1}$ along the real axis by integration of the function $e^{2\pi irz/\omega}[z + ip_4 + \tilde{\Sigma}(z,\ p_4)]^{-1}$ around the contour shown in Fig. 3. According to Eq. (17) the pole of the integrand is given to accuracy $(p_0f_0)^2$ by the expression

$$z_0(p_4) = -ip_4m^*/m + \Delta\mu - i\tau^{-1}(1 - 2\beta^2p_4^2/\pi^2),$$

and to accuracy $(p_0f_0)^2$ the residue at the point z_0 is unity. Therefore the final expression for $\mathfrak{N}_r^{osc}$ is

$$\mathfrak{N}_r^{osc} = \frac{m}{\pi}\left(\frac{m\omega}{r}\right)^{1/2}\frac{1}{\beta}\sin\left[\frac{2\pi r}{\omega}(\mu+\Delta\mu)-\frac{\pi}{4}\right]$$
$$\times\sum_{k=0}^{\infty}\exp\left\{-\frac{2\pi^2r}{\beta\omega}\,\frac{m^*}{m}(2k+1)-\frac{4\pi r}{\omega\tau}\left[(2k+1)^2-\frac{1}{2}\right]\right\}. \qquad (22)$$

Integrating the expression (22) for the density of the Fermi gas with respect to μ and neglecting terms proportional to the gas parameter p_0f_0, we get the following expression for Ω, the thermodynamic potential per unit volume:

$$\Omega = \Omega_0 + 2\sum_{r=1}^{\infty}(-1)^r\Omega_r,$$

$$\Omega_r^{osc} = \frac{1}{2\pi^2}\left(\frac{m\omega}{r}\right)^{3/2}\frac{1}{\beta}\cos\left[\frac{2\pi r}{\omega}(\mu+\Delta\mu)-\frac{\pi}{4}\right]$$
$$\times\sum_{k=0}^{\infty}\exp\left\{-\frac{2\pi^2r}{\beta\omega}\,\frac{m^*}{m}(2k+1)-\frac{4\pi r}{\omega\tau}\left[(2k+1)^2-\frac{1}{2}\right]\right\}. \qquad (23)$$

Using the formula (3), we find the oscillating part of the magnetic moment

$$M_r^{osc} = -\frac{1}{\pi}\,\frac{e}{c}\left(\frac{m}{r\omega}\right)^{1/2}\frac{\mu}{\beta}\sin\left[\frac{2\pi r}{\omega}(\mu+\Delta\mu)-\frac{\pi}{4}\right]$$
$$\times\sum_{k=0}^{\infty}\exp\left\{-\frac{2\pi^2r}{\beta\omega}\,\frac{m^*}{m}(2k+1)-\frac{4\pi r}{\omega\tau}\left[(2k+1)^2-\frac{1}{2}\right]\right\}. \qquad (24)$$

6. If the condition $\omega\tau \gg 1$ is satisfied, as it is in the temperature range

$$\mu(\omega/\mu)^2(p_0f_0)^2 \ll \beta^{-1} \ll \mu(\omega/\mu)^{1/2}(p_0f_0)^{-1},$$

the formula (24) takes the form

$$M_r^{osc} = -\frac{1}{2\pi}\,\frac{e}{c}\left(\frac{m}{r\omega}\right)^{1/2}\frac{\mu}{\beta}\sin\left[\frac{2\pi r}{\omega}(\mu\right.$$
$$\left.+\Delta\mu)-\frac{\pi}{4}\right]\sinh^{-1}\frac{2\pi^2r}{\beta\omega}\,\frac{m^*}{m}. \qquad (25)$$

This same sort of expression for the oscillating part of the magnetic moment is obtained, according to a paper by I. M. Lifshitz and Kosevich,[2] if one starts from a dispersion law which is of the form

$$\varepsilon(p) = \frac{1}{2m}p^2 - \Delta\mu + \frac{m^*-m}{m}\,\frac{p_0}{m}(p-p_0)$$

near the Fermi surface.

In the temperature range $\mu \gg \beta^{-1} \gtrsim \mu(\omega/\mu)^{1/2} \times (p_0f_0)^{-1}$ we can confine ourselves to the first term of the sum in Eq. (24). This gives a formula for M_r^{osc} which is analogous to that obtained in a paper by Dingle,[3]

$$M_r^{osc} = -\frac{1}{\pi}\,\frac{e}{c}\left(\frac{m}{r\omega}\right)^{1/2}\frac{\mu}{\beta}\sin\left[\frac{2\pi r}{\omega}(\mu\right.$$
$$\left.+\Delta\mu)-\frac{\pi}{4}\right]\exp\left\{-\frac{2\pi^2r}{\beta\omega}\,\frac{m^*}{m}-\frac{2\pi r}{\omega\tau}\right\}, \qquad (26)$$

where $\Delta\mu$, m^*, and τ are defined by the formulas (18).

The writers express their gratitude to A. I. Akhiezer and I. M. Lifshitz for valuable advice, and to Yu. A. Bychkov for helpful discussions.

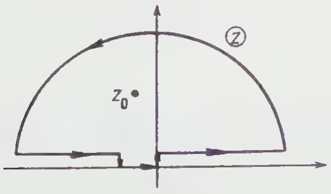

FIG. 3

---

[1] Appendix to article by D. Shoenberg, Proc. Roy. Soc. **A170**, 341 (1939).

[2] I. M. Lifshitz and A. M. Kosevich, Doklady Akad. Nauk SSSR **96**, 963 (1954).

[3] R. B. Dingle, Proc. Roy. Soc. **A211**, 517 (1952).

[4] Abrikosov, Gor'kov, and Dzyaloshinskiĭ, JETP **36**, 900 (1959), Soviet Phys. JETP **9**, 636 (1959).

[5] E. S. Fradkin, JETP **36**, 1286 (1959), Soviet Phys. JETP **9**, 912 (1959).

[6] V. M. Galitskiĭ, JETP **34**, 151 (1958), Soviet Phys. JETP **7**, 104 (1958).

[7] V. G. Skobov, JETP **37**, 1467 (1959), Soviet Phys. JETP **10**, 1039 (1960).

Translated by W. H. Furry
242

SOVIET PHYSICS JETP VOLUME 12, NUMBER 5 MAY, 1961

SOME PROPERTIES OF DRESSED PARTICLE OPERATORS IN FIELD THEORY

M. A. BRAUN and Yu. V. NOVOZHILOV

Leningrad State University

Submitted to JETP editor May 25, 1960

J. Exptl. Theoret. Phys. (U.S.S.R.) 39, 1317-1322 (November, 1960)

We investigate the properties of dressed particle operators, defined as producing single particle states when acting on the vacuum. Haag[1] has shown that the dressed particle creation operators have a strong-convergence limit for infinite time. We show that this is also true for the annihilation operators. Assuming the possibility of a coupling-constant expansion, we show that the dressed operators cannot satisfy the causality condition in its usual form.

1. INTRODUCTION

IF one could construct a field theory based on "dressed" particle operators (as opposed to the usual "bare" particle operators), one would no longer need to go through the renormalization procedure; in principle such an approach, making use of no nonphysical quantities, would be the more systematic one. Nevertheless, the actual use of dressed operators is still restricted to the Schrödinger representation, for the properties of the corresponding Heisenberg operators are not yet well enough understood. It is known only that for a large time the dressed creation operators converge strongly to the so-called in and out creation operators[1] and that the dressed operators cannot satisfy the bare-operator commutation relations so long as the interaction fails to vanish.[1,2]

In this communication we establish some other properties of dressed operators. Section 2 discusses some equivalent definitions of dressed operators. Section 3 extends Haag's results[1] to annihilation operators [strictly speaking, we shall prove not that the dressed annihilation operators converge strongly to the bare one, but, like Haag, the somewhat weaker result of Eq. (13)]. Section 4 is devoted to causality properties of dressed operators. In it we show that these operators cannot satisfy the causality condition in its usual form, i.e., that their commutator does not vanish on a space-like surface. The proof is based on perturbation theory.

For simplicity we shall deal only with scalar particles of a single kind.

2. THE CONDITION THAT THE OPERATORS DESCRIBE DRESSED PARTICLES

Let us define a local Lorentz-invariant dressed particle operator $Q(x)$ by the condition that

$$Q^{(+)}(k,\ t)\,|0\rangle = |k\rangle. \tag{1}$$

Here $|0\rangle$ is the physical vacuum, $|k\rangle$ is a single-particle state corresponding to 4-momentum k (with $k^2 = \mu^2$) and such that

$$\langle k\,|\,k'\rangle = 2k_0\delta(\mathbf{k}-\mathbf{k}'), \tag{2}$$

and, as usual,

$$Q^{(\pm)}(k,\ x_0) = \mp i\int d^3x\,Q(x)\frac{\overleftrightarrow{\partial}}{\partial x_0}e^{\mp ikx}$$
$$\equiv \mp i\int d^3x\left\{Q(x)\frac{\partial}{\partial x_0}e^{\mp ikx} - e^{\mp ikx}\frac{\partial}{\partial x_0}Q(x)\right\}. \tag{3}$$

Condition (1) agrees well with the physical meaning of a dressed operator.

We now define in and out operators according to

$$A^{out}_{in}(x) = Q(x) + \int \Delta^{adv}_{ret}(x-x')\,j(x')\,d^4x',\quad j(x')$$
$$\equiv (\Box - \mu^2)\,Q(x'). \tag{4}$$

It is known[1-3] that the $A^{out}_{in}(k,\ t)$ operators are independent of t and that they satisfy the usual free-particle commutation relations. It is known also that

$$A^{(+)}_{in}(k_1)\ \ldots\ A^{(+)}_{in}(k_n)\,|0\rangle \equiv |k_1\ \ldots\ k_n\rangle_{in}$$

is an energy-momentum eigenstate describing n particles with 4-momenta $k_1 \ldots k_n$ (with $k_i^2 = \mu^2$) before collision (and similarly for out operators). Further,

$$A^{(+)}_{in}(k)\,|0\rangle = A^{(+)}_{out}(k)\,|0\rangle = |k\rangle.$$

The relation between $Q^{(\pm)}(k,\ t)$ and, for instance, $A^{(\pm)}_{in}(k)$ is, according to (3) and (4), of the form

$$A^{(\pm)}_{in}(k) = Q^{(\pm)}(k,\ t) \pm i\int d^4x\,\theta(t-x)\,j(x)\,e^{\mp ikx}. \tag{5}$$

Condition (1) that the operators describe dressed particles states that

$$[A_{in}^{(+)}(k) - Q^{(+)}(k,\ t)]\,|0\rangle$$

$$= i\int d^4x\,\theta(t-x)\,j(x)\,e^{-ikx}\,|0\rangle = 0,$$

from which it follows immediately that

$$j(x)\,|0\rangle = 0. \qquad (6)$$

Note that this equation has been obtained as a consequence of (1). It is clear also that (1) is a consequence of (6). Furthermore, it is seen from (5) that (6) implies also that

$$[A_{in}^{(-)}(k) - Q^{(-)}(k,\ t)]\,|0\rangle = 0,$$

so that

$$Q^{(-)}(k,\ t)\,|0\rangle = 0. \qquad (7)$$

Thus conditions (1), (6), and (7) are shown to be equivalent. Any one of them may be used as the condition that the operators describe dressed particles.

We remark also that together (1) and (7) lead to yet another form of this condition, likewise equivalent to those above, namely

$$Q(x)\,|0\rangle = A_{in}^{out}(x)\,|0\rangle. \qquad (8)$$

This condition was used by Greenberg.[2]

As a further remark we point out that all this can also be formulated in terms of state vectors.[4,5] To do this we introduce the asymptotic states Ψ^a, satisfying the conditions

$$\langle\Psi_1^a\,|\,\Psi_2^a\rangle = G(1,\ 2) = \delta(1,\ 2) + g(1,\ 2),$$

$$\langle\Psi_1^a\,|\,2\rangle_{in} = \delta(1,\ 2) + T^{(\pm)}(1,\ 2)/(E_1 - E_2 \mp i0), \qquad (9)$$

(where $g(1,2)$ and $T^{(\pm)}(1,2)$ are smooth functions) as well as the requirement that the vacuum and single-particle states of Ψ^a are $|0>$ and $|k>$, respectively. The relation of this to the previously defined dressed operators is given by

$$\Psi^{ac}(k_1 \ldots k_n) = Q^{(+)}(k_1,\ 0) \ldots Q^{(+)}(k_n,\ 0)\,|0\rangle. \qquad (10)$$

3. STRONG CONVERGENCE

To study the behavior of the dressed operators as $t \rightarrow \pm\infty$, we go over in the usual way to wave packets and introduce the $Q_\alpha^{(\pm)}(x_0)$ operators, which are defined analogously to those of Eq. (3), except that $e^{\mp ikx}$ is replaced by $f_\alpha^{(\pm)}(x)$, a positive- or negative-frequency solution of the Klein-Gordon equation with mass μ, orthonormalized according to

$$\pm i\int d^3x\,f_\alpha^{(\pm)*}(x)\,\frac{\overleftrightarrow{\partial}}{\partial x_0}\,f_\beta^{(\pm)}(x) = \delta_{\alpha\beta} \qquad (11)$$

and such that $(f_\alpha^{(+)})^* = f_\alpha^{(-)}$.

By postulating the behavior of the vacuum expectation values $Q(x)$ for equal times, Haag[1] has shown that

$$Q_{\alpha_1}^{(+)}(t) \ldots Q_{\alpha_n}^{(+)}(t)\,|0\rangle \rightrightarrows |\alpha_1 \ldots \alpha_n\rangle_{in\,(out)}. \qquad (12)$$

Here the symbol $\rightrightarrows$ indicates strong convergence, and $|\alpha_1 \ldots \alpha_n>_{in(out)}$ is an n-particle in (or out) state in which the wave function of the m-th particle in x-space is $f_{\alpha_m}(x)$.

We shall show that if the vacuum expectation values behave according to Haag's postulate, then in addition to (12) we have

$$Q_{\beta_1}^{(-)}(t) \ldots Q_{\beta_n}^{(-)}(t)\,Q_{\alpha_1}^{(+)}(t) \ldots Q_{\alpha_m}^{(+)}(t)\,|0\rangle$$

$$\underset{t\rightarrow-(+)\infty}{\rightrightarrows}\begin{cases} 0, & m<n \\ \sum \delta_{\beta_1\alpha_{i_1}} \ldots \delta_{\beta_n\alpha_{i_n}}\,|\alpha_{i_{n+1}} \ldots \alpha_{i_m}\rangle_{in\,(out)}, & m \geqslant n \end{cases} \qquad (13)$$

(the sum is taken over all permutations $i_1 \ldots i_n$ of $1 \ldots m$).

It is known that (12) does not, strictly speaking, imply

$$Q_\alpha^{(+)} \rightrightarrows A_{\alpha\,in\,(out)}^{(+)} \quad \text{as} \quad t \rightarrow -(+)\infty,$$

although this convergence seems highly probable (see, for instance, Haag[1]). Similar considerations relating to (13) lead one to believe that

$$Q_\alpha^{(-)} \rightrightarrows A_{\alpha\,in\,(out)}^{(-)} \quad \text{as} \quad t \rightarrow -(+)\infty$$

and that therefore the difference between $Q(x)$ and $A_{in\,(out)}(x)$ converges strongly to zero as $t \rightarrow -(+)\infty$.

Equation (13) is proved in analogy with Haag's proof of (12). For simplicity we consider the case $m = n = 1$. Consider the expression

$$\langle 0|\,[Q_\beta^{(-)}(t)\,Q_\alpha^{(+)}(t) - Q_\alpha^{(+)}(t)\,Q_\beta^{(-)}(t) - \delta_{\alpha\beta}]^+$$
$$\times\,[Q_\beta^{(-)}(t)\,Q_\alpha^{(+)}(t) - Q_\alpha^{(+)}(t)\,Q_\beta^{(-)}(t) - \delta_{\alpha\beta}]\,|0\rangle \qquad (14)$$

for large $|t|$. As Haag has shown, the vacuum expectation value of products of $Q_\alpha^{(\pm)}(t)$ operators reduce, as $|t| \rightarrow \infty$ (up to terms of order t^{-3}) to the sum of products of vacuum expectation values of pairs of $Q_\alpha^{(+)}(t)$ and $Q_\beta^{(-)}(t)$ operators taken in the same order as in the original product. In particular, for (14) we have, as $|t| \rightarrow \infty$,

$$\langle 0|\,Q_\alpha^{(-)}\,Q_\beta^{(+)}\,|0\rangle\,\langle 0|\,Q_\beta^{(-)}\,Q_\alpha^{(+)}\,|0\rangle$$
$$-\,\langle 0|\,Q_\beta^{(+)}\,Q_\alpha^{(-)}\,|0\rangle\,\langle 0|\,Q_\beta^{(-)}\,Q_\alpha^{(+)}\,|0\rangle$$
$$-\,\langle 0|\,Q_\alpha^{(-)}\,Q_\beta^{(+)}\,|0\rangle\,\langle 0|\,Q_\alpha^{(+)}\,Q_\beta^{(-)}\,|0\rangle$$
$$+\,\langle 0|\,Q_\beta^{(+)}\,Q_\alpha^{(-)}\,|0\rangle\,\langle 0|\,Q_\alpha^{(+)}\,Q_\beta^{(-)}\,|0\rangle$$
$$-\,2\delta_{\alpha\beta}\,\langle 0|\,Q_\alpha^{(-)}\,Q_\beta^{(+)}\,|0\rangle + 2\delta_{\alpha\beta}\,\langle 0|\,Q_\alpha^{(+)}\,Q_\beta^{(-)}\,|0\rangle + \delta_{\alpha\beta}.$$

We now find by using conditions (1) and (17) that this expression vanishes, or that

$$\lim_{|t|\to\infty} \| [Q_\beta^{(-)}(t) Q_\alpha^{(+)}(t) - Q_\alpha^{(+)}(t) Q_\beta^{(-)}(t) - \delta_{\alpha\beta}] |0\rangle \| = 0.$$

On the other hand, we know that $Q_\beta^{(-)}(t)|0\rangle = 0$, so that

$$Q_\beta^{(-)}(t) Q_\alpha^{(+)}(t)|0\rangle \underset{t\to\pm\infty}{\rightrightarrows} \delta_{\alpha\beta}|0\rangle,$$

q.e.d.

4. CAUSAL PROPERTIES OF DRESSED OPERATORS

It is well known that the condition that Q (x) be a dressed operator does not define it uniquely. One is then led naturally to look for additional restrictions which will pick out the most "physical" or "convenient" of all possible Q (x) operators. One would suppose that the causality condition would serve this function (see, for instance, Greenberg[2]); we write the condition in the form

$$[Q(x), Q(y)] = 0 \quad \text{for} \quad (x-y)^2 < 0. \tag{15}$$

In this section we will show that dressed operators cannot satisfy (15). Since the commutation relations of the Q (x) operators are not known, we shall make use of perturbation theory. Actually what we will show is that the condition that the operators describe dressed particles leads to

$$[A_{in(out)}(y), j(x)] \neq 0 \quad \text{for} \quad (x-y)^2 < 0. \tag{16}$$

This means that in the first approximation in the coupling constant g, the commutator [Q (y), j (x)] ≠ 0 for $(x-y)^2 < 0$. It follows then that [Q (y), Q (x)] ≠ 0 for $(x-y)^2 < 0$, also in the first approximation in g. If the perturbation theory expansion converges at least asymptotically, this means that the causality condition (15) cannot be fulfilled (except perhaps for special values of g such that the higher approximations cancel the first).

We proceed to prove (16). Let us expand the current j (x) in a Fock series in the A_{in} (or, equivalently, A_{out}) operators:

$$j(x) = \sum_{m,\,n=0}^{\infty} \int \frac{d^2p_1}{2p_{10}} \cdots \frac{d^3q_1}{2q_{10}} \cdots \frac{f_{mn}(p_1 \ldots p_m | q_1 \ldots q_n | x)}{\sqrt{m!\,n!}}$$
$$\times A_{in}^{(+)}(p_1) \ldots A_{in}^{(+)}(p_m) A_{in}^{(-)}(q_1) \ldots A_{in}^{(-)}(q_n) \tag{17}$$

(here $p_i^2 = q_k^2 = \mu^2$). Considerations of Lorentz invariance lead to

$$f_{mn}(p_1 \ldots p_m | q_1 \ldots q_n | x)$$
$$= \exp\left\{i\left(\sum p - \sum q\right)x\right\} \varphi_{mn}(p_1 \ldots p_m | q_1 \ldots q_n),$$

where φ_{mn} is a scalar function symmetric in the p_i and q_i separately. Because the current is Hermetian,

$$\varphi_{mn}(p_1 \ldots p_m | q_1 \ldots q_n) = \varphi_{nm}^*(q_1 \ldots q_n | p_1 \ldots p_m).$$

Let us think of the φ_{mn} functions as expanded in a power series in the coupling constant, and let us consider only those terms linear in g (which we shall denote henceforth simply as φ_{mn}). We remark that all the φ_{mn} cannot vanish in the first approximation in g, for this would contradict the very meaning of a coupling constant.

As a basis for proving (16) we shall use conditions (6), which leads obviously to

$$\varphi_{m0} = \varphi_{0m} = 0. \tag{18}$$

The commutation relations of the A_{in} are well known, and there is no difficulty in calculating the matrix elements of the commutator of $A_{in}(y)$ and j (x) between any in states. We obtain

$$Z_{mn}(y, x) = \frac{1}{\sqrt{m!\,n!}}\, {}_{in}\langle p_1 \ldots p_m | [A_{in}(y), j(x)] | q_1 \ldots q_n \rangle_{in}$$
$$\frac{1}{(2\pi)^{3/2}} \exp\left\{i\left(\sum p - \sum q\right)x\right\} \int \frac{d^3k}{2k_0}$$
$$\times \{\varphi_{m+1,\,n}(kp_1 \ldots p_m | q_1 \ldots q_n) e^{-ik(y-x)} \sqrt{m+1}$$
$$- \varphi_{m,\,n+1}(p_1 \ldots p_m | kq_1 \ldots q_n) e^{ik(y-x)} \sqrt{n+1}\} \tag{19}$$

(in the integrand $k^2 = \mu^2$).

Let m = 0, n ≠ 0. It then follows from (18) that

$$Z_{0n}(y, x)$$
$$= (2\pi)^{-3/2} \exp\left\{-ix\sum q\right\} \int \frac{d^3k}{2k_0} e^{-ik(y-x)} \varphi_{1n}(k | q_1 \ldots q_n). \tag{20}$$

The right side of (20) cannot vanish for $(x-y)^2 < 0$ so long as $\varphi_{1n} \not\equiv 0$. Indeed, for $x_0 = y_0$ we are left with the ordinary Fourier transform. If the right side is to have a δ-function singularity, the integrand must contain a polynomial in |k|, which is clearly impossible because of the $2k_0$ in the denominator. Thus if $[A_{in}(y), j(x)] = 0$ for $(x-y)^2 < 0$, we obtain

$$\varphi_{1n} = \varphi_{n1} = 0.$$

Now consider the case m = 1, n ≠ 0, 1. We have

$$Z_{1n} = \sqrt{2}(2\pi)^{-3/2} \exp\left\{i\left(p - \sum q\right)x\right\}$$
$$\times \int \frac{d^3k}{2k_0} e^{-ik(y-x)} \varphi_{2n}(k, p | q_1 \ldots q_n).$$

Similar considerations lead to the conclusion that

$$\varphi_{2n} = \varphi_{n2} = 0.$$

Continuing in this way we can prove finally that if $[A_{in}(y), j(x)] = 0$ for $(x-y)^2 < 0$, all the φ_{mn} functions vanish, contrary to assumption. Thus we have proven (16).

In conclusion we should like to mention that it seems to us quite natural that the dressed operators do not satisfy the causality condition in the form of (15). This must, of course, be related to the smearing out of the physical particles over some region whose radius is of the order of $1/\mu$. This behavior of the dressed operators, however, is a serious obstacle to using them in constructing a Lorentz invariant formalism for scattering theory. To obtain such a formalism is the foremost problem in the theory of dressed particles.

---

[1] R. Haag, Phys. Rev. **112**, 669 (1958); see also Nuovo cimento suppl. **1**, 131 (1959).

[2] O. W. Greenberg, Phys. Rev. **115**, 706 (1959).

[3] W. Zimmerman, Nuovo cimento **10**, 597 (1958).

[4] L. Van Hove, Physica **21**, 901 (1955); **22**, 343 (1956).

[5] Yu. V. Novozhilov, JETP **35**, 742 (1958), Soviet Phys. JETP **8**, 515 (1959); Vestnik, Leningrad State Univ. **22**, 93 (1958); Nucl. Phys. **15**, 469 (1960).

Translated by E. J. Saletan
243

SOVIET PHYSICS JETP VOLUME 12, NUMBER 5 MAY, 1961

CONTRIBUTION TO THE THEORY OF FERRO- AND ANTIFERROMAGNETISM

V. L. GINZBURG and V. M. FAĬN

Radiophysics Institute, Gor'kiĭ State University

Submitted to JETP editor May 26, 1960

J. Exptl. Theoret. Phys. (U.S.S.R.) **39**, 1323-1338 (November, 1960).

A simple approximate method is developed for the determination of the magnetization of the lattice or sublattice and of other quantities in ferro- and antiferromagnetic materials. The method is applicable over the entire range of temperatures, and takes into account the dependence on the dimensions and form of the magnetic system. The question is discussed of the antiferromagnetism and ferromagnetism of small particles and polymer chains, an aggregate of which may be considered, under given conditions, to form a "paramagnetic fluid."

ONE of the highly interesting current problems is the study of ferromagnetism, and especially antiferromagnetism, of finely-disperse substances, polymers, and possibly, individual macromolecules. (We are concerned here also with the paramagnetic region, i.e., with temperatures above the transition temperature.) It is clear even from general considerations that magnetic methods can be highly effective in the study of the cited objects. Hence we shall limit ourselves here only to referring to the experimental data that point to the anomalous magnetic properties of certain nucleic acids and artificial polymers.[1] The nature of these effects has not yet been elucidated, but even if it is not related to antiferromagnetism, as we assume,[2] an analysis of the properties of ferro- and antiferromagnetic materials of the "polymeric type" will nevertheless be necessary. For this purpose, we must have a simple method for the approximate calculation of the magnetization of the lattice or sublattice and of other quantities, as functions of the dimensions and form of the specimens (small particles, films, polymer chains, etc.) over as wide a temperature range as possible.

Such a method is developed below, based on a certain self-consistent generalization of the theory of spin waves. The results obtained may also be of interest in the case of bulk ferro- and antiferromagnetic materials, since the expressions derived are approximately correct for all temperatures. Here we have based our treatment on the ordinary model of localized spins with exchange interaction (see, e. g., reference 3), which in itself deviates greatly from reality. However, the results thus obtained have, to a considerable degree, a general character. That is, they are independent of the model within broad limits, and may be derived in a semi-phenomenological manner.[4-6] It would be somewhat more consistent to develop the theory directly by the latter method, but both approaches are permissible in the final analysis. However, we found it more convenient to proceed from the model representation. (Besides, while in the semi-phenomenological approach one commonly limits the treatment to the terms which are quadratic in the components of the wave vector, we have used more general expressions.)

1. FERROMAGNETISM

We shall write the Hamiltonian of a system of spins $\hbar\mathbf{S}_j$ in the usual form:[3,7]

$$\mathcal{H} = -J\sum_{jl}\mathbf{S}_j\mathbf{S}_{j+l} - \mu H\sum_{j} S_j^z - \mu H_A\sum_{j} S_j^z,$$

$$\mu = ge\hbar/2mc, \quad J > 0, \tag{1}$$

$$\{S_j^x S_k^y\} = S_j^x S_k^y - S_k^y S_j^x$$

$$= i\delta_{jk}S_j^z, \ldots, (S_j^x)^2 + (S_j^y)^2 + (S_j^z)^2 = S(S+1). \tag{2}$$

In Eq. (1), the summation over l is carried out over nearest neighbors, each pair of spins being represented twice. (Thus, the quantity commonly designated as the exchange integral is exactly equal to J, while the interaction energy of a pair of spins is equal to $2J\mathbf{S}_j\mathbf{S}_k$.) H is the magnetic field intensity, and H_A is the effective field of the magnetic anisotropy, both lying in the direction of the z axis. In Eq. (1), we can also easily take into account anisotropic terms of a more general form, but shall not do this here.

We transform to the variables

$$\mathrm{S}_\lambda = N^{-1/2}\sum_{\mathrm{j}} \exp(i\boldsymbol{\lambda}\mathrm{j})\,\mathrm{S}_{\mathrm{j}}, \qquad \mathrm{S}_{\mathrm{j}} = N^{-1/2}\sum_{\lambda} \mathrm{S}_\lambda \exp(-i\boldsymbol{\lambda}\mathrm{j})$$

$$\sum_{\mathrm{j}} \exp i(\boldsymbol{\mu} - \mathrm{j}\boldsymbol{\lambda}) = N\delta_{\lambda\mu}, \tag{3}$$

where N is the total number of particles (spins), **j** is the radius vector of the j-th lattice point, and the wave vector **λ** also takes on N different values. If the spins are located at the points of a simple rectangular (orthorhombic) lattice with lattice parameters a_1, a_2, and a_3 along the axes $x \equiv 1$, $y \equiv 2$, and $z \equiv 3$, while the specimen has dimensions n_1a_1, n_2a_2, and n_3a_3 along these axes,

$$N = n_1n_2n_3, \qquad \lambda_i = 2\pi m_i / n_i a_i, \quad -n_i/2 \leqslant m_i \leqslant n_i/2,$$
$$m_i = 0, \pm 1, \pm 2 \ldots .$$

Here we assume that $n_i \gg 1$; in the contrary case, boundary conditions are essential, and then, for example, $m_i \leq n_i/2 - 1$. The limitation to the case in which $n_i \gg 1$ is not obligatory, and does not prevent an approximate study of very small objects, for example, with $n_i \gtrsim 10$.

In terms of the new variables,

$$\mathscr{H} = -JZ\sum_\lambda \gamma_\lambda \mathrm{S}_\lambda \mathrm{S}_{-\lambda} - \mu(H + H_A)N^{1/2}S_0^z,$$

$$\{S_\lambda^x S_\rho^y\} = iN^{-1/2}S_{\lambda+\rho}^z \text{ etc.}, \qquad Z\gamma_\lambda = \sum_{\mathrm{l}} \exp(i\boldsymbol{\lambda}\mathrm{l}), \tag{4}$$

where Z is the number of nearest neighbors. Hence,

$$\dot{S}_\rho^x = \frac{i}{\hbar}\{\mathscr{H}S_\rho^x\} = (\omega_H + \omega_A)S_\rho^y$$
$$+ \frac{\omega_0}{2}N^{-1/2}\sum_\lambda (\gamma_\lambda - \gamma_{\lambda-\rho})(S_\lambda^z S_{\rho-\lambda}^y - S_\lambda^y S_{\rho-\lambda}^z);$$
$$\dot{S}_\rho^y = -(\omega_H + \omega_A)S_\rho^x$$
$$+ \frac{\omega_0}{2}N^{1/2}\sum_\lambda (\gamma_\lambda - \gamma_{\lambda-\rho})(S_\lambda^x S_{\rho-\lambda}^z - S_\lambda^z S_{\rho-\lambda}^x),$$
$$\omega_H = \mu H/\hbar = geH/2mc, \quad \omega_A = \mu H_A/\hbar, \qquad \omega_0 = 2JZ/\hbar. \tag{5}$$

We shall now consider that the system has been magnetized along the z axis, so that the mean value of the z component of the total spin $S_{\text{total}}^z = \sum S_j^z = N^{1/2}S_0^z$ is large in comparison with the root-mean-square values of the quantities $S_{\text{total}}^{x,y} = \sum S_j^{x,y} = N^{1/2}S_0^{x,y}$. The quantity S_0^z will be considered to be a classical quantity, and will be conveniently designated as $N^{1/2}\eta S$, where ηS is the mean value of the z component of the total spin per particle. This condition has the following form, where the brackets < > denote the statistical mean value:

$$N\eta S = \langle S_{\text{total}}^z\rangle \gg \langle (S_{\text{total}}^{x,y})^2\rangle^{1/2}. \tag{6}$$

As we shall see, this condition is not at all sufficient, but when it is obeyed, the linearization of Eq. (5) may lead to reasonable results. Proceeding thus, i.e., replacing S_0^z by $\langle S_0^z\rangle = N^{1/2}\eta S$, we have

$$\dot{S}_\lambda^x = \omega_\lambda S_\lambda^y, \qquad \dot{S}_\lambda^y = -\omega_\lambda S_\lambda^x,$$
$$\omega_\lambda = \omega_H + \omega_{A0}\eta + \omega_0\eta S[1 - (\gamma_\lambda + \gamma_{-\lambda})/2], \tag{7}$$

Here we assume that $\omega_A = \omega_{A_0}\eta$, since the field H_A itself vanishes for $\eta = 0$ in the self-consistent approximation, and in the simplest case, H_A is proportional to η (i.e., $H_A = H_{A_0}\eta$, where H_{A_0} = const.). Equation (7) is derived from the Hamiltonian*

$$\mathscr{H}_0 = \sum_\lambda{}' \frac{\hbar\omega_\lambda}{\eta S}(S_\lambda^x S_{-\lambda}^x + S_\lambda^y S_{-\lambda}^y)$$
$$= \sum_\lambda{}' \frac{\omega_\lambda}{2}(P_{\lambda 1}^2 + Q_{\lambda 1}^2 + P_{\lambda 2}^2 + Q_{\lambda 2}^2)$$
$$= \sum_\lambda{}' \hbar\omega_\lambda(n_{\lambda 1} + n_{\lambda 2} + 1) = \sum_\lambda \hbar\omega_\lambda\left(n_\lambda + \frac{1}{2}\right),$$
$$\{S_\lambda^x S_{-\lambda}^y\} = iN^{-1/2}S_0^z = i\eta S, \qquad S_{\pm\lambda}^x = \sqrt{\eta S/2\hbar}\,(Q_{\lambda 1} \pm iQ_{\lambda 2}),$$
$$S_{\pm\lambda}^y = \sqrt{\eta S/2\hbar}\,(P_{\lambda 1} \pm iP_{\lambda 2}), \quad \{P_{\lambda l}Q_{\mu m}\} = -i\hbar\delta_{lm}\delta_{\lambda\mu}. \tag{8}$$

Thus, the excitation energy is equal to a sum of oscillator energies.

If we assume that $\eta = 1$, the expression obtained obviously corresponds exactly with the ordinary spin-wave approximation. At low temperatures, under the assumption that saturation ($\eta = 1$) occurs at T = 0, the spin-wave approximation for ferromagnetic materials is very good.[3,7] On the contrary, at increased temperatures, and especially at T ~ Θ (Θ is the Curie point), the ordinary spin-wave approximation is completely unsuitable. This latter situation is quite understandable, since with the decrease in the mean spin ηS occurring as the temperature is raised, the frequency of the spin waves must decrease [see Eq. (7)], a fact not taken into account. In this regard, we may hope that, without fixing the parameter η, but rather, by determining it by the self-consistent method, we may construct a theory having a region of applicability considerably greater than that in which η = const.

To determine η, we shall use the exact operator equation

$$(S_{\mathrm{j}}^x)^2 + (S_{\mathrm{j}}^y)^2 + (S_{\mathrm{j}}^z)^2 = S(S+1),$$

averaged over the states of the system. If we also take into account [see Eq. (8)] the fact that

---

*The prime denotes summation over positive values only of $\boldsymbol{\lambda} = (\lambda_1, \lambda_2, \lambda_3)$. In order to avoid introduction of the quantum numbers n_{λ_1} and n_{λ_2} into Eq. (8), we have assumed that $n_\lambda = n_{\lambda_1}$ $(\lambda \geq 0)$ and $n_\lambda = n_{\lambda_2}$ $(\lambda < 0)$.

$$\langle S_j^x S_j^x + S_j^y S_j^y \rangle = \frac{1}{N} \left\langle \sum_\lambda (S_\lambda^x S_{-\lambda}^x + S_\lambda^y S_{-\lambda}^y) \right\rangle - 2\eta \frac{S}{N} \sum \left(n_\lambda + \frac{1}{2} \right),$$

we have

$$\frac{2\eta S}{N} \sum n_\lambda + \eta S + \langle (S_j^z)^2 \rangle = S(S+1). \tag{9}$$

Obviously, for spin ½, $(S_j^Z)^2 = 1/4$. Then, in a state of thermal equilibrium,* in which $\overline{n}_\lambda = [\exp(\hbar\omega_\lambda/kT) - 1]^{-1}$, we obtain the following equation for η:

$$\eta = 1 - \frac{2\eta}{N} \sum_\lambda \left[\exp \frac{\hbar\omega_\lambda}{kT} - 1 \right]^{-1},$$

$$\omega_\lambda = \omega_H + \omega_{A0}\eta + \frac{\omega_0}{2} \left(1 - \frac{\gamma_\lambda + \gamma_{-\lambda}}{2} \right) \eta. \tag{10}$$

At low temperatures, at which $1 - \eta \ll 1$, Eq. (10) coincides with the result of the ordinary spin-wave theory:[3]

$$SN(1-\eta) = \sum_\lambda \left[\exp \frac{\hbar\omega_\lambda}{kT} - 1 \right]^{-1},$$

$$\omega_\lambda = \omega_H + \omega_{A0} + \omega_0 S \left(1 - \frac{\gamma_\lambda + \gamma_{-\lambda}}{2} \right). \tag{11}$$

If in Eq. (9) we assume that $\langle (S_j^Z)^2 \rangle = \eta^2 S^2$ for spin $S > 1/2$, then on going to low temperatures we obtain Eq. (11), with the substitution of $S + 1/2$ for S. In order to establish complete correspondence, we may assume that

$$\langle (S_j^z)^2 \rangle = \eta^2 S^2 - S(\eta^2 - 1)/2.$$

Then the equation for η is:

$$(\eta^2 - 1)\left(S - \frac{1}{2} \right) + \eta = 1 - \frac{2\eta}{N} \sum \left(\exp \frac{\hbar\omega_\lambda}{kT} - 1 \right)^{-1},$$

$$\omega_\lambda = \omega_H + \omega_{A0}\eta + \omega_0 S \left(1 - \frac{\gamma_\lambda + \gamma_{-\lambda}}{2} \right) \eta. \tag{12}$$

For $S = 1/2$, this equation goes over into Eq. (10); at $T \to 0$, it goes over into Eq. (11); while for $T \to \Theta$ it gives a reasonable result (see below). In other respects, however, it is not as firmly based as Eq. (10).

In the high-temperature region (near the Curie point Θ), the parameter $\eta \ll 1$, and $\eta(\Theta) = 0$. Hence, by using the expansion

$$(e^x - 1)^{-1} = 1/x - 1/2 + x/12 - x^3/720 + \ldots$$

in the first-order approximation, for $H = 0$, we obtain

$$\eta^2 = A(1 - T/\Theta), \qquad \Theta = (S + 1/2) SJ/kF,$$

$$F = \frac{1}{N} \sum \left(\delta + Z - \sum_{\mathbf{l}} \cos \boldsymbol{\lambda}\mathbf{l} \right)^{-1}, \quad A = \frac{S + 1/2}{S - 1/2 + (1+\delta) JSZ/3k\Theta},$$

$$\frac{1}{N} \sum_\lambda \left(Z - \sum_{\mathbf{l}} \cos \boldsymbol{\lambda}\mathbf{l} \right) = Z, \qquad \delta = \frac{\mu H_{A0}}{2JS}. \tag{13}$$

Such a law for the magnetization

$$M = \mu SN\eta/V = \text{const} \sqrt{1 - T/\Theta}$$

(here V is the volume of the specimen) must be obtained when fluctuations are neglected.[8]

For a simple cubic lattice (with the number Z of nearest neighbors = 6, and with lattice parameter a), upon replacing summation by integration, for $\delta = 0$, we obtain

$$F = \frac{a^3}{(2\pi)^3} \int \frac{d\boldsymbol{\lambda}}{\left(6 - \sum_{\mathbf{l}} \cos \boldsymbol{\lambda}\mathbf{l} \right)} = \frac{1}{2\pi^3} \iiint_0^\pi \frac{du\, dv\, dw}{3 - \cos u - \cos v - \cos w} = 0.2526. \tag{14}$$

Thus, for spin $S = 1/2$, we have $k\Theta/J = 1.98$ and $\eta^2 = 1.98(1 - T/\Theta)$. In addition, calculations carried out in the paramgnetic region for the model being studied under the same conditions give values $k\Theta/J = 1.93$, 1.92, and 1.83.[9-11] The excellent agreement obtained is better than might be expected. This may apparently be explained by the smallness of the role of large values of λ. For the relatively long wavelengths in Eq. (14), the spin-wave approximation, starting with a state with magnetic moment $M(T) = \mu\eta(T)SN$, must be good.

We note that attempts to widen the field of applicability of the spin-wave theory by means of some self-consistent treatment have been made previously.[12-15] However, the method of calculation used by Heber[12] and Schafroth[13] seems to us to be more complex, while the results either do not apply at all[12] to the region $T \sim \Theta$, or are poorly applicable. In the papers of Bogolyubov and Tyablikov,[14,15] double-time retarded and advanced Green's functions were used, and then Eq. (10) was derived approximately for spin ½, with $\omega_{A_0} = 0$. The method given above for deriving this equation seems to us to be not only simpler, but also physically clearer. In addition to the comparison of values of $k\Theta/J$ given above, the results obtained by Tyablikov[15] and the comparison of the latter with other solutions give evidence that Eq. (10) is correct at low temperatures within an accuracy of terms of the order of $T^{-5/2}$, inclusive. For $H \neq 0$ and $T > \Theta$, it is correct within an curacy of terms of the order of $1/T$.

Thus, there is every ground to consider that the very simple self-consistent treatment applied here gives good results. The character of the approximation is not associated here with concrete expressions for the frequencies ω_λ. In other words, by using Eqs. (10) and (12) with frequencies $\omega_\lambda = \omega_H + \omega_A + f(\lambda)\eta$, where f is some reasonably selected function, we arrive at a phenomenological self-consistent theory of spin waves. The essential limitation here is actually the fact that the original Hamiltonian in Eq. (1) commutes with $S^z_{\text{total}} = \sum S^z_j$. We shall not carry out here the possible generalization of the self-consistent theory to the case in which there is an anisotropic interaction of a more general type. Rather, we shall consider further only ferromagnetic materials of small dimensions.

---

*In the case of a spectrum of quasi-particles having energy levels depending on the energy, as is known, the ordinary formula for $\overline{n}$ may be derived from the expression for the entropy.

Within the framework of theory being discussed, we retain Eqs. (10) — (13) in this case, except that we cannot go from summation to integration in all directions.* Thus, for thin films, we must retain the summation in the direction perpendicular to the plane of the film. For long "fibers" we must apply summation in two directions, and for parallelepipeds, in all three directions. In the case of a simple cubic lattice with dimensions n_1a, n_2a, and n_3a: $N = n_1n_2n_3$, and

$$F \quad \frac{4}{n_1 n_2 n_3} \sum_{l_1 l_2 l_3} \left(\frac{\delta}{2} + 3 - \cos\frac{2\pi m_1}{n_1} - \cos\frac{2\pi m_2}{n_2} - \cos\frac{2\pi m_3}{n_3} \right)^{-1},$$

$$\frac{\delta}{2} = \frac{\mu H_{A0}}{4JS}, \qquad m_i = 0, 1, \ldots, n_i/2. \qquad (15)$$

In the three-dimensional case in sufficiently large systems, the factor taking into account anisotropy plays in certain respects simply the role of a convergence factor, eliminating the infinite term in F for the case $m_1 = m_2 = m_3 = 0$ [see Eq. (15)].* However, in the one- and two-dimensional problems, the results already depend fundamentally on δ. Thus, for an infinite chain of spins we have:

$$F = \frac{1}{2\pi} \int_0^\pi \frac{du}{\delta/2 + 1 - \cos u} \approx \frac{1}{2\sqrt{\delta}}, \qquad \delta \ll 1. \qquad (16)$$

In view of Eqs. (13) and (14), we have for such a chain,

$$\Theta = \left[\sqrt{2S} \left(S + \tfrac{1}{2} \right) / k \right] \sqrt{\mu H_{A0} J}.$$

At the same time, it follows from general statistical considerations[18] that a phase transition in an infinite one-dimensional system is impossible, i.e., $\Theta = 0$. The same is naturally true in the Ising model,[19] which corresponds to the limit of strong anisotropy.

With regard to the discussion above, we note firstly that the introduction of the field $H_A = H_{A_0}\eta$ is in itself an approximate method, and introduces an additional element of self-consistency. Actually, the true interaction in one separate direction has the form $\sum S^z_j S^z_{j+1}$, but this expression has been replaced by one of the type $\langle S^z \rangle \sum S^z_j = \eta S \sum S^z_j$. As a result, the effect of the anisotropy field is equivalent to the effect of a certain external magnetic field bringing about the appearance of a magnetic moment in the chain for $T \neq 0$. Secondly, even independently of the problem of the nature of the anisotropy field, the original introduction of the mean quantity $\langle S^z_j \rangle = \eta S$ is permissible in the statistical calculations, in general, only under the condition that the fluctuations are small. In other words, in addition to condition (6), the following condition must be fulfilled:

$$\langle (\Delta\eta)^2 \rangle \ll \langle \eta \rangle^2 \equiv \eta^2, \qquad \Delta\eta = \eta - \langle \eta \rangle \qquad (17)$$

(to avoid complicating the notation, we shall write

---

*The presence of spontaneous magnetization in ferromagnetic materials and the magnetic effects associated therewith may be taken into account to a certain degree by the introduction of the field H_A. However, this field depends on the form and dimensions of the specimen, just as does the magnetization itself. We shall not consider this important magnetic moment in this article, just as we shall not in general analyze the question of the nature and magnitude of the anisotropy field H_A. For the antiferromagnetic materials, in which we are chiefly interested, the entire problem of the relation of H_A to the dimensions and form is, in a certain respect, considerably less critical, owing to the lack of spontaneous magnetization. However, in the case of the ferromagnetic materials, the corresponding relation may be taken into account to a certain degree as the result of the solution of magnetostatic problems. Besides, in both the ferromagnetic and the antiferromagnetic materials, the form and dimensions of the specimens exhibit, of course, an influence on sufficiently long waves. Hence, in the region of sufficiently low temperatures, the problem of the dependence of various quantities on the dimensions and form requires special study (for the latter remark, the authors wish to thank M. I. Kaganov).

*In this regard, one of the ways of calculating sums of the type of (15) is simply the omission of terms with $m_1 = m_2 = m_3 = 0$, anisotropy being simultaneously neglected (see, e.g., reference 16). The results of such a calculation are given below for illustration (for the most recent experimental data on films, see the paper of Neugebauer[17]):

$(n_1n_2n_3)=$	$(\infty\infty\infty)$	(64,64,64)	(32,32,32)	(16,16,16)	(4,4,4)	(4,4,16)	(4,4,64)
F=	0.2526	0.29	0.32	0.37	0.66	0.75	1.7

$(n_1n_2n_3)=$	(8,8,64)	(4,16,16)	(4,64,64)	(8,16,16)	(8,32,32)	(8,64,64)	(8,128,128)
F=	0.67	0.55	0.61	0.32	0.41	0.42	0.44

It is clear from Eqs. (13) and (15) that it is possible to neglect the terms with $m_1 = m_2 = m_3 = 0$ if $N\delta \gg 1$. When $N\delta \ll 1$, obviously $F \approx (N\delta)^{-1}$. However, in this case the conditions for validity of the approximation are not fulfilled (see criterion (21) below). Hence, and also in view of the requirement $n_i \gg 1$, by no means all given values of F can be used.

η for $<\eta>$ whenever this does not lead to confusion).

For a concrete application of condition (17), as well as for a more complete test of the linear approximation used here, we would, of course, have to determine all of the physical quantities from the next order of approximation. However, we shall not go through this involved procedure here, but rather, shall estimate the fluctuation of η within the framework of the semi-thermodynamic theory. Near the Curie point, neglecting fluctuations,[8] the thermodynamic potential per unit volume can be expressed in the form

$$\Phi = \Phi_0 + \alpha\eta^2 + \tfrac{1}{2}\beta\eta^4 + \rho(\operatorname{grad}\eta)^2 - \eta H\mu SNV^{-1}, \quad (18)$$

where $\eta(r)$ is the characteristic parameter,[18,8] for which we may also select the quantity $<\eta>$ used above, as applied to a state of incomplete thermodynamic equilibrium. Assuming that

$$\Delta\eta = \sum \eta_\lambda e^{i\lambda r},$$

as usual, we then determine the thermodynamic fluctuations at $H = 0$ (for more detail, see reference 8 and the literature cited there):

$$\langle|\eta_\lambda|^2\rangle = kT/(\Phi_0'' + 2\rho\lambda^2)V,$$

$$\langle(\Delta\eta)^2\rangle = \left\langle\int(\Delta\eta(\mathrm{r}))^2\,dV\right\rangle = \sum_\lambda \langle|\eta_\lambda|^2\rangle,$$

$$\Phi_0'' = (\partial^2\Phi/\partial\eta^2)_{\eta=\eta_0}, \qquad \Phi_0'' = -4\alpha \quad (\text{at } T < \Theta),$$

$$\eta_0^2 \equiv \langle\eta\rangle^2_{\mathbf{equil}} = -\alpha/\beta \approx \alpha'_\Theta(\Theta - T)/\beta_\Theta \quad (\text{at } T < \Theta),$$

$$\eta_0^2 = 0 \quad (\text{at } T > \Theta). \quad (19)$$

Equation (18) may be used under condition (17) at temperatures not too far from the Curie point (for $\eta \ll 1$), and for wave vectors $\lambda \ll \lambda_{\max} = \pi/a$. However, in order to make the estimates in Eq. (19), we must carry out the summation or integration up to values $\lambda \sim \lambda_{\max}$. As a result of such an estimate and the use of condition (17) for the three-dimensional case, criteria may be obtained, which have previously been discussed in reference 8. In real ferromagnetic materials, the situation is rather unclear, but apparently condition (17) is well obeyed when $\Delta T \gg 10^{-2}\Theta$ (in the case of metals this condition may be even weaker).

It is obvious from Eq. (19)that the fluctuations are greater in the two-dimensional, and especially in the one-dimensional case, than in the three-dimensional case. Thus, for an infinite chain

$$\langle(\Delta\eta)^2\rangle \sim \frac{kT}{2\pi}\int_0^{\lambda_{max}}\frac{d\lambda}{\Phi_0'' + 2\rho\lambda^2}$$

$$= \frac{kT}{2\pi\sqrt{2\rho\Phi_0''}}\tan^{-1}\left(\sqrt{\frac{2\rho}{\Phi_0''}}\,\lambda_{max}\right) \approx \frac{kT}{4\sqrt{2\rho\Phi_0''}} \qquad (20)$$

Further, from Eqs. (13) and (16) we obtain

$$\eta^2 \sim (k\Theta/J)(1 - T/\Theta), \qquad k\Theta \sim S^{3/2}\sqrt{\mu H_{A0}J};$$

In view of (18) (or more exactly, from the condition that $\partial\Phi/\partial\eta = 0$), in the region $T > \Theta$ in the presence of a magnetic field

$$\eta = \mu SNH/2V\alpha = \mu SNH/2V\alpha'_\Theta(T - \Theta).$$

At the same time, we may derive from Eq. (12), for $H \neq 0$ and $T \gg \Theta$, the equation $\eta = (S + \tfrac{1}{2}) \times \mu H/2kT$. Hence $\alpha'_\Theta \sim kN/V = k/a$ (in the one-dimensional case, $N/V = N/L = 1/a$, where L is the length of the chain and a is the distance between neighboring spins). Finally, the coefficient $\rho \sim Ja$, since for the shortest waves ($\lambda \sim \lambda_{\max} = \pi/a$), the energy $\rho(d\eta/dz)^2 \sim \rho\lambda^2_{\max} \sim \rho/a^2$ must be of the order of the exchange energy J/a per unit length of chain.

In view of all that has been said, condition (17) acquires the form

$$\eta^2 \sim \frac{k}{J}(\Theta - T) \gg \langle(\Delta\eta)^2\rangle \sim kT/10\sqrt{k(\Theta - T)J}$$

or

$$(\Theta - T)/\Theta \gg (J/k\Theta)^{1/3} \gtrsim 1$$

(We assume that $T \sim \Theta$, since all of the estimates refer to the region near the Curie point, and have been made with a corresponding degree of precision). The condition which we have derived obviously cannot be fulfilled. Thus, for an infinite chain the approximation is indeed inapplicable, in agreement with the general results. From this example, the procedure is clear by which we may test the region of applicability of our approximation.

We note that a finite chain (two- and three-dimensional systems not yet being discussed) can be ferromagnetic (possess a magnetic moment) even for $T \neq 0$ (for an infinite chain, long-range order essentially vanishes, while any finite set of spins may possess a magnetic moment differing from zero as the result of short-range order). In the case of finite systems, condition (6) is also essential. According to Eqs. (3) and (8),

$$S^x_{\mathbf{total}} = \sum_j S^x_j = N^{1/2}S^x_0,$$

$$\langle(S^x_{\mathbf{total}})^2\rangle = N\langle(S^x_0)^2\rangle$$

$$= \eta SN\left(\bar{n}_0 + \tfrac{1}{2}\right) = \eta SN\left\{\left(\exp\frac{\hbar\omega_{\lambda=0}}{kT} - 1\right)^{-1} + \tfrac{1}{2}\right\},$$

$$\omega_{\lambda=0} = \omega_H + \omega_{A0}\eta.$$

Hence, condition (6), within the region in which $\hbar\omega_{\lambda=0}/kT \ll 1$ and $\omega_H \ll \omega_{A_0}\eta$, acquires the form

$$\eta \gg \sqrt{kT/\hbar\omega_{A0}SN} = \sqrt{kT/\mu S H_{A0} N}. \tag{21}$$

However, if $\omega_H \gg \omega_{A0}\eta$, the following inequality must be satisfied

$$\eta \gg kT/\hbar\omega_H SN = kT/\mu SHN.$$

When $T \rightarrow 0$, we have the condition $\eta \gg 1/N$ in place of Eq. (21). For example, condition (21) for $T \sim \Theta$, $S \sim 1$, and $k\Theta/\mu H_{A_0} \sim 10^6$ ($\Theta \sim 10^3$ deg K, $H_{A_0} \sim 10$ oe) is reduced to the requirement that $\eta \gg 10^3/\sqrt{N}$. Then, for $\eta \sim 0.1$, only sufficiently small particles having $N \lesssim 10^8$ fail to fulfill the condition.

The problem of the behavior of systems having Hamiltonians of the type of Eq. (1) in cases in which conditions (6) and (7) are not fulfilled is highly interesting. Here we may expect very peculiar properties, in particular a high susceptibility χ, showing a tendency toward saturation even at not very strong fields. More concretely, we have in mind systems for which the Curie point $\Theta \ll J/k$ (and as a particular case, $\Theta = 0$). Then, in the region $\Theta < T < J/k$, a law of the type $\chi \sim 1/(T - \Theta)$ apparently need not hold true, since the interaction between the spins $\sim J/k$ is still very strong. A system of spins in such a state may be designated as an "incoherent ferromagnetic material" or a "paramagnetic fluid" with ferromagnetic interaction (see also Sec. 3).

2. ANTIFERROMAGNETISM (GENERAL STUDY)

The Hamiltonian of the model being studied of an antiferromagnetic material in an external field **H** and an anisotropy field $\mathbf{H}_A$ has the form

$$\mathcal{H} = \sum_{j,k} J_{jk}\mathbf{S}_j\mathbf{S}_k - \mu\mathbf{H}\sum_{j,k}(\mathbf{S}_j + \mathbf{S}_k) - \mu\mathbf{H}_A\sum_{jk}(\mathbf{S}_j - \mathbf{S}_k). \tag{22}$$

Here the subscripts j and k denote the spins situated at the points of the two sublattices 1 and 2, while the sign is chosen such that the exchange integral for the antiferromagnetic interaction $J_{jk} > 0$. N is the total number of spins. We shall introduce the operators $\mathbf{S}_{1,2\lambda}$:

$$\mathbf{S}_\mathbf{j} = \left(\frac{2}{N}\right)^{1/2}\sum_\lambda \mathbf{S}_{1,\lambda}\exp(-i\boldsymbol{\lambda}\mathbf{j}),$$

$$\mathbf{S}_\mathbf{k} = \left(\frac{2}{N}\right)^{1/2}\sum_\lambda \mathbf{S}_{2,\lambda}\exp(-i\boldsymbol{\lambda}\mathbf{k}),\quad \mathbf{S}_{1,\lambda} = \left(\frac{2}{N}\right)^{1/2}\sum_\mathbf{j} \mathbf{S}_\mathbf{j}\exp(i\boldsymbol{\lambda}\mathbf{j}), \tag{23}$$

where

$$\{S^x_{l,\lambda} S^y_{m\mu}\} = i\sqrt{2/N}\,\delta_{lm}S^z_{l,\lambda+\mu} \quad \text{and its cyclic permutations;} \quad l, m = 1, 2;$$

$$\sum_\mathbf{j}\exp\{i(\boldsymbol{\lambda} - \boldsymbol{\mu})\mathbf{j}\} = (N/2)\,\delta_{\lambda\mu}.$$

Further, the operator (22) acquires the form

$$\mathcal{H} = 4DJ\sum_\lambda \gamma_\lambda \mathbf{S}_{1,\lambda}\mathbf{S}_{2,-\lambda} - \mu\left(\frac{N}{2}\right)^{1/2}\mathbf{H}(\mathbf{S}_{1,0} + \mathbf{S}_{2,0})$$

$$- \mu\left(\frac{N}{2}\right)^{1/2}\mathbf{H}_A(\mathbf{S}_{1,0} - \mathbf{S}_{2,0}),$$

$$2DJ\gamma_\lambda = \sum_{\mathbf{k}-\mathbf{j}} J_{\mathbf{jk}}\exp\{i\boldsymbol{\lambda}(\mathbf{k} - \mathbf{j})\},$$

$$J = (2D)^{-1}\sum_{\mathbf{k}-\mathbf{j}} J_{\mathbf{jk}},\ \gamma_0 = 1,\ \gamma_\lambda = \gamma_{-\lambda}. \tag{24}$$

Here the fact has been taken into account that we encounter identical terms twice in summing over j and k in Eq. (22). D is the number of dimensions of the simple lattice being studied. Only nearest neighbors are assumed to interact (i.e., 2D = Z = the number of neighbors). We then obtain the equations of motion from Eq. (24):

$$\dot{\mathbf{S}}_{1,\lambda} = \frac{i}{\hbar}\{\mathcal{H}\mathbf{S}_{1,\lambda}\}$$

$$\omega_0\sqrt{\frac{2}{N}}\sum_\mu \gamma_\mu[\mathbf{S}_{2,-\mu}\mathbf{S}_{1,\lambda+\mu}] + \frac{\mu}{\hbar}[\mathbf{S}_{1,\lambda},\ \mathbf{H} + \mathbf{H}_A],$$

$$\dot{\mathbf{S}}_{2,\lambda} = \omega_0\sqrt{\frac{2}{N}}\sum_\mu \gamma_\mu[\mathbf{S}_{1,-\mu}\mathbf{S}_{2,\lambda+\mu}]$$

$$+ \frac{\mu}{\hbar}[\mathbf{S}_{2,\lambda},\ \mathbf{H} - \mathbf{H}_A],\ \omega_0 = \frac{4DJ}{\hbar}. \tag{25}$$

We shall now linearize Eqs. (25) in the vicinity of the mean values:

$$\langle S^1_{\mathbf{total}\,z}\rangle = \sum\langle S_{j,z}\rangle = \sqrt{\frac{N}{2}}\,S^z_{1,0}$$

$$= \frac{N}{2}\langle S_{jz}\rangle = \frac{N}{2}\eta_1 S,$$

$$\langle S^2_{\mathbf{total}\,z}\rangle = \sum_k\langle S_{kz}\rangle = \sqrt{\frac{N}{2}}\,S^z_{2,0} = -\frac{N}{2}\eta_2 S. \tag{26}$$

We have obviously made here the common assumption of the theory of antiferromagnetism that both sublattices possess a large mean spin (magnetization) directed along z or in the opposite direction.[3,6,20-23] Here we shall consider, in the absence of an external field **H**, that $\eta_1 = \eta_2$, i.e., the system as a whole possesses no magnetic moment.* As is known, unlike in the ferromagnetic case, the problem of the quantum-mechanical nature of the original state used in Eq. (26) is not yet very clear,[3] but we shall not take up this important problem now.

After linearization, Eq. (25) may be written as follows (with the fields **H** and $\mathbf{H}_A$ directed along the z axis):

---

*We may consider analogously the case of ferromagnetism in which the magnetic moments of the sub-lattices are not equal in absolute value, even at H = 0.

$$\dot{S}^x_{1,\lambda} = (\omega_0 S\eta_2 + \omega_{A0}\eta_2 + \omega_H)\,S^y_{1,\lambda} + \omega_0 S\eta_1\gamma_\lambda S^y_{2,\lambda},$$
$$\dot{S}^x_{2,\lambda} = -(\omega_0 S\eta_1 + \omega_{A0}\eta_1 - \omega_H)\,S^y_{2,\lambda} - \omega_0 S\eta_2\gamma_\lambda S^y_{1,\lambda},$$
$$\dot{S}^y_{1,\lambda} = -(\omega_0 S\eta_2 + \omega_{A0}\eta_2 + \omega_H)\,S^x_{1,\lambda} - \omega_0 S\eta_1\gamma_\lambda S^x_{2,\lambda},$$
$$\dot{S}^y_{2,\lambda} = (\omega_0 S\eta_1 + \omega_{A0}\eta_1 - \omega_H)\,S^x_{2,\lambda} + \omega_0 S\eta_2\gamma_\lambda S^x_{1,\lambda},$$

$$\{S^x_{1,\lambda}S^y_{1,-\lambda}\} = i\eta_1 S, \quad \omega_H = \mu H/\hbar, \quad \omega_{A0} = \mu H_{A0}/\hbar,$$
$$\omega_0 = 4DJ/\hbar, \quad \gamma_\lambda = \gamma_{-\lambda}, \qquad \{S^x_{2,\lambda}S^y_{2,-\lambda}\} = -i\eta_2 S. \quad (27)$$

Here, in the equations for $S^{x,y}_{1,\lambda}$ we have assumed that $(\mu\hbar)H_A = \omega_{A_0}\eta_2$ and in the equations for $S^{x,y}_{2\,\lambda}$, that $(\mu\hbar)H_A = \omega_{A_0}\eta_1$, where $\omega_{A_0} = (\mu\hbar)H_{A_0}$ = const. Of course this means in essence that we have had to introduce two fields H_A differing for the two sublattices, from Eq. (22) on. By considering the fields H_A to be proportional to $\eta_{1,2}$, we take into account very simply the fact that the anisotropy field H_A itself vanishes when $\eta_{1,2} = 0$. The system (27) is derived from the Hamiltonian

$$\mathcal{H} = \frac{\hbar}{S}\sum_\lambda \frac{1}{2\eta_1}(\omega_0 S\eta_2 + \omega_{A0}\eta_2 + \omega_H)(S^x_{1,\lambda}S^x_{1,-\lambda} + S^y_{1,\lambda}S^y_{1,-\lambda})$$
$$+ \frac{1}{2\eta_2}(\omega_0 S\eta_1 + \omega_{A0}\eta_1 - \omega_H)(S^x_{2,\lambda}S^x_{2,-\lambda} + S^y_{2,\lambda}S^y_{2,-\lambda})$$
$$+ \omega_0 S\gamma_\lambda(S^x_{1,\lambda}S^x_{2,-\lambda} + S^y_{1,\lambda}S^y_{2,-\lambda}). \quad (28)$$

We shall now transform to new variables

$$S^x_{1,\lambda} = (c_{1,\lambda}Q_{1,\lambda} + c_{2,\lambda}Q_{2,-\lambda})\sqrt{\eta_1 S},$$
$$S^y_{1,\lambda} = (c_{1,\lambda}P_{1,-\lambda} - c_{2,\lambda}P_{2,-\lambda})\sqrt{\eta_1 S},$$
$$S^x_{2,-\lambda} = (c_{2,\lambda}Q_{1,-\lambda} + c_{1,\lambda}Q_{2,\lambda})\sqrt{\eta_2 S},$$
$$S^y_{2,-\lambda} = (c_{2,\lambda}P_{1,\lambda} - c_{1,\lambda}P_{2,-\lambda})\sqrt{\eta_2 S},$$
$$\{Q_{l\lambda}P_{m\mu}\} = i\delta_{lm}\delta_{\lambda\mu}.$$

where

$$c_{1,\lambda} = c_{1,-\lambda}, \qquad c_{2\lambda} = c_{2,-\lambda}, \qquad c^2_{1,\lambda} - c^2_{2,\lambda} = 1,$$
$$c_{1,\lambda} = \rho_\lambda/\sqrt{\rho^2_\lambda - \gamma^2_\lambda}, \qquad c_{2,\lambda} = -\gamma_\lambda/\sqrt{\rho^2_\lambda - \gamma^2_\lambda},$$
$$\rho_\lambda = (1+\delta)\left(\frac{\eta_1+\eta_2}{2\sqrt{\eta_1\eta_2}}\right) + \left[(1+\delta)^2\left(\frac{\eta_1+\eta_2}{2\sqrt{\eta_1\eta_2}}\right)^2 - \gamma^2_\lambda\right]^{1/2},$$
$$\delta_a \equiv \delta - \frac{\omega_{A0}}{\omega_0 S}.$$

In terms of these new variables, the Hamiltonian acquires the form

$$\mathcal{H} = \frac{\hbar}{2}\sum_\lambda \omega^+_\lambda(Q_{1,\lambda}Q_{1,-\lambda} + P_{1,\lambda}P_{1,-\lambda})$$
$$+ \omega^-_\lambda(Q_{2,\lambda}Q_{2,-\lambda} + P_{2,\lambda}P_{2,-\lambda}),$$

where

$$\omega^+_\lambda = \omega_0 S\frac{(1+\delta)(\eta_1\gamma^2_\lambda + \eta_2\rho^2_\lambda) - 2\sqrt{\eta_1\eta_2}\,\gamma^2_\lambda\rho_\lambda}{\rho^2_\lambda - \gamma^2_\lambda} + \omega_H,$$
$$\omega^-_\lambda = \omega_0 S\frac{(1+\delta)(\eta_2\gamma^2_\lambda + \eta_1\rho^2_\lambda) - 2\sqrt{\eta_1\eta_2}\,\gamma^2_\lambda\rho_\lambda}{\rho^2_\lambda - \gamma^2_\lambda} - \omega_H. \quad (29)$$

If we assume that $\eta_1 = \eta_2 = \eta$,

$$\omega^\pm_\lambda = \eta\omega_0 S\sqrt{(1+\delta)^2 - \gamma^2_\lambda} \pm \omega_H = \omega_\lambda \pm \omega_H. \quad (29a)$$

In order to express the Hamiltonian as a sum of Hamiltonians of harmonic oscillators, we shall transform to the variables

$$Q_{1,\pm\lambda} = \sqrt{\tfrac{1}{2}}\,(q_{1,\lambda} \pm iq_{2,\lambda}), \qquad P_{1,\pm\lambda} = \sqrt{\tfrac{1}{2}}\,(p_{1,\lambda} \mp ip_{2,\lambda}),$$
$$Q_{2,\pm\lambda} = \sqrt{\tfrac{1}{2}}\,(q_{3,\lambda} \pm iq_{4,\lambda}),$$
$$P_{2,\pm\lambda} = \sqrt{\tfrac{1}{2}}\,(p_{3,\lambda} \mp ip_{4,\lambda}); \quad \{q_{l\lambda}p_{m\mu}\} = i\delta_{lm}\delta_{\lambda\mu}. \quad (30)$$

In terms of these variables, the Hamiltonian operator becomes

$$\mathcal{H} = \sum_{\lambda\geq 0}{}' \{\tfrac{1}{2}(q^2_{1,\lambda} + p^2_{1,\lambda} + q^2_{2,\lambda} + p^2_{2,\lambda})\hbar\omega^+$$
$$+ \tfrac{1}{2}(q^2_{3,\lambda} + p^2_{3,\lambda} + q^2_{4,\lambda} + p^2_{4,\lambda})\hbar\omega^-\}.$$

The matrix elements of the operators q and p are equal to:

$$(q_{l,\lambda})_{n,\,n+1} = \sqrt{(n+1)/2} = (q_{l,\lambda})_{n+1,\,n},$$
$$(p_{l,\lambda})_{n,\,n+1} = -(p_{l,\lambda})_{n+1,\,n} = -i\sqrt{(n+1)/2}. \quad (32)$$

The eigenvalues of the energy of the spin waves are:

$$\mathcal{H} = \sum_{\lambda\geq 0}{}'(n_{1,\lambda} + \tfrac{1}{2} + n_{2,\lambda} + \tfrac{1}{2})\hbar\omega^+_\lambda$$
$$+ (n_{3,\lambda} + \tfrac{1}{2} + n_{4,\lambda} + \tfrac{1}{2})\hbar\omega^-_\lambda,$$

or

$$\mathcal{H} = \sum_\lambda (n^+_\lambda + \tfrac{1}{2})\hbar\omega^+_\lambda + (n^-_\lambda + \tfrac{1}{2})\hbar\omega^-_\lambda. \quad (33)$$

We shall use the following equations as conditions of self-consistency:

$$\langle(S^x_j)^2 + (S^y_j)^2\rangle = \frac{2}{N}\sum_\lambda\langle S^x_{1,\lambda}S^x_{1,-\lambda}$$
$$+ S^y_{1,\lambda}S^y_{1,-\lambda}\rangle = S(S+1) - \langle(S^z_j)^2\rangle,$$
$$\langle(S^x_k)^2 + (S^y_k)^2\rangle = \frac{2}{N}\sum_\lambda\langle S^x_{2,\lambda}S^x_{2,-\lambda}$$
$$+ S^y_{2,\lambda}S^y_{2,-\lambda}\rangle = S(S+1) - \langle(S^z_k)^2\rangle, \quad (34)$$

which may be written in the form

$$\eta_1 S(G_D + G^{(1)}_{DT}) = S(S+1) - \langle(S^z_j)^2\rangle,$$
$$\eta_2 S(G_D + G^{(2)}_{DT}) = S(S+1) - \langle(S^z_k)^2\rangle;$$

$$G_D = \frac{2}{N}\sum_\lambda\frac{\rho^2_\lambda + \gamma^2_\lambda}{\rho^2_\lambda - \gamma^2_\lambda}$$
$$= \frac{2}{N}\sum_\lambda\frac{(1+\delta)(\eta_1+\eta_2)/2\sqrt{\eta_1\eta_2}}{\{(1+\delta)^2[(\eta_1+\eta_2)/2\sqrt{\eta_1\eta_2}]^2 - \gamma^2_\lambda\}^{1/2}};$$

$$G^{(1)}_{DT} = \frac{4}{N}\sum_\lambda\frac{\rho^2_\lambda\overline{n^+_\lambda} + \gamma^2_\lambda\overline{n^-_\lambda}}{\rho^2_\lambda - \gamma^2_\lambda}, \quad G^{(2)}_{DT} = \frac{4}{N}\sum_\lambda\frac{\gamma^2_\lambda\overline{n^+_\lambda} + \rho^2_\lambda\overline{n^-_\lambda}}{\rho^2_\lambda - \gamma^2_\lambda},$$

$$\overline{n^\pm_\lambda} = \left[\exp\frac{\hbar\omega^\pm_\lambda}{kT} - 1\right]^{-1}. \quad (35)$$

For the case of spin $\frac{1}{2}$, to which we shall limit ourselves for simplicity, $(S_j^Z)^2 = (S_k^Z)^2 = \frac{1}{4}$, and

$$\eta_1 (G_D + G_{DT}^{(1)}) = 1, \qquad \eta_2 (G_D + G_{DT}^{(2)}) = 1. \tag{36}$$

In the absence of a magnetic field, $\eta_1 = \eta_2 = \eta$ for an antiferromagnetic material, Eqs. (35) and (36) coincide, and for spin $S = \frac{1}{2}$ we have

$$\eta\,(J_D + J_{DT}) = 1, \qquad J_D = \frac{2}{N} \sum \frac{1+\delta}{[(1-\delta)^2 - \gamma_\lambda^2]^{1/2}},$$

$$J_{DT} = \frac{4}{N} \sum \frac{1+\delta}{[(1+\delta)^2 - \gamma_\lambda^2]^{1/2}} (e^{\hbar\omega_\lambda/kT} - 1)^{-1},$$

$$\omega_\lambda = \frac{\eta\omega_0}{2} [(1+\delta)^2 - \gamma_\lambda^2]^{1/2}, \quad \delta = \frac{2\omega_{A0}}{\omega_0}, \quad \omega_0 = \frac{4DJ}{\hbar}. \tag{37}$$

Obviously, when $T = 0$,

$$\eta(0) = J_D^{-1}. \tag{38}$$

For two- and three-dimensional lattices of large dimensions, the integral J_D converges even when $\delta = 0$. Then $J_D = (2\pi)^{-D} \int d\lambda \sqrt{1-\gamma_\lambda^2}$, and according to Anderson,[20] $J_2 = 1.393$ and $J_3 = 1.156$. Thus, for the two- and three-dimensional cases, respectively, $\eta(0) = 0.72$ and $\eta(0) = 0.865$. The latter result agrees with references 3 and 20, but is more precise. For an infinite linear chain with $\delta \ll 1$, $J_D = J_1 \approx \pi^{-1} |\ln \delta|$. Hence, the value of $\eta(0)$ is not zero. In fact, as in the ferromagnetic case, there is no long-range order in a linear antiferromagnetic chain. However, the result obtained by neglecting fluctuations seems more natural than that stated by Anderson.[20]

Near the Néel point, when $\eta \ll 1$, we have

$$\eta^2 = A\left(1 - \frac{T}{\Theta}\right), \quad \Theta = \frac{DJ}{kF_a}, \quad F_a = \frac{2}{N} \sum \frac{1+\delta}{(1+\delta)^2 - \gamma_\lambda^2},$$

$$A^{-1} = \frac{2}{3N} \sum (1+\delta) \frac{DJ}{k\Theta} = (1+\delta) \frac{DJ}{3k\Theta}. \tag{39}$$

For the three-dimensional case, as $\delta \to 0$,

$$F_a = \frac{2}{N} \sum \frac{1}{1-\gamma_\lambda^2} = \frac{1}{(2\pi)^3} \int \frac{d\lambda}{1-\gamma_\lambda^2}$$

$$\frac{1}{\pi^3} \iiint_0^\pi \frac{du\,dv\,dw}{1 - [(\cos u + \cos v + \cos w)/3]^2}$$

$$\frac{1}{\pi^3} \iiint_0^\pi \frac{du\,dv\,dw}{1 - (\cos u + \cos v + \cos w)/3} = 1.516. \tag{40}$$

Hence, the ratio $k\Theta/J = 3J/kF_a = 1.98$, i.e., it is the same as in ferromagnetic materials (see above). Unfortunately, there have been no completely reliable statistical calculations of $k\Theta/J$ for antiferromagnetic materials, at least as known to us. According to the calculations in reference 24, which seem to be the most reliable,[23] $k\Theta/J = 2.004$ for a simple cubic lattice. The necessary condition for the applicability of the self-consistent approximation has a form of the type of Eq. (6), namely

$$N\eta S \gg \sqrt{\langle (S_{1,2\,\mathrm{total}}^{x,y})^2 \rangle}.$$

It is easy to see that this condition (for high temperatures with $H = 0$) coincides with criterion (21). As $T \to 0$, for antiferromagnetic materials the following inequality must be satisfied, instead of Eq. (21)

$$\eta \gg 1/N\sqrt{\delta} \qquad (\eta \ll 1). \tag{41}$$

We note that a certain self-consistent treatment in the theory of antiferromagnetism has already been carried out by Ziman[21] for the purpose of deriving corrections to the ordinary theory of spin waves; a paper on this latter subject by Oguchi[25] has recently appeared. In addition, P'u Fu-C'ho[26] recently extended the method of Bogolyubov and Tyablikov[14] to the case of antiferromagnetism with spin $\frac{1}{2}$ in the absence of anisotropy. In the assumptions just given, the result obtained by P'u Fu-C'ho[26] and that derived above [see Eqs. (38) — (41)] agree; this may serve as a test of the correctness of the methods of calculation. The use of different methods here seems essential to us, since the comparison with the results of references 24 and 26 gives us additional confidence in the effectiveness, and in general, in the quite high accuracy of the method of calculation which we have used.

In order to calculate the parallel susceptibility $\chi_{\parallel}$, we must know η_1 and η_2 in the presence of a magnetic field. We shall assume that

$$\hbar\omega_H / kT \ll 1, \qquad \eta_1 = \eta + \eta_1', \qquad \eta_2 = \eta + \eta_2',$$

where

$$|\eta_{1,2}'| = O(\hbar\omega_H / kT) \ll \eta.$$

Then, we obtain from Eqs. (36) and (37), by expansion in series to an accuracy of first-order terms in $\hbar\omega_H/kT$, η_1', and η_2',

$$\eta_1' (J_D + J_{DT}) + \eta\, [\partial (G_D + G_{DT}^{(1)}) / \partial\eta_1]_0\, \eta_1'$$
$$+ \eta\, [\partial (G_D + G_{DT}^{(1)}) / \partial\eta_2]_0\, \eta_2'$$
$$\eta R \hbar\omega_H / kT = 0.$$

$$\eta_2' (J_D + J_{DT}) + \eta\, [\partial (G_D + G_{DT}^{(2)}) / \partial\eta_1]_0\, \eta_1'$$
$$+ \eta\, [\partial (G_D + G_{DT}^{(2)}) / \partial\eta_2]_0\, \eta_2' + \eta R \hbar\omega_H / kT = 0,$$

$$R = \frac{1}{N} \sum_\lambda \left[\left(\coth \frac{\hbar\omega_\lambda}{2kT}\right)^2 - 1\right] = \frac{1}{N} \sum_\lambda \left(\sinh \frac{\hbar\omega_\lambda}{2kT}\right)^{-2},$$

$$\eta\,(J_D + J_{DT}) = 1. \tag{42}$$

The subscript zero in the derivatives with respect to η_1 and η_2 indicates that they are taken for η_1

$= \eta_2 = \eta$, where

$$\left[\frac{\partial}{\partial\eta_{1,2}}\left(G_{DT}^{(1)} - G_{DT}^{(2)}\right)\right]_0 = \frac{4}{N}\sum\left|\frac{\partial(n^+ - n^-)}{\partial\eta_{1,2}}\right|_0$$

$$= \frac{\hbar}{NkT}\sum_\lambda\left[\left(\coth\frac{\hbar\omega_\lambda}{2kT}\right)^2 - 1\right]\left(\frac{\partial(\omega_\lambda^- - \omega_\lambda^+)}{\partial\eta_{1,2}}\right)_0,$$

$$(\omega_\lambda^- - \omega_\lambda^+) = \omega_0 S(1+\delta)(\eta_1 - \eta_2) - 2\omega_H.$$

Hence, as may be easily seen

$$\eta_1' = -\eta_2', \qquad \eta_1' - \eta_2' = \frac{2\eta R\hbar\omega_H / kT}{(\hbar\omega_0 S / kT)(1+\delta)\eta R + \eta^{-1}},$$

$$S = {}^1/_2, \qquad \hbar\omega_H = \mu H, \qquad \mu = \frac{ge\hbar}{2mc}, \qquad \hbar\omega_0 = 4DJ,$$

$$M_z = (\eta + \eta_1')\frac{N}{2}S\mu - (\eta + \eta_2')\frac{N}{2}S\mu$$

$$= \frac{\mu^2\eta^2 RNH}{\hbar\omega_0(1+\delta)\eta^2 R + 2kT} = V\chi_\parallel H, \tag{43}$$

where M_Z is the total magnetic moment, V is the volume, and $\chi_{||}$ is the susceptibility per unit volume.

At low temperatures, when $\hbar\omega_0(1+\delta)\eta^2 R \ll 2kT$,

$$\chi_\parallel = \frac{\mu^2\eta^2}{2kTV}\sum_\lambda \sinh\frac{\hbar\omega_\lambda}{2kT})^{-2}. \tag{44}$$

For $\eta = 1$, this formula coincides with that derived in the ordinary spin-wave approximation.[21] However, even at low temperatures Eq. (43) is more accurate, since $\eta \approx \eta(0) = J_D^{-1} \neq 1$. Near the Néel point

$$R \approx [2/\eta^2(1+\delta)][k\Theta/2DJ)^2 F_a = {}^1/_2 F_a(1+\delta)\eta^2$$

[see Eq. (39)], and consequently,

$$\chi_\parallel(\Theta) = \frac{\mu^2 N}{8k(1+\delta)F_a V\Theta} = \frac{\mu^2 N}{8D(1+\delta)JV}. \tag{45}$$

3. ANTIFERROMAGNETISM OF SMALL PARTICLES AND CHAINS. PARAMAGNETIC FLUIDS

The formulas derived in Sec. 2 permit us within certain limits to explain the dependence of the magnetization of the sublattices $M_{1,2}(T)$, the Néel temperature Θ, the susceptibility $\chi_{||}$, and certain other quantities on the form and dimensions of the system, as well as on various parameters (J, δ, etc). However, we cannot go into detail here on this set of problems, but shall limit ourselves to a few remarks.

In the antiferromagnetic case [in distinction from a ferromagnetic system with the Hamiltonian of Eq. (1)], the magnetization of the sublattices $M_{1,2} = + NS\eta(T)/2$ depends on the form and dimensions of the spin system even at T = 0. This fact is especially clear from Eqs. (37) — (39) and (43) — (44) in the limiting case of very small particles, as is also the fact of the corresponding dependences of the quantities Θ, $\chi_{||}$, and $\eta(T)$. The point is that in a sufficiently small system, the first term having $\lambda = 0$, which is neglected when we go over to integration, plays the predominant role in the sums. At the same time, if we retain only this first term having $\lambda = 0$, we obtain (for $\delta \ll 1$)

$$J_D = \sqrt{2}/N\sqrt{\delta}, \qquad F_a = 1/N\delta,$$

$$\Theta = DJ/kF_a = 2JN\delta/k = \mu H_{A0}N/2k, \quad \eta(0) = N\sqrt{\delta/2}, \tag{46}$$

where

$$\delta = 2\omega_{A0}/\omega_0, \qquad \omega_0 = 4DJ/\hbar, \qquad \omega_{A0} = \mu H_{A0}/\hbar.$$

For a large three-dimensional spin system, $\eta(0) = 0.856$, and $F_a = 1.516$; hence it seems that the expressions in (46) might be applied, respectively, under the conditions $N\sqrt{\delta} \ll 1$ [for $\eta(0)$], and $N\delta \ll 1$ (for Θ). However, in fact, there is no region in which the formulas of (46) are applicable, in line with the fact that the inequalities (21) and (41) are not fulfilled. Nevertheless, it follows from (46), just as from a more detailed analysis, that $\eta(0)$ and Θ become less in small particles.* The change in the quantities $\eta(T)/\eta(0)$ and $\chi_{||}(T)$ with decreasing dimensions of the system is even clearer. In fact, under the condition $NkT\mu H_{A_0}/(\hbar\omega_0)^2 \ll 1$, which is compatible with (41), in the temperature region in which $\hbar\omega_{\lambda=0} = \omega_0\sqrt{\delta/2}\eta \ll kT \ll k\Theta$, we may easily derive (for $N\sqrt{\delta} \gg 1$):

$$J_{DT} = 2kT/\mu H_{A0}N\eta, \qquad \eta(T) = \eta(0)(1 - 2kT/\mu H_{A0}N), \tag{47}$$

$$\chi_\parallel(T) = (2\mu^2/VkT)(kT/\hbar\sqrt{\omega_0\omega_{A0}})^2. \tag{48}$$

Thus, within a certain definite region, the difference $1 - \eta(T)/\eta(0)$ and the susceptibility $\chi_{||}$ differ considerably from the values given by the expressions

$$1 - \eta(T)/\eta(0) \sim (kT/\hbar\omega_0)^2 \text{ and } \chi_\parallel \sim (\mu^2 N/kTV)(kT/\hbar\omega_0)^3,$$

applicable to large systems.[22] The result (45) is also of interest; according to it the value of $\chi_{||}$ at the transition point for a given J is independent of Θ (for $\delta \ll 1$). Hence it is clear that in the general case in the region $T < \Theta$ (for a given temperature T and for constant values of the other parameters), the susceptibility increases with the decrease in Θ which takes place in small particles, films, and fibers.

---

*Naturally, as the dimensions of the system are decreased, the transition becomes less sharp, and strictly speaking, we cannot speak then of a phase transition. In practice, when $N \gg 1$ this fact is not essential.

Thus, the properties of antiferromagnetic finely-dispersed substances, polymer chains and structures may be appreciably different from those of the ordinarily studied antiferromagnetic substances (above all, it would be expedient to compare the properties of one and the same substance as depending on the dimensions and form of the crystals).

In the region in which the limiting formulas (47) and (48) are valid, the difference between antiferromagnetic specimens of differing forms is obliterated. This is understandable, since the role of the form decreases as all dimensions are decreased. In addition, for sufficiently thin films and fibers, the differences from the three-dimensional case may be very great, since long-range order is generally absent in an infinite chain, as it is also in a two-dimensional system with $\delta = 0$. In fact, according to Eqs. (37) — (39), for an infinite chain, $\eta(0) \approx \pi/|\ln \delta|$, and $\Theta = J\sqrt{2\delta}/k$. However, in this case the approximation itself is not valid, in connection with the increase in fluctuations (see the analogous estimate for ferromagnetic substances at the end of Sec. 1).

However, for finite chains, especially if they are short enough, antiferromagnetic ordering may take place. It is sufficient to say that we cannot make a strict distinction between long-range and short-range order in a finite system. However, with regard to short-range antiferromagnetic order, the latter is observed in a series of substances (e. g., by neutron scattering) even at temperatures considerably above the Néel point. In this regard, we may also refer to the calculation of the short-range order in an infinite chain.[27,28] On the other hand, as has been mentioned, our formulas are inapplicable to sufficiently small particles, as well as to antiferromagnetic systems above the Néel point. This is associated with the use, along with the other magnetic moments, of the anisotropy field $H_A = H_{A_0}\eta$, which vanishes when the mean magnetization of the sublattice equals zero. The fact is that the appearance of short-range order is also associated with a certain anisotropy field H'_A, which apparently is of the order of H_{A_0} for the given small group of spins.

The region of very small particles and chains, as well as the paramagnetism of those systems having thermal transitions $\Theta \ll \Theta_0 \sim J/k$, is nevertheless very interesting. Hence, in spite of the fact that we have no pertinent quantitative results, we shall consider this problem too.

Ordinarily, $\Theta \sim \Theta_0 \sim J/k$, and correspondingly, when $\Theta \ll \Theta_0$ (in particular, when $\Theta = 0$), we may expect that the formula $\chi \sim \text{const}/(T + \Theta)$ will not be valid over the wide temperature range $\Theta < T < \Theta_0 \sim J/k$. (A law of the type $\chi \sim \text{const}/(T + \Theta)$ will probably hold true for $T \gtrsim \Theta_0$.) In the temperature range $\Theta < T \gtrsim \Theta_0$ (this range has no sharp upper boundary), the substance may be called either an "incoherent antiferromagnetic substance" or a "paramagnetic fluid" with antiferromagnetic interaction (the analogous concepts for the ferromagnetic case have already been taken up at the end of Sec. 1; in connection with this subject, the experimental data of Ryan, Pugh, and Smoluchowski[29] may be of interest). As in the case of other fluids, it seems impossible, in general, to construct a consistent and sufficiently exact theory for such a state. Individual special cases may be exceptions (a long chain at low temperatures, etc).* We hope yet to take up this problem in its various aspects, but shall mention at present only the following.

One of the possibilities for a qualitative understanding is the comparison of the properties of fluids with those of a very highly-disperse crystalline medium (the quasi-crystalline model). Individual "crystallites" of such a medium contain a small number of spins each. According to the hypothesis, these crystallites retain their high degree of order, i.e., within them $\eta \sim 1$ (or, say, $\eta \sim 0.1$) and $H'_A = H_{A_0}$. Then, as might be supposed, the lowest excited state of the "crystallite" has an energy of $\hbar\omega_{\lambda=0}$, where

$$\omega_{\lambda=0} = \eta\omega_0 S\sqrt{2\delta} \pm \omega_H \sim \sqrt{\omega_0\omega_{A0}} \pm \omega_H$$

[see Eq. (29a)]. The susceptibility of such a system is determined by Eq. (48), which had also been derived by us previously.[2] Here, in the region $\hbar\sqrt{\omega_0\omega_{A_0}}/k \ll T \ll \Theta$, the susceptibility increases in proportion to T^2. Then, probably, χ goes through a gentle maximum at $T \sim \Theta_0 \sim J/k$, and beyond this, decreases according to a law of the type $1/(T + \Theta_0)$. We note also that χ depends on H even in fields of the order of $\hbar\sqrt{\omega_0\omega_{A_0}}/\mu$. Such a model is very crude, and the corresponding estimate of χ is not very convincing, but we should expect just this sort of dependence $\chi(T, H)$ in qualitative terms for a "paramagnetic fluid" of the antiferromagnetic type.

In view of what has been said, the attempt which we made[2] to explain the experimental data of Blyumenfel'd et al.[1] retains its content, but refers now to the region of "incoherent antiferromagnetism." Besides, within the framework of the model which we have studied, the very boundary between the properties of a very finely-dispersed antiferromagnetic system and those of a paramagnetic fluid of the antiferromagnetic type is obliterated to a considerable degree. In particular, internal magnetic fields must be observable (e. g., by the nuclear magnetic resonance method) in "paramagnetic fluids" also, while a strong broadening of the paramagnetic resonance lines will take place as well.

---

*We are familiar only with the result for the Ising model.[19,30] In this case, $\chi_{\parallel}$ has a gentle maximum at $kT \sim J$.

The theoretical and experimental study of "paramagnetic fluids" is of great interest. However, it was possible above, of course, only to pose questions and give some qualitative conceptions which will be necessary in the subsequent analysis. In this regard, it may not be superfluous to emphasize in conclusion that the basic content of this article has not been connected at all with the concept of "paramagnetic fluids", since it has involved the region below the transition temperature.

---

[1] Blyumenfel'd, Kalmanson, and Sheng, Dokl. Akad. Nauk SSSR **124**, 1144 (1959), Soviet Phys.-Doklady **4**, 260 (1959). L. A. Blyumenfel'd, Биофизика (Biophysics) **4**, 515 (1959).

[2] V. L. Ginzburg and V. M. Faĭn, Dokl. Akad SSSR **131**, 785 (1960), Soviet Phys.-Doklady **5**, 328 (1960).

[3] J. Van Kranendonk and J. H. Van Vleck, Revs. Modern Phys. **30**, 1 (1958).

[4] E. M. Lifshitz, JETP **15**, 97 (1945).

[5] C. Herring and C. Kittel, Phys. Rev. **81**, 869 (1951).

[6] M. Kaganov and V. Tsukernik, JETP **34**, 106 (1958), Soviet Phys. JETP **7**, 73 (1958).

[7] F. J. Dyson, Phys. Rev. **102**, 1217 (1956).

[8] V. L. Ginzburg, Физика твердого тела **2**, 2031 (1960), Soviet Phys.-Solid State **2** in press.

[9] V. Zehler, Z. Naturforsch. **5a**, 344 (1950).

[10] G. S. Rushbrooke and P. J. Wood, Proc. Phys. Soc. **A68**, 1161 (1955).

[11] C. Domb and M. F. Sykes, Proc. Roy. Soc. (London) **A240**, 214 (1957).

[12] G. Heber, Z. Naturforsch. **9a**, 91 (1954).

[13] M. R. Schlafroth, Proc. Phys. Soc. **A67**, 33 (1954).

[14] N. N. Bogolyubov and S. V. Tyablikov, Dokl. Akad. Nauk SSSR **126**, 53 (1959), Soviet Phys.-Doklady **4**, 589 (1959).

[15] S. V. Tyablikov, Ukr. Mat. Zhur. **11**, 287 (1959).

[16] M. J. Klein and R. S. Smith, Phys. Rev. **81**, 378 (1951).

[17] C. A. Neugebauer, Phys. Rev. **116**, 1441 (1959).

[18] L. D. Landau and E. M. Lifshitz, Статистическая физика (Statistical Physics), Sec. 144, Gostekhizdat (1951); [Engl. transl. Addison-Wesley, 1958].

[19] G. F. Newell and E. W. Montroll, Revs. Modern Phys. **25**, 353 (1953).

[20] P. W. Anderson, Phys. Rev. **86**, 694 (1952).

[21] J. M. Ziman, Proc. Phys. Soc. **A65**, 540, 548 (1952).

[22] R. Kubo, Phys. Rev. **87**, 568 (1952).

[23] Nagamiya, Yosida, and Kubo, Adv. in Phys. **4**, 1 (1955).

[24] Yin Yuan-li, Phys. Rev. **84**, 721 (1951).

[25] T. Oguchi, Phys. Rev. **117**, 117 (1960).

[26] P'u Fu-C'ho, Dokl. Akad. Nauk SSSR **130**, 1244 and **131**, 546 (1960), Soviet Phys.-Doklady **5**, 128 (1960) and **5**, 321 (1960).

[27] R. Orbach, Phys. Rev. **112**, 309 (1958).

[28] L. R. Walker, Phys. Rev. **116**, 1089 (1959).

[29] Ryan, Pugh, and Smoluchowski, Phys. Rev. **116**, 1106 (1959).

[30] C. Domb, Adv. in Physics, **9**, 150 (1960).

Translated by M. V. King
244

SOVIET PHYSICS JETP VOLUME 12, NUMBER 5 MAY, 1961

CALCULATION OF AVERAGE PARAMETERS OF EXTENSIVE COSMIC-RAY AIR SHOWERS

S. I. NIKOL'SKIĬ and A. A. POMANSKIĬ

P. N. Lebedev Physics Institute, Academy of Sciences, U.S.S.R.

Submitted to JETP editor June 3, 1960

J. Exptl. Theoret. Phys. (U.S.S.R.) 39, 1339-1346 (November, 1960)

Results of a calculation of nuclear-cascade showers containing a given number of electrons at the observation level are presented. The distribution of the production levels is determined for extensive air showers containing 10^4, 10^5, and 10^6 particles at sea level and at 3860 m altitude. Various shower parameters, averaged over different production levels, are compared with experimental data.

THE experiments[1,2] carried out in Pamir (3860 m altitude) in the course of many years have yielded very detailed information on the average parameters of extensive air showers (EAS) with a total number of particles from 10^4 to 10^6 at mountain altitudes. The question arises as to what extent the experimental data correspond with present views concerning the elementary act of nuclear interaction over a wide energy range of the interacting particles.

In experimental studies of the different parameters of EAS, the total number of charged particles (i.e., shower size) at the observation level is determined, rather than the energy of the primary particle producing the shower. Because of fluctuations in the shower production level,[3] in the nuclear interactions of the "leading" particle along the depth of the atmosphere,[4] and in the characteristics of the elementary act of nuclear interaction,* the total number of particles at the observation level reflects the primary-particle energy only on an average basis. In our calculations, we have taken the fluctuations in the shower-production level into account. Other fluctuations are not essential for the assumed model of the elementary act of nuclear interaction upon which the calculations are based. The presence of nuclei with Z > 1 in the primary cosmic radiation has also not been taken into account, which leads to a slight overestimate of the fluctuations in the shower-production level.

1. NUCLEAR-CASCADE SHOWERS PRODUCED BY PARTICLES OF A GIVEN ENERGY

The EAS that are within the size range of interest at the observation level are nuclear-cascade showers produced by primary particles of 10^{12} to 10^{16} ev.

The calculation of nuclear-cascade showers was carried out under the following assumptions:

1. The cascade of nuclear-active particles consists of nucleons and $\pi^\pm$ mesons which, in nuclear interactions, lose energy for the production of π^0 mesons. The number of $\pi^\pm$ mesons decreases also as a result of the $\pi \to \mu$ decay. The possibility of the production of other nuclear-active particles and their influence on the cascade process was not taken into account.

2. To describe the elementary act of nuclear interactions of nucleons and $\pi^\pm$ mesons with air nuclei at $E_0 > 10^{13}$ ev, the hydrodynamical model was used,[6] taking the traveling wave[7] into account. The particle energy corresponding to the traveling wave was assumed to be $0.8\,E_0\,(E_0/\mu c^2)^{-1/15}$, where μ is the rest mass of the meson. The production probability of nucleons or π mesons of such an energy corresponds to the fraction of nucleons or π mesons among all secondary particles, assumed to be 0.27* and 0.73 respectively.

---

*The hypothesis that there is a strong influence of such fluctuations on the development of EAS has been discussed by Grigorov and Shestoperov.[5] In quantitative estimates, however, the fluctuations in the characteristics of the elementary act of interaction have been reduced to fluctuations in the shower production level.

*Such a fraction of nucleons among all secondary particles corresponds to a disintegration temperature of the hydrodynamical system $T_K \sim 1.5\,\mu c^2$. Preliminary calculations based on the fraction of nucleons corresponding to a disintegration temperature $T_K \sim \mu c^2$ have yielded a lower number of nuclear-active particles in EAS at the observation level than that obtained in experiments. It is possible that, by taking hyperons into account within the framework of the hydrodynamical theory, we shall obtain a sufficient number of particles different from π mesons even for $T_K \sim \mu c^2$. Incidentally, the value of 0.27 as the fraction of π mesons does not contradict certain available emulsion data.[8]

3. The relations used for the description of the nuclear interaction of nucleons with energy $E_0 < 10^{13}$ ev differ from the above-mentioned hydrodynamical model only in one additional assumption, namely that the particle corresponding to the traveling wave is a nucleon. For $\pi^\pm$ mesons with energy $E_0 < 10^{13}$ ev, the same hydrodynamical model was used, but without taking the traveling wave into account. Although this formal extrapolation into the low-energy region (down to 10^{10} ev) of the hydrodynamical-model relations does not have sufficient physical justification, the required characteristics of nuclear interactions obtained in this manner nevertheless do not contradict the experimental data in the corresponding energy range.[9]

4. The nuclear-interaction mean free path in air was assumed to be $\lambda_0 = 75$ g/cm^2. In the following discussion, length is measured in units of λ_0.

5. The minimum energy of the particles taking part in the nuclear-cascade process was assumed to be 3.7×10^9 ev.

In carrying out the calculations, the method of successive generations[10] was used. The number of nucleons of the i-th generation of energy E found in a shower produced by a primary particle of energy E_0 was assumed to be

$$N_i(E, E_0) = \int_E^{E_0} N_{i-1}(\varepsilon, E_0) \frac{dn^n}{d\ln\varepsilon} d\ln\varepsilon + \int_E^{E_0} \pi_{i-1}^{\pm}(\varepsilon, E_0) \frac{dn^{\pi}}{d\ln\varepsilon} d\ln\varepsilon \tag{1}$$

and, correspondingly, the number of $\pi^\pm$ mesons is

$$\pi_i^{\pm}(E, E_0) = A_i(E) \int_E^{E_0} N_{i-1}(\varepsilon, E_0) \frac{d\pi^n}{d\ln\varepsilon} d\ln\varepsilon + A_i(E) \int_E^{E_0} \pi_{i-1}^{\pm}(\varepsilon, E_0) \frac{d\pi^{\pi}}{d\ln\varepsilon} d\ln\varepsilon, \tag{2}$$

where $A_i(E) = [1 + k(E)/i]^{-1}$ is a coefficient accounting for the decay of charged π mesons of energy E, and $k(E)$ is given by the expression[10]

$$k(E) = l_0 \lambda_0 / \rho_0 (E/\mu c) \tau_0 \cos\theta.$$

Here ρ_0 is the mean air density in g/cm^3 at the depth l_0 corresponding to sea level, μ the $\pi^\pm$ meson mass, and τ_0 the lifetime of the $\pi^\pm$ meson. An isothermic atmosphere was assumed. In Eqs. (1) and (2), $dn^n/d\ln\epsilon$ and $dn^\pi/d\ln\epsilon$ are the spectra of secondary nucleons produced in the interaction between a nucleon or $\pi^\pm$ meson respectively and an air nucleus, and $d\pi^n/d\ln\epsilon$ and $d\pi^\pi/d\ln\epsilon$ are the spectra of secondary $\pi^\pm$ mesons produced in the interaction between a nucleon or $\pi^\pm$ meson respectively and an air nucleus. The total number of nucleons and $\pi^\pm$ mesons of energy $\geq E$ at a depth x is given by the equations[10]

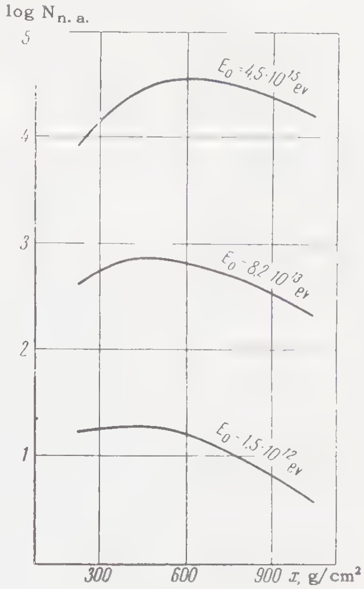

FIG. 1

$$\begin{aligned} N(\geqslant E, x) &= \sum_i^{\infty} \int_E^{E_0} \frac{e^{-x} x^i}{i!} N_i(E', E_0)\, dE', \\ \pi^{\pm}(\geqslant E, x) &= \sum_i^{\infty} \int_E^{E_0} \frac{e^{-x} x^i}{i!} \pi_i^{\pm}(E', E_0)\, dE'. \end{aligned} \tag{3}$$

The variation of $N_{na} = N(\geq E, x) + \pi^\pm(\geq E, x)$ with depth x for $E \geq 3.7 \times 10^9$ ev is shown in Fig. 1 for three values of E_0. In the summation, we cut the series off at that generation whose contribution to the nuclear-active component of the shower amounts to < 1% of the total number of nuclear-active particles at the given depth.*

In order to obtain the variation of the number of electrons with the depth x, it is necessary to add together the cascade showers from the photons produced in the decay of the π^0 mesons. The number of γ rays of energy E of the i-th generation, produced by the π^0 mesons in a shower with total energy E_0, can be assumed to be

$$\gamma_i(E/2, E_0) = \pi_i^{\pm}(E, E_0) / A_i(E).$$

The quantity $\pi_i^\pm(E, E_0)$ is determined by Eq. (2). The total number of electrons at a depth x, produced by photons of energy $\geq E$ produced directly in the decay of the π^0 mesons, is given by the equation[10]

---

*The calculation was carried out by numerical approximation. The error of the results is less than 10%.

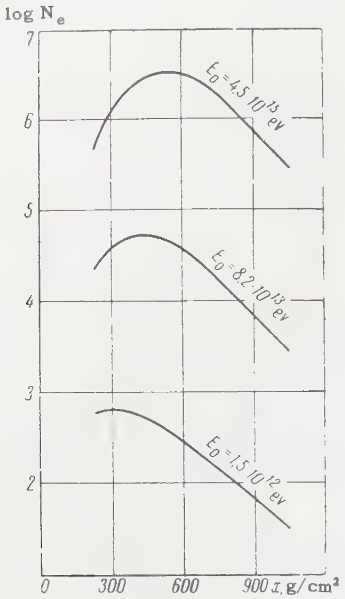

FIG. 2

$$N_e(x) = \sum_i \int_E \gamma_i (E, E_0) \int_0^x e^{-(x-t)} \frac{(x-t)^{i-1}}{(i-1)!} P(E, t)\, dt\, dE, \quad (4)$$

where P(E, t) is the total number of cascade electrons produced by a photon of energy E if the cascade has traversed the depth t.[11] This expression represents a good approximation for $E \gg \beta$, where $\beta = 7.2 \times 10^7$ ev is the critical energy for air. For $E < 10^9$ ev, cascade curves calculated by the moment method were used. The variation of $N_e(x)$ with the depth x for three values of E_0 is shown in Fig. 2.

2. INFLUENCE OF FLUCTUATIONS IN THE PRODUCTION LEVEL OF EAS

By measuring any parameter of an EAS with a given number of particles at the observation level, we obtain an average over a certain energy range of the primary particles that have interacted at different altitudes above the observation level. The results of the calculations of the preceding section refer to showers produced by primary particles of a given energy. The distribution of the production levels and of the energies of the primary particles can be found if we know the energy spectrum of the cosmic radiation at the upper edge of the atmosphere $f(E_0)\,dE_0 = A\,dE_0/E^{\gamma+1}$, the depth of the observation level x_0, the mean free path of nuclear interaction λ_0, and the relation between the primary-particle energy and the total number of charged particles in the shower at various depths in the atmosphere. In the range of production levels and shower sizes of interest we can, with sufficient accuracy, substitute the number of electrons $N(E_0, x) \approx N_e(E_0, x_0 - \bar{x})$ (where $\bar{x}$ is the shower production depth) for the total number of charged particles in the shower.

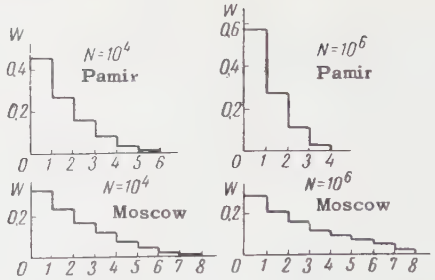

FIG. 3. Production probability W at a given atmospheric depth of a shower having a given size at the observation level (Moscow or Pamir). (The depth is measured in nuclear-interaction mean free paths.)

The number of showers observed at the depth x_0 with a number of particles N and produced at depth $\bar{x}$, is given by the expression

$$C(N, \bar{x})\, dN d\bar{x} = Ae^{-\bar{x}} E_0^{-\gamma} \frac{\partial E_0}{\partial N}\, dN d\bar{x}, \qquad (5)$$

where $E_0 = E_0(N, x_0 - \bar{x})$. The probability of shower production at various depths in the atmosphere, given by Eq. (5), is shown by the histograms in Fig. 3 for two given values of N at mountain altitudes and at sea level. It can be seen that the maximum contribution is due to the showers produced along the first nuclear-interaction mean free path. However, while the only appreciable contribution at mountain altitudes is made by the showers produced along the first three interaction mean free paths, at sea level it is also necessary to take the showers produced at greater depths into account.

From a known distribution of the shower-production levels, we can calculate the energy distribution of the particles producing showers of a given size at the observation level. Such distributions are represented by the histograms in Fig. 4 for showers with a total number of particles $N = 10^5$. The y axis denotes the shower-production probability W for a particle with a given energy. The dotted and solid lines show the distribution for sea level and for the mountain altitude (depth 675

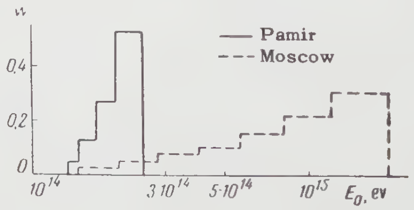

FIG. 4.

TABLE I

Observation level, m	N		
	10^4	10^5	10^6
3860	$2.6\cdot10^{13}$	$2\cdot10^{14}$	$1.6\cdot10^{15}$
0	$1.3\cdot10^{14}$	$0.9\cdot10^{15}$	$0.7\cdot10^{16}$

g/cm^2) respectively. The mean energy (in ev) of the primary particles which produce showers of a given size N at sea level, obtained from analogous distributions, is shown in Table I.

It can be seen from the table that the relation between the mean energy of the primary particles and the total number of charged particles at the observation level differs little from the usual factor relating the number of particles with the energy of the shower-producing primary particle.[12]

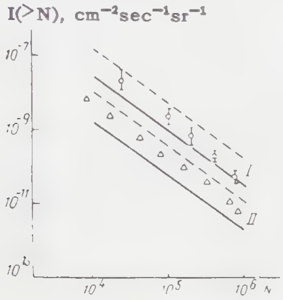

FIG. 5. Intensity of EAS with size greater than N. I – calculation for mountain altitudes, II – calculation for sea level, o – experimental data[15] for mountain altitudes, Δ – experimental data[15] for sea level.

The number of showers of a given size at the observation level (x_0) can be obtained from Eq. (5) by integrating over $\bar{x}$. The frequency of showers of size $>N$ is shown in Fig. 5.

$$J(>N)=\int_N^\infty dN\int_0^{x_0} C(N,\bar{x})\,dx.$$

The absolute intensity of the primary cosmic radiation was taken as $f(E_0)\,dE_0 = AE_0^{-2.7}dE_0$, where the coefficient A was normalized to experimental data[13] for 10 Bev. The results of this calculation are shown by the solid line in Fig. 5. A calculation was also carried out based on the data on the spectrum of primary cosmic radiation from underground measurements.[14] The result is shown by the dotted line in Fig. 5. Experimental data on the intensity of EAS are taken from reference 15. It can be seen from the figure that the experimental data on the absolute frequency of EAS can be made to agree well with the calculation if, for the intensity of primary cosmic radiation, we assume an intermediate value between the results of references 13 and 14.

Table II. Mean free path for particle absorption in showers, g/cm^2

Observation level, m	Number of particles in the shower		
	10^4	10^5	10^6
3860	230	280	340
0	170	175	180
From the calculated altitude dependence between the levels 3860 and 0 m	210	210	—

The altitude variation of the number of EAS calculated by us is in agreement with experimental data, within the statistical spread of the latter.

Showers with a given number of particles at the observation level are produced at a different altitude, and consequently have a different absorption coefficient than at the observation level. The average calculated values of the absorption mean free path of the particles in showers observed at sea level and at mountain altitudes are shown in Table II. It can be seen from the table that the altitude variation of the showers does not depend on the average parameters of individual showers (see also reference 5). Using the altitude variation of EAS obtained before (Fig. 5) and the size spectrum of showers, one can determine the absorption coefficients of the shower particles[12] neglecting the fluctuations in shower development (lower row of Table II).

3. ENERGY FLUX CARRIED BY SHOWER PARTICLES AT THE OBSERVATION LEVEL

The total energy of the nuclear-active component in showers of a given size at the observation level x_0 was calculated from the energy spectra of nuclear-active particles at different depths in the atmosphere in a shower produced by a primary particle with energy E_0. Nucleons and charged π mesons, calculated according to Eq. (3), were regarded as nuclear-active particles. If the differential energy spectrum of nuclear-active particles in the shower produced by a primary particle with energy E_0 at a depth $x = x_0 - \bar{x}$ is $f(E, x_0 - \bar{x}, E_0)\,dE$, then the total energy carried by nuclear-active particles at the observation level in showers of size N is

$$\varepsilon(N, x_0)=\frac{1}{C(N)}\int_0^{x_0} C(N,\bar{x})\,d\bar{x}\int_{E_{min}}^{E_{max}} Ef(E, x_0-\bar{x}, E_0)\,dE,$$

where

$$C(N)=\int_0^{x_0} C(N,\bar{x})\,d\bar{x}.$$

TABLE III

N	Altitude, m	Energy of nuclear-active shower component, ev	
		Calculation	Experiment
10^4	3860	$6\cdot 10^{12}$	$\sim 4{,}4\cdot 10^{12}$
	0	$8{,}8\cdot 10^{12}$	$>1{,}7\cdot 10^{12}$
10^5	3860	$4{,}6\cdot 10^{13}$	$\gtrsim 1{,}1\cdot 10^{13}$
	0	$7{,}7\cdot 10^{13}$	$> 2\cdot 10^{13}$
10^6	3860	$4\cdot 10^{14}$	$\sim 2{,}3\cdot 10^{14}$
	0	$8{,}2\cdot 10^{14}$	$\gtrsim 1{,}2\cdot 10^{14}$

Moreover, the distribution of shower-production levels $\overline{x}$ and the relation between $\overline{x}$ and E_0 is given by Eq. (5). The limits of integration $E_{min} = 3.7 \times 10^9$ ev and $E_{max} < E_0$ represent the minimum energy of the nuclear-active particles that were taken into account and the maximum energy of the nuclear-active particles encountered in the calculated spectrum. The values of $\epsilon (x_0, N)$ obtained in the calculation are shown in Table III. The same table also shows the experimental data on the energy flux carried by the nuclear-active component of EAS.[18,19] A comparison of the experimental data with the calculation reveals an agreement only for showers with a total number of particles $N = 10^4$ at an altitude of 3860 m above sea level. For the remaining cases, the calculated energy fluxes of the nuclear-active component agree with experimental data only in their order of magnitude.

TABLE IV

N	Altitude, m	Energy of electron-photon shower component, ev		$\bar{\varepsilon}(N, x_0)$, ev
		Calculation	Experiment	
10^4	3860	$2{,}8\cdot 10^{12}$	$2.3\cdot 10^{12}$	$4.1\cdot 10^{12}$
	0	$2{,}3\cdot 10^{12}$	$2\cdot 10^{12}$	$3{,}5\cdot 10^{12}$
10^5	3860	$3{,}2\cdot 10^{13}$	$2{,}3\cdot 10^{13}$	$3.8\cdot 10^{13}$
	0	$2.4\cdot 10^{13}$	$2\cdot 10^{13}$	$3.5\cdot 10^{13}$
10^6	3860	$3.4\cdot 10^{14}$	$2{,}2\cdot 10^{14}$	$4.1\cdot 10^{14}$
	0	$2.5\cdot 10^{14}$	$2\cdot 10^{14}$	$3.5\cdot 10^{14}$

The energy of the electron-photon component in showers of a given size at the observation level cannot be obtained directly from the calculations, since the energy spectrum of electrons and photons was not calculated by us. The energy flux carried by the electron-photon shower component can be estimated, assuming that the shower-particle absorption coefficient corresponds to the average cascade parameter $\overline{s}$ at the observation level. The results of such an estimate and the experimental data on the energy of the electron-photon component are shown in Table IV. The agreement of the calculated values with the experiment can be regarded as sufficient, especially since the method used can lead to an underestimate of the parameter $\overline{s}$ and, consequently, to an overestimate of the energy.

We can calculate more exactly the energy lost below the observation level by the electron-photon component of showers of a given size. This energy $\bar{\epsilon}(N, x_0)$, in addition to the energy of the electron-photon component at the observation level, includes the energy transferred to π^0 mesons below this level. Using the notation introduced above, we can express the calculation procedure by the relation

$$\bar{\varepsilon}(N, x_0) = \frac{1}{C(N)} \int_0^{x_0} C(N, \bar{x})\, d\bar{x} \int_{x_0-\bar{x}}^{\infty} N_e(x')\, dx',$$

where $N_e(x') = N$ for $x' = x_0 - \overline{x}$. The results are shown in the last column of Table IV.

The corresponding quantity cannot be measured experimentally, and is usually estimated from the absorption of showers in the atmosphere as $4.4 \times 10^8 N_e$, where N_e is the number of electrons in the shower at observation level. A comparison with the values in the table shows that, by taking the fluctuations in the observation level into account, we cause a small decrease in the calculated energy lost by the electron-photon component in the atmosphere.

4. CONCLUSIONS

1. The above calculations of various parameters of EAS of a given size at the observation level show that the study of the shower structure, for the purpose of obtaining information on the variation of the elementary nuclear act of interaction with the energy of the primary particle, can be carried out more efficiently at mountain altitudes, near the maximum of the nuclear-cascade shower development. At mountain altitudes, the number of particles (shower size) at the observation level represents sufficiently well the energy of the primary particle which produced the shower. In the interpretation of experimental data obtained at sea level, the distribution of shower-production levels may already change the energy of the primary particle producing a shower of a given size by a factor of ten.

2. The assumptions on which the calculations are based lead to a satisfactory description of the composition of EAS at mountain altitudes, and agree with the experimentally observed altitude dependence of the showers. However, a number of parameters referring to the number of nuclear-active particles and the energy carried by them at sea level are markedly different from experimental data. The main reasons for this discrepancy

are the assumption that the inelasticity coefficient of nucleon interactions decreases in the $10^{11} - 10^9$ ev energy range, and the identification of all those secondary nuclear-active particles which are not π mesons as nucleons.

The authors wish to thank Prof. G. T. Zatsepin for his many comments on the results of the calculations, and G. Ya. Goryacheva for carrying out many of the calculations.

---

[1] Dobrotin, Zacepin, Nikol'skiĭ, and Hristiansen, Nuovo cimento **3**, Suppl. No. 4, 635 (1956).

[2] Dovzhenko, Zatsepin, Murzina, Nikol'skiĭ, Rakobol'skaya, and Tukish, Dokl. Akad. Nauk SSSR **118**, 899 (1958), Soviet Phys.-Doklady **3**, 122 (1958).

[3] G. T. Zatsepin and L. I. Sarycheva, Dokl. Akad. Nauk SSSR **99**, 951 (1954).

[4] G. T. Zatsepin and L. G. Dedenko, Proceedings of the Moscow Conference on Cosmic Rays **2**, (1960) (in press).

[5] N. L. Grigorov and V. Ya. Shestoperov, JETP **34**, 1539 (1958), Soviet Phys. JETP **7**, 1061 (1958).

[6] L. D. Landau and S. Z. Belen'kiĭ, Usp. Fiz. Nauk **56**, 309 (1955).

[7] N. M. Gerasimova and D. S. Chernavskiĭ, JETP **29**, 372 (1955), Soviet Phys. JETP **2**, 344 (1956).

[8] Edwards, Losty, Perkins, Pinkau, and Reynolds, Phil. Mag. **3**, 237 (1958).

[9] N. L. Grigorov, Usp. Fiz. Nauk **58**, 599 (1956).

[10] G. T. Zatsepin and I. L. Rozental', Dokl. Akad. Nauk SSSR **99**, 369 (1954).

[11] S. Z. Belen'kiĭ, Лавинные процессы в космических лучах (Cascade Processes in Cosmic Rays), Gostekhizdat, 1948.

[12] K. Greisen, Progress in Cosmic-Ray Physics **3**, North-Holland Publishing Co., Amsterdam, 1956.

[13] A. N. Charakhch'yan and T. N. Charakhch'yan, JETP **35**, 1088 (1958), Soviet Phys. JETP **8**, 761 (1959).

[14] Barett, Bollinger, Cocconi, Eisenberg, and Greisen, Revs. Mod. Phys. **24**, 133 (1952).

[15] Kulikov, Nesterova, Nikol'skiĭ, Solov'eva, Khristiansen, and Chudakov, Тр. международной конференции по космическим лучам (Proceedings of the Moscow International Conference on Cosmic Rays) **2**, 1960.

[16] S. I. Nikol'skiĭ and A. A. Pomanskiĭ, JETP **35**, 618 (1958), Soviet Phys. JETP **8**, 430 (1959).

[17] S. I. Nikol'skiĭ and E. I. Tukish, Proceedings of the Moscow International Conference on Cosmic Rays **2**, 1960.

[18] V. A. Dmitriev, Dissertation, Moscow State University, 1960.

[19] N. N. Goryunov, Dissertation, Moscow State University, 1960.

Translated by H. Kasha
245

SOVIET PHYSICS JETP VOLUME 12, NUMBER 5 MAY, 1961

ELECTRON SCATTERING IN THE THOMAS-FERMI MODEL

T. TIETZ

Lodz University, Poland

Submitted to JETP editor June 4, 1960

J. Exptl. Theoret. Phys. (U.S.S.R.) 39, 1347-1348 (November, 1960)

We calculate the differential cross section for electron scattering by atoms in the Thomas-Fermi approximation with the Latter potential.[1] Results of numerical integration are presented for Ne, Si, and S, and these are compared with results obtained by the Hartree method.[3]

SEVERAL authors have used numerous different kinds of statistical potentials to calculate atomic energy levels and the corresponding eigenfunctions. Latter[1] and Gambos[2] have given complete reviews of the literature concerned with these problems.

According to Latter the best results for the eigenfunctions and eigenvalues are obtained when one uses a statistical potential of the form

$$V(r)=\begin{cases}-(Ze^2/r)\,\Phi(x), & Z\Phi(x)>1\\ -e^2/r, & Z\Phi(x)<1,\end{cases}\qquad (1)$$

where $\Phi(x)$ is the well known Thomas-Fermi function for a neutral atom. He has shown that this potential gives more accurate values for the atomic energy levels than can be obtained in a calculation using the Hartree method.[3] It is thus of interest to calculate the differential cross section for elastic electron scattering using this potential, and to compare the result so obtained with the result of a numerical calculation by the Hartree method in the first Born approximation.

In the first Born approximation the differential cross section for the potential of (1) is given by the expression

$$I(\vartheta)=\frac{3^{8/3}h^4Z^{2/3}}{2^{34/3}\pi^{4/3}e^4m^2P^2}\left[\int\limits_0^{x_0}\Phi(x)\sin Px\,dx+\frac{1}{Z}\int\limits_{x_0}^{\infty}\sin Px\,dx\right]^2.\qquad (2)$$

The quantity P appearing in (2) is defined by the formula

$$P=\frac{3^{2/3}hv\sin(\vartheta/2)}{2^{7/3}\pi^{1/3}e^2Z^{1/3}}=\frac{3^{2/3}h^2}{2^{7/3}\pi^{1/3}e^2mZ^{1/3}}\,\frac{\sin(\vartheta/2)}{\lambda},\qquad (3)$$

where ϑ is the scattering angle, v is the electron velocity, and λ is the corresponding wave length. The parameter x_0 in Eq. (2) is obtained from the relation $Z\Phi(x_0)=1$.

Noting that

$$\int\limits_{x_0}^{\infty}\sin Px\,dx=\lim_{\alpha\to 0}\int\limits_{x_0}^{\infty}e^{-\alpha x}\sin Px\,dx,\qquad (4)$$

we find that $I(\vartheta)$ is given by

$$I(\vartheta)=\frac{3^{8/3}h^4Z^{2/3}}{2^{34/3}\pi^{4/3}e^4\,.n^2P^2}\left[\int\limits_0^{x_0}\Phi(x)\sin Px\,dx+\frac{\cos Px_0}{ZP}\right]^2.\qquad (5)$$

Numerical values of x_0 and $\Phi(x)$ are found in the tables of Kobayashi and Taima.[4]

The Table gives the dependence of $I(\vartheta)/5.66\times 10^{-20}$ on $\lambda^{-1}\sin(\vartheta/2)\times 10^{-8}$ for three values of Z, as obtained from numerical calculations based on Eq. (5). For comparison we give also the results obtained using the Hartree method.[3] Detailed comparison shows that the two methods give equal results for large Z, whereas they differ considerably for low Z.

$\frac{10^{-8}}{\lambda}\sin\frac{\vartheta}{2},\ \frac{1}{\text{cm}}$	$\frac{10^{20}}{5.66}I(\vartheta)$, cm²					
	Ne		Si		S	
	Hartree method	Equation (5)	Hartree method	Equation (5)	Hartree method	Equation (5)
0,1	4900	26708	70000	38346	57600	44555
0.2	3900	6315	13200	11053	17400	13707
0.3	2180	2936	4150	5189	6130	6428
0,4	1220	1465	1830	2468	2600	3021
0,5	700	716	1000	1206	1340	1487
0,6	420	375	610	660	770	832
0.7	256	221	400	412	480	527
0,8	156	146	275	275	324	350
0,9	106	101	188	185	222	233
1,0	72	70	130	125	160	141
1,1	49	49	94	89	116	97

The author expresses his gratitude to Professor P. Gambos for interest in the work. The author is likewise grateful to Ya. Vatso for aid in the numerical calculations.

---

[1] R. Latter, Phys. Rev. 99, 510 (1955).

[2] P. Gambos, Die statistische Theorie des Atoms und ihre Anwendungen, Springer-Wien, 1949.

[3] N. Mott and H. Massey, Theory of Atomic Collisions, Oxford 1949.

[4] S. Kobayashi and T. Taima, Table of the Exact Values of the T. F. Function, Memoires of the Faculty of Liberal Arts, Education Kagawa, Japan, 1957.

Translated by E. J. Saletan
246

SOVIET PHYSICS JETP VOLUME 12, NUMBER 5 MAY, 1961

RECURRENT CONSTRUCTION OF ANGULAR OPERATORS. II

Introduction of an Integral Spin and an Arbitrary Orbital Momentum

J. FISCHER[*] and S. CIULLI[†]

Joint Institute for Nuclear Research

Submitted to JETP editor June 8, 1960

J. Exptl. Theoret. Phys. (U.S.S.R.) **39**, 1349-1356 (November, 1960)

The method previously proposed by the authors[1] for practical construction of angular operators, in which one uses only differential operations, is applied to studying the change in the form of the angular operators resulting from the adding of a new orbital angular momentum or an integer spin to the process. Formulas for practical computations and examples are given.

INTRODUCTION

IN studying processes in which more than four particles participate, the computation of the angular operators (their definition and properties can be found in references 1 – 3) becomes very complicated and long. The practical question therefore arises of obtaining a complete set of angular operators for a given process on the assumption that one knows the angular operators for a simpler process. In its simplest form[*] this question can be expressed in the form of the relation

$$\Omega_0 \mathcal{Y}(a_1 + a_2 \to \sum_1^n a_i') = \mathcal{Y}(a_1 + a_2 \to \sum_1^n a_i' + s), \qquad (1)$$

or

$$\Omega_0 \mathcal{Y}(a \to \sum_1^n a_i') = \mathcal{Y}(a + s \to \sum_1^n a_i').$$

In other words, the operator Ω_0 "adds" a new scalar particle to the process. However, it is not difficult to show that this question can be formulated as a special case of the problem of finding an operator Ω, which changes the quantum number of one of the angular momenta in the reaction from l to l', without changing the number of particles participating in the process. This enables us to find a complete set of angular operators for the process if we know just one term of the set. Therefore we shall first find the explicit form of the operator Ω, and then in Sec. 3 express Ω_0 in terms of Ω.

It will also be shown that the proposed method can be used also for finding angular operators for a process in which, compared with the initial process, one scalar particle has been replaced by a vector or a tensor particle.

1. CHANGE IN QUANTUM NUMBER OF AN ORBITAL ANGULAR MOMENTUM

Let us consider reactions of the type

$$a_1 + a_2 \to a_1' + a_2' + \ldots + a_k' \qquad (2a)$$

and decays of the type

$$a \to a_1' + a_2' + \ldots + a_k'. \qquad (2b)$$

In processes of type (2a) there is one initial and k – 1 final unknown orbital angular momenta in the system of the center of mass. [In the decays (2b) there are no initial orbital angular momenta.] If we also include the spins of all the particles in the processes (2a) and (2b), then there are altogether M initial and N final independent angular momenta, where

$$0 \leqslant M \leqslant 3, \quad k-1 \leqslant N \leqslant 2k-1,$$

depending on how many particles with non-zero spin are present. If M and N are greater than unity, these angular momenta can combine with one another into total angular momenta; in this process the number of initial angular momenta increases up to 2M – 1 and the number of final angular momenta to 2N – 1. All these angular momenta and the corresponding quantum numbers will be denoted (without distinguishing orbital, spin, and total angular momenta) by the symbol l with different subscripts.

---

[*] Associate of the Physics Institute of the Czechoslovak Academy of Sciences, Prague.

[†] Associate of the Institute for Atomic Physics, Bucharest, Rumania.

[‡] The symbols a, a_i, a_i' denote any particles or nuclei, s is a particle with spin zero, $\mathcal{Y}$ is the angular operator for the process written inside the parentheses.

Let us consider any process of type (2a) or (2b). Let us assume that its initial and final states are characterized by complete sets of quantum numbers for the angular momenta. Let us consider three angular momenta $\mathbf{l}_a, \mathbf{l}_b, \mathbf{l}_c$ of the set for the final state, and assume that they are connected by the relation

$$\mathbf{l}_a+\mathbf{l}_b=\mathbf{l}_c. \tag{3}$$

As yet we make no assumptions concerning the nature of the angular momenta $\mathbf{l}_a$ and $\mathbf{l}_b$. The angular operator $\mathcal{J}$ with the quantum numbers l_a, l_b, and l_c can be written in the form

$$\mathcal{J}(\ldots l_a l_b l_c \ldots)=\sum_{M=-l_c}^{l_c} X_{l_c M}\Psi_{l_c M}^{l_a l_b}, \tag{4}$$

where

$$\Psi_{l_c M}^{l_a l_b}=\sum_{m=-l_a}^{l_a} C_{l_c M}^{l_a m l_b M-m}\psi_{l_a m}\varphi_{l_b M-m}$$

and where the $X_{l_c M}$ are functions of the other variables in the process, and do not depend on l_a and l_b. If on the right side of (4) we substitute in place of the function Ψ the functions Ψ' with the same values of l_c and M, but with different l_a' and l_b', then the expression

$$\sum_M X_{l_c M}\Psi_{l_c M}^{l_a' l_b'}=\mathcal{J}(\ldots l_a' l_b' l_c \ldots)$$

is another angular operator for the same process. Therefore the transition from $\mathcal{J}(\ldots l_a l_b l_c \ldots)$ to $\mathcal{J}(\ldots l_a' l_b' l_c \ldots)$ is equivalent to a transition on the right-hand side of (4) from Ψ to Ψ', and can be described formally as follows:

$$\Omega\mathcal{J}(\ldots l_a l_b l_c \ldots)=\mathcal{J}(\ldots l_a' l_b' l_c \ldots), \tag{5}$$

i.e., we have

$$\Omega\Psi_{l_c M}^{l_a l_b}=\Psi_{l_c M}^{l_a' l_b'}, \tag{5'}$$

where the operator Ω depends on l_a and l_b and is a scalar with respect to simultaneous rotations of the spaces characterizing $\mathbf{l}_a$ and $\mathbf{l}_b$.*

The fundamental problem is to find the explicit form of Ω^{rs} for the case $l_a' = l_a + r$, $l_b' = l_b + s$, where $r, s = 1, 0, -1$. All the other cases are solved by repeated application of the Ω^{rs} (cf. Sec. 3).

Let us use Johnson's theorem:[4] If there are vector operators $\mathbf{A}$, $\mathbf{B}$ with the commutation relations

$$[l_{ai}, A_j]=i\sum_k \varepsilon_{ijk}A_k, \qquad [l_{bi}, A_j]=0, \qquad [l_{ai}, B_j]=0,$$

$$[l_{bi}, B_j]=i\sum_k \varepsilon_{ijk}B_k \qquad (ijk=xyz,\ \varepsilon_{xyz}=1), \tag{6}$$

then the matrix elements of their scalar product are equal [cf., for example, reference 5, formula (3.101)] to

$$\begin{aligned}&\langle l_a+r, l_b+s, l_c', M' \,|\, \mathbf{AB} \,|\, l_a, l_b, l_c, M\rangle\\ &\quad=\langle l_a+r \vdots A \vdots l_a\rangle\langle l_b+s \vdots B \vdots l_b\rangle \chi^{rs}\delta_{l_c' l_c}\delta_{M'M},\end{aligned} \tag{7}$$

where the χ^{rs} are numerical coefficients having the values

$$\begin{aligned}\chi^{11}&=-\tfrac{1}{2}[(l_a+l_b+l_c+3)(l_a+l_b+l_c+2)\\ &\quad\times(l_a+l_b+2-l_c)(l_a+l_b+1-l_c)]^{1/2},\\ \chi^{10}&=-\tfrac{1}{2}[(l_c+l_a-l_b+1)(l_c+l_b-l_a)\\ &\quad\times(l_c+l_a+l_b+2)(l_a+l_b-l_c+1)\}^{1/2},\\ \chi^{1-1}&=\tfrac{1}{2}[(l_c+l_a-l_b+1)(l_c+l_a-l_b+2)\\ &\quad\times(l_c-l_a+l_b-1)(l_c-l_a+l_b)]^{1/2},\\ \chi^{0-1}&=\tfrac{1}{2}[(l_c-l_a+l_b)(l_c+l_a-l_b+1)\\ &\quad\times(l_c+l_a+l_b+1)(l_a+l_b-l_c)]^{1/2},\\ \chi^{-1-1}&=-\tfrac{1}{2}[(l_a+l_b+l_c+1)(l_a+l_b+l_c)\\ &\quad\times(l_a+l_b-l_c)(l_a+l_b-l_c-1)]^{1/2},\end{aligned}$$

with the symmetry properties $\chi^{rs}(l_a, l_b, l_c) = (-1)^{r+s}\chi^{sr}(l_b, l_a, l_c)$. The symbol $\langle l_a + r \vdots A \vdots l_a\rangle$ is defined by the relations

$$\begin{aligned}\langle l_a+1 \vdots A \vdots l_a\rangle&=[(l_a+1)^2-m_a^2]^{-1/2}\langle l_a+1, m_a \,|\, A_z \,|\, l_a, m_a\rangle,\\ \langle l_a \vdots A \vdots l_a\rangle&=m_a^{-1}\langle l_a, m_a \,|\, A_z \,|\, l_a, m_a\rangle,\\ \langle l_a-1 \vdots A \vdots l_a\rangle&=(l_a^2-m_a^2)^{-1/2}\langle l_a-1, m_a \,|\, A_z \,|\, l_a, m_a\rangle.\end{aligned} \tag{8}$$

Analogous relations hold for $\langle l_b + s \vdots B \vdots l_b\rangle$.

To raise or lower l_a and l_b we need operators Ω^{rs} whose matrix elements are all equal to zero, except for the one where we have on the left $\langle l_a + r, l_b + s, l_c, m|$ and on the right $|l_a, l_b, l_c, m\rangle$. We shall write them as scalar products of two vectors $\mathbf{A}^{(r)}$, $\mathbf{B}^{(s)}$ of the type of Eq. (6) which, according to Johnson's theorem, should have the form

$$\begin{aligned}\langle l_a+r' \vdots A^{(r)} \vdots l_a\rangle&=\langle l_a+r \vdots A^{(r)} \vdots l_a\rangle\delta_{rr'},\\ \langle l_b+s' \vdots B^{(s)} \vdots l_b\rangle&=\langle l_b+s \vdots B^{(s)} \vdots l_b\rangle\delta_{ss'}.\end{aligned} \tag{9}$$

Then, according to Eq. (7), the matrix elements of $\mathbf{A}^{(r)}\cdot\mathbf{B}^{(s)}$ will be

$$\begin{aligned}&\langle l_a+r', l_b+s', l_c', M' \,|\, \mathbf{A}^{(r)}\mathbf{B}^{(s)} \,|\, l_a l_b l_c M\rangle=\langle l_a+r \vdots A^{(r)} \vdots l_a\rangle\\ &\qquad\langle l_b+s \vdots B^{(s)} \vdots l_b\rangle\chi^{rs}\delta_{rr'}\delta_{ss'}\delta_{l_c l_c'}\delta_{MM'}.\end{aligned} \tag{10}$$

---

*The angular operators $\mathcal{J}$ are scalar with respect to simultaneous rotations of all the orbital and spin dynamical variables of the process.

Consequently, the operators

$$\Omega^{rs}(l_a l_b l_c) = \mathbf{A}^{(r)}\mathbf{B}^{(s)} / \chi^{rs}\langle l_a + r \vdots A^{(r)} \vdots l_a\rangle\langle l_b + s \vdots B^{(s)} \vdots l_b\rangle \tag{11}$$

have the required properties [cf. Eqs. (5) and (5′)]:

$$\Omega^{rs}(l_a l_b l_c)\Psi^{l_a l_b}_{l_c, M} = \Psi^{l_a+r,\, l_b+s}_{l_c, M}$$

In other words,

$$\Omega^{rs}(l_a l_b l_c)\mathcal{Y}(\ldots l_a, l_b, l_c\ldots) = \mathcal{Y}(\ldots l_a + r, l_b + s, l_c\ldots), \tag{12}$$

where r, s = 1, 0, −1.

In order for formulas (12) and (11) to be practical, one must find the explicit form of the vectors $\mathbf{A}^{(r)}$ and $\mathbf{B}^{(s)}$ having the properties (6) and (9). The next section is devoted to this problem.

2. EXPLICIT FORM OF THE VECTORS $\mathbf{A}^{(r)}$

The explicit form of the vectors $\mathbf{A}^{(r)}$ depends on whether the angular momentum $\mathbf{l}_a$ is the sum of two (or more) angular momenta or not.[*]

1. Let us first assume that the eigenfunction $\psi_{l_a m_a}$ is a spherical harmonic:

$$\psi_{l_a m_a} = Y_{l_a m_a}(\mathbf{p}), \tag{13}$$

where $\mathbf{l}_a = -i\,[\mathbf{p} \times \partial/\partial\mathbf{p}]$.

If $\mathbf{l}_a$ is an angular momentum, then $\mathbf{p}$ will be the unit momentum vector $\mathbf{p} = \mathbf{P}/P$; if on the other hand $\mathbf{l}_a$ denotes an integer spin, then $\mathbf{p}$ will be the spin variable α.

Omitting the mathematical derivations (cf. reference 8), we give only the final results[†]

$$\mathbf{A}^{(1)} = \nabla^{+1} \equiv P^{l+2}\frac{\partial}{\partial\mathbf{P}}P^{-(l+1)}, \quad \mathbf{A}^{(0)} = \nabla^0 \equiv \mathbf{l} = -i\left[\mathbf{P}\times\frac{\partial}{\partial\mathbf{P}}\right],$$

$$\mathbf{A}^{(-1)} = \nabla^{-1} \equiv P^{-(l-1)}\frac{\partial}{\partial\mathbf{P}}P^{l}. \tag{14}$$

It can be shown by direct calculation that the vectors ∇^{+1}, ∇^0, ∇^{-1} satisfy the commutation relations (6) and have the property (9). From (8) and (13) it also follows that

$$\langle l+1 \vdots \nabla^{+1} \vdots l\rangle = -\sqrt{\frac{2l+1}{2l+3}}, \qquad \langle l \vdots \nabla^0 \vdots l\rangle = 1,$$

$$\langle l-1 \vdots \nabla^{-1} \vdots l\rangle = \sqrt{\frac{2l+1}{2l-1}}. \tag{15}$$

2. Now let us assume that the function ψ_{lm} is a combination of two or more spherical harmonics:

$$\psi_{lm} = \sum C^{l_1\mu l_2 m-\mu}_{lm}\chi_{l_1\mu}\varkappa_{l_2 m-\mu}. \tag{13′}$$

This corresponds to the addition of angular momenta $\mathbf{l} = \mathbf{l}_1 + \mathbf{l}_2$. If now we apply to ψ_{lm} a vector operator l_{1i} (i = x, y, z), then, according to the general theory (cf. reference 5), we obtain a mixture of states ψ_{l+1}, ψ_l and ψ_{l-1}. It is then sufficient to apply the projection operators $Z_0 Z_-$, $Z_- Z_+$ and $Z_+ Z_0$ where

$$Z_0 = \mathbf{l}^2 - l(l+1), \qquad Z_- = \mathbf{l}^2 - l(l-1),$$

$$Z_+ = \mathbf{l}^2 - (l+1)(l+2),$$

in order to obtain the pure states ψ_{l+1}, ψ_l, and ψ_{l-1} respectively. Thus it is easy to see that the operators $\mathbf{A}^{\pm1}$ will have the form:

$$\mathbf{A}^{(\pm1)} = \mathbf{V}^{\pm1} \equiv Z_{\mp}Z_0\mathbf{l}_1. \tag{16}$$

The computation of $\mathbf{V}^{\pm1}$ from formula (16) (cf. reference 8) gives the result

$$\begin{aligned}\mathbf{V}^{\pm1} = {} & 2\mathbf{l}_1\{l(l+1) - l_1(l_1+1) + l_2(l_2+1)\} \\ & - 2\mathbf{l}_2\{l(l+1) + l_1(l_1+1) \\ & - l_2(l_2+1)\} + 4i\left(\pm l + \tfrac{1}{2} \pm \tfrac{1}{2}\right)[\mathbf{l}_1\mathbf{l}_2].\end{aligned} \tag{17}$$

The operator $\mathbf{A}^0$ is obviously the total angular momentum:

$$\mathbf{A}^0 = \mathbf{V}^0 \equiv \mathbf{l} = \mathbf{l}_1 + \mathbf{l}_2 \tag{17′}$$

[cf. Eq. (14)].

The matrix elements of the vectors $\mathbf{V}^{+1}$, $\mathbf{V}^0$ and $\mathbf{V}^{-1}$ are equal to

$$\begin{aligned}&\langle l_1 l_2 l+1 \vdots V^1 \vdots l_1 l_2 l\rangle \\ &\quad = 2\sqrt{\frac{2l+1}{2l+3}}[(l+1-l_1+l_2)(l+1+l_1-l_2) \\ &\quad \times (l_1+l_2+l+2)(l_1+l_2-l)]^{1/2}, \\ &\langle l_1 l_2 l \vdots V^0 \vdots l_1 l_2 l\rangle = 1, \\ &\langle l_1 l_2 l-1 \vdots V^{-1} \vdots l_1 l_2 l\rangle = 2\sqrt{\frac{2l+1}{2l-1}}[(l-l_1+l_2)(l+l_1-l_2) \\ &\quad \times (l_1+l_2+1)(l_1+l_2+1-l)]^{1/2}.\end{aligned} \tag{18}$$

All the other matrix elements are equal to zero, as they should be according to formula (9).

3. ANALYSIS OF RESULTS

1. Formula (11) determines the operator Ω^{rs} by means of which we can, according to (12), change the quantum numbers characterizing the angular operators $\mathcal{Y}$ of a given process by one unit. The vectors $\mathbf{A}^{(r)}$ have the form either of the vectors $\mathbf{V}^r$ of formula (17) or the vectors ∇^r of formula (14), depending on whether the corresponding angular momentum $\mathbf{l}_a$ (whose quantum number is to be changed) can be written as a sum of two other angular momenta $\mathbf{l}_{a1}$ and $\mathbf{l}_{a2}$ or not.

---

[*] All the formulas of this section are obtained only for vectors $\mathbf{A}^{(r)}$. The corresponding formulas for $\mathbf{B}^{(s)}$ are obtained by the trivial replacements

$$\mathbf{A}\to\mathbf{B}, \quad r\to s, \quad l_a\to l_b, \quad m_a\to m_b, \quad \psi\to\varphi.$$

[*] Here and in what follows we drop the subscript a on l_a, m_a, etc.

2. Increasing or decreasing l_a, l_b by any integer > 1 is achieved by repeated application of the operator Ω^{rs}. Thus, if we know one angular operator for the given process, we can by means of Ω^{rs} obtain all the others.

3. As was already stated in the introduction, the operator Ω can also be used for going over to a more complicated process containing one more scalar particle than participates in the original process [cf. formula (1)]. This is related to the fact that the spherical harmonic Y_{00} is equal to the constant $1/\sqrt{4\pi}$ so that the introduction in the process of a new orbital angular momentum l with quantum number l equal to zero reduces to multiplying the whole set of angular operators by $1/\sqrt{4\pi}$. For example

$$\frac{1}{\sqrt{4\pi}}\cdot\mathcal{Y}\left(a_1+a_2\to\sum_1^n a_i'\right)=\mathcal{Y}\left(a_1+a_2\to\sum_1^n a_i'+s'\right),$$

$$l_{s'}=0.$$

Having determined in this way the angular operators for the new process for $l_{s'} = 0$, we can by using Ω^{1i} $(0, l, l)$ increase the value of $l_{s'}$ to unity. Similarly, the operator $\Omega^{1i}(1, l', l)$ increases $l_{s'}$ from 1 to 2, etc.

Let us take, for example, the process $s_1 + s_2 \to s_1' + s_2'$, characterized by the following angular operators, ($\mathscr{P}_l$ is a Legendre polynomial):

$$\mathcal{Y}_l(s_1+s_2\to s_1'+s_2')=\frac{2l+1}{4\pi}\mathscr{P}_l(\mathbf{pr}),\quad l=0,1,2,\ldots \tag{19}$$

Multiplying by $1/\sqrt{4\pi}$ we obviously obtain $\mathcal{Y}l_{s_1'}, l, l$ $(s_1 + s_2 \to s_1' + s_2' + s_3')$, where $l_{s_3'} = 0$ and $l = 0, 1, 2\ldots$ According to (11), (15), the operator

$$\Omega^{1r}(0,l,l)=\nabla_R^{+1}\nabla_Q^r/\chi^{1r}\langle 1\,\vdots\,\nabla_R^{+1}\,\vdots\,0\rangle\langle l+r\,\vdots\,\nabla_Q^r\,\vdots\,l\rangle$$

increases $l_{s_3'}$ from zero to unity:

$$\Omega^{1r}(0,l,l)\,\mathcal{Y}_{0,l,l}=\mathcal{Y}_{1,l+r,l}.$$

For convenience we give the following general formulae which are useful in particular computations:

$$\nabla_R^0(l)f(\mathbf{pr})=-i\left[\mathbf{R}\times\frac{\partial}{\partial\mathbf{R}}\right]f(\mathbf{pr})=i[\mathbf{p}\times\mathbf{r}]f',$$

$$\nabla_R^{+1}(l)f(\mathbf{pr})=R^{l+2}\frac{\partial}{\partial\mathbf{R}}R^{-(l+1)}f(\mathbf{pr})$$

$$=-(l+1)\mathbf{r}f+(\mathbf{p}-\mathbf{r}(\mathbf{pr}))f',$$

$$\nabla_R^{-1}(l)f(\mathbf{pr})=R^{-(l-1)}\frac{\partial}{\partial\mathbf{R}}R^{l}f(\mathbf{pr})=l\mathbf{r}f+(\mathbf{p}-\mathbf{r}(\mathbf{pr}))f', \tag{20}$$

and note that

$$\nabla_R^{+1}(l=0)\cdot 1=-\mathbf{r}. \tag{20$'$}$$

By means of these formulas we obtain, for example, for $r = 0$,

$$\mathcal{Y}_{1,l,l}=-\frac{1}{(4\pi)^{3/2}}\frac{i(2l+1)\sqrt{3}}{\sqrt{l(l+1)}}\mathbf{r}[\mathbf{p}\times\mathbf{q}]\mathscr{P}_l' \tag{21}$$

and similarly for $l + r = l + 1$ ($\mathscr{P}_l$ depends on $\mathbf{p}\cdot\mathbf{q}$). Continuing further, we can obtain $\mathcal{Y}l_{s_3'}, l, l$ for $l_{s_3'} = 2$, 3, etc. For example,

$$\mathcal{Y}_{2ll}=-\frac{\sqrt{5}}{(4\pi)^{3/2}}\frac{2l+1}{[l(l+1)(2l-1)(2l+3)]^{1/2}}\{l(l+1)\mathscr{P}_l$$

$$-3(\mathbf{pq}-(\mathbf{pr})(\mathbf{qr}))\mathscr{P}_l'-3(\mathbf{r}[\mathbf{p}\times\mathbf{q}])^2\mathscr{P}_l''\}. \tag{22}$$

4. The introduction of an integral spin can be done in similar fashion. One need only make the formal substitution

$$r_i\to\mathbf{e}_i\sqrt{4\pi/3},\quad i=x,y,z. \tag{23}$$

In this way, we obtain angular operators for processes of the type

$$s_1+s_2\to s_1'+v_2',$$

where v_2' is a particle with spin 1, 2, 3 etc. For example, in the case of a particle with spin 2, we obtain from (22) by using (23)

$$\mathcal{Y}=-\frac{\sqrt{5}}{3\sqrt{4\pi}}\frac{2l+1}{[l(l+1)(2l-1)(2l+3)]^{1/2}}\{\delta_{\alpha\beta}l(l+1)\mathscr{P}_l$$

$$-3(\mathbf{pq}\,\delta_{\alpha\beta}-p_\alpha q_\beta)\mathscr{P}_l'-3[\mathbf{p}\times\mathbf{q}]_\alpha[\mathbf{p}\times\mathbf{q}[_\beta\,\mathscr{P}_l''\}\,\mathbf{e}_\alpha\mathbf{e}_\beta.$$

We note that for spin 1 the form of the operators Ω simplifies considerably if we use (20′) and (23):

$$\Omega^1=\frac{1}{\sqrt{(l+1)(2l+1)}}V^{+1},\qquad\Omega^0=\frac{1}{\sqrt{l(l+1)}}\nabla^0,$$

$$\Omega^{-1}=\frac{1}{\sqrt{l(2l+1)}}\nabla^{-1}.$$

It is known that these operators transform the spherical harmonics Y_l^m into spherical vectors.

5. Let us show on a few examples how one can, by this method, obtain from the operators for the reaction

$$s+N\to s'+N' \tag{24}$$

the angular operators for the reaction

$$s+N\to s_1+s_2+N',$$

which were given in Tables I, II and III of our earlier paper.[3] It is known that the angular operators for the process (24) have the form*

$$\{(l'+1)\mathscr{P}_{l'}+i\sigma\mathbf{P}_y\mathscr{P}_{l'}'\}/4\pi\ \text{for}\ j'=l'+1/2=l+1/2=j, \tag{25.1}$$

$$\{-(l'+1)\sigma\mathbf{p}\mathscr{P}_{l'}+\sigma\mathbf{P}_x\mathscr{P}_l'\}/4\pi\ \text{for}\ j'=l'+1/2=l-1/2=j, \tag{25.2}$$

$$\{-l'\sigma\mathbf{p}\mathscr{P}_{l'}-\sigma\mathbf{P}_x\mathscr{P}_{l'}'\}/4\pi\ \text{for}\ j'=l'-1/2=l+1/2=j, \tag{25.3}$$

---

*In the following we shall use the notation introduced in reference 3 and also used in Sec. 5 of reference 1. In particular we recall that $\mathbf{P}_y = [\mathbf{p}\times\mathbf{r}]$, $\mathbf{P}_x = \mathbf{r} - \mathbf{p}(\mathbf{p}\cdot\mathbf{r})$.

$$\{l'\mathscr{P}_{l'} - i\boldsymbol{\sigma}\mathbf{P}_y\mathscr{P}'_{l'}\}\,/\,4\pi \text{ for } j' = l' - {}^1/_2 = l - {}^1/_2 = j, \quad (25.4)$$

where l' is the orbital angular momentum of the final state and the Legendre polynomials $\mathscr{P}_{l'}$ depend on $\mathbf{p}\cdot\mathbf{r} = \cos\theta$. We note that s, s′, s_1 and s_2 correspond to particles with spin zero and without definite parity; if the parities of s and s′ are the same, only the first and fourth channels are allowed.

a) The four angular operators of Table I in reference 3, corresponding to the quantum numbers $l_1 = 0$, $l_2 = l'$, can be obtained from (25.1) – (25.4) by multiplying by $1/\sqrt{4\pi}$: (I 1) = $(4\pi)^{-1/2}$ × (25.1), (I 2) = $(4\pi)^{-1/2}$ × (25.2), etc.

b) The first four angular operators (III 1 – 4) of Table III in reference 3 can be obtained from (I 1 – 4) in the following fashion:

$$\Omega^{10}\left(l_1 = 0,\ \tfrac{1}{2},\ j = \tfrac{1}{2}\right)(\mathrm{I}\ 1;2;3;4) = (\mathrm{III}\ 1;2;3;4), \quad (26)$$

where*

$$\Omega^{10} = \nabla^1_Q\nabla^0_\sigma\,/\,\chi^{10}\langle 1 \vdots \nabla^1 \vdots 0\rangle\langle \tfrac{1}{2} \vdots \nabla^0 \vdots \tfrac{1}{2}\rangle = -\boldsymbol{\sigma}\mathbf{q}.$$

Let us, for example, verify the second of the relations (26). We have

$$-\boldsymbol{\sigma}\mathbf{q}\,(\mathrm{I}\ 2) = (4\pi)^{-3/2}\{l_2 + 1)(\boldsymbol{\sigma}\mathbf{q})(\boldsymbol{\sigma}\mathbf{p})\mathscr{P}_{l_2}$$
$$-(\boldsymbol{\sigma}\mathbf{q})(\boldsymbol{\sigma}\mathbf{P}_x)\mathscr{P}'_{l_2}\} = (\mathrm{III}.\ 2).$$

We note that the angular operators (I 3) and (II 7) can be associated with diagrams which clearly show the connection of the orbital angular momenta (cf. Fig. 1). The angular momenta of the initial state are on the right, those of the final state on the left. To each angular momentum there corresponds one line, where a spin ½ is indicated by an arrow. From the diagram it is also clear how the operators Ω act.

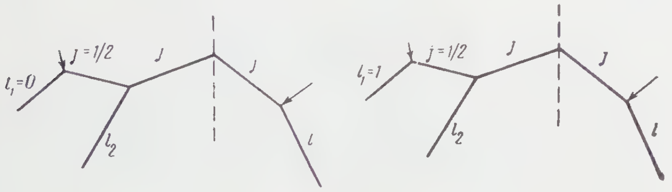

FIG. 1

c) Let us calculate the angular operator (III 7) by means of (III 1) (cf. Fig. 2). We have

$$\Omega^{10} = \mathbf{V}^1_j\,\nabla^0_{l_2}\,/\,\chi^{10}\langle \tfrac{3}{2} \vdots V^1 \vdots \tfrac{1}{2}\rangle\langle l_2 \vdots \nabla^0 \vdots l_2\rangle$$
$$= -\mathbf{V}^1_j\,\nabla^0_{l_2}\,/\,4\sqrt{l_2(2l_2+3)},$$

where $\mathbf{V}^1_j$ and $\nabla^0_{l_2}$ are equal, according to (14) and (17), to the following expressions:

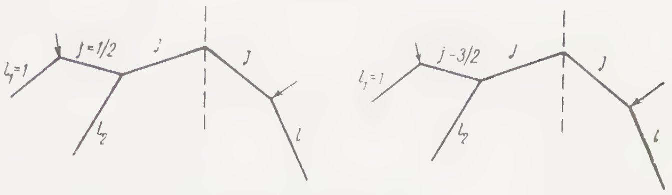

FIG. 2

$$\mathbf{V}^1_j = -\mathbf{l}_1 - 2\boldsymbol{\sigma} - 3i[\boldsymbol{\sigma}\mathbf{l}_1], \qquad \mathbf{l}_1 = -i[\mathbf{Q}\times\partial/\partial\mathbf{Q}];$$
$$\nabla^0_{l_2} = \mathbf{l}_2, \qquad \mathbf{l}_2 = -i[\mathrm{R}\times\partial/\partial\mathrm{R}].$$

The computation gives the result

$$\Omega^{10}(\mathrm{III}\ 1) = -(4\pi)^{-3/2}[l_2(2l_2+3)]^{-1/2}\{(i(2l_2+3)\mathbf{P}_y\mathbf{q}$$
$$-(l_2+3)(\boldsymbol{\sigma}\mathbf{r})(\mathbf{pq}) + l_2(\boldsymbol{\sigma}\mathbf{p})(\mathbf{rq}) + (\boldsymbol{\sigma}\mathbf{q})(\mathbf{pr}))\mathscr{P}'_{l_2}$$
$$-(3(\boldsymbol{\sigma}\mathbf{P}_y)(\mathbf{P}_y\mathbf{q}) + \boldsymbol{\sigma}\mathbf{q}((\mathbf{pr})^2 - 1))\mathscr{P}''_{l_2}\}. \quad (27)$$

We note that in this way we can obtain the angular operators in a much simpler form than they were given in reference 3.

CONCLUSION

From the analysis given we see that the proposed method for computing angular operators is simpler than the algebraic methods which are usually used. In particular, it is simpler than the method given by the authors in reference 3, and besides it has a more general applicability. As is known, the algebraic methods (which make use of the Clebsch-Gordan and Racah coefficients) lead to difficult computations which restrict their applicability in angular and polarization analysis to only the simplest processes. On the other hand, the differential methods retain their simplicity even in the case of complex processes. Besides, if one knows one or more angular operators, the computation is simplified, since the proposed method is a recursion method.

[1] J. Fischer and S. Ciulli, JETP **38**, 1740 (1960), Soviet Phys. JETP **11**, 1256 (1960).

[2] V. I. Ritus, JETP **32**, 1536 (1957) and **37**, 217 (1959), Soviet Phys. JETP **5**, 1249 (1957) and **10**, 153 (1960).

[3] S. Ciulli and J. Fischer, Nuovo cimento **12**, 264 (1959).

[4] M. H. Johnson, Phys. Rev. **38**, 1628 (1931).

[5] E. Condon and G. Shortley, Theory of Atomic Spectra, Cambridge, University Press (1951).

[6] M. E. Rose, Multipole Fields, Wiley (1955).

[7] A. R. Edmonds, Angular Momentum in Quantum Mechanics, Princeton University Press (1957).

[8] J. Fischer and S. Ciulli, Recurrent Construction of Angular Operators. Preprint D-482, Joint Institute for Nuclear Research.

Translated by M. Hamermesh
247

---

*The results of Sec. 2 are valid for an orbital angular momentum and an integer spin, but the relation $\nabla^0 = \sigma/2$ analogous to the second of formulas (14), is also valid.

SOVIET PHYSICS JETP VOLUME 12, NUMBER 5 MAY, 1961

A RESONANCE MODEL FOR THE REACTIONS $N + \pi \rightarrow N + \pi + \pi$ *AND* $\gamma + N \rightarrow N + \pi + \pi$

V. V. ANISOVICH

Leningrad Physico-Technical Institute, Academy of Sciences, U.S.S.R.

Submitted to JETP editor June 9, 1960

J. Exptl. Theoret. Phys. (U.S.S.R.) **39**, 1357-1362 (November, 1960)

The reaction $N + \pi \rightarrow N + \pi + \pi$ for 300 to 550 Mev incident mesons and the reaction $\gamma + N \rightarrow N + \pi + \pi$ for 450 to 700 Mev γ quanta are studied phenomenologically. It is shown that a simple model, according to which the production of a meson in meson-nucleon collisions proceeds mainly via the transition $D_{3/2} \rightarrow P_{3/2}\, s_{3/2}$, is in agreement with all available experimental data.

THE reaction $N + \pi \rightarrow N + \pi + \pi$ for incident mesons with energies of 300 to 450 Mev has been considered earlier[1] under the assumption that in the final state one of the mesons and the nucleon are created in the resonance state $(^3/_2, {}^3/_2)$ with an energy which is in most cases of the order of the resonance energy. The interaction of the second meson, which requires little energy, can in this case be neglected in comparison with the resonance interaction of the first meson with the nucleon. For incident meson energies above 450 Mev this approach becomes incorrect, since the second meson will require more energy, and the interaction of this meson with the nucleon must also be included. The interaction of the two mesons with the nucleon must be considered also for energies below 450 Mev, if the reaction proceeds in such a way that the first meson and the nucleon do not in most cases interact with an energy of the order of the resonance energy. In this case both mesons have an energy which is somewhat below the resonance energy and interact rather strongly with the nucleon.

In the present paper we consider the reactions $N + \pi \rightarrow N + \pi + \pi$ and $\gamma + N \rightarrow N + \pi + \pi$ for the case when the interaction of both mesons with the nucleon has to be accounted for in the final state. We shall use the approximation of a static nucleon; everywhere in the following we shall consider the mass of the nucleon infinitely large. As in reference 1, we assume that the energy dependence of the matrix element is determined solely by the interaction of the particles in the final state and that the meson-meson interaction is small. We assume further that the additional meson is created in such a way that in the final state one of the mesons and the nucleon are in the resonance state $(^3/_2, {}^3/_2)$, while the other meson has an angular momentum L which is either zero or unity. If the second meson has angular momentum one, it can enter into a resonance interaction with the nucleon. This interaction leads to the appearance of an additional factor in the transition amplitude $q_2^{-2} \sin \delta(q_2)$, where q_2 is the momentum of the second meson, and $\delta(q)$ is the meson-nucleon scattering phase in the state $(^3/_2, {}^3/_2)$.

1. THE REACTION $N + \pi \rightarrow N + \pi + \pi$ FOR MESON ENERGIES OF 300 TO 550 MEV

In this case the following transitions are possible (the notation is the same as in reference 1):

$$D_{3/2} \rightarrow P_{3/2}S_{3/2}, \qquad P_{1/2} \rightarrow P_{3/2}p_{1/2}, \qquad P_{3/2} \rightarrow P_{3/2}p_{3/2}. \tag{1}$$

The matrix element corresponding to these transitions has the form

$$C^{jM}_{\lambda 0 ^1/_2 M} a^t_{jL} q_1^{-2} \sin \delta (q_1)\, q_2^{-2L} \sin^L \delta (q_2) \times \sum_m C^{jM}_{LM-m\, ^3/_2 m} C^{^3/_2 m}_{1m-\mu\, ^1/_2 \mu} Y_{1m-\mu} (\mathbf{q}_1) Y_{LM-m} (\mathbf{q}_2); \tag{2}$$

$\mathbf{q}_1$ and $\mathbf{q}_2$ are the momenta of the mesons, t is the isotopic spin of the system, λ is the orbital angular momentum of the incident meson, a^t_{jL} are constants which must be determined by comparison of the calculated expressions for the cross sections with the experimental data. Since L is either 0 or 1, the factor $q_2^{-2} \sin \delta(q_2)$ comes into play only if L = 1.

The connection between the imaginary and real parts of a^t_{jL} can be found in the same way as, for example, in reference 2, by using the unitarity of S matrix:

$$\operatorname{Im}(a^t_{jL}) = a^t_{jL} \exp(-i\eta^t_{j\lambda}) \sin \eta^t_{j\lambda}, \tag{3a}$$

where $\eta^t_{j\lambda}$ is the meson-nucleon scattering phase. As intermediate states we used here only one-meson states. It follows from (3a) that

$$a^t_{jL} = b^t_{jL} \exp(i\eta^t_{j\lambda}), \tag{3b}$$

where b^t_{jL} is a real quantity.

ε	$E_{\pi\ \mathrm{lab}}$, Mev	$E_{\gamma\ \mathrm{lab}}$, Mev		I_2	I_3	I_4	I_5
2,65	290	450	0.2	0.005	0.03	0.042	0.154
2.9	340	500	0,4	0.018	0.08	0.09	0,30
3.1	380	540	0,9	0.049	0.20	0,24	0.66
3,3	420	575	1.3	0,110	0.35	0,43	0.86
3,5	470	620	1.6	0.190	0.55	0.70	0.90
3.7	510	660	1.7	0,200	0,60	1.00	0,76

With the help of computations analogous to those done by us in reference 1, we obtain from (2) the following expression for the angular distribution of the mesons in the center-of-mass system (c.m.s.)

$$4\pi d\sigma / d\Omega = b_0 + b_1 \cos\theta + b_2 (3\cos^2\theta - 1)/2;$$

$$b_0 = (A_1 + A_2) I_1 + BI_2, \quad b_1 = CI_3, \quad b_2 = DI_1 + EI_2. \quad (4)$$

The quantities I_1, I_2, and I_3 depend only on the total energy of the system. Their values are given in the table; there we also list the value of the energy of the incident meson or γ quantum in the laboratory system. The constant coefficients A_1, A_2, ..., E depend on the type of reaction and on the meson whose angular distribution we are considering. All these constants for all reactions N + π → N + π + π are expressed in terms of six real parameters b^t_{jL}. The explicit form of the coefficients for various reactions is given in the Appendix.

We can also obtain the energy distribution of the mesons,

$$\frac{d\sigma}{d\omega} = \Big(A_1 \frac{\sin^2\delta(\omega)}{(\omega^2 - 1)^2} + A_2 \frac{\sin^2\delta(\varepsilon - \omega)}{((\varepsilon - \omega)^2 - 1)^2}$$

$$+ B \frac{\sin^2\delta(\omega)\sin^2\delta(\varepsilon - \omega)}{(\omega^2 - 1)^2((\varepsilon - \omega)^2 - 1)^2}\Big) \frac{\sqrt{1 + k^2}\sqrt{M^2 + k^2}}{k^2(\sqrt{1 + k^2} + \sqrt{M^2 + k^2})}$$

$$+ \omega(\varepsilon - \omega)\sqrt{\omega^2 - 1}\sqrt{(\varepsilon - \omega)^2 - 1}, \quad (5)$$

where $\omega = \sqrt{1 + q^2}$ is the energy of the meson under consideration, $\epsilon = \omega_1 + \omega_2$ is the total energy of the two mesons, and k is the momentum of the incident meson in the c.m.s. As in formula (4), the coefficients A_1, A_2, and B depend on the type of reaction and on the meson whose energy distribution we are considering.

The behavior of the cross section (4) as a function of the energy is determined by the coefficients b_0, b_1, and b_2. These coefficients depend on the energy only through the functions I_1, I_2, and I_3. In the region of 300 to 450 Mev the behavior of I_1, I_2, and I_3 is the same as that of the analogous functions introduced in reference 1; therefore, the behavior of the coefficients b_0, b_1, and b_2 in this energy region will also be the same as that of the analogous coefficients in reference 1. Formula (4) will thus also be in good agreement with the available experimental data in the region of 300 to 450 Mev, just as the corresponding formulas of reference 1. For higher energies there are not yet any data available with the help of which the energy dependence of the coefficients b_0, b_1, and b_2 could be tested.

It is seen from the foregoing and from formula (4) that our present formulas for the total cross sections are in complete agreement with the formulas of reference 1, if the main contribution to the meson creation process comes from the transition $D_{3/2} \rightarrow P_{3/2}\, s_{3/2}$. In this case and also for higher energies, the same relations between the total cross sections of the various processes must obtain as in reference 1 [formula (4)]. It follows from these relations that the ratio of the total cross sections of the processes

$$\pi^+ + p \rightarrow p + \pi^0 + \pi^+ \text{ and } \pi^+ + p \rightarrow n + \pi^+ + \pi^+$$

is equal to three. This does not contradict the experimental value $1.5^{+1.5}_{-0.5}$ (reference 3). This can, perhaps be regarded as evidence that the process mainly involves the transition $D_{3/2} \rightarrow P_{3/2}\, s_{3/2}$ also at higher energies.

Below we shall treat in more detail the case when the main contribution to the cross section comes from the transition $D_{3/2} \rightarrow P_{3/2}\, s_{3/2}$. In this case the cross sections for the five reactions N + π → N + π + π are expressed in terms of the two unknown real parameters $b^{1/2}_{3/2,0}$ and $b^{3/2}_{3/2,0}$ and the meson-nucleon scattering phases $\eta^{1/2}_{3/2,2}$ and $\eta^{3/2}_{3/2,2}$ in a wide region of energies (300 to 550 Mev). The phases enter in the cross section in the form $\cos(\eta^{1/2}_{3/2,2} - \eta^{3/2}_{3/2,2})$. The phase $\eta^{3/2}_{3/2,2}$ is small; the same cannot be said of the phase $\eta^{1/2}_{3/2,2}$ since there is a resonance in the state $D_{3/2}$ at the energy 650 Mev. However, according to Burrowes et al.,[4] $\cos\eta^{1/2}_{3/2,2}$ is not smaller than 0.85 for the energies under consideration. We shall therefore regard $\cos(\eta^{1/2}_{3/2,2} - \eta^{3/2}_{3/2,2})$ as equal to unity.

The two parameters $b^{1/2}_{3/2,0}$ and $b^{3/2}_{3/2,0}$ can be determined from the data of Willis[3] on the summed cross section of the reactions $\pi^+ + p \rightarrow p + \pi^0 + \pi^+$ and $\pi^+ + p \rightarrow n + \pi^+ + \pi^+$ and from the data of

Perkins et al. on the cross section of the reaction $\pi^- + p \rightarrow n + \pi^- + \pi^+$ (reference 5). Then the cross sections of the possible reactions $N + \pi \rightarrow N + \pi + \pi$ in the energy interval 300 to 550 Mev are given by the following expressions (cross sections in millibarns):

$$\begin{aligned}
&\sigma(\pi^+ + p \rightarrow n + \pi^+ + \pi^+) = 0{,}5 I_1,\\
&\sigma(p + \pi^- \rightarrow n + \pi^+ + \pi^-) = 2.3 I_1,\\
&\sigma(\pi^+ + p \rightarrow p + \pi^0 + \pi^+) = 1.6 I_1,\\
&\sigma(p + \pi^- \rightarrow n + \pi^0 + \pi^0) = 3.2 I_1,\\
&\sigma(p + \pi^- \rightarrow p + \pi^- + \pi^0) = 2.1 I_1.
\end{aligned} \tag{6}$$

Of further interest is the ratio of the number of fast mesons over the number of slow mesons for various reactions and various energies. This ratio can be obtained with the help of formula (5). It is equal to unity for the π^+ in the reaction $\pi^+ + p \rightarrow n + \pi^+ + \pi^+$ and for the π^0 in the reaction $\pi^- + p \rightarrow n + \pi^0 + \pi^0$. For the other reactions we have from (5):

$$\begin{aligned}
&N(p + \pi^+ \rightarrow p + \pi^0 + \pi^+;\ \pi^0)\\
&\quad = (I_4 + 0.35 I_5)/(0.35 I_4 + I_5),\\
&N(p + \pi^- \rightarrow n + \pi^- + \pi^+;\ \pi^-)\\
&\quad = (0{,}71 I_4 + 1{,}7 I_5)/(1{,}7 I_4 + 0{,}71 I_5),\\
&N(p + \pi^- \rightarrow p + \pi^- + \pi^0;\ \pi^-)\\
&\quad = (1{,}3 I_4 + 0{,}8 I_5)/(0{,}8 I_4 + 1{,}3 I_5).
\end{aligned} \tag{7a}$$

If $\epsilon = \omega_1 + \omega_2$, the summed energy of the two mesons in the c.m.s., then $N(\pi^+ + p \rightarrow p + \pi^0 + \pi^+;\ \pi^0)$ is the ratio of the number of neutral mesons with an energy larger than $\epsilon/2$ over the number of neutral mesons with an energy smaller than $\epsilon/2$ in the reaction $\pi^+ + p \rightarrow p + \pi^0 + \pi^+$. For the π^+ mesons this ratio is given by the expression

$$\begin{aligned}
&N(\pi^+ + p \rightarrow p + \pi^0 + \pi^+;\ \pi^+)\\
&\quad = 1/N(\pi^+ + p \rightarrow p + \pi^0 + \pi^+;\ \pi^0).
\end{aligned} \tag{7b}$$

I_4 and I_5 are functions of the total energy only. It follows from the data of Batusov, Bogachev, and Sidorov (see reference 5, p. 81) that for π^- and π^+ in the reaction $\pi^- + p \rightarrow n + \pi^+ + \pi^-$ at the energy 290 Mev, these ratios are equal to 1.0 ± 0.5 and 0.45 ± 0.25, respectively. Formulas (7) give the values 1.5 and 0.65 for these ratios, which is in agreement with the experimental data.

2. THE REACTION $\gamma + N \rightarrow N + \pi + \pi$ FOR γ QUANTUM ENERGIES OF 450 TO 700 MEV

Two mesons can be created by photoproduction in the following reactions:

$$\begin{aligned}
&\gamma + p \rightarrow p + \pi^+ + \pi^-, && \gamma + n \rightarrow n + \pi^- + \pi^+,\\
&\gamma + p \rightarrow n + \pi^+ + \pi^0, && \gamma + n \rightarrow p + \pi^- + \pi^0,\\
&\gamma + p \rightarrow p + \pi^0 + \pi^0, && \gamma + n \rightarrow n + \pi^0 + \pi^0.
\end{aligned} \tag{8}$$

Since one of the mesons and the nucleon are necessarily in a state with the total isotopic spin $^3/_2$, the transition amplitudes corresponding to these six reactions can be expressed in terms of the three independent amplitudes with total isotopic spin $^1/_2$ and projection $^1/_2$, total isotopic spin $^1/_2$ and projection $-^1/_2$, and total isotopic spin $^3/_2$ (reference 6). With this assumption, each of these reactions can proceed via the following transitions:

$$E1 \rightarrow P_{3/2} S_{3/2}, \tag{9a}$$

$$M1 \rightarrow P_{3/2} p_{1/2}, \qquad M1,\ E2 \rightarrow P_{3/2} p_{3/2}, \qquad E2 \rightarrow P_{3/2} p_{5/2}. \tag{9b}$$

The expression for the differential cross section can be obtained in the usual way; we find

$$\begin{aligned}
4\pi d\sigma/d\Omega &= A I_1 + B I_2 + C I_3 \cos\theta\\
&\quad + (D I_1 + E I_2)(3\cos^2\theta - 1)/2.
\end{aligned} \tag{10}$$

According to (8) and (9), the constants A, B, ..., E will in this process be expressed in terms of 12 constants. It is meaningless to express the coefficients A, B, ..., E in terms of such a large number of unknown constants. The constants A, B, ..., E should therefore be considered independent for each of the reactions (8). Formula (10) allows us only to determine the energy dependence of the cross sections.

Sellen, Cocconi, Cocconi, and Hart[7] have measured the cross section of the reaction $\gamma + p \rightarrow p + \pi^+ + \pi^-$ in a wide energy interval. They obtained small coefficients in front of cos θ for the angular distributions of the π^- and π^+ mesons in the region of 500 to 700 Mev. This indicates, perhaps, that the process goes mainly via the transition $E1 \rightarrow P_{3/2}S_{3/2}$. Estimates show that the magnitude of the coefficient in front of cos θ in the angular distribution of the mesons can be explained by a ratio of 0.2 between the contributions from the transitions (9b) and the total cross section.

If the process goes mainly via the transition $E1 \rightarrow P_{3/2}S_{3/2}$, the total cross section has the form

$$\sigma = A I_1. \tag{11}$$

The coefficients A for the various processes will be expressed in terms of the three constants d_t (t are the isotopic spin variables). The explicit dependence of the coefficients A on d_t is given in the Appendix. The imaginary and real parts of the coefficients d_t are connected by a relation that follows from the unitarity condition.

By a method analogous to that leading to (3), we obtain

$$d_t = c_t \exp(i\varphi_t), \qquad \sin\varphi_t = c_t^{-1}\gamma^t_{3/2\,2} b^t_{3/2\,0} \sin\eta^t_{3/2\,2}. \tag{12}$$

The quantities $b^t_{3/2,0}$ and $\eta^t_{3/2,2}$ were introduced in (3), and c_t is a real constant. We have written the matrix element for the photoproduction of a single meson in the state $D_{3/2}$ in the form

$$\langle\gamma \mid N\pi\rangle = \gamma^t_{3/2\,2} \sin\eta^t_{3/2\,2} \exp(i\eta^t_{3/2\,2}).$$

Thus the six photoproduction cross sections (8) are in this case expressed in terms of three real parameters.

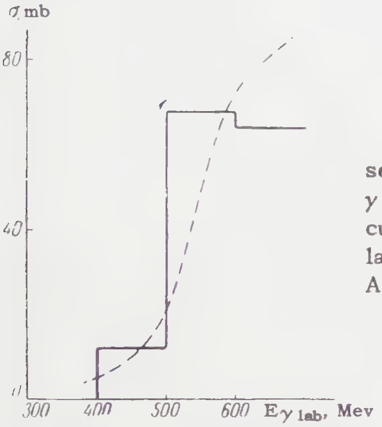

Solid curve: total cross section of the reaction $\gamma + p \to p + \pi^+ + \pi^-$;[7] dashed curve: cross section calculated by formula (11) with A = 49 mb.

Formula (11) gives satisfactory agreement with the experimental data,[7] as is seen from the figure. The expression for the cross section obtained by formula (11) leads to a value which is smaller than the experimental value by a fourth in the interval 500 to 600 Mev and larger by a fifth in the region 600 to 700 Mev.

In the present paper and in reference 1 we consider a rather simple model according to which the process $N + \pi \to N + \pi + \pi$ goes mainly through the transition $D_{3/2} \to P_{3/2}S_{3/2}$. This model predicts correctly the energy dependence of the coefficients in the angular distribution of the created particles.[1] Moreover, in this model all cross sections are expressed in terms of only two unknown parameters $b^{1/2}_{3/2,0}$ and $b^{3/2}_{3/2,0}$. In this model it is therefore possible to express all total cross sections and energy distributions of the created particles solely in terms of known functions of the energy, I_1, I_2, etc., once two arbitrary different experimental quantities are known. The three quantities predicted in this way (the ratio of the cross sections for $p + \pi^+ \to n + \pi^+ + \pi^+$ and $p + \pi^+ \to p + \pi^+ + \pi^0$, the ratio of the number of fast π^+ mesons over the number of slow π^+ mesons and the ratio of the number of fast π^- mesons over the number of slow π^- mesons in the reaction $p + \pi^- \to n + \pi^+ + \pi^-$ for an incident meson energy of 290 Mev) are in agreement with the experimental values.

The energy dependence of the total cross section for the reaction $\gamma + p \to n + \pi^+ + \pi^-$ is in qualitative agreement with the predictions of the model. However, owing to the paucity of the experimental data on the photoproduction of two π mesons, it is impossible to make a detailed comparison.

APPENDIX

We give the expressions for the coefficients A_1, A_2, ..., E entering in formula (4) for the π mesons denoted in reference 1 by the symbol $\pi(1)$:

$$A_1 = \frac{2}{5}\sum_{tt'} \alpha_t\alpha_{t'} \operatorname{Re}(a^{t*}_{3/2\,0} a^{t'}_{3/2\,0}),$$

$$B = \sum_{tt'}\Big\{\left(\tfrac{1}{3}\alpha_t\alpha_{t'} + \tfrac{2}{9}\alpha_t\beta_{t'} + \tfrac{1}{3}\beta_t\beta_{t'}\right)\operatorname{Re}(a^{t*}_{1/2\,1} a^{t'}_{1/2\,1})$$
$$+ \left(\tfrac{2}{3}\alpha_t\alpha_{t'} - \tfrac{8}{9}\alpha_t\beta_{t'} + \tfrac{2}{3}\beta_t\beta_{t'}\right)\operatorname{Re}(a^{t*}_{3/2\,1} a^{t'}_{3/2\,1})\Big\},$$

$$C = \sum_{tt'}\Big\{\left(-\tfrac{2}{3}\sqrt{\tfrac{2}{15}}\alpha_t\beta_{t'} - 2\sqrt{\tfrac{2}{15}}\beta_t\beta_{t'}\right)\operatorname{Re}(a^{t*}_{1/2\,1} a^{t'}_{3/2\,0})$$
$$+ \left(-\frac{8}{15\sqrt{3}}\alpha_t\beta_{t'} + \frac{4}{5\sqrt{3}}\beta_t\beta_{t'}\right)\operatorname{Re}(a^{t*}_{3/2\,1} a^{t'}_{3/2\,0})\Big\},$$

$$D = \sum_{tt'}\frac{2}{5}\alpha_t\alpha_{t'} \operatorname{Re}(a^{t*}_{3/2\,0} a^{t'}_{3/2\,0}),$$

$$E = \sum_{tt'}\Big\{\left(-\tfrac{4}{3}\sqrt{\tfrac{2}{5}}\alpha_t\alpha_{t'} + \tfrac{4}{9}\sqrt{\tfrac{2}{5}}\alpha_{t'}\beta_t - \tfrac{2}{9}\sqrt{\tfrac{2}{5}}\alpha_t\beta_{t'}\right.$$
$$\left. - \tfrac{2}{3}\sqrt{\tfrac{2}{5}}\beta_t\beta_{t'}\right)\operatorname{Re}(a^{t*}_{1/2\,1} a^{t'}_{3/2\,1})$$
$$+ \left(-\tfrac{2}{15}\alpha_t\alpha_{t'} + \tfrac{32}{45}\alpha_t\beta_{t'} - \tfrac{8}{15}\beta_t\beta_{t'}\right)\operatorname{Re}(a^{t*}_{3/2\,1} a^{t'}_{3/2\,1})\Big\}. \tag{A.1}$$

A_2 is obtained from A_1 by replacing α_t and $\alpha_{t'}$ by β_t and $\beta_{t'}$. The numbers α_t and β_t for various processes are given in reference 1.

We give now the expression for A in formula (11) in terms of d_t:

$$A = \frac{1}{5}\sum_{tt'}(a_t\alpha_{t'} + \beta_t\beta_{t'})\operatorname{Re}(d_t^* d_{t'}). \tag{A.2}$$

α_t and β_t are numbers which for the various processes are equal to

$$\alpha_t = C^{t\tau}_{1\mu\,3/2\,\lambda+\nu} C^{3/2\,\lambda+\nu}_{1\nu\,1/2\,\lambda}, \qquad \beta_t = C^{t\tau}_{1\nu\,3/2\,\lambda+\mu} C^{3/2\,\lambda+\mu}_{1\mu\,1/2\,\lambda}.$$

t and τ are the total isotopic spin and its projection on the z axis in the final state, μ and ν are the isotopic spins of the mesons, and λ is the isotopic spin of the nucleon in the final state.

---

[1] V. V. Anisovich, JETP **39**, 97 (1960), Soviet Phys. JETP **12**, 71 (1961).

[2] V. N. Gribov, JETP **33**, 1431 (1957), Soviet Phys. JETP **6**, 1102 (1958). E. Fermi, Nuovo cimento Suppl. **2**, 1 (1955).

[3] W. J. Willis, Phys. Rev. **116**, 753 (1960).

[4] Burrowes, Caldwell, Frisch, Hill, Ritson, Schluter, and Wahlig, Phys. Rev. Lett. **2**, 119 (1959).

[5] B. Pontecorvo, The Scattering of Pions by Nucleons and Single Pion Production in Pion-Nucleon and Nucleon-Nucleon Interactions, report at the Kiev Conference 1959, p. 86.

[6] K. M. Watson, Phys. Rev. **85**, 852 (1952).

[7] Sellen, Cocconi, Cocconi, and Hart, Phys. Rev. **113**, 1323 (1959).

Translated by R. Lipperheide
248

SOVIET PHYSICS JETP VOLUME 12, NUMBER 5 MAY, 1961

ANISOTROPIC PROPAGATION OF LONGITUDINAL ELECTROACOUSTICAL WAVES IN A DRIFTING PLASMA

V. A. LIPEROVSKIĬ

Moscow Power Institute

Submitted to JETP editor June 11, 1960

J. Exptl. Theoret. Phys. (U.S.S.R.) 39, 1363-1366 (November, 1960)

The experimentally observed anisotropy in the propagation of low-frequency electroacoustical waves in a low-pressure gas-discharge plasma is explained theoretically within the hydrodynamic approximation by including collisions between charged particles and neutral atoms. From the derived dispersion equation it is found that plane waves of a given frequency will propagate under certain conditions from cathode to anode with an increase in amplitude and from anode to cathode with a decrease in amplitude. This anisotropy is due mainly to the combined effect of charged particle — atom collisions and constant drift motion. In the presence of boundaries the anisotropy is enhanced.

LET us consider the propagation of a plane longitudinal low-frequency wave in a plasma consisting of two kinds of charged particles, electrons and ions, drifting in opposite directions in a region filled with a neutral gas. The neutral gas is of such density, moreover, that the collision frequency of electrons and ions with atoms is about the same as their wave frequencies in coordinate systems moving with the drift velocities.

To describe the oscillation process we shall make use of Vlasov's[1] hydrodynamic approximation to the equations of motion, with an additional term to allow for collisions on the following model. We assume that in every collision with a neutral atom a charged particle loses its excess momentum due to the superimposed oscillation. If this excess momentum is directed against the drift velocity, the charged particle will be accelerated in the drift direction by the collision, and vice versa.

Let Δn denote the totality of electrons with velocity $u_0 + u_1$. During a time Δt some of them ($\tilde{q}_1 \Delta t$) will collide with neutral atoms ($\tilde{q}_1$ is the fraction of the electron gas that collides with neutral atoms per unit time). We assume that in the collision the electrons lose a fraction, κ_1, of their excess momentum. Thus, the total momentum change is $\Delta p_1 = -\tilde{q}_1 \kappa_1 m_1 u_1 \Delta n \Delta t$. If we set $\tilde{q}_1 \kappa_1 = q_1$, then the "friction" per unit mass due to collisions with the neutral gas is $-q_1 u_1$, and, correspondingly, $-q_2 v_1$ for the ion gas. We assume that the wave oscillations are small and take the direction from the cathode to the anode as positive.

The basic linearized equations for one-dimensional flow are as follows:

$$\begin{aligned} \frac{\partial u_1}{\partial t} + u_0 \frac{\partial u_1}{\partial x} &= -\frac{v_{T_1}^2}{\rho_0} \frac{\partial \rho_1}{\partial x} + \frac{e_1}{m_1} E_1 - q_1 u_1, \\ \frac{\partial v_1}{\partial t} - v_0 \frac{\partial v_1}{\partial x} &= -\frac{v_{T_2}^2}{d_0} \frac{\partial d_1}{\partial x} + \frac{e_2}{m_2} E_1 - a_2 v_1; \end{aligned} \tag{1}$$

$$\rho_0 \frac{\partial u_1}{\partial x} + u_0 \frac{\partial \rho_1}{\partial x} = -\frac{\partial \rho_1}{\partial t}, \qquad d_0 \frac{\partial v_1}{\partial x} - v_0 \frac{\partial d_1}{\partial x} = -\frac{\partial d_1}{\partial t}, \tag{2}$$

$$\frac{\partial E_1}{\partial x} = 4\pi \left(\frac{e_1}{m_1} \rho_1 + \frac{e_2}{m_2} d_1 \right). \tag{3}$$

Here (1) is the Bernoulli-Euler equation, (2) the equation of continuity for the electron and ion gas respectively, and (3) Poisson's equation.

In these equations u_0 and v_0 represent the drift velocities, $v_{T_1} = \sqrt{3kT_1/m_1}$ and $v_{T_2} = \sqrt{3kT_2/m_2}$ the sound velocities, u_1 and v_1 the velocity perturbations, ρ_1 and d_1 the density perturbations, T_1 and T_2 the temperature, e_1 and e_2 the charge, m_1 and m_2 the mass of the electron and ion gas respectively, and q_1, q_2 the collision rate between charged and neutral particles multiplied by the average fractional loss of excess momentum.

Since we are concerned with the propagation of a plane wave with a given frequency ω, we seek solutions of the form

$$\rho_1 = \rho_1^0 e^{i(\omega t + kx)}, \qquad d_1 = d_1^0 e^{i(\omega t + kx)}. \tag{4}$$

Proceeding in the usual way we obtain the dispersion equation:

$$\begin{aligned} &\omega_{01}^2 / [(\omega + u_0 k)^2 - v_{T_1}^2 k^2 - i q_1 \omega - i q_1 u_0 k] \\ &+ \omega_{02}^2 / [(\omega - v_0 k)^2 - v_{T_2}^2 k^2 - i q_2 \omega + i q_2 v_0 k] = 1, \end{aligned} \tag{5}$$

where

$$\omega_{01}^2 = 4\pi (e_1 / m_1)^2 \rho_0, \qquad \omega_{02}^2 = 4\pi (e_2 / m_2)^2 d_0.$$

For frequencies, wave numbers, and drift velocities that satisfy the relations

$$\frac{\omega}{\omega_{01}}, \ \frac{\omega}{\omega_{02}}, \ \frac{|k| v_{T_1}}{\omega_{01}}, \ \frac{|k| v_{T_2}}{\omega_{02}}, \ \frac{|k| u_0}{\omega_{01}}, \ \frac{|k| v_0}{\omega_{02}}, \ \frac{q_1}{\omega_{01}}, \ \frac{q_2}{\omega_{02}} \ll 1, \tag{6}$$

we can neglect fourth-order terms in comparison with those of the second order.

Equation (5) can be reduced to the form

$$\omega^2 + 2A\omega k + Bk^2 - iDk - iCk = 0, \tag{7}$$

$$A = u_0 m_1 / m_2 - v_0, \qquad B = v_0^2 - v_{T_2}^2 + (u_0^2 - v_{T_1}^2) m_1 / m_2,$$
$$C = q_1 m_1 / m_2 + q_2, \qquad D = q_1 u_0 m_1 / m_2 - q_2 v_0,$$

where we have used the fact that $\omega_{01}^2 / \omega_{02}^2 = m_2 / m_1$, $N_1 = N_2$, and $m_2 \gg m_1$. Substituting $k = \alpha + i\beta$ and equating the coefficients in the real and imaginary parts to zero, we obtain

$$\beta = \tfrac{1}{2} (\alpha D + \omega C) / (\alpha B + \omega A). \tag{8}$$

The dispersion equation for α appears as

$$\omega^2 + 2A\omega\alpha + B\alpha^2 = \frac{B}{4} \left(\frac{\alpha D + \omega C}{\alpha B + \omega A} \right)^2 - \frac{D}{2} \left(\frac{\alpha D + \omega C}{\alpha B + \omega A} \right). \tag{9}$$

Equation (9) has two real roots α_1 and α_2, with a negative sign for a wave propagating from the cathode to the anode and a positive sign for one from the anode to the cathode, while β_1 and β_2 represent the attenuation coefficients of the corresponding waves. If $|D| > |\omega C/\alpha|$ and $|B| > |\omega A/\alpha|$ then β_1 and β_2 have the same sign when α_1 and α_2 are of unlike sign. When $\beta_{1,2} < 0$, the wave from the anode to the cathode decreases exponentially in amplitude, while one from the cathode to the anode increases (the equations are valid as long as the linearization is). This anisotropy is due mainly to the presence of the coefficient D, i.e., to collisions with the atoms at a constant drift velocity. The mechanism responsible for the increase in the wave amplitude can probably be discovered only by kinetic analysis. It should be noted merely that the mechanisms of increase in longitudinal oscillations in the plasma currents, investigated by Filimonov,[2] have nothing to do with collisions.

The oscillations discussed above are of an electroacoustical nature, as can be seen if one obtains the relationship of the wave amplitude on the carrier concentrations.

Equation (9) explains the experimentally observed anisotropy[3] in the propagation of electroacoustical waves in a gas discharge plasma, and yields for the phase velocity of the wave a value that coincides with the experimental value.

The following are the specific data for one of the experiments[3]: a discharge with $i = 30$ ma, $E_0 = 2$ v/cm, and $T_1 = 2.05 \times 10^{5\circ}$ K was ignited in a He-filled tube with a radius of 1.5 cm and $p = 0.01$ mm Hg. Induced oscillations with a frequency $\nu = 250$ kc/sec were found to move only from the cathode to the anode. Under these conditions (see Engel's book[4]) $u_0 = 1.18 \times 10^8$ cm/sec $v_0 = 1.20 \times 10^5$ cm/sec, the cross section for electron collisions with helium atoms is $\sigma_1 = 2.53 \times 10^{-16}$ cm^2 while that of ions with helium atoms is $\sigma_2 = 10 \times 10^{-16}$ cm^2. The density of the neutral gas is $N_0 = 3.31 \times 10^{14}$ atoms/cm^3 at 20° C and $T_2 \approx 2000$° K.

On the assumption that the electrons and ions have Maxwellian distributions, the fraction of electrons colliding with neutral atoms per unit time was found to be

$$\tilde{q}_1 = \frac{\sigma_1 N_0 v_{\mathbf{av}}^2}{\sqrt{\pi}\, u_0} \left[\frac{u_0}{v_{\mathbf{av}}} \exp \left\{ - \left(\frac{u_0}{v_{\mathbf{av}}} \right)^2 \right\} + \left(\frac{1}{2} + \frac{u_0^2}{v_{\mathbf{av}}^2} \right) \sqrt{\pi} \Phi \left(\frac{u_0}{v_{\mathbf{av}}} \right) \right], \tag{10}$$

where

$$\Phi(x) = \int_0^x e^{-t^2} dt, \qquad v_{\mathbf{av}} = \sqrt{\frac{2kT_1}{m_1}}.$$

The formula for $\tilde{q}_2$ is similar.

Let us assume that in collisions with the walls, just as in collisions with neutral atoms, the charged particles lose the excess momentum acquired from the wave. For the fraction of particles colliding per unit time at the point (x, t), let us now take the ratio of the number of particles that have collided with the neutral gas and with the wall to the total number of particles in a volume contained between two sections perpendicular to the tube axis.

The result is that the collisions with the wall add a term $v_{av}/R\sqrt{\pi}$ to Eq. (10) (R is the radius of the tube). An analogous term is also added to the formula for $\tilde{q}_2$.

Under the above conditions, assuming $\kappa_1 = \kappa_2 = 1$, we find that $q_1 = 1.19 \times 10^8$ sec^{-1} and $q_2 = 2.20 \times 10^5$ sec^{-1}. A graphical solution of Eq. (9) yields

$$\alpha_1 = -0.48 \text{cm}^{-1}, \qquad \beta_1 = -0.05 \text{cm}^{-1},$$
$$\alpha_2 = 0.45 \text{cm}^{-1}, \qquad \beta_2 = 0.12 \text{cm}^{-1}.$$

Hence the phase velocity of the wave is

$$V_{\text{ph}} = 32{,}1 \cdot 10^5 \text{ cm/sec}.$$

Since the wave is described by the factor $\exp(i\omega t + i\alpha x - \beta x)$, we see that the first solution describes a wave with slowly increasing amplitude propagating from cathode to anode. No increase in amplitude was observed experimentally, but the phase velocity of the observed wave[3] (31.8×10^5 cm/sec) agrees quite well with the computed value.

The second solution applies to a rapidly attenuated wave from the anode to the cathode, which was not observed experimentally. If the boundaries are ignored, the anisotropy under the same conditions and in the same qualitative circumstances will be less.

In conclusion I wish to thank Prof. A. A. Vlasov for his interest and critical review of this paper and A. A. Zaĭtsev for his aid with the experimental comparison.

[1] A. A. Vlasov, Теория многих частиц (The Many Body Problem), Gostekhizdat, 1950.

[2] G. F. Filimonov, Радиофизика и электроника (Radio Engineering and Electronics) **4**, 75 (1959).

[3] Vasil'eva, Zaĭtsev, and Andryukhina, Izv. Akad. Nauk SSSR, Ser. Fiz. **23**, 995 (1959), Columbia Tech. Transl. p. 982.

[4] A. von Engel, Ionized Gases, (Clarendon Press, Oxford, 1955).

Translated by A. Skumanich
249

SOVIET PHYSICS JETP VOLUME 12, NUMBER 5 MAY, 1961

THE RADIATION FROM A CHARGE MOVING IN AN INHOMOGENEOUS MEDIUM

S. P. KAPITZA

Institute of Physics Problems, Academy of Sciences, U.S.S.R.

Submitted to JETP editor June 15, 1960

J. Exptl. Theoret. Phys. (U.S.S.R.) 39, 1367-1370 (November, 1960)

The problem considered is that of the radiation from a uniformly moving charge in a medium with random inhomogeneities. Expressions are obtained for the intensity, the polarization, and the directivity of the radiation. It is pointed out that as the threshold for the Cerenkov effect is approached there is a logarithmic increase of the radiated intensity.

A charge moving uniformly in an inhomogeneous medium must give rise to radiation due to the polarization of the medium. If the inhomogeneities of the medium are randomly distributed, then we get incoherent radiation caused by the polarization of these inhomogeneities. This effect can be regarded as a special type of transition radiation at the inhomogeneities of the medium. It is obvious that these phenomena are analogous to the scattering of light and can be described in terms of the scattering of the waves that accompany the motion of the particle. Unlike the Cerenkov effect, the radiation at inhomogeneities of the medium will occur also at speeds smaller than the phase velocity of light in the medium.

For the calculation we represent the field caused by the motion of the charge as a sum of plane waves (cf. e. g., reference 1). When a charge moves with the velocity v the field produced is excited by the charge and current density distributions

$$\rho = e\delta(\mathbf{r} - \mathbf{v}t), \qquad j = e\mathbf{v}\delta(\mathbf{r} - \mathbf{v}t).$$

When the electromagnetic field from these sources is represented as Fourier integrals describing the variation with the coordinates, the field is described by the following Fourier components $\mathbf{A_k}$ of the vector potential and $\varphi_\mathbf{k}$ of the scalar potential

$$\mathbf{A_k} = \frac{e}{2\pi^2 c}\frac{\mathbf{v}}{k^2 - \omega^2\varepsilon/c^2}e^{-i\omega t}, \qquad \varphi_\mathbf{k} = \frac{e}{2\pi^2\varepsilon}\frac{1}{k^2 - \omega^2\varepsilon/c^2}e^{-i\omega t}.$$

From this we have for the spatial Fourier components of the electric field, which depend on the time,

$$\mathbf{E_k} = \frac{i\omega}{c}\mathbf{A_k} - i\mathbf{k}\varphi_\mathbf{k} = \frac{ie}{2\pi^2}\frac{\omega\mathbf{v}/c^2 - \mathbf{k}/\varepsilon}{k^2 - \omega^2\varepsilon/c^2}e^{-i\omega t}, \tag{1}$$

where k is the wave vector; $\epsilon = \epsilon(\omega)$ is the dielectric constant at frequency ω; $\omega = \mathbf{k}\cdot\mathbf{v} = k_x v$; v is the speed of motion along the x axis.

Let us consider the radiation from the fields at the inhomogeneities of the medium, using the usual arguments of scattering theory. For scalar scattering on random inhomogeneities of the dielectric constant of the medium, the radiation is emitted from volumes that are small in comparison with the wavelength. This corresponds to Rayleigh scattering at small particles or at fluctuations of the density of the medium, on the assumption of dipole radiation from the scatterers.

The total intensity of the incoherent radiation in the frequency range $d\omega$ is obtained by summing the intensities radiated from the individual scatterers over the entire volume V:

$$dI_\omega = \frac{8\pi\omega^4\sqrt{\varepsilon}}{3c^3}\int\limits_V N\,|\mathbf{P}_\omega|^2\,dV\,d\omega,$$

where N is the number of scattering centers in unit volume, and P_ω is the Fourier component of the dipole moment of a scattering element with the polarizability α. Since $\mathbf{P}_\omega = \alpha\mathbf{E}_\omega$, the total intensity is given by

$$dI_\omega = \frac{8\pi\omega^4\sqrt{\varepsilon}N\alpha^2}{3c^3}\int|\mathbf{E}_\omega|^2\,dV\,d\omega.$$

We see that the scattering properties of the medium are entirely determined by the extinction coefficient

$$s = \frac{8\pi\omega^4}{3c^4}N\alpha^2 \doteq \frac{\omega^4}{6\pi c^4}V\overline{\delta\varepsilon}^2. \tag{2}$$

The extinction coefficient has the dimensions of an inverse length. The distance $L = 1/s = 1/N\sigma$ is essentially the range of radiation in the scattering medium; L is determined by the scattering either at fluctuations of ϵ or at scattering particles which are characterized by a cross section σ.

The integral of $|\mathbf{E}_\omega|^2$ over a volume that is unlimited in the y and z directions and is of length l in the x direction can be expressed in terms of the Fourier components $\mathbf{E_k}$ by the formula

$$\iiint |\mathbf{E}_\omega|^2\, dx\, dy\, dz = \frac{4\pi^2}{v^2}\int_0^l dx \iint_{-\infty}^{+\infty} \mathbf{E_k}\mathbf{E_k^*}\, dk_y\, dk_z .$$

Thus we get for the radiation from unit path length in the frequency range $d\omega$ the expression

$$J_\omega = \frac{dI_\omega}{l\, d\omega} = \frac{4\pi^2 sc\sqrt{\varepsilon}}{v^2}\iint_{-\infty}^{+\infty} \mathbf{E_k}\mathbf{E_k^*}\, dk_y\, dk_z .$$

Using the relations (1) and (2), we break the integrand up into two parts,

$$J_\omega = \frac{2sc^2\sqrt{\varepsilon}}{c\beta^2\varepsilon^2}\iint\left\{\frac{(\omega/v)^2(\varepsilon\beta^2-1)^2}{[(\omega/v)^2(1-\varepsilon\beta^2)+k_y^2+k_z^2]^2}\right.$$
$$\left.+\frac{k_y^2+k_z^2}{[(\omega/v)^2(1-\varepsilon\beta^2)+k_y^2+k_z^2]^2}\right\}dk_y\, dk_z, \tag{3}$$

where $\beta = v/c$. For the integration it is convenient to change to polar coordinates in the plane of k_y and k_z:

$$p^2 = k_y^2 + k_z^2.$$

In the first part of the integral we have separated out the terms that are due to the polarization of the volume by the field E_x directed along the motion of the charge. This integral converges at all values of p^2 and gives

$$J_{\omega x} = \frac{2\pi e^2 s}{c\beta^2\varepsilon^{3/2}}(1-\varepsilon\beta^2). \tag{4}$$

The integration of the second part of Eq. (3) gives the radiation that is due to the polarization of the volume by cylindrical waves with the fields E_y, E_z,

$$J_{\omega yz} = \frac{2\pi e^2 s}{c\beta^2\varepsilon^{3/2}}\left(\ln\frac{p_\infty^2 v^2}{\omega^2(1-\varepsilon\beta^2)}-1\right), \tag{5}$$

where p_∞ denotes the upper limit of the integration with respect to p.

Let us examine the behavior of the integrals for $\epsilon\beta^2 < 1$, i.e., below the threshold of the Cerenkov effect. Unlike the integral (4), the integral (5) diverges logarithmically at the upper limit, which corresponds to small distances. At small distances, however, the microscopic treatment of the scattering is illegitimate, and therefore we can simply introduce a certain limiting frequency $\omega_\infty = p_\infty/v$, corresponding to this restriction. Thus the complete spectral density of the energy radiated by the charge per unit path length is given by

$$J = \frac{\pi e^2 s}{c\varepsilon^{3/2}\beta^2}\left(2\ln\frac{\omega_\infty}{\omega\sqrt{1-\varepsilon\beta^2}}-\varepsilon\beta^2\right). \tag{6}$$

Let us find the distribution of the polarization and intensity of this radiation. In view of the dipole character of the radiation from the scatterers, we get for the angular distribution of the radiation

$$dJ = \frac{3}{8\pi}\left[J_{\omega x}\sin^2\vartheta + \tfrac{1}{2}J_{\omega yz}(1+\cos^2\vartheta)\right]d\sigma, \tag{7}$$

where $d\sigma$ is an element of solid angle and ϑ is the angle between the direction of observation and the motion of the charge.

A quantity of practical importance is the ratio of the intensities emitted in directions along the path and transverse to the path, which is given by

$$\frac{J_\parallel}{J_\perp} = \frac{\ln[\omega_\infty/\omega\sqrt{1-\varepsilon\beta^2}]-{}^1\!/_2}{\ln[\omega_\infty/\omega\sqrt{1-\varepsilon\beta^2}]-\varepsilon\beta^2+{}^1\!/_2}.$$

Since the radiation from J_x is directed only transverse to the path of the particle, the radiation directed along the path of the particle is not polarized, as is already clear from considerations of symmetry. The degree of polarization P of the radiation directed transverse to the path depends on the velocity:

$$\frac{P_\parallel}{P_\perp} = \frac{\ln[\omega_\infty/\omega\sqrt{1-\varepsilon\beta^2}]-{}^1\!/_2}{1-\varepsilon\beta^2}. \tag{8}$$

Let us express the formula (6) for the total intensity of the radiation in terms of the number dn of quanta of energy $\hbar\omega$ that are emitted in the frequency range $d\omega$ in unit path length:

$$dn = \frac{e^2 s\lambda}{\hbar c\pi\varepsilon\beta^2}\left[2\ln\frac{\omega_\infty}{\omega}-\ln(1-\varepsilon\beta^2)-\varepsilon\beta^2\right]\frac{d\omega}{c}, \tag{9}$$

where $\lambda = 2\pi c/\omega\epsilon^{1/2}$ is the wavelength in the medium.

A basic feature of the radiation at random inhomogeneities of the medium is its logarithmic increase with approach to the condition $\epsilon\beta^2 \rightarrow 1$, since the velocity dependence of the other terms is small. The value of the limiting frequency ω_∞, or the corresponding value of the minimum impact parameter, determines the part of the radiation that has only a weak velocity dependence for large β.

The magnitude of the effect itself can be compared with the intensity of the Cerenkov radiation, which occurs in the medium for $\epsilon\beta^2 > 1$. In the notations we have been using the intensity of the Cerenkov radiation is

$$dn_C = \frac{e^2}{\hbar c\varepsilon\beta^2}(\varepsilon\beta^2-1)\frac{d\omega}{c}.$$

In the case of a gas the ratio of intensities n/n_C for $\beta \sim 1$ is given in order of magnitude by the ratio of the polarizability of the medium to its scattering properties,

$$n/n_C \approx \alpha/\lambda^3,$$

i.e., it is determined by the ratio of the polarizability χ of a molecule or particle to the cube of the wavelength, and does not depend on the number density.

The possibility of studying the effect depends on the size of the scattering in the medium. It is obvious that the size of the volume in which radiation from the charge occurs must be smaller than the range L of the radiation, in order for it to be permissible to neglect secondary scattering and depolarization of the radiation.

It would be interesting to observe the smearing of the Cerenkov radiation near the threshold owing to the logarithmic increase of the radiation from inhomogeneities of the medium.

If the medium contains atoms that give resonance scattering, they will also be excited, since the medium scatters strongly at these frequencies. This excitation of atoms will occur even if the density and effective cross section of these atoms does not lead to local reaching of the threshold for Cerenkov radiation at the resonance frequency. Thus there can be excitation of small impurities in a gas if the main substance does not have an anomalous polarizability at the frequency in question.

The writer thanks L. D. Landau and L. A. Vaĭnshteĭn for helpful discussions.

---

[1] L. D. Landau and E. M. Lifshitz, Электродинамика сплошных сред (Electrodynamics of Continuous Media), Fizmatgiz, 1957.

Translated by W. H. Furry
250

SOVIET PHYSICS JETP VOLUME 12, NUMBER 5 MAY, 1961

THE POSSIBILITY OF EXPERIMENTAL CHECK OF THE MODEL OF A NON-AXIAL ROTATOR BY STUDYING THE INFLUENCE OF THE MEDIUM ON THE ANGULAR CORRELATION OF CASCADE GAMMA RAYS

D. P. GRECHUKHIN

Submitted to JETP editor June 15, 1960

J. Exptl. Theoret. Phys. (U.S.S.R.) **39**, 1371-1373 (November, 1960)

An experiment is proposed for the purpose of checking the assumptions of the model of a non-axial rotator for even-even nuclei. The experiment is based on measurement of the attenuation factor for angular correlation of γ quanta for similar cascades in isotopes of the same element placed in identical media.

THE model of the non-axial rotator which was developed by Davydov and Filippov[1] predicts a quite marked dependence of the quadrupole moment of the nucleus Q_2 in the excited states of the rotator on the parameter γ of non-axial deformation of the nucleus.

According to this model, we have for the matrix element of the nuclear quadrupole moment operator

$$\langle\psi^*_{IM_1i}(\beta,\gamma,\theta_j)|\hat{Q}_{2\mu}|\psi_{IM_2i}(\beta,\gamma,\theta_j)\rangle$$

$$= \frac{3}{4\pi} ZR_0^2 \sqrt{\frac{4\pi}{5}} \beta f_{Ii}(\gamma) C^{IM_1}_{IM_2 2\mu},$$

$$\hat{Q}_{2\mu} = \sqrt{\frac{4\pi}{5}} \sum_{i=1}^{Z} r_i^2 Y_{2\mu}(\mathbf{n}_i); \qquad (1)$$

θ_j are the Euler angles for the orientation of the rotator; β, γ are the deformation parameters for the nucleus; $C^{\cdot\cdot}_{\cdot\cdot}$ are the Clebsch-Gordan coefficients. In particular, for the first and second excited states with spin $I = 2^+$, the functions $f_{Ii}(\gamma)$ are equal to

$$f_{21} = -f_{22} = -3\cos 3\gamma/\sqrt{1 + 8\cos^2 3\gamma}. \qquad (2)$$

Investigation of the dependence of Q_2 on γ is of interest as an experimental test of the assumptions of the non-axial rotator model. Measurement of quadrupole moments of nuclei in excited states is possible by investigating the attentuation of the angular correlation of cascade γ quanta as a result of the interaction of the quadrupole moment Q_2 in the intermediate state of the nucleus with the electric field of the source medium.[2] However, the application of this method is seriously limited by the fact that the field of the medium is not known precisely and can only be estimated crudely with difficulty. This difficulty can be eliminated if we compare the moments Q_2 of different isotopes of the same element, as determined from the attenuation of the correlation in one and the same medium. In this case, the unknown value of the field intensity (or the corresponding derivatives) and other parameters of the medium drop out of the final result for the ratio of the quadrupole moments.

Such a possibility exists in the case of the even-even isotopes of Nd, Sm, Gd, W, Os, and Pt. In this group of nuclear isotopes, according to the non-axial rotator model, as the number of neutrons is changed there occurs a change in the parameter of non-axial deformation γ from 0 to 30°. Thus, measurement of the ratio of values of Q_2 for nuclei of this group enables one to check the dependence (2).

Especially interesting is the study of the quenching of the angular correlation when we use a liquid as the source medium. In this case, as it turns out, there is no need to know exactly the lifetime of the intermediate state of the nucleus, τ, which in general enters in the result in other cases.[2]

From observation of the angular correlation of the γ-γ cascade $I_i \to I_B \to I_f$,

$$W(\theta) = 1 + \sum_{\varkappa} G_{2\varkappa} A_{2\varkappa} P_{2\varkappa}(\cos\theta)$$

one determines experimentally the attenuation coefficients $G_{2\kappa}$, since the $A_{2\kappa}$ are known exactly for a given form of cascade with known spins I_i, I_B and I_f.[2] For liquid sources under the condition that the resolving time of the apparatus is much greater than the lifetime τ of the nucleus in the intermediate state with spin I_B, we have for the coefficients $G_{2\kappa}$[2]

$$G_{2\varkappa} = (1 + \lambda_{2\varkappa}\tau)^{-1}. \qquad (3)$$

Here (cf. reference 2)

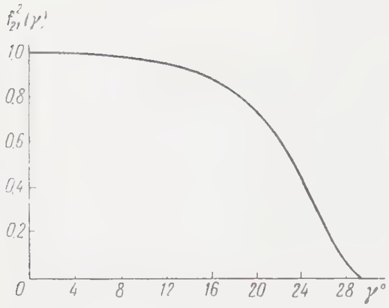

$$\lambda_{2\varkappa} = \frac{3}{80}\left(\frac{eQ_2}{\hbar}\right)^2 \left\langle\frac{\partial^2 V}{\partial z^2}\right\rangle^2 \tau_c$$
$$\times \frac{2\varkappa(2\varkappa+1)[4I_B(I_B+1)-2\varkappa(2\varkappa+1)-1]}{I_B^2(2I_B-1)^2}, \qquad (4)$$

$< \partial^2 V/\partial z^2 >^2$ is the mean square of the second derivative of the fluctuation field in the medium; τ_c is the correlation time in the liquid, Q_2 is the quadrupole moment of the nucleus in the state I_B.

Now let us compare $\lambda_{2K}\tau$ for two isotopes of the same element whose nuclei have respectively $\gamma = 0$ and $\gamma \neq 0$, i.e., let us find the ratio $(\lambda_{2K}\tau)_\gamma/(\lambda_{2K}\tau)_0$. It is assumed that the values of G_{2K} for the isotopes are measured in similar cascades $I_i \rightarrow I_B \rightarrow I_f$ in the same medium.

The probability of the γ transition for collective E2 transitions of a rotator $I_B \rightarrow I_f$ has the form:[1]

$$\frac{1}{\tau} = W(E2;\ I_B \rightarrow I_f)$$
$$= \frac{3}{8\pi} 10^{-3}\left(\frac{e^2}{\hbar c}\right)^5 Z^2 R_0^4 k^5 \beta^2 b(E2;\ I_B \rightarrow I_f)\ \frac{m_e c^2}{\hbar}. \qquad (5)$$

Here R_0 is the nuclear radius in units $r_0 = 1.4 \times 10^{-13}$ cm; $r_0 = e^2/2m_e c^2$; k is the energy of the radiated quantum in units of $m_e c^2$ (0.511 Mev). The values of $b(E2;\ I_B \rightarrow I_f)$ are given in reference 1 for various transitions.

Assuming that one uses the same medium and the same type of cascade for the isotopes with $\gamma = 0$ and $\gamma \neq 0$, we obtain from (3), (4), and (5) for the ratio $(\lambda_{2K}\tau)_\gamma/(\lambda_{2K}\tau)_0$ the result

$$\frac{(\lambda_{2\varkappa}\tau)_\gamma}{(\lambda_{2\varkappa}\tau)_0} = \frac{k_0^5}{k_\gamma^5}\frac{[b(E2;\ I_B \rightarrow I_f)]_0}{[b(E2;\ I_B \rightarrow I_f)]_\gamma} f^2_{I_B}(\gamma). \qquad (6)$$

Here $f_{I_B}(\gamma)$ is the function $f_{I_i}(\gamma)$ for the state I_B of the rotator [cf. (1)]; k_0 and k_γ are energies of the E2 transitions $I_B \rightarrow I_f$ for the isotopes with $\gamma = 0$ and $\gamma \neq 0$.

Of primary interest is a cascade where the intermediate level is the first excited state of the nucleus with spin $I_B = 2^+$. In this case $b(E2;\ 21 \rightarrow 0)$ varies between the limits 0.933 and 1[1], i.e., it is practically independent of γ. Thus we have

$$f^2_{21}(\gamma) = \frac{(\lambda_{2\varkappa}\tau)_\gamma k_\gamma^5}{(\lambda_{2\varkappa}\tau)_0 k_0^5} = \frac{k_\gamma^5}{k_0^5}\frac{[(1-G_{2\varkappa})/G_{2\varkappa}]_\gamma}{[(1-G_{2\varkappa})/G_{2\varkappa}]_0}. \qquad (7)$$

The function $f^2_{21}(\gamma)$ is shown in the figure. The right side of (7) can easily be measured experimentally, while γ is known from the ratio of the energies of the first and second excited states of the nucleus which have spins 2^+.[1] Thus there is the possibility for checking the dependence of $Q_2(\gamma)$ in the model of the non-axial rotator.

---

[1] A. S. Davydov and G. F. Filippov, JETP **35**, 440 (1958), Soviet Phys. JETP **8**, 303 (1959).

[2] A. Abragam and R. V. Pound, Phys. Rev. **92**, 943 (1953). R. M. Steffen, Advances in Phys. **4**, 293 (1955).

Translated by M. Hamermesh
251

SOVIET PHYSICS JETP VOLUME 12, NUMBER 5 MAY, 1961

A SCHEME OF WEAK INTERACTIONS WITH NEUTRAL CURRENTS

V. N. BAĬER and I. B. KHRIPLOVICH

Submitted to JETP editor June 15, 1960

J. Exptl. Theoret. Phys. (U.S.S.R.) **39**, 1374-1380 (November, 1960)

The cross sections for scattering and annihilation in the collision of light particles due to weak interaction are calculated. The degree of logitudinal polarization in such nucleon-nucleon scattering is estimated. Effects caused by weak interaction between the electrons in the medium are considered.

1. INTRODUCTION

IT is well known that in the V — A scheme of weak interactions,[1] it is possible for charged particles to be scattered by neutral ones, along with decay processes. It is not excluded, however, that the weak interaction has a universal character not only in the sense of the coupling constant and the interaction structure, but is also universal in that it is realized between all the fermions. If this assumption is adopted, the following law results: the weaker the interaction (from strong to gravitational), the more universal it is in the sense of the particles participating in it.[2]

It must be considered, however, that many processes (for example, the decay $\mu^\pm \rightarrow 2e^\pm + e^\mp$) are experimentally forbidden. In order to circumvent the difficulty, it is necessary to introduce supplementary exclusions: thus, Feynman and Gell-Mann exclude the neutral current containing terms of the type $(\bar{e}e)$, $(\bar{\mu}e)$, $(\bar{n}n)$, etc.[1]

Certain interest therefore attaches to a scheme in which the class of possible weak interactions is broadened, and at the same time the forbidden processes are automatically excluded. Such a scheme was proposed, for example, by Bludman.[3] It contains many new processes, but this does not contradict the experimental data known at present. Although we adhere to this scheme in the article, it should be noted it is not the only one, and that the authors are primarily interested in the consequences of introducing neutral currents into the theory of weak interactions. For the sake of simplicity, we do not consider strange particles.

We introduce the charge space of weak interactions. We consider in this space the doublets $(\nu\mu)$, (νe), and (pn), and assume that the weak interaction is invariant with respect to rotations in this space. Then the weak-interaction Lagrangian can be represented in the form

$$L = \frac{1}{4}\frac{G}{\sqrt{2}}\sum_{ij}[\bar{\psi}_i\gamma_\mu(1-i\gamma_5)\tau\psi_i][\bar{\psi}_j\gamma_\mu(1-i\gamma_5)\tau\psi_j]$$
$$= \frac{G}{\sqrt{2}}\sum_{ij}\Big\{[\bar{\psi}_i\gamma_\mu(1-i\gamma_5)\tau_+\psi_i][\bar{\psi}_j\gamma_\mu(1-i\gamma_5)\tau_-\psi_j]$$
$$+\tfrac{1}{4}[\bar{\psi}_i\gamma_\mu(1-i\gamma_5)\tau_3\psi_i][\bar{\psi}_j\gamma_\mu(1-i\gamma_5)\tau_3\psi_j]\Big\}. \qquad (1)$$

In the usual notation, the Lagrangian (1) can be written as

$$L = L_\pm + L_3; \qquad (2)$$

$$L_\pm = (\bar{p}n)(\bar{e}\nu) + (\bar{n}p)(\bar{\nu}e) + (\bar{p}n)(\bar{\mu}\nu)$$
$$+ (\bar{n}p)(\bar{\nu}\mu) + (\bar{\nu}\mu)(\bar{e}\nu) + (\bar{\mu}\nu)(\bar{\nu}e)$$
$$+ (\bar{\nu}e)(\bar{e}\nu) + (\bar{\nu}\mu)(\bar{\mu}\nu) + (\bar{p}n)(\bar{n}p), \qquad (3)$$

$$L_3 = (\bar{p}p)(\bar{\nu}\nu) - (\bar{n}n)(\bar{\nu}\nu) - \tfrac{1}{2}(\bar{p}p)(\bar{e}e) + \tfrac{1}{2}(\bar{n}n)(\bar{e}e)$$
$$- \tfrac{1}{2}(\bar{p}p)(\bar{\mu}\mu) + \tfrac{1}{2}(\bar{n}n)(\bar{\mu}\mu) + \tfrac{1}{4}(\bar{p}p)(\bar{p}p)$$
$$+ \tfrac{1}{4}(\bar{n}n)(\bar{n}n) + (\bar{\nu}\nu)(\bar{\nu}\nu) + \tfrac{1}{4}(\bar{e}e)(\bar{e}e) + \tfrac{1}{4}(\bar{\mu}\mu)(\bar{\mu}\mu)$$
$$+ \tfrac{1}{2}(\bar{\mu}\mu)(\bar{e}e) - \tfrac{1}{2}(\bar{p}p)(\bar{n}n) - (\bar{\mu}\mu)(\bar{\nu}\nu) - (\bar{e}e)(\bar{\nu}\nu). \qquad (4)$$

Here $L_\pm$ is the usual weak-interaction Lagrangian (1); the Lagrangian L_3 is new; it is seen to contain the interaction of the neutral currents.

By virtue of the known symmetry property of the V — A interaction

$$(\bar{A}B)(\bar{C}D) = (\bar{C}B)(\bar{A}D),$$

the terms $(\bar{\nu}e)(\bar{e}\nu)$, $(\bar{\nu}\mu)(\bar{\mu}\nu)$, $-(\bar{\mu}\mu)(\bar{\nu}\nu)$, $-(\bar{e}e)(\bar{\nu}\nu)$ cancel out of the total Lagrangian. Thus, this scheme does not contain the interaction between the neutrino and electrons or muons,[4] which is so widely discussed at present.

The scattering of a proton by a neutron is described in the theory of weak interactions[1] by the term $(\bar{p}n)(\bar{n}p)$, and in the proposed scheme this process is described in addition by the term $-\frac{1}{2}(\bar{p}p)(\bar{n}n)$. These terms are not given here, since the nucleon currents cannot be written in the form of a pure V — A variant in view of the influence of the strong interactions.

We investigate below the processes brought about by the Lagrangian L_3.

2. LEPTON-LEPTON PROCESSES

Along with the decay $\mu \rightarrow e + \nu + \bar{\nu}$, and scattering $\mu + e \rightarrow \nu + \nu$, processes known from the usual theory of weak interactions, other lepton scattering processes are also possible in this scheme, viz: $e + e \rightarrow e + e$, $\mu + \mu \rightarrow \mu + \mu$, $\nu + \nu \rightarrow \nu + \nu$, $e + \mu \rightarrow e + \mu$, and also the weak annihilation $e + e \rightarrow \mu + \mu$. The total cross section for each of these processes can be written in the form

$$\sigma = \sigma_e + \sigma_i + \sigma_w, \tag{5}$$

where σ_e is the electromagnetic interaction cross section, σ_w the weak interaction cross section, and σ_i the term for the interference between the electromagnetic and weak interactions. In this section, all the cross sections are written out in the c.m.s. for ultrarelativistic particles.

In the case of scattering of identical leptons, the weak-interaction cross section is of the form

$$\sigma_w(\theta) = r_0^2 \left(\frac{Gm^2}{e^2}\right)^2 \left(\frac{\mathscr{E}}{m}\right)^2 (5 + \cos^2\theta), \tag{6}$$

and the interference term is of the form

$$\sigma_i(\theta) = \frac{1}{\sqrt{2}} r_0^2 \frac{Gm^2}{e^2} \frac{5 + 3\cos^2\theta}{\sin^2\theta}. \tag{7}$$

The following symbols are used here: r_0 is the classical radius of the electron, m is the electron mass, G is the weak-interaction constant, $\mathscr{E}$ is the particle energy, and θ is the scattering angle. In the case of the scattering of a neutrino, the weak interaction cross section has an additional factor 16, and there is no interference term.

The cross section for the scattering $e + \mu \rightarrow e + \mu$ has the form

$$\sigma_w(\theta) = 8r_0^2 \left(\frac{Gm^2}{e^2}\right)^2 \left(\frac{\mathscr{E}}{m}\right)^2 \cos^4\frac{\theta}{2}, \tag{8}$$

$$\sigma_i(\theta) = \sqrt{2} r_0^2 \frac{Gm^2}{e^2} \frac{\cos^4(\theta/2)}{\sin^2(\theta/2)}. \tag{9}$$

For the cross sections of the weak annihilation $e + e \rightarrow \mu + \mu$ we obtain

$$\sigma_w(\theta) = 8r_0^2 \left(\frac{Gm^2}{e^2}\right)^2 \left(\frac{\mathscr{E}}{m}\right)^2 \cos^4\frac{\theta}{2}, \tag{10}$$

$$\sigma_i(\theta) = \sqrt{2} r_0^2 \frac{Gm^2}{e^2} \cos^4\frac{\theta}{2}. \tag{11}$$

Comparing the energy dependence of different cross sections, we see that with increasing energy the electromagnetic cross section decreases as $\mathscr{E}^{-2}$, the interference cross section is independent of the energy, and the weak-interaction increases as $\mathscr{E}^2$. It is clear therefore that, starting with a certain energy, the contribution of the weak interaction to the cross section will exceed all others and will become decisive.

To estimate the orders of magnitude of the quantities, we consider the cross section for the scattering of an electron by an electron. At a scattering angle of 15° and an energy of 3 Bev, the contribution of the interference term amounts to 0.01% of the contribution of the electromagnetic term, and the contribution of the weak term is negligibly small. But even at 100 Bev both the interference and the weak scattering cross sections become greater than the electromagnetic cross-section. At a scattering angle of 90°, the effects are even more noticeable: at 3 Bev the contribution of the interference term is 0.2% of the contribution of the electromagnetic term, but even at 70 Bev the contribution of both the interference and the weak terms of the interactions become comparable with the contribution from the electromagnetic term.

Thus, in the local theory the cross section for the scattering of an electron by an electron has a minimum at an energy of several times 10 Bev, and the absolute magnitude of the cross section is very small ($\sim 10^{-34}$ cm^2). If, however, the interactions are "smeared out" then the cross sections are multiplied by the corresponding form factors, and the absolute values of the cross sections become even smaller. Unfortunately, nothing is known at present regarding either the form factors or in general regarding the applicability of the V − A variant at such high energies. We note that if the weak interaction is produced through an intermediate boson whose mass is usually assumed to be several Bev, this leads to an appreciable distortion of the angular cross sections given above; this circumstance could in principle permit the detection of this boson.

Along with the processes considered above, the weak interaction between electrons will naturally lead to new effects in optics and in solid state physics.

The parity nonconserving part of the weak interaction will contribute to the antisymmetrical part of the polarization tensor, the presence of which leads to natural optical activity.[5] It is clear that this effect will be of order v/c.

Calculation in first order in G yields the following expression for the angle of rotation of the plane of polarization

$$\theta = \frac{16}{9}\pi^2 N \frac{n^2 + 2}{\lambda} \operatorname{Im} \sum_{n,k} \frac{\hbar\omega}{(E_n - E_0)^2 - \hbar^2\omega^2} \times \left[\frac{\overset{*}{\pi}_{nk}\mathbf{p}_{0k}\mathbf{M}_{n0} + \pi_{nk}\mathbf{p}_{n0}\mathbf{M}_{k0}}{E_n - E_k} + \frac{\overset{*}{\pi}_{0k}\mathbf{p}_{0n}\mathbf{M}_{nk} + \pi_{0k}\mathbf{p}_{kn}\mathbf{M}_{n0}}{E_0 - E_k}\right]. \tag{12}$$

Here N is the concentration, p_{0k}, M_{n0}, and π_{nk} are the matrix elements of the electric dipole moment, magnetic dipole moment, and weak interaction, respectively. For liquid helium $\theta \sim 10^{-15}$ rad/cm,

$$\frac{\pi_{kn}}{E_k - E_n} \sim 10^{-18},$$

$$p_{0k} M_{n0} \sim \left(\frac{v}{c}\right) p_{0k} p_{n0} \sim \left(\frac{v}{c}\right) |p_{0k}|^2$$

$$\sim \frac{e\hbar^2}{2m(E_0 - E_k)} \frac{v}{c} f_{0k} \sim 10^{-36},$$

where f_{0k} is the oscillator strength.

In addition, weak interaction between electrons will lead (in first order in G) to a shift of the levels of the atomic electrons. Thus, for singlet levels of helium the shift will be of order 0.1 cps (in the nonrelativistic approximation the shift for triplet levels is equal to 0).

It is clear that the probability of forbidden transitions due to weak interactions will be of order G^2, although the corrections to the probabilities of the allowed transitions will be of order G.

Were the weak interaction between electrons capable of leading to bound states, this could lead to effects of the superconductivity type. Unfortunately, this effect cannot be estimated by virtue of the well known difficulties with higher approximations of the 4-fermion interaction.

3. LEPTON-NUCLEON PROCESSES

The scheme which we consider contains additional processes of scattering of leptons by nucleons, such as p(n) + e(μ, ν) → p(n) + e(μ, ν) (their probability was previously estimated by Zel'dovich[6]), and annihilation processes such as e(μ, ν) + e(μ, ν) → p(n) + p(n). We shall again write the cross sections in the form (5).

The electromagnetic nucleon current can be represented in the form

$$j_\mu = \bar{\psi}' \left[\gamma_\mu F_1^{p(n)} - \frac{\mu^{p(n)}}{4M} (\gamma_\mu \hat{q} - \hat{q}\gamma_\mu) F_2^{p(n)}\right] \psi, \tag{13}$$

where $F_1^{p(n)}$, $F_2^{p(n)}$ are the electric and magnetic form factors of the proton (neutron), $\mu^{p(n)}$ is the anomalous magnetic moment of the proton (neutron), M is the nucleon mass, and q = p′ − p the momentum transfered.

Allowing for G invariance,[7] we obtain for the weak nucleon current the expression

$$V_\mu + A_\mu = \bar{\psi}' \left[\gamma_\mu F_1 - \frac{\mu}{4M} (\gamma_\mu \hat{q} - \hat{q}\gamma_\mu) F_2 - i\gamma_\mu\gamma_5 g_1 \right.$$
$$\left. - i\gamma_5 q_\mu g_3 \right] \psi, \tag{14}$$

where F_1 and F_2 are the isovector parts of the corresponding electromagnetic nucleon form factors, $\mu = \mu_p - \mu_n$, and g_1 is the axial form factor. The terms proportional to g_3 make a contribution $\sim m^2/M^2$ (and are neglected).

For the scattering of an electron by a nucleon at rest, we obtain

$$\sigma_w(\theta) = 4r_0^2 \left(\frac{Gm^2}{e^2}\right)^2 \left(\frac{\mathcal{E}}{m}\right)^2 \frac{\cos^2(\theta/2)}{[1+2(\mathcal{E}/M)\sin^2(\theta/2)]^3}$$
$$\left\{F_1^2 - \frac{q^2}{4M^2}\left[2(F_1 + \mu F_2)^2 \tan^2\frac{\theta}{2}\right.\right.$$
$$+ \mu^2 F_1^2 + 2g_1^2 \tan^2\frac{\theta}{2} - 4g_1(F_1 + \mu F_2)$$
$$\left.\left.\left(\frac{M}{\mathcal{E}}\sec^2\frac{\theta}{2} + \tan^2\frac{\theta}{2}\right)\right]\right\}, \tag{15}$$

$$\sigma_i(\theta) = \sqrt{2} r_0^2 \frac{Gm^2}{e^2} \frac{\cot^2(\theta/2)}{[1+2(\mathcal{E}/M)\sin^2(\theta/2)]^2} \left\{F_1 F_1^{p(n)}\right.$$
$$- \frac{q^2}{4M}\left[2(F_1 + \mu F_2)(F_1^{p(n)} + \mu^{p(n)} F_2^{p(n)}) \tan^2\frac{\theta}{2}\right.$$
$$+ \mu\mu^{p(n)} F_2 F_2^{p(n)} - 2g_1 (F_1^{p(n)}$$
$$\left.\left. + \mu^{p(n)} F_2^{p(n)}) \left(\frac{M}{\mathcal{E}}\sec^2\frac{\theta}{2} + \tan^2\frac{\theta}{2}\right)\right]\right\}. \tag{16}$$

In the derivation of (15) and (16) we neglected m^2 compared with M^2 and q^2. Neglect of the latter limits the applicability of these formulas in the small angle region. Comparison with the formula of Rosenbluth[8] shows that the ratio of the interference cross section to the electromagnetic cross section amounts to ~ 0.003% for the proton, and ~ 0.006% for the neutron in backward scattering of 1-Bev electrons.

For weak annihilation of an electron-positron pair and a pair of nucleons we obtain in the c.m.s.

$$\sigma_w(\theta) = 2r_0^2 \left(\frac{Gm^2}{e^2}\right)^2 \left(\frac{\mathcal{E}}{m}\right)^2 v \{(F_1^2 + g_1^2)(1 + v^2\cos^2\theta)$$
$$+ \frac{M^2}{\mathcal{E}^2}(F_1^2 - g_1^2) + 4\mu F_1 F_2 + \mu^2 F_2^2 \left[\frac{\mathcal{E}^2}{M^2}(1 - v^2\cos^2\theta) + 1\right]$$
$$+ 4g_1(F_1 + \mu F_2) v\cos\theta\}, \tag{17}$$

$$\sigma_i(\theta) = \frac{1}{\sqrt{2}} r_0^2 \frac{Gm^2}{e^2} v \left\{F_1 F_1^{p(n)} \left(1 + v^2\cos^2\theta + \frac{M^2}{\mathcal{E}^2}\right)\right.$$
$$+ 2(\mu^{p(n)} F_2^{p(n)} F_1 + \mu F_2 F_1^{p(n)})$$
$$+ \mu\mu^{p(n)} F_2 F_2^{p(n)} \left[\frac{\mathcal{E}^2}{M^2}(1 - v^2\cos^2\theta) + 1\right]$$
$$\left. + 2g_1(F_1^{p(n)} + \mu^{p(n)} F_2^{p(n)}) v\cos\theta\right\}, \tag{18}$$

where v is the velocity of the nucleon. Near the threshold, σ_i amounts to 0.1% of σ_e.

All the foregoing pertains also to processes in which muons participate, the only difference being that the neglect of m_μ^2 can result in an error of several percent. For processes in which neutrinos participate, obviously $\sigma_i = 0$ and σ_w must, according to (4), be multiplied by 4.

4. SCATTERING OF NUCLEONS BY NUCLEONS

To describe the scattering of nucleons by nucleons, we use the phenomenological transition matrix in the c.m.s.:[9]

$$M_0 = \alpha + \beta(\boldsymbol{\sigma}_1\mathbf{n})(\boldsymbol{\sigma}_2\mathbf{n}) + \gamma_1(\boldsymbol{\sigma}_1\mathbf{n}) + \gamma_2(\boldsymbol{\sigma}_2\mathbf{n})$$
$$+ \delta(\boldsymbol{\sigma}_1\mathbf{m})(\boldsymbol{\sigma}_2\mathbf{m}) + \varepsilon(\boldsymbol{\sigma}_1\mathbf{l})(\boldsymbol{\sigma}_2\mathbf{l}), \tag{19}$$

where α, β, $\gamma_{1,2}$, δ, ϵ are functions of the energy and the transferred momentum; $\boldsymbol{\sigma}_1$ and $\boldsymbol{\sigma}_2$ are the spin operators of particles 1 and 2, $\mathbf{l}$, $\mathbf{m}$, and $\mathbf{n}$ are the unit vectors in the directions $\mathbf{p}_1' + \mathbf{p}_1$, $\mathbf{p}_1' - \mathbf{p}_1$ and $(\mathbf{p}_1' + \mathbf{p}_1) \times (\mathbf{p}_1' - \mathbf{p}_1)$. This matrix includes all the interactions which are invariant under space reflection, including electromagnetic interactions, and the parity-conserving part of the weak interactions. Thus, considering weak interaction between nucleons we should take additional account only of the parity nonconserving part of the Lagrangian

$$L_{\mathbf{nc}} = a\frac{G}{\sqrt{2}}\Big\{\Big[\bar{u}_2'\Big(\gamma_\mu F_1 - \frac{\mu}{4M}(\gamma_\mu\hat{q} - \hat{q}\gamma_\mu)$$
$$\times F_2\Big)u_2\Big][\bar{u}_1'(-i\gamma_\mu\gamma_5 g_1)u_1] + [\bar{u}_2'(-i\gamma_\mu\gamma_5 g_1)u_2]$$
$$\times\Big[\bar{u}_1'(\gamma_\mu F_1 + \frac{\mu}{4M}(\gamma_\mu\hat{q} - \hat{q}\gamma_\mu)F_2)u_1\Big]\Big\}, \tag{20}$$

where a = 1/4 for pp and nn scattering; a = 1/2 for pn scattering.*

We note that the interference contribution from (19) and (20) to the cross section averaged over the spins is 0. Actually, this contribution should be a pseudo-scalar, and after averaging over the spins the scattering process is characterized by 2 vectors, from which a pseudo-scalar cannot be constructed.

Weak interaction between nucleons is apparently simplest to observe in polarization experiments. The interference term between (19) and (20) leads to the occurrence of longitudinal polarization. Since the dominating contribution to (19) is made by strong interactions, we shall assume M_0 invariant in isotopic space, that is, $\gamma_1 = \gamma_2 = \gamma$.

With the aid of several cumbersome transformations we can obtain from (20) the parity nonconserving scattering matrix, written in the two-component form in the c.m.s.

$$M_1 = a\frac{Gg_1}{2\pi}p\cos\frac{\theta}{2}\Big\{\Big[F_1 - \frac{\mathcal{E}-M}{M}\mu F_2\sin^2\frac{\theta}{2}\Big](\boldsymbol{\sigma}_1 - \boldsymbol{\sigma}_2)\mathbf{l}$$
$$+ i\frac{\mathcal{E}-M}{2\mathcal{E}}\sin\theta\Big[F_1 + \frac{\mathcal{E}+M}{M}\mu F_2\Big]\Big[(\boldsymbol{\sigma}_2\mathbf{l})(\boldsymbol{\sigma}_1\mathbf{n})$$
$$- (\boldsymbol{\sigma}_2\mathbf{n})(\boldsymbol{\sigma}_1\mathbf{l})\Big]\Big\}. \tag{21}$$

The total transition matrix is of the form

$$M = M_0 + M_1. \tag{22}$$

Let us calculate, in first order in G, the polarization of the scattered nucleons, brought about in the scattering of unpolarized particles. The polarization vector will be represented in form

$$\mathbf{P} = \mathbf{P}_\perp + \mathbf{P}_\parallel. \tag{23}$$

The longitudinal-polarization vector, in the scattering of protons by protons or of neutrons by neutrons, is

$$\mathbf{P}_\parallel = \frac{Gg_1p\cos(\theta/2)}{4\pi(|\alpha|^2 + |\beta|^2 + 2|\gamma|^2 + |\delta|^2 + |\varepsilon|^2)}$$
$$\times\Big\{\Big(F_1 - \frac{\mathcal{E}-M}{M}\sin^2\frac{\theta}{2}\mu F_2\Big)[\mathbf{l}\,\mathrm{Re}(\alpha + \beta + \delta - \varepsilon)$$
$$- 2\mathbf{m}\,\mathrm{Im}\gamma] - \frac{\mathcal{E}-M}{2\mathcal{E}}\sin\theta\Big(F_1 + \frac{\mathcal{E}+M}{M}\mu F_2\Big)$$
$$\times[2\mathbf{l}\,\mathrm{Im}\gamma + \mathbf{m}\,\mathrm{Re}(\alpha + \beta - \delta - \varepsilon)]\Big\}, \tag{24}$$

and in the scattering of neutrons by protons

$$\mathbf{P}_\parallel = \frac{Gg_1p\cos(\theta/2)}{2\pi(|\alpha|^2 + |\beta|^2 + 2|\gamma|^2 + |\delta|^2 + |\varepsilon|^2)}$$
$$\times\Big\{\Big(F_1 - \frac{\mathcal{E}-M}{M}\sin^2\frac{\theta}{2}\mu F_2\Big)[\mathbf{l}\,\mathrm{Re}(\alpha - \varepsilon) - \mathbf{m}\,\mathrm{Im}\gamma]$$
$$- \frac{\mathcal{E}-M}{2\mathcal{E}}\sin\theta\Big(F_1 + \frac{\mathcal{E}+M}{M}\Big)\mu F_2[\mathbf{l}\,\mathrm{Im}\gamma + \mathbf{m}\,\mathrm{Re}(\beta - \varepsilon)]\Big\}. \tag{25}$$

Here p is the momentum of the scattered nucleon.

The up-down asymmetry coefficient can be written in the form

$$\varkappa = (1 - P_\parallel)/(1 + P_\parallel) \approx 1 - 2P_\parallel. \tag{26}$$

Unfortunately, the moduli and phases of the coefficients α, β, γ, δ, and ϵ are still unknown. We can therefore only make a rough estimate of the longitudinal polarization. It is found to be $10^{-6} - 10^{-7}$ at 200 – 300 Mev.

It is clear that an analogous calculation can also be made for the lepton and the lepton-nucleon scattering, in which case the coefficient of longitudinal polarization will be of order $10^{-3} - 10^{-4}$ at an energy of several Bev.

---

*In the examination of scattering of neutrons by protons, we shall take into account only the term $-\frac{1}{2}(\bar{p}p)(\bar{n}n)$ in the Lagrangian, and disregard the term $(\bar{p}n)(\bar{n}p)$, although they are of the same order, since lack of experimental information enables us to obtain only rough estimates for the matrix M_0.

[1] R. P. Feynman, and M. Gell-Mann, Phys. Rev. **109**, 193 (1958).

[2] K. Aizu. Progr. Theoret. Phys. **22**, 192 (1959).

[3] S. Bludman, Nuovo cimento **9**, 433 (1958).

[4] B. M. Pontecorvo, JETP **36**, 1615 (1959), Soviet Phys. JETP **9**, 1148 (1959); G. M. Gandel'man and V. S. Pinaev, JETP **37**, 1072 (1959), Soviet Phys. JETP **10**, 764 (1960).

[5] M. V. Vol'kenshtein, Молекулярная оптика (Molecular Optics), Gostekhizdat, 1951.

[6] Ya. B. Zel'dovich, JETP **36**, 1952 (1959), Soviet Phys. JETP **9**, 1389 (1959).

[7] L. B. Okun', Usp. Fiz. Nauk **68**, 449 (1959), Ann. Revs. Nuc. Sci. Vol 9, p. 61.

[8] R. Hofstadter, Revs. Modern Phys. **28**, 214 (1958).

[9] L. Wolfenstein, and J. Ashkin, Phys. Rev. **85**, 947 (1952).

Translated by J. G. Adashko
252

SOVIET PHYSICS JETP VOLUME 12, NUMBER 5 MAY, 1961

THE SHAPE OF THE ELECTRON RESONANCE LINE IN A SYSTEM OF PARTICLES WITH AN ANISOTROPIC g FACTOR

A. K. CHIRKOV and A. A. KOKIN

Ural Polytechnical Institute

Submitted to JETP editor June 17, 1960

J. Exptl. Theoret. Phys. (U.S.S.R.) 39, 1381-1386 (November, 1960)

The moments and the line shape are calculated for a system of randomly oriented noninteracting particles with an anisotropic g factor, for the case of no thermal motion. The results of the calculation are compared with experimental data on resonance absorption in powders, glasses, and undercooled solutions.

1. In observations of electron magnetic resonance in powders, glasses, solid solutions, undercooled solutions, and so on, one finds at sufficiently high frequencies a considerable distortion of the shape of the absorption line, which is caused by the manifestation of anisotropy of the g factors of the individual particles and of the hyperfine structure constant.[1-3]

A characteristic feature of the distortions caused by anisotropy of the g factor is an increase of the asymmetry of the line with increase of the magnetic field. The distortions of the line shape that appear because hyperfine structure shows up in sufficiently strong magnetic fields do not depend on the strength of the field.

There have been a number of papers[4,5] on the analysis of the effect of the anisotropy of the g factor of the randomly oriented particles on the line shape of magnetic resonance in glasses and organic compounds. These papers, however, have dealt only with a uniaxial anisotropy of the g factor.

The unsymmetrical character of the absorption line in a powder of the free organic radical diphenyl-picryl hydrazyl (DPPH) has been observed experimentally at the frequency 25,500 Mc/sec.[6]

An attempt to explain the observed asymmetry of the line by the presence of a uniaxial anisotropy of the g factor of the individual single crystals has been made in a paper by Kikuchi and Cohen.[7] In calculating the line shape they used results obtained by measurements of the g factor made with individual, relatively large, single crystals of DPPH. Lack of the necessary experimental data prevented these authors from making a comparison of theory with experiment.

A temperature dependence of the anisotropy of the g factor of a single crystal of DPPH has been discovered by Singer and Kikuchi.[8]

In such complicated paramagnetic compounds as free organic radicals it is natural to expect that there will be not uniaxial, but triaxial anisotropy.[9] In this case the shape of the absorption line can be still more complex.

In the present paper the moments and the line shape are calculated for a system consisting of particles that have a weak triaxial or uniaxial anisotropy of the g factor and are randomly oriented in space.

2. The absorption spectrum of electronic magnetic resonance in a specimen with anisotropy of the g factor is determined by the eigenvalues of the spin Hamiltonian

$$\hat{\mathscr{H}} = \mu_0 (\mathbf{S}\mathbf{g}\mathbf{H}_0), \qquad (1)$$

where μ_0 is the Bohr magneton. In its principal axes the tensor **g** has the components $g + \Delta g_i$ $(i = 1, 2, 3)$, where g is the average value, so that

$$\Delta g_1 + \Delta g_2 + \Delta g_3 = 0.$$

We shall assume that the internal interactions lead only to a broadening of the spectrum lines.

If the external magnetic field H_0 is directed along the z axis, then for an arbitrary orientation of the particle relative to the external field the expression (1) takes the form

$$\hat{\mathscr{H}} = \mu_0 H_0 (g_{xz}\hat{S}_x + g_{yz}\hat{S}_y + g_{zz}\hat{S}_z). \qquad (2)$$

In the case of small anisotropy, $\Delta g_{1,2,3} \ll g$, the nondiagonal terms g_{xz}, g_{yz} can be neglected in first approximation, and the component g_{zz} of the tensor g can be represented in the form

$$g_{zz}(\vartheta, \varphi, \psi) = g + \Delta g_{zz}(\vartheta, \varphi, \psi), \qquad (3)$$

where ϑ, φ, ψ are the Euler angles that determine the orientation of the principal magnetic axes of the particle relative to a fixed coordinate system.

The quantity $\Delta g_{zz}(\vartheta, \varphi, \psi)$ is calculated from

$$\Delta g_{zz}(\vartheta, \varphi, \psi) = (\mathbf{A}^{-1}\mathbf{\Delta g}\mathbf{A})_{zz},$$

where $\mathbf{\Delta g}$ is the anisotropic part of the tensor in the system of the principal axes and $\mathbf{A}$ is the matrix of the rotation of the principal axes of the particle relative to the coordinate system; we get as the result

$$\Delta g_{zz} = \Delta g_1 \sin^2\vartheta \sin^2\psi + \Delta g_2 \sin^2\vartheta \cos^2\psi + \Delta g_3 \cos^2\vartheta. \quad (4)$$

We now find as the expression for the resonance frequency

$$\omega_0^* = \mu_0 g_{zz} H_0/\hbar = \omega_0 + \frac{\mu_0 H_0}{\hbar} \Delta g_{zz}(\vartheta, \varphi, \psi), \quad (5)$$

where $\omega_0 = \mu_0 g H_0/\hbar$.

For comparison with the experimental data it is convenient to express this result in field units:

$$H_0^* = H_0 + \Delta H_1 \sin^2\vartheta \sin^2\psi + \Delta H_2 \sin^2\vartheta \cos^2\psi + \Delta H_3 \cos^2\vartheta = H_0 + \Delta H_z, \quad (6)$$

where $\Delta H_i = \Delta g_i H_0/g$. The values of the anisotropy constants ΔH_i can be determined from the displacement of the maxima of the resonance absorption lines for three independent rotations of a single crystal around its principal axes ($\vartheta = \pi/2$, $\psi = 0$, $\psi = \pi/2$) in the plane perpendicular to the direction of the external magnetic field.

3. On the assumption that the orientations of the individual particles are randomly distributed in space, the total shape of the absorption line can be found by averaging the spectra of the individual particles over all possible directions:

$$J(H - H_0) = \frac{1}{\pi} \int_0^{\pi/2} \sin\vartheta \, d\vartheta \int_0^{\pi} d\psi I(H - H_0^*), \quad (7)$$

where $I(H - H_0^*)$ is the function, normalized to unity, for the line shape of the individual particle, which can be represented in the form

$$I(H - H_0^*) = \frac{1}{2\pi} \int_{-\infty}^{+\infty} G(t) \exp\{i(H - H_0^*)t\} \, dt. \quad (8)$$

Then

$$J(H - H_0) = \frac{1}{2\pi} \int_{-\infty}^{+\infty} \mathfrak{G}(t) \exp\{i(H - H_0)t\} \, dt, \quad (9)$$

$$\mathfrak{G}(t) = \frac{1}{\pi} \int_0^{\pi/2} \sin\vartheta \, d\vartheta \int_0^{\pi} d\psi \, G(t) \exp\{i(H - H_0^*)t\} \, dt. \quad (10)$$

To find the moments of the line shape we expand the expression for the function $G(t)$, which is obtained from Eq. (8) by the inverse Fourier transformation, in a power series in t. Comparing the coefficients of identical powers of t, we get

$$M_n = \int_{-\infty}^{+\infty} I(x) x^n \, dx = (-i)^n \frac{d^n}{dt^n} G(0). \quad (11)$$

Here M_n are the moments of the absorption line for the individual particle relative to the field H_0^*. In a similar way we can determine the moments of the total absorption curve relative to the field H_0

$$\mathfrak{M}_n = \int_{-\infty}^{+\infty} J(x) x^n \, dx = (-i)^n \frac{d^n}{dt^n} \mathfrak{G}(0). \quad (12)$$

Assuming that the absorption line for the individual particle is symmetrical and that its shape does not depend on the orientation, by using Eqs. (10) and (12) we find

$$\mathfrak{M}_0 = 1, \quad \mathfrak{M}_1 = 0, \quad \mathfrak{M}_2 = M_2 + \overline{\Delta H_z^2},$$

$$\mathfrak{M}_3 = -\overline{\Delta H_z^3}, \quad \mathfrak{M}_4 = M_4 + 6\overline{\Delta H_z^2} M_2 + \overline{\Delta H_z^4}, \quad (13)$$

where

$$\overline{\Delta H_z^n} = \frac{1}{4\pi} \int (\Delta H_z)^n \sin\vartheta \, d\vartheta \, d\varphi. \quad (14)$$

We have

$$\begin{aligned}
\overline{\Delta H_z^2} &= \tfrac{1}{5}(\Delta H_1^2 + \Delta H_2^2 + \Delta H_3^2) \\
&\quad + \tfrac{2}{15}(\Delta H_1 \Delta H_2 + \Delta H_1 \Delta H_3 + \Delta H_2 \Delta H_3), \\
\overline{\Delta H_z^3} &= \tfrac{1}{7}(\Delta H_1^3 + \Delta H_2^3 + \Delta H_3^3) + \tfrac{3}{35}(\Delta H_1^2 \Delta H_2 + \Delta H_1 \Delta H_2^2 \\
&\quad + \Delta H_1^2 \Delta H_3 + \Delta H_3^2 \Delta H_1 \\
&\quad + \Delta H_2^2 \Delta H_3 + \Delta H_2 \Delta H_3^2) + \tfrac{2}{35}(\Delta H_1 \Delta H_2 \Delta H_3), \\
\overline{\Delta H_z^4} &= \tfrac{1}{9}(\Delta H_1^4 + \Delta H_2^4 + \Delta H_3^4) + \tfrac{4}{63}(\Delta H_3^3 \Delta H_1 \\
&\quad + \Delta H_3 \Delta H_1^3 + \Delta H_2^3 \Delta H_1 + \Delta H_1^3 \Delta H_2 + \Delta H_2^3 \Delta H_3 \\
&\quad + \Delta H_3^3 \Delta H_2) + \tfrac{2}{35}(\Delta H_1 \Delta H_2 \Delta H_3^2 \\
&\quad + \Delta H_1 \Delta H_2^2 \Delta H_3 + \Delta H_1^2 \Delta H_2 \Delta H_3). \quad (15)
\end{aligned}$$

The presence of odd moments ($\mathfrak{M}_3 \neq 0$) is evidence of the unsymmetrical character of the total absorption curve.

To obtain the function for the shape of the total absorption curve we assume that the absorption curve of the individual particle has the Lorentz shape:

$$I(H - H_0^*) = \frac{1}{\pi \Delta H} \left[\left(\frac{H - H_0^*}{\Delta H} \right)^2 + 1 \right]^{-1}, \quad (16)$$

where ΔH is the half-width of the line.

Substituting this expression in Eq. (7) and integrating over $d\vartheta$, we get

$$J(H - H_0) = \frac{1}{2\pi^2 \Delta H} \int_0^{\pi} d\psi \Bigl\{ \frac{1}{\gamma} \Bigl[\frac{1}{2\alpha} \ln \frac{\beta + \gamma + \alpha}{\beta + \gamma - \alpha} + \frac{1}{p} \Bigl(\tan^{-1} \frac{2\beta + \alpha}{p} + \tan^{-1} \frac{2\beta - \alpha}{p} \Bigr) \Bigr\}, \quad (17)$$

$$\alpha = \left[2\beta\left(\gamma - \frac{H-H_0}{\Delta H} + \beta + \frac{2}{3}\,\frac{\Delta H_3 - \Delta H_1}{\Delta H}\right)\right]^{1/2},$$

$$\gamma = \pm\left[1 + \left(\frac{H-H_0}{\Delta H} - \beta - \frac{2}{3}\,\frac{\Delta H_3 - \Delta H_1}{\Delta H}\right)^2\right]^{1/2},$$

$$p = \sqrt{4\beta\gamma - \alpha^2}, \qquad \beta = \frac{\Delta H_1 - \Delta H_3 + (\Delta H_1 - \Delta H_2)\cos^2\psi}{\Delta H}. \tag{18}$$

The upper sign is for $\beta > 0$ and the lower for $\beta < 0$. In the general case the further integration can be accomplished only by numerical methods.

To determine the function for the shape of the total absorption curve when the anisotropy of the hyperfine structure constant is taken into account we must make the replacements

$$H_0 \to H_0 + Am, \quad \Delta H_i \to \Delta H_i + \Delta A_i m \tag{19}$$

in the expression (17). Thus in this case the change of intensity of the individual components of the hyperfine structure follows a law analogous to that for the change of the intensity of the absorption line owing to the existence of an anisotropy of the g factors of the individual particles.

From the results given in the paper of Kikuchi and Cohen,[7] which were obtained for a single crystal of the organic free radical carbazyl, it follows that for rotations of the crystal around the magnetic symmetry axes in a field $H_0 = 8000$ oe

$$\Delta H = 0.25 \text{ oe}, \qquad \Delta H_1 - \Delta H_2 = -2.4 \text{ oe},$$

$$\Delta H_1 - \Delta H_3 = 3.6 \text{ oe}, \qquad \Delta H_2 - \Delta H_3 = 6.0 \text{ oe}, \tag{20}$$

and the hyperfine structure is not manifested here. Unfortunately from the paper in question we cannot establish the direction of the axes with sufficient accuracy.

The results of a numerical integration of Eq. (17) are shown in Fig. 1.

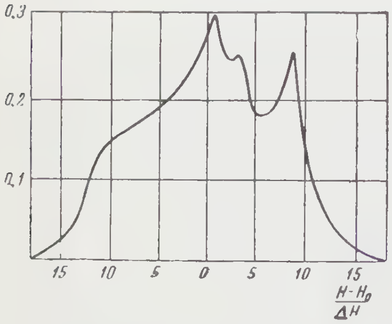

FIG. 1. The function for the shape of the total absorption curve in the case of triaxial anisotropy of the g factor. The numerical integration was performed with the values (20); the quantity plotted as ordinate is $J(H-H_0)\Delta H \cdot 5$.

A small difference in the magnetic properties of the individual particles, caused by defects of the crystal lattice,[2] can lead to a smoothing out of the shape of the total curve. This is evidently the explanation of the absence of distinct maxima of this sort on the experimental curves for polycrystalline specimens of free radicals.

Observations of the resonance absorption of complicated complex ions Cu^{++} in undercooled solutions actually give curves analogous to that shown in Fig. 1,[10] owing to the identity of the individual molecules.

In the case of axial symmetry $\Delta H_1 = \Delta H_2 = -\Delta H_3/2$. Then after integrating the expression (17) we get

$$J(H-H_0) = \frac{1}{2\pi\Delta H\gamma}\left[\frac{1}{2\alpha}\ln\frac{\beta+\gamma+\alpha}{\beta+\gamma-\alpha} + \frac{1}{p}\left(\tan^{-1}\frac{2\beta+\alpha}{p} + \tan^{-1}\frac{2\beta-\alpha}{p}\right)\right], \tag{21}$$

where α, β, γ are defined in Eq. (18) and $\beta = 3\Delta H_1/\Delta H$. Curves drawn for various values of β are shown in Fig. 2. This shape of the absorption curves is characteristic of glasses, undercooled solutions, and so on, whose paramagnetic complexes possess symmetries close to the axial type.[1,3,4]

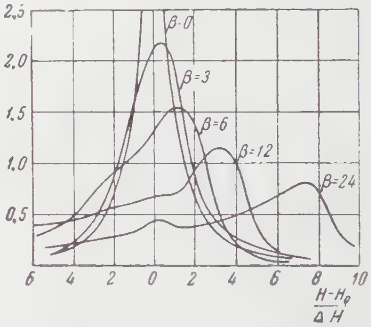

FIG. 2. The function for the shape of the total absorption curve in the case of uniaxial anisotropy of the g factor, for various values of the parameter $\beta = 3\Delta H_1/\Delta H$; the quantity plotted as ordinate is $J(H-H_0)\Delta H \cdot 10$.

Both in the case of uniaxial anisotropy and in that of triaxial anisotropy the position of the main maximum is shifted relative to the position that corresponds to weak fields.

In strong fields the absorption curve has supplementary maxima in addition to the main maximum (Fig. 2). In weak fields the curve has a single maximum, whose position corresponds to the isotropic part of the g factor.

4. The widths and shapes of the resonance absorption curves for the free organic radicals $(XC_6H_4)\ (C_6H_5)N - NC_6H_2(NO_2)_3$, DPPH (X = H), ClPPH (X = Cl), and carbazyl $(C_6H_4)(C_6H_4)N - NC_6H_2(NO_2)_3$,[11] in powder form, have been studied in the low-frequency range, 9 Mc to 800 Mc, by means of the method described in references 12 and 13.

The width and shape of the absorption curve at frequencies 10,000 and 36,000 Mc were determined by means of videospectroscopes with resonators of the pass-band type. The absorption curves were photographed from the screen of the oscilloscope. The magnetic field was modulated at low frequency and amplitudes up to 200 oe. Nuclear resonance was used for the measurement and stabilization of the magnetic field.

The specimen was placed in the central part of a resonator oscillating in the H_{011} mode and could be turned around one of the axes.

The results of the measurements showed that the width and shape of the absorption curve in the low-frequency region is practically independent of the strength of the constant field, and in weak fields, for all the radicals studied, the width is the same as that of the absorption line of an individual single crystal.

It can be seen from the curves of Fig. 2 that as the field is increased the line width increases; at the same time the curve becomes more asymmetrical. A similar phenomenon is also observed in the case of triaxial anisotropy.

The experimental dependence of the line width on the constant magnetic field for a number of organic free radicals, which is shown in Fig. 3, can be satisfactorily explained on the basis of the anisotropy of the g factors of the individual single crystals.

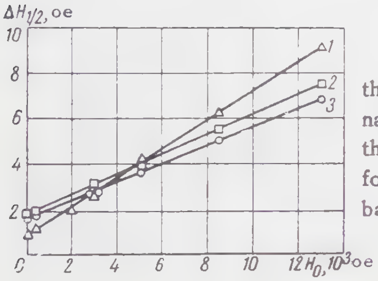

FIG. 3. Dependence of the half-width of the resonance absorption curve on the constant magnetic field for free radicals: 1 – carbazyl, 2 – ClPPH, 3 – DPPH.

Thus in the analysis of the data on the width and shape of the absorption lines in powders, glasses, solid solutions, undercooled solutions, etc., in the case of strong fields ($H_0 > 1000$ oe) one must take into account the fact that a considerable part of the line width is caused by the anisotropy of the g factor. But the considerations we have given about the effect of the anisotropy of the g factor of the individual particle on the shape of the line are not always taken into account. For example, in references 14 and 15 analyses of the shape of the absorption line in strong fields for powders of free radicals are made the basis of unconvincing deductions about the effect of various substituted atoms on the size of the exchange interactions.

In a paper by Singer and Kikuchi[8] it has been found that with decrease of the temperature there is an increase of the absorption line width and of the anisotropy constants in an individual single crystal of DPPH, and also an increase of the absorption line width for a polycrystalline specimen in a strong field (8000 oe). The temperature dependence of the absorption line in the powder also gives evidence of the important part played by the anisotropy of the g factor of the individual particles.

---

[1] Ghosh, Gordy, and Hill, Phys. Rev. **96**, 36 (1954).

[2] G. Berthet, Ann. de phys. **3**, 629 (1958).

[3] Gordy, Miyagawa, Watabe, and Wilbur, Proc. Natl. Acad. Sci. U.S. **44**, 613 (1958).

[4] R. H. Sands, Phys. Rev. **99**, 1222 (1955).

[5] Searl, Smith, and Wyard, Proc. Phys. Soc. **74**, 491 (1959).

[6] Hutchison, Pastor, and Kowalsky, J. Chem. Phys. **20**, 534 (1952).

[7] C. Kikuchi and V. W. Cohen, Phys. Rev. **93**, 394 (1954).

[8] L. S. Singer and C. Kikuchi, J. Chem. Phys. **23**, 1738 (1955).

[9] M. Sternberg, Compt. rend. **240**, 990 (1955).

[10] A. I. Rivkind, Report at Conference on Paramagnetic Resonance (in Russian), Kazan', 1959.

[11] Matevosyan, Postovskiĭ, and Chirkov, Журнал общей химии (J. of Gen. Chem.) **29**, 858 (1959).

[12] A. K. Chirkov and R. O. Matevosyan, JETP **33**, 1053 (1957), Soviet Phys. JETP **6**, 811 (1958).

[13] A. K. Chirkov and A. A. Kokin, JETP **35**, 50 (1958), Soviet Phys. JETP **8**, 36 (1959).

[14] Walter, Codrington, D'Adamo, and Torrey, J. Chem. Phys. **25**, 319 (1956).

[15] R. G. Bennett and A. Henglein, J. Chem. Phys. **30**, 1117 (1959).

Translated by W. H. Furry
253

SOVIET PHYSICS JETP VOLUME 12, NUMBER 5 MAY, 1961

ON THE NATURE OF THE FIRST EXCITED STATES OF EVEN-EVEN SPHERICAL NUCLEI

S. T. BELYAEV

Submitted to JETP editor June 21, 1960

J. Exptl. Theoret. Phys. (U.S.S.R.) 39, 1387-1400 (November, 1960)

Possible collective excitations are investigated, and their microscopic structure is analyzed. It is shown that the excitations are bound states of the particle-particle or particle-hole types, depending on the interaction. The quadrupole excitations correspond to the excitations previously found by macroscopic study. The significance of the polarizability of the core is investigated.

1. INTRODUCTION

THE spectra of the excited states of even-even undeformed nuclei are subject to definite laws.[1] The first excited state is 2^+, and its energy increases monotonically as the closed shell is approached.* The probability of the E2 transition to the ground state decreases thereby monotonically, and its magnitude exceeds considerably the single-particle value. The second excited state (4^+, 2^+, or 0^+) lies approximately twice as high, and in many nuclei a nearby doublet is found (4^+, 2^+), and in some a triplet (4^+, 2^+, 0^+). Definite laws have also been established for electromagnetic transitions from these states.

The presence of these laws suggests that the excitations are collective. The model of hydrodynamic surface oscillations is inconsistent, since the theoretical value of the mass coefficient must be increased by several times 10 to explain the experimental values of the energy levels. In addition, this model does not explain the strong dependence of the vibrational energy (of the first 2^+ level) on the filling of the upper shell.

The author has shown earlier,[2] that if the pair correlation of the nucleons and their "quadrupole" interaction are taken into account, a new form of oscillation of the spherical nucleus arises, which is essentially non-hydrodynamic in nature. These "oscillations" are connected essentially with the variation of the configurations of the internal nucleons, and can be realized even if the nuclear surface is fixed. The energies of the obtained oscillations, the mass coefficient, and their dependence on the filling of the upper shell are in qualitative agreement with experimental data.

In the present article we shall consider the microscopic structure of these excitations, so that their nature can be explained in greater detail and the connection with the single-particle description established. To ascertain whether it is legitimate to take into account only the interaction that causes pairing and the quadrupole interaction of the nucleons, we investigate the possible collective excitations for an arbitrary form of interaction. The influence of the polarizability of the core on the effective interaction between the nucleons is also established.

With a view towards explaining the principal questions on the nature of collective excitations and the conditions under which they arise, we confine ourselves to an examination of the particular case of an unfilled shell with one j level. The results obtained, however, are valid qualitatively in the general case, too.

2. MACROSCOPIC DESCRIPTION OF THE EXCITATIONS

Let us consider briefly the macroscopic picture of quadrupole oscillations,[2] which will help to establish the connection with the microscopic description. We shall consider nucleons of one kind on the subshell $j \gg 1$. The Hamiltonian in the second quantization has the form

$$H = H_0 + H_{int} = \sum_m (\varepsilon - \lambda)\, a_m^+ a_m + \tfrac{1}{2} \sum_m \langle m_1 m_2 | V | m_2' m_1' \rangle\, a_{m_1}^+ a_{m_2}^+ a_{m_2'} a_{m_1'}, \qquad (2.1)$$

where a_m^+ and a_m are the operators of creation and annihilation of the nucleon in the state $|jm\rangle$, and the chemical potential λ has been introduced, as usual, to eliminate difficulties with the determination of the number of particles in the system.

Let us calculate, first, the nucleon interaction that describes the pairing of two particles in a state with total momentum J = 0:

$$H_{int}'' = -\tfrac{1}{4} G \sum_{mm'} (-1)^{j+m} a_m^+ a_{-m}^+ (-1)^{j+m'} a_{-m'} a_{m'}, \qquad (2.2)$$

---

*A similar behavior, but to a lesser extent, is observed also for certain subshells.

where G is the interaction constant. The Hamiltonian (2.2) describes the interaction of the pair in the state $J = 0$. The particles do not interact in any other state. Therefore, the breaking of a pair with $J = 0$ leads to the same excitation energy, independently of the final state of the "broken" pair. The real interaction naturally removes this degeneracy, but qualitatively such an excitation picture remains correct.

Along with the "single-particle" excitations, connected with the breaking of one pair, there exist excitations of the collective type, in which a slight realignment of all the pairs takes place. Here, strictly speaking, the system is no longer an aggregate of independent pairs, and it must be described by certain "collective" parameters. We choose as such a parameter the total quadrupole moment Q.* Corresponding to the ground state is $Q = 0$, and the collective excited states of a given type correspond to a certain realignment of the single-particle states, and the appearance of a nonvanishing Q. Assuming an adiabetic variation of the collective parameter Q, we find first the energy of the system for a fixed value of Q, and then consider small oscillations in Q.

An important role is played in the indicated collective excitations by the interactions between particles of the self-consistent field type. We shall take into account the part of such an interaction, connected with the quadrupole asymmetry ("quadrupole interaction"):

$$H'_{int} = -\tfrac{1}{2}\varkappa \sum_{mm'} q_m q_{m'} a^+_m a^+_{m'} a_{m'} a_m, \qquad (2.3)$$

where $q_m = \langle jm|\hat{q}\,|jm\rangle$ is the matrix element of the single-particle quadrupole moment, and κ is the interaction parameter.

To find the ground state of the system for a fixed value of Q, it is convenient to take account of the additional condition $Q = \text{const}$ by the method of Lagrange multipliers, adding to the Hamiltonian a term $-\sigma\hat{Q}$ ($\hat{Q} = \Sigma q_m a_m a^+_m a_m$ is the quadrupole-moment operator), and determine σ from the condition $\langle\hat{Q}\rangle = Q$.

Thus, let us consider the auxiliary Hamiltonian

$$\bar{H} = H - \sigma\hat{Q} = \sum_m (\varepsilon - \lambda - \sigma q_m)\, a^+_m a_m + H''_{int} + H'_{int}. \qquad (2.4)$$

Let us carry out a canonical transformation to new Fermi operators[3]

$$\alpha_m = U_m a_m - (-1)^{j+m} V_m a^+_{-m}, \qquad U_m^2 + V_m^2 = 1 \quad (2.5)$$

and require that $\bar{H}$ be a minimum for the ground state $\Psi_0(Q)$, defined by the condition $\alpha_m \Psi_0(Q) = 0$ ("vacuum" in the quasi-particles). We obtain here an equation for U_m and V_m

$$(\varepsilon - \lambda - \tilde{\sigma} q_m)\, 2U_m V_m - \Delta\,(U_m^2 - V_m^2) = 0, \qquad (2.6)$$

where

$$\Delta = \tfrac{1}{2} G \sum_m U_m V_m, \qquad Q = \sum_m q_m V_m^2, \qquad \tilde{\sigma} = \sigma + \varkappa Q. \quad (2.7)$$

Expressing U_m and V_m in terms of Δ and using the connection between the chemical potential λ and the total number of particles ($N = \Sigma V_m^2$), we obtain a system of equations for the determination of Δ and λ:

$$\frac{G}{4}\sum_m \frac{1}{[\Delta^2 + (\varepsilon - \lambda - \tilde{\sigma} q_m)^2]^{1/2}} = 1,$$

$$\sum_m \frac{\varepsilon - \lambda - \tilde{\sigma} q_m}{[\Delta^2 + (\varepsilon - \lambda - \tilde{\sigma} q_m)^2]^{1/2}} = 2\,(\Omega - N), \qquad (2.8)$$

where $2\Omega = 2j + 1$ is the total number of states in the sub-shell.

The energy of the ground state of the system, W, is defined as the average value of the initial Hamiltonian $H = H_0 + H'_{int} + H''_{int}$ in the state $\Psi_0(Q)$. As a result we obtain

$$W = \langle \Psi_0(Q),\ H\Psi_0(Q)\rangle = (\varepsilon - \lambda)\,N - \tfrac{1}{2}\varkappa Q^2 - \Delta^2/G. \qquad (2.9)$$

For the energy of the quasi-particle we obtain analogously

$$E_m = \langle \Psi_0(Q),\ \alpha_m H \alpha^+_m\ \Psi_0(Q)\rangle - W = \sqrt{\Delta^2 + (\varepsilon - \lambda - \tilde{\sigma} q_m)^2}. \qquad (2.10)$$

For small σ the solution (2.8) for Δ, U_m, and V_m is of the form

$$\Delta \approx \tfrac{1}{2}\,\Omega\, G \sin\vartheta \left\{1 - \frac{\tilde{\sigma}^2}{(\Omega G)^2}\frac{1}{\Omega}\sum_m q_m^2\right\}, \qquad (2.11)$$

$$U_m \approx U - V\frac{\tilde{\sigma}}{\Omega G}\, q_m \sin\vartheta, \quad V_m = V + U\frac{\tilde{\sigma}}{\Omega G}\, q_m \sin\vartheta, \quad (2.12)$$

where

$$V = (N/2\Omega)^{1/2}, \quad U = (1 - N/2\Omega)^{1/2}, \quad \sin\vartheta = 2UV. \quad (2.13)$$

(The magnitude of $\sin\vartheta$ characterizes the degree of filling the shell, and varies from unity for a half-filled shell, to 0 on the edge of the shell.) The parameter $\tilde{\sigma}$ is connected with the quadrupole moment:

$$Q = \sum_m q_m V_m^2 = \frac{\tilde{\sigma}}{\Omega G}\sin^2\vartheta \sum_m q_m^2. \qquad (2.14)$$

The wave function of state with a non vanishing Q and $\Psi_0(Q)$ can be expressed in terms of the "spherical-nucleus" functions $\Psi(0)$. For this purpose, we introduce the quasi-particles for the spherical nucleus $\alpha_m^{(0)}$, defined from (2.5) with

---

*We have in mind the quadrupole moment of the mass, not of the charge.

$U_m = U$ and $V_m = V$. It is easy to see that the following relation holds

$$\alpha_m \approx (UU_m + VV_m)\,\alpha_m^{(0)} + (VU_m - UV_m)(-1)^{j+m}\,\alpha_{-m}^{(0)+},$$

from which it follows that

$$\Psi_0(Q) = \exp\left\{\frac{1}{2}\sum_m \frac{UV_m - VU_m}{UU_m + VV_m}(-1)^{j+m}\;\alpha_m^{(0)+}\;\alpha_{-m}^{(0)+}\right\}\Psi_0(0),$$

and for small Q

$$\Psi_0(Q) = \exp\Big\{Q\left(2\sin\vartheta\sum q_m^2\right)^{-1} \times\sum_m(-1)^{j+m}q_m\,\alpha_m^{(0)+}\alpha_{-m}^{(0)+}\Big\}\,\Psi_0(0). \qquad (2.15)$$

For the energy in the ground state, in the same approximation of small Q, we obtain from (2.9), (2.11), and (2.14)

$$W(Q) - W(0) = \tfrac{1}{2}\,\Omega G\,(1 - \Theta_0^{-1}\sin^2\vartheta)\,Q^2\,(\sin^2\vartheta\sum q_m^2)^{-1} \equiv \tfrac{1}{2}\,C_Q\,Q^2, \qquad (2.16)$$

where

$$\frac{1}{\Theta_0} = \frac{\varkappa}{\Omega G}\sum_m q_m^2.$$

(The quantity Θ_0 defines the critical filling at which the spherical shape of the nucleus becomes unstable.) Expression (2.16) determines the dependence of the energy of the system on the collective parameter Q, i.e., it is the "potential energy" of the collective motion. The total Hamiltonian of the collective motion, for small values of Q, has the form

$$H_Q = \tfrac{1}{2}\,B_Q\,\dot{Q}^2 + \tfrac{1}{2}\,C_Q\,Q^2,$$

where the "mass coefficient" and B_Q is determined by the following expression ($\hbar = 1$):

$$B_Q = 2\sum_{i\neq 0}\left|\left\langle\Psi_i,\ \frac{\partial}{\partial Q}\Psi_0\right\rangle\right|^2\Big/(W_i - W_0). \qquad (2.17)$$

From (2.15) we obtain

$$\left[\frac{\partial}{\partial Q}\Psi_0(Q)\right]_{Q=0} = \left(2\sin\vartheta\sum q_m^2\right)^{-1}\sum_m(-1)^{j+m}q_m\,\alpha_m^{(0)+}\,\alpha_{-m}^{(0)+}\;\Psi_0(0),$$

from which it is clearly seen that the operator $\partial/\partial Q$ transfers the system to a state with 2 quasiparticles; therefore $W_i - W_0 = 2E = \Omega G$. After simple transformations we obtain

$$B_Q = (\Omega G\sin^2\vartheta\sum q_m^2)^{-1}. \qquad (2.18)$$

For the oscillation energy we obtain, according to (2.6) and (2.18),

$$\omega = \sqrt{C_Q/B_Q} = 2E\sqrt{1 - \Theta_0^{-1}\sin^2\vartheta}\,. \qquad (2.19)$$

As follows from (2.19), the energy of the resultant collective excitation is actually less than the energy required to break the pair, $2E = \Omega G$ ("single-particle" excitation), and ω decreases monotonically as the filling is increased ($\sin^2\vartheta \to 1$).

3. MICROSCOPIC ANALYSIS OF QUADRUPOLE EXCITATIONS

In this section we consider the same problem by a different method, which will enable us to establish the microscopic structure of the resultant excitations. Where possible we shall emphasize the analogy with infinite systems, for which the character of the excitations has been sufficiently well investigated.

As is well known, the lower excited states of a many-particle system can be approximately described as an aggregate of elementary excitations—quasi-particles. In an ideal degenerate Fermi gas, the quasi-particles are holes below the Fermi level and particles above it. The switching on of the interaction leads, firstly, to a change of the effective mass of the quasi-particles, and secondly to the appearance of an interaction between the quasi-particles themselves. If the latter does not lead to the appearance of bound states, but only to scattering processes, it can usually be neglected, since the scattering of quasi-particles yields only corrections proportional to Ω^{-1} (Ω is the volume of the system).

In the case when bound states become possible, new "collective" excitations appear. Thus, in the repulsion between particles, new bound states of the particle and hole at the Fermi boundary can occur in the Fermi system, and this leads to a new type of excitation — zero sound.[4] It can be stated that an excited state with two quasi-particles is unstable under the formation of a bound pair of these quasi-particles. In the case of attraction, the properties of the Fermi system change more radically; bound states become possible between particles near the Fermi surface, and this leads to instabilities even in the ground state relative to pairing between particles, and the sharp Fermi boundary becomes diffuse. The quasi-particles near the new ground state are superpositions of holes and particles.

One multiply-degenerate level ($j \gg 1$) is equivalent to an infinitesimally thin spherical layer below the diffuse Fermi level. The number of states $2\Omega = 2j + 1$ plays the role of the "volume" of the system. According to the foregoing, solving the problem of the interacting nucleons at this

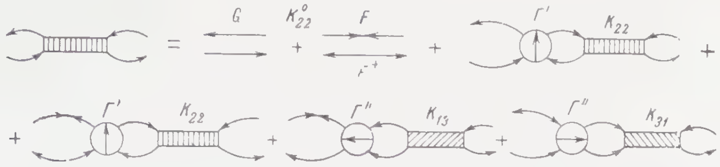

FIG. 1

level, accurate to Ω^{-1}, denotes firstly finding the quasi-particles, and secondly finding the "bound states." (In a system of finite dimensions, the concept of a bound state is rather arbitrary, and we shall use it to denote strongly correlated states.)

To investigate the excitations of a many-particle system, it is best to use the method of Green's functions.[5] Single-particle excitations (the spectrum of quasi-particles) are described by single-particle functions. In the presence of pairing in the ground state, it is necessary to use three functions (see Gor'kov[6]):

$$G(m;\ t_1-t_2)=-i\langle T\{a_m(t_1)\,\overset{+}{a}_m(t_2)\}\rangle,$$

$$F(m;\ t_1-t_2)=-ie^{i\lambda(t_1+t_2)}\langle T\{a_m(t_1)\,a_{-m}(t_2)\}\rangle,$$

$$F^+(m;\ t_1-t_2)=-ie^{-i\lambda(t_1+t_2)}\langle T\{\overset{+}{a}_m(t_1)\,\overset{+}{a}_{-m}(t_2)\}\rangle, \qquad (3.1)$$

which in our case (spherical symmetry) have the following Fourier transforms

$$G(m;\ \varepsilon)=\frac{U^2}{\varepsilon-E+i\delta}+\frac{V^2}{\varepsilon+E-i\delta} \qquad (\delta\to+0),$$

$$F(m;\ \varepsilon)=-F^+(m;\ \varepsilon)$$

$$=-(-1)^{j+m}UV\left(\frac{1}{\varepsilon-E+i\delta}-\frac{1}{\varepsilon+E-i\delta}\right), \qquad (3.2)$$

when U and V are as defined in (2.13) while E is the energy of the quasi-particle (in the first approximation, its value is ΩG/2).

To investigate the collective excitations, it is necessary to consider two-particle Green's functions. In the presence of pairing we cannot in general write down a closed equation for a single function, and we must introduce three different functions, for example

$$K_{22}=\langle T\{a_1\overset{+}{a}_2 a_3\overset{+}{a}_4\}\rangle, \qquad K_{13}=\langle T\{\overset{+}{a}_1\overset{+}{a}_2\, a_3\overset{+}{a}_4\}\rangle,$$

$$K_{31}=\langle T\{a_1a_2a_3\overset{+}{a}_4\}\rangle. \qquad (3.3)$$

Thus, the equation for K_{22} has the form (see Fig. 1)

$$K_{22}(12;\,34)=K_{22}^0(12;\,34)+i\{G(1;\,5)\,G(7;\,2)$$

$$+F(17)\,F^+(25)\}\,\Gamma'(56;\,78)\,K_{22}(86;\,34)$$

$$+iF(17)\,G(8;\,2)\,\Gamma''(56;\,78)\,K_{13}(56;\,34)$$

$$+iG(1;\,5)\,F^+(26)\,\Gamma''(56;\,78)\,K_{31}(87;\,34) \qquad (3.4)$$

(integration over repeated indices 5 — 8 is implied). Here Γ is a compact (irreducible) fourpole, which in the first approximation is equal to the corresponding interaction matrix element (see 2.1):

$$2\Gamma_0''(12;\ 2'1')=\Gamma_0'(12;\,2'1')=\langle 12|V|2'1'\rangle$$

$$-\langle 12|V|1'2'\rangle, \qquad (3.5)$$

In higher approximations in Γ it is necessary to distinguish between directions of "irreducibility" (Fig. 2). The aggregate of the graphs, which is irreducible in the direction of motion of the two particles, is denoted by Γ″, and the aggregate which is irreducible in the particle — hole direction is denoted by Γ′.

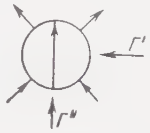

FIG. 2

In the right half of (3.4) there are contained, along with K_{22}, two other functions, so that in general it is necessary to consider a system of three equations. It will prove advantageous to uncouple the functions K. Assuming that $t_1,\ t_2 > t_3,\ t_4$, we write

$$K_{22}=\sum_s\varphi_s(12)\,\tilde{\varphi}_s(34); \qquad K_{31}=\sum_s\chi_s(12)\,\tilde{\varphi}_s(34),$$

$$K_{13}=\sum_s\bar{\chi}_s(12)\,\tilde{\varphi}_s(34),$$

where

$$\varphi_s(12)=\langle 0|T\{a_1\overset{+}{a}_2\}|s\rangle, \qquad \tilde{\varphi}_s(34)=\langle s|T\{a_3\overset{+}{a}_4\}|0\rangle,$$

$$\chi_s(12)=\langle 0|T\{a_1a_2\}|s\rangle, \qquad \bar{\chi}_s(12)=\langle 0|T\{\overset{+}{a}_1\,\overset{+}{a}_2\}|s\rangle. \qquad (3.6)$$

In the investigation of bound states we can discard the inhomogeneities in the equations for K [the term K_{22}^0 in (3.4)].[7,5] Then, using the fact that $\tilde{\varphi}_s(34)$ is contained in each term, we can "divide" all the equations by $\tilde{\varphi}_s(34)$. As a result we obtain a system of homogeneous equations for φ_s, χ_s, and $\bar{\chi}_s$.

For further simplification, we shall assume that Γ describes a non-retarded interaction.* Then both times in the functions φ_s, χ_s, and $\bar{\chi}_s$ can be taken to be equal ($t_1 - t_2 \to -0$), so that the problem reduces to a determination of the three functions

---

*The time delay of the interaction of the nucleons in the nucleus is $\sim\varepsilon_F^{-1}$ (ε_F is the Fermi boundary energy), which is much shorter than the times ω^{-1} of interest to us.

$$\varphi_{\omega\mu}(m) = \langle 0 | \overset{+}{a}_m a_{m+\mu} | \omega\mu\rangle, \quad \chi_{\omega\mu}(m) = \langle 0 | a_{-m} a_{m+\mu} | \omega\mu\rangle,$$
$$\overline{\chi}_{\omega\mu}(m) = \langle 0 | a_m^{+} a_{-m-\mu}^{+} | \omega\mu\rangle, \qquad (3.7)$$

where the state $|s\rangle$ is characterized by an energy ω, and a momentum projection μ. The system of equations for (3.7) has the form

$$(4E^2 - \omega^2)\varphi_{\omega\mu}(m) = -2E\sin^2\vartheta \sum_{m'} \Gamma'_{\mu}(m;\, m')\varphi_{\omega\mu}(m')$$
$$- E\sin\vartheta\cos\vartheta \sum_{m'} \Gamma''_{\mu}(m;\, m')\chi^{(+)}_{\omega\mu}(m')$$
$$- \tfrac{1}{2}\omega\sin\vartheta \sum_{m'} \Gamma''_{\mu}(m;\, m')\chi^{(-)}_{\omega\mu}(m'), \qquad (3.8a)$$

$$(4E^2 - \omega^2)\chi^{(+)}_{\omega\mu}(m) = -2E\cos^2\vartheta \sum_{m'} \Gamma''_{\mu}(m;\, m')\chi^{(+)}_{\omega\mu}(m')$$
$$- \omega\cos\vartheta \sum_{m'} \Gamma''_{\mu}(m;\, m')\chi^{(-)}_{\omega\mu}(m')$$
$$- 4E\sin\vartheta\cos\vartheta \sum_{m'} \Gamma'_{\mu}(m;\, m')\varphi_{\omega\mu}(m'),$$

$$(4E^2 - \omega^2)\chi^{(-)}_{\omega\mu}(m) = -2E \sum_{m'} \Gamma''_{\mu}(m;\, m')\chi^{(-)}_{\omega\mu}(m')$$
$$- \omega\cos\vartheta \sum_{m'} \Gamma''_{\mu}(m;\, m')\chi^{(+)}_{\omega\mu}(m')$$
$$- 2\omega\sin\vartheta \sum_{m'} \Gamma'_{\mu}(m;\, m')\varphi_{\omega\mu}(m'), \qquad (3.8b)$$

where instead of χ and $\bar{\chi}$ we introduce their linear combinations

$$\chi^{(\pm)}_{\omega\mu}(m) = (-1)^{j+m}\{\chi_{\omega\mu}(m) \pm (-1)^{\mu}\overline{\chi}_{\omega\mu}(m)\} \qquad (3.9)$$

and for the sake of abbreviation we put

$$\Gamma'_{\mu}(m;\, m') = \tfrac{1}{2}\{\Gamma'(m+\mu, m';\, m'+\mu, m)$$
$$+ (-1)^{\mu}\Gamma'(-m, m';\, m'+\mu, -m-\mu)\},$$
$$\Gamma''_{\mu}(m;\, m')$$
$$= (-1)^{j+m}\Gamma''(m+\mu, -m;\, -m', m'+\mu)(-1)^{j+m'}. \qquad (3.10)$$

So far we did not refer to any specific interaction between particles. Let us consider now the particular case of "quadrupole" interaction (2.3), for which we obtain, according to (3.5) and (3.10),

$$\Gamma'_{\mu}(m;\, m') = -\delta_{\mu 0}\varkappa q_m q_{m'}, \qquad \Gamma''_{\mu} = 0. \qquad (3.11)$$

Substituting (3.11) in (3.8), we get

$$(4E^2 - \omega^2)\varphi_{\omega}(m) = 2\varkappa E\sin^2\vartheta\, q_m \sum_{m'} q_{m'}\varphi_{\omega}(m'), \qquad (3.12a)$$

$$(4E^2 - \omega^2)\chi^{(+)}_{\omega}(m) = 4\varkappa E\cos\vartheta\sin\vartheta\, q_m \sum_{m'} q_{m'}\varphi_{\omega}(m'), \qquad (3.12b)$$

$$(4E^2 - \omega^2)\chi^{(-)}_{\omega}(m) = 2\varkappa\omega\sin\vartheta\, q_m \sum_{m'} q_{m'}\varphi_{\omega}(m'). \qquad (3.12c)$$

The first equation contains only φ_ω. From the condition of solvability of this equation, we obtain the energy of the bound state

$$\omega = 2E\Big[1 - \frac{\varkappa}{2E}\sin^2\vartheta \sum_m q_m^2\Big]^{1/2}, \qquad (3.13)$$

which coincides exactly with (2.19).

The function φ_ω (3.7) describes a particle-hole pair, and consequently the resultant excitation is a bound state of the hole and the particle. In this sense, it is an analog of the zero sound of an infinite Fermi system. However, the state obtained is not described by the function φ_ω alone. It is seen from (3.12b and c) that the functions $\chi_\omega^{(\pm)}$ are also different from zero. This can be understood by recalling that in the presence of pairing, the quasi-particles are superpositions of holes with particles. In quadrupole interaction, the "hole" component of one quasi-particle is bound with the "particle" component of its partner, but in the bound state there exist also other components. It must be emphasized that the possibility of production of a balanced state of a particle with a hole occurs only when the system contains pairs with J = 0, of the Cooper type (particle – particle). This is seen, in particular, from expression (3.13) for the energy of the bound state, where the energy of the Cooper pairing 2E is contained in explicit form.

As can be seen from (3.12), the dependence of the functions φ_ω, $\chi_\omega^{(\pm)}$ on the projection of the momentum m is determined by the quantity q_m, which is proportional to the Clebsch-Gordan coefficient (jm j − m | 20), and consequently the state found is characterized by a momentum J = 2.

Let us consider now the pairing interaction (2.2), for which we obtain from (3.5) and (3.10)

$$\Gamma'_{\mu}(m;\, m') = 0, \qquad \Gamma''_{\mu}(m;\, m') = -\delta_{\mu 0}G/2. \qquad (3.14)$$

When Γ′ = 0, the energy of the bound state is determined actually from the last two equations of (3.8), which contain in this case only $\chi^{(\pm)}$, describing pairs of particles or holes. Consequently, in this case the bound state is caused by pairing of the Cooper type (particle – particle or hole – hole). The solution of the secular equation for the interaction (3.14) yields $\omega = 0$ for the energy of the bound state. This result is obvious, since the bound pairs of the Cooper type with J = 0 [which are described by the interaction (2.2)] have already been taken into account in the ground state of the system. We note that in the solution of Eqs. (3.8) the interaction that describes the pairing, and the quadrupole interaction can be considered independently, since they lead to bound states with different momenta.

We emphasize that although formulas (2.19) and (3.13) coincide formally, there is an essential difference between them. In the derivation of (2.19) we used the adiabaticity requirement, which formally limits the region of its application to the condition $\omega \leq 2E$, whereas expression (3.13) is free of this limitation. Another advantage of the microscopic analysis is the possibility of expressing the wave functions of the "collective" state in terms of single-particle functions (the functions φ_ω, and $\chi_\omega^{(\pm)}$ give directly the contribution of the various single-particle combinations).

Thus, in the presence of an interaction that describes the pairing (2.2) and a quadrupole interaction (2.3), collective excitations are possible in the system; these excitations can be considered macroscopically as oscillations of the quadrupole moment, and microscopically as a bound state of a hole and a particle with $J = 2$. The question arises: what justifies the special choice of the Hamiltonian, and how essential is it? Will the character of the excitations change when a more real interaction is examined? These questions are analyzed in the next section.

4. COLLECTIVE EXCITATIONS IN AN ARBITRARY INTERACTION

As was established in the preceding section, the quantities Γ' and Γ'', which describe the effective interaction, lead to bound states of different nature. Γ'' binds a particle to a particle (a hole to a hole), while Γ' binds a particle to a hole. So far we have considered only pairs of the first type, with momentum $J = 0$, and pairs of the second type, with $J = 2$. In the general case Γ' and Γ'' describe an interaction in states with all possible momenta.* It is convenient to represent Γ' and Γ'', in the form of a sum of terms corresponding to pairing with a definite J.

We consider first Γ' and Γ'' of the first approximation (3.5). To determine the dependence of the matrix element on the projections of the single-particle momenta, it is convenient to separate in the interaction potential the angular dependence, writing it in terms of spherical tensor operators:[8]

$$V(\mathbf{r}_1, \mathbf{r}_2) = \sum_k v_k(r_1 r_2)\,(T^k(1)\,T^k(2)). \tag{4.1}$$

From this we obtain for an arbitrary matrix element between the single particle states $|1\rangle = |n_1 l_1 j_1 m_1\rangle$:[8]

$$\langle 12|V|2'1'\rangle = -\sum_{k\mu}(-1)^{\mu}F'_k(-1)^{j'_1-m'_1}(j_1m_1\,j'_1-m'_1|k\mu)$$
$$\times(-1)^{j'_2-m'_2}(j_2m_2\,j'_2-m'_2|k-\mu), \tag{4.2}$$

where the quantities F'_k, which are independent of m, are defined as

$$F'_k = -(2k+1)^{-1}(1\|T^k\|1')(2\|T^k\|2')F^{(k)}(122'1'). \tag{4.3}$$

[Here $F^{(k)}$ are the Slater radial integrals, and $(1\,\|\,T^k\,\|\,1')$ are the reduced matrix element of the tensor operators.]

Using (4.2), we can write the interaction Hamiltonian in the form

$$H_{int} \approx -\tfrac{1}{2}\sum_{\substack{122'1'\\ k\mu}} F'_k(122'1')(-1)^{\mu}(a_1^+\,a_{1'})_{k\mu}(a_2^+\,a_{2'})_{k-\mu}, \tag{4.4}$$

where the quantity

$$(a_1^+\,a_{1'})_{k\mu} = \sum_m (-1)^{j'_1-m'_1}(j_1m_1\,j'_1-m'_1|k\mu)\,a_1^+\,a_{1'} \tag{4.5}$$

can be considered as an operator that describes a particle and a hole in a state with momentum k. Along with (4.4), it is possible to expand H_{int} in states in which the particle—particle and hole—hole pairs have definite momenta

$$H_{int} = -\tfrac{1}{2}\sum_{\substack{122'1'\\ k\mu}} f_k(a_1^+\,a_2^+)_{k\mu}(a_{2'}\,a_{1'})_{k\mu}, \tag{4.6}$$

corresponding to a representation of the matrix element in the form

$$\langle 12|V|2'1'\rangle = -\sum_{k\mu} f_k(j_1m_1j_2m_2|k\mu)(j'_1\,m'_1\,j'_2\,m'_2|k\mu). \tag{4.7}$$

Using the algebra of the Clebsch-Gordan coefficients (see, for example, references 8 and 9), we can relate the coefficients of expansions (4.2) and (4.7). As a result we get

$$f_k = (-1)^{j_1+j'_2-k}\sum_l (2l+1)\,W(j_1\,j_2\,j'_1\,j'_2;\;kl)\,F'_l, \tag{4.8}$$

where W is the Racah coefficient. Analogously we can obtain expressions for the "exchange" matrix element in (3.5), the addition of which is equivalent to changing the quantities F'_k and f_k in (4.2) and (4.8). In the case of a single j-level the exchange corrections to f_k and F'_k are equal to f_k and $-f_k$, respectively. As a result we obtain, with account of (3.5) and (3.10) ($F_k = F'_k - f_k$):

$$\Gamma'_\mu(m;\;m') = -\sum_k F_k(-1)^{j-m}(j, m+\mu, j, -m|k\mu)$$
$$\times(-1)^{j-m'}(j, m'+\mu, j, -m'|k\mu),$$
$$\Gamma''_\mu(m;\;m') = -\sum_k f_k(-1)^{j-m}(j, m+\mu, j, -m|k\mu)$$
$$\times(-1)^{j-m'}(j, m'+\mu, j, -m'|k\mu). \tag{4.9}$$

---

*Even momenta $0 \leq J \leq 2j-1$ are possible for the j^N configuration.

We note that in the derivation of (4.9), the expansion (4.2) was used only to separate the regular dependence on the projection of the momentum, that is, the geometrical factor. Therefore expressions (4.9) are valid not only in the first approximation in the interaction potential, but also in the general case (neglecting delay).

The quantity F_k in (4.9) is the effective interaction (binding energy) between a particle and a hole in a state with momentum k, and f_k is the analogous characteristic of two particles (holes).* Relation (4.8) between the quantities f_k and F_k does not take place in general, since the four-poles Γ'' and Γ' correspond to different irreducible aggregates of diagrams, but it becomes valid for Γ which are irreducible in both direction [see text following formula (3.5)].

Substituting (4.9) in (3.8) and using the orthogonality of the Clebsch-Gordan coefficients, we can obtain a system of algebraic equations for the wave functions of the pairs with definite momentum k (and its projection μ)

$$\varphi_{\omega k} = \sum_m (-1)^{j-m}(j, m+\mu, j, -m \mid k\mu)\, \varphi_{\omega\mu}(m),$$

$$\chi^{(\pm)}_{\omega k} = \sum_m (-1)^{j-m}(j, m+\mu, j, -m \mid k\mu)\, \chi^{(\pm)}_{\omega\mu}(m); \qquad (4.10)$$

$$(4E^2 - \omega^2 - 2F_k E \sin^2\vartheta)\,\varphi_{\omega k}$$
$$- f_k E \sin\vartheta \cos\vartheta\, \chi^{(+)}_{\omega k} - \tfrac{1}{2} f_k \omega \sin\vartheta\, \chi^{(-)}_{\omega k} = 0, \qquad (4.11a)$$

$$(4E^2 - \omega^2 - 2f_k E \cos^2\vartheta)\,\chi^{(+)}_{\omega k} - f_k \omega \cos\vartheta \chi^{(-)}_{\omega k}$$
$$- 4F_k E \sin\vartheta \cos\vartheta\, \varphi_{\omega k} = 0, \qquad (4.11b)$$

$$(4E^2 - \omega^2 - 2f_k E)\,\chi^{(-)}_{\omega k} - f_k \omega \cos\vartheta \chi^{(+)}_{\omega k}$$
$$- 2F_k \omega \sin\vartheta\, \varphi_{\omega k} = 0. \qquad (4.11c)$$

The condition for the solvability of the system (4.11) has the form

$$(4E^2 - \omega^2)^2 [(2E - f_k)^2$$
$$- (2E - f_k)(F_k - f_k)\sin^2\vartheta - \omega^2] = 0, \qquad (4.12)$$

from which we obtain for the energy of the bound state with momentum k

$$\omega_k = (2E - f_k)\left[1 - \frac{F_k - f_k}{2E - f_k}\sin^2\vartheta\right]^{1/2}. \qquad (4.13)$$

If there is no pairing of the Cooper type ($f_k = 0$), then (4.14) goes into (3.13) as $F_k \rightarrow F_2 = \kappa \Sigma q_m^2$. In the general case the bound state is determined by the pairing of both types (particle—particle and particle—hole). If $F_k > f_k$, then, as can be seen from (4.13), account of f_k leads only to a renormalization of the quantities E and F_k, and the dependence of ω_k on the filling of the shell remains the same.

In the case when $F_k < f_k$ this dependence changes considerably. Thus, in the limiting case $F_k = 0$, we get

$$\omega_k = 2E\left[\left(1 - \frac{f_k}{2E}\right)\left(1 - \frac{f_k}{2E}\cos^2\vartheta\right)\right]^{1/2}. \qquad (4.14)$$

It is impossible to establish a general relation between f_k and F_k. For orientation purposes, we consider the case when relation (4.8) is valid. When $j \gg 1$ the main contribution to the right half of (4.8) is given by terms with large l, and we can use the following approximation[9] ($j, l \gg k$)

$$W(jjjj;\, kl) \approx -(2j+1)^{-1} P_k(\cos\alpha_l),$$
$$\cos\alpha_l = [l(l+1) - 2j(j+1)] / 2j(j+1).$$

In this approximation (4.8) assumes the form

$$f_k \approx \tfrac{1}{2}(j + \tfrac{1}{2}) \int_{-1}^{1} P_k(\cos\alpha_l)\, F'_l \, d\cos\alpha_l. \qquad (4.15)$$

We consider the case of a δ interaction $V_{12} \sim (\mathbf{r}_1 - \mathbf{r}_2)$, for which[10]

$$F'_0 = 2G(j + \tfrac{1}{2});\; F'_2 = \tfrac{1}{4}F'_0, \ldots,$$
$$F'_{l \gg 1} \approx \frac{2G}{\pi}\sqrt{\left(\frac{2j+1}{l}\right)^2 - 1} \approx \frac{2G}{\pi}\tan\frac{\alpha_l}{2}, \qquad (4.16)$$

where G is a constant connected with the radial integral. Substituting (4.16) in (4.15), we get

$$f_k \approx \frac{4G}{\pi}(j + \tfrac{1}{2}) \int_0^{\pi/2} P_k(\cos 2\beta)\sin^2\beta\, d\beta. \qquad (4.17)$$

In particular, $f_0 = G(j + 1/2)$, $f_2 = 1/4\, f_0$, and from a comparison with (4.16) it follows that for a δ interaction $f_k = 1/2\, F'_k = F_k$. When the interaction radius if finite, this relation is violated, and F_k diminishes more rapidly with k than f_k.* As a result we have $F_k > f_k$ for small k ($k \ll 2j - 1$), and $F_k < f_k$ for large k. We emphasize that these estimates are only tentative, since the effective interaction Γ cannot be approximated in general by means of a potential, and the quantities F_k and f_k may be non-monotonic functions of k. Thus, account of polarizability of the core, as will be shown in the next section, leads to a sharp increase in the effective quadrupole interaction F_2.

5. EFFECT OF POLARIZATION OF THE CORE

Interaction between particles at the j level occurs both directly and through the nucleons of the core. The part Γ' that corresponds to such an interaction can be represented in the following form (see Fig. 3)

---

*With the sign used in (4.3), F_k and f_k are positive in the case of attraction.

*This can be seen from the limiting case of "long-range action," when $F_k \sim \delta_{k0}$. It follows then from (4.8) that $f_k \approx F_0/(2j+1) = \text{const}$.

$$\widetilde{\Gamma}'(13;24) = -i\gamma(15;26)\widetilde{K}(65;87)\gamma(73;84), \tag{5.1}$$

where γ is the effective interaction of the outer nucleon with the core nucleon (the wavy line on Fig. 3), and K is the Green's function for the core.

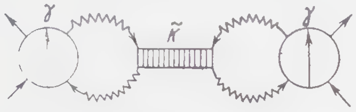

FIG. 3

Going over to a representation in which the momentum of the particle — hole pair is fixed, we obtain

$$\widetilde{F}_k = i\sum_{\alpha\beta}\gamma_k(\alpha)\widetilde{K}_k(\alpha;\beta)\gamma_k(\beta), \tag{5.2}$$

where $\widetilde{F}_k$ is the part of F_k connected with the interaction through the core, $\gamma_k(\alpha)$ describes the transition of the particle — hole pair with momentum k from the j level to the core. The two-particle function of the core is given by the equation

$$\widetilde{K}_k(\alpha;\beta;t-t') = \langle T\{(a^+(t)a(t))_{\alpha k}(a^+(t')a(t'))_{\beta k}\}\rangle. \tag{5.3}$$

Here $(a^+a)_{\alpha k}$ denotes a pair state characterized by momentum k and the remaining quantum numbers α. We assume that γ_k does not contain a delay, and therefore we can consider in $\widetilde{K}$ the times of the ends to be pairwise equal. Breaking up $\widetilde{K}$ similar to (3.6), we obtain

$$\widetilde{K}_k(\alpha;\beta;\tau) = \begin{cases}\sum_s e^{-iE_{s0}\tau}\langle 0|(a^+a)_{\alpha k}|s\rangle\langle s|(a^+a)_{\beta k}|0\rangle, & \tau>0\\ \sum_s e^{iE_{s0}\tau}\langle 0|(a^+a)_{\beta k}|s\rangle\langle s|(a^+a)_{\alpha k}|0\rangle, & \tau<0.\end{cases} \tag{5.4}$$

For the Fourier transform of $\widetilde{K}_k$ we obtain from (5.4)

$$\widetilde{K}_k(\alpha;\beta;\omega) = i\sum_s\left\{\frac{\langle 0|(a^+a)_{\alpha k}|s\rangle\langle s|(a^+a)_{\beta k}|0\rangle}{E_{s0}-\omega} + \frac{\langle 0|(a^+a)_{\beta k}|s\rangle\langle s|(a^+a)_{\alpha k}|0\rangle}{E_{s0}+\omega}\right\}. \tag{5.5}$$

The excitation energy of the core, $E_{s0} = E_s - E_0$, is equal in order of magnitude to the energy difference between the shells, whereas the ω of interest to us correspond to the pairing energies of the outer nucleons; therefore $\omega \ll E_{s0}$. Substituting (5.5) in (5.2) and neglecting ω, we get

$$\widetilde{F}_k = -\sum_{\alpha\beta}\gamma_k(\alpha)\gamma_k(\beta)\sum_s\frac{2}{E_{s0}}\langle 0|(a^+a)_{\alpha k}|s\rangle\langle s|(a^+a)_{\beta k}|0\rangle$$
$$\equiv\sum_{\alpha\beta}\gamma_k(\alpha)\gamma_k(\beta)h_k(\alpha\beta). \tag{5.6}$$

Introducing $\overline{F}_k$, namely that part of F_k connected with the direct interaction ($F_k = \overline{F}_k + \widetilde{F}_k$), we can write

$$\widetilde{F}_k = \eta_k\overline{F}_k, \tag{5.7}$$

where

$$\eta_k = \sum_{\alpha\beta}\frac{\gamma_k(\alpha)\gamma_k(\beta)}{\overline{F}_k}h\ (\alpha\beta) \equiv \overline{\gamma}_k\sum_{\alpha\beta}h\ (\alpha\beta). \tag{5.8}$$

Let us show that the coefficient of renormalization of the direct interaction, η_k, can be connected with the polarizability of the core by the external nucleon. The interaction of the external nucleon (b, b^+) with the core can be written, in analogy with (4.4), as

$$\widetilde{H} = \sum_{\alpha k\mu}\gamma_k(\alpha)(-1)^\mu(b^+b)_{k-\mu}(a^+a)_{\alpha k\mu}. \tag{5.9}$$

In the first approximation we can neglect the reaction of the core on the nucleon, and assume the state of the latter to be specified (that is, consider the nucleon as an external field). Averaging (5.9) over the nucleon state $|jm_0\rangle$, we obtain the additional energy of the core in the presence of an external particle

$$\langle\widetilde{H}\rangle_b = \sum_{\alpha k}\varphi_k\gamma_k(\alpha)(a^+a)_{\alpha k}, \tag{5.10}$$

where

$$\varphi_k = \langle(b^+b)_{k0}\rangle = (-1)^{j-m_0}(jm_0 j-m_0|k0). \tag{5.11}$$

Considering (5.10) as a perturbation, we obtain the change in the wave function of the core

$$\Psi_0^{(1)} = -\sum_{\alpha k}\varphi_k\gamma_k(\alpha)\sum_s\frac{\langle s|(a^+a)_{\alpha k}|0\rangle}{E_{s0}}\Psi_s^0. \tag{5.12}$$

In the presence of an external nucleon, the core loses its spherical symmetry and its polarization can be characterized by the following average values of the multipole moments

$$\hat{Q}_l = \sum_{12}\left\langle 1\left|\sqrt{\frac{2l+1}{4\pi}}r^lY_{l0}\right|2\right\rangle a_1^+a_2$$
$$= \sum\left(1\left\|\frac{r^l}{\sqrt{4\pi}}Y_{l0}\right\|2\right)(-1)^{j_2-m}(j_1mj_2-m|l0)a_1^+a_2$$
$$\equiv\sum_\alpha q_l(\alpha)(a^+a)_{\alpha l}. \tag{5.13}$$

Using (5.12), we obtain the induced moment of the core

$$\langle 0|\hat{Q}_l|0\rangle = -\varphi_l\sum_{\alpha\beta}[q_l(\alpha)\gamma_l(\beta)+q_l(\beta)\gamma_l(\alpha)]\sum_s\frac{1}{E_{s0}}$$
$$\times\langle 0|(a^+a)_{\alpha l}|s\rangle\langle s|(a^+a)_{\beta l}|0\rangle. \tag{5.14}$$

Introducing the multipole moment of the external nucleon $\langle Q_l\rangle_p = \varphi_l q_l$, we can rewrite (5.14) in the form

$$\langle 0 | \hat{Q}_l | 0 \rangle = \eta'_l \langle Q_l \rangle_p, \tag{5.15}$$

where η'_l, the polarizability of the core, is determined from the relation

$$\eta'_l = \sum_{\alpha\beta} \frac{1}{2q_l} [q_l(\alpha)\gamma_l(\beta) + q_l(\beta)\gamma_l(\alpha)]\, h_l(\alpha\beta) \equiv \bar{\gamma}'_l \sum_{\alpha\beta} h_l(\alpha\beta). \tag{5.16}$$

From a comparison of (5.16) and (5.8) we see that the quantities η_l and η'_l actually coincide. (The small difference is due only to a somewhat different determination of the average quantities $\bar{\gamma}$ and $\bar{\gamma}'$.) Thus, the increase in the direct interaction of the external nucleons due to the coupling with the core is determined by the polarizability of the latter.*

The quadrupole polarizability of the core (η_2) is measured experimentally from the value of the quadrupole moment for the magic nuclei plus one nucleon, and lies in the range $1 < \eta_2 < 3$.[11] The polarizability of the higher multipolarities is apparently much less, leading to a "selective" increase in the quadrupole interaction.

We note that the influence of the core on the interaction between the external nucleons is not confined to the considered effect. The remaining effects, however, particularly the renormalization of Γ'', are not connected with the presence of the surface, and exist also in infinite nuclear matter.

6. CONCLUSION

The main results obtained above can be formulated in the following manner:

Depending on the character of the interaction there can be formed in spherical nuclei "bound" (correlated) states of pairs with non-vanishing momenta of both the Cooper type and of the particle — hole type. This possibility arises only in the presence of pairing, that is, a condensate of Cooper pairs with zero momentum.

The polarizability of the core leads to a strong increase in the effective quadrupole interaction between the outer nucleons, and this contributes to the formation of a bound state of a particle and a hole with momentum J = 2. Macroscopically these excitations can be considered as oscillations of a quadrupole moment of external nucleons. The surface oscillations arising thereby are only a consequence of the static polarizability of the core, and have nothing in common with the hydrodynamic surface oscillations.

These general results are not connected with the specific model of a single j level used in the calculation. (The more general case leads only to a mathematical complication of non-principal nature.*)

Which of the possible bound states are realized in real nuclei is a question that calls for a comparison of the experimental data with the results of quantitative calculations. For quadrupole excitations, such a comparison was carried out by Kisslinger and Sorensen.[13] One can classify as this type of excitation the first level 2^+, and in most cases also the following levels (2^+, 4^+), which correspond to two bound pairs. The question of the existence of bound states with higher moments (and also with odd moments in the case of mixture of several j levels) calls for a thorough analysis of the experimental data. Apparently they lie somewhat above the "two-phonon" state of the quadrupole branch.

The author is grateful to V. M. Galitskiĭ and A. B. Migdal for numerous discussions.

---

*For the quadrupole interaction this result was obtained by the author[2] from macroscopic considerations.

*Veneroni and Arvieu have considered a case of several j levels, but without Cooper pairing.

[1] A. Bohr, and B. Mottelson, Kgl. Danske Videnskab Selskab, Mat.-fys. Medd. **27**, No. 16 (1953).

[2] S. T. Beliaev, Kgl. Danske Videnskab Selskab, Mat.-fys. Medd. **31**, No. 11 (1959).

[3] Bogolyubov, Tolmachev, and Shirkov, Новый метод в теории сверхпроводимости (A New Method in the Theory of Superconductivity), Acad. of Sci. Press, 1959.

[4] L. D. Landau, JETP **32**, 59 (1957), Soviet Phys. JETP **5**, 101 (1957); Yu. L. Klimontovich and V. P. Silin, JETP **23**, 151 (1952).

[5] V. M. Galitskiĭ and A. B. Migdal, JETP **34**, 139 (1958), Soviet Phys. JETP **7**, 96 (1958).

[6] L. P. Gor'kov, JETP **34**, 735 (1958), Soviet Phys. JETP **7**, 505 (1958).

[7] M. Gell-Mann, and F. Low, Phys. Rev. **84**, 350 (1951).

[8] J. P. Elliot, and A. M. Lane, Handbuch d. Physik, 39, (1957).

[9] A. R. Edmonds, Angular Momentum in Quantum Mechanics, Princeton University Press, (1957).

[10] K. Helmers, Nucl. Phys. **12**, 647 (1959).

[11] Z. Śzymański, Nucl. Phys. **11**, 454 (1959).

[12] M. Veneroni and R. Arvieu, Compt. rend. **250**, 2155 (1960).

[13] L. S. Kisslinger and R. A. Sorensen, Preprint, 1960.

Translated by J. G. Adashko
254

SOVIET PHYSICS JETP VOLUME 12, NUMBER 5 MAY, 1961

THE INFLUENCE OF IMPURITIES ON THE DE HAAS-VAN ALPHEN EFFECT

Yu. A. BYCHKOV

Institute of Physics Problems, Academy of Sciences of the U.S.S.R.

Submitted to JETP editor June 22, 1960

J. Exptl. Theoret. Phys. (U.S.S.R.) **39**, 1401-1410 (November, 1960)

The methods of quantum field theory are used to study the influence of the elastic scattering by impurities on the quantum oscillations of the magnetic susceptibility of the electron gas in a metal (the de Haas-van Alphen effect). The quasi-classical case is considered, for which the condition $\hbar\omega/\zeta \ll 1$ is satisfied, where ω is the frequency of revolution in the magnetic field and ζ is the chemical potential; a quadratic dispersion law is assumed. It is shown that if $1/\omega\tau_0 \gg \hbar\omega/\zeta$ the effect of the scattering by impurities is described by the Dingle factor[3] with $\tau_D = 4\tau_0/\pi$ (τ_0 is the mean free time for $H = 0$). If $1/(\omega\tau_0) \lesssim \hbar\omega/\zeta$, a more complicated situation exists. In particular, if $\zeta = \hbar\omega(M_0 + 1/2) + \Delta$ and $|\Delta| \leq \hbar\omega/2$, then for $\hbar^2\omega^2/\zeta \ll |\Delta| \lesssim \hbar\omega/2$ the effect of impurities reduces, as before, to the Dingle factor. In the region $|\Delta| \lesssim \hbar^2\omega^2/\zeta$ the effect of the impurities is extremely complicated.

It is well known that at sufficiently strong magnetic fields, for which the quantization of the energy of an electron becomes important, the electron gas in a metal has an appreciable magnetic susceptibility.[1-2] The susceptibility $\chi(H)$ is the sum of two terms: $\chi(H) = \chi_1 + \chi_2(H)$, where χ_1 does not depend on the magnitude of the magnetic field, while $\chi_2(H)$ is an oscillating function of H.

In calculating $\chi_2(H)$ the overwhelming majority of authors have concerned themselves only with the dependence of χ_2 on the magnetic field and the topology of the Fermi surface and have not studied the effect of the scattering of the electrons on $\chi_2(H)$. An exception is the work of Dingle,[3] who has made an attempt to take into account the effect on χ_2 of the elastic scattering of the electrons by impurities. For this purpose Dingle used the artificial method of introducing into all the formulas for χ_2 a certain averaging factor, which subsequently received the name of the Dingle factor.

In the present paper we use the methods of quantum field theory, as developed for application to scattering by impurities by Edwards[4] and by Abrikosov and Gor'kov,[5] to study the problem of the effect of the elastic scattering of the electrons by impurities on the oscillating part of the susceptibility.

To find the magnetic moment of a system of electrons it is necessary to calculate the free energy F. Since we are considering only elastic collisions with the impurities, the distribution function is not changed, so that we can write at once:

$$F = N\zeta - 2kT\int_0^\infty \frac{dZ}{d\varepsilon}\ln\left(1 + e^{\frac{\zeta-\varepsilon}{kT}}\right)d\varepsilon, \qquad (1)$$

where ζ is the chemical potential of the system, N is the number of electrons per unit volume, and $dZ/d\epsilon$ is the number density of electron states per unit energy range, in the presence of the magnetic field H and chaotically distributed impurities. The factor 2 in the term with the integral is due to the spin of the electron (we are not concerned with the spin part of the susceptibility).

The problem thus reduces to that of calculating the density of states $dZ/d\epsilon$. For simplicity we shall adopt the dispersion law $\epsilon = p^2/2m$. The results can be extended in a very simple way to an arbitrary quadratic dispersion law.

In the absence of impurities

$$\left(\frac{dZ}{d\varepsilon}\right)_0 = \frac{m^{3/2}\omega}{2^{3/2}\pi^2}\sum_M \frac{1}{\sqrt{\varepsilon - \omega(M + 1/2)}} \qquad (2)$$

(we have set $\hbar = c = 1$). Here the summation over M is taken for positive values of the radicand, and $\omega = eH/m$ is the frequency of revolution of an electron in the magnetic field.

It is very convenient to represent the energy in the form

$$\varepsilon = \omega(M_0 + 1/2) + \Delta, \qquad |\Delta| \leqslant \omega/2. \qquad (3)$$

It can be seen from Eq. (3) that for $\Delta = 0$ the density of levels $dZ/d\epsilon$ is a discontinuous function: it approaches a finite limit for $\Delta \to -0$, and goes to infinity like $\Delta^{-1/2}$ for $\Delta \to +0$. Inclusion of the scattering by the impurities must destroy this discontinuity and make $dZ/d\epsilon$ a smooth function.

1. CALCULATION OF $dZ/d\epsilon$

Let us consider the Green's function of an electron

$$G(\mathbf{r}, \mathbf{r}'; \varepsilon) = \sum_n \frac{\psi_n(\mathbf{r})\psi_n^*(\mathbf{r}')}{E_n - \varepsilon - i\delta}, \qquad \delta \to 0. \tag{4}$$

Here n is a set of quantum numbers that characterize the state of the electron in the presence of the magnetic field H and of the impurities; E_n and $\psi_n(\mathbf{r})$ are the energy and wave function of the electron in the corresponding stationary state. If we now use the orthonormality of $\psi_n(\mathbf{r})$ and the definition of $dZ/d\epsilon$, according to which

$$dZ/d\varepsilon = \sum_n \delta(E_n - \varepsilon)$$

(where $\delta(x)$ is the usual δ function), it is easy to establish a connection between the density of states $dZ/d\epsilon$ and the Green's function $G(\mathbf{r}, \mathbf{r}'; \epsilon)$:

$$\frac{dZ}{d\varepsilon} = \frac{1}{\pi}\operatorname{Im}\int G(\mathbf{r}, \mathbf{r}; \varepsilon)\, d\mathbf{r}. \tag{5}$$

The Green's function $G(\mathbf{r}, \mathbf{r}'; \epsilon)$ satisfies the equation:[5]

$$G(\mathbf{r}, \mathbf{r}'; \varepsilon) = G_0(\mathbf{r}, \mathbf{r}'; \varepsilon) - \int G_0(\mathbf{r}, \mathbf{r}''; \varepsilon) V(\mathbf{r}'') G(\mathbf{r}'', \mathbf{r}'; \varepsilon)\, d\mathbf{r}'', \tag{6}$$

where $G_0(\mathbf{r}, \mathbf{r}'; \epsilon)$ is the Green's function of the electron in the absence of impurities and

$$V(\mathbf{r}) = \sum_\alpha v(\mathbf{r} - \mathbf{r}_\alpha) \tag{7}$$

is the potential of the field of the chaotically distributed impurities.

Let $E_n^0 = \omega(M + \tfrac{1}{2}) + p_z^2/2m$ and $\psi_n^0(\mathbf{r})$ be the energies and wave functions of the stationary states in the absence of impurities. The set of quantum numbers n consists of the magnetic quantum number M, the momentum p_z ($\mathbf{H}$ is directed along the z axis), and a wave number p_y, which is connected with the center of the orbit of the electron on the x axis by the relation $x_0 = p_y/eH$. Let us expand $G(\mathbf{r}, \mathbf{r}'; \epsilon)$ in terms of these functions. Obviously

$$G_0(\mathbf{r}, \mathbf{r}'; \varepsilon) = \sum_n \psi_n^0(\mathbf{r})\, g_n \psi_n^{0*}(\mathbf{r}'),$$

$$G(\mathbf{r}, \mathbf{r}'; \varepsilon) = \sum_{n, m} \psi_n^0(\mathbf{r})\, G_{nm} \psi_m^{0*}(\mathbf{r}'), \tag{8}$$

where the summations over n, m mean summation over the magnetic quantum number M and integration over dp_z and dp_y; $g_n = (E_n^0 - \epsilon - i\delta)^{-1}$.

By using the relations (6) and (8), we easily get the equation that is satisfied by G_{nm}:

$$G_{nm} = \delta_{nm} g_n - g_n \sum_k V_{nk} G_{km}, \tag{9}$$

$$V_{nk} = \int \psi_n^{0*}(\mathbf{r}) V(\mathbf{r}) \psi_k^0(\mathbf{r})\, d\mathbf{r}.$$

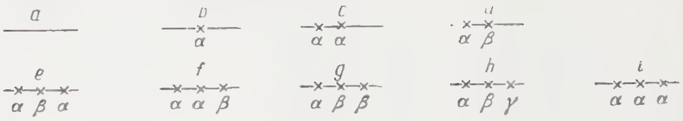

FIG. 1

Here V_{nk} is the matrix element of the operator for the interaction of the electron with the impurities. The function for the energy density of the states is simply related to G_{nn}:

$$\frac{dZ}{d\varepsilon} = \frac{1}{\pi}\operatorname{Im}\sum_n G_{nn}. \tag{10}$$

Let us now proceed to the solution of Eq. (9). For this purpose we use the results of the paper of Abrikosov and Gor'kov.[5] According to Eq. (7)

$$V_{nk} = \sum_\alpha v_{nk}^\alpha, \qquad v_{nk}^\alpha = \int \psi_n^{0*}(\mathbf{r})\, v(\mathbf{r} - \mathbf{r}_\alpha)\, \psi_k^0(\mathbf{r})\, d\mathbf{r}.$$

If in a diagram we use a cross with the index α to correspond to the expression v_{lk}^α, and a straight line to correspond to g_l, then G_{nm} can be represented up to terms of third order in V by the diagrams shown in Fig. 1. The transition from a diagram to the corresponding algebraic expression is made by means of a simple rule: one places in correspondence with each line a factor g_l and with each cross a factor v_{lk}^α; as we move along the diagram, the indices l and k change only when we pass through a cross; to the initial and final lines there correspond the indices n and m. After the expression is written out, it must be summed over all indices corresponding to intermediate lines and over the indices of the various impurities, which are denoted by Greek letters, and then multiplied by $(-1)^s$, where s is the number of crosses in the given diagram.

To illustrate this rule by examples, let us write out the expressions for diagrams c and e of Fig. 1:

$$g_n \sum_{k, \alpha} v_{nk}^\alpha g_k v_{km}^\alpha g_m, \tag{c}$$

$$-g_n \sum_{\substack{k, l \\ \alpha \neq \beta}} v_{nk}^\alpha g_k v_{kl}^\beta g_l\, v_{lm}^\alpha g_m. \tag{e}$$

From the diagrams drawn it is clear than we have first a perturbation-theory series with respect to the scattering by a given impurity (for example, b and c in Fig. 1), and second a perturbation-theory series corresponding to successive scatterings by different impurities (b, d, h in Fig. 1).

Obviously the summation of the diagrams of types b and c in Fig. 1 is simply the transition from v_{lk}^α to the complete amplitude for scattering of the electron by the given impurity, a_{lk}. We have

$$a^{\alpha}_{lk} = v^{\alpha}_{lk} - \sum_{s} v^{\alpha}_{ls} g_s v^{\alpha}_{sk} + \sum_{s,\,t} v^{\alpha}_{ls} g_s v^{\alpha}_{st} g_t v^{\alpha}_{tk} \ldots \tag{11}$$

We shall therefore not consider henceforth diagrams in which a given impurity is encountered two or more times in succession (types c, f, etc.), and shall put in correspondence with a cross the complete amplitude a_{lk} (there remain, however, diagrams like e in Fig. 1, in which, between successive scatterings by an impurity α, the electron is scattered by one or more impurities $\beta \neq \alpha$). If we make this stipulation, then up to the fourth order we need consider only the diagrams shown in Fig. 2, where crosses for the same impurity are connected by dashed lines.

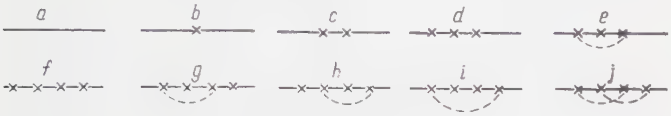

FIG. 2

Some remarks must be made regarding the total amplitude a_{lk} for scattering by a given impurity. For metals with a quadratic dispersion law, i.e., a small number of carriers, the wavelength of the electron is much larger than the range of the potential of an impurity. Therefore the potential of the impurity can be treated like a δ function. In this case the scattering amplitude has the form[6]

$$a^{\alpha}_{lk} = F(\varepsilon)\, \psi^{0*}_{l}(\mathbf{r}_{\alpha})\, \psi^{0}_{k}(\mathbf{r}_{\alpha}). \tag{12}$$

The function $F(\epsilon)$ can be determined very simply. Obviously

$$a^{\alpha}_{lk} = \int \psi^{0*}_{l}(\mathbf{r})\, v(\mathbf{r} - \mathbf{r}_{\alpha})\, \psi_{k}(\mathbf{r})\, d\mathbf{r},$$

where $\psi_k(\mathbf{r})$ satisfies an integral equation that is equivalent to the Schrödinger equation:

$$\psi_k(\mathbf{r}) = \psi^{0}_{k}(\mathbf{r}) - \int G(\mathbf{r}, \mathbf{r}';\ \varepsilon)\, v(\mathbf{r} - \mathbf{r}_{\alpha})\, \psi_k(\mathbf{r})\, d\mathbf{r}.$$

It is clear that to find the amplitude a_{lk} it is necessary to know $\psi_k(\mathbf{r})$ in the region of action of the potential. But in this region, i.e., for small values of $\mathbf{r}$ and $\mathbf{r}'$, the Greens function satisfies

$$G(\mathbf{r}, \mathbf{r}';\ \varepsilon) \approx G_0(\mathbf{r}, \mathbf{r}') + g(\varepsilon),$$

where $G_0(\mathbf{r}, \mathbf{r}')$ is the Green's function of the electron for $\epsilon = 0$ in the absence of the magnetic field. If we take all these points into account, we get for $F(\epsilon)$:

$$F(\varepsilon) \approx f - f^2 g(\varepsilon), \tag{13}$$

where f is the scattering amplitude of the electron for $\epsilon = 0$ and $H = 0$.

The expression (13) is nothing other than the expansion of $F(\epsilon)$ in powers of the small ratio of the scattering amplitude for $\epsilon = 0$ to the wavelength of the electron; it is incorrect only in the narrow range of values of the magnetic field in which $\Delta \ll \omega$,[6] since in this region $fg \gg 1$ and therefore it is necessary to take into account subsequent terms in an expansion of $F(\epsilon)$ in series of powers of fg. We shall assume, however, that when collisions with impurities are taken into account $fg \ll 1$. We shall discuss this condition later in more detail.

It is easy to establish the connection of $g(\epsilon)$ with the sum $\sum_n g_n$. It can be shown[6] that the separation out of $g(\epsilon)$ is equivalent to dropping from the sum $\sum_n g_n$ the divergent part that arises from summation over very large magnetic quantum numbers M.

In the specific calculation of G_{nm} we shall assume that the following conditions are satisfied: $\zeta \gg \omega$, i.e., we have the quasi-classical case, and $\omega\tau > 1$ (as we shall see later, for $\omega\tau \lesssim 1$ the quantum effects are exponentially small).

The simplest diagrams in Fig. 2 are b, c, d, and f. For these diagrams the averagings over the positions of the impurities for the various crosses are independent of each other. The averages can be taken over the whole volume of the crystal. In particular, for diagram c we have

$$g_n g_m \sum_{\substack{k \\ \alpha \neq \beta}} \langle a^{\alpha}_{nk} \rangle\, g_k\, \langle a^{\beta}_{km} \rangle = \delta_{nm} g^3_n c^2 F^2(\varepsilon), \tag{14}$$

where c is the concentration of impurities. The relation (14) follows from the obvious formula

$$\sum_{\alpha} \langle a^{\alpha}_{nk} \rangle = F(\varepsilon)\, c \int \psi^{0*}_{n}(\mathbf{r}_{\alpha})\, \psi^{0}_{k}(\mathbf{r}_{\alpha})\, d\mathbf{r}_{\alpha} = F(\varepsilon)\, c\, \delta_{nk}.$$

Obviously to each impurity there must correspond a term cf^2g, since the term cf is simply the change of the reference level for the energy. If we take this into account, the expression (14) is equal to $\delta_{nm} g^3_n c^2 f^4 g^2$.

We can at once calculate the expression for an arbitrary diagram in which a given impurity is encountered only once (types b, c, and so on). We have

$$\delta_{nm} g^{s+1}_n c^s f^{2s} g^s (-1)^s. \tag{15}$$

In order of magnitude such a diagram gives

$$\Delta^{-1} (cf^2 g/\Delta)^s, \tag{16}$$

i.e., for $\Delta \sim cf^2 g$ they give the same contribution.

Let us now study the simplest diagrams in which

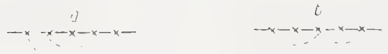

FIG. 3

a given impurity is encountered twice (e in Fig. 2). It is easy to show that after the averaging the diagram e gives

$$-\delta_{nm}g_n^2c^2f^4g\frac{\partial g}{\partial\varepsilon}\sim\frac{1}{\Delta}\left(\frac{cf^2g}{\Delta}\right)^2.$$

For $\Delta\sim cf^2g$ this diagram is of the same order as diagram c. By similar arguments it is easy to show that for $\Delta\sim cf^2g$ we get the same contribution from all diagrams in which a given impurity is encountered not more than twice. These include, in particular, diagrams of the type a of Fig. 3.

An exception to this rule is formed by diagrams of the type j of Fig. 2. Simple estimates show that for arbitrary Δ the ratio of the expression corresponding to this diagram to that for diagram c of Fig. 2 is $1/M_0$, where $M_0\sim\epsilon/\omega$. But since we are assuming that $M_0\gg 1$, this means that the "overlapping" diagrams can be omitted. We note here that the dropping of diagrams $\sim 1/M_0$ is practically equivalent to the neglect of corrections $\sim 1/(\epsilon\tau)$ in comparison with $\sim 1/(\omega\tau_0)$. Since we are interested only in corrections to ω, we shall omit diagrams of the type j of Fig. 2.

Diagrams are possible in which a given impurity is encountered more than twice. An example is the diagram b of Fig. 3. A simple estimate shows that in order of magnitude this diagram is equal to $\Delta^{-1}(cf^2g/\Delta)^3fg$, i.e., as compared with the diagrams considered previously, it contains the extra factor $fg\ll 1$. This factor occurs in all diagrams in which a given impurity is encountered more than twice.

Our final conclusion is that in the expansion (10) we need include only terms in which each impurity is encountered not more than two times, and that we must omit overlapping diagrams of the type j of Fig. 2. In addition to this, after the averaging only the diagonal elements of the matrix G_{nm} will be different from zero:

$$\langle G_{nm}\rangle=\delta_{nm}G_n.$$

If we take all these facts into account, it is easy to get the equation that G_n satisfies. Obviously

$$G_n^{-1}=E_n^0-\varepsilon+cF-cF^2(G-g),\qquad G=\sum_n G_n,$$

or, if we use the fact that $F=f-f^2g$,

$$G_n^{-1}=E_n^0-\varepsilon+cf-cf^2G. \tag{17}$$

Finally we get for $G(\epsilon)$ the following equation (we have dropped the term cf, which means a change of the reference level for energies and is of no interest):

$$G=\sum_n(E_n^0-\varepsilon-cf^2G)^{-1}.$$

If we perform the integration over p_z, we get

$$G=i\frac{m^{3/2}\omega}{2^{3/2}\pi}\left\{\sum_{M=0}^{\infty}[\varepsilon+cf^2G-\omega(M+1/2)]^{-1/2}-A\right\}, \tag{18}$$

where the subtraction of A is equivalent to the subtraction of the divergent term caused by summation over very large values of M.

According to Eq. (9), the density of levels is connected with $G(\epsilon)$ by the relation

$$\frac{dZ}{d\varepsilon}=\frac{1}{\pi}\operatorname{Im}G(\varepsilon). \tag{10'}$$

Since the calculation is being made in the quasiclassical domain $\omega/\zeta\ll 1$, G is essentially equal to an integral with respect to M plus an added term G_1 which goes to zero for H = 0 and is in general small in comparison with the integral, except for a narrow range of values of the magnetic field, in which $|\Delta|\ll\omega$. We take for the integral the value $G_0=im^{3/2}\epsilon^{1/2}(2\pi)^{-1/2}$, since we must neglect the corrections to ϵ caused by the scattering. Thus we have

$$G=G_0+i\frac{m^{3/2}\omega}{2^{3/2}\pi}\left\{\sum_{M=0}^{\infty}\frac{1}{\sqrt{\varepsilon+cf^2G-\omega(M+1/2)}}\right.$$
$$\left.-\int_0^{\infty}\frac{dM}{\sqrt{\varepsilon+cf^2G-\omega M}}\right\}. \tag{19}$$

For not too small Δ the ratio G_1/G_0 is in order of magnitude $(\omega/\epsilon)^{1/2}\ll 1$. Thus in this range of values of H Eq. (19) can be solved by the method of successive approximations; that is, we simply substitute G_0 in the expression in curly brackets. Furthermore,

$$cf^2G_0=i\pi/2\tau_0, \tag{20}$$

where τ_0 is the mean free time for H = 0.

The calculation of G_1 can be carried out by means of the Poisson summation formula:

$$\sum_{M=0}^{\infty}f(M+1/2)=\sum_{-\infty}^{\infty}(-1)^l\int_0^{\infty}f(x)e^{2\pi ilx}dx,$$

from which we have

$$G(\varepsilon)=G_0(\varepsilon)+i\frac{m^{3/2}\omega}{2^{3/2}\pi}\sum_{-\infty}^{\infty}{}'(-1)^l\int_0^{\infty}\frac{e^{2\pi ilx}dx}{\sqrt{\varepsilon+i\pi/2\tau_0-\omega x}}; \tag{21}$$

the prime on the summation sign means that the term with $l=0$ is omitted.

For the oscillating part G_1 we have

$$i\frac{m^{3/2}\omega^{1/2}}{2^{3/2}\pi}\sum_{1}^{\infty}(-1)^l e^{2\pi il\varepsilon/\omega}\int_{-\infty}^{\infty}\frac{e^{-2\pi ilx}dx}{\sqrt{x+i\pi/2\omega\tau_0}}.$$

The calculation of this integral is not difficult, and therefore we simply state the result,

$$i\,\frac{m^{3/2}\omega^{1/2}}{2\pi}\sum_{1}^{\infty}\frac{(-1)^{l}}{\sqrt{l}}\exp\left(2\pi i l\,\frac{\varepsilon}{\omega}-i\,\frac{\pi}{4}-\frac{\pi^{2}l}{\omega\tau_{0}}\right). \qquad (22)$$

From this we get as the expression for $(dZ/d\epsilon)$:

$$\left(\frac{dZ}{d\varepsilon}\right)_{\mathrm{osc}}=\frac{m^{3/2}\omega^{1/2}}{2\pi^{2}}\sum_{1}^{\infty}\frac{(-1)^{l}}{\sqrt{l}}\exp\left(-\pi^{2}l/\omega\tau_{0}\right)\cos\left(2\pi l\,\frac{\varepsilon}{\omega}-\frac{\pi}{4}\right). \qquad (23)$$

The factor $\exp(-\pi^2 l/\omega\tau_0)$ is indeed the Dingle factor.[3]*

The maximum value of G_1 is reached near $\Delta = 0$; this maximum value is of the order of magnitude $m^{3/2}\omega\tau_0^{1/2}$, and therefore if $(\omega\tau_0)^{-1} \gg \omega/\epsilon$ Eq. (23) is valid for arbitrary values of Δ. A more complicated situation arises in the case $(\omega\tau_0)^{-1} \lesssim \omega/\epsilon$. Here too, however, Eq. (23) is valid as before for $|\Delta| \gg \omega^2/\epsilon$.

For small values of Δ ($|\Delta| \ll \omega$) Eq. (19) becomes much simpler, and takes the form

$$G=G_{0}+\frac{im^{3/2}\omega}{2^{3/2}\pi}\,\frac{1}{\sqrt{\Delta+cf^{2}G}}. \qquad (24)$$

Equation (24) is obviously an algebraic equation of the third degree in G. We shall only study some of its properties.

An elementary analysis shows that $\mathrm{Im}\,G_1$ falls off rapidly with increase of $|\Delta|$, but remains positive. At $\Delta_0 = \pi(2\cdot 3^{1/2}\tau_0)^{-1} \ll \omega$ the function $\mathrm{Im}\,G_1$ has a maximum, and

$$(\mathrm{Im}\,G_{1})_{max}\approx \mathrm{Im}\,G_{0} \qquad (1/\omega\tau_{0}\sim\omega/\varepsilon). \qquad (25)$$

In particular, for $(\omega\tau_0)^{-1} \ll \omega/\epsilon$

$$(\mathrm{Im}\,G)_{max}=\mathrm{Im}\,G_{0}\,\frac{\sqrt{3}}{\pi^{1/3}2^{4/3}}\left(\frac{\omega^{2}\tau_{0}}{\varepsilon}\right)^{1/3}. \qquad (25')$$

Equation (24) is valid only in a narrow range of energies near $\Delta = 0$. In order to calculate the position of the minimum of Im G it is necessary to use Eq. (19). We shall not do this.

Let us now return to the condition (13). It is quite obvious that Eq. (13) will be satisfied if we have $f(\mathrm{Im}\,G)_{\max} \ll 1$. It is easy to show, when one uses Eq. (25), that this condition is equivalent to the following restriction on the concentration of impurities:

$$c \gg \sqrt{\sigma}\,(eH)^{2}, \qquad (26)$$

where σ is the total cross section for elastic scattering of an electron by an impurity for $H = 0$, $\epsilon = 0$.

2. CALCULATION OF THE MAGNETIC SUSCEPTIBILITY AND THE MAGNETIC MOMENT

It now remains for us to calculate the formulas for the magnetic moment and the susceptibility. Since we are interested in only the oscillating parts of these quantities, we shall hereafter always give formulas for χ_2 and M_2. If we use the relations (1) and (10′), we get

$$M_{2}=\frac{2kT}{\pi}\int_{0}^{\infty}\mathrm{Im}\left(\frac{\partial G_{1}}{\partial H}\right)\ln\left(1+\exp(\zeta-\varepsilon)/kT\right)d\varepsilon. \qquad (27)$$

It can be seen from Eq. (19) that G_1 is a function of the variables ω and $\Delta = \epsilon - \omega(M_0 + 1/2)$. It is obvious that in Eq. (27) we must differentiate G_1 only with respect to Δ, since then each differentiation with respect to H will involve multiplication by the quantity $M_0 \gg 1$, and therefore

$$\frac{\partial G_{1}}{\partial H}=-\left(\frac{e}{m}\right)\left(\frac{\varepsilon}{\omega}\right)\frac{\partial G_{1}}{\partial\varepsilon}. \qquad (28)$$

This means that we must know the functional relationship $G_1(\Delta)$ over the whole periodicity interval $|\Delta| \le \omega/2$. But for arbitrary Δ this can be obtained in closed form only in the case $(\omega\tau_0)^{-1} \gg \omega/\epsilon$ (cf. Eq. (23)):

$$M_{2}=-\frac{m^{3/2}\omega^{1/2}}{\pi}\left(\frac{e}{m}\right)\left(\frac{\zeta}{\omega}\right)kT \times\sum_{1}^{\infty}\frac{(-1)^{l}\exp\left(-\pi^{2}l/\omega\tau_{0}\right)}{\sqrt{l}\,\sinh(2\pi^{2}lkT/\omega)}\sin\left(2\pi l\,\frac{\zeta}{\omega}-\frac{\pi}{4}\right). \qquad (29)$$

Actually this formula is also valid for arbitrary $(\omega\tau_0)^{-1}$. In fact, it can be seen from Eq. (29) that $M_2 \sim (e/m)\,m^{3/2}\omega^{1/2}\zeta$. At the same time the contribution to M_2 given by the integration in Eq. (27) in the region $|\Delta| \sim \omega^2/\zeta$ is $(e/m)\,m^{3/2}\zeta\Delta^{1/2}$. But the ratio of this correction to M_2 is $\sim(\omega/\zeta)^{1/2} \ll 1$, so that the contribution from the region $\Delta \sim 0$ is relatively small, and thus M_2 depends only very weakly on the exact behavior of $\mathrm{Im}\,G_1$ for $\Delta \sim 0$.

We have written out the expression for the magnetic moment in the case in which there is a single group of electrons with an isotropic dispersion law. This formula can be extended very simply to the case of several groups of electrons corresponding to different ellipsoids with arbitrary quadratic dispersion laws $\epsilon = \frac{1}{2}m_{ik}^{-1}p_i p_k$, where m_{ik} is the mass tensor. If we take the z axis in the direction of **H**, then the frequency of revolution of the electrons that belong to the ith ellipsoid is $\omega_i = eH(m_{zz}^{i}/|m^{i}|)^{1/2}$ ($|m^{i}|$ is the determinant of the mass tensor). With this notation we have instead of Eq. (29)

---

*We note that the quantity τ_D, which in Dingle's paper[3] plays the role of a mean free time, is actually connected with the true mean free time τ_0 for $H = 0$ by the relation $\tau_D = 4\tau_0/\pi$.

$$M_2 = -e\sum_i \frac{|m^i|^{1/2}\omega_i^{1/2}}{\pi}\sqrt{\frac{m^i_{zz}}{|m^i|}}\left(\frac{\zeta}{\omega_i}\right)$$

$$\times kT\sum_1^\infty \frac{(-1)^l \exp(-\pi^2 l/\omega_i\tau_0)}{\sqrt{l}\sinh(2\pi^2 l\, kT/\omega_i)}\sin\left(2\pi l\frac{\zeta}{\omega_i}-\frac{\pi}{4}\right), \qquad (29')$$

where τ_0 is the mean free time in the absence of the magnetic field. Thus the effect of the scattering by impurities on the oscillating part M_2 of the magnetic moment has the character of a Dingle factor for an arbitrary value of the ratio $1/(\omega\tau_0)$.

Besides M_2, the susceptibility $\chi_2 = \partial M_2/\partial H$ is of interest. If we use the same arguments as in the derivation of Eq. (28), we easily find that

$$\chi_2 = -\frac{2}{\pi}\left(\frac{e}{m}\right)^2\left(\frac{\zeta}{\omega}\right)^2\int_0^\infty \operatorname{Im} G_1\frac{\partial f_0}{\partial\varepsilon}\,d\varepsilon$$

$$\left(f_0 = \left\{1+\exp\frac{\varepsilon-\zeta}{kT}\right\}^{-1}\right). \qquad (30)$$

In particular, for $T = 0$

$$\chi_2 = \frac{2}{\pi}\left(\frac{e\zeta}{m\omega}\right)^2 \operatorname{Im} G_1, \qquad (31)$$

i.e., χ_2 is directly connected with Im G_1, whose properties we have already elucidated in the preceding section.

We can finally summarize as follows the results relating to the effect of the scattering by impurities on the magnetic susceptibility χ_2. If $(\omega\tau_0)^{-1} \gg \omega/\zeta$, the effect of the scattering is described by the Dingle factor for all values of the magnetic field **H**. For $(\omega\tau_0)^{-1} \lesssim \omega/\zeta$ and $|\Delta| \gg \omega^2/\zeta$ this is still true, but in the region $|\Delta| \lesssim \omega^2/\zeta$ the dependence on the impurities is more complicated.

We note here that for $T \gg \omega^2/\zeta$ and arbitrary $\omega\tau_0$ we have as a valid formula for χ_2:

$$\chi_2 = 2\frac{m^{3/2}}{\omega^{1/2}}\left(\frac{e}{m}\right)^2\left(\frac{\zeta}{\omega}\right)^2 kT\sum_1^\infty(-1)^l\sqrt{l}\,\frac{\exp(-\pi^2 l/\omega\tau_0)}{\sinh(2\pi^2 l\,kT/\omega)}$$

$$\times\cos\left(2\pi l\frac{\zeta}{\omega}-\frac{\pi}{4}\right). \qquad (32)$$

In conclusion I express my deep gratitude to Academician L. D. Landau, and also to A. A. Abrikosov, L. P. Gor'kov, and I. M. Khalatnikov for helpful advice and discussions.

---

[1] L. D. Landau, Z. Physik **64**, 629 (1930).

[2] I. M. Lifshitz and A. M. Kosevich, JETP **29**, 730 (1955), Soviet Phys. JETP **2**, 636 (1956).

[3] R. B. Dingle, Proc. Roy. Soc. **A211**, 517 (1952).

[4] S. F. Edwards, Phil. Mag. **3**, 1020 (1958).

[5] A. A. Abrikosov and L. P. Gor'kov, JETP **35**, 1558 (1958), Soviet Phys. JETP **8**, 1090 (1959).

[6] Yu. A. Bychkov, JETP **39**, 689 (1960), Soviet Phys. JETP **12**, 483 (1961).

Translated by W. H. Furry
255

SOVIET PHYSICS JETP VOLUME 12, NUMBER 5 MAY, 1961

ACCOUNT OF THE NUCLEAR COULOMB FIELD IN THE INTERACTION BETWEEN ELECTRONS AND AN ELECTROMAGNETIC FIELD

V. G. GORSHKOV

Leningrad Physico-Technical Institute, Academy of Sciences, U.S.S.R.

Submitted to JETP editor June 22, 1960

J. Exptl. Theoret. Phys. (U.S.S.R.) **39**, 1411-1421 (November, 1960)

Convenient expressions for practical calculations are derived for the matrix elements of the interaction between electrons and an electromagnetic field near the nucleus. The Coulomb field is taken into account with an accuracy up to terms proportional to $(\alpha Z)^2$.

It is known that it is impossible to find a convenient analytic expression for the exact relativistic wave functions of electrons in a Coulomb field. As approximations to the wave function one may use the Furry-Sommerfeld-Maue (FSM) function[1] or the Born series with respect to the Coulomb field, cut off at some term. If the small angular momenta cannot be neglected, the FSM function is valid only with an accuracy up to terms proportional to αZ for arbitrary energies. The Born series for the wave function, which is useful only for large energies, has been employed only for the calculation of the correction proportional to αZ (see, for example, reference 2). An exception to this is the problem of the elastic scattering of electrons by a Coulomb field, for which the probability has been calculated up to terms proportional to $(\alpha Z)^2$ (reference 3).

In the first section of the present paper we establish the connection between the FSM function and the Born series; on the basis of this connection the correction proportional to $(\alpha Z)^2$ to the FSM function will be separated out. In the second section we shall derive convenient working formulas for the general matrix elements of the considered processes in second Born approximation, i.e., with an accuracy up to terms $(\alpha Z)^2$. As the perturbing potential we take an initially screened Coulomb potential. The screening parameter will be set equal to zero in the final result, and it will be shown that the terms which are divergent under this operation cancel out.

1. WAVE FUNCTIONS OF THE FREE PARTICLES

The matrix element for electronic processes near the nucleus (photoeffect, conversion, bremsstrahlung and pair creation, elastic scattering of the electron) can be written in the form

$$W = \int \psi_2^+(\mathbf{r})\widetilde{B}(\mathbf{r})\psi_1(\mathbf{r})\,d\mathbf{r}, \qquad \widetilde{B} = \boldsymbol{\alpha}\mathbf{B} - B^0, \tag{1}$$

where $\psi(\mathbf{r})$ are the electron wave functions of the continuous or discrete spectrum in the Coulomb field of the nucleus, and $B(\mathbf{r})$ is the four-potential of the electromagnetic field.

In momentum space formula (1) takes the form

$$W = \iint \varphi_2^+(\mathbf{f}_2)\widetilde{B}(\mathbf{k})\varphi_1(\mathbf{f}_1)\,d\mathbf{f}_1\,d\mathbf{f}_2,$$
$$B(\mathbf{k}) = \int e^{-i\mathbf{k}\mathbf{r}}B(\mathbf{r})\,d\mathbf{r}, \quad \mathbf{k} = \mathbf{f}_2 - \mathbf{f}_1. \tag{2}$$

For our later discussion it is convenient to separate out only the functions of the discrete spectrum in the matrix element. If, therefore, one of the wave functions (for example, φ_1) belongs to the discrete spectrum, we write expression (2) in the form

$$W = \int \varphi_2^+(\mathbf{f})\,d\mathbf{f}\int \widetilde{B}(\mathbf{k})\varphi_1(\mathbf{f}-\mathbf{k})\,d\mathbf{k}$$
$$= \int \varphi^+(\mathbf{p},\mathbf{f})J(\mathbf{v})\,d\mathbf{f} = \langle \mathbf{p}|J,$$
$$J(\mathbf{v}) = \int B(\mathbf{k})\varphi_1(\mathbf{v})\,d\mathbf{k}, \qquad \varphi(\mathbf{p}) = \varphi_2, \qquad \mathbf{v} = \mathbf{f}-\mathbf{k}. \tag{3a}$$

We shall deal with the function J as a function of $\mathbf{v}$, assuming that the integration over $\mathbf{f}$ is done before the integration over $\mathbf{k}$.

In order to make the notation consistent, we write, if both functions belong to the continuous spectrum, the matrix element (2) also in the form

$$W = \int \varphi^+(\mathbf{p}_2,\mathbf{f}_2)J(\mathbf{v})\varphi(\mathbf{p}_1,\mathbf{f}_1)\,d\mathbf{f}_1\,d\mathbf{f}_2 = \langle \mathbf{p}_2|J|\mathbf{p}_1\rangle, \tag{3b}$$

where now $J(\mathbf{v}) = \widetilde{B}(\mathbf{v})$, $\mathbf{v} = \mathbf{k} = \mathbf{f}_2 - \mathbf{f}_1$.

We use Dirac's integral equation with a screened Coulomb potential $-eZe^{-\lambda r}/r$ for "incoming" waves in the momentum representation:

$$\varphi(\mathbf{p},\mathbf{f}) = \delta(\mathbf{p}-\mathbf{f})u(\mathbf{p}) + \beta\frac{m - i\hat{f}}{\mathbf{f}^2 - \mathbf{p}^2 - i\varepsilon}\int\frac{\gamma_4}{\mathbf{q}_{fs}^2 + \lambda^2}\varphi(\mathbf{s})\,d\mathbf{s}, \tag{4}$$

where

$$\mathbf{q}_{fs} = \mathbf{f} - \mathbf{s}, \qquad \beta = \alpha Z / 2\pi^2, \qquad f^0 = p^0 = E, \qquad \hat{f} = \gamma_i f_i,$$

$$(i\hat{p} + m)\, u(p) = 0, \qquad \hbar = c = 1.$$

The wave function can be expressed in the form of a power series in β:

$$\varphi(\mathbf{p}, \mathbf{f}) = \Big\{ \delta(\mathbf{f} - \mathbf{p}) + \beta \frac{(m - i\hat{f})\gamma_4}{(\mathbf{f}^2 - \mathbf{p}^2 - i\varepsilon)(\mathbf{q}_{fp}^2 + \lambda^2)}$$
$$+ \beta^2 \frac{(m - i\hat{f})\gamma_4}{\mathbf{f}^2 - \mathbf{p}^2 - i\varepsilon} \int \frac{(m - i\hat{s})\gamma_4\, ds}{(\mathbf{q}_{fs}^2 + \lambda^2)(\mathbf{s}^2 - \mathbf{p}^2 - i\varepsilon)(\mathbf{q}_{sp}^2 + \lambda^2)} + \ldots$$
$$+ \beta^n \frac{(m - i\hat{f})\gamma_4}{\mathbf{f}^2 - \mathbf{p}^2 - i\varepsilon}$$
$$\times \int \frac{(m - i\hat{s}_{n-1})\gamma_4 \ldots (m - i\hat{s}_1)\gamma_4\, ds_{n-1} \ldots ds_1}{(\mathbf{q}_{fs_{n-1}}^2 + \lambda^2) \ldots (\mathbf{s}_1^2 - \mathbf{p}^2 - i\varepsilon)(\mathbf{q}_{s_1 p}^2 + \lambda^2)} + \ldots \Big\} u(\mathbf{p}), \tag{5}$$

where $s_k^0 = E = p^0$.

Expressions for the matrix elements calculated from a finite number of terms of (5) can be used only for large momenta owing to the presence of terms proportional to $(\alpha ZE/p)^n$ (see Sec. 2). To obtain an expansion in αZ which is valid for arbitrary values of p, we must sum up all those terms in (5) which lead to the appearance of the parameter $\alpha ZE/p$.

For this purpose we use the identity

$$(m - i\hat{s})\gamma_4 = 2E + \tilde{q}_{sp} + \gamma_4(i\hat{p} + m),$$

to transform expression (5) to the new series

$$\varphi(\mathbf{p}, \mathbf{f}) = \varphi_0(\mathbf{p}, \mathbf{f}) + \varphi_{\mathrm{I}}(\mathbf{p}, \mathbf{f}) + \varphi_{\mathrm{II}}(\mathbf{p}, \mathbf{f}) + \ldots, \tag{6}$$

which is constructed in the following way: φ_0 contains all terms of (5) with numerators which do not involve Dirac matrices, i.e., which are proportional to $(2E)^n$ $(n = 0, 1, 2, \ldots)$; φ_{I} contains all terms with numerators of the form $\tilde{q}_{fp}(2E)^{n-1}$, i.e., proportional to the remaining part of the numerator of the second term of (5); in φ_{II} we include all terms with numerators of the form $(m - i\hat{f})\gamma_4 \times \tilde{q}_{s_{n-1}p}(2E)^{n-2}$, i.e., proportional to the remaining part of the numerator of the third term of (5), etc.

We thus obtain

$$\varphi_0(\mathbf{p}, \mathbf{f}) = \Big\{ \delta(\mathbf{f} - \mathbf{p}) + \frac{2E\beta}{(\mathbf{f}^2 - \mathbf{p}^2 - i\varepsilon)(\mathbf{q}_{fp}^2 + \lambda^2)} + \frac{(2E\beta)^2}{\mathbf{f}^2 - \mathbf{p}^2 - i\varepsilon}$$
$$\times \int \frac{ds}{(\mathbf{q}_{fs}^2 + \lambda^2)(\mathbf{s}^2 - \mathbf{p}^2 - i\varepsilon)(\mathbf{q}_{sp}^2 + \lambda^2)} + \ldots \Big\} u(\mathbf{p}) = |0,0\rangle$$
$$+ 2E\beta\,|1,0\rangle + (2E\beta)^2\,|2,0\rangle + \ldots, \tag{7a}$$

$$\varphi_{\mathrm{I}}(\mathbf{p}, \mathbf{f}) = \beta \sum_{k=1}^{\infty} (2E\beta)^{k-1}\, |k, \mathrm{I}\rangle = \frac{1}{2E}\, \tilde{q}_{fp}\varphi_0(\mathbf{p}, \mathbf{f}),$$
$$|k, \mathrm{I}\rangle = \tilde{q}_{fp}\, |k, 0\rangle; \tag{7b}$$

$$\varphi_{\mathrm{II}}(\mathbf{p}, \mathbf{f}) = \beta^2 \sum_{k=2}^{\infty} (2E\beta)^{k-2}\, |k, \mathrm{II}\rangle = \beta \frac{(m - i\hat{f})\gamma_4}{\mathbf{f}^2 - \mathbf{p}^2 - i\varepsilon} \int \frac{\varphi_{\mathrm{I}}(\mathbf{p}, \mathbf{s})}{\mathbf{q}_{fs}^2 + \lambda^2}\, ds,$$
$$|k, \mathrm{II}; \mathbf{f}\rangle = \frac{(m - i\hat{f})\gamma_4}{\mathbf{f}^2 - \mathbf{p}^2 - i\varepsilon} \int \frac{|k-1, \mathrm{I}; \mathbf{s}\rangle}{\mathbf{q}_{fs}^2 + \lambda^2}\, ds. \tag{7c}$$

It is easily seen that φ_0 without the spinor factor $u(\mathbf{p})$ is a solution of the ordinary Schrödinger equation:

$$\varphi_0(\mathbf{p}, \mathbf{f}) = \delta(\mathbf{p} - \mathbf{f}) + \frac{2E\beta}{\mathbf{f}^2 - \mathbf{p}^2 - i\varepsilon} \int ds\, \frac{\varphi_0(\mathbf{p}, \mathbf{s})}{(\mathbf{q}_{fs}^2 + \lambda^2)}.$$

The solution of this equation in coordinate space has the form

$$\psi_0(\mathbf{p}, \mathbf{r}) = N e^{i\mathbf{pr}}\, {}_1F_1(-i\xi; 1; i\rho),$$

where

$$N^2 = 2\pi\xi / (1 - e^{2\pi\xi}), \quad \xi = \alpha ZE / p, \quad \rho = pr - \mathbf{pr}.$$

By going over to coordinate space in (7b), we obtain an expression for $\psi_0 + \psi_{\mathrm{I}}$:

$$\psi_0 + \psi_{\mathrm{I}} = \Big\{ 1 - i\frac{1}{2E}\, \tilde{\nabla}_r - \frac{1}{2E}\, \tilde{p} \Big\} \psi_0(\mathbf{p}, \mathbf{r}). \tag{8}$$

This is the FSM function (see, for example, reference 1). Except for the terms with small l in the expansion of the total ψ in terms of eigenfunctions of the angular momentum, the function (8) is an exact solution of the Dirac equation for large E.[1] We do not wish to restrict ourselves to problems in which the small l do not play any role, and we shall therefore regard expression (8) as an expansion in αZ which is valid for all momenta. The matrix elements for many problems (as the ones enumerated above) can be easily computed with the help of the function (8). However, in those cases where the small l cannot be neglected, the resulting expressions will be correct only with an accuracy up to terms proportional to αZ.

It follows from the discussion above that we must add the function (7c) to the function (8) if we want to take account of the corrections proportional to $(\alpha Z)^2$. If we restrict ourselves to large energies only, it suffices to substitute in (7c) only the first term. Using the identity

$$(m - i\hat{f})\gamma_4\tilde{q}_{sp} u(\mathbf{p}) = [2(\mathbf{p}\mathbf{q}_{sp}) + \tilde{q}_{fs}\tilde{q}_{sp}]\, u(\mathbf{p}),$$

this term can be written in the form

$$\varphi'_{\mathrm{II}}(\mathbf{p}, \mathbf{f}) = \beta^2 \Big\{ \frac{1}{\mathbf{f}^2 - \mathbf{p}^2 - i\varepsilon} \int \frac{2(\mathbf{p}\mathbf{q}_{sp})\, ds}{(\mathbf{q}_{fs}^2 + \lambda^2)(\mathbf{s}^2 - \mathbf{p}^2 - i\varepsilon)(\mathbf{q}_{sp}^2 + \lambda^2)}$$
$$+ \frac{\tilde{\mathbf{q}}_{fp}}{\mathbf{f}^2 - \mathbf{p}^2 - i\varepsilon} \int \frac{\tilde{q}_{sp}\, ds}{(\mathbf{q}_{fs}^2 + \lambda^2)(\mathbf{s}^2 - \mathbf{p}^2 - i\varepsilon)(\mathbf{q}_{sp}^2 + \lambda^2)} \Big\} u(\mathbf{p})$$
$$\equiv \beta^2 \{ |2, \mathrm{II}\rangle^A + |2, \mathrm{II}\rangle^{\mathbf{B}} \}. \tag{7c'}$$

We note that the magnitude of the matrix element computed with the help of the function (7c′) may serve as a criterion for the legitimacy of neglecting the terms with small l.

Writing the function $\varphi_{\mathrm{II}}(\mathbf{p}, \mathbf{f})$ in coordinate space,

$$\psi_{\mathrm{II}}(\mathbf{p},\mathbf{r})=\int e^{i\mathbf{f}\mathbf{r}}\varphi_{\mathrm{II}}(\mathbf{p},\mathbf{f})\,d\mathbf{f},$$

we obtain the following expressions for the matrix elements (1) to (3):

a) One of the functions belongs to the discrete spectrum:

$$W=\int[\psi_0(\mathbf{p},\mathbf{r})+\psi_{\mathrm{I}}(\mathbf{p},\mathbf{r})]^{+}J(\mathbf{r})\,d\mathbf{r}+\int\varphi_{\mathrm{II}}^{+}(\mathbf{p},\mathbf{f})\,J(\mathbf{v})\,d\mathbf{f}, \tag{9a}$$

where $J(\mathbf{r})=\widetilde{B}(\mathbf{r})\psi_1(\mathbf{r})$; $J(\mathbf{v})$ is defined by formula (3a).

b) Both functions belong to the continuous spectrum:

$$W=\int[\psi_0(\mathbf{p}_2,\mathbf{r})+\psi_{\mathrm{I}}(\mathbf{p}_2,\mathbf{r})]^{+}\widetilde{B}(\mathbf{r})\,[\psi_0(\mathbf{p}_1,\mathbf{r})+\psi_{\mathrm{I}}(\mathbf{p}_1,\mathbf{r})]\,d\mathbf{r}+\left\{\int\varphi_{\mathrm{II}}^{+}(\mathbf{p}_2,\mathbf{f})\,J_1(\mathbf{v})\,d\mathbf{f}+(2\rightleftarrows 1)\right\}, \tag{9b}$$

where

$$J_s(\mathbf{v})=\int e^{-i\mathbf{f}\mathbf{r}}\widetilde{B}(\mathbf{r})\,\psi_0(\mathbf{p}_s,\mathbf{r})\,d\mathbf{r}=\int\widetilde{B}(\mathbf{k})\,\varphi_0(\mathbf{p}_s,\mathbf{v})\,d\mathbf{k},$$

$$\mathbf{v}=\mathbf{f}-\mathbf{k}.$$

The symbol $(2\rightleftarrows 1)$ denotes the interchange of the indices 1 (initial state) and 2 (final state).

Thus, if the matrix elements can be computed with the help of the function (8), the correction quadratic in αZ to the probability is determined by the integral

$$\langle 2,\mathrm{II}\,|\,J=\int\varphi_{\mathrm{II}}^{+}(\mathbf{p},\mathbf{f})\,J(\mathbf{v})\,d\mathbf{f}. \tag{9c}$$

This integral will be calculated in Sec. 2, using the function (7c′).

2. CALCULATIONS IN THE SECOND BORN APPROXIMATION

For large energies the first three terms of the series (6) coincide with the first three terms of the series (5) with an accuracy up to and including terms proportional to $(\alpha Z)^2$. Therefore, if it is impossible for some reason to calculate a matrix element with the function (8), one can use the series (5), which gives a result which is valid only in the region of large energies. However, in this case the matrix elements will in general contain terms which are logarithmically divergent for $\bar{\lambda}\to 0$. This is connected with the presence of the term $[(\mathbf{s}^2-\mathbf{p}^2-i\epsilon)(q_{sp}^2+\lambda^2)]^{-1}$ with two coinciding (for $\lambda\to 0$) poles at the point $s=p$ under the integral sign. Since the divergence is logarithmic, the smallest decrease in the order of the pole suffices to remove the divergence. Terms containing q_{sp} in the numerator will, therefore, not be divergent.

The remaining divergences must cancel out in the expression for the probability. This is seen most easily if we use the expansions (6) and (7) for (5) and go up to and including terms proportional to β^2. It is clear that the divergences of φ_0 must cancel each other, the divergences in the interference terms from φ_0 and φ_{I} must be compensated again by interference divergences, etc.

1. Let us first consider the case in which the initial state belongs to the discrete spectrum. With the notations (7) and (3a), we write the matrix element in the form

$$\begin{aligned}\langle\mathbf{p}\,|\,J&=\langle 0\,|\,J+\beta\langle 1\,|\,J+\beta^2\langle 2\,|\,J\\&=(\langle 0{,}0\,|\,J+2E\beta\langle 1{,}0\,|\,J+(2E\beta)^2\langle 2{,}0\,|\,J)+\beta(\langle 1,\mathrm{I}\,|\,J\\&\quad+2E\beta\langle 2,\mathrm{I}\,|\,J)+\beta^2(\langle 2,\mathrm{II}\,|^{A}J+\langle 2,\mathrm{II}\,|^{\mathrm{B}}J).\end{aligned} \tag{10}$$

Here

$$\begin{aligned}&\langle 0{,}0\,|\,J=J(\mathbf{v}_0),\qquad \mathbf{v}_0=\mathbf{p}-\mathbf{k};\\&\langle 1,(0,\mathrm{I})\,|\,J=u^{+}(\mathbf{p})\int\frac{(1,\widetilde{\mathbf{q}}_{fp})\,J(\mathbf{v})\,d\mathbf{f}}{(\mathbf{f}^2-\mathbf{p}^2-i\varepsilon)(\mathbf{q}_{fp}^2+\lambda^2)},\\&\langle 2(0,\mathrm{I})\,|\,J=u^{+}(\mathbf{p})\int\frac{(1,\widetilde{\mathbf{q}}_{fp})\,J(\mathbf{v})\,d\mathbf{f}}{\mathbf{f}^2-\mathbf{p}^2-i\varepsilon}\\&\qquad\times\int\frac{d\mathbf{s}}{(\mathbf{q}_{fs}^2+\lambda^2)(\mathbf{s}^2-\mathbf{p}^2-i\varepsilon)(\mathbf{q}_{sp}^2+\lambda^2)};\\&\langle 2,\mathrm{II}\,|^{A}J=u^{+}(\mathbf{p})\int\frac{2(\mathbf{p}\mathbf{q}_{sp})\,d\mathbf{s}}{(\mathbf{q}_{sp}^2+\lambda^2)(\mathbf{s}^2-\mathbf{p}^2-i\varepsilon)(\mathbf{q}_{fs}^2+\lambda^2)}\\&\qquad\times\int\frac{J(\mathbf{v})\,d\mathbf{f}}{\mathbf{f}^2-\mathbf{p}^2-i\varepsilon};\\&\langle 2,\mathrm{II}\,|^{\mathrm{B}}J=u^{+}(\mathbf{p})\int\frac{\widetilde{q}_{sp}\,d\mathbf{s}}{(\mathbf{q}_{sp}^2+\lambda^2)(\mathbf{s}^2-\mathbf{p}^2-i\varepsilon)(q_{fs}^2+\lambda^2)}\\&\qquad\times\int\frac{\widetilde{q}_{fp}\,J(\mathbf{v})\,d\mathbf{f}}{\mathbf{f}^2-\mathbf{p}^2-i\varepsilon}.\end{aligned} \tag{11}$$

According to the above-said, only the terms $<1,0\,|\,J$ and $<2,(0,\mathrm{I})\,|\,J$ will contain divergent parts.

Using the formulas given in the Appendices A and B, letting λ go to zero in all non-divergent terms, and considering that in (A.2) $\nabla_{\mathrm{B}}=-\nabla_{\mathrm{k}}$ we obtain

$$\begin{aligned}&\langle 0.0\,|\,J=F(1),\qquad \langle 1.0\,|\,J=\pi^2ip^{-1}(a+A(x)F(1),\\&\langle 1,\mathrm{I}\,|\,J=\pi^2i\widetilde{G}(1),\\&\langle 2{,}0\,|\,J=(\pi^2i/p)^2\tfrac{1}{2}\{(a+A(x))^2-\pi^2/6\}F(1),\\&\langle 2.\,\mathrm{I}\,|\,I=(\pi^2i)^2p^{-1}(a+A(x))\widetilde{G}(1),\\&a=\ln(2p/\lambda),\qquad F(x)=u^{+}(\mathbf{p})\,xf(x),\end{aligned} \tag{12}$$

$$\mathbf{G}(x)=-u^{+}(\mathbf{p})\int_0^x dx_1\{\mathbf{n}f(x_1)+\nabla_kR(x_1)\},\qquad \mathbf{n}=\mathbf{p}/p;$$

$$\langle 2,\mathrm{II}\,|^{A}J=(\pi^2i)^2\,2u^{+}(\mathbf{p})\left\{\int_0^1\frac{dx_1}{x_1}\int_0^{x_1}\frac{dx_2}{x_2-1}f(x_2)+\int_0^1dx\int_0^1dy\,(\mathbf{n}\nabla_B)\int_\infty^{1-x}\frac{dt}{\Lambda_t}f_{2t}(x,y)\right\},$$

$$\langle 2, \mathrm{II}|^{\mathbf{B}}J = (\pi^2 i)^2 \Big\{ -\tilde{n} \int_0^1 \frac{dx_1}{x_1} \tilde{G}(x_1)$$
$$+ u^+(\mathbf{p}) \int_0^1 dx \int_0^1 dy\, \tilde{\nabla}_B \int_\infty^{1-x} dt \Big[\frac{\tilde{B}y - \tilde{n}}{\Lambda_t} f_{2t}(x, y)$$
$$- \tilde{\nabla}_k R_{2t}(x, y) \Big] \Big\},$$
$$\mathbf{B} = \mathbf{n}x, \quad \Lambda_t = \Lambda_{2t}/p = (1 - B^2 y)(1 - y) + t^2 y,$$
$$\mathbf{P}_2 = p\mathbf{B}y - \mathbf{k}. \tag{13}$$

Substituting (12) and (13) in the expression for the probability

$$|\langle \mathbf{p}|J|^2 = |\langle 0,0|J|^2 + 2\beta\,\mathrm{Re}\,\{2E\langle 1,0|J(\langle 0,0|J)^+$$
$$+ \langle 1,\mathrm{I}|J(\langle 0,0|J)^+\} + \beta^2\{(2E)^2[2\mathrm{Re}\,\{\langle 2,0|J(\langle 0,0|J)^+\}$$
$$+ |\langle 1,0|J|^2] + 2E\cdot 2\mathrm{Re}\,[\langle 2,\mathrm{I}|J(\langle 0,0|J)^+$$
$$+ \langle 1,\mathrm{I}|J(\langle 1,0|J)^+]$$
$$+ |\langle 1,\mathrm{I}|J|^2 + 2\mathrm{Re}\,[\langle 2,\mathrm{II}|J(\langle 0,0|J)^+]\}, \tag{14}$$

we easily verify that the terms containing $a = \log(2p/\lambda)$ drop out.

The correct expression for the amplitude (10) is thus given by formulas (12) and (13) with $a = 0$. The expression for (9c) is given by formulas (13).

2. If the function $J(\mathbf{v})$ has a multiple pole at the point $v = \alpha Z$, the residue of $J(\mathbf{v})$ (see Appendix A) at this point may be proportional to $(\alpha Z)^{-n}$. In order to take account of all the corrections proportional to $(\alpha Z)^2$, we must therefore include more terms of the series (5). However, we may again only consider the first three terms of the series, if we change the expression for $J(\mathbf{v})$. We show this on the example of the photoeffect; the other possibilities can be treated in an analogous way.

For the photoeffect, $J(\mathbf{v})$ has the form[2]

$$J(\mathbf{v}) = J_0(\mathbf{v}) + C/(\mathbf{v}^2 + \eta^2)^2, \qquad \eta = \alpha Z, \qquad C = \mathrm{const}$$

or

$$J(\mathbf{v}) = J_0(\mathbf{v}) - \frac{1}{2\eta}\frac{\partial}{\partial\eta}\left(\frac{C}{v^2 + \eta^2}\right). \tag{15}$$

Let us consider the internal integral in the matrix element which contains $J(\mathbf{v})$ in the integrand:

$$L = \int \frac{\gamma_4 (m - i\hat{s}_n) J(\mathbf{v}_n)\, ds_n}{(\mathbf{q}^2_{s_{n-1}s_n} + \lambda^2)(\mathbf{s}_n^2 - p^2 - i\varepsilon)}, \qquad \mathbf{v}_n = \mathbf{s}_n - \mathbf{k}, \qquad \mathbf{s}_n = \mathbf{f}.$$

Substituting the expression (15) for $J(\mathbf{v})$ in this integral and using the residue of the second term, we find

$$L = L_0 + \frac{\pi^2 C}{\eta} \frac{\gamma_4 (m - i\hat{k})}{(\mathbf{k}^2 - \mathbf{p}^2)(\mathbf{v}^2_{n-1} + \lambda^2)}, \qquad \mathbf{v}_{n-1} = \mathbf{s}_{n-1} - \mathbf{k}. \tag{16}$$

L_0 does not contain terms proportional to $1/\eta$.

The second term in (16) comes from that part of (15) which is equal to

$$-\frac{C}{2\eta}\left\{\frac{\partial}{\partial\eta}\frac{1}{\mathbf{v}^2 + \eta^2)}\right\}_{\eta\to 0} = \frac{\pi^2 C}{\eta}\delta(\mathbf{v}), \tag{17}$$

it gives a contribution to the $(n-1)$-st matrix element. A similar term from the $(n+1)$-st matrix element enters in the n-th matrix element.

To remain within a given n-th order, we therefore must subtract expression (17) from $J(\mathbf{v})$ and add the second term of (16), multiplied by β, i.e., we must replace $J(\mathbf{v})$ by

$$J(\mathbf{v}) - \frac{C}{2\beta}\delta(\mathbf{v}) + \frac{C}{2}\gamma_4(m - i\hat{k})\frac{1}{\mathbf{v}^2 + \lambda^2}. \tag{18}$$

3. Let us now consider the case in which both functions in (1) belong to the continuous spectrum. We shall assume that electrons are present in the initial (index 1) and final state (index 2). The expressions for the matrix elements involving a single positron state were considered by Krutov and the author.[4]

The matrix element has the form (up to terms proportional to β^2 inclusively)

$$\langle \mathbf{p}_2|J|\mathbf{p}_1\rangle = \langle 0|J|0\rangle + \beta(\langle 1|J|0\rangle + \langle 0|J|1\rangle)$$
$$+ \beta^2(\langle 2|J|0\rangle + \langle 1|J|1\rangle + \langle 0|J|2\rangle). \tag{19a}$$

Recalling that in our case

$$\langle m|J|n\rangle = \langle n|J|m\rangle_{(2\rightleftarrows 1)},$$

we can write

$$\langle \mathbf{p}_2|J|\mathbf{p}_1\rangle = \langle 0|J|0\rangle + \{\beta\langle 1|J|0\rangle + \beta^2\langle 2|J|0\rangle$$
$$+ (2\rightleftarrows 1)\} + \beta^2\langle 1|J|1\rangle. \tag{19b}$$

Owing to the equality $J(\mathbf{f}_2 - \mathbf{f}_1)|0\rangle = J(\mathbf{f}_2 - \mathbf{p}_1)$, the terms in the curly brackets in (19b) agree with the terms entering in (10), if there we replace $\mathbf{k}$ by $\mathbf{p}_1$ and $\mathbf{p}$ by $\mathbf{p}_2$.

The last term of (19b) can be rewritten in the form

$$1|J|1\rangle = 2E_1 2E_2\langle 1,0|J|1,0\rangle + (2E_1\langle 1,\mathrm{I}|J|1,0\rangle$$
$$+ (2\rightleftarrows 1) + \langle 1,\mathrm{I}|J|1,\mathrm{I}\rangle,$$
$$\langle 1, (0,\mathrm{I})_\alpha|J|1, (0,\mathrm{I})_\beta\rangle$$
$$= u^+(\mathbf{p}_2)\iint(d\mathbf{f}_2\, d\mathbf{f}_1\{(1, \tilde{q}_{f_2p_2})_\alpha J(k)(1, \tilde{q}_{f_1p_1})_\beta$$
$$\times [(\mathbf{q}^2_{f_2p_2} + \lambda^2)(\mathbf{f}_2^2 - \mathbf{p}_2^2 - i\varepsilon)(\mathbf{q}^2_{f_1p_1}$$
$$+ \lambda^2)(\mathbf{f}_1^2 - \mathbf{p}_1^2 - i\varepsilon)]^{-1}\}\, u(p_1), \tag{20}$$

where $\mathbf{k} = \mathbf{f}_2 - \mathbf{f}_1$.

Using formulas (A.10) and (A.11), we obtain (setting $\lambda = 0$ in the non-divergent terms)

$$\langle 1,0|J|1,0\rangle=(\pi^2 i/p_1p_2)^2\{a_2+A(x_2)\}\{a_1$$
$$+A(x_1)\}R(\alpha,1|\alpha,1),$$
$$\langle 1,\mathrm{I}|J|1,0\rangle=(\pi^2 i)^2 p_1^{-1}\{a_1+A(x_1)\}R(\beta,1|\alpha,1),$$
$$\langle 1,\mathrm{I}|J|1,\mathrm{I}\rangle=(\pi^2 i)^2 R(\beta,1|\beta,1), \tag{21}$$
$$R(\alpha,x_2|\beta,x_1)=u^+(\mathbf{p}_2)O_2^\alpha O_1^\beta R(x_2|x_1)u(\mathbf{p}_1),$$
$$O_i^\alpha=x_i\frac{\partial}{\partial\Lambda_i},\quad O_i^\beta=\int_0^{x_i}dx_i'\left(-\widetilde{p}_i\frac{\partial}{\partial\Lambda_i}+\widetilde{\nabla}_{B_i}\right),\ a_i=\ln\frac{2p_i}{\lambda}.$$

In complete analogy to the preceding considerations, it can be shown that the terms containing a_i cancel out after substitution of (21), (12), and (13) (replacing **k** by $\mathbf{p}_1$ and **p** by $\mathbf{p}_2$) in the expression for the probability

$$|\langle\mathbf{p}_2|J|\mathbf{p}_1\rangle|^2=|\langle 0|J|0\rangle|^2+\{2\beta\,\mathrm{Re}\langle 1|J|0\rangle\langle 0|J|0\rangle^+$$
$$+\beta^2[2\mathrm{Re}\langle 2|J|0\rangle\langle 0|J|0\rangle^++|\langle 1|J|0\rangle|^2]+(2\rightleftarrows 1)\}$$
$$+2\beta^2\,\mathrm{Re}\{\langle 1|J|1\rangle\langle 0|J|0\rangle^++\langle 1|J|0\rangle\langle 0|J|1\rangle^+\}. \tag{22}$$

If both functions belong to the continuous spectrum, the correct expression for the amplitude is thus given by formulas (19), (21) and (12), (13) (with the above-mentioned replacement of coordinates), where we must set $a_i = 0$ in all formulas.

4. Let us consider an example. Assume that the function J(**v**) varies so slowly for finite values of **v** that it can be taken outside of the integral without appreciable error. [In some cases this step can be justified even if the function J depends strongly on **v**, since for most terms only the real part of the matrix elements enters in the formulas for the probability (14) and (22) (see reference 4).] In this case the "dimensionality" of the integral in $<2,\ \mathrm{II}|^{B}J$, is equal to zero, so that the integral diverges logarithmically for large momenta. This divergence is connected with the well-known divergence of the Dirac wave function with $l = 0$ at the origin in coordinate space and is a consequence of our choice of a point nucleus. This divergence disappears if we take account of the finite dimensions of the nucleus. However, we shall, as before, consider a point nucleus, but with the assumption that J(**v**) goes to zero for $\mathbf{v}\to\infty$. This is equivalent to discarding the divergent parts in $<2,\ \mathrm{II}|^{B}J$, where the function J(**v**) has been taken outside of the integral. That this is so can be easily verified by integration by parts, for example.

Recalling that

$$R(x)=\Lambda J(\mathbf{v}_0),\qquad R(x_2|x_1)=\Lambda_2\Lambda_1 J(\mathbf{v}_0),$$

and computing the integrals in formulas (12), (13), and (21), we obtain the following values for the probabilities (14) and (22):

$$|\langle\mathbf{p}|J|^2=|\langle 0|J|^2\{(1+\pi\xi+\tfrac{1}{3}\pi^2\xi^2)+\tfrac{1}{4}(\alpha Z)^2+\sigma\}, \tag{14'}$$
$$|\langle\mathbf{p}_2|J|\mathbf{p}_1\rangle|^2=|\langle 0|J|0\rangle|^2\{1+[\pi\xi_2+\tfrac{1}{3}\pi^2\xi_2^2+(2\rightleftarrows 1)]$$
$$+\pi\xi_1\pi\xi_2+\tfrac{1}{2}(\alpha Z)^2+2\sigma\}; \tag{22'}$$

here $\sigma = 2(\alpha Z)^2\{1-\frac{1}{3}(\log 2+\frac{1}{6})\}$ represents the contribution from the function φ'_{II} [see formula (6)].

The probability in our example is thus expressed in the form of a product of the probability in zeroth order Born approximation and a certain factor which depends on Z and the energy of the particle. The constant function J(**v**) corresponds in coordinate space to a function of the form $J(\mathbf{v}_0)\,\delta(\mathbf{r})$. Hence the probabilities (14) and (22) can also be written in the form

$$|\langle\mathbf{p}|J|^2=|\psi^+(\mathbf{p},0)J(\mathbf{v}_0)|^2, \tag{14''}$$
$$|\langle\mathbf{p}_2|J|\mathbf{p}_1\rangle|^2=|\psi^+(\mathbf{p}_2,0)J(\mathbf{v}_0)\psi(\mathbf{p}_1,0)|^2. \tag{22''}$$

It is easily shown that, if we substitute the function (8) with $\mathbf{r} = 0$ instead of $\psi(\mathbf{p}, 0)$, we obtain formulas (14′) and (22′) without the last term σ, with an accuracy up to and including terms proportional to $(\alpha Z)^2$. We note that this last term is in our case independent of the energy and, therefore, is not small at large energies. This is connected with the fact that the terms with small l in ψ cannot be neglected for a δ-function-like J(**v**).

In conclusion the author expresses his deep gratitude to L. A. Sliv, B. A. Volchok, and V. A. Krutov for their interest in this work.

APPENDIX A

In order to make our expressions more uniform and facilitate the calculation of the integrals, we introduce the notation

$$\{K_f(\mathbf{r},a),\mathbf{K}_f(\mathbf{r},a)\}J(\mathbf{v})=\int\frac{\{1,\mathbf{q}_{fp}\}J(\mathbf{v})\,d\mathbf{f}}{(\mathbf{f}^2-\mathbf{p}^2-i\varepsilon)(\mathbf{q}_{fr}^2-a^2)},$$
$$\mathbf{v}=\mathbf{f}-\mathbf{k}. \tag{A.1}$$

Applying the Feynman device to the denominator of (A.1) (see reference 4, Appendix C), we obtain

$$\{K_f(\mathbf{r},a),\mathbf{K}_f(\mathbf{r},a)\}J(\mathbf{v})=\pi^2 i\left(\int_0^1 dx\,\frac{\{1,\mathbf{B}-\mathbf{p}\}}{\Lambda}f(x)\right.$$
$$\left.+\int_0^1 dx\,\{0,\nabla_B\}R(x)\right),$$

$$f(x)=\frac{\partial}{\partial\Lambda}R(x),\qquad \pi^2 iR(x)=\frac{1}{2}\int\frac{J(\mathbf{v})\,d\mathbf{v}}{(\mathbf{P}-\mathbf{v})^2-\Lambda^2}, \tag{A.3a}$$
$$\Lambda^2=(\mathbf{p}^2-\mathbf{r}^2x)(1-x)+a^2x+i\varepsilon(1-x),$$
$$\mathbf{P}=\mathbf{B}-\mathbf{k},\qquad \mathbf{B}=\mathbf{r}x. \tag{A.3b}$$

The single integrals (11) are obtained by setting $\mathbf{r} = \mathbf{p}$, $a = i\lambda$, where Λ and B are given by formulas (A.7).

We separate out the angular part of $J(\mathbf{v})$ in the form of an expansion in multipole fields and restrict ourselves for simplicity to a single term of the expansion, i.e., we set $J(\mathbf{v}) = A_l(v)\,\tilde{Y}_{jlm}(\mathbf{v}/v)$. Performing the integration in (A.3a) as in reference 4 (Appendix C), we find

$$R(x) = \frac{1}{2P}\Big\{\int\limits_{-P+\Lambda}^{P+\Lambda} A_l(v)\,P_l(\zeta)\,v\,dv + 2Q_l(\zeta)\,v\,\mathrm{Res}_i A_l(v)\,|_{\omega_i}\Big\}\,\tilde{Y}_{jlm}\Big(\frac{\mathbf{P}}{P}\Big),$$

$$f(x) = \frac{1}{2}\big(A_lP_l\,|_{P+\Lambda} + A_lP_l\,|_{-P+\Lambda}\big)\,\tilde{Y}_{jlm}\Big(\frac{\mathbf{P}}{P}\Big) + \Lambda\chi(\Lambda)\,\tilde{Y}_{jlm}\Big(\frac{\mathbf{P}}{P}\Big),$$

$$\chi(\Lambda) = \frac{1}{2P}\,A_lP_l\,\Big|_{-P+\Lambda}^{P+\Lambda} + \frac{1}{P}\,\frac{\partial}{\partial\Lambda^2}\,Q_l(\zeta)\,v\,\mathrm{Res}_i A_l(v)\,|_{\omega_i} - \frac{1}{(2P)^2}\int\limits_{-P+\Lambda}^{P+K} A_l(v)\,P_l'(\zeta)\,dv, \tag{A.4}$$

where $\zeta = (v^2 + P^2 - \Lambda^2)/2vP$, P_l is a Legendre polynomial, and $\mathrm{Res}_i A_l$ denotes the sum of the residues of A_l in the points ω_i. It follows from (A.4) and (A.3b) that

$$f(1) = J(\mathbf{v}_0) + O(a). \tag{A.5}$$

The property (A.5) is independent of the form of the function $J(\mathbf{v})$.

In the special case $J(\mathbf{v}) = 1/(v^2 + \lambda^2)$ we obtain from (A.4)

$$R(x) = \frac{1}{2P}\ln\frac{P+\Lambda+i\lambda}{-P+\Lambda+i\lambda} = \int\limits_{\infty}^{\Lambda+i\lambda}\frac{dt}{P^2-t^2},$$

$$f(x) = \frac{1}{P^2-(\Lambda+i\lambda)^2}.$$

We therefore have for the internal integrals of the double integrals (11)

$$\int\frac{\{1,\,\mathbf{q}_{sp}\}\,ds}{(\mathbf{q}_{fs}^2+\lambda^2)(s^2-\mathbf{p}^2-i\varepsilon)(\mathbf{q}_{sp}^2+\lambda^2)} = \{K_s(\mathbf{p},\,i\lambda),\ \mathbf{K}_s(\mathbf{p},\,i\lambda)\}\,\frac{1}{\mathbf{q}_{fs}^2+\lambda^2}$$

$$= \pi^2 i\Big(\int\limits_0^1\frac{\{1,\,\mathbf{B}_1-\mathbf{p}\}}{\Lambda_1}\,\frac{dx}{P_f^2-(\Lambda_1+i\lambda)^2} + \int\limits_0^1\{0,\,\nabla_{B_1}\}\int\limits_{\infty}^{\Lambda_1+i\lambda}\frac{dt}{P_f^2-t^2}\Big), \tag{A.6}$$

$$\Lambda_1^2 = \mathbf{p}^2(1-x)^2 - \lambda^2 x, \qquad \mathbf{B}_1 = \mathbf{p}x, \qquad \mathbf{P}_f = \mathbf{B}_1 - \mathbf{f}. \tag{A.7}$$

For the double integrals in (11) we obtain, respectively,

$$\int\frac{\{1,\,\mathbf{q}_{sp}\}_\alpha\,ds}{(\mathbf{q}_{sp}^2+\lambda^2)(s^2-\mathbf{p}^2-i\varepsilon)(\mathbf{q}_{fs}^2+\lambda)^2}\int\frac{\{1,\,\mathbf{q}_{fp}\}_\beta\,J(\mathbf{v})\,d\mathbf{f}}{\mathbf{f}^2-\mathbf{p}^2-i\varepsilon} = \pi^2 i\Big(\int\limits_0^1\frac{\{1,\,\mathbf{B}_1-\mathbf{p}\}_\alpha}{\Lambda_1}\,\{K_f(\mathbf{B}_1,\,\Lambda_1+i\lambda),\ \mathbf{K}_f(\mathbf{B}_1,\,\Lambda_1+i\lambda)\}_\beta\,dx$$

$$+ \int\limits_0^1\{0,\,\nabla_{B_1}\}_\alpha\int\limits_{\infty}^{\Lambda_1+i\lambda} dt\,\{\mathbf{K}_f(\mathbf{B}_1,\,t),\ \mathbf{K}_f(\mathbf{B}_1,\,t)\}_\beta\Big) = (\pi^2 i)^2\Big(\int\limits_0^1\frac{\{1,\,\mathbf{B}_1-\mathbf{p}\}}{\Lambda_1}\,dx\Big[\int\limits_0^1 dy\,\frac{\{1,\,\mathbf{B}_2-\mathbf{p}\}_\beta}{\Lambda_2}\,f_2(x,\,y) + \int\limits_0^1 dy\,\{0,\,\nabla_{B_2}\}_\beta\,R_2(x,\,y)\Big]$$

$$+ \int\limits_0^1\{0,\,\nabla_{B_1}\}_\alpha\int\limits_{\infty}^{\Lambda_1+i\lambda} dt\,\Big[\int\limits_0^1 dy\,\frac{\{1,\,\mathbf{B}_2-\mathbf{p}\}_\beta}{\Lambda_{2t}}\,f_{2t}(x,\,y) + \int\limits_0^1 dy\,\{0,\,\nabla_{B_2}\}_\beta R_{2t}(x,\,y)\Big]\Big), \tag{A.8}$$

$$\Lambda_2^2 = \mathbf{p}^2(1-xy)^2 - \lambda^2 xy + 2i\lambda\Lambda_1 y - \lambda^2 y, \qquad \mathbf{P}_2 = \mathbf{B}_2 - \mathbf{k}, \qquad \mathbf{B}_2 = \mathbf{B}_1 y, \quad \Lambda_{2t}^2 = (\mathbf{p}^2 - \mathbf{B}_1^2 y)(1-y) + t^2 y, \qquad \mathbf{P}_{2t} = \mathbf{P}_2. \tag{A.9}$$

The indices on the functions f and R correspond to the indices on Λ and $\mathbf{P}$.

For the double integrals (20) we find

$$\iint d\mathbf{f}_2 d\mathbf{f}_1\,\{1,\,\mathbf{q}_{f_2p_2}\}_\alpha\,J(\mathbf{k})\,\{1,\,\mathbf{q}_{f_1p_1}\}_\beta \times [(\mathbf{q}_{f_2p_2}^2+\lambda^2)(\mathbf{f}_2^2-\mathbf{p}_2^2-i\varepsilon)(\mathbf{q}_{f_1p_1}^2+\lambda^2)(\mathbf{f}_1^2-\mathbf{p}_1^2-i\varepsilon)]^{-1}$$

$$= \{K_{f_2}(\mathbf{p}_2,\,i\lambda),\ \mathbf{K}_{f_2}(\mathbf{p}_2,\,i\lambda)\}_\alpha\,\{K_{f_1}(\mathbf{p}_1,\,i\lambda),\ \mathbf{K}_{f_1}(\mathbf{p}_1,\,i\lambda)\}_\beta\,J(\mathbf{k})$$

$$= (\pi^2 i)^2\int\limits_0^1 dx_2\Big\{\frac{1}{\Lambda_2}\frac{\partial}{\partial\Lambda_2},\ \frac{\mathbf{B}_2-\mathbf{p}_2}{\Lambda_2}\frac{\partial}{\partial\Lambda_2} + \nabla_{B_2}\Big\}_\alpha \times \int\limits_0^1 dx_1\Big\{\frac{1}{\Lambda_1}\frac{\partial}{\partial\Lambda_1},\ \frac{\mathbf{B}_1-\mathbf{p}_1}{\Lambda_1}\frac{\partial}{\partial\Lambda_1} + \nabla_{B_1}\Big\}_\beta\,R(x_2\,|\,x_1), \tag{A.10}$$

where

$$(\pi^2 i)^2 R(x_2\,|\,x_1) = \frac{1}{4}\int J(\mathbf{k})\,d\mathbf{f}_2\,d\mathbf{f}_1\,/\,[(\mathbf{B}_2-\mathbf{f}_2)^2 - \Lambda_2^2]\,[(\mathbf{B}_1-\mathbf{f}_1)^2-\Lambda_1^2], \qquad \Lambda_2^2 = \mathbf{p}_2^2(1-x_2)^2 - \lambda^2 x_2,$$

$$\mathbf{B}_2 = \mathbf{p}_2 x_2,\ \Lambda_1 = \mathbf{p}_1^2(1-x_1)^2 - \lambda^2 x_1,\ \mathbf{B}_1 = \mathbf{p}_1 x_1,\ \mathbf{k} = \mathbf{f}_2 - \mathbf{f}_1. \tag{A.11}$$

APPENDIX B

In this Appendix we shall separate out of the expressions (A.2), (A.8), and (A.10) those parts which diverge for $\lambda \to 0$.

Since the expressions (A.4) remain finite for $\lambda \to 0$, all divergences are contained in those parts of (A.2), (A.8), and (A.10) which have $\Lambda_{1,2}$ in the denominators; the divergences show up in the integration near $x = y = 1$, where $\Lambda_{1,2}$ has a simple pole (for $\lambda \to 0$). Terms whose numerators vanish at these points are not divergent.

Considering that owing to (A.9) the functions f_2 and R_2 are functions of the product xy with an accuracy up to terms of order λ, we make the transformation of variables $x = x_1$, $xy = x_2$ in all integrals which do not involve an integration over t. Then all divergent terms can be reduced to the following two integrals:

$$I_1 = \int_0^1 \frac{dx_1}{x_1\Lambda_1} F(x_1) = \int_0^1 F(x_1)\, d\Phi_1(x_1), \tag{B.1}$$

$$I_2 = \int_0^1 \frac{dx_1}{x_1\Lambda_1} \int_0^x \frac{dx_2}{x_2\Lambda_2} F(x_2) = \int_0^1 d\Phi_1(x_1) \int_0^1 F(x_2)\, d\Phi_2(x_2), \tag{B.2}$$

where $d\Phi_s(x_s) = dx_s/x_s\Lambda_s$ with $F(0) = 0$.

Integrating (B.1) by parts, we obtain

$$I_1 = \Phi_1(1)\, F(1) - \int_0^1 \Phi_1(x)\, dF(x) = \int_0^1 \{\Phi_1(1) - \Phi_1(x)\}\, dF(x).$$

Analogously, we find for (B.2)

$$\begin{aligned} I_2 = &\int_0^1 \Phi_1(x_1)\, F(x_1)\, d\Phi_1(x_1) \\ &- \int_0^1 d\Phi_1(x_1) \{\Phi_1(x_1 - \Phi_2(x_1)\}\, F(x_1) \\ &- \int_0^1 d\Phi_1(x_1) \int_0^x \Phi_2(x_2)\, dF(x_2). \end{aligned}$$

Considering that $\Lambda_2|_{x_2=x_1} = \Lambda_1 + i\lambda$, we have

$$\Phi_2(x_2)\,|_{x_2=x_1} = \Phi_2(x_2, \Lambda_2)\,|_{x_2=x_1} = \Phi_1(x_1, \Lambda_1 + i\lambda) + O(\lambda)$$

and hence

$$\Phi_1(x_1) - \Phi_2(x_1) = -\sum_{k=1}^{\infty} \frac{1}{k!} \frac{\partial^k}{\partial\Lambda_1^k} \Phi_1(x_1, \Lambda_1)\,(i\lambda)^k.$$

Then we obtain with an accuracy up to terms proportional to λ

$$I_2 = \frac{1}{2} \int_0^1 \{\Phi_1(1) - \Phi_1(x)\}^2\, dF(x) - \zeta F(1),$$

$$\zeta = -\int_0^1 \frac{dx_1}{\Lambda_1} \sum_{k=1}^{\infty} \frac{1}{k!} \frac{\partial^k}{\partial\Lambda_1^k} \Phi_1(x_1, \Lambda_1)\,(i\lambda)^k.$$

Using the explicit form of $\Phi_1(x)$:

$$\Phi_1(x) = \frac{1}{p} \ln \frac{2x}{1 - x + \Lambda_1/p}, \qquad \Phi_1(1) = \ln \frac{2p}{i\lambda}$$

and setting λ equal to zero whereever possible, we obtain finally (with $\zeta = \pi^2/12$)

$$I_1 = \frac{1}{p} \int_0^1 \left(\ln \frac{2p}{\lambda} + \ln \frac{1-x}{ix}\right) dF(x) = \frac{1}{p}\,(a + A(x))\, F(1), \tag{B.3}$$

$$\begin{aligned} I_2 &= \frac{1}{p^2} \frac{1}{2} \left\{ \int_0^1 \left(\ln \frac{2p}{\lambda} + \ln \frac{1-x}{ix}\right)^2 dF(x) - \frac{\pi^2}{6} F(1) \right\} \\ &= \frac{1}{2p^2} \left[(a + A(x))^2 - \frac{\pi^2}{6} \right] F(1); \end{aligned} \tag{B.4}$$

$$a = \ln \frac{2p}{\lambda}, \qquad A^k(x)\, F(1) = \int_0^1 \ln^k \frac{1-x}{ix}\, dF(x).$$

---

[1] R. H. Boyer, Phys. Rev. **117**, 475 (1960).

[2] M. Gavrila, Phys. Rev. **113**, 514 (1959).

[3] H. Mitter and P. Urban, Acta Physica Austriaca **7**, 311 (1953).

[4] V. A. Krutov and V. G. Gorshkov, JETP **39**, 591 (1960), Soviet Phys. JETP **12**, 417 (1961).

Translated by R. Lipperheide
256

SOVIET PHYSICS JETP VOLUME 12, NUMBER 5 MAY, 1961

DISPERSION RELATIONS IN THE NONRELATIVISTIC SCATTERING THEORY WITH SPIN-ORBIT INTERACTION

V. S. BUSLAEV

Leningrad State University

Submitted to JETP editor June 22, 1960

J. Exptl. Theoret. Phys. (U.S.S.R.) **39**, 1422-1426 (November, 1960)

Dispersion relations for the scattering of spin-$\frac{1}{2}$ particles by a potential containing the spin-orbit interaction are derived in the nonrelativistic theory. The behavior of the Green's function of the total Hamiltonian at large complex energies is investigated.

DISPERSION relations (d.r.) for the nonrelativistic scattering amplitude have been considered in a number of papers (see references 1 to 3 and others). These authors assumed that the Hamiltonian is independent of the spin. The simplest method of derivation was based on a study of the behavior of the Green's function of the total Hamiltonian at complex energies E.[3]

In the present paper we consider the scattering of a spin-$\frac{1}{2}$ particle by a potential which includes the spin-orbit interaction. A proof of the d.r. for this case will be given. First we shall study some properties of the Green's function, leaving out a large part of the mathematical details. The latter will be published in a different place. Here we shall make only a few general remarks concerning these questions.

Two estimates are important for the proof of the d.r. with the help of the Green's function: one on the positive half of the real axis, which requires a detailed analysis of the integral equation for the Green's function at finite energies, and another at large energies in the complex plane, based on the Born series, which converges rapidly in this region.

For finite values of E we can investigate the Green's function for our problem with the help of the usual methods.[4,5] However, at large energies these methods must be modified somewhat, since the Born series converges poorly in the presence of the lS interaction. In this connection we propose a certain transformation of the Born series which improves its convergence properties (for large E). This transformation is made possible by the fact that we have been able to calculate explicitly the first term of the asymptotic Green's function for $E \to \infty$.

1. PROPERTIES OF THE GREEN'S FUNCTION

The energy operator of the system has the form

$$H = H_0 + V, \tag{1}$$

where

$$H_0 = -\nabla^2, \qquad V = -iV_1(r)\,[\mathbf{r}\times\nabla]\,\mathbf{S} + V_0(r), \tag{2}$$

and **S** is the vector for spin $\frac{1}{2}$.

The Green's function satisfies the integro-differential equation

$$R(E) = R_0(E) - R_0(E)\,VR(E), \tag{3}$$

where

$$R_0(E) = \frac{1}{4\pi\,|\mathbf{r}-\mathbf{r}'|}\exp\left(i\sqrt{E}\,|\mathbf{r}-\mathbf{r}'|\right). \tag{4}$$

We assume that

$$|V_0(r)| \leqslant \frac{Ce^{-\varkappa r}}{(1+r)^{3+\varepsilon}}; \qquad |V_1(r)|,\ |V_1'(r)| \leqslant \frac{Ce^{-\varkappa r}}{(1+r)^{4+\varepsilon}}$$
$$(\varepsilon > 0,\ \varkappa \geqslant 0). \tag{5}$$

Equation (3) can be written as an integral equation

$$R(E) = R_0(E) - R_0^V(E)\,R(E), \tag{6}$$

where

$$R_0^V(E) \equiv -iV_1(r')[\mathbf{r}'\times\nabla']R_0(\mathbf{r},\mathbf{r}';E)\,\mathbf{S} + V_0(r')\,R_0(\mathbf{r},\mathbf{r}';E). \tag{7}$$

Equation (6) can be investigated by the same methods as in the case where $V_1(\mathbf{r}) = 0$. It can be established that, first, $R(\mathbf{r}, \mathbf{r}', E)$ is analytic in the complex E plane with a cut along the positive part of the real axis with the exception of a finite number of negative poles E_j at the positions of the eigenvalues; second,

$$\operatorname{Res} R(\mathbf{r}, \mathbf{r}'; E)|_{E=E_j} = \sum_k \psi_{jk}(\mathbf{r}) \overline{\psi_{jk}(\mathbf{r}')}, \tag{8}$$

where ψ_{jk} is an orthonormalized eigenfunction corresponding to the eigenvalue E_j; and third,

$$|R(\mathbf{r}, \mathbf{r}'; E)| \leqslant K(|\mathbf{r} - \mathbf{r}'|^{-1} + 1) \tag{9}$$

on the cut.

The direct method of successive approximations for Eq. (6) (Born series) converges poorly even for large energies, since the kernel $R_0^V(E)$ contains $\sqrt{E}$ linearly. This implies that all terms of the series contain contributions which do not vanish as $E \to \infty$. However, by integration by parts, these terms can be separated out explicitly and summed up. As a result we obtain the following expression* for the nonvanishing term $P(E)$ of the asymptotic Green's function $R(E)$ as $E \to \infty$:

$$P(\mathbf{r}, \mathbf{r}'; E) = R_0(\mathbf{r}, \mathbf{r}'; E) \exp\left\{\tfrac{1}{8} iS[\mathbf{r}\times\mathbf{r}'] \int_{-1}^{1} V_1\left(\tfrac{1}{2}(1-\eta)\mathbf{r} + \tfrac{1}{2}(1+\eta)\mathbf{r}'\right) d\eta\right\}. \tag{10}$$

Formula (10) can be proved rigorously by transforming Eq. (6) to the form

$$R(E) = P(E) + \Pi(E) - \Pi^V(E) R(E), \tag{11}$$

$$\Pi(E) = R_0(E) - P(E) - P(E) V R_0(E), \tag{12}$$

where $\Pi^V(E)$ is constructed from $\Pi(E)$ in the same way as $R_0^V(E)$ is from $R_0(E)$.

The method of successive approximations applied to Eq. (11) at high energies converges in the same way as the Born series in the absence of the spin-orbit interaction. We thus obtain the estimate (for large E)

$$|R(\mathbf{r}, \mathbf{r}', E) - P(\mathbf{r}', \mathbf{r}'; E)| \leqslant F(\mathbf{r}, \mathbf{r}'; E) \exp(-\operatorname{Im}\sqrt{E}|\mathbf{r} - \mathbf{r}'|), \tag{13}$$

where $F(\mathbf{r}, \mathbf{r}'; E) \to 0$ for $E \to \infty$ uniformly for any finite region of variation of $\mathbf{r}$ and $\mathbf{r}'$.

2. DERIVATION OF THE DISPERSION RELATIONS

As a complete set of asymptotic states for the scattering we choose the set of functions

$$\Phi_a(\mathbf{r}, \sigma) = \exp(i\sqrt{E}\boldsymbol{\alpha}\mathbf{r}) \chi_m^\alpha(\sigma). \tag{14}$$

Here $a = (E, \boldsymbol{\alpha}, m)$, $\boldsymbol{\alpha}\cdot\boldsymbol{\alpha} = 1$, $m = \pm\frac{1}{2}$, and $\chi_m^\alpha(\sigma)$ is a spinor which has the components $\delta_{m\sigma}$ in a system oriented along the vector $\boldsymbol{\alpha}$.

For the scattering amplitude we use the following expression:

$$f_{ba} = -\frac{1}{4\pi}(\Phi_b; V\Psi_a), \tag{15}$$

where $b = (E, \boldsymbol{\beta}, n)$, $\boldsymbol{\beta}\cdot\boldsymbol{\beta} = 1$, $n = \pm\frac{1}{2}$, and $\Psi_a(\mathbf{r}, \sigma)$ is a solution of the scattering problem

$$\Psi_a = \Phi_a - R(E + i0) V\Phi_a. \tag{16}$$

We then find for f_{ba}

$$f_{ba} = -(1/4\pi)(\Phi_b, V\Phi_a) + (1/4\pi)(V\Phi_b, R(E + i0)V\Phi_a). \tag{17}$$

We introduce the usual notations

$$\boldsymbol{\pi} = |\boldsymbol{\pi}|\mathbf{n} = \tfrac{1}{2}\sqrt{E}(\boldsymbol{\beta} + \boldsymbol{\alpha}); \qquad \boldsymbol{\Delta} = \sqrt{E}(\boldsymbol{\beta} - \boldsymbol{\alpha}), \qquad \mathbf{n}\boldsymbol{\Delta} = 0;$$
$$\boldsymbol{\nu} = [\boldsymbol{\beta}\times\boldsymbol{\alpha}]/\sin\theta, \qquad \cos\theta = \boldsymbol{\beta}\boldsymbol{\alpha}. \tag{18}$$

We shall regard f_{ba} as a function of E, with fixed Δ, $\mathbf{n}$ $(\Delta \leq \kappa/2)$, and spinor variables (f_{ba} depends practically only on E, Δ, and the spinor variables).

We expand the spinors χ_m^α and χ_m^β in terms of the constant spinors $\chi_m^\mathbf{n}$:

$$\chi_m^\alpha = \sum_k \tau_{mk}\left(\frac{\theta}{2}\right)\chi_k^\mathbf{n}, \qquad \chi_m^\beta = \sum_k \tau_{mk}\left(\frac{\theta}{2}\right)(-1)^{m-k}\chi_k^\mathbf{n},$$
$$\tau_{mk}(\theta) = \delta_{mk}\cos\frac{\theta}{2} + i\delta_{m,-k}\sin\frac{\theta}{2}. \tag{19}$$

It is now easily seen that the first term on the right-hand side of formula (17) is analytic in E with a cut along the positive half of the real axis and with a singularity of the type $1/\sqrt{E}$ at $E = 0$.

The second term has the following form in the new variables:

$$\frac{1}{4\pi}(V\Phi_b, R(E)V\Phi_a) = \frac{1}{4\pi}\sum_{k,k'} \tau_{mk}\left(\frac{\theta}{2}\right)\tau_{nk'}\left(\frac{\theta}{2}\right)$$
$$\times \int d\mathbf{r}\, d\mathbf{r}' \exp\left\{-\frac{i}{2}\Delta(\mathbf{r} + \mathbf{r}')\right\} \exp\left\{-i\sqrt{E - \frac{\Delta^2}{4}}\,\mathbf{n} \times (\mathbf{r} - \mathbf{r}')\right\} \{\chi_{k'}^\mathbf{n}, (\sqrt{E}V_1(r)[\mathbf{r}\times\boldsymbol{\beta}]S + V_0(r)) R(\mathbf{r}, \mathbf{r}'; E)$$
$$\times (\sqrt{E}V_1(r')[\mathbf{r}'\times\boldsymbol{\alpha}]S + V_0(r'))\chi_k^\mathbf{n}\}, \qquad \sin\frac{\theta}{2} = \frac{\Delta}{2\sqrt{E}}. \tag{20}$$

If we separate out the poles of $R(\mathbf{r}, \mathbf{r}'; E)$ and apply the integral analog of the Weierstrass theorem,[7] using (9) and (13), we can conclude that the analytic properties of the second term differ from those of the first term described above only by the presence of the additional poles at the points E_j.

It follows from the estimate (13) that the function f_{ba} does not grow faster than E as $E \to \infty$; the leading term of the amplitude f_{ba}^0 for $E \to \infty$ can be easily calculated:

$$f_{ba}^0 = -\frac{1}{4\pi}\sqrt{E}(S[\mathbf{r}\times\boldsymbol{\beta}]V_1\Phi_b, \Psi_a^0), \tag{21}$$

where

---

*Similar formulas [see also Eqs. (21) and (22)] have been considered by many authors for the case $V_1(r) = 0$ in the determination of correction terms to the Born approximation (see, for example, reference 6).

$$\Psi_a^0 = e^{i\sqrt{E}\alpha r} \exp\left\{\frac{i}{4} S[\alpha \times r] \int_0^\infty d\eta V_1(r - \alpha\eta)\right\} \chi_m^\alpha \tag{22}$$

is the leading term of the solution Ψ_a.

We separate out the dependence of $f_{nm}(\Delta, n; E)$ on n, m by writing $f_{nm}(\Delta, n; E)$ in the matrix form

$$f(\Delta, n; E) = A(\Delta, E) + B(\Delta, E) \nu S, \tag{23}$$

where the functions $A(\Delta, E)$ and $B(\Delta, E)$ do not depend any more on m and n. These functions have the properties

$$A(\Delta, E - i0) = \overline{A(\Delta, E + i0)},$$
$$B(\Delta, E - i0) = \overline{B(\Delta, E + i0)}, \tag{24}$$

which probably are most easily obtained by expanding $f(\Delta, E)$ in terms of spherical functions. We conclude from (24) that the residues of $A(\Delta, E)$ and $B(\Delta, E)$ at the points E_j are real.

Thus we have obtained the following dispersion relation for the function $g(E) = A(\Delta, E)$, $B(\Delta, E)$:

$$\operatorname{Re} g(E) = P \frac{1}{\pi} \int_0^\infty \frac{1}{E' - E} \frac{E - E_0}{E' - E_0} \operatorname{Im} g(E') \, dE'$$
$$+ \operatorname{Re} g(E_0) + \sum_j \frac{1}{E - E_j} \frac{E - E_0}{E_j - E_0} d_j^g, \tag{25}$$

where

$$d_j^g = \operatorname{Res} g(E)\big|_{E=E_j}, \tag{26}$$

and E_0 is an arbitrary positive energy. The residues d_j^g are given in terms of the eigenfunctions of the discrete spectrum.

The dispersion relation for $B(\Delta, E)$ can, apparently, be given in a different form, since $\operatorname{Im} B(\Delta, E)$ increases more slowly than $\sqrt{E}$; however, this requires a more detailed investigation of the asymptotic form of $B(\Delta, E)$.

The values of $\operatorname{Im} g(E)$ in the unphysical region $E < \frac{1}{4}\Delta^2$ which enter in the d.r. can be obtained in the usual manner[2,8] by analytic continuation from the physical region, using, for example, the expansion in spherical functions.

In conclusion we note that the modified Born approximation for the scattering amplitude (21) has possible interest for quantitative calculations in cases where the lS interaction cannot be neglected.

The author thanks Prof. O. A. Ladyzhenskaya for her interest in this work and L. D. Faddeev for valuable comment and advice.

---

[1] D. Y. Wong, Phys. Rev. **107**, 302 (1957).

[2] N. N. Khuri, Phys. Rev. **107**, 1148 (1957).

[3] L. D. Faddeev, JETP **35**, 433 (1958), Soviet Phys. JETP **8**, 299 (1959).

[4] R. Jost and A. Pais, Phys. Rev. **82**, 840 (1951).

[5] A. N. Povzner, Математ. сборник (Math Collection) **32**, 1 (1953); Doklady Akad. Nauk SSSR **104**, 360 (1955).

[6] D. S. Saxon and L. I. Schiff, Nuovo cimento **6** 614 (1957).

[7] V. I. Smirnov, Курс высшей математики (Course in Higher Mathematics) **3**, pt. II, GITTL (1953).

[8] A. Klein and S. Zemach, Ann. of Phys. **7**, 440 (1959).

Translated by R. Lipperheide
257

SOVIET PHYSICS JETP VOLUME 12, NUMBER 5 MAY, 1961

ANOMALOUS MAGNETIC MOMENTS OF THE MUON AND OF THE ELECTRON

V. B. BERESTETSKIĬ

Submitted to JETP editor June 2, 1960

J. Exptl. Theoret. Phys. (U.S.S.R.) 39, 1427-1429 (November, 1960)

The dispersion relations and unitarity conditions yield a simple method for calculating the radiative corrections to quantum electrodynamics. A correction to the magnetic moment is calculated by taking into account the "cutoff" at high momenta.

1. Krokhin, Khlebnikov, and the author[1] calculated the anomalous moment of the muon, $\delta\mu$, with allowance for the possible inapplicability of quantum electrodynamics in the region of high momenta. By introducing the Feynman cutoff factor with end-point momentum λ_0, an expression was obtained for $\delta\mu/\mu = (\alpha/2\pi)(1 - \delta F)$. When $m_\mu^2/\lambda_0^2 \ll 1$ (m_μ is the muon mass), the deviation from the Schwinger correction amounts to

$$\delta F = 2m_\mu^2 / 3\lambda_0^2. \tag{1}$$

Recently de Tollis[2] called attention to the fact that the introduction of cutoff multipliers by other methods leads to somewhat different values for δF. The purpose of the present note is to derive an expression $\delta\mu$ with the most illustrative introduction of the end-point momentum, so that the numerical estimate of the value of the expected effect is facilitated.

2. The amplitude of interaction between a muon and an electromagnetic wave, A_σ is characterized by two invariant form factors a and b, according to the general expression

$$\begin{aligned} A_\sigma &= e\bar{u}(p_2)\left\{a(t)\gamma_\sigma + \tfrac{1}{4}b(t)m_\mu^{-1}(\gamma_\sigma\hat{q} - \hat{q}\gamma_\sigma)\right\}u(p_1) \\ &= e\bar{u}(p_2)\left\{[a(t) + b(t)]\gamma_\sigma - \tfrac{1}{2}b(t)m_\mu^{-1}p_\sigma\right\}u(p_1). \end{aligned} \tag{2}$$

Here p_1 and p_2 are the momenta of the muon, $u(p_i)$ are the spinor amplitudes,

$$(\hat{p}_i - m_\mu)u(p_i) = 0, \qquad q = p_1 - p_2, \quad p = p_1 + p_2, \quad t = q^2.$$

The region $t < 0$ corresponds to the radiation or absorption of a wave accompanied by a muon momentum change $p_1 \to p_2$, while the region $t > 4m_\mu^2$ corresponds to the production or annihilation of a pair (with momenta p_1 and $-p_2$). The anomalous magnetic moment is defined by the quantity

$$b(0) = \delta\mu/\mu.$$

To find $b(t)$, we use the dispersion relation

$$b(t) = \frac{1}{\pi}\int\frac{\operatorname{Im} b(t')}{t' - t}\,dt', \tag{3}$$

and to calculate $\operatorname{Im} b(t)$, we can use the unitarity relation

$$2\operatorname{Im} A_\sigma = \sum_n \langle n|q\rangle^* \langle n|p_1, p_2\rangle, \tag{4}$$

where the first bracket in the right half of the equation denotes the amplitude of the transformation of an electromagnetic wave into a certain aggregate of particles n, while the second denotes the amplitude of the conversion of the pair into these particles.

We assume that for values $t < \lambda_0^2$ these amplitudes can be calculated by using the formulas of quantum electrodynamics. If the laws of quantum electrodynamics are violated when $t > \lambda_0^2$, then for lack of something better we must cut off the integral (3) at the value $t' = \lambda_0^2$. Here λ_0 is the limiting value of the pair energy, which is annihilated according to the laws of quantum electrodynamics.

We can now estimate the quantity λ_0 by comparing it with the average electromagnetic radius $(\overline{r^2})^{1/2}$ of the nucleon $\lambda_0^2 \sim 6/\overline{r^2}$. Using the data of Hofstadter, $\overline{r^2} \approx {}^1/_3 m_\pi^2$, where m_π, is the pion mass, we obtain

$$\lambda_0^2 \sim 18m_\pi^2 \approx 36m_\mu^2. \tag{5}$$

3. If we confine ourselves to first-order approximation in $e^2 = \alpha$, the states n can only be two-particle states (an electron or muon pair). Then

$$\langle n|q\rangle^* = e\bar{u}(k_2)\gamma_\sigma u(k_1), \tag{6}$$

where k_1 and $-k_2$ are the momenta of the pair components, and $< n|p_1, p_2 > \equiv < k_1, k_2|p_1, p_2 >$ is the amplitude of the conversion of an electron pair into a muon pair, or the amplitude of scattering of a muon by an antimuon, calculated in the first approximation (in α). The summation in (4) reduces in this case to summation over the polarizations of the particles k_1 and k_2, and integration over the values of k_1 and k_2, as permitted by the conservation laws.

The amplitude of the scattering of a muon by an antimuon has the form

$$\langle k_1,\ k_2 | p_1,\ p_2\rangle = -M + M^{(a)}$$

$$M = \alpha\,[\bar{u}(p_2)\gamma_\rho u(k_2)]\,[\bar{u}(k_1)\gamma_\rho u(p_1)]/(k_1 - p_1)^2, \quad (7)$$

$$M^{(a)} = \alpha\,[\bar{u}(p_2)\gamma_\rho u(p_1)]\,[\bar{u}(k_1)\gamma_\rho u(k_2)]/t. \quad (8)$$

The exchange (annihilation) part of this amplitude $M^{(a)}$ is independent of p_1 and p_2. Therefore the result of its substitution in (4) will not contain p and will make no contribution to Im b. The amplitude of the conversion of an electron pair into a muon pair is also of the form (8), and this process likewise does not contribute to Im b. We note that the corresponding terms in the amplitude A_σ are usually not related to the vertex part Γ_σ, but are described as an effect of vacuum polarization (Π_σ). Thus, if we represent the amplitude A_σ in the form

$$A_\sigma = e\bar{u}(p_2)\{\Gamma_\sigma + \Pi_\sigma\}\,u(p_1),$$

then the form factor b will be contained only in Γ_σ, and for its calculation it is enough to take into account in (3) only the amplitude M.

Substituting in (4) the expressions (6) and (8), we obtain

$$\operatorname{Im}\Gamma_\sigma = -\frac{\alpha}{2\pi}\int \gamma_\rho(\hat{k}_2 + m_\mu)\gamma_\sigma(\hat{k}_1 + m_\mu)\gamma_\rho\delta(k_1^2 - m_\mu^2)\,\delta(k_2^2 - m_\mu^2)\,\frac{d^4k_1 d^4k_2}{(k_1 - p_1)^2} = -\frac{\alpha}{8}\frac{1}{\sqrt{t(t - 4m_\mu^2)}}\int\limits_{-(t-4m_\mu^2)}^{t-4m_\mu^2}\gamma_\rho(\hat{k}_2 + m)\gamma_\sigma(\hat{k}_1 + m)\gamma_\rho\frac{d\nu}{\nu + t - 4m_\mu^2}, \quad (9)$$

where $\nu = (k_1 + k_2)(p_1 + p_2)$. We note that this expression can be obtained from the Feynman diagram for the vertex part, by replacing the product of the Green's function of the muons by double the product of their imaginary parts.[3]

From (9) we obtain

$$\operatorname{Im} b(t) = \frac{\alpha}{4}\frac{4m_\mu^2}{\sqrt{t(t - 4m_\mu^2)}}. \quad (10)$$

This gives, after substitution in (3),

$$b(0) = \frac{1}{\pi}\int\limits_{4m_\mu^2}^{\lambda_0^2}\frac{\operatorname{Im} b(t)}{t}\,dt = \frac{\alpha}{2\pi}\sqrt{1 - \frac{4m_\mu^2}{\lambda_0^2}}, \quad (11)$$

that is,

$$1 - \delta F = \sqrt{1 - 4m_\mu^2/\lambda_0^2}. \quad (12)$$

Using estimate (5), we obtain $\delta F \sim 0.06$.

4. The anomalous magnetic moment of the electron, with allowance for the finiteness of λ_0 (reference 4) can be calculated by the same method. This yields

$$\delta F = 2m_e^2/\lambda_0^2, \quad (13)$$

where m_e is the electron mass.

In view of the smallness of m_e, this correction can be taken into account only with the radiative corrections on the order of α^2 and α^3. At the present time only the correction of order α^2 has been calculated. It corresponds to taking into account also three-particle states (a pair plus a photon). Here

$$2\operatorname{Im} A_\sigma = \Sigma(\Gamma_\sigma M + CB),$$

where Γ_σ is the vertex part, M is the amplitude of scattering of an electron by an electron, calculated with allowance for the first radiative corrections, C is the amplitude of the Compton effect, and B is the amplitude of the bremsstrahlung on the electron (the last two in the first approximation).

For calculation of order α^3, it is necessary to take into account four-particle states (a pair plus two photons and two pairs). We have

$$2\operatorname{Im} A_\sigma = \Sigma(\Gamma_\sigma M + CB + C_{II}B_{II} + BP + C_{II}D),$$

where C_{II} is the amplitude of the double Compton effect, B_{II} is the amplitude of the bremsstrahlung of two photons, P is the amplitude of pair production upon collision of an electron with a positron, and D is the amplitude of scattering of a photon by a photon, taken in first approximation. In amplitudes C and B account should be taken of the first radiative corrections, while second correction should be taken into account in Γ_σ and M.

I am grateful to M. Terent'ev for useful discussions.

---

[1] Berestetskiĭ, Krokhin, and Khlebnikov, JETP **30**, 788 (1959), Soviet Phys. JETP **3**, 761 (1956).

[2] B. de Tollis, Nuovo cimento **16**, 203 (1960).

[3] Mandelstam, Phys. Rev. **115**, 1741 (1959).

Translated by J. G. Adashko
258

SOVIET PHYSICS JETP VOLUME 12, NUMBER 5 MAY, 1961

THE SCATTERING OF SLOW NEUTRONS IN FERRITES AND ANTIFERROMAGNETICS

V. G. BAR'YAKHTAR and S. V. MALEEV

Leningrad Physico-Technical Institute, Academy of Sciences, U.S.S.R. and Physico-Technical Institute, Academy of Sciences, Ukrainian S.S.R.

Submitted to JETP editor July 2, 1960

J. Exptl. Theoret. Phys. (U.S.S.R.) 39, 1430-1436 (November, 1960)

We use the spin-wave method to evaluate cross sections for the elastic scattering of a neutron in ferrites and antiferromagnetics and the cross sections for the scattering of a neutron accompanied by the emission or absorption of one spin wave.

RECENTLY the scattering of slow neutrons has gained ever greater importance as a method for studying solids and liquids. This refers in particular to the study of the energy spectra of different substances. One can, for instance, point to the investigations[1] to determine the spectrum of the elementary excitation in He II, to the steadily increasing number of investigations to study the phonon dispersion law in different crystals, and also to the first attempt to determine the spin wave dispersion law in magnetite.[2]

All these papers are based upon the following fact, first noted by Placzek and Van Hove,[3] that when a neutron is scattered coherently while at the same time one elementary excitation (a phonon, spin wave, and so on) is absorbed or emitted the laws of conservation of energy and momentum are of the form

$$\hbar^2 p^2/2m \mp \varepsilon(\mathbf{k}) = \hbar^2 p'^2/2m, \qquad \mathbf{p} \mp \mathbf{k} = \mathbf{p}' - \boldsymbol{\tau}, \tag{1}$$

where $\hbar\mathbf{p}$ and $\hbar\mathbf{p}'$ are the neutron momenta before and after the scattering, $\hbar\mathbf{k}$ the quasi-momentum of the elementary excitation, $\epsilon(\mathbf{k})$ its energy, and τ a reciprocal lattice vector multiplied by 2π. Here and henceforth the upper sign refers to the scattering of a neutron accompanied by the emission of a quantum and the lower one to the scattering accompanied by the absorption of a quantum.

For given values of $\mathbf{p}$, $\mathbf{p}'$, and τ, the set of equations (1) determines the values of $\mathbf{k}$ and $\epsilon(\mathbf{k})$ uniquely. If the values of $\mathbf{p}$ and τ are given and also the direction of the scattering (the direction of $\mathbf{p}'$), then, for a given dispersion law $\epsilon(\mathbf{k})$, the magnitude of $\mathbf{p}'$ can only take on a finite number of values. At the same time one verifies easily that if more than one elementary excitation quantum takes part in the scattering, the magnitude of $\mathbf{p}'$ can take on a continuous range of values for given values of $\mathbf{p}$, τ, and the direction of the scattering. The energy distribution of neutrons scattered in a given direction has thus steep maxima corresponding to single-quantum scattering events. By determining the positions of these maxima for different scattering angles one can establish the dispersion law for the elementary excitations, using Eqs. (1).

In the present paper we use the phenomenological spin-wave theory to obtain an expression for the cross section for elastic magnetic scattering in antiferromagnetics and ferrites. These yield, in particular, the temperature dependence of the Bragg maxima and also expressions for the cross sections for scattering accompanied by the absorption or emission of one spin wave. These expressions determine also the intensities of the above-mentioned maxima of the single-quantum scattering in the cases considered.

One may also think that processes involving a large number of spin waves will play a small part in substances with a sufficiently high Curie temperature. This statement is proved in the case where the spin-wave energy[4] is $\epsilon(\mathbf{k}) \approx J(ak)^2$, where J is the exchange integral and a the lattice constant.*

It is well known[6] that the matrix element of the magnetic scattering of a neutron by a system of spin waves is of the form

$$V^{A'\mathbf{p}'}_{A\mathbf{p}} = -\frac{4\pi\hbar^2}{m} r_0 \gamma_0 \Big(A' \Big| \sum_l e^{i\mathbf{q}\mathbf{R}_l} F_l(q) S_l^\alpha \Big| A\Big) \{s_n^\beta - e^\alpha(\mathbf{s}_n \mathbf{e})\}, \tag{2}$$

where m is the neutron mass, r_0 the classical electron radius, γ_0 the neutron magnetic moment in nuclear magnetons, A the state of the system before the scattering, A' the state after the scattering, $\mathbf{q} = \mathbf{p} - \mathbf{p}'$ the momentum transfer, $\mathbf{e} = (\mathbf{q}\cdot\mathbf{q})^{-1}$, $\mathbf{s}_n$ the neutron spin, and $\mathbf{S}_l$, $F_l(q)$, and $\mathbf{R}_l$ the spin, the magnetic form factor, and the coordinate of the l-th atom; the summation over l is over all the magnetic atoms of the system.

---

*We use this opportunity to note that although Maleev's statement[4] that multi-magnon scattering processes play a small role is correct, the classification of these processes given by him[4,5] is not altogether correct.

It is convenient to split the sum over l into a sum over the elementary cells of the magnetic lattice and one over the atoms inside the elementary cell.* We then get

$$\sum_l e^{i\mathbf{qR}_l}\mathbf{S}_l = \sum_j e^{i\mathbf{qR}_j}\sum_\nu e^{i\mathbf{qr}_\nu}F_\nu(q)\mathbf{S}_{j\nu}, \tag{3}$$

where j is the index of the elementary cell, and ν the index of the atom inside the elementary cell.

As at the present there exists no consistent microscopic spin-wave theory for antiferromagnetics or ferrites, we shall in the following use the results of a recently developed phenomenological spin-wave theory.[7,8] In this theory the basic role is played by the densities of the magnetic moments $\mathbf{M}_\nu(\mathbf{r})$ of the magnetic sublattices; these can be connected with the atomic spins through the following relation

$$\mathbf{S}_{j\nu} \to (v_0/\mu n)\,\mathbf{M}_\nu(\mathbf{R}_j), \tag{4}$$

where n is the number of atoms in the elementary cell, v_0 the volume of the elementary cell, and μ the electronic magnetic moment. Using Eqs. (3) and (4) we can write the matrix element for the magnetic scattering of a neutron in the form

$$V_{A'A} = -\frac{4\pi\hbar^2}{m}\frac{v_0}{\mu n}r_0\gamma_0\langle A'|\sum_j e^{i\mathbf{qR}_j}\sum_\nu e^{i\mathbf{qr}_\nu}F_\nu(q)M_\nu^\alpha(\mathbf{R}_j)|A\rangle$$
$$\times\ \{s_n^\alpha - e^\alpha(\mathbf{s}_n\mathbf{e})\}. \tag{5}$$

We first of all shall consider elastic scattering. The vectors $\mathbf{M}_\nu(\mathbf{R}_j)$ have non-vanishing diagonal matrix elements only for the components along the corresponding axes of the spontaneous magnetization. Taking the translational symmetry of the sublattice into account, we get thus

$$\langle A|\mathbf{M}_\nu(\mathbf{R}_j)|A\rangle = \boldsymbol{\varepsilon}_\nu M_{0\nu}\{1 - (\mu n/M_{0\nu}v_0)\,n_\nu(A)\}, \tag{6}$$

where $\boldsymbol{\epsilon}_\nu$ is a unit vector in the direction of the magnetization of the sublattice, $M_{0\nu}$ is the maximum density of the magnetic moment, and $(\mu n/M_{0\nu}v_0)\,n(A)$ is the relative average deviation from the maximum magnetization in the state A.

Using Eqs. (5) and (6) we can obtain the following expression for the cross section for the elastic scattering of a neutron

$$\frac{d\sigma_0}{d\Omega} = r_0^2\gamma_0^2\frac{(2\pi)^3}{v_0}\sum_\tau\delta(\mathbf{q}+\tau)\frac{1}{n}\sum_{\nu\nu'}[\boldsymbol{\varepsilon}_\nu\boldsymbol{\varepsilon}_{\nu'} - (\mathbf{e}\boldsymbol{\varepsilon}_\nu)(\mathbf{e}\boldsymbol{\varepsilon}_{\nu'})]S_\nu S_{\nu'}$$
$$\times F_\nu(q)F_{\nu'}^*(q)\exp\{i\mathbf{q}(\mathbf{r}_\nu - \mathbf{r}_{\nu'})\}\exp\{-W_{\nu q}$$
$$-W_{\nu'q}\}[1 - G_\nu(T) - G_{\nu'}(T)], \tag{7}$$

where $S_\nu = v_0M_{0\nu}/n\mu$ is the effective spin of the atoms in the sublattice, $\exp(-W_{\nu q})$ the thermal Debye-Waller factor for the atoms in the sublattice, which is introduced in the usual way, and

$$G_\nu(T) = \langle\frac{\mu n}{M_{\nu 0}v_0}n(A)\rangle_T = \frac{M_{\nu 0} - M_\nu(T)}{M_{\nu 0}} \ll 1 \tag{8}$$

the relative deviation from the spontaneous magnetization of the sublattice from its maximum value ($T \ll \Theta_c$). When deriving Eq. (8) we have used the following well-known relation[9]

$$\frac{n}{N}\sum_{lj}\exp\{i\mathbf{q}(\mathbf{R}_l - \mathbf{R}_j)\} = \frac{(2\pi)^3}{v_0}\sum_\tau\delta(\mathbf{q}+\tau), \tag{9}$$

where N is the number of atoms in the scatterer.

We note that since the magnetic elementary cell is larger than the nuclear elementary cell the Bragg maxima of the magnetic scattering will include some that do not coincide with maxima of nuclear scattering. This fact has already often been used to study the magnetic structure of antiferromagnetics (see, for instance, reference 10). We must also note that the temperature dependence of the Bragg maxima is determined, together with the Debye-Waller factor, by the quantities $G_\nu(T)$. The experimental determination of the temperature dependence of these quantities enables us to find the change in the magnetic moment of the sublattices with temperature. The comparison of this dependence with the theoretically evaluated one is an additional check on the theory.

For a scatterer consisting of two sublattices magnetized in the opposite direction, Eq. (7) can be simplified considerably. We have in that case for antiferromagnetics

$$\frac{d\sigma_0}{d\Omega} = r_0^2\gamma_0^2 S^2\frac{(2\pi)^3}{v_0}|F(q)|^2[1 - 2G(T)]e^{-2W_q}\sum_\tau\delta(\mathbf{q}$$
$$+\tau)(1 - e_z^2)(1 + \cos\mathbf{r}_{12}\tau). \tag{10}$$

When deriving Eq. (10) we took into account the equivalence of the magnetic lattices in an antiferromagnetic.

For ferrites we have

$$\frac{d\sigma_0}{d\Omega} = \frac{1}{2}r_0^2\gamma_0^2\frac{(2\pi)^3}{v_0}\{S_1^2|F_1(q)|^2[1 - 2G_1(T)]e^{-2W_{1q}}$$
$$+ S_2^2|F_2(q)|^2[1 - 2G_2(T)]e^{-2W_{2q}} - 2S_1S_2[1 - G_1(T)$$
$$- G_2(T)]e^{-W_{1q}-W_{2q}}\mathrm{Re}\,F_1(q)F_1^*(q)e^{i(\mathbf{q},\,\mathbf{r}_1-\mathbf{r}_2)}\}\sum_\tau\delta(\mathbf{q}$$
$$+\tau)(1 - e_z^2), \tag{11}$$

---

*In the following we shall talk simply about "an elementary cell" instead of about "a magnetic elementary cell" wherever this cannot leed to any misunderstanding.

where e_z is the component of $\mathbf{e}$ in the direction of the magnetization.

$G(T) =$ [illegible]

For ferrites we have

$G_{1,2}(T) =$ [illegible]

Here β is the magnetic anisotropy constant, and $\gamma \sim \Theta_c/\mu M_0$ (the notation is the same as in reference 11).

We now consider the inelastic scattering of neutrons. We restrict ourselves for the sake of simplicity to the case where the scatterer consists of two sublattices magnetized in opposite directions. To evaluate the matrix elements corresponding to the scattering of a neutron accompanied by the emission or absorption of spin waves we follow Holstein and Primakoff[12] and go over from the operators of the moments $\mathbf{M}_\nu$ to the spin-wave creation operators c_k^+ and annihilation operators c_k. If we are interested in the scattering of a neutron with the emission or absorption of one spin wave, we can restrict ourselves to the first terms in the expansion of the operators of the moments in terms of the spin-wave creation and annihilation operators; this expansion is of the form[11]

$$M_{1k}^{\mp} = M_{1k}^{x} \pm iM_{1k}^{y} = \sqrt{\mu M_{10}} \begin{cases} -u_k c_{1k} + v_k c_{2,-k}^{+} \\ -u_k c_{1,-k}^{+} + v_k c_{2k} \end{cases}, \quad (12)$$

$$M_{2k}^{\mp} = M_{2k}^{x} \pm iM_{2k}^{y} = \sqrt{\mu M_{20}} \begin{cases} -u_k c_{2,-k}^{+} + v_k c_{1,k} \\ -u_k c_{2k} + v_k c_{1,-k}^{+} \end{cases}, \quad (13)$$

where c_{1k}^+ and c_{1k} are the creation and annihilation operators of spin waves with energy ϵ_{1k}, while c_{2k}^+ and c_{2k} are those for spin waves with energy ϵ_{2k}.

In the case of a ferrite, when $M_{10} \sim M_{20}$, the quantities u_k, v_k, and ϵ_k are determined by the equations[11] [for the case where $(ka)^2 \ll 1$]

$$u_k \approx \sqrt{\frac{M_{10}}{M_{10} - M_{20}}} = \sqrt{\frac{s_1}{s_1 - s_2}},$$

$$v_k \approx \sqrt{\frac{M_{20}}{M_{10} - M_{20}}} = \sqrt{\frac{s_2}{s_1 - s_2}}; \quad (14)$$

$$\varepsilon_{1k} \approx \mu (M_{10} - M_{20})^{-1} (\alpha_1 k^2 M_{10}^2$$

$$+ \alpha_2 k^2 M_{20}^2 - 2\alpha_{12} k^2 M_{10} M_{20}) + \mu H,$$

$$\varepsilon_{2k} \approx \mu (M_{10} - M_{20})^{-1} M_{10} M_{20} (\alpha_1 + \alpha_2 - 2\alpha_{12}) k^2$$

$$+ \mu [\gamma (M_{10} - M_{20}) - H]. \quad (15)$$

According to the spin-wave theory, the function $G_\nu(T)$ has for an antiferromagnetic the form

[illegible]

In the case of an antiferromagnetic[13]

$$u_k \approx v_k \approx \sqrt{\gamma\mu M_0/2\varepsilon_k} \gg 1; \quad (16)$$

$$\varepsilon_{1,2} = \mu M_0 \sqrt{2\gamma [\beta + (\alpha - \alpha_{12}) k^2]} \mp \mu H,$$

$$\alpha_1 \sim \alpha_2 \sim \alpha_{12} \sim \Theta_c a^2 (\mu M_0)^{-1}. \quad (17)$$

Using Eqs. (5), (12), and (13) one obtains easily the cross section for the scattering of a neutron accompanied by the emission or absorption of one spin wave

$$\frac{d\sigma_{\pm 1,2}}{d\Omega\, dE'} = \frac{r_0^2 \gamma_0^2}{4} \sqrt{S_1 S_2} \int d\mathbf{k}\, \frac{p'}{p} \sum_{\tau} \delta (\mathbf{q} \mp \mathbf{k} + \tau) \left(n_{1,2} + \frac{1}{2} \pm \frac{1}{2}\right)$$

$$\times \{u_k^2 |F_1(q)|^2 e^{-2W_{1q}} + v_k^2 |F_2(q)|^2 e^{-2W_{2q}}$$

$$- 2u_k v_k e^{-W_{1q} - W_{2q}} \operatorname{Re} F_1(q) F_2^*(q) e^{i\mathbf{q}(\mathbf{r}_1 - \mathbf{r}_2)}\} (1$$

$$+ e_z^2)\, \delta (E - E' \mp \varepsilon_{1,2}(\mathbf{k})),$$

$$n_{1,2}(k) = [\exp \{\varepsilon_{1,2}(k)/T\} - 1]^{-1}. \quad (18)$$

The integration with respect to $\mathbf{k}$ is over the volume of the elementary cell that contains the origin. Consequently, the only terms that do not vanish, in the sum over τ, which occurs in Eq. (18), are those for which the vector $\mathbf{q} + \tau$ lies in the elementary cell of the reciprocal lattice centered about the origin. Then, if $a|\mathbf{q} + \tau| \ll 1$, it is convenient to write Eq. (18) in the form

$$\frac{d\sigma_{\pm 1,2}}{d\Omega\, dE'} \approx \frac{1}{4} S r_0^2 \gamma_0^2 \frac{p'}{p} \frac{\gamma\mu M_0}{\varepsilon (\mathbf{q} + \tau)} \Big[n_{1,2} (\mathbf{q} + \tau)$$

$$+ \frac{1}{2} \pm \frac{1}{2}\Big] |F(\tau)|^2 e^{-2W\tau}$$

$$\times (1 - \cos \mathbf{r}_{12} \mathbf{q}) (1 + \tau_z^2)\, \delta [E - E' \mp \varepsilon_{1,2} (\mathbf{q} + \tau)] \quad (19)$$

in the antiferromagnetic case* and

$$\frac{d\sigma_{\pm 1,2}}{d\Omega dE'} \approx r_0^2 \gamma_0^2 \frac{\sqrt{S_1 S_2}}{4 (S_1 - S_2)} \frac{p'}{p} \Big[n_{1,2} (\mathbf{q} + \tau)$$

$$+ \frac{1}{2} \pm \frac{1}{2}\Big] \{S_1 |F_1(\tau)|^2 e^{-2W_{1\tau}} + S_2 |F_2(\tau)|^2 e^{-2W_{2\tau}}$$

$$- 2\sqrt{S_1 S_2} \operatorname{Re} F_1(\tau) F_2^*(\tau) e^{i(\mathbf{r}_1 - \mathbf{r}_2,\, \tau)}\, e^{-W_{1\tau} - W_{2\tau}}\}$$

$$\times (1 + \tau_z^2)\, \delta [E - E' \mp \varepsilon_{1,2} (\mathbf{q} + \tau)] \quad (20)$$

in the ferrite case.

---

*Elliott and Lowde were the first[14] to obtain this equation from a microscopic spin-wave theory for antiferromagnetics.

One can see from these formulae that the cross section for the scattering of a neutron accompanied by the absorption or emission of a spin wave is proportional to the first power of the temperature in the temperature range $\Theta_C \gg T \gg \epsilon(q + \tau)$, and the scattering in ferrites occurs mainly only when spin waves with energy ϵ_1 take part, since the number of spin waves with energy ϵ_2 is exponentially small $[\sim \exp(-\Theta_C/T)]$. If the temperature is such that $T \ll \epsilon(q + \tau)$ the cross section for the scattering accompanied by the absorption of one spin wave is proportional to $\exp\{-\epsilon(q + \tau)/T\}$ and the cross section for the scattering accompanied by the emission of one spin wave tends to a constant limit which is independent of the temperature.

Let us consider in more detail the scattering cross section in antiferromagnetics. From the expression for the spin wave energy in antiferromagnetics when there is no magnetic field it follows that when

$$|\mathbf{q} + \boldsymbol{\tau}|^2 \ll \beta/(\alpha - \alpha_{12}) \sim \beta\mu M_0/\Theta_c a^2 \ll a^{-2} \qquad (21)$$

the energy of the scattered neutrons is independent of the direction and is given by the expression

$$E' = E \mp \mu M_0 \sqrt{2\beta\gamma}. \qquad (22)$$

The quantity $\mu M_0\sqrt{2\beta\gamma}$ is of the order of several degrees for several antiferromagnetics (MnF_2 and others), and for neutrons with energies of the order of several hundreds of degrees the change in energy is thus several percent. One verifies easily that this lack of dependence of the energy on the scattering angle occurs near those angles where the Bragg condition $|p + \tau| = p$ is satisfied and for which elastic scattering is possible.

It is well known that if the antiferromagnetic is placed in a constant external magnetic field, the structure of the ground state changes,[8,15] in fields $H = \sqrt{2\beta\gamma}(1 + \beta/4\gamma)$. If the magnetic moments are oriented along a chosen axis of the antiferromagnetic, in the absence of a field, then a field $H \gtrsim \sqrt{2\beta\gamma}(1 + \beta/4\gamma)$ causes the magnetic moments of the sublattices to be oriented almost perpendicular to the chosen axis. Together with the change in the ground state, the character of the spin-wave dispersion law is also changed.[8,16] Magnetic and thermal measurements[17] on $CuCl_2 \cdot 2H_2O$ indicate that such a transition indeed takes place. It would be of interest to observe by neutron diffraction the change in the structure of the ground state and, in particular, the change in the spin-wave dispersion law.

We must note that it is experimentally simplest to observe inelastic magnetic scattering in substances with a high Curie temperature (several hundred degrees). The reason is, first, that when inelastic scattering takes place in such substances one can more easily discover a change in the neutron energy (which, roughly speaking, is proportional to Θ_C), and second that the scatterer can be at a relatively high temperature.

Borovik-Romanov[18] has recently studied in detail the magnetic properties of antiferromagnetics with weak ferromagnetism ($MnCO_3$, $CoCO_3$, and others) comparing the experimental data with the results obtained from spin-wave theory. He noted a considerable discrepancy between the experimental and the theoretical results. In view of this it would be very important to establish the spin-wave dispersion law in those substances by studying experimentally neutron scattering accompanied by the absorption or emission of one spin wave. Neutron-scattering experiments with these substances are, however, extremely complicated, as they have a very low Curie temperature (tens of degrees).

The authors express their deep gratitude to A. I. Akhiezer for suggesting this topic and for his interest in this paper.

Note added in proof (October 12, 1960). One should note that near the Bragg maximum for which $\cos(\mathbf{r}_{12} \cdot \boldsymbol{\tau}) = 1$ the cross section for the inelastic scattering in antiferromagnetics [which is given by Eq. (19)] becomes very small. It is then no longer possible to assume that $u_k = v_k$ and we must use Eq. (18) to evaluate the cross section, substituting into it the exact expressions for v_k and u_k given in reference 11.

---

[1] Palevsky, Otnes, Larsson, Pauli, and Stedman, Phys. Rev. **108**, 1346 (1957).

[2] B. N. Brockhouse, Phys. Rev. **106**, 859 (1957).

[3] G. Placzek and L. Van Hove, Phys. Rev. **93**, 1207 (1954).

[4] S. V. Maleev, JETP **34**, 1518 (1958), Soviet Phys. JETP **7**, 1048 (1958).

[5] S. V. Maleev, JETP **33**, 1010 (1957), Soviet Phys. JETP **6**, 776 (1958).

[6] O. Halpern and M. Johnson, Phys. Rev. **55**, 898 (1939).

[7] M. I. Kaganov and V. M. Tsukernik, JETP **34**, 106 (1958), Soviet Phys. JETP **7**, 73 (1958).

[8] E. Turov and Yu. Irkhin, Izv. Akad. Nauk SSSR, Ser. Fiz. **22**, 1168 (1958), Columbia Tech Translations, p. 1158.

[9] A. I. Akhiezer and I. Ya. Pomeranchuk, Некоторые вопросы теории ядра (Some Problems in Nuclear Theory), Gostekhizdat, 1950.

[10] C. G. Shull and J. S. Smart, Phys. Rev. **76**, 1256 (1949).

[11] V. G. Bar'yakhtar and G. I. Urushadze, JETP **38**, 1253 (1960), Soviet Phys. JETP **11**, 905 (1960).

[12] T. Holstein and H. Primakoff, Phys. Rev. **58**, 1098 (1940).

[13] G. I. Urushadze, JETP **39**, 680 (1960), Soviet Phys. JETP **12**, 476 (1960).

[14] R. J. Elliott and R. D. Lowde, Proc. Roy. Soc. (London) **A230**, 46 (1955).

[15] A. Amatuni, Физика металлов и металловедение (Phys. Metals and Metallography) **3**, 411 (1959).

[16] E. A. Turov, JETP **36**, 1254 (1959), Soviet Phys. JETP **9**, 890 (1959).

[17] Van den Handel, Gijsman, and Poulis, Physica **18**, 862 (1952).

[18] A. S. Borovik-Romanov, JETP **36**, 766 (1959), Soviet Phys. JETP **9**, 539 (1959); A. S. Borovik-Romanov and V. Ozhogin, Seventh All-Union Low Temperature Conference, Khar'kov, 1960.

Translated by D. ter Haar
259

SOVIET PHYSICS JETP VOLUME 12, NUMBER 5 MAY, 1961

TEMPERATURE GREEN'S FUNCTION FOR ELECTRONS IN A SUPERCONDUCTOR

G. M. ÉLIASHBERG

Leningrad Physico-Technical Institute, Academy of Sciences, U.S.S.R.

Submitted to JETP editor July 4, 1960

J. Exptl. Theoret. Phys. (U.S.S.R.) **39**, 1437-1441 (November, 1960)

The temperature Green's function for electrons in a superconductor are computed by the diagram technique for $T \neq 0$. An estimate is made of the region near the critical temperature for which the usual analysis, which makes use of a temperature-dependent gap in the excitation spectrum, is no longer valid. The magnitude of this temperature range is of the order of $(2\Delta(0)/\omega_0)^4 T_c$.

A characteristic of the electron excitation spectrum in superconductors is the appearance of an energy gap. Strictly speaking, the gap exists only at zero temperature. However, if we neglect scattering, then we can determine the temperature-dependent gap $\Delta(T)$ for $T > 0$.[1] Scattering leads to the appearance of finite damping in the excitations, which vanishes at $T = 0$ for minimum energy $\Delta(0)$.[2,3] For $T > 0$, even the excitations with energy $\Delta(T)$ have a finite lifetime. The very concept of the gap loses its meaning when the damping becomes comparable with $\Delta(T)$. Further, it will be shown that the temperature range in which it is not possible to use the gap concept is very small.

The most convenient way for studying this problem is the calculation of the Green's function. Without taking damping into account, Gor'kov[4] determined the damping at $T > 0$ for a superconductor with four-fermion interaction. For the problem under consideration, a model with electron-phonon interaction would be more suitable.

In a paper by the author[3] equations were obtained for the functions $G(\epsilon, p)$ and $F(\epsilon, p)$ for $T = 0$. (Similar equations are contained in the work of Buĭkov.[2] The notation used henceforth is that introduced in reference 3.) Using the diagram technique[5,6] for $T \neq 0$, we can immediately write down the corresponding equations for $T > 0$:

$$G(\varepsilon_n, p) = \frac{\varepsilon_n + \xi(p) + \Sigma_1(-\varepsilon_n, p)}{\Omega(\varepsilon_n, p)}, \qquad F(\varepsilon_n, p) = \frac{\Sigma_2(\varepsilon_n, p)}{\Omega(\varepsilon_n, p)}. \tag{1}$$

$$\Omega(\varepsilon_n, p) = [\varepsilon_n - \xi(p) - \Sigma_1(\varepsilon_n, p)][\varepsilon_n + \xi(p) + \Sigma_1(-\varepsilon_n, p)] - [\Sigma_2(\varepsilon_n, p)]^2; \tag{2}$$

$$\Sigma_1(\varepsilon_n, p) = -\frac{T}{(2\pi)^3} \sum_{n'} d\mathbf{p}' \, G(\varepsilon_{n'}, p') D(\varepsilon_n - \varepsilon_{n'}; p - p'),$$

$$\Sigma_2(\varepsilon_n, p) = \frac{T}{(2\pi)^3} \sum_{n'} \int d\mathbf{p}' \, F(\varepsilon_{n'}, p') D(\varepsilon_n - \varepsilon_{n'}; p - p'). \tag{3}$$

Here

$$\varepsilon_n = i(2n+1)\pi T, \qquad \xi(p) = v_0(p - p_0),$$

$$D(\omega_n, q) = \alpha_q^2 \, 2\omega_q / (\omega_n^2 - \omega_q^2), \qquad \omega_n = i2n\pi T.$$

For $q \ll q_{\max}$, the value $\alpha_q^2 = \lambda_0 \pi^2 sq / \sqrt{1 - \lambda_0}\, p_0$, $\omega_q = \sqrt{1 - \lambda_0}\, sq$, s is the velocity of sound ($\hbar = m = 1$).[7]

The function $G(\epsilon_n, p)$ coincides with the analytic continuation of the retardation function $G_R(\epsilon, p)$ $(n > 0)$ and the advance function $G_A(\epsilon, p)$ $(n < 0)$.[5] The same applies to the functions $F(\epsilon_n, p)$, $\Sigma_1(\epsilon_n, p)$ and $\Sigma_2(\epsilon_n, p)$. Making use of these properties, we can go from Eqs. (1) — (3) to integral equations. For this purpose, we note that when $n > 0$ we have the equality

$$\int_{C_1} dz \, G_R(z, p') \, D(\varepsilon_n - z, q) \tanh \frac{z}{2T}$$

$$= 4\pi i T \sum_{n'=0}^{\infty} G(\varepsilon_{n'}, p') D(\varepsilon_n - \varepsilon_{n'}; q)$$

$$+ 2\pi i \alpha_q^2 \left[G_R(\varepsilon_n + \omega_q; p') \tanh \frac{\varepsilon_n + \omega_q}{2T} \right.$$

$$\left. - G_R(\varepsilon_n - \omega_q; p') \tanh \frac{\varepsilon_n - \omega_q}{2T} \right],$$

$$\int_{C_2} dz \, G_A(z, p') D(\varepsilon_n - z, q) \tanh \frac{z}{2T}$$

$$= 4\pi i T \sum_{n'=-1}^{-\infty} G(\varepsilon_{n'}; p') D(\varepsilon_n - \varepsilon_{n'}; q).$$

The contours C_1 and C_2 encompass the upper and lower halfplanes, respectively, while integration over both contours is carried out in a counterclockwise direction. The real axis is a cut.

Since the integrals over the large semicircles are equal to zero, and since we have $G_A(\epsilon') = G_R^*(\epsilon')$ for real $z = \epsilon'$, we can then write

$$\Sigma_1(\varepsilon_n, p) = \frac{i}{2(2\pi)^4}\int_{-\infty}^{\infty} d\varepsilon' \tanh\frac{\varepsilon'}{2T}\, d\mathbf{p}' \,[G_R(\varepsilon', p')$$

$$-G_R^*(\varepsilon', p')]\, D(\varepsilon_n - \varepsilon', p - p')$$

$$+\frac{1}{2(2\pi)^3}\int d\mathbf{p}'\, \alpha^2_{p-p'}\,[G_R(\varepsilon_n + \omega_{p-p'}; p')$$

$$+ G_R(\varepsilon_n - \omega_{p-p'}, p')]\coth\frac{\omega_{p-p'}}{2T}$$

in place of (2). The first component contains only Im G_R. Making use of the well-known relation

$$G_R(\varepsilon, p) = -\frac{1}{\pi}\int_{-\infty}^{\infty}\frac{\operatorname{Im} G_R(\varepsilon', p')}{\varepsilon - \varepsilon' + i\delta}\, d\varepsilon',$$

we can also express the second component in terms of Im G_R. Continuing both sides of the equation analytically from the upper halfplane to the real axis, we get

$$\Sigma_{1R}(\varepsilon, p) = -\frac{1}{(2\pi)^4}\int_{-\infty}^{\infty} d\varepsilon' \int d\mathbf{p}' \operatorname{Im} G_R(\varepsilon', p')$$

$$\times\, \alpha^2_{p-p'}\, \frac{\tanh(\varepsilon'/2T) - \coth(\omega_{p-p'}/2T)}{\varepsilon' - \varepsilon - \omega_{p-p'} - i\delta}$$

$$-\frac{\tanh(\varepsilon'/2T) + \coth(\omega_{p-p'}/2T)}{\varepsilon' - \varepsilon + \omega_{p-p'} - i\delta}\Bigg]. \tag{4}$$

In the isotropic case under consideration, Σ_1 and Σ_2 are practically independent of p for $p \sim p_0$. We divide $\Sigma_{1R}(\epsilon)$ into an odd $f_0(\epsilon)$ and even $\mu_1 + if_1(\epsilon)$. Since the imaginary part of Σ_{1R} is an even function of ϵ, $f_0(\epsilon)$ is real. Let us consider Im $G_R(\epsilon, p)$. Bearing in mind that $\Sigma_1(-\epsilon_n)$ goes over into $\Sigma^*_{1R}(-\epsilon)$ upon analytic continuation from the upper half-plane, we can write

$$G_R(\varepsilon, p) = \frac{\varepsilon - f_0(\varepsilon) - if_1(\varepsilon)}{\Omega(\varepsilon, p)} + \frac{\xi(p) + \mu_1}{\Omega(\varepsilon, p)}.$$

Upon substitution of the second component in (4), we obtain an expression in which the important region of integration is far from the Fermi surface. This gives for the chemical potential μ a correction that is practically independent of T. The contribution of the first component comes from the region close to p_0. Therefore, we can go from integration over p′ to integration over $q = |p - p'|$, $\xi = v_0(p' - p_0)$, and the angle φ. As a result, we obtain the following after integration over ξ:

$$f(\varepsilon) = f_0(\varepsilon) + if_1(\varepsilon) = \frac{1}{8\pi^2 v_0}\int_{-\infty}^{\infty} d\varepsilon' \operatorname{Re}\left\{\frac{\varepsilon' - f(\varepsilon')}{\Omega_1(\varepsilon')}\right\} \operatorname{sign} \operatorname{Im} \Omega_1(\varepsilon')\, \varphi_1(\varepsilon', \varepsilon);$$

$$\varphi_1(\varepsilon', \varepsilon) = \int_0^{q_1} dq\, q\alpha_q^2 \left[\frac{\tanh(\varepsilon'/2T) - \coth(\omega_q/2T)}{\varepsilon' - \varepsilon - \omega_q - i\delta} - \frac{\tanh(\varepsilon'/2T) + \coth(\omega_q/2T)}{\varepsilon' - \varepsilon + \omega_q - i\delta}\right];$$

$$\Omega_1^2(\varepsilon) = [\varepsilon - f(\varepsilon)]^2 - \Sigma_2^2(\varepsilon), \qquad q_1 = \min\{2p_0,\ q_{max}\}.$$

We can establish the fact that sign Im $\Omega_1(\epsilon') = \operatorname{sign} \epsilon'$. If we neglect the imaginary parts of the functions f and Σ_2 in Ω_1 under the integral sign, then it is evident that Re $\Omega_1(\epsilon) = 0$ for $|\epsilon| \leq \Delta$, where $\pm\Delta$ are the roots of the equation $[\epsilon - f_0(\epsilon)]^2 - [\operatorname{Re}\Sigma_2(\epsilon)]^2 = 0$.

Therefore, in the same approximation,

$$\operatorname{Re}\left\{\frac{\varepsilon - f(\varepsilon)}{\Omega_1(\varepsilon)}\right\} = \begin{cases}(\varepsilon - f_0(\varepsilon))/\Omega_1(\varepsilon), & |\varepsilon| > \Delta,\\ 0, & |\varepsilon| < \Delta,\end{cases}$$

and hence

$$f(\varepsilon) = \frac{1}{8\pi^2 v_0}\int_{-\infty}^{\infty} d\varepsilon' \frac{\varepsilon' - f_0(\varepsilon')}{\Omega_1(\varepsilon')}\,\theta(\varepsilon'^2 - \Delta^2)\,\varphi_1(\varepsilon', \varepsilon)\operatorname{sign}\varepsilon',$$

$$\Omega_1(\varepsilon) = [[\varepsilon - f_0(\varepsilon)]^2 - [\operatorname{Re}\Sigma_2(\varepsilon)]^2]^{1/2}. \tag{5}$$

An estimate will be given below of the imaginary parts, from which the limits of applicability of the approximations will be clear.

We note that only the possibility of discarding the imaginary parts for $\epsilon \lesssim \Delta$ is of importance for us. As will be seen, this possibility vanishes only in the immediate vicinity of the transition point. As in reference 3, we define the function $Q(\epsilon) = \Sigma_2(\epsilon)(1 - f(\epsilon)/\epsilon)^{-1}$. From the definition of Δ as a root of the equation $\Omega_1^2(\epsilon) = 0$, it follows that $\Delta = Q(\Delta)$. Replacing $Q(\epsilon)$ under the radical in the expression for Ω_1 by the constant Δ, we rewrite (5) in the following form:

$$f(\varepsilon) = \frac{1}{8\pi^2 v_0}\int_{\Delta}^{\infty} d\varepsilon' \frac{\varepsilon'}{\sqrt{\varepsilon'^2 - \Delta^2}}\int_0^{q_1} dq\, q\alpha_q^2 \left[\left(\tanh\frac{\varepsilon'}{2T} + \coth\frac{\omega_q}{2T}\right)\right.$$

$$\times\left(\frac{1}{\varepsilon' + \varepsilon + \omega_q + i\delta} - \frac{1}{\varepsilon' - \varepsilon + \omega_q - i\delta}\right)$$

$$+\left(\tanh\frac{\varepsilon'}{2T} - \coth\frac{\omega_q}{2T}\right)\left(\frac{1}{\varepsilon' - \varepsilon - \omega_q - i\delta}\right.$$

$$\left.\left.-\frac{1}{\varepsilon' + \varepsilon - \omega_q + i\delta}\right)\right]. \tag{6}$$

The real part of this expression $f_0(\epsilon)$ does not differ appreciably from its value for T = 0. We consider the imaginary part $f_1(\epsilon)$ in more detail:

$$f_1(\varepsilon) = -\frac{1}{8\pi^2 v_0}\int_{\Delta}^{\infty} d\varepsilon' \frac{\varepsilon'}{\sqrt{\varepsilon'^2-\Delta^2}}\int_0^{q_1} dq\, q\alpha_q{}^2 \Big[\Big(\tanh\frac{\varepsilon'}{2T}$$

$$+ \coth\frac{\omega_q}{2T}\Big)\left(\delta(\varepsilon'+\varepsilon+\omega_q)+\delta(\varepsilon'-\varepsilon+\omega_q)\right)$$

$$+\Big(\coth\frac{\omega_q}{2T}-\tanh\frac{\varepsilon'}{2T}\Big)\big(\delta(\varepsilon'-\varepsilon-\omega_q)$$

$$+\delta(\varepsilon'+\varepsilon-\omega_q)\big)\Big]. \tag{7}$$

The first component vanishes for $|\epsilon| \leq \Delta$. The second component is different from zero for all ϵ but vanishes for $T = 0$. The greatest interest for us lies in $f_1^{(2)}(\epsilon)$, since it determines the magnitude of the damping of excitations with minimum energy Δ. Moreover, the imaginary part of $G_R(\epsilon, p)$ is connected with $f_1^{(2)}(\epsilon)$ for $\epsilon \leq \Delta$.

Since the small $\omega_q \sim T \ll \Theta$ (Θ is the Debye temperature) make a contribution to $f_1^{(2)}$, we can write

$$f_1^{(2)}(\varepsilon) = -\frac{\pi\lambda_0}{(1-\lambda_0)^2}\frac{1}{\omega_0{}^2}\int_{\Delta}^{\infty} d\varepsilon' \frac{\varepsilon'}{\sqrt{\varepsilon'^2-\Delta^2}}$$

$$\times\left\{\frac{\varepsilon'^2+\varepsilon^2}{e^{\varepsilon'/T}+1}+\frac{(\varepsilon'-\varepsilon)^2}{e^{(\varepsilon'-\varepsilon)/T}-1}+\frac{(\varepsilon'+\varepsilon)^2}{e^{(\varepsilon'+\varepsilon)/T}-1}\right\}, \tag{8}$$

where $\omega_0 = 2sp_0$.

Let us consider some limiting cases.

1. $T \ll \Delta$, $(\Delta - \epsilon)/T \gg 1$. In this case, the imaginary part is an exponentially small quantity:

$$f_1^{(2)}(\varepsilon) = -\frac{\pi^{3/2}\lambda_0}{(1-\lambda_0)^2}\left(\frac{T}{2\Delta}\right)^{1/2}\frac{1}{\omega_0^2}[\varepsilon^2+\Delta^2$$

$$+(\varepsilon+\Delta)^2 e^{-\varepsilon/T}+(\Delta-\varepsilon)^2 e^{\varepsilon/T}]\, e^{-\Delta/T}\Delta. \tag{9}$$

2. $T \ll \Delta$, $(\Delta - \epsilon)/T \ll 1$. For ϵ sufficiently close to Δ, the dependence of $f_1^{(2)}$ on T become a power dependence:

$$f_1^{(2)}(\varepsilon) = -\frac{\pi^{3/2}\lambda_0}{(1-\lambda_0)^2}\left(\frac{T}{\omega_0}\right)^2\left(\frac{T}{2\Delta}\right)^{1/2}\Delta. \tag{10}$$

3. $T \gg \Delta$, $\epsilon \lesssim \Delta$. In this case the expression does not contain Δ and therefore coincides with that part of the damping of the excitations in the normal metal which is connected with the absorption of phonons:

$$f_1^{(2)}(\varepsilon) = -\frac{4\pi\lambda_0}{(1-\lambda_0)^2}\left(\frac{T}{\omega_0}\right)^2 T\int_0^{\infty} dx\, \frac{x^2 e^x}{e^{2x}-1}$$

$$\approx -\frac{8{,}2\,\pi\lambda_0}{(1-\lambda_0)^2}\left(\frac{T}{\omega_0}\right)^2 T. \tag{11}$$

The equation for $\Sigma_2(\epsilon)$ can be obtained by starting out from the same considerations as in the derivation of (6). We write out the result:

$$Q(\varepsilon) \equiv \frac{\Sigma_2(\varepsilon)}{1-f(\varepsilon)/\varepsilon} = \frac{1}{8\pi^2 v_0}\frac{1}{1-f(\varepsilon)/\varepsilon}\int_{\Delta}^{\infty} d\varepsilon' \frac{C(\varepsilon')}{\sqrt{\varepsilon'^2-\Delta^2}}$$

$$\times\int_0^{q_1} dq\,q\,\alpha_q^2\Big[\Big(\tanh\frac{\varepsilon'}{2T}+\coth\frac{\omega_q}{2T}\Big)\Big(\frac{1}{\varepsilon'+\varepsilon+\omega_q+i\delta}$$

$$+\frac{1}{\varepsilon'-\varepsilon+\omega_q-i\delta}\Big)+\Big(\coth\frac{\omega_q}{2T}-\tanh\frac{\varepsilon'}{2T}\Big)$$

$$\times\Big(\frac{1}{\varepsilon'-\varepsilon-\omega_q-i\delta}+\frac{1}{\varepsilon'+\varepsilon-\omega_q+i\delta}\Big)\Big]. \tag{12}$$

Here $C(\epsilon) = \operatorname{Re} Q(\epsilon)$. It is not difficult to prove that the equation can be written in the following form, with accuracy up to quantities of the order of $(T_c/\omega_0)^2$:

$$C(\varepsilon) = \frac{1}{4\pi^2 v_0}\frac{1}{1-f_0(\varepsilon)/\varepsilon}\int_{\Delta}^{\infty} d\varepsilon' \frac{C(\varepsilon')}{\sqrt{\varepsilon'^2-\Delta^2}}$$

$$\tanh\frac{\varepsilon'}{2T}\int dq\,q\,\alpha_q^2\Big(\frac{1}{\varepsilon'+\varepsilon+\omega_q}+\frac{1}{\varepsilon'-\varepsilon+\omega_q}\Big). \tag{13}$$

This equation differs from Eq. (37) of reference 3 only in the presence of $\tanh(\epsilon'/2T)$. Thanks to this, the usual relation between T_c and $\Delta(0)$ is preserved. The imaginary part of $\Sigma_2(\epsilon)$, together with Δ, vanishes for $T = T_c$ and therefore is of no interest to us.

In conclusion, let us consider the problem of at what temperatures $f_1(\epsilon)$ becomes comparable with Δ and when the concept of shell loses its meaning. It follows from (11) that $|f_1|/\Delta \sim 1$ for $\Delta/T_c \sim (8\pi\lambda_0/(1-\lambda_0)^2)(T_c/\omega_0)^2$, i.e.,

$$T_c - T \sim \frac{64\,\lambda_0^2}{(1-\lambda_0)^4}\left(\frac{T_c}{\omega_0}\right)^4 \approx \frac{0.4\lambda_0^2}{(1-\lambda_0)^4}\left(\frac{2\Delta(0)}{\omega_0}\right)^4.$$

Since $T_c \ll \omega_0$ for all known superconductors, the interval of temperatures close to T_c in which the usual approach becomes unsuitable is very small. Even for lead, for which T_c/ω_0 is comparatively large (~ 0.1), the value $(T_c - T)/T_c \lesssim 0.01$.

The author is very grateful to L. É. Gurevich for his constant attention to the research.

---

[1] Bardeen, Cooper, and Schrieffer, Phys. Rev. **108**, 1175 (1957).

[2] M. V. Buĭkov, Doklady Akad. Nauk SSSR **132**, 561 (1960), Soviet Phys.-Doklady **5**, 544 (1960).

[3] G. M. Eliashberg, JETP **38**, 966 (1960), Soviet Phys. JETP **11**, 689 (1960).

[4] L. P. Gor'kov, JETP **34**, 735 (1958), Soviet Phys. JETP **7**, 505 (1958).

[5] Abrikosov, Gor'kov, and Dzyaloshinskiĭ, JETP **36**, 900 (1959), Soviet Phys. JETP **9**, 636 (1959).

[6] E. S. Fradkin, JETP **36**, 1286 (1959), Soviet Phys. JETP **9**, 912 (1959).

[7] A. B. Migdal, JETP **34**, 1438 (1958), Soviet Phys. JETP **7**, 996 (1958).

Translated by R. T. Beyer
260

SOVIET PHYSICS JETP VOLUME 12, NUMBER 5 MAY, 1961

SEMI-ANALYTICAL SOLUTION OF EQUATIONS OF THE CHEW-MANDELSTAM TYPE

Yu. A. SIMONOV and K. A. TER-MARTIROSYAN

Submitted to JETP editor July 23, 1960

J. Exptl. Theoret. Phys. (U.S.S.R.) **39**, 1442-1449 (November, 1960)

A simple method for solving equations of the Chew-Mandelstam type is proposed, which rapidly yields an approximate solution. The method is applied to the Chew-Mandelstam equation for the interaction of neutral and charged pions. The results of the first approximation in the case of charged pions are compared with the numerical calculation of Chew, Mandelstam, and Noyes.

1. INTRODUCTION

As is well known, the unitarity conditions and the analyticity properties lead in the two-particle approximation[1-4] to a closed system of equations[5,6] for the spectral functions $A_{ij}(s, s')$ and $a_i(s)$ $(i = 1, 2, 3)$ of the Mandelstam representation. The Chew-Mandelstam equation[4] for the functions $a_i(s)$ results from the above equations if the contributions from the functions $A_{ij}(s, s')$ are neglected. With the help of the solutions of these equations a first approximation can also be obtained for the functions $A_{ij}(s, s')$, and then first-order corrections to the solution $a_i(s)$ of the Chew-Mandelstam equation. Thus the solution of a Chew-Mandelstam type equation may be viewed as the first step of an iteration procedure for the solution of the complete set of equations for the spectral functions $A_{ij}(s, s')$ and $a_i(s)$. We outline below a simple method for solving equations of the Chew-Mandelstam type, which makes it possible to obtain rapidly an approximate solution and investigate its properties.

The method to be proposed is analogous to the well-known method of Dalitz, Dyson, and Castillejo.[7] If the values of the coupling constant lie in a certain region the solution is obtained in the form of analytic functions, the coefficients of these functions being solutions of a system of algebraic equations. They depend on the coupling constant and can be determined by numerical calculations (or even analytically, in the simplest approximation).

The method is applicable in the low-energy region, i.e., precisely where the two-particle approximation, used in the derivation of the equations, makes sense. Even the first approximation gives usually good results in this region.

In the present note we shall demonstrate the basic ideas of this solution on the simplest example: the $\pi\pi$ interaction between neutral and charged mesons. We hope to report later on a number of other cases of physical interest.

2. THE INTERACTION OF NEUTRAL PIONS

The Chew-Mandelstam equation for the amplitude for the interaction of neutral pions

$$A_0(\nu) = [(1+\nu)/\nu]^{1/2} e^{i\delta_0} \sin\delta_0$$

$(\nu = q^2/\mu^2$, q is the momentum in the barycentric frame, δ_0 is the phase shift) has the following form:[4,6]

$$A_0(\nu) = -\lambda + \frac{1}{\pi}\int_0^\infty \sqrt{\frac{\nu'}{1+\nu'}}\left(\frac{1}{\nu'-\nu} - \frac{1}{\nu'-\nu_0}\right)|A_0(\nu')|^2 d\nu' + \frac{2}{\pi}\int_{-\infty}^{-1}\left(\frac{1}{\nu'-\nu} - \frac{1}{\nu'-\nu_0}\right)\frac{d\nu'}{\nu'}\int_0^{-\nu'-1}\sqrt{\frac{\nu''}{1+\nu''}} \times |A_0(\nu'')|^2 d\nu'', \qquad (1)$$

where $\lambda = -A_0(\nu_0)$, ν_0 being the point at which the subtraction was performed.

Similar to the case of the πN interaction in the static model,[7] it is convenient to deal with the inverse amplitude $h(\nu) = A_0^{-1}(\nu)$. At that we shall consider only that solution of Eq. (1) which has no zeros in the complex ν plane. Then $h(\nu)$ has the same analyticity properties as $A_0(\nu)$; the imaginary part of $h(\nu)$ along the cuts is easily determined from Eq. (1).

As a result we obtain for $h(\nu)$ the equation

$$h(\nu) = -\frac{1}{\lambda} - \frac{1}{\pi}\int_0^\infty \sqrt{\frac{\nu'}{1+\nu'}}\left(\frac{1}{\nu'-\nu} - \frac{1}{\nu'-\nu_0}\right)d\nu' - \frac{2}{\pi}\int_{-\infty}^{-1}\left(\frac{1}{\nu'-\nu} - \frac{1}{\nu'-\nu_0}\right)|h(\nu')|^2\frac{d\nu'}{\nu'}\int_0^{-1-\nu'}\sqrt{\frac{\nu''}{1+\nu''}} \times \frac{d\nu''}{|h(\nu'')|^2}. \qquad (2)$$

This equation is inconvenient as it stands, because the integrations on the right hand side extend to infinity (and divergent integrals are obtained when the integrands are expanded in powers of ν'). It is useful to introduce in place of ν the variable $x = \nu/(1+\nu)$, which covers the range $0 \leq x \leq 1$ when $0 \leq \nu \leq \infty$, and in place of ν' the variable $y = \nu'/(1+\nu')$ in the first integral and $y = (1+\nu')/\nu'$ in the second integral. Equation (2) then reduces to the simple form $(\eta = \nu''/(1+\nu''))$:

$$h(x) = C + \frac{x}{\pi}\int_0^1 \frac{dy}{\sqrt{y}\,(x-y)} + \frac{2}{\pi}\int_0^1 \frac{y^{3/2}v(y)\,dy}{1/x - y}, \tag{3}$$

$$v(y) = \frac{1-y}{y^{3/2}}\int_0^y \left|\frac{h(1/y)}{h(\eta)}\right|^2 \frac{\sqrt{\eta}\,d\eta}{(1-\eta)^2}, \tag{4}$$

where $C = h(0)$.

To the value $\nu = \nu_0$ corresponds $x = x_0$, with $h(x_0) = -\lambda^{-1}$. Setting in Eq. (3) $x = x_0$ we obtain

$$C = -\lambda^{-1} - \frac{x_0}{\pi}\int_0^1 \frac{dy}{\sqrt{y}\,(x_0-y)} - \frac{2}{\pi}\int_0^1 \frac{y^{3/2}v(y)\,dy}{1/x_0 - y}. \tag{5}$$

To the value $\nu_0 = -2/3$ corresponds $x_0 = -2$.

We next study the properties of the function $v(y)$. In order to solve the Eqs. (3) and (4) it is sufficient to determine $v(y)$ in the region $0 \leq y \leq 1$; it follows from Eq. (4) that in that region $v(y) > 0$. Transposing in Eq. (4) the factor multiplying the integral to the left and differentiating with respect to y we obtain

$$\frac{d}{dy}\left[\frac{y^{3/2}v(y)}{(1-y)\,|h(1/y)|^2}\right] = \frac{y^{1/2}}{(1-y)^2\,|h(y)|^2}, \tag{6}$$

$$y(1-y)(\tilde{u}v' - \tilde{u}'v)u + \tfrac{1}{2}(3-y)\tilde{u}uv = \tilde{u}^2, \tag{7}$$

where $u(y) = |h(y)|^2$, $\tilde{u}(y) = |h(1/y)|^2$ and the prime denotes everywhere differentiation with respect to y.

One deduces easily from Eqs. (4) and (3) [or (6) and (3)] that $v(0)$ is a finite quantity. Furthermore, it can be shown that $y = 0$ is altogether not a singular point of the function $v(y)$, i.e., that $v(y)$ can be expanded in a Taylor series about $y = 0$. In addition, it follows from Eqs. (4) and (6) that the function $v(y)$ is finite at $y = 1$ and that as y approaches 1 the function $v(y)$ becomes

$$v(y) \approx 1 + a[\ln(1/y)]^{-1}, \tag{8}$$

where a is some constant.

Thus $v(y)$ is a positive function varying between $v(0) = \alpha_0$ at $y = 0$ and $v = 1$ at $y = 1$. We shall seek an expression for it in the form of a polynomial of degree N:

$$v(y) = \sum_{n=0}^{N} \alpha_n y^n. \tag{9}$$

To find the coefficients α_n we choose N+1 points in the interval $0 \leq y \leq 1$ and require Eq. (7) to be satisfied at these points. We then obtain a system of N+1 nonlinear algebraic equations for the N+1 coefficients α_n.

The main idea of our method has to do with the circumstance that the Eq. (1) was derived in the two-particle approximation and therefore can be valid only for small values of x (not close to unity). The whole scheme will be self consistent if on the right hand side of Eq. (3) values of $v(y)$ for y near unity are unimportant. It is therefore natural to require Eq. (7) to be satisfied at the point $y = 0$ for the case $N = 0$, at the points $y = 0$ and $y = 1/2$ for the case $N = 1$, etc.

In the first approximation we set $v(y) = \alpha_0$. Then Eq. (7), evaluated at the point $y = 0$, yields

$$\tfrac{3}{2}\alpha_0 u(0) = \tilde{u}(0). \tag{10}$$

On the other hand, substituting Eq. (9) into Eq. (3) we obtain

$$h(x) = C + \frac{2}{\pi}\Big[xJ_0(1/x) + 2\sum_{n=0}^{N}\alpha_n J_{2n+4}(x)\Big]$$
$$- i\sqrt{x}\,\theta(1-x) + 2ix^{-3/2}\sum_{n=0}^{N}\alpha_n x^{-n}\theta(x-1),$$

$$J_n(x) = \tfrac{1}{2}\,\mathrm{P}\int_0^1 \frac{y^{n-1)/2}}{1/x - y}\,dy = -\frac{1}{n-1} + \frac{1}{x}J_{n-2}(x). \tag{11}$$

Here P denotes the principal-value integral.

In order to calculate $u(0) = |h(0)|^2$ and $\tilde{u}(0) = |h(\infty)|^2$ we make use of Eq. (11) in which we keep only the first term in the summation over n. As a result we obtain from Eq. (10)

$$\alpha_0 = \frac{2}{3}\,\frac{(1-\eta)^2}{1 - 8\eta(1-\eta)/9 + \sqrt{1 - 16\eta(1-\eta)/9}},$$

$$\eta = -\frac{2}{\pi C}. \tag{12}$$

In this approximation the constant η is related to the four-boson interaction constant λ by

$$\frac{2}{\pi\eta} = \frac{1}{\lambda} + \frac{2}{\pi}x_0 J(1/x_0) + \frac{4}{\pi}\alpha_0 J_4(x_0). \tag{13}$$

In the next higher approximation we seek a $v(y)$ in the form $v(y) = \alpha_0 + \alpha_1 y$ and determine α_0 and α_1 from Eq. (7) evaluated at the points $y = 0$ and $y = 1/2$. The equations for α_0 and α_1 are of the form

$$\tfrac{3}{2}\alpha_0 = \Big[1 - \eta\Big(1 - \tfrac{2}{3}\alpha_0 - \tfrac{2}{5}\alpha_1\Big)\Big]^2,$$

$$\alpha_1 = 2\,\frac{4\tilde{u}^2(1/2) - 5\tilde{u}(1/2)\,u(1/2)\,\alpha_0 + \tilde{u}'(1/2)\,u(1/2)\,\alpha_0}{u(1/2)\,[7\tilde{u}(1/2) - \tilde{u}'(1/2)]}. \tag{14}$$

Here $\tilde{u}(1/2)$, $u(1/2)$, and $\tilde{u}'(1/2)$ are expressed in terms of α_0 and α_1 according to Eq. (11). These equations are solved very simply by the iteration

TABLE I

η	-0.4	-0.3	-0.2	-0.1	0	0.1	0.15
α_0	0.82	0.84	0.8	0.74	0.67	0.57	0.49
α_1	-0.34	-0.05	-0.02	0.06	0.19	0.48	0.88

method, where we ignore in the first approximation those terms in the right hand sides which contain α_1. Then the first equation in (14) yields for α_0 the same value as is given by Eq. (12), and the second equation in (14) gives α_1 in terms of C and α_0, whose dependence on λ is already determined with the help of (14).

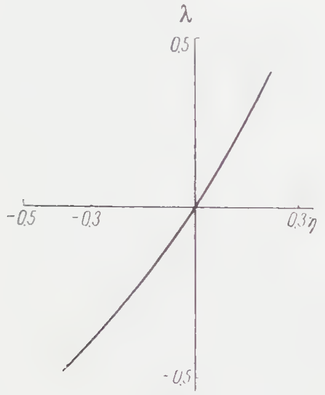

FIG. 1

We have solved the system (14) numerically. In Table I we give values of α_0 and α_1 for various values of η. If we substitute into Eq. (5) $v(y) = \alpha_0 + \alpha_1 y$ and use for α_0 and α_1 values from Table I, we can obtain η as a function of λ (Fig. 1). From here one obtains easily α_0 and α_1 as functions of λ (Fig. 2). A solution for the system (14) exists only in the region $-0.4 \leq \eta \leq 0.15$ or $-0.5 \leq \lambda \leq 0.25$. At the limits of this region α_1 becomes infinite from which it follows that the amplitude $A_0(\nu)$ vanishes identically.

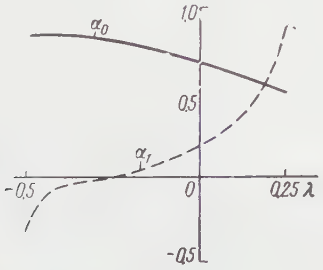

FIG. 2

Equation (1) was also solved numerically. The limiting values for λ as obtained by this method were almost the same: $-0.6 \leq \lambda \leq 0.25$. The curves in Figs. 3 and 4 represent the dependence of $-\frac{1}{2}\pi\eta\sqrt{x}\cot\delta_0 = -\frac{1}{2}\pi\eta \operatorname{Re} h(x)$ on $\nu = 1/(1-x) = q^2/\mu^2$. The solid curves represent the first approximation constructed according to Eqs. (11) and (14). For all λ, with the exception of values in the immediate vicinity of the limiting values, the first and second approximations practically coincide (for such λ a single curve is shown in Fig. 3). For values close to the limiting values the second approximation gives a significant correction. The second approximation curves are shown in Figs. 3 and 4 by dotted lines.

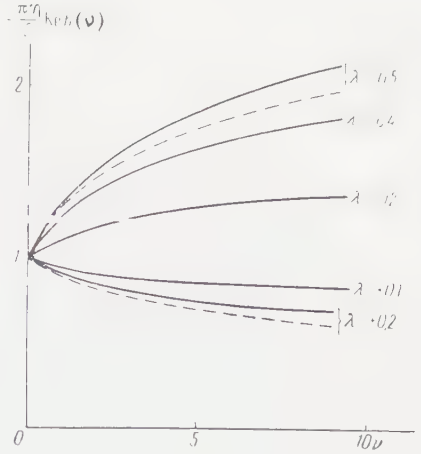

FIG. 3

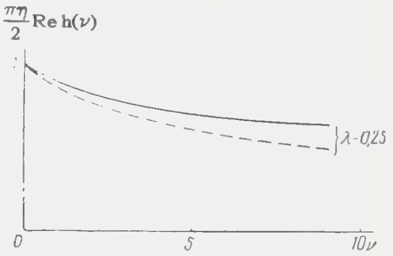

FIG. 4

3. INTERACTION OF CHARGED MESONS

The equations appropriate to this case were given by Chew and Mandelstam.[4] As in the neutral mesons case we introduce the quantities $h_0(x) = [A_0^0(x)]^{-1}$, $h_2(x) = [A_0^2(x)]^{-1}$, $h_1(x) = [A_1^1(x)]^{-1}$; the upper index denotes the isotopic spin, the lower index denotes the orbital angular momentum. We then obtain the following system of equations for the functions $h_i(x)$ $(i = 0, 2)$ and $h_1(x)$:

$$h_i(x) = C_i + \frac{x}{\pi}\int_0^1 \frac{dy}{\sqrt{y}\,(x-y)} + \frac{1}{\pi}\int_0^1 \frac{y^{3/2} v_i(y)\,dy}{1/x-y}, \quad (15)$$

$$h_1(x) = C_1 + \frac{x}{\pi}\int_0^1 \frac{\sqrt{y}\,dy}{x-y} + \frac{1}{\pi}\int_0^1 \frac{y^{5/2} v_1(y)\,dy}{1/x-y}; \quad (16)$$

$$C_i = -\binom{(5\lambda)^{-1}}{(2\lambda)^{-1}} - \frac{x_0}{\pi}\int_0^1 \frac{dy}{\sqrt{y}\,(x_0-y)} - \frac{1}{\pi}\int_0^1 \frac{y^{3/2} v_i(y)\,dy}{1/x_0-y}, \quad (17)$$

$$C_1 = \left\{ \frac{1}{\pi} \int_0^1 \left[\frac{\sqrt{y}}{|h_1(y)|^2} - \frac{y^{3/2} v_1(y)}{|h_1(1/y)|^2} \right] dy \right\}^{-1}. \quad (18)$$

The expressions for $v_i(y)$ and $v_1(y)$ are of the form

$$v_i(y) = (1-y) \left| h_i\left(\frac{1}{y}\right) \right|^2 y^{-3/2} \int_0^y \frac{\eta d\eta}{(1-\eta)^2} \left\{ \frac{\alpha_{i0}}{|h_0(\eta)|^2} \right.$$

$$\left. + \frac{\alpha_{i2}}{|h_2(\eta)|^2} + \alpha_{i1} 3 \left(1 - 2\frac{y(1-\eta)}{\eta(1-y)}\right) \frac{\eta^2}{|h_1(\eta)|^2} \right\}, \quad (19)$$

$$v_1(y) = (1-y) \left| h_1\left(\frac{1}{y}\right) \right|^2 y^{-3/2} \int_0^y \frac{\sqrt{\eta}d\eta}{(1-\eta)^2} \left(1 - \frac{1-y}{1-\eta}\right)$$

$$\times \left\{ \frac{\alpha_{10}}{|h_0(\eta)|^2} + \frac{\alpha_{12}}{|h_2(\eta)|^2} \right.$$

$$\left. + 3\alpha_{11} \left(1 - 2\frac{y(1-\eta)}{\eta(1-y)}\right) \frac{\eta^2}{|h_1(\eta)|^2} \right\}, \quad (20)$$

where α_{ik} is a known matrix:[4]

$$\alpha_{ik} = \begin{pmatrix} 2/3 & 10/3 & 2 \\ 2/3 & 1/3 & -1 \\ 2/3 & -5/3 & 1 \end{pmatrix}. \quad (21)$$

Transfering the factor multiplying the integrals on the right hand sides of the Eqs. (19) and (20), and differentiating with respect to y, we obtain equations for $v_i(y)$ and $v_1(y)$ analogous to Eq. (7) in the case of neutral mesons. These equations are now much more involved:

$$y(1-y)(v_i'\tilde{u}_i - v_i\tilde{u}_i') + \frac{1}{2}(3-y)\tilde{u}_i v_i = \tilde{u}_i^2 \left\{ \frac{\alpha_{i0}}{u_0(y)} + \frac{\alpha_{i2}}{u_2(y)} \right.$$

$$\left. - \frac{3\alpha_{i1} y^2}{u_1(y)} - 6\alpha_{i1} y^{-1/2} \int_0^y \frac{\eta^{3/2} d\eta}{(1-\eta)|h_1(\eta)|^2} \right\}, \quad i = 0.2; \quad (22)$$

$$y(1-y)(v_1'\tilde{u}_1 - v_1\tilde{u}_1') + \frac{1}{2}(3-y)\tilde{u}_1 v_1$$

$$= \tilde{u}_1^2 y^{-1/2} \left\{ (1-y)^2 \int_0^y \frac{\sqrt{\eta} d\eta}{(1-\eta)^3} \left[\frac{2}{3u_0(\eta)} - \frac{5}{3u_2(\eta)} \right. \right.$$

$$\left. + 3\left(1 - \frac{2y(1-\eta)}{\eta(1-y)}\right) \frac{\eta^2}{u_1(\eta)} \right]$$

$$\left. - 6 \int_0^y \frac{\eta^{3/2} d\eta}{(1-\eta)} \left(1 - \frac{1-y}{1-\eta}\right) [u_1(\eta)]^{-1} \right\}. \quad (23)$$

It is easy to show from Eqs. (22) and (23) that $v_0(0)$ and $v_2(0)$ are not equal to zero, whereas $v_1(0)$ equals zero. As in the preceding section it can be shown that $y = 0$ is not a singular point of the functions $v_i(y)$. Following our method we now look for $v_i(y)$ in the form of a polynomial in y. The problem is then reduced to the solution of nonlinear algebraic equations, whose number equals the number of unknown coefficients of the various powers of y in the polynomials (24):

$$v_0(y) = \sum_{k=0}^{N} \alpha_k y^k; \quad v_2(y) = \sum_{k=0}^{N} \beta_k y^k; \quad v_1(y) = \sum_{k=1}^{N} \gamma_k y^k. \quad (24)$$

In the first approximation we may substitute $v_0(y) = \alpha_0$, $v_2(y) = \beta_0$ and $v_1(y) = \gamma_0 y$ into the Eqs. (22) and (23) and then set in them $y = 0$. We then obtain for α_0, β_0, and γ_0 the following system of equations:

$$\frac{3}{2}\alpha_0 = \tilde{u}_0(0)(2/3\, u_0(0) + 10/3\, u_2(0)),$$

$$\frac{3}{2}\beta_0 = \tilde{u}_2(0)(2/3\, u_0(0) + 1/3\, u_2(0)),$$

$$\frac{5}{2}\gamma_0 = \frac{2}{3}\tilde{u}_1(0)(2/3\, u_0(0) - 5/3\, u_2(0)), \quad (25)$$

where

$$\tilde{u}_i(x) = |h_i(1/x)|^2, \qquad u_i(x) = |h_i(x)|^2.$$

As in the neutral meson case, $h_i(x)$, $u_i(x)$ and $\tilde{u}_i(x)$ may be expressed in terms of the coefficients α_k, β_k and γ_k. For example

$$h_0(x) = C_0 + \frac{2}{\pi}\left[xJ_0\left(\frac{1}{x}\right) + \sum_{n=0}^{N} \alpha_n J_{2n+4}(x) \right]$$

$$+ i\sqrt{x}\theta(1-x) + i\theta(x-1)x^{-3/2} \sum_{n=0}^{N} \alpha_n x^{-n}. \quad (26)$$

Keeping in Eq. (26) only the coefficients α_0, β_0 and γ_0 we obtain after substitution into (25)

$$u_i(0) = C_i^2, \quad \tilde{u}_0(0) = \left[C_0 + \frac{2}{\pi}\left(1 - \frac{1}{3}\alpha_0\right) \right]^2,$$

$$\tilde{u}_2(0) = \left[C_2 + \frac{2}{\pi}\left(1 - \frac{1}{3}\beta_0\right) \right]^2,$$

$$\tilde{u}_1(0) = \left[C_1 + \frac{2}{\pi}\left(\frac{1}{3} - \frac{1}{7}\gamma_0\right) \right]^2. \quad (27)$$

The first two equations in (25) are quadratic in α_0 and β_0 and do not contain γ_0. Solving these equations yields the functions $\alpha_0(C_0, C_2)$ and $\beta_0(C_0, C_2)$. On the other hand by making use of Eq. (17) we can express C_0 and C_2 in terms of α_0 and α_2:

$$C_0 = -\frac{1}{5\lambda} - \frac{2}{\pi}\left[x_0 J_0\left(\frac{1}{x_0}\right) + \alpha_0 J_4(x_0) \right], \quad (28)$$

$$C_2 = -\frac{1}{2\lambda} - \frac{2}{\pi}\left[x_0 J_0\left(\frac{1}{x_0}\right) + \beta_0 J_4(x_0) \right]. \quad (29)$$

From here α_0 and β_0 are obtained by iteration of which the first step is obtained by substituting for C_0 and C_2 in $\alpha_0(C_0, C_2)$ and $\beta_0(C_0, C_2)$ the values given by Eqs. (28) and (29) with $\alpha_0 = \beta_0 = 0$.

The third equation in (25) is quadratic in γ_0; solving it using the already determined $\alpha_0(\lambda)$ and $\beta_0(\lambda)$ yields $\gamma_0(C_1, \lambda)$. According to Eq. (18)

$$C_1^{-1} = \frac{1}{\pi} \int_0^1 \left[\frac{\sqrt{y}}{u_1(y)} - \frac{\gamma_0 y^{5/2}}{\tilde{u}_1(y)} \right] dy. \quad (30)$$

Finally $\gamma_0(\lambda)$ is obtained by iteration of which the first step is obtained by substituting in $\gamma_0(C_1, \lambda)$ the value $C_1^{(0)}$ obtained from Eq. (30) with $\gamma_0 = 0$. Table II lists the coefficients $\alpha_0(\lambda)$ and $\beta_0(\lambda)$ obtained in this manner.

TABLE II

λ	0	0.1	0.3	1
α_0	0.8	0.58	0.305	0.04
β_0	3	2.1	1.05	0.18

The dashed lines in Fig. 5 depict the dependence of $-5\lambda\sqrt{x}\ \cot\delta_0 = -5\lambda\ \mathrm{Re}\ h_0(x)$ on $\nu = 1/(1-x) = q^2/\mu^2$ in the first approximation constructed according to Eqs. (15) and (24). The dashed lines in Fig. 6 depict the dependence of the function $-2\lambda\sqrt{x}\ \cot\delta_2$ on ν.

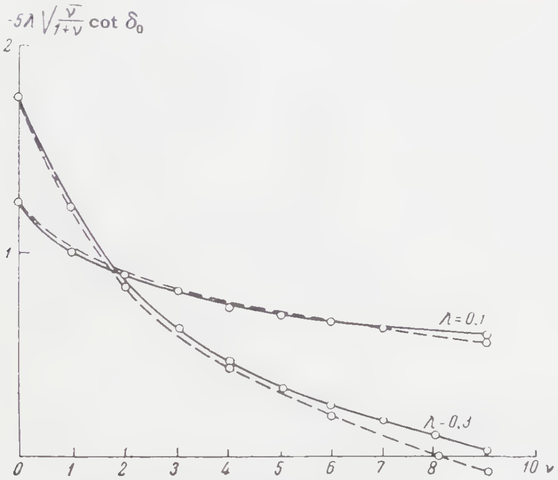

FIG. 5

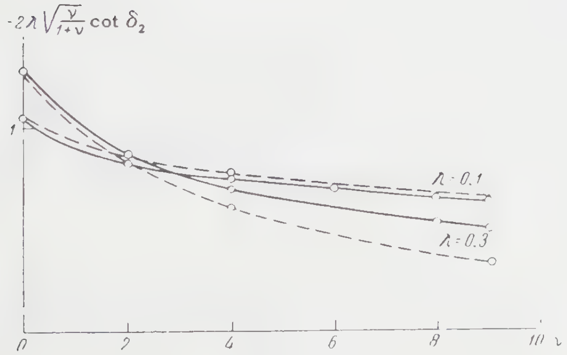

FIG. 6

4. CONCLUSIONS

A comparison of the results of the first and second approximations for the function $-(\pi\eta/2) \times \sqrt{x}\ \cot\delta = -(\pi\eta/2)\ \mathrm{Re}\ h(x)$ (Figs. 3 and 4) shows, that the second order corrections may be neglected, except for values of λ close to the limiting values when $\alpha_1(\lambda)$ becomes large. However, as is seen from Fig. 2, this exceptional region is not large. It must also be remembered that the range of validity of Eqs. (1) and (2) is restricted to the limits $0 \leq \nu \lesssim 3$. This is just the region in which the corrections attain their smallest values and for $\nu = 0$ the first and second approximations are identical. Furthermore our first approximation is in good agreement with the numerical solution of Eq. (1) (E. P. Vedeneev and A. L. Krylov, private communication).

We may also check the appropriateness of our first approximation in the charged meson theory. The comparison of our first approximation (dashed lines) and of the numerical solutions of the Chew-Mandelstam equations for the scattering of charged mesons[8] (solid lines) is given in Figs. 5 and 6 for the functions $-5\lambda\sqrt{x}\ \cot\delta_0$ and $-2\lambda\sqrt{x}\ \cot\delta_2$. It is seen that the agreement, particularly in the region $0 \leq \nu \lesssim 3$, is very good. It is not surprising that the solution found by us in the first approximation is, in essence, the S-wave dominant solution of Chew, Mandelstam, and Noyes. The reason for this is that in the first approximation the S-wave scattering amplitudes are obtained independently of the P-wave scattering amplitude [the first two equations in (25) are not coupled to the third one].

Thus, in all cases considered, already the first approximation yields reasonably good results. When it is noted that the first approximation can be obtained quite easily it becomes clear that the method here outlined could be very useful for the investigation of solutions of equations of the Chew-Mandelstam type.

Our method was applied here to the Chew-Mandelstam equations for the scattering of neutral and charged pions. It may also be applied to other equations of analogous structure, say πN or πK scattering.

---

[1] S. Mandelstam, Phys. Rev. **112**, 1344 (1958).

[2] S. Mandelstam, Phys. Rev. **115**, 1741 (1959).

[3] S. Mandelstam, Phys. Rev. **115**, 1752 (1959).

[4] G. Chew and S. Mandelstam, UCRL 8728, April 1959.

[5] K. A. Ter-Martirosyan, JETP **39**, 827 (1960), Soviet Phys. JETP **12**, 575 (1961), Nucl. Phys. (in press).

[6] M. Cini and S. Fubini, Ann. of Phys. (in press).

[7] Castillejo, Dalitz, and Dyson, Phys. Rev. **101**, 453 (1956).

[8] Chew, Mandelstam, and Noyes, preprint.

Translated by A. M. Bincer
261

SOVIET PHYSICS JETP VOLUME 12, NUMBER 5 MAY, 1961

ELECTRIC FORCES IN A TRANSPARENT DISPERSIVE MEDIUM

L. P. PITAEVSKIĬ

Institute for Terrestial Magnetism, Ionosphere, and Radio Transmission,
Academy of Sciences, U.S.S.R.

Submitted to JETP editor July 27, 1960

J. Exptl. Theoret. Phys. (U.S.S.R.) **39**, 1450-1458 (November, 1960)

It is shown that the expression for the stress tensor of a variable electric field in a transparent dispersive medium is the same as the usual expression for a nondispersive medium. It is also shown that if the parameters of the medium are time-dependent an imaginary part appears in the dielectric susceptibility, which is a real quantity for time-independent parameters. An expression is derived for the stress tensor of a variable electric field in a transparent liquid located in a constant magnetic field.

1. THE STRESS TENSOR OF A VARIABLE ELECTRIC FIELD IN A TRANSPARENT LIQUID DISPERSIVE MEDIUM

In the present work we investigate the form of the stress tensor of a variable electric field in a transparent liquid dispersive medium. We are interested here, of course, in the average of the tensor over an oscillation period of the field. As is well known, the stress in a dielectric placed in a constant electric field is given by the Maxwell-Abraham stress tensor. For an isotropic liquid it has the form

$$\sigma_{ik} = -p_0\delta_{ik} - \frac{E^2}{8\pi}\left[\varepsilon - \rho\left(\frac{\partial\varepsilon}{\partial\rho}\right)_T\right]\delta_{ik} + \varepsilon\frac{E_iE_k}{4\pi}, \qquad (1)$$

Here $p_0 = p_0(\rho, T)$ is the pressure in the liquid in the absence of the electric field as a function of ρ and T, ϵ is the dielectric susceptibility of the liquid, and ρ is its density. The derivation of (1) is based on the expression for the energy density of a constant electric field in a dielectric,

$$U = U_0 + \frac{D^2}{8\pi\varepsilon} = U_0 + \frac{\varepsilon E^2}{8\pi}, \qquad (2)$$

Here U_0 is the energy density in the absence of the field.

Let us now consider a liquid dielectric whose dielectric permittivity is a function of the frequency of the field. Let it be located in an electric field which varies with a frequency at which the dielectric is transparent, i.e., such that $\epsilon(\omega)$ is a real quantity. A typical example of such a medium is an electron plasma at $\omega \gg \nu$ (ν is the effective collision frequency). The expression for the time average of the energy density of the electric field in such a medium is different from (2), and contains the derivative of ϵ with respect to ω (see reference 1):

$$U = U_0 + \frac{d\omega\varepsilon}{d\omega}\frac{\overline{E^2}}{8\pi}. \qquad (3)$$

One might naturally expect additional terms containing $d\epsilon/d\omega$ to appear in this case in the expression for the stress tensor. However, we shall see that this is not so, i.e., that the stress tensor in this case is given by expression (1), but is averaged over the time.

For a proof of this assertion we first give a very simple derivation of expression (1) for a constant field. Consider a capacitor filled with a dielectric of dielectric constant ϵ, and which carries on its plates a constant charge Q. The energy of such a capacitor is

$$\mathcal{U} = \mathcal{U}_0 + Q^2/2C = \mathcal{U}_0 + C\varphi^2/2. \qquad (4)$$

Here $\mathcal{U}_0$ is the energy of the uncharged capacitor, C its capacity, and φ the potential difference between its plates.

Let us now subject the capacitor to some continuous deformation. First we displace its plates or its lateral surfaces. The work performed on it by the external force will then be

$$\delta A = \sigma_{ik}\xi_i n_k S \qquad (i, k = 1, 2, 3), \qquad (5)$$

where n_k is the normal to the displaced surface, ξ_i its displacement, and S its area. However, since a capacitor with constant charge is an electrically closed system, the work (5) will simply be equal to the change of its energy:

$$\delta A = \sigma_{ik}\xi_i n_k S = \delta\mathcal{U}_0 - \frac{Q^2}{2C^2}\delta C = \delta\mathcal{U}_0 - \tfrac{1}{2}\varphi^2\delta C. \qquad (6)$$

If we now express δC in terms of the displacement of the plates (taking into account the change of the density of the dielectric during deformation), we immediately find from Eq. (6) the expression (1) for σ_{ik}.

Now we show that the expression for the tensor in a variable field is determined by an equation that agrees exactly with the time average of Eq. (6). Consider a capacitor filled with a dielectric of dielectric constant $\epsilon(\omega)$; to its plates we apply an alternating potential,

$$\varphi = \tfrac{1}{2}\left(\varphi_0 e^{-i\omega t} + \overset{*}{\varphi}_0 e^{i\omega t}\right) \tag{7}$$

of frequency ω such that $\operatorname{Im}\epsilon(\omega) = 0$. Such a capacitor, however, is no longer a closed system. In order to avoid calculating the work of the current source we therefore consider a simpler, electrically closed, oscillating system, consisting of a capacitor and an inductance, i.e., an oscillating circuit with natural frequency ω.

The energy of a capacitor filled with a dispersive dielectric is given by the following expression, which takes the place of Eq. (4),

$$\mathcal{U} = \mathcal{U}_0 + \frac{d\omega C}{d\omega}\,\frac{\overline{\varphi^2}}{2}, \tag{8}$$

This is easily obtained by comparing Eqs. (2) and (3) and taking it into account that $C \sim \epsilon$. The energy in the inductance is $L\overline{I^2}/2c^2 = C\overline{\varphi^2}/2$, where c is the speed of light, and I the current through the inductance (here we assume that the inductance does not depend on frequency, and we have used the well known relation between current and voltage in an oscillating circuit). Therefore the total energy of our closed system is equal to

$$\mathcal{U} = \mathcal{U}_0 + \frac{d\omega C}{d\omega}\,\frac{\overline{\varphi^2}}{2} + \frac{C\overline{\varphi^2}}{2} = \mathcal{U}_0 + \frac{1}{\omega}\,\frac{d\omega^2 C}{d\omega}\,\frac{\overline{\varphi^2}}{2}. \tag{9}$$

Now let us subject the capacitor in our circuit to an infinitesimal deformation. The accompanying work of the stress forces will be, as before,

$$\delta A = \sigma_{ik}\xi_i n_k S.$$

To calculate the change of energy in the system, which equals δA, we note that, as is known from mechanics, the so-called adiabatic invariant remain constant during an infinitesimal change of the parameters of any linear oscillating system. For linear systems this invariant is defined as the ratio of the oscillation energy to the natural frequency of the system:

$$\mathcal{U}_{\mathrm{osc}}/\omega = \mathrm{const.} \tag{10}$$

We note that Eq. (10) has a simple quantum-mechanical basis. In fact, the energy levels of every linear quantum-mechanical system have (after subtracting the zero-point energy) the form

$$E_n = \hbar\omega n \qquad (n = 0, 1, \ldots),$$

where ω is the eigenfrequency and n the quantum number. Therefore

$$\mathcal{U}/\omega = E_n/\omega = \hbar n.$$

But during an infinitesimal change of external conditions the quantum state of the system does not change, i.e., n remains constant.

From (10) it is clear that the energy changes in direct proportion to the frequency, and in our case we obtain

$$\delta\mathcal{U} = \delta\mathcal{U}_0 + \frac{d\omega^2 C}{\omega\, d\omega}\,\frac{\overline{\varphi^2}}{2}\,\frac{\delta\omega}{\omega}, \tag{11}$$

where $\delta\omega$ is the change in natural frequency of the circuit due to the deformation of the capacitor. Since $\omega = c/\sqrt{LC}$ we find

$$\delta\omega/\omega = -\tfrac{1}{2}\,\delta C/C, \tag{12}$$

where δC is the change in capacitance.

We must, however, take into account that the capacitance changes not only by deformation, but also because of the change in the oscillation frequency of the circuit, since the capacitance depends on frequency. Therefore,

$$\delta C = \delta C_{\mathrm{st}} + (dC/d\omega)\,\delta\omega, \tag{13}$$

where δC_{st} is expressed in terms of the displacement ξ_i like in the static case.

Eliminating $\delta C/C$ from (12) and (13) we find

$$\frac{\delta\omega}{\omega}\left(\frac{1}{\omega}\,\frac{d\omega^2 C}{d\omega}\right) = -\,\delta C_{\mathrm{st}}. \tag{14}$$

Substituting $\delta\omega/\omega$ from (14) into (11) we finally obtain

$$\delta\mathcal{U} = \delta\mathcal{U}_0 - \tfrac{1}{2}\,\overline{\varphi^2}\,\delta C_{\mathrm{st}}, \tag{15}$$

i.e., an expression which agrees with the average of Eq. (6). If we now note that δC_{st} is expressed in terms of the deformation (like in the static case) we immediately conclude without additional calculation that the tensor is also given by the average of Eq. (1),

$$\sigma_{ik} = -\,p_0\delta_{ik} - \frac{\overline{E^2}}{8\pi}\left[\varepsilon - \rho\left(\frac{\partial\varepsilon}{\partial\rho}\right)_T\right]\delta_{ik} + \varepsilon\,\frac{\overline{E_i E_k}}{4\pi} \tag{16}$$

even in the presence of dispersion.

Formula (15) can be presented from a somewhat different point of view. We assume that the capacitance changes only because of changes in permittivity of the dielectric. Then

$$\delta C = (S/4\pi d)\,\delta\varepsilon$$

(S is the surface area of the plates and d their separation), and the infinitesimal work of the external forces is

$$\delta A = \delta\mathcal{U} = \delta\mathcal{U}_0 - \frac{1}{8\pi}\frac{\overline{\varphi^2}}{d}S\delta\varepsilon = \delta\mathcal{U}_0 - \frac{\overline{E^2}}{8\pi}V\delta\varepsilon \qquad (17)$$

(V is the volume of the capacitor). If we now consider instead of the capacitor an arbitrary volume filled with dielectric, then instead of Eq. (17) we obtain

$$\delta\mathcal{U} = \delta\mathcal{U}_0 - \int\frac{\overline{E^2}}{8\pi}\delta\varepsilon\,dV. \qquad (18)$$

Formula (18) is correct for changes occurring at a constant entropy of the medium. However, since at constant entropy and temperature small additions to the energy and free energy, respectively, are equal, exactly the same formula applies for the change in the free energy $\mathcal{F}$ at a given temperature and at zero work of the sources of the field:

$$\delta\mathcal{F} = \delta\mathcal{F}_0 - \int\frac{\overline{E^2}}{8\pi}\delta\varepsilon\,dV. \qquad (18a)$$

This formula agrees with the formula for the change in the free energy for fixed field sources in the static case [see reference (1), formula 14.1)].

As is well known, the components σ_{ik}, together with U and the components of the energy-flux vector $\mathbf{S} = (c/4\pi)\,\mathbf{E}\times\mathbf{H}$, form the four-dimensional energy-momentum tensor $T_{\alpha\beta}$ of the system. From our results it follows that in a static medium the only component of $T_{\alpha\beta}$ containing the derivative of ϵ with respect to ω is T_{44}. Knowing $T_{\alpha\beta}$ in a static medium, we can find its value in a moving medium from the Lorentz transformation formula. Then $d\epsilon/d\omega$ will enter also into the other components of the tensor. We write down as an example the equation for the energy flux of the field in a medium moving with velocity v [with accuracy up to terms $\sim(v/c)^2$]:

$$\mathbf{S} = \frac{c}{4\pi}\overline{[\mathbf{E}\times\mathbf{H}]} + \frac{\overline{E^2}}{8\pi}\left(\omega\frac{\partial\varepsilon}{\partial\omega} - \rho\frac{\partial\varepsilon}{\partial\rho}\right)\mathbf{v}. \qquad (19)$$

2. PERMITTIVITY OF MEDIA WITH TIME-DEPENDENT PARAMETERS

Let the state of our liquid be described by some parameter λ. (In particular, this may be the density or the pressure of the liquid.) In this case the dielectric permittivity will of course be a function of this parameter $[\epsilon = \epsilon(\omega, \lambda)]$. Now let the parameter λ depend on time. Then we can introduce the idea of a time-dependent permittivity. Since also in this case the connection between **E** and **D** for weak field remains linear we may write

$$\mathbf{D}(t) = \mathbf{E}(t) + \int_0^\infty f(\tau, t)\,\mathbf{E}(t-\tau)\,d\tau. \qquad (20)$$

(If the properties of the medium did not depend on time, the function f would depend only on τ and not on t.)

Putting $\mathbf{E}(t) = \mathbf{E}_0 e^{-i\omega t}$ we obtain

$$\mathbf{D}(t) = \varepsilon(\omega, t)\,\mathbf{E}_0 e^{-i\omega t}, \qquad (21)$$

where it is natural to call the quantity

$$\varepsilon(\omega, t) = 1 + \int_0^\infty f(\tau, t)\,e^{i\omega\tau}\,d\tau \qquad (22)$$

the permittivity of the medium with time-dependent parameters.

The function $\epsilon(\omega, t)$, however, will by no means agree with the function $\epsilon_0(\omega, t) = \epsilon(\omega, \lambda(t))$, i.e., with the function of the static value of λ, in which we put $\lambda = \lambda(t)$. This is connected with the fact that the function $\epsilon(\omega, t)$ in general will not be determined by the value of λ at the same moment of time, but will depend also on the time derivatives of λ. If λ changes slowly (compared to atomic frequencies) then the dependence of ϵ can be limited to $d\lambda/dt$ only, and we can take only the first term of the expansion in this quantity. Thus

$$\varepsilon(\omega, t) = \varepsilon_0(\omega, t) + a(\omega, \lambda(t))\,d\lambda/dt. \qquad (23)$$

(ϵ must of course tend toward ϵ_0 as $d\lambda/dt \to 0$).

The second term is usually taken to be only a negligibly small correction to the first. However, if the medium is transparent when the parameters are time-independent, i.e., if $\operatorname{Im}\epsilon(\omega, \lambda) = 0$, then, generally speaking, $\operatorname{Im} a \neq 0$. Therefore the dependence of λ on time leads to the appearance of an imaginary part of ϵ, which represents a qualitatively new effect.

We now show that if $\operatorname{Im}\epsilon(\omega, \lambda) = 0$, then Im a can be found in closed form (the real part of a gives only a small correction to ϵ_0 and is uninteresting). For the derivation consider a capacitor filled with a dielectric whose parameters vary slowly with time. We shall consider that a potential difference

$$\varphi = \tfrac{1}{2}(\varphi_0 e^{-i\omega t} + \varphi_0^* e^{i\omega t}),$$

is maintained between the plates of the capacitor. Here φ_0 is a complex constant.

The current through the capacitor now has the form

$$I(t) = \tfrac{1}{2}\,[I_0(t)\,e^{-i\omega t} + I_0^*(t)\,e^{i\omega t}], \tag{24}$$

where $I_0(t)$ is a slow function of the time. The capacitance is given by the formula

$$C(\omega, t) = \varepsilon(\omega, t)\,S/4\pi d. \tag{25}$$

Then the charge on the capacitor plates is

$$Q = \tfrac{1}{2}\,[C(\omega, t)\,\varphi_0 e^{-i\omega t} + C^*(\omega, t)\,\varphi_0^* e^{i\omega t}]. \tag{26}$$

Since $I = dQ/dt$, we find

$$I_0 = [-i\omega C(\omega, t) + \partial C(\omega, t)/\partial t]\,\varphi_0. \tag{27}$$

Let us now apply the law of conservation of energy to our condensor. In this case it means that the change of energy of the capacitor equals the work needed to change its dielectric constant at a fixed current source, plus the work of the source to maintain the given potential across the capacitor. According to (15) the work for the change $\delta\epsilon$ (per unit time) equals $\tfrac{1}{2}\overline{\varphi^2}\,\partial C/\partial t$, and the work of the current source is $\overline{I\varphi}$, i.e.,

$$\frac{\partial}{\partial t}\left(\frac{1}{2}\,\frac{d\omega C}{d\omega}\,\overline{\varphi^2}\right) = -\frac{\overline{\varphi^2}}{2}\,\frac{\partial C}{\partial t} + \overline{I\varphi}. \tag{28}$$

With accuracy up to terms of higher order of smallness, we can regard here C as a real quantity in all expressions containing $\partial C/\partial t$, since $\operatorname{Im} C$ is of the order $d\lambda/dt \sim \partial C/\partial t$.

Substituting (27) into (28) we find

$$\frac{\overline{\varphi^2}}{2}\,\frac{\partial C}{\partial t} + \frac{\overline{\varphi^2}}{2}\,\frac{\partial^2 C}{\partial\omega\,\partial t} = \frac{\overline{\varphi^2}}{2}\,\frac{\partial C}{\partial t} + \frac{\overline{\varphi^2}}{2}\operatorname{Im} C, \tag{29}$$

$$\operatorname{Im} C = \frac{1}{2}\,\frac{\partial^2 C}{\partial\omega\,\partial t} = \frac{1}{2}\,\frac{\partial^2 C}{\partial\lambda\,\partial\omega}\,\frac{d\lambda}{dt}. \tag{30}$$

Substituting (23) and (25) into (30) we finally find

$$\operatorname{Im} a(\omega, \lambda) = \frac{1}{2}\,\frac{\partial^2\varepsilon(\omega, \lambda)}{\partial\omega\,\partial\lambda}, \tag{31}$$

$$\varepsilon(\omega, t) = \varepsilon_0(\omega, t) + \frac{i}{2}\,\frac{\partial^2\varepsilon_0(\omega, t)}{\partial\omega\,\partial t}. \tag{32}$$

(The real part of a, as already indicated, is negligible and can be omitted). The formula (32) clearly is correct also in the case when ϵ depends on several parameters.

We note in conclusion that formula (32), like formula (15), can be derived not only by applying the theorem on adiabatic invariants, but also directly from the fundamental formulas of quantum mechanics, if one expresses the left and right sides of these formulas by the corresponding matrix elements of quantum-mechanical perturbation theory. However, we shall not dwell upon these rather cumbersome calculations. (These calculations were first performed by I. E. Dzyaloshinskiĭ to derive formulas equivalent to (15).)

3. THE STRESS TENSOR OF A VARIABLE ELECTRIC FIELD IN A LIQUID LOCATED IN A STRONG MAGNETIC FIELD

Consider a liquid placed in a strong constant magnetic field and a weak electric field varying with a frequency at which the liquid is transparent. Here we shall suppose that when there is no electric field the liquid does not have any magnetic properties, i.e., that its magnetic permeability is $\mu = 1$.

The permittivity of the liquid in the magnetic field in the absence of absorption is a Hermitian tensor of the form

$$\varepsilon_{ik}(\omega, \mathbf{H}) = \varepsilon_1(\omega, H^2)\,\delta_{ik} + \varepsilon_2(\omega, H^2)\,H_i H_k + i\varepsilon_3(\omega, H^2)\,e_{ikl}H_l, \tag{33}$$

where $\mathbf{H}$ is the constant magnetic field intensity, and e_{ikl} a totally antisymmetric unit tensor. Here ϵ_1, ϵ_2, and ϵ_3 are functions of H^2 and ω which tend toward some finite limit as $H^2 \to 0$. In particular, for an electron plasma,

$$\varepsilon_1 = 1 - \frac{\omega_0^2}{\omega^2 - \omega_H^2}, \qquad \varepsilon_2 = \frac{e^2}{m^2c^2}\,\frac{\omega_0^2}{(\omega^2 - \omega_H^2)\,\omega^2},$$

$$\varepsilon_3 = -\frac{e}{mc}\,\frac{\omega_0^2}{(\omega^2 - \omega_H^2)\,\omega},$$

$$\omega_H^2 = e^2H^2/m^2c^2, \qquad \omega_0^2 = 4\pi ne^2/m, \tag{34}$$

(n is the number of electrons per unit volume, e the charge, and m the mass of the electron).

Consider some volume filled by a dielectric of permittivity (33). By generalizing some arguments of the preceding section, it is not difficult to show that in this case the following relation holds for the variation of the free energy [instead of formula (18a)]

$$\delta\mathcal{F} = \int\left\{\delta F_0 - \frac{1}{16\pi}\,E_{0i}^* E_{0k}\,\delta\varepsilon_{ik}\right\}dV, \tag{35}$$

where F_0 is the density of the free energy in the absence of an electric field, and $\mathbf{E}_0$ is the complex amplitude of the electric field:*

$$\mathbf{E} = \tfrac{1}{2}\,(\mathbf{E}_0 e^{-i\omega t} + \mathbf{E}_0^* e^{i\omega t}).$$

We note first that although our medium is by assumption nonmagnetic ($\mathbf{B} = \mathbf{H}$) when there is no electric field, this is no longer so when the electric field is taken into account. Therefore we determine first the connection between **B** and **H**, accurate to terms $\sim E^2$. For this we use the well known thermodynamic equation

---

*To derive (35), strictly speaking, it is not enough to consider only the field in a capacitor, since we cannot produce in that way a field of the most general form, say a rotating one. This difficulty can easily be avoided by considering, instead of an oscillating circuit, a cavity resonator of arbitrary form. Simple calculations lead to the same formula (35) in this case, too.

$$\mathbf{H} = 4\pi \partial F / \partial \mathbf{B}.$$

Carrying out the differentiation with the help of formula (35), and taking into account that $\mu = 1$ by assumption, i.e.,

$$4\pi \partial F_0 / \partial \mathbf{B} = \mathbf{B}, \qquad F_0 = F_{00} + B^2 / 8\pi$$

(F_{00} is the density of free energy in the absence of both the electric and magnetic fields) we find

$$\mathbf{H} = \mathbf{B} - \tfrac{1}{4} E^*_{0i} E_{0k} \partial \varepsilon_{ik} / \partial \mathbf{B} \tag{36}$$

or, to the same accuracy,

$$\mathbf{B} = \mathbf{H} + \tfrac{1}{4} E^*_{0i} E_{0k} \partial \varepsilon_{ik} / \partial \mathbf{H}. \tag{36a}$$

We note that since $\partial \epsilon_{ik} / \partial H \neq 0$ when $H = 0$, $B \neq 0$ even when $H = 0$, i.e., a variable electric field can create in the medium an average magnetic moment proportional to E^2. It is easy to see that for this the electric field must rotate, i.e., it must not be linearly polarized.

Now we subject our dielectric to a deformation at constant induction **B**, the displacement vector of its points being $\delta\mathbf{r}(\mathbf{r})$. Then we must recognize that when a volume element is displaced its permittivity changes, and consequently the magnetic field changes from point to point. Taking this into account we obtain

$$\delta \varepsilon_{ik} = -(\delta \mathbf{r} \nabla) \varepsilon_{ik} - \frac{\partial \varepsilon_{ik}}{\partial \rho} \rho \operatorname{div} \delta \mathbf{r} + \frac{\partial \varepsilon_{ik}}{\partial B_l} (\delta \mathbf{r} \nabla) B_l. \tag{37}$$

Since the deformation takes place at constant **B**, we have

$$\delta F_0 = \delta F_{00} = -(\delta \mathbf{r} \nabla) F_{00} - \frac{\partial F_{00}}{\partial \rho} \rho \operatorname{div} \delta \mathbf{r}.$$

Substituting into (35) and integrating by parts we obtain

$$\delta \mathcal{F} = \int \Big\{ \nabla \Big(\rho \frac{\partial F_{00}}{\partial \rho} - F_{00} \Big) - \frac{1}{16\pi} \nabla \Big(E^*_{0i} E_{0k} \rho \frac{\partial \varepsilon_{ik}}{\partial \rho} \Big) - \frac{E^*_{0i} E_{0k}}{16\pi} \Big(\nabla \varepsilon_{ik} + \frac{\partial \varepsilon_{ik}}{\partial B_l} \nabla B_l \Big) \Big\} \delta \mathbf{r} \, dV. \tag{38}$$

On the other hand, the change in free energy equals the work of the forces

$$\delta \mathcal{F} = -\int \mathbf{f} \delta \mathbf{r} \, dV, \tag{39}$$

where **f** is the force acting on a unit volume of the dielectric. Equating (38) and (39) and recalling that

$$F_{00} - \rho \partial F_{00} / \partial \rho = -p_{00}$$

[$p_{00} = p_{00}(\rho, T)$ is the pressure in the absence of the fields as a function of ρ and T], we find the final expression for the force

$$\mathbf{f} = -\operatorname{grad} p_{00} + \frac{1}{16\pi} \operatorname{grad} \Big[E^*_{0i} E_{0k} \Big(\frac{\partial \varepsilon_{ik}}{\partial \rho} \Big)_T \rho \Big] - \frac{E^*_{0i} E_{0k}}{16\pi} \Big[\operatorname{grad} \varepsilon_{ik} - \frac{\partial \varepsilon_{ik}}{\partial B_l} \operatorname{grad} B_l \Big] \tag{40}$$

or, substituting $E^*_{0i} E_{0k} \partial \epsilon_{ik} / \partial B_l$ from (36),

$$\mathbf{f} = -\nabla p_{00} + \frac{1}{16\pi} \nabla \Big[E^*_{0i} E_{0k} \Big(\frac{\partial \varepsilon_{ik}}{\partial \rho} \Big) \rho \Big] - \frac{E^*_{0i} E_{0k}}{16\pi} \nabla \varepsilon_{ik} + \frac{(B_l - H_l) \nabla B_l}{4\pi}. \tag{41}$$

To find the tensor σ_{ik} we must transform the right side of (41) into the form $\partial \sigma_{ik} / \partial x_k$. For this we note that in virtue of the Maxwell equations

$$\begin{aligned} E^*_{0l} E_{0m} \frac{\partial \varepsilon_{lm}}{\partial x_i} &= \frac{\partial}{\partial x_i} (E^*_{0l} E_{0m} \varepsilon_{lm}) - \Big(E^*_{0l} \varepsilon_{lm} \frac{\partial E_{0m}}{\partial x_i} + \text{compl. conj.} \Big) = \frac{\partial}{\partial x_i} (E^*_{0l} E_{0m} \varepsilon_{lm}) - \Big(\frac{\partial E_{0l}}{\partial x_m} D^*_{0m} \\ &+ \text{compl. conj.} \Big) = \frac{\partial}{\partial x_i} (E^*_{0l} E_{0m} \varepsilon_{lm}) - \Big(\frac{\partial E_{0l} D^*_{0m}}{\partial x_m} + \text{compl. conj.} \Big), \end{aligned}$$

$$\begin{aligned} (B_k - H_k) \frac{\partial B_k}{\partial x_i} &= \frac{\partial}{\partial x_i} \Big(\frac{B^2}{2} - \mathbf{BH} \Big) - \frac{\partial H_k}{\partial x_i} B_k = \frac{\partial}{\partial x_i} \Big(\frac{B^2}{2} - \mathbf{BH} \Big) + \frac{\partial H_i B_k}{\partial x_k} = \frac{\partial}{\partial x_i} \Big\{ -\frac{H^2}{2} - \frac{(\mathbf{B} - \mathbf{H})^2}{2} \Big\} + \frac{\partial H_i B_k}{\partial x_k} \\ &\approx -\frac{1}{2} \frac{\partial H^2}{\partial x_i} + \frac{\partial H_i B_k}{\partial x_k}. \end{aligned}$$

We obtain

$$\sigma_{ik} = -p_{00} \delta_{ik} + \frac{1}{8\pi} \Big\{ \frac{E^*_{0l} E_{0m}}{2} \Big(\rho \frac{\partial \varepsilon_{lm}}{\partial \rho} - \varepsilon_{lm} \Big) - H^2 \Big\} \delta_{ik} + \frac{1}{4\pi} H_i B_k + \frac{1}{16\pi} (E^*_{0i} D_{0k} + \text{compl. conj.}) \tag{42}$$

or, expressing **D** by **E** and **B** by **H**,

$$\begin{aligned} \sigma_{ik} = &-\Big(p_{00} + \frac{H^2}{8\pi} \Big) \delta_{ik} + \frac{1}{4\pi} H_i H_k + \frac{1}{16\pi} \Big\{ E^*_{0l} E_{0m} \Big(\rho \frac{\partial \varepsilon_{lm}}{\partial \rho} - \varepsilon_{lm} \Big) \Big\} \delta_{ik} \\ &+ \frac{1}{16\pi} \Big\{ H_i \frac{\partial \varepsilon_{lm}}{\partial H_k} E^*_{0l} E_{0m} + (\varepsilon_{km} E^*_{0i} E_{0m} + \text{compl. conj.}) \Big\}. \end{aligned} \tag{43}$$

The tensor σ_{ik} in the liquid must satisfy two conditions. First, the tangential components of the forces acting on the surface must be continuous on the interface between two adjoining liquids. This is necessary in order that the liquids be in mechanical equilibrium. If we recall that the tangential components of **E** and **H**, and the normal components of **D** and **B**, are continuous in virtue of the boundary conditions, then it follows at once from (42) that this condition is fulfilled, i.e., that

$$\sigma_{ik}n_k = \sigma'_{ik}n_k$$

(n is the normal to the surface).

Secondly, in virtue of the law of conservation of angular momentum, the tensor σ_{ik} must be symmetric. To verify that this condition is fulfilled we express ϵ_{ik} through ϵ_1, ϵ_2, and ϵ_3 in (43). We obtain

$$\begin{aligned}\sigma_{ik} = &-\left(p_{00} + \frac{H^2}{8\pi}\right)\delta_{ik} + \frac{1}{4\pi} H_i H_k \\ &+ \frac{1}{16\pi}\left\{E^*_{0l}E_{0m}\left(\rho\frac{\partial\varepsilon_{lm}}{\partial\rho} - \varepsilon_{lm}\right)\right\}\delta_{ik} \\ &+ \frac{1}{16\pi}\left\{[\varepsilon_1 E^*_{0i}E_{0k} + \varepsilon_2(\mathbf{E}_0\times\mathbf{H})(E^*_{0i}H_k + E^*_{0k}H_i)\right. \\ &+ i\varepsilon_3 E^*_{0i}[\mathbf{E}_0\times\mathbf{H}]_k + \text{compl. conj.}] + 2H_iH_k\left[\frac{\partial\varepsilon_1}{\partial H^2}\mathbf{E}_0\times\mathbf{E}^*_0\right. \\ &+ \left.\left.\frac{\partial\varepsilon_2}{\partial H^2}|[\mathbf{E}_0\times\mathbf{H}]|^2 + i\frac{\partial\varepsilon_3}{\partial H^2}[\mathbf{E}^*_0\times\mathbf{E}_0]\times\mathbf{H}\right] + i\varepsilon_3 H_i[\mathbf{E}^*_0\times\mathbf{E}_0]_k\right\}.\end{aligned} \tag{44}$$

We can verify the correctness of the identity

$$\begin{aligned}iE^*_{0i}[\mathbf{E}_0\times\mathbf{H}]_k + \text{compl. conj.} = &-iH_i[\mathbf{E}^*_0\times\mathbf{E}_0]_k \\ &+ i[\mathbf{E}^*_0\times\mathbf{E}_0]\mathbf{H}\delta_{ik},\end{aligned} \tag{45}$$

with the help of which we now write σ_{ik} in the manifestly symmetric form

$$\begin{aligned}\sigma_{ik} = &-\left(p_{00} + \frac{H^2}{8\pi}\right)\delta_{ik} + \frac{1}{4\pi}H_iH_k + \frac{1}{16\pi}\left\{E^*_{0l}E_{0m}\left(\rho\frac{\partial\varepsilon_{lm}}{\partial\rho}\right.\right. \\ &- \left.\left.\frac{\varepsilon_{lm}+\varepsilon^*_{lm}}{2}\right)\right\}\delta_{ik} + \frac{1}{16\pi}\{\varepsilon_1E^*_{0i}E_{0k} + \varepsilon_2(\mathbf{E}_0\mathbf{H})(E^*_{0i}H_k \\ &+ H_iE^*_{0k}) + \text{compl. conj.}\} + \frac{H_iH_k}{8\pi}\left\{\frac{\partial\varepsilon_1}{\partial H^2}\mathbf{E}_0\mathbf{E}^*_0\right. \\ &+ \left.\frac{\partial\varepsilon_2}{\partial H^2}|[\mathbf{E}_0\times\mathbf{H}]|^2 + i\frac{\partial\varepsilon_3}{\partial H^2}[\mathbf{E}^*_0\times\mathbf{E}_0]\mathbf{H}\right\}.\end{aligned} \tag{46}$$

The expression (46) can be generalized without difficulty to the case where the medium possesses magnetic properties even when the electric field vanishes.

In conclusion I express my thanks to L. D. Landau for advice and discussion, and V. L. Ginzburg and I. E. Dzyaloshinskiĭ for a discussion of the results. I also thank M. A. Leontovich who called to my attention the question considered in Sec. 3 of the present paper.

---

[1] L. D. Landau and E. M. Lifshitz, Электродинамика сплошных сред (Electrodynamics of Continuous Media), Gostekhizdat, 1957.

Translated by D. Brill
262

SOVIET PHYSICS JETP VOLUME 12, NUMBER 5 MAY, 1961

SCATTERING THEORY FOR A THREE-PARTICLE SYSTEM

L. D. FADDEEV

Mathematics Institute, Academy of Sciences, U.S.S.R.

Submitted to JETP editor July 30, 1960

J. Exptl. Theoret. Phys. (U.S.S.R.) **39**, 1459-1467 (November, 1960)

It is shown that the eigenfunctions of the Hamiltonian of a three-particle system with pair interaction can be represented in a natural fashion as the sum of three terms, for each of which there exists a linked set of equations. This set can be written down with the help of the solutions of the pair problems, and can be solved uniquely, in contrast to the equations of the Lippman-Schwinger type. In the limit of zero range, the well-known Skornyakov-Ter-Martirosyan equations are obtained.

AT the present time, the basic premises of scattering theory, with redistribution of the particles, have been worked out in as much detail as in the theory of elastic scattering. To be precise, nonstationary (Ekstein[1]) and the stationary (Gerjuoy[2]) statements of the scattering problem have been given, a unique procedure has been formulated for the writing down of the element of the S matrix for any possible process, and the asymptotic value of the eigenfunctions of the Hamiltonian of the system in configuration space has been expressed in terms of these matrix elements. However, integral equations of the Lippman-Schwinger type,[3,4] which are easily derived for these functions even in this general case,[4,5] possess a number of inadequacies. In the first place, these equations possess solutions for both the homogeneous and inhomogeneous equation, so that the solution is not determined uniquely by the free term. In the second place, it is difficult in these equations to proceed to the case in which the pair interactions are specified not by means of potentials, but, for example, by means of boundary conditions (solid spheres) or by the specifying of the logarithmic derivative of the solution for r = 0 (zero-range forces).

We obtain below for the eigenfunctions equations that are free of these inadequacies. It is shown that the eigenfunctions can be represented in a natural way as sums of three terms, for which there exists a linked set of equations. In the case of three particles with pair interaction, there are three such terms and all the equations are inhomogeneous, while the homogeneous equation has a solution only for energies corresponding to the bound state of the entire system. To determine the kernels of the integral equations it is necessary to solve only the pair problem. These kernels are generalizations of the so-called T matrix, and can easily be constructed for different limiting cases, in which there is no potential. We note that the natural division of the wave function in the three particle problem into three terms has appeared in several researches devoted to the question (see, for example, references 7 and 8).

The derivation of the equations is given in the first section. We begin by recalling well-known premises of scattering theory. In the second section, the equations are written down in the momentum representation. The meaning of pair kernels is explained there in detail. The equations are written in terms of these kernels. In the third section, a number of remarks are made in connection with the equations that have been derived.

1. FORMAL THEORY

The method will be illustrated by an example of three nonrelativistic spinless particles with masses m_1, m_2, m_3. The particles are assumed to be different. The Hamiltonian of the system has the form ($\hbar = 1$)

$$H = T_1 + T_2 + T_3 + V_{23} + V_{31} + V_{12}, \tag{1}$$

$$T_i = -(1/2m_i)\nabla_i^2, \qquad i = 1, 2, 3; \tag{2}$$

V_{ij} acts only on the variable $\mathbf{r}_{ij} = \mathbf{r}_i - \mathbf{r}_j$ of the wave function and vanishes as $r_{ij} \rightarrow \infty$.

In this system, infinite motions are possible, whether of all three particles or of the bound state of any pair plus the third particle. We shall prove that each pair can form bound states. This situation is expressed in the asymptotic behavior of the wave functions of the system. The asymptotic basis functions Φ_n are generally separated into four classes. The functions

$$\Phi_{n_0} = \exp\{i\mathbf{k}_1\mathbf{r}_1 + i\mathbf{k}_2\mathbf{r}_2 + i\mathbf{k}_3\mathbf{r}_3\} \tag{3}$$

with energies

$$E_{n_0} = k_1^2/2m_1 + k_2^2/2m_2 + k_3^2/2m_3 \tag{4}$$

describe the free motion of all three particles.

The free motion of the bound state of particles 2 and 3 and of particle 1 is described by the functions

$$\Phi_{n_{23}} = \exp\{i\mathbf{k}_1\mathbf{r}_1 + i\mathbf{K}_{23}\mathbf{R}_{23}\}\,\varphi_{23}^{(l)}(\mathbf{r}_{23}), \tag{5}$$

$$\mathbf{R}_{23} = (m_2\mathbf{r}_2 + m_3\mathbf{r}_3)/(m_2 + m_3), \qquad \mathbf{r}_{23} = \mathbf{r}_2 - \mathbf{r}_3. \tag{6}$$

Here $\varphi_{23}^{(l)}(\mathbf{r})$ is the solution of the equation

$$[-(1/2\mu_{23})\nabla_r^2 + v_{23}(\mathbf{r})]\,\varphi_{23}^{(l)}(\mathbf{r}) = -\lambda_{23}^{(l)}\varphi_{23}^{(l)}(\mathbf{r}), \tag{7}$$

where

$$\mu_{23} = m_2m_3/(m_2 + m_3), \qquad \lambda_{23}^{(l)} > 0, \qquad l = 1, 2, \ldots,$$

i.e., the function that describes the bound state. The corresponding energy is determined by the formula

$$E_{n_{23}} = k_1^2/2m_1 + K_{23}^2/2(m_2 + m_3) - \lambda_{23}^{(l)}. \tag{8}$$

The functions $\Phi_{n_{31}}$ and $\Phi_{n_{12}}$ can be constructed similarly.

The element of the S matrix that characterizes the transition from the state described asymptotically by the function Φ_i to the state described by the function Φ_f is determined by the expression

$$R_{fi} = \langle\Phi_f, V_f\,\Psi_i\rangle, \qquad E_i = E_f. \tag{9}$$

Here V_f is the part of the interaction which is not taken into account in the state Φ_f, while the function Ψ_i is determined by means of the resolvent

$$G(z) = (H - z)^{-1} \tag{10}$$

according to the formula

$$\Psi_n = -\underset{\varepsilon\to+0}{i\varepsilon G}(E_n + i\varepsilon)\,\Phi_n. \tag{11}$$

The functions Ψ_n are the eigenfunctions of the total Hamiltonian H with eigenvalues E_n. Equations of the Lippman-Schwinger type for these functions are easily constructed from the corresponding equation for the resolvent G(z):

$$G(z) = G_0(z) - G_0(z)\,VG(z), \tag{12}$$

$$G_0(z) = (H_0 - z)^{-1},$$

$$H_0 = T_1 + T_2 + T_3, \qquad V = H - H_0. \tag{13}$$

Multiplying both sides of (12) by $-i\epsilon$ and applying the equation to Φ_n, we get

$$\Psi_n = -\underset{\varepsilon\to+0}{i\varepsilon G_0}(E_n + i\varepsilon)\,\Phi_n - G_0(E_n + i0)\,V\Psi_n. \tag{14}$$

It is not difficult to see that

$$-\underset{\varepsilon\to+0}{i\varepsilon\,G_0}(E_{n_0} + i\varepsilon)\,\Phi_{n_0} = \Phi_{n_0}, \tag{15}$$

so that we get an equation of the Lippman-Schwinger type for Ψ_{n_0}:

$$\Psi_{n_0} = \Phi_{n_0} - G_0(E_{n_0} + i0)\,V\Psi_{n_0}. \tag{16}$$

Here,

$$-\underset{\varepsilon\to+0}{i\varepsilon G_0}(E_{n_{23}} + i\varepsilon)\,\Phi_{n_{23}} = 0, \tag{17}$$

since

$$\begin{aligned} G_0(z)\,\Phi_{n_{23}} &= \exp\{i\mathbf{k}_1\mathbf{r}_1 + i\mathbf{K}_{23}\mathbf{R}_{23}\} \\ &\times \frac{2\mu_{23}}{4\pi}\int \frac{\exp\{i\,[2\mu_{23}(z - k_1^2/2m_1 - K_{23}^2/2\,(m_2 + m_3))]^{1/2}\,|\,\mathbf{r}_{23} - \mathbf{r}_{23}'\,|\}}{|\,\mathbf{r}_{23} - \mathbf{r}_{23}'\,|} \\ &\times \varphi_{23}^{(l)}(\mathbf{r}_{23}')\,d^3r_{23}' \end{aligned} \tag{18}$$

does not possess a singularity for $z = E_{n_{23}}$. Thus $\Psi_{n_{23}}$ is the solution of the homogeneous equation in terms of the Green's function G_0:

$$\Psi_{n_{23}} = -G_0(E_{n_{23}} + i0)\,V\Psi_{n_{23}}. \tag{19}$$

If we use the Green's function

$$G_{23}(z) = (H_0 + V_{23} - z)^{-1}, \tag{20}$$

then we get inhomogeneous equations for Ψ_{n_0} and $\Psi_{n_{23}}$. However, the equations for $\Psi_{n_{31}}$ and $\Psi_{n_{12}}$, expressed in terms of this Green's function, will be homogeneous.

Actually we have, for example,

$$\begin{aligned} G_{23}(z)\,\Phi_{n_{31}} &= \exp\{i\mathbf{K}\mathbf{R}\}\int d^3p\,\exp\{i\mathbf{p}\boldsymbol{\rho}_1\}\left[\left(\frac{1}{2\pi}\right)^3\int\varphi_{31}(\mathbf{r})\right. \\ &\left.\times\exp\left\{-i\mathbf{r}\left(\mathbf{p} + \frac{m_1}{m_1 + m_3}\mathbf{p}_2\right)\right\}d^3\mathbf{r}\right] \\ &\times\left[\int g_{23}\left(\mathbf{r}_{23},\ \mathbf{r}',\ z - \frac{p^2}{2\mu_1} - \frac{K^2}{2M}\right)\right. \\ &\left.\times\exp\left\{-i\mathbf{r}'\left(\frac{m_2}{m_2 + m_3}\mathbf{p} + \mathbf{p}_2\right)\right\}d^3\mathbf{r}'\right]. \end{aligned} \tag{21}$$

Here $g_{23}(\mathbf{r}, \mathbf{r}', z)$ is the solution of the equation

$$[-(2\mu_{23})^{-1}\nabla_r^2 + v_{23}(\mathbf{r}) - z]\,g_{23}(\mathbf{r}, \mathbf{r}', z) = \delta^3(\mathbf{r} - \mathbf{r}'), \tag{22}$$

which, as is known, has poles at $z = -\lambda_{23}^{(l)}$, $l = 1, 2, \ldots$;

$$\mathbf{R} = M^{-1}(m_1\mathbf{r}_1 + m_2\mathbf{r}_2 + m_3\mathbf{r}_3),$$

$$\boldsymbol{\rho}_1 = (m_2 + m_3)^{-1}(m_2\mathbf{r}_2 + m_3\mathbf{r}_3) - \mathbf{r}_1, \qquad \mathbf{K} = \mathbf{K}_{31} + \mathbf{k}_2,$$

$$\mu_1 = m_1(m_2 + m_3)/M, \qquad \mathbf{p}_2 = M^{-1}(m_2\mathbf{K}_{31} - (m_1 + m_3)\,\mathbf{k}_2),$$

$$M = m_1 + m_2 + m_3. \tag{23}$$

After integration over p we get a smooth function of z, such that

$$- i\varepsilon G_{23} (E_{n_{31}} + i\varepsilon) \Phi_{n_{31}} = 0. \quad (24)$$
$$\scriptstyle \varepsilon \to +0$$

Thus, in the case under examination, equations of the Lippman-Schwinger type do not have unique solutions, and the choice of the latter must be carried out through additional requirements, for example, asymptotic behavior in all directions in configuration space. But this means that the equations do not satisfy the fundamental role of integral equations — that of combining the differential equation and the boundary conditions in a single relation. Therefore, these equations are ill-suited for finding the solutions in practice.

We shall begin the derivation of our equations for the eigenfunctions by revising Eq. (12) for $G(z)$. We shall seek $G(z)$ in the form

$$G(z) = G_0(z) - G_0(z) T(z) G_0(z). \quad (25)$$

We have for $T(z)$ the equation

$$T(z) = V - VG_0(z) T(z). \quad (26)$$

We now consider the successive approximations for this equation:

$$\begin{aligned} T(z) &= V_{23} + V_{31} + V_{12} \\ &\quad - (V_{23} + V_{31} + V_{12}) G_0(z) (V_{23} + V_{31} + V_{12}) + \ldots \end{aligned} \quad (27)$$

and reconstruct the series in the following way:

$$\begin{aligned} T(z) &= V_{23} - V_{23}G_0(z) V_{23} + V_{23}G_0(z) V_{23}G_0(z) V_{23} - \ldots \\ &\quad + V_{31} - V_{31}G_0(z) V_{31} + \ldots + V_{12} - V_{12}G_0(z) V_{12} + \ldots \\ &\quad + (V_{23} - V_{23}G_0(z) V_{23} + \ldots) G_0(z) \\ &\quad \times (V_{31} - V_{31}G_0(z) V_{31} + \ldots) + \ldots \end{aligned} \quad (28)$$

We denote by $T_{23}(z)$ the sum of the chain

$$T_{23}(z) = V_{23} - V_{23}G_0(z) V_{23} + \ldots \quad (29)$$

Obviously, $T_{23}(z)$ is the solution of the equation

$$T_{23}(z) = V_{23} - V_{23}G_0(z) T_{23}(z), \quad (30)$$

which is obtained from (26) if we set the two potentials V_{31} and V_{12} equal to zero. In Eq. (30) the variables are separated trivially (this is done below in detail) and the operator $T_{23}(z)$ is characterized only by the pair interaction of particles 2 and 3. $T_{31}(z)$ and $T_{12}(z)$ are introduced similarly. It is not difficult to write down the series for (27) by means of these operators. It suffices to replace all V_{ij} in (27) by the corresponding $T_{ij}(z)$ and to omit terms that contain a factor of the type $T_{23}(z) G_0(z) T_{23}(z)$, i.e., where $T_{ij}(z)$ with the same indices appear side by side.

It is not possible to write down the equation for which the resultant series would be the successive-approximation series. However, if we represent $T(z)$ as a sum of three terms

$$T(z) = T^{(1)}(z) + T^{(2)}(z) + T^{(3)}(z), \quad (31)$$

where, for example,

$$T^{(1)}(z) = V_{23} - V_{23}G_0(z) T(z) \quad (32)$$

and $T^{(2)}(z)$ and $T^{(3)}(z)$ are similarly defined, then these components satisfy a linked set of equations, which are conveniently written in matrix form:

$$\begin{pmatrix} T^{(1)}(z) \\ T^{(2)}(z) \\ T^{(3)}(z) \end{pmatrix} = \begin{pmatrix} T_{23}(z) \\ T_{31}(z) \\ T_{12}(z) \end{pmatrix} - \begin{pmatrix} 0 & T_{23}(z) & T_{23}(z) \\ T_{31}(z) & 0 & T_{31}(z) \\ T_{12}(z) & T_{12}(z) & 0 \end{pmatrix} G_0(z) \begin{pmatrix} T^{(1)}(z) \\ T^{(2)}(z) \\ T^{(3)}(z) \end{pmatrix}. \quad (33)$$

It is not difficult to verify that the successive approximations for this equation duplicate the series described above. Naturally, the validity of the resultant system does not depend on the convergence of this series. A derivation of Eq. (33) without the use of perturbation theory will be published elsewhere.

We now obtain the corresponding equations for the functions Ψ_n. In accord with the expansion (31), we have

$$G(z) = G_0(z) + G^{(1)}(z) + G^{(2)}(z) + G^{(3)}(z), \quad (34)$$

where the functions

$$G^{(i)}(z) = - G_0(z) T^{(i)} G_0(z), \qquad i = 1, 2, 3, \quad (35)$$

satisfy the equation

$$\begin{pmatrix} G^{(1)} \\ G^{(2)} \\ G^{(3)} \end{pmatrix} = \begin{pmatrix} G_{23} - G_0 \\ G_{31} - G_0 \\ G_{12} - G_0 \end{pmatrix} - G_0 \begin{pmatrix} 0 & T_{23} & T_{23} \\ T_{31} & 0 & T_{31} \\ T_{12} & T_{12} & 0 \end{pmatrix} \begin{pmatrix} G^{(1)} \\ G^{(2)} \\ G^{(3)} \end{pmatrix}. \quad (36)$$

Here the argument z is everywhere omitted,

$$G_{ij}(z) = (H_0 + V_{ij} - z)^{-1}. \quad (37)$$

Applying both sides of this equation (multiplied by $-i\epsilon$) to the functions Φ_{n_0} and $\Phi_{n_{23}}$, and taking into account equalities of the type (17) and (24), we get equations of the following form for Ψ_{n_0} and $\Psi_{n_{23}}$:

$$\Psi_{n_0} = \Phi_{n_0} + \Psi_{n_0}^{(1)} + \Psi_{n_0}^{(2)} + \Psi_{n_0}^{(3)} \qquad (z = E_{n_0} + i0), \quad (38)$$

$$\begin{pmatrix} \Psi^{(1)} \\ \Psi^{(2)} \\ \Psi^{(3)} \end{pmatrix} = \begin{pmatrix} \Phi_{n_0}^{(23)} - \Phi_{n_0} \\ \Phi_{n_0}^{(31)} - \Phi_{n_0} \\ \Phi_{n_0}^{(12)} - \Phi_{n_0} \end{pmatrix} - G_0(z) \begin{pmatrix} 0 & T_{23}(z) & T_{23}(z) \\ T_{31}(z) & 0 & T_{31}(z) \\ T_{12}(z) & T_{12}(z) & 0 \end{pmatrix} \begin{pmatrix} \Psi^{(1)} \\ \Psi^{(2)} \\ \Psi^{(3)} \end{pmatrix}; \quad (39)$$

$$\Psi_{n_{23}} = \Psi_{n_{23}}^{(1)} + \Psi_{n_{23}}^{(2)} + \Psi_{n_{23}}^{(3)} \qquad (z = E_{n_{23}} + i0), \quad (40)$$

$$\begin{pmatrix} \Psi^{(1)} \\ \Psi^{(2)} \\ \Psi^{(3)} \end{pmatrix} = \begin{pmatrix} \Phi_{n_{23}} \\ 0 \\ 0 \end{pmatrix} - G_0(z) \begin{pmatrix} 0 & T_{23}(z) & T_{23}(z) \\ T_{31}(z) & 0 & T_{31}(z) \\ T_{12}(z) & T_{12}(z) & 0 \end{pmatrix} \begin{pmatrix} \Psi^{(1)} \\ \Psi^{(2)} \\ \Psi^{(3)} \end{pmatrix} \quad (41)$$

Here, in order to avoid encumbering the formulas, we have omitted at many places a number of indices characterizing the corresponding functions.

The equations for $\Psi_{n_{31}}$ and $\Psi_{n_{12}}$ are similar to the equation for $\Psi_{n_{23}}$ except that the free term differs from zero in the second and third place, respectively. In Eqs. (39) we denote by $\Phi_{n_0}^{(ij)}$ the limits

$$\Phi_{n_0}^{(ij)} = \underset{\varepsilon\to+0}{-\,i\varepsilon G_{ij}}\,(E_{n_0}+i\varepsilon)\,\Phi_{n_0}. \tag{42}$$

It is not difficult to establish that, for example,

$$\Phi_{n_0}^{(23)} = \exp\,\{i\mathbf{k}_1\mathbf{r}_1 + i\mathbf{K}_{23}\mathbf{R}_{23}\}\,\varphi_{23}(\mathbf{r}_{23},\ \mathbf{k}_{23}), \tag{43}$$

where $\varphi_{23}(\mathbf{r},\mathbf{k})$ is a solution of the equation

$$[-(2\mu_{23})^{-1}\nabla_r^2 + v_{23}(\mathbf{r})]\,\varphi_{23}(\mathbf{r},\ \mathbf{k}) = k^2\varphi_{23}(\mathbf{r},\ \mathbf{k}), \tag{44}$$

such that $\varphi_{23}(\mathbf{r},\mathbf{k}) - e^{i\mathbf{k}\cdot\mathbf{r}}$ is a diverging wave in which

$$\mathbf{K}_{23} = \mathbf{k}_2 + \mathbf{k}_3, \qquad \mathbf{k}_{23} = (m_2\mathbf{k}_2 - m_3\mathbf{k}_2)/(m_2+m_3). \tag{45}$$

2. MOMENTUM REPRESENTATION

The momentum representation is especially suitable for writing down these equations. We can introduce three different systems of coordinates in place of the coordinates $\mathbf{k}_1$, $\mathbf{k}_2$, $\mathbf{k}_3$ in this representation. For example, in the set

$$\mathbf{K} = \mathbf{k}_1 + \mathbf{k}_2 + \mathbf{k}_3, \qquad \mathbf{k}_{23} = (m_3\mathbf{k}_2 - m_2\mathbf{k}_3)\,/\,(m_2+m_3),$$
$$\mathbf{p}_1 = M^{-1}\,[m_1(\mathbf{k}_2+\mathbf{k}_3) - (m_2+m_3)\,\mathbf{k}_1], \quad M = m_1+m_2+m_3 \tag{46}$$

the kernel of the operator $T_{23}(z)$ assumes an especially simple form:

$$T_{23}(\mathbf{k}_1,\ \mathbf{k}_2,\ \mathbf{k}_3,\ \mathbf{k}_1',\ \mathbf{k}_2',\ \mathbf{k}_3';\ z)$$
$$= \delta^3(\mathbf{K}-\mathbf{K}')\,\delta^3(\mathbf{p}_1-\mathbf{p}_1')\,t_{23}(\mathbf{k}_{23},\ \mathbf{k}_{23}';\ z - K^2/2M$$
$$- p_1^2/2\mu_1), \tag{47}$$

where $\mu_1 = m_1(m_2+m_3)/M$, and $t_{23}(\mathbf{k},\mathbf{k}';z)$ is a solution of an equation of the type

$$t(\mathbf{k},\ \mathbf{k}';\ z) = v(\mathbf{k}-\mathbf{k}') - \int\frac{v(\mathbf{k}-\mathbf{k}'')\,t(\mathbf{k}'',\ \mathbf{k}';\ z)}{\mathbf{k}''^2/2\mu - z}\,d^3k''. \tag{48}$$

In operator form, (48) has the form

$$t(z) = v - vg_0(z)\,t(z), \tag{49}$$

$$g_0(z) = (h_0 - z)^{-1}, \qquad h_0 = -(1/2\mu)\,\nabla^2. \tag{50}$$

We see that $t(\mathbf{k},\mathbf{k}';z)$ represents a kernel of the pair T matrix, where all the arguments have independent values. The scattering amplitude of particles 2 and 3 on one another is proportional in their center-of-mass system to $t_{23}(\mathbf{k},\mathbf{k}';z)$ for $2\mu_{23}z = k^2 + i0 = k'^2 + i0$.

It is convenient to write down the kernels of the operators $T_{31}(z)$ and $T_{12}(z)$ in the coordinates $\mathbf{K}$, $\mathbf{k}_{31}$, $\mathbf{p}_2$ and $\mathbf{K}$, $\mathbf{k}_{12}$, $\mathbf{p}_3$, respectively. Expressions for these coordinates and for the kernels of the operators $T_{31}(z)$ and $T_{12}(z)$ are obtained by interchanging of the indices in the given formulas.

The operator $G_0(z)$ is the operator of multiplication by the function

$$\left(\frac{K^2}{2M}+\frac{k_{23}^2}{2\mu_{23}}+\frac{p_1^2}{2\mu_1}-z\right)^{-1} = \left(\frac{K^2}{2M}+\frac{k_{31}^2}{2\mu_{31}}+\frac{p_2^2}{2\mu_2}-z\right)^{-1}$$
$$= \left(\frac{K^2}{2M}+\frac{k_{12}^2}{2\mu_{12}}+\frac{p_3^2}{2\mu_3}-z\right)^{-1}. \tag{51}$$

All the Φ_n functions contain the factor $\delta^3(\mathbf{K}-\mathbf{K}_0)$, where $\mathbf{K}_0$ is the total momentum of the system.* It is not difficult to transform to the center-of-mass system, dropping this factor and introducing a new reference point for the energy

$$\overline{E}_n = E_n - K_0^2/2M. \tag{52}$$

Below we shall operate in the center-of-mass system and will not write the bar over E_n.

Our system becomes especially simple if we introduce separate coordinates for each component $\Psi^{(i)}$:

$$\Psi^{(1)} = \Psi^{(1)}(\mathbf{k}_{23},\ \mathbf{p}_1), \qquad \Psi^{(2)} = \Psi^{(2)}(\mathbf{k}_{31},\ \mathbf{p}_2),$$
$$\Psi^{(3)} = \Psi^{(3)}(\mathbf{k}_{12},\ \mathbf{p}_3). \tag{53}$$

For these functions, the equation take on the following form:

$$\overline{\Psi}_n(\mathbf{k},\ \mathbf{p}) = \overline{\Phi}_n(\mathbf{k},\ \mathbf{p}) - \int A(\mathbf{k},\ \mathbf{p},\ \mathbf{k}',\ \mathbf{p}';$$
$$z = E_n + i0)\,\overline{\Psi}_n(\mathbf{k}',\ \mathbf{p}')\,d^3k'd^3p'. \tag{54}$$

Here $\overline{\Psi}_n$ and $\overline{\Phi}_n$ are columns of three components, while A is a three-row square matrix. The elements $a^{(ij)}$ of this matrix have the form

$$a^{(11)} = a^{(22)} = a^{(33)} = 0,$$
$$a^{(12)} = \left(\frac{k^2}{2\mu_{23}}+\frac{p^2}{2\mu_1}-z\right)^{-1} t_{23}\left(\mathbf{k},\ -\frac{m_2}{(m_2+m_3)}\mathbf{p}-\mathbf{p}',\ z-\frac{p^2}{2\mu_1}\right)$$
$$\times\,\delta^3\left(\mathbf{k}'-\mathbf{p}-\frac{m_1}{(m_1+m_3)}\mathbf{p}'\right),$$
$$a^{(13)} = \left(\frac{k^2}{2\mu_{23}}+\frac{p^2}{2\mu_1}-z\right)^{-1} t_{23}\left(\mathbf{k},\ \frac{m_3}{(m_2+m_3)}\mathbf{p}+\mathbf{p}';\ z-\frac{p^2}{2\mu_1}\right)$$
$$\times\,\delta^3\left(\mathbf{k}'+\mathbf{p}+\frac{m_1}{(m_1+m_2)}\mathbf{p}'\right). \tag{55}$$

The expressions for $a^{(23)}$ and $a^{(31)}$ or for $a^{(21)}$ and $a^{(32)}$ are obtained from expressions for $a^{(12)}$ or $a^{(13)}$ by the corresponding interchange of the indices in the right hand sides of (55).

Equations (54) and (55) are the final forms of the equations used. The potentials V_{ij} do not appear explicitly in these equations. The mathematical solvability of these equations will be treated elsewhere.

---

*Here and throughout we denote the quantum numbers by an upper or lower index 0 to distinguish them from the arguments of the wave functions.

3. DISCUSSION OF THE DERIVED EQUATIONS

1. The equations become simplified in the case of identical particles. Thus, as an example, all the $\Psi^{(i)}(\mathbf{k},\mathbf{p})$ coincide for a symmetric eigenfunction Ψ_{sym}, so that we replace the set by the single equation

$$\Psi_n(\mathbf{k},\mathbf{p}) = \Phi_n(\mathbf{k},p) - \frac{m}{k^2+3p^2/4-mz}\int\Big[t\Big(\mathbf{k},-\frac{1}{2}\mathbf{p}-\mathbf{p}';\ z-\frac{3}{4}\frac{p^2}{m}\Big) \times \Psi_n\Big(\mathbf{p}+\frac{1}{2}\mathbf{p}',\ \mathbf{p}'\Big) + t\Big(\mathbf{k},\ \frac{1}{2}\mathbf{p}+\mathbf{p}';\ z-\frac{3}{4}\frac{p^2}{m}\Big) \times \Psi_n\Big(-\mathbf{p}-\frac{1}{2}\mathbf{p}',\ \mathbf{p}'\Big)\Big]\,d^3p',$$
$$z = E_n + i0. \tag{56}$$

If Ψ_{sym} corresponds to scattering by a bound system, then

$$\Phi_n(\mathbf{k},\mathbf{p}) = \delta^3(\mathbf{p}-\mathbf{p}_0)\,\varphi(\mathbf{k}), \qquad E_n = 3p_0^2/4 - \lambda, \tag{57}$$

where $\varphi(\mathbf{k})$ is the function describing the bound state. By solution of Eq. (56), Ψ_{sym} is expressed in the form

$$\Psi_{sym} = \Psi_n(\mathbf{k}_{23},\mathbf{p}_1) + \Psi_n(\mathbf{k}_{31},\mathbf{p}_2) + \Psi_n(\mathbf{k}_{12},\mathbf{p}_3) = 3\operatorname*{sym}_{\mathbf{k},\mathbf{p}}[\Psi(\mathbf{k}_{23},\mathbf{p}_1)]. \tag{58}$$

The symbol sym denotes symmetry with respect to the variables written beneath it.

If Ψ_{sym} corresponds to free motion of all three particles, then

$$\Phi_n(\mathbf{k},\mathbf{p}) = m\frac{t(\mathbf{k},\mathbf{k}_0;\ k_0^2/m+i0)}{k^2-k_0^2-i0}\,\delta^3(\mathbf{p}-\mathbf{p}_0),$$
$$E_n = \frac{k_0^2}{m} + \frac{3}{4}\frac{p_0^2}{m}, \tag{59}$$

$$\Psi_{sym} = \operatorname*{sym}_{\mathbf{k},\mathbf{p};\mathbf{k}^0,\mathbf{p}^0}[\delta^3(\mathbf{k}_{23}-\mathbf{k}_{23}^0)\,\delta^3(\mathbf{p}_1-\mathbf{p}_1^0) + 3\Psi_n(\mathbf{k}_{23},\mathbf{p}_1;\ \mathbf{k}_{23}^0,\mathbf{p}_1^0)]. \tag{60}$$

In the approximation of zero range of forces, $t(\mathbf{k},\mathbf{k}';z)$ does depend on neither $\mathbf{k}$ nor $\mathbf{k}'$:

$$t(\mathbf{k},\mathbf{k}';z) = [(2\pi)^2\mu(\alpha+i\sqrt{2\mu z})]^{-1}, \quad \operatorname{Im}\sqrt{z} \geqslant 0. \tag{61}$$

Here α is the inverse scattering length. If $\alpha > 0$, then the pair problem has a bound state, in which the corresponding $\varphi(\mathbf{k})$ has the form

$$\varphi(\mathbf{k}) = N/(k^2+\alpha^2), \tag{62}$$

where N is a normalizing factor. Equation (56) shows that in the corresponding problem with three particles, the symmetric function for scattering on a bound state is determined by Eq. (58), where $\Psi_n(\mathbf{k},\mathbf{p})$ has the form

$$\Psi_n(\mathbf{k},\mathbf{p}) = \frac{Nm}{k^2+3p^2/4-mz}\left(\delta^3(\mathbf{p}-\mathbf{p}_0) - \frac{1}{\pi^2}\frac{\varphi(\mathbf{p},\mathbf{p}_0)}{\alpha+i\sqrt{mz-3p^2/4}}\right), \tag{63}$$

where the following equation is valid for $\varphi(\mathbf{p},\mathbf{p}_0)$:

$$\varphi(\mathbf{p},\mathbf{p}_0) = (p^2+\mathbf{p}\mathbf{p}_0+p_0^2-mz)^{-1} - \frac{1}{\pi^2}\int\frac{\varphi(\mathbf{p}',\mathbf{p}_0)\,d^3p'}{(p^2+\mathbf{p}\mathbf{p}'+p'^2-mz)(\alpha+i\sqrt{mz-3p'^2/4})}. \tag{64}$$

This equation is identical with the equation of Skornyakov–Ter-Martirosyan.[9] This is not difficult to prove by making the substitution

$$\varphi(\mathbf{p},\mathbf{p}_0) = \frac{3}{8}\frac{a(\mathbf{p},\mathbf{p}_0)}{\alpha-i\sqrt{mz-3p^2/4}}. \tag{65}$$

2. The potentials can be entirely eliminated from the expressions for the matrix elements of the S matrix. We shall carry out the corresponding derivation for the case of a process in which particle 3 is scattered from a bound state of particles 1 and 2 to produce a bound state of particles 3 and 1 and a free particle 2, i.e., for the process

$$(1,2)+3\to 2+(1,3). \tag{66}$$

The matrix element is determined by the expression

$$R_{fi} = \langle\Phi_f,\ V_f\,\Psi_i\rangle, \qquad E_f = E_i, \tag{67}$$

where

$$\Phi_f = \Phi_{n_{31}}, \qquad V_f = V_{23}+V_{12},$$
$$E_f = 2\mu_2(p_2^0)^2 - \lambda_{31}, \qquad E_i = 2\mu_3(p_3^0)^2 - \lambda_{12},$$
$$\Psi_i = \Psi_{n_{12}} = \Psi^{(1)}+\Psi^{(2)}+\Psi^{(3)}. \tag{68}$$

Here λ_{31} and λ_{12} are the corresponding positive binding energies.

With the help of an equation of the type (30) for T_{23} and (41) for $\Psi_{n_{12}}$, we get

$$V_{23}\Psi^{(1)} = -V_{23}G_0T_{23}(\Psi^{(2)}+\Psi^{(3)}) = -V_{23}(\Psi^{(2)}+\Psi^{(3)}) + T_{23}(\Psi^{(2)}+\Psi^{(3)}) \tag{69}$$

and, consequently,

$$V_{23}\Psi_i = T_{23}(\Psi^{(2)}+\Psi^{(3)}). \tag{70}$$

Similarly,

$$V_{12}\Psi_i = V_{12}\Phi_{n_{12}} + T_{12}(\Psi^{(1)}+\Psi^{(2)}) \tag{71}$$

and thus

$$\langle\Phi_f,\ V_f\,\Psi_i\rangle = \langle\Phi_{n_{31}},\ V_{12}\,\Phi_{n_{12}}\rangle + \langle\Phi_{n_{31}},\ T_{23}(z)(\Psi^{(2)}+\Psi^{(3)}) + T_{12}(z)(\Psi^{(1)}+\Psi^{(2)})\rangle,$$
$$z = E_i + i0. \tag{72}$$

The potential V_{12} can also be eliminated from the first term. Simple calculation with the aid of the equation for $\varphi_{12}(r)$ shows that

$$\langle\Phi_{n_{31}}, V_{12}\Phi_{n_{12}}\rangle = -\left[\frac{1}{2\mu_{12}}\left(\mathbf{p}_2^0 + \frac{m_2}{m_1+m_2}\mathbf{p}_3^0\right)^2 + \lambda_{12}\right] \times \varphi_{12}\left(\mathbf{p}_2^0 + \frac{m_2}{m_1+m_2}\mathbf{p}_3^0\right)\varphi_{31}\left(\mathbf{p}_3^0 + \frac{m_3}{m_1+m_3}\mathbf{p}_2^0\right), \qquad (73)$$

where $\varphi_{12}(\mathbf{k})$ and $\varphi_{31}(\mathbf{k})$ are functions describing the bound states in the momentum representation.

The matrix elements for other processes can be transformed in a similar fashion. A special paper will be devoted to various similar formulas, to the proof of the completeness of the eigenfunctions and the unitarity of the S matrix, and to other premises of the so-called formal scattering theory.

3. Obviously, the re-formulation of the equations of scattering theory given here can be carried out in the case of an arbitrary number of particles $n \geq 3$. If there are only pair interactions, then the number of equations in the system will be $N = n(n-1)/2$. These equations will be useful if only there are no more bound states than pairs of particles, since otherwise solutions of the homogeneous equations will exist. If triple or more complicated bound states exist, then a more complex construction must be used for $n \geq 4$. In this case, it is natural to assume the existence of triple or more complicated interactions.

In any case, for pair interactions in which repulsion predominates, equations similar to those obtained can be shown to be useful. An especially great simplification is obtained for the problem with identical particles. In this case, the system reduces to a single equation. We note that in the nonstationary formulation (more precisely, in the problem of statistical physics, where the inverse temperature plays a role similar to the time) the reconstruction of a series similar to (27) has been carried out by Yang and Lee.[10] However, these authors did not write out any integral equation, of which there is one in our case, since the particles are considered to be identical. It is possible that this equation can be useful for the problems of statistical physics.

The author thanks F. A. Berezin, V. N. Gribov, S. V. Maleev, and L. V. Prokhorov for discussions and useful remarks.

---

[1] H. Ekstein, Phys. Rev. **101**, 880 (1956).

[2] E. Gerjuoy, Ann. Phys. **5**, 58 (1958).

[3] B. A. Lippman and J. Schwinger, Phys. Rev. **79**, 469 (1950).

[4] M. Gell-Mann and M. L. Goldberger, Phys. Rev. **91**, 398 (1953).

[5] B. A. Lippman, Phys. Rev. **102**, 264 (1956).

[6] L. L. Foldy and W. Tobocman, Phys. Rev. **105**, 1099 (1957).

[7] V. N. Gribov, JETP **38**, 553 (1960), Soviet Phys. JETP **11**, 400 (1960).

[8] L. Eyges, Phys. Rev. **115**, 1643 (1959).

[9] G. V. Skornyakov and K. A. Ter-Martirosyan, JETP **31**, 775 (1956), Soviet Phys. JETP **4**, 648 (1957).

[10] T. D. Lee and C. N. Yang, Phys. Rev. **113**, 1165 (1959).

Translated by R. T. Beyer
263

Letters to the Editor

THE REACTION (α, t) ON Li^7, Be^9, *AND* Na^{23}

N. A. VLASOV, S. P. KALININ, A. A. OGLOBLIN, and V. I. CHUEV

Submitted to JETP editor July 23, 1960

J. Exptl. Theoret. Phys. (U.S.S.R.) **39**, 1468-1470 (November, 1960)

SEVERAL reports[1-3] have appeared recently on the investigation of the reactions (p, α), (α, p), (d, α), etc. The angular distributions of the particles in these reactions recall in many cases the Butler curves, and it is therefore sometimes concluded that these reactions proceed via stripping or pickup. However, it is impossible to draw final conclusions concerning the mechanism of these reactions from the form of the angular distribution, which is the same for all direct processes. It may be that a comparison of the probabilities of excitation of the same states in the investigated reaction and in a reaction of known mechanism [for example (d, p) or (d, n)] is more sensitive to the mechanism of the process.

We have investigated the reaction (α, t) on the nuclei Li^7, Be^9, and Na^{23} at α-particle energies of 40 Mev over a broad interval of excitation energies. The residual nuclei Be^8, B^{10}, and Mg^{24} were obtained also in the stripping reaction (d, n),[4-5] and in the pickup reaction (d, t).[6-7] The reaction (α, t) has heretofore been investigated only in individual cases.[8-10]

The triton spectra were determined, as in the investigation of the (d, t) reaction[6] from the activity of the tritium accumulated in stacks of foils located around the target. The targets used were foils made of the investigated elements, 4 mg/cm^2 thick.

Figure 1 shows typical angular distributions of tritons in the reaction (α, t).

Figure 2 shows the triton spectra at small angles. In all three cases lines corresponding to many different states of the residual nuclei are observed. The angular distributions of most of the groups are well described by the square of the spherical Bessel function $[j_{l+\frac{1}{2}}(qR_0)]^2$, and the value of the orbital momentum of the captured proton is almost always in agreement with the values of the spins and parities of the investigated levels. The value used here for the radius R_0 coincides with that obtained from the stripping reaction on these nuclei.

In Figure 3 are compared the probabilities of excitation of the same levels of the final nuclei in the reactions (α, t), (d, n), and (d, t). A comparison of the reactions (α, t) and (d, n) on Na^{23} for levels with energy greater than 5 Mev must be made with caution, since transitions with $l = 0$, which are observed in this region in the reaction (d, n), may not be noticed in the reaction (α, t).

The great difference between the reaction (α, t) and (d, t) is not surprising, for in the (d, t) reaction it is the hole levels that are predominantly excited. But the spectra of the (α, t) reaction also differ greatly from the spectra of the reaction (d, n), in which, as in the (α, t) reaction a proton is captured. This means that in the (α, t) reaction the single-particle proton levels are not excited predominantly, as in the (d, n) reaction, and the mechanism of the (α, t) reaction differs appreciably from the stripping mechanism of the (d, n) reaction.

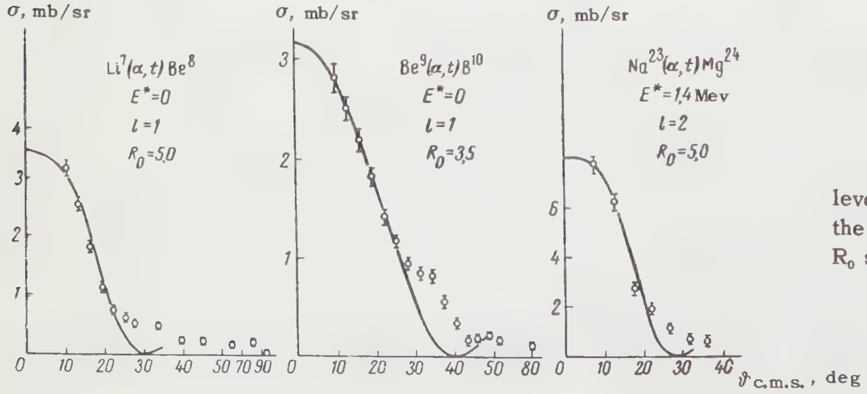

FIG. 1. Angular distributions of tritons. E* – level of residual nucleus. Solid curve – square of the spherical Bessel function for values of l and R_0 shown in the figure.

---

[1] P. Herrman and G. F. Pieper, Phys. Rev. **105**, 1556 (1957).

[2] C. B. Fulmer and B. L. Cohen, Phys. Rev. **112**, 1672 (1958).

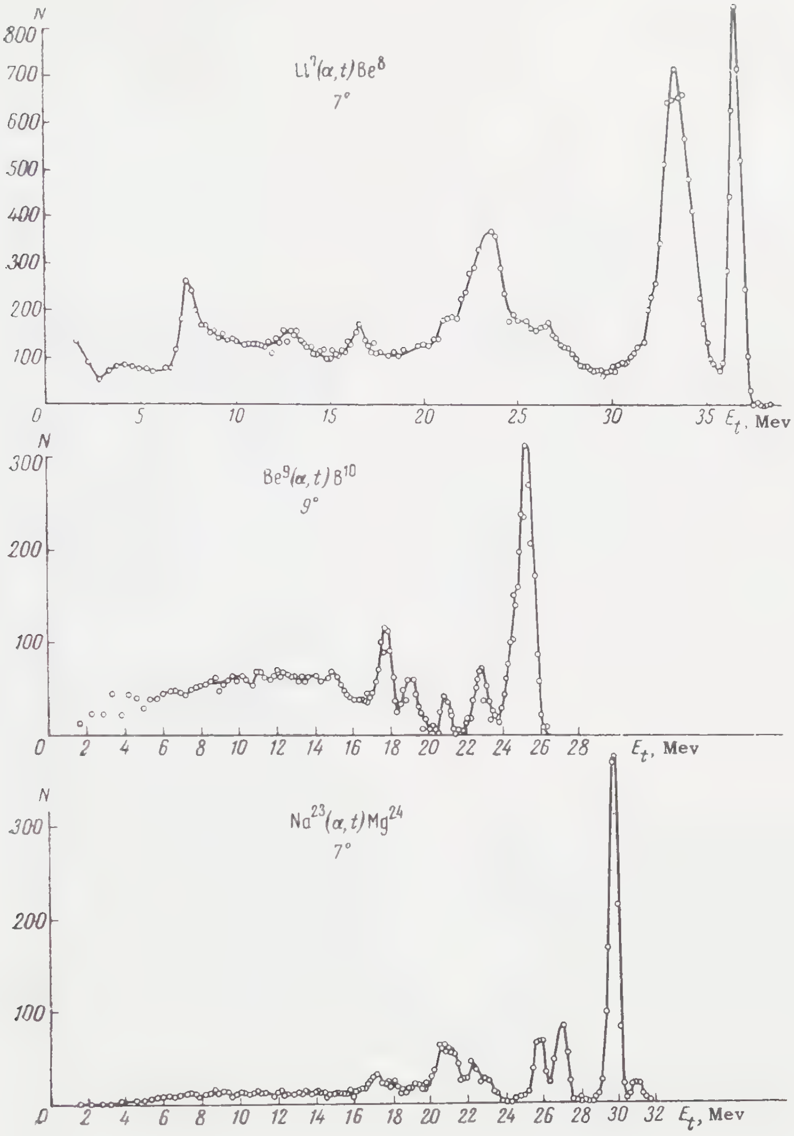

FIG. 2

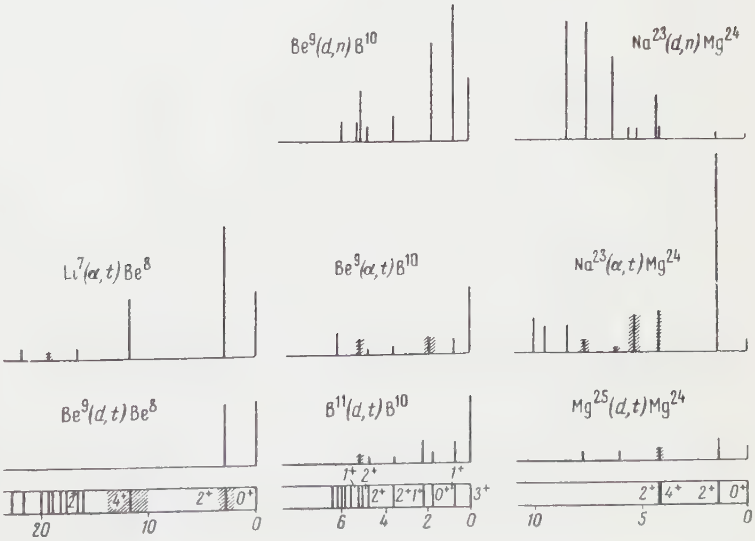

FIG. 3. Probabilities of excitation of the levels of the nuclei Be^8, B^{10}, and Mg^{24} in the reactions (d, n), (α, t), and (d, t). The ordinates represent the values of the differential cross section at the maximum [for the reactions (α, t) and for $Na^{23}(d, n)Mg^{24}$], and the reduced widths [for the reactions (d, t) and $Be^9(d, n)B^{10}$].

[3] M. El Nadi and M. El Khishin, Proc. Phys. Soc. 73, 705 (1959).

[4] W. E. Meyerhof and L. F. Chase, Phys. Rev. **111**, 1348 (1958).

[5] Calvert, Jaffe, Litherland, and Maslin, Proc. Phys. Soc. **A68**, 1017 (1955).

[6] N. A. Vlasov and A. A. Ogloblin, JETP **37**, 54 (1959), Soviet Phys. JETP **10**, 39 (1960).

[7] Vlasov, Kalinin, Ogloblin, and Chuev, Paper at the 10th Conference of Nuclear Spectroscopy, 1960 (in press).

[8] S. V. Starodubtsev and K. V. Makaryunas, JETP **36**, 1594 (1959), Soviet Phys. JETP **9**, 1133 (1959).

[9] J. L. Yntema, Bull. Am. Phys. Soc. **5**, 77 (1960).

[10] Gonzalez-Vidal, Conzett, and Wade, Bull. Am. Phys. Soc. **5**, 230 (1960).

Translated by J. G. Adashko
264

ANISOTROPY OF THE EVEN PHOTOMAGNETIC EFFECT IN n-TYPE GERMANIUM AT LOW TEMPERATURES

I. K. KIKOIN and S. D. LAZAREV

Submitted to JETP editor August 20, 1960

J. Exptl. Theoret. Phys. (U.S.S.R.) **39**, 1471-1473 (November, 1960)

THE anisotropy of the even photomagnetic emf observed in germanium[1] is at room temperatures satisfactorily described by the phenomenological equations of Kagan and Smorodinskiĭ[2] right up to magnetic fields of 20,000 oe.

A study of the temperature dependence of the even photomagnetic effect showed that at low temperatures its anisotropy becomes anomalous. The investigation was performed on single crystal specimens of n-type germanium.

The orientation of the crystal axes and the direction in which the even photomagnetic emf was measured were chosen in such a way that only the anisotropic component was measured.[3] In order to do this the specimen which was cut in the form of a circular disc was mounted such that the [111] axis coincided with the normal **n** to the illuminated surface. If we take the direction of the magnetic field H to be along the x axis, and the direction of the light ray along the y axis, we measured the even photomagnetic emf in the z direction. The odd photomagnetic emf which occurs along the same direction was eliminated by measuring for two opposite directions of the magnetic field. Under those conditions the expression for the even photomagnetic emf E_q is of the form (see also reference 3)

$$E_q = \frac{1}{3\sqrt{2}} LH^2 \sin^2\theta \cos 3\varphi, \qquad (1)$$

if we assume that the above mentioned phenomenological equations can be applied; in Eq. (1) φ is the angle over which the specimen is turned around the normal **n**, θ the angle between the normal **n** and z (the direction of the magnetic field), and L a material constant.

The specimen studied could be rotated both in its own plane around the normal **n** (to change the angle φ) and also around the z axis (to change the angle θ).

The dependence of the even photomagnetic emf on the angle φ (which at the same time determines the anisotropy) which was obtained at liquid nitrogen temperatures agreed completely with Eq. (1), as it does at room temperatures. As far as the dependence of this emf on the angle θ is concerned, at a temperature of 78°K it is essentially different from that at room temperature ($\sin^2\theta$). The dependence is depicted in Fig. 1 where along the ordinate axis the extremum values of the even photomagnetic emf are given which correspond to $\varphi = \pi/3, 2\pi/3, \ldots.$ The different

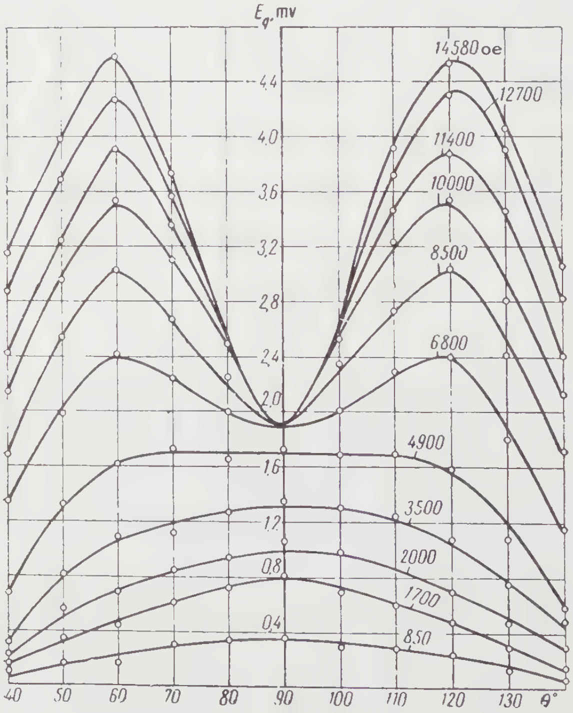

FIG. 1

curves correspond to the different values of the magnetic field given in the figure. While for small values of the field the angular dependence $E_q(\theta)$ approximately satisfies Eq. (1), at large values of the field $(H > 6000$ oe$)$ it behaves anomalously. The value of the emf goes through a minimum at $\theta = \pi/2$, shows a maximum at $\theta = 54°$ and $126°$ and decreases to zero at $\theta = 0°$ and $180°$.

It is essential to note that the dependence of the even photomagnetic emf on the magnetic field is different for different angles θ, as can be seen from Fig. 2. Along the ordinate axis we have again given the extremum values of the even photomagnetic emf. For $\theta = \pi/2$ (the plane of the specimen is then parallel to the magnetic field) the even photomagnetic emf reaches saturation in relatively small fields, H = 6000 oe. At $\theta = 80°$ the value of the field for which saturation is reached is equal to 10,000 oe. For larger angles θ saturation does apparently not set in until fields which are larger than those attained in our experimental conditions are reached.

Qualitatively similar curves have been obtained for the emf produced when illumination is replaced by an electrical current from an external emf source flowing through the specimen, in the direction of the incident light.

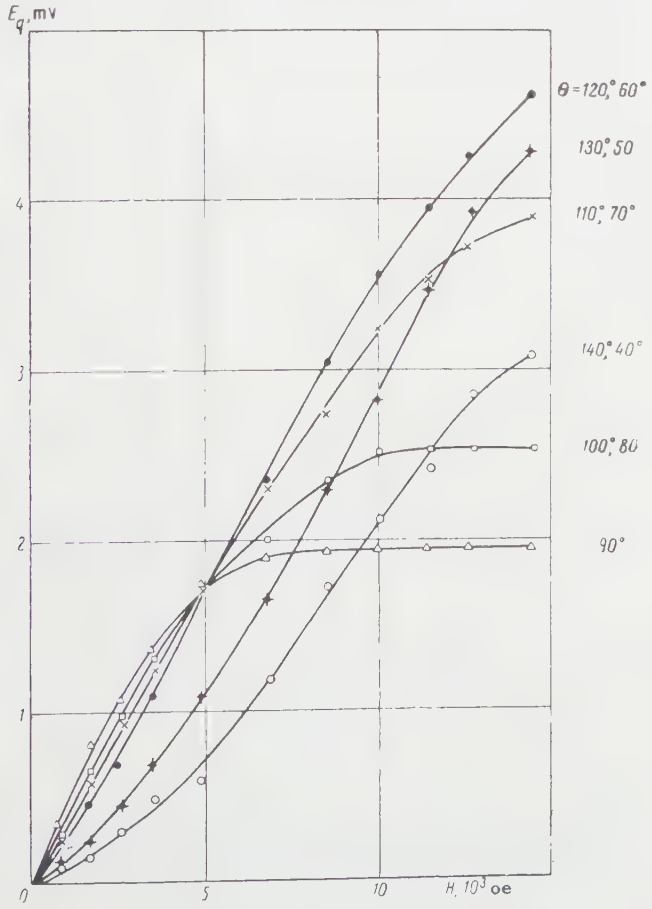

FIG. 2

At the moment we cannot suggest a satisfactory explanation of the observed anomalies. It is possible that they are connected with the presence of many carrier effective masses[4] each of which "shows up" at an appropriate angle θ.

---

[1] I. K. Kikoin and Yu. A. Bykovskiĭ, Doklady Akad. Nauk SSSR **116**, 381 (1957), Soviet Phys. Doklady **2**, 477 (1958).

[2] Yu. Kagan and Ya. A. Smorodinskiĭ, JETP **34**, 1346 (1958), Soviet Phys. JETP **7**, 929 (1958).

[3] I. K. Kikoin and S. D. Lazarev, Doklady Akad. Nauk SSSR, in press.

[4] Yu. Kagan, JETP **38**, 1854 (1960), Soviet Phys. JETP **11**, 1333 (1960).

Translated by D. ter Haar
265

CONCERNING THE RADIATION OF A NUCLEUS IN THE PRESENCE OF UNEXCITED NUCLEI OF THE SAME TYPE

M. I. PODGORETSKIĬ and I. I. ROĬZEN

Joint Institute for Nuclear Research

Submitted to JETP editor May 31, 1960

J. Exptl. Theoret. Phys. (U.S.S.R.) **39**, 1473-1475 (November, 1960)

If the emission of a γ quantum by an excited nucleus takes place in the presence of one or several nuclei of the same type, it becomes possible for the γ quantum to "wander" inside such a system. As will be shown below, in many cases this may lead to a change in the observed frequency and to a damping of the radiation (see also reference 1). It is assumed that the nuclei can be regarded as isotropic classical oscillators.

1. We consider the question of the radiation of a nucleus which is a component of a symmetric diatomic molecule, the axis a of which is fixed in space $(a \gg \lambda$, where λ is the radiated wavelength$)$. The radiation field of such a molecule at a point far from the molecule and at an angle ϑ to its axis (which is assumed directed from the oscillator with dipole moment P_0 to the oscillator with dipole moment P_1), can be determined by solving the system of equations

$$\ddot{P}_0(t) + \beta\ddot{P}_1(t - a/c) + 2\gamma\dot{P}_0(t) + \omega^2 P_0(t) = 0,$$
$$\ddot{P}_1(t) + \beta\ddot{P}_0(t - a/c) + 2\gamma\dot{P}_1(t) + \omega^2 P_1(t) = 0,$$
$$E(\mathbf{R}_0, t) \sim \frac{1}{R_0 c^2}\left[\ddot{P}_0\left(t - \frac{R_0}{c}\right) + \ddot{P}_1\left(t - \frac{R_0}{c} + \frac{a\cos\vartheta}{c}\right)\right], \quad (1)$$

where $\gamma = \tau/2$, τ is the average lifetime, $\beta = (3/4\pi)(\lambda/a)(\gamma/\omega)$, and the distance $\mathbf{R}_0$ is measured from P_0. For the sake of simplicity we assume here that the radiation is polarized in a plane perpendicular to the axis of the molecule.

We specify the following initial conditions:

$$P_k(t) = \dot{P}_k(t) \equiv 0 \text{ for } t < 0,$$
$$P_k(0) = A\delta_{k0},\ \dot{P}_k(0) = 0,\ k = 0.1. \quad (2)$$

The solution of the system (1) with initial conditions (2) leads, accurate to quantities of order γ/ω, to the following result:

$$P_0(t) = \tfrac{1}{2}A\left[\cos\omega_1 t \exp(-|\gamma_1|t) + \cos\omega_2 t \exp(-|\gamma_2|t)\right],$$
$$P_1(t) = \tfrac{1}{2}A\left[\cos\omega_1 t \exp(-|\gamma_1|t) - \cos\omega_2 t \exp(-|\gamma_2|t)\right], \quad (3)$$

where

$$\omega_1 = \omega\left(1 - \tfrac{1}{2}\beta\cos\frac{\omega a}{c}\right), \qquad \omega_2 = \omega\left(1 + \tfrac{1}{2}\beta\cos\frac{\omega a}{c}\right),$$
$$\gamma_1 = -\gamma - \tfrac{1}{2}\beta\omega\sin\frac{\omega a}{c} < 0, \qquad \gamma_2 = -\gamma + \tfrac{1}{2}\beta\omega\sin\frac{\omega a}{c} < 0. \quad (4)$$

Substituting (3) into the expression for the field intensity E from (1), we see that a rather complicated time-dependent situation results and, in particular, the decay curve is non-exponential, becoming such only after the lapse of a time

$$\tau' > 1/|\gamma_1 - \gamma_2| = 1/\beta\omega|\sin(\omega a/c)|.$$

The corresponding decay constant is less than γ by an amount

$$\frac{\beta\omega}{2}\sin\frac{\omega a}{c} = \left(\frac{3}{8\pi}\frac{\lambda}{a}\sin\frac{\omega a}{c}\right)\gamma.$$

It is obvious that the initial assumption, that the position of the molecule axis is fixed in space, is not essential for these conclusions.

2. In order to obtain an idea concerning the radiation of an excited nucleus contained in a crystal, we consider the subsidiary problem of the radiation of an oscillator contained in a one-dimensional chain with a period a. This problem already includes all the characteristic features inherent in the radiation from a crystal. At the same time, it can be completely solved in analytic form.

In order to obtain the radiation field at a certain point, we must know the function

$$F(t) = \sum_k \frac{1}{R_k} P_k\left(t - \frac{R_k}{c}\right), \quad (5)$$

where R_k is the distance from this point to the k-th oscillator, and the summation is carried out over all the oscillators of the chain. It is easy to see that F(t) obeys the following equation

$$\ddot{F}(t) + \beta\sum_k\sum_{n\neq 0}\frac{1}{R_k|n|}\ddot{P}_{k+n}\left(t - \frac{a|n|}{c} - \frac{R_k}{c}\right)$$
$$+ 2\gamma\dot{F}(t) + \omega^2 F(t) = 0. \quad (6)$$

In the case when the distance to the point of observation is much greater than the length of the chain, equation (6) can be rewritten in closed form:*

$$\ddot{F}(t) + \beta\sum_{\substack{n=-\infty \\ n\neq 0}}^{n=\infty}\frac{1}{|n|}\ddot{F}\left(t - \frac{a|n| + bn}{c}\right)$$
$$+ 2\gamma\dot{F}(t) + \omega^2 F(t) = 0, \quad (7)$$

where $b = a\cos\vartheta$, and ϑ is the angle between $\mathbf{R}_0$ and the axis of the chain, which is assumed directed towards positive indices k. If we specify an initial condition analogous to (2), the solution of (7) will have the following form:

$$F(t) \sim A\exp(-|\gamma(\vartheta)|t)\cos\omega(\vartheta)t, \quad (8)$$

where

$$\omega(\vartheta) = \omega\left\{1 + \frac{\beta}{4}\ln\left[4\sin^2\frac{\omega(a+b)}{2c} + \frac{\gamma^2(\vartheta)(a+b)^2}{c^2}\right]\right.$$
$$\left.\times\left[4\sin^2\frac{\omega(a-b)}{2c} + \frac{\gamma^2(\vartheta)(a-b)^2}{c^2}\right]\right\},$$
$$\gamma(\vartheta) = -\gamma + \frac{1}{4}\omega\beta\left\{\left[(2n_1 + 1)\pi - \frac{\omega(a+b)}{c}\right]\right.$$
$$\left. + \left[(2n_2 + 1)\pi - \frac{\omega(a-b)}{c}\right]\right\}. \quad (9)$$

Here n_1 and n_2 are integers, which must be chosen such that the absolute values of the expressions in the square brackets in (9) do not exceed π.

It is seen from (8) that at each angle there is a different frequency $\omega(\vartheta)$, and different damping $\gamma(\vartheta)$. It is interesting to note that the character of the dependence of ω and γ on ϑ recalls the distribution of intensity in the case of diffraction by a one-dimensional grating. The change in frequency is

$$\Delta\omega = |\omega - \omega(\vartheta)| \sim \omega\beta/4 = (3/16\pi)\lambda\gamma/a. \quad (10)$$

However, near angles ϑ for which $\sin[\omega(a \pm b)/2c] \sim 0$, its magnitude becomes considerably greater. From (9) we get that

$$\max||\gamma(\vartheta)| - \gamma| \sim 3\gamma\lambda/8a, \quad (11)$$

that is, the change in the damping can become quite appreciable. As time goes on, the radiation remains only at those angles corresponding to minimum damping.

In conclusion, we give an equation for the amplitude $\chi(t)$ of the radiation from a crystal with cubic lattice at a point the direction to which is given by the vector $\mathbf{m}$, $|\mathbf{m}| = 1$:

$$\ddot{\chi}(t) + \beta \sum_{\mathbf{k} \neq 0} \frac{1}{|\mathbf{k}|} \ddot{\chi}\left[t - \frac{a}{c}(|\mathbf{k}| + \mathbf{km})\right]$$
$$- \beta \sum_{\mathbf{k} \neq 0} \frac{\mathbf{k}}{|\mathbf{k}|^3}\left(\mathbf{k}, \ddot{\chi}\left[t - \frac{a}{c}(|\mathbf{k}| + \mathbf{km})\right]\right)$$
$$+ 2\gamma\dot{\chi}(t) + \omega^2\chi(t) = 0. \tag{12}$$

The similarity between (7) and (12) gives grounds for expecting that their solutions will also be essentially similar. The described variation in frequency can be observed, in principle, by the procedure proposed by Mössbauer.[2,3]

The authors are grateful to V. I. Ogievetskiĭ, V. M. Faĭn, Ya. I. Khanin, D. S. Chernavskiĭ, and F. L. Shapiro for participating in a discussion of this work and for significant comments.

---

*For the approximations made in the derivation of (7), it is also necessary that the condition $1 \pm \cos\vartheta \gg 2\pi\gamma/\omega$ be satisfied; this condition is violated only for angles ϑ which are exceedingly close to $\vartheta = 0$ and $\vartheta = \pi$.

---

[1] M. I. Podgoretskiĭ and I. I. Roĭzen, preprint, Joint Institute for Nuclear Research, R-546g.

[2] R. L. Mössbauer, Z. Phys. **151**, 124 (1958).

[3] R. L. Mössbauer, Z. Naturforsch. **14a**, 211 (1959).

Translated by J. G. Adashko
266

SCATTERING MATRIX OF NUCLEONS ON A TARGET WITH SPIN 1

P. VINTERNITTS

Leningrad State University

Submitted to JETP editor July 8, 1960

J. Exptl. Theoret. Phys. (U.S.S.R.) **39**, 1476 (November, 1960)

THE article by Budyanskiĭ[1] contains the general form of the scattering matrix of a particle with spin $\frac{1}{2}$ by a particle with spin 1, and 12 observable quantities are calculated, making up one of the possible complete sets of experiments. It appears to us that this matrix has not been written down quite correctly.

Using the Oehme method[2] we can write the matrix for the scattering of nucleons on any target in the form

$$M = a + b\,\boldsymbol{\sigma}\mathbf{n} + c\,\boldsymbol{\sigma}\mathbf{m} + d\,\boldsymbol{\sigma}\mathbf{l} \tag{1}$$

(the notation is the same as used by Oehme[2]). The coefficients in (1) should have the following form:

$$a = \alpha_1 I + \alpha_2 S_n + \alpha_3 S_m^2 + \alpha_4 S_l^2,$$
$$b = \beta_1 I + \beta_2 S_n + \beta_3 S_m^2 + \beta_4 S_l^2,$$
$$c = \gamma_1 S_m + \gamma_2 (S_n S_m + S_m S_n), \quad d = \delta_1 S_l + \delta_2 (S_n S_l + S_l S_n). \tag{2}$$

If we transform the scattering matrix given by Budyanskiĭ[1] to the form (1), we obtain

$$a = A_1 I + A_2 S_n + A_3 (S_m^2 + S_l^2),$$
$$b = B_1 I + B_2 S_n + B_3 (S_m^2 + S_l^2),$$
$$c = C_1 S_m + C_2 S_n S_m + C_3 S_m S_n,$$
$$d = D_1 S_l + D_2 S_n S_l + D_3 S_l S_n. \tag{3}$$

It is obvious that no general considerations lead to $\alpha_3 = \alpha_4$ and $\beta_3 = \beta_4$. On the other hand, the complete system of orthonormal basis matrices of the spin space of the particle with spin 1 do not contain expressions of the type $S_i S_k$ and $S_k S_i$ individually, but of the type $S_i S_k + S_k S_i$ (see, for example, reference 3), and consequently one must assume $C_2 = C_3$ and $D_2 = D_3$. The number of complex scalar coefficients should actually be 12 (this follows from general relations given by Puzikov[4]), and this is satisfied by the scattering matrix both in form (2) and (3). It is naturally necessary to use the formula (2), and not (3), for all calculations and suitably correct all the expressions for the cross sections, the polarization, and the correlation functions obtained in reference 1.

---

[1] G. M. Budyanskiĭ, JETP **33**, 889 (1957), Soviet Phys. JETP **6**, 684 (1958).

[2] R. Oehme, Phys. Rev. **98**, 147 (1955).

[3] A. S. Davydov, Теория атомного ядра (Theory of the Atomic Nucleus), M., Fizmatgiz, 1958.

[4] L. D. Puzikov, JETP **34**, 947 (1958), Soviet Phys. JETP **7**, 655 (1958).

Translated by J. G. Adashko
267

OBSERVATION OF POSITRONIUM REACTIONS IN AQUEOUS SOLUTIONS

V. I. GOL'DANSKIĬ, O. A. KARPUKHIN, and G. G. PETROV

P. N. Lebedev Physics Institute, Academy of Sciences, U.S.S.R. and Institute of Chemical Physics, Academy of Sciences, U.S.S.R.

Submitted to JETP editor August 2, 1960

J. Exptl. Theoret. Phys. (U.S.S.R.) 39, 1477-1478 (November, 1960)

SEVERAL reports have recently been published on the annihilation of positrons in aqueous solutions, or on the effect of different additives on this annihilation,[1-4] and the proposed treatment of the observed results is based on attempts to introduce the thermodynamic oxidation-reduction potential of positronium.[3,4] Such a treatment, however, is not completely correct for the following reasons: a) in connection with the fast annihilation of the positrons, chemical processes of the type

$$\mathrm{Ox} + \mathrm{Ps} \rightarrow \mathrm{Red} + \mathrm{Ps}^{+}$$

(Ox — oxidizer, Red — reducer, $\mathrm{Ps} = e^{+}e^{-}$, $\mathrm{Ps}^{+} = e^{+}$) are essentially irreversible; b) for the same reason and because of the exceedingly small stationary concentrations of Ps and Ps^{+}, one cannot use for the analysis of the positronium reactions the potentials of multi-electron transitions of the type $\mathrm{Me}^{++} + 2\mathrm{Ps} \rightarrow \mathrm{Me} + 2\mathrm{Ps}^{+}$ (Me — metal); c) no macroscopic metallic phase is produced in reactions in which positronium participates, so that there is no justification for operating with standard metal-ion potentials. We note furthermore that the experiments described in references 1 — 4 were carried out essentially in highly concentrated (2M) solutions of multi-valent ions, in which the activity of the ions is, as is well known, a highly indeterminate quantity. In order to demonstrate the essentially kinetic character of the action of different substances on the annihilation of positronium in aqueous solutions, and in order to arrive at a systematic comparison of such an action with oxidation-reduction and magnetic characteristics of different ions, we have carried out a series of experiments to investigate the rate of 3γ annihilation of positrons from a Na^{22} source (0.1 mC) in aqueous solutions. Without going into details of the apparatus, which is similar to that described by McGervey and de Benedetti,[3] we shall indicate only the basic results.

1) The table indicates the decrease in the rate of 3γ annihilation compared with pure water under the influence of various additives (essentially, different cations with a Cl^{-} anion inert to positronium). In the presence of a general tendency towards reduction of the counting rate $C_{3\gamma}$ on going over to stronger oxidizers, there are, however, also serious deviations from such a sequence.

Substance	Concentration, mole/liter	Standard oxidation-reduction potential for the oxidizer-reducer pair indicated in parentheses	No. of unpaired electrons	Difference in $C_{3\gamma}$ (min^{-1}) relative to water
KOH	1	+2.92 ($\mathrm{K}^{+}/\mathrm{K}$)		—0.02±0.31
$\mathrm{BaCl_2}$	2	+2.92 ($\mathrm{Ba}^{++}/\mathrm{Ba}$)		—0.55±0.39
NaCl	2	+2.71 ($\mathrm{Na}^{+}/\mathrm{Na}$)		+0.07±0.25
$\mathrm{MnCl_2}$	2	+1.10 ($\mathrm{Mn}^{++}/\mathrm{Mn}$)	5	—0.57±0.26
$\mathrm{ZnCl_2}$	2	+0.76 ($\mathrm{Zn}^{++}/\mathrm{Zn}$)		+0.24±0.34
$\mathrm{FeCl_2}$	0.1	+0.44 ($\mathrm{Fe}^{++}/\mathrm{Fe}$)	4	—0.99±0.27
$\mathrm{CrCl_3}$	2	+0.41 ($\mathrm{Cr}^{+++}/\mathrm{Cr}^{++}$)	3	—1.70±0.28
$\mathrm{TlNO_3}$	saturation	+0.34 ($\mathrm{Tl}^{+}/\mathrm{Tl}$)		—1.24±0.29
$\mathrm{CoCl_2}$	2	+0.27 ($\mathrm{Co}^{++}/\mathrm{Co}$)	3	—1.17±0.40
$\mathrm{NiSO_4}$	2	+0.23 ($\mathrm{Ni}^{++}/\mathrm{Ni}$)	2	—1.03±0.36
$\mathrm{CuCl_2}$	2	—0.34 ($\mathrm{Cu}^{++}/\mathrm{Cu}$)	1	—1.85±0.31
$\mathrm{FeCl_3}$	2	—0.77 ($\mathrm{Fe}^{+++}/\mathrm{Fe}^{++}$)	5	—2.62±0.33
$\mathrm{FeCl_3}$	0.1	—0.77 ($\mathrm{Fe}^{+++}/\mathrm{Fe}^{++}$)	5	—1.41±0.28
$\mathrm{KMnO_4}$	saturation	—1.63 ($\mathrm{MnO'_4} + 3e/\mathrm{MnO_2}$)		—2.44±0.42
$\mathrm{H_2O_2}$	30% by weight	—1.78 ($\mathrm{H_2O_2} + 2e/\mathrm{H_2O}$)		—1.55±0.28

These deviations can be partially due to the $^3S_1 \rightarrow {}^1S_0$ conversion on unpaired electrons of paramagnetic ions, but there is likewise no unambiguous connection between the magnetic properties of the ions and the value of $C_{3\gamma}$. Thus, in spite of the similarity of the data in the Table with the results of McGervey and de Benedetti,[3] and also with the results of Trumpy[4] (in those cases where we investigated the same additives), we do not consider it established that a systematic variation of $C_{3\gamma}$ takes place with standard oxidation-reduction potentials of the additives.

2) In accordance with the results of Green and Bell[1] and of Trumpy,[4] we have also observed a strong quenching of the counting rate $C_{3\gamma}$ by additions of the oxidizer anion $\mathrm{NO_3^-}$, and found in addition that $\mathrm{MnO_4^-}$ has an even stronger action. But the action of $\mathrm{MnO_4^-}$ (0.01 M) was found to be perfectly identical in strongly acid (pH = 2), neutral (pH = 7) and alkali (pH = 12) solutions: the respective values of $C_{3\gamma}$ were 5.13 ± 0.16, 5.01 ± 0.16, and 5.15 ± 0.27 min^{-1} (the value for water being 6.04 ± 0.09). This demonstrates convincingly the decisive role of the concentration of $\mathrm{MnO_4^-}$, and not of the oxidation-reduction potential of the system. We can arrive at an analogous conclusion from data on the quenching of $C_{3\gamma}$ by means of additives of Fe^{+++} and Fe^{++}, taken at different concentrations.

3) The counting rate $C_{3\gamma}$ as a function of the concentration of the $\mathrm{MnO_4^-}$ additive (in neutral solution) is given by the following figures:

Concentration of MnO_4, mole/liter	Saturated solution	0.1	0.01	0.001	0 (water)
$C_{3\gamma}$, min^{-1}	3.6±0.42	5.08±0.45	5.08±0.12	5.50±0.30	6.04±0.09

It is obvious that the quenching of $C_{3\gamma}$ appears quite strongly even at low concentrations. In experiments with high concentrations of highly active additives, the value of $C_{3\gamma}$ tends to a limit corresponding to the contribution of free 3γ annihilation. Therefore a quantitative comparison of the effects of different additives on the formation and conversion of positronium makes it obligatory to perform the experiments at small concentrations. At the present time we continue systematic investigations of the kinetic characteristics of different reactions of positronium in aqueous solutions.

The authors are grateful to Academician A. N. Frumkin for a discussion of the obtained results.

---

[1] R. Green and R. Bell, Can. J. Phys. **35**, 398 (1957); **36**, 1684 (1958).

[2] R. de Zafra, Phys. Rev. **113**, 1457 (1959).

[3] J. McGervey and S. de Benedetti, Phys. Rev. **114**, 495 (1959).

[4] G. Trumpy, Phys. Rev. **118**, 668 (1960).

Translated by J. G. Adashko
268

ASYMMETRY OF MOTT DOUBLE SCATTERING AND ABSOLUTE VALUES OF LONGITUDINAL POLARIZATION OF BETA PARTICLES

P. E. SPIVAK, L. A. MIKAÉLYAN, I. E. KUTIKOV, and V. F. APALIN

Submitted to JETP editor August 24, 1960

J. Exptl. Theoret. Phys. (U.S.S.R.) **39**, 1479-1481 (November, 1960)

As a result of relative measurements of longitudinal polarization of the β particles emitted in the decay of P^{32}, Sm^{153}, Lu^{177}, Ho^{166}, In^{114}, and Au^{198}, differences up to 12% have been observed in the magnitude of the longitudinal polarization. This result showed the presence of deviations of the magnitude of the polarization from the predicted value, which for electrons is equal to v/c. The size of these deviations was obtained from results of absolute measurements of the polarization of the electrons from Sm^{153}.[2] The longitudinal polarization of the electrons was converted to a transverse polarization in crossed magnetic and electric fields and was found from the asymmetry of the scattering by gold from the relation

$$\langle\sigma\rangle = (1 + J_l / J_r) / (1 - J_l / J_r)\, S,$$

where $\langle\sigma\rangle$ is the degree of polarization, J_l and J_r are the scattered intensities to left and right, and S is a function of angle, energy and charge. Using the values of S computed by Sherman,[3] we found that in the case of Ho^{166} and In^{114} the differences of the values of the polarization from the value of v/c reached 12 — 15%.

As we have noted,[1,2] for a final judgment concerning the magnitude of the deviation of the polarization from the value v/c we must have trustworthy values of the function S. The existing experimental data concerning this question are in most cases not sufficiently exact, while for the angles and energies which are of interest to us there are no data at all.

In this connection, we undertook a measurement of the quantity S in an experiment on double scattering of unpolarized electrons by gold. In the following we give a brief description of the apparatus and the results of measurements for energies of 245 and 290 kev and scattering angles $\theta_1 = \theta_2 = 120°$. At present, we are carrying out measurements over an energy range 50 — 250 kev and scattering angles 90 — 150°. The detailed description of the work will be published soon.

The geometry of the experiment is shown in the figure. A beam of accelerated electrons 2, after passing through a system of diaphragms, entered a chamber in which there was placed the first scatterer 1. The second scatterer 4 was in a separate chamber at a distance of ~ 1 meter from the first. The twice-scattered electrons were recorded by ring Geiger counters 3 placed at a distance of about 20 cm from the second scatterer. To reduce scattering from the walls of the appa-

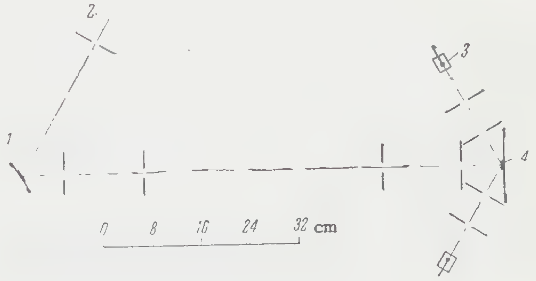

ratus, the linear dimensions of the chambers were chosen to be large (around 400 mm) and the internal surface was covered with Plexiglas on which a conducting layer of graphite was deposited. Careful study of the effect of scattering of the electrons from the walls of the first chamber showed that under the conditions of the experiment the relative number of such electrons which impinge on the second scatterer amounts to (0.4 ± 0.2)%. The effect of scattering in the second chamber did not exceed 0.25%.

Measurement of the energy spectrum of the electrons showed that for the electrons impinging on the second scatterer the energy spread corresponds to a width at half-height of ± 1.5%. The apparatus asymmetry was eliminated by replacing the first gold scatterer by an aluminim scatterer of thickness 1.4 mg/cm². Since the electrons scattered by the aluminum also have some polarization, the experimentally measured quantity differs from S^2_{Au} and is equal to $S^2_{Au}(1 - S_{Al}/S_{Au})$. According to Sherman, $S_{Al}/S_{Au} = 0.1$.

The effect of multiple scattering in the scatterers was determined by making measurements for different thicknesses of the first and second scatterers. Altogether we used four first and four second scatterers whose thicknesses lay in the range from 70 to 300 μg/cm². The statistical accuracy of each measurement of the quantity S was ± 3%. The counting rate was usually 500 — 1500 pulses/min, while the relative magnitude of the background did not exceed 5%. Corrections were made on the experimentally determined scattering asymmetries for: a) scattering from the walls of the first chamber — (0.4 ± 0.2)%; b) scattering from the backing of the scatterer material — from 2 to 4% depending on the thicknesses of the scatterers; c) for the finiteness of the angles of observation — 0.5%. As a result we obtained the values given in the table.

Electron energy, kev	S^2	S	S/S_T
245	0,168±4 %	0.411±2 %	0.960±2 %
290	0,161±4 %	0,401±2 %	0.941±2 %

Here S/S_T denotes the ratio of the experimentally measured values to the values obtained from Sherman's tables.

The results obtained show that the absolute values of longitudinal polarization previously given by us[2] should be increased by 5%.

In the present work we also had the possibility for experimentally finding the magnitude of the depolarization of the electrons along their path from the source to the scatterer in the system of crossed fields which was used by us earlier.[2] The measurements consisted in first finding the scattering asymmetry for a given pair of scatterers. Then we placed between the scatterers the system with crossed fields and repeated the asymmetry measurement, where the field magnitudes were chosen so that the angle through which the spin turned was 180°. These measurements were carried out for electrons of energy 170 kev, which under our conditions could still have their spin rotated through 180°.

As a result of these measurements, it was found that the depolarization along the path from source to scatterer in the crossed field system reduces the magnitude of the asymmetry by (2 ± 2)% in agreement with the estimate made by us earlier.[2]

We give below the absolute values of longitudinal polarization of electrons for an energy of 300 kev, obtained using the results of the present work.

	P^{32}	Sm^{153}	Lu^{177}	Ho^{166}	In^{114}	Au^{198}
Polarization $\langle\sigma\rangle/(v/c)$	1.02	0.97	0.92	0.91	0.93	0.94
Error of relative measurements, %	1.5	—	1.5	1.5	2.5	2.0

The error of the absolute measurements amounts to 3.3%.

Thus it has been established that deviation of the degree of longitudinal polarization from the value v/c is not an exceptional phenomenon, as was thought earlier. The magnitude of these deviations in the cases considered by us reached 8 — 9%. Apparently the observed deviations must be ascribed to an effect of the structure of the nucleus.

---

[1] L. A. Mikaélyan and P. E. Spivak, JETP **37**, 1168 (1959), Soviet Phys. JETP **10**, 831 (1960).

[2] P. E. Spivak and L. A. Mikaélyan, JETP **39**, 1479 (1960), this issue p. 1027. Nucl. Phys. (in press).

[3] N. Sherman, Phys. Rev. **103**, 1601 (1956).

Translated by M. Hamermesh
269

ANTIFERROMAGNETISM OF $CoCO_3$

R. A. ALIKHANOV

Institute of Physics Problems, Academy of Sciences, U.S.S.R.

Submitted to JETP editor August 26, 1960

J. Exptl. Theoret. Phys. (U.S.S.R.) **39**, 1481-1483 (November, 1960)

THE magnetic susceptibility of cobalt carbonate, which is isomorphous with the $MnCO_3$ and $FeCO_3$ crystals investigated in earlier work,[1] exhibits typically antiferromagnetic behavior from room temperature to 40° K, according to Bizette.[2] The decrease of the reciprocal susceptibility below this temperature range is especially rapid from 20° to 14° K, like that of a ferromagnet. Borovik-Romanov and Orlova[3] later obtained more detailed measurements of the susceptibility of powdered $CoCO_3$, finding less ferromagnetism than one would expect from ferromagnetic saturation. By analogy with the ideas of Matarrese and Stout[4] regarding the ferromagnetism of NiF_2, it was suggested that the observed weak ferromagnetism can result if the antiferromagnetic sublattices are not exactly antiparallel. According to Borovik-Romanov and Orlov, the ferromagnetism of $CoCO_3$ is relatively large (~ 3% of the saturation moment) and can be detected by means of neutron diffraction.

We first began to study $CoCO_3$ in 1958, when, since other sources were unavailable, we used the native $CoCO_3$ mineral spherocobaltite from the vicinity of Riegelsdorf, Germany.* However, the observed neutron-diffraction pattern could not be interpreted on the basis of the known $CoCO_3$ parameters,[5] since neither the Bragg angles nor the reflection intensities agreed with the calculated values. Cooling to 4.2° K produced no change in the pattern. It was evident that the spherocobaltite specimen did not possess the sought magnetic properties.

We have now investigated a finely crystalline hydrothermal specimen† of $CoCO_3$, the neutron-diffraction pattern of which at 4.2° K is shown in Fig. 1. The small-angle (111) and (100) reflections are of magnetic origin; they are absent at 20.4° K. Unlike the case of $MnCO_3$, the relative intensities I of these peaks show that magnetic scattering contributes mainly to the (100) reflection, whose intensity is more than twice that of the (111) reflection. This indicates that the magnetic moments of Co^{++} ions, unlike those of Mn^{++} ions in the analogous situation, depart from the (111) planes in such a way that the sum of the projections of moments on (100) planes considerably exceeds that on (111) planes. Calculation of the direction of antiferromagnetism relative to the rhombohedral axis, using the magnetic intensity ratio, indicates an angle of 46 ± 4° between the moments and the [111] axis. Erickson's value for the form factor of Co^{++} was used.

In addition to the (111) and (100) magnetic reflections, as the temperature was reduced from 20.4° to 4.2° K some intensity increase was observed in the case of (110) and (211) reflections. In a number of successive runs the latter oscillated from 2 to 6.5% of the (211) nuclear intensity. The small magnetic contribution to reflections with even sums of indices for the given structure results from weak ferromagnetism. Dzyaloshinskiĭ's thermodynamic theory[7] proposes three possible magnetic states of Mn, Fe, and Co carbonates at temperatures below T_N. For the present case the most suitable of these is state II, with the following conditions for the minimum of the thermodynamic potential:

$$\beta \approx \pi/2 - d/a, \quad \varphi = \pi/2, \quad m_x = q/B, \quad m_y = m_z = 0,$$

where β is the angle between the spins and (111),

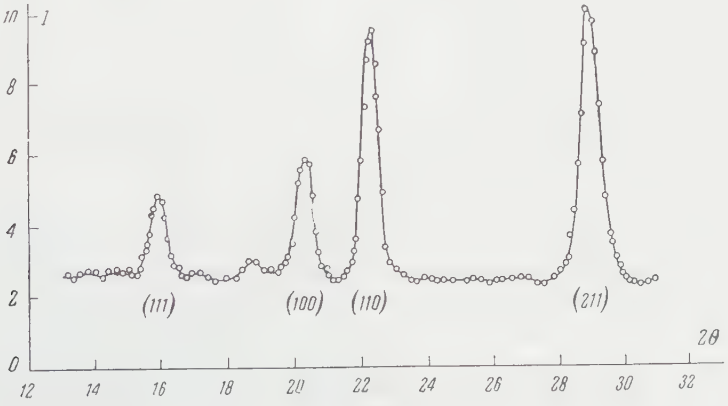

FIG. 1

φ is the angle between the spin projections on (111) and the twofold symmetry axis, $\mathbf{m}$ is the ferromagnetic moment, and d, a, g, B are expansion coefficients [see Eq. (3a) in reference 7]. Figure 2 gives the experimentally observed arrangement of magnetic moments in $CoCO_3$, corresponding to state II. It should be noted that the angle β is very close to the direction of the shortest distance from the central ion to its nearest neighbor. This picture differs somewhat from the theoretical prediction for state II, since the coefficient ratio d/a is of the order of unity, whereas the theory predicts the very small ratio $\sim v^2/c^2$.

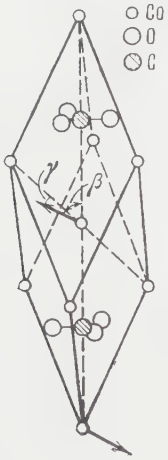

FIG. 2

In connection with this additional observed type of antiferromagnetic structure for isomorphous carbonates of the iron group, it should be remembered that in $FeCO_3$ magnetic moments are directed along the [111] axis, while in $MnCO_3$ they lie in the (111) plane.

The weak ferromagnetism of $CoCO_3$, which is indicated by the small magnetic contribution to the (211) reflections, shows that the magnetic moments of the ions form a small angle γ with the plane of symmetry, thus producing a total ferromagnetic moment along the twofold axis (Fig. 2). The ratio between ferromagnetic and antiferromagnetic contributions to the (211) and (100) reflections indicates $15 \pm 5°$ as the magnitude of γ. The existence of the ferromagnetic moment (8.6%) in the (111) plane was recently observed by Borovik-Romanov and Ozhogin,[8] who investigated the weak ferromagnetism of $CoCO_3$ in crystals obtained from the same source as ours.† They calculated $\gamma = 7°$, from their absolute data for the ferromagnetic moment and the calculated saturation moment of the ion. Aside from experimental errors, uncertainty regarding the saturation moment of Co^{++} is the most likely source of a discrepancy regarding γ.

I am deeply grateful to Academician P. L. Kapitza for his continued interest in this work. I also wish to thank A. S. Borovik-Romanov and I. E. Dzyaloshinskiĭ for valuable discussions, N. Yu. Ikornikova and N. N. Mikhaĭlov for producing and classifying the crystal specimen, and I. P. Karpikhin for experimental assistance.

---

*The author is greatly indebted to Prof. S. D. Chetverikov, P. V. Kalinin, M. G. Spiridonova, and B. M. Shmakin for their assistance in preparing the mineral specimen.

†This specimen was prepared by I. Yu. Ikornikova at the Institute of Crystallography, Academy of Sciences, U.S.S.R.

---

[1] R. A. Alikhanov, JETP **36**, 1690 (1959), Soviet Phys. JETP **9**, 1204 (1959).

[2] H. Bizette, Ann. phys. **1**, 233 (1946).

[3] A. S. Borovik-Romanov and M. P. Orlova, JETP **31**, 579 (1956), Soviet Phys. JETP **4**, 531 (1957).

[4] L. M. Matarrese and J. W. Stout, Phys. Rev. **94**, 1792 (1954).

[5] R. W. G. Wyckoff, The Structure of Crystals, Chem. Catalog. Co., New York, 1931.

[6] R. A. Erickson, Phys. Rev. **90**, 779 (1953).

[7] I. E. Dzyaloshinskiĭ, JETP **32**, 1547 (1957), Soviet Phys. JETP **5**, 1259 (1957).

[8] A. S. Borovik-Romanov and V. I. Ozhogin, JETP **39**, 27 (1960), Soviet Phys. JETP **12**, 18 (1961).

Translated by I. Emin
270

DIPOLE MOMENT OF UNSTABLE ELEMENTARY PARTICLES

Ya. B. ZEL'DOVICH

Submitted to JETP editor September 7, 1960

J. Exptl. Theoret. Phys. (U.S.S.R.) **39**, 1483-1485 (November, 1960)

PARITY nonconservation makes it possible for an elementary particle with spin to have a dipole moment.[1] Landau's theory of combined inversion[2] leads to time-reversal invariance, from which Landau concludes that elementary particles do not have an electric dipole moment.

However, this conclusion cannot be extended to apply to decaying unstable particles. To prove Landau's assertion, we consider a particle with spin and a dipole moment. Time reversal changes the spin direction, but leaves the direction of the dipole moment unchanged; it follows that there can be no time-reversal-invariant relation between spin and dipole moment.

An unstable particle is represented by an exponentially-decaying state amplitude surrounded by outgoing waves for the decay products. Under time reversal, an unstable particle is transformed not into the same particle with reversed spin but into something entirely different — into a state with exponentially-increasing amplitude surrounded by incoming waves for the decay products. Therefore, the proof that a dipole moment is not present does not apply to unstable particles.

We shall use an example to show the connection between a particle's instability and its dipole moment. We consider a neutral particle A^0 with spin $\frac{1}{2}$. Suppose the Hamiltonian contains terms corresponding to the two different reactions

$$A^0 \rightleftarrows B^+ + C^-, \quad A^0 \rightleftarrows D^0 + E^0.$$

Further suppose that $m_B + m_C > m_A > m_D + m_E$, so that A^0 actually decays into D^0 and E^0, while the transformation of A^0 into B^+ and C^- proceeds virtually, i.e., the B^+ and C^- particles form a cloud around the A^0, but do not escape to infinity.

The dipole moment depends only on the distribution of the charged B^+ and C^- particles. We assume that the interaction $A^0 \rightleftharpoons B^+ + C^-$ is parity nonconserving, so that the B^+ and C^- cloud is a superposition of $S_{1/2}$ and $P_{1/2}$ waves. Let B^+ have spin $\frac{1}{2}$ and C^- have spin 0; the wave function of the system has two components corresponding to the two possible spin orientations of B^+.

Suppose A^0 is in the state with $s_Z = +\frac{1}{2}$. Then the wave function for B^+ and C^- has the form

$$\psi = \begin{vmatrix} af_0(r) - ib\sqrt{1/3}\, f_1(r)\cos\theta \\ ib\sqrt{2/3}\, f_1(r)\sin\theta\, e^{i\varphi} \end{vmatrix},$$

where r, θ, φ describe the relative position of B^+ and C^-.

$$f_0(r) = r^{-1}e^{-\varkappa r}, \ f_1(r) = df_0/dr = -(r^{-2} + \varkappa r^{-1})\, e^{-\varkappa r},$$

$$\varkappa = \sqrt{2\mu\Delta}, \ \mu = m_B m_C/(m_B + m_C), \ \Delta = E_B + E_C - E_A.$$

The charge density is $|\psi|^2 = \psi^*\psi$. As has been shown by the author[3] (cf. the derivation of the corresponding formulae), a and b are real in a time-reversal-invariant theory, so that if κ is real the interference term (proportional to $\cos\theta$) in the charge density vanishes and the dipole moment is identically equal to zero.

For an unstable particle, time-reversal invariance requires that the constants coupling the A particle to the S- and P-wave states of B and C (and consequently, also the amplitudes, a and b, of these waves) remain real. The difference lies in the fact that, owing to the decay of the A^0 into D^0 and E^0, the energy of the A^0 becomes complex: $E_A = m_A c^2 - iw/2$, where w is the decay probability of the A (units with $\hbar \equiv 1$). Therefore, κ also becomes complex; for small w, we have $\kappa = \kappa_0(1 + iw/4\Delta)$. With this, the dipole moment is easily found to be*

$$d_z = e\int r\cos\theta\, \psi^*\psi\, dv = -\frac{\pi}{3\sqrt{3}}\frac{e}{\varkappa_0}\frac{w}{\Delta}ab.$$

The integral which gives d_z converges, although $\int \psi^*\psi\, dv$ diverges at the origin.

Thus, with a time-reversal-invariant Hamiltonian, the combination of parity nonconservation and particle instability leads to the appearance of a dipole moment, i.e., to an apparent violation of time-reversal invariance. In this sense, the result agrees with that of Behrends,[4] who discussed the radiative decay $\Lambda \rightarrow n + \gamma$ along with the main decay channel $\Lambda \rightarrow p + \pi^-$. In this case the result contains terms obviously contradicting time-reversal invariance, notwithstanding the time-reversal invariance of the Hamiltonian.

From a general point of view, this problem is of interest as an example of the special properties of unstable particles; statements which are true for stable particles cannot be automatically extended to unstable particles.

---

*Note that the non-zero result comes from the term κr^{-1} in $f_1(r)$ and not from $\exp(-\kappa r)$.

---

[1] T. D. Lee and C. N. Yang, Phys. Rev. **104**, 254 (1956).

[2] L. D. Landau, JETP **32**, 407 (1957), Soviet Phys. JETP **5**, 336 (1957).

[3] Ya. B. Zel'dovich, JETP **33**, 1488 (1957), Soviet Phys. JETP **6**, 1148 (1958).

[4] R. E. Behrends, Phys. Rev. **111**, 1691 (1958).

Translated by M. Bolsterli
271

ON THE PION-PION RESONANCE IN THE p STATE

HO TSO-HSIU and CHOU KUANG-CHAO

Joint Institute for Nuclear Research

Submitted to JETP editor September 30, 1960

J. Exptl. Theoret. Phys. (U.S.S.R.) **39**, 1485-1486 (November, 1960)

QUITE recently there has been great interest in the question of the existence of a p resonance (isobar) in pion-pion scattering.[1] From a study of the structure of nucleons by the method of dispersion relations, Frazer and Fulco have concluded that an isobar with mass 435 Mev and half-width 10 Mev must exist in the p state of pion-pion systems.[2] Similar results on the presence of a p resonance in pion-pion scattering have also been obtained by other authors.[3] On the other hand, the integral equations for pion-pion scattering have been derived more accurately by means of the ordinary theory of one-dimensional dispersion relations.[4] Preliminary results on the solution of these equations, obtained by means of an electronic computing machine, show that the amplitude of the p wave is very small. It is as yet unknown whether there is another solution with a large p amplitude. Therefore a direct experimental test of the presence of a p isobar in the pion-pion system is of great importance. For this purpose Chew and others[5] have suggested the reactions

$$e^+ + e^- \to \pi^+ + \pi^-, \quad e^- + e^- \to e^- + e^- + \pi^+ + \pi^-, \qquad (1)$$

studies of which could help to provide information about the interaction of pions in the p state. These processes are interesting because the theoretical interpretation of the results is simple and clear. But because of the lack of high-energy clashing electron and positron beams, it is difficult to conduct such experiments at present.

In the present note we suggest the study of the following processes:

$$\pi^\pm + \mathrm{He}^4 \to \mathrm{He}^4 + \pi^\pm + \pi^0, \qquad (2a)$$

$$\pi^\pm + d \to d + \pi^\pm + \pi^0, \qquad (2b)$$

$$p + p \to d + \pi^+ + \pi^0. \qquad (2c)$$

For all of these processes the initial isotopic spin is $I = 1$. Consequently, the pair of pions in the final state has the isotopic spin $I = 1$ and is in a state with odd orbital angular momentum. In the low energy region these pions are mainly in the p state.

Let us assume that there is an isobar with mass 435 Mev and half-width 10 Mev in the p state. Then in the reactions (2) the pairs of pions come from the decay of isobars that have been produced together with nuclei He^4 or d. Because of this it is to be expected that there will be a sharp maximum in the spectrum of the He^4 (or d).

Let us consider, for example, the reaction (2a). Suppose the energy of the incident pion beam is 700 Mev in the laboratory system. (l.s.). Then in the center-of-mass system (c.m.s.) one should observe a maximum in the spectrum of the He^4 at energy 11 Mev and with half-width 2 Mev. In the case of the reaction (2c) with incident beam energy 1.4 Bev in the l.s. the deuteron spectrum in the c.m.s. must have a maximum at energy 36 Mev and with half-width 3 Mev.

If the p isobar does not exist, then the shape of the spectrum of the He^4 (d) varies smoothly and is determined mainly by the statistical phase-volume factor. Therefore measurements of the spectra of the nuclei in the reactions (2) will give information about the existence of a p resonance in the pion-pion system.

We note that the process $d + d \to \mathrm{He}^4 + \pi^0 + \pi^+ + \pi^-$ is also useful for studying the isobaric structure of pion-pion systems in the iso-scalar state.

---

[1] S. D. Drell, Proceedings of Annual International Conference on High Energy Physics, CERN, 1958.

[2] W. R. Frazer and J. R. Fulco, Phys. Rev. Letters 2, 365 (1959).

[3] F. Cerulus, Nuovo cimento **14**, 827 (1959).

[4] Hsien Ting-Ch'ang, Ho Tso-Hsiu, and W. Zoellner, Preprint D-547, Joint Institute of Nuclear Studies.

[5] G. F. Chew, preprint, 1960; N. Cabibbo and R. Gatto, Phys. Rev. Letters **4**, 313 (1960); L. M. Brown and F. Calogero, Phys. Rev. Letters **4**, 315 (1960).

Translated by W. H. Furry
272

POSSIBILITY OF USING INDIRECT TRANSITIONS TO OBTAIN NEGATIVE TEMPERATURES IN SEMICONDUCTORS

N. G. BASOV, O. N. KROKHIN, and Yu. M. POPOV

P. N. Lebedev Physics Institute, Academy of Sciences, U.S.S.R.

Submitted to JETP editor October 3, 1960

J. Exptl. Theoret. Phys. (U.S.S.R.) **39**, 1486-1487 (November, 1960)

In some semiconductors, particularly germanium and silicon, the edge of the infrared absorption and emission band corresponds to "indirect" transitions, i.e., processes in which the emission and absorption of a photon is accompanied by simultaneous emission and absorption of a phonon[1-3] This is due to the structure of the bands and takes place when the extrema of the energy with respect to the quasi-momentum of the carriers in the conduction and valence bands correspond to different values of quasimomentum.[4-5]

The radiation of longest wavelength will correspond in such transitions to simultaneous emission of a photon and one phonon (multi-phonon processes can be disregarded as having low probability compared with single-phonon processes). The inverse of the aforementioned process is the simultaneous absorption of a photon and a phonon. Therefore if a sample is at a sufficiently low temperature, when the lattice has practically none of the phonons needed for absorption, radiation of longer wavelength will not be absorbed, and the sample will be practically transparent to such radiation.

If some mechanism (optical illumination, external electric field, etc) increases the concentration of carriers above their equilibrium value, then a negative temperature can be produced relative to the transition under consideration. Estimates show that to produce a negative temperature it is necessary to satisfy the inequality $\omega_r/\omega_f < T_{eff}/T$, where ω_r and ω_f are the photon and phonon frequencies, T the sample temperature, and T_{eff} the effective temperature that determines the filling of the conduction-band levels relative to the valence-band levels. For example, in germanium $\omega_r/\omega_f \sim 25$, i.e., $T_{eff}/T > 25$, which is apparently feasible in the case of a sample cooled to helium temperatures, if the excitation is produced by presently-available radiation sources or an external electric field. However, in order for amplification of radiation to take place in such a system, it is necessary that the induced photon emission prevail over the various absorption processes in the semiconductor (absorption on free carriers, on impurities, etc).[6]

We note that there exists another possibility of producing negative-temperature states in semiconductors. In several papers,[7-10] the observed spectra of recombination radiation of some semiconductors were interpreted as simultaneous emission of a photon and a phonon from exciton states. The mechanism for production of negative temperatures, described above, is fully applicable to such states, too.

---

[1] Hall, Bardeen, and Blatt, Phys. Rev. **95**, 559 (1954).

[2] W. H. Brattain and H. B. Briggs, Phys. Rev. **75**, 1705 (1949).

[3] G. C. MacFarlane and V. Roberts, Phys. Rev. **97**, 1714 (1955) and **98**, 1865 (1955).

[4] F. Herman, Phys. Rev. **88**, 1210 (1952).

[5] Dresselhaus, Kip, and Kittel, Phys. Rev. **92**, 827 (1953).

[6] Basov, Krokhin, and Popov, Usp. Fiz. Nauk **72**, 161 (1960), Soviet Phys.-Uspekhi **3**, 702 (1961).

[7] MacFarlane, McLean, Quarrington, and Roberts, Phys. Chem. Solids **8**, 388 (1959).

[8] Haynes, Lax, and Flood, ibid **8**, 392 (1959).

[9] Zwerdling, Roth, and Lax, ibid. **8**, 397 (1959).

[10] Haynes, Lax, and Flood, International Conference on Semiconductor Physics, Prague, 1960.

Translated by J. G. Adashko
273

SOVIET PHYSICS JOURNALS

Published in English by the American Institute of Physics

Soviet Physics—JETP

A translation, beginning with 1955 issues of "Zhurnal Eksperimental'noi i Teoreticheskoi Fiziki" of the USSR Academy of Sciences. Leading physics journal of Soviet Union. Similar to "The Physical Review" in quality and range of topics. Outstanding new work is most likely to appear in this journal.

Twelve issues, approximately 4000 pages. $75 domestic, $79 foreign. Libraries $35 domestic, $39 foreign. Single copies, $8.*

Soviet Physics—SOLID STATE

A translation, beginning with 1959 issues of "Fizika Tverdogo Tela" of the USSR Academy of Sciences. Offering results of theoretical and experimental investigations in the physics of semiconductors, dielectrics, and on applied physics associated with these problems. Also publishes papers on electronic processes taking place in the interior and on the surface of solids.

Twelve issues, approximately 2000 pages. $55 domestic, $59 foreign. Libraries $25 domestic, $29 foreign. Single copies, $8.*

Soviet Physics—TECHNICAL PHYSICS

A translation, beginning with 1956 issues of "Zhurnal Tekhnicheskoi Fiziki" of the USSR Academy of Sciences. Contains work on plasma physics and magnetohydrodynamics, aerodynamics, ion and electron optics, and radio physics. Also publishes articles in mathematical physics, the physics of accelerators, and molecular physics.

Twelve issues, approximately 2000 pages, $55 domestic, $59 foreign. Libraries $25 domestic, $29 foreign. Single copies, $8.*

Soviet Physics—ACOUSTICS

A translation, beginning with 1955 issues of "Akusticheskii Zhurnal" of the USSR Academy of Sciences. Devoted principally to physical acoustics but includes electro-, bio-, and psychoacoustics. Mathematical and experimental work with emphasis on pure research.

Four issues, approximately 500 pages. $12 domestic, $14 foreign. (No library discounts.) Single copies, $4.

Soviet Physics—DOKLADY

A translation, beginning with 1956 issues of the physics sections of "Doklady Akademii Nauk SSSR," the proceedings of the USSR Academy of Sciences. All-science journal offering four-page reports of recent research in physics and borderline subjects.

Six issues, approximately 1500 pages. $35 domestic, $38 foreign. Libraries $15 domestic, $18 foreign. Single copies Vols. 1 and 2, $5; Vol. 3 and later issues, $7.*

Soviet Physics—CRYSTALLOGRAPHY

A translation, beginning with 1957 issues of the journal "Kristallografiya" of the USSR Academy of Sciences Experimental and theoretical papers on crystal structure, lattice theory, diffraction studies, and other topics of interest to crystallographers, mineralogists, and metallurgists.

Six issues, approximately 1000 pages. $25 domestic, $27 foreign. Libraries $10 domestic, $12 foreign. Single copies, $5.*

SOVIET ASTRONOMY—AJ

A translation, beginning with 1957 issues of "Astronomicheskii Zhurnal" of the USSR Academy of Sciences. Covers various problems of interest to astronomers and astrophysicists including solar activity, stellar studies, spectroscopic investigations of radio astronomy.

Six issues, approximately 1100 pages. $25 domestic, $27 foreign. Libraries $10 domestic, $12 foreign. Single copies, $5.*

Soviet Physics—USPEKHI

A translation, beginning with September, 1958, issue of "Uspekhi Fizicheskikh Nauk" of the USSR Academy of Sciences. Offers reviews of recent developments comparable in scope and treatment to those carried in "Reviews of Modern Physics." Also contains reports on scientific meetings within the Soviet Union, book reviews, and personalia.

Six issues, approximately 1700 pages. (Contents limited to material from Soviet sources.) $45 domestic, $48 foreign. Libraries $20 domestic, $23 foreign. Single copies $9.*

*For libraries of nonprofit academic institutions.
Subscription prices subject to annual variation, depending on size of Russian originals.

Please send orders and inquiries to

American Institute of Physics
335 East 45 Street, New York 17, N.Y.